

# World Journal of *Gastroenterology*

*World J Gastroenterol* 2021 May 14; 27(18): 2054-2250



### EVIDENCE REVIEW

- 2054** Role of microbial dysbiosis in the pathogenesis of esophageal mucosal disease: A paradigm shift from acid to bacteria?

*D'Souza SM, Houston K, Keenan L, Yoo BS, Parekh PJ, Johnson DA*

### REVIEW

- 2073** Immune disorders and rheumatologic manifestations of viral hepatitis

*Maslennikov R, Ivashkin V, Efremova I, Shirokova E*

### MINIREVIEWS

- 2090** Neurological manifestations of hepatitis E virus infection: An overview

*Jha AK, Kumar G, Dayal VM, Ranjan A, Suchismita A*

- 2105** Stroma-targeting strategies in pancreatic cancer: Past lessons, challenges and prospects

*Polani F, Grierson PM, Lim KH*

- 2122** Magnetic resonance imaging-based artificial intelligence model in rectal cancer

*Wang PP, Deng CL, Wu B*

- 2131** Remaining issues of recommended management in current guidelines for asymptomatic common bile duct stones

*Saito H, Kadono Y, Shono T, Kamikawa K, Urata A, Nasu J, Imamura H, Matsushita I, Tada S*

### ORIGINAL ARTICLE

#### Basic Study

- 2141** Alleviation of acute pancreatitis-associated lung injury by inhibiting the p38 mitogen-activated protein kinase pathway in pulmonary microvascular endothelial cells

*Zhang XX, Wang HY, Yang XF, Lin ZQ, Shi N, Chen CJ, Yao LB, Yang XM, Guo J, Xia Q, Xue P*

- 2160** Partially hydrolyzed guar gum attenuates non-alcoholic fatty liver disease in mice through the gut-liver axis

*Takayama S, Katada K, Takagi T, Iida T, Ueda T, Mizushima K, Higashimura Y, Morita M, Okayama T, Kamada K, Uchiyama K, Handa O, Ishikawa T, Yasukawa Z, Okubo T, Itoh Y, Naito Y*

#### Retrospective Cohort Study

- 2177** Factors influencing the failure of interferon-free therapy for chronic hepatitis C: Data from the Polish EpiTer-2 cohort study

*Janczewska E, Kolek MF, Lorenc B, Klapaczynski J, Tudrujek-Zdunek M, Sitko M, Mazur W, Zarębska-Michaluk D, Buczyńska I, Dybowska D, Czauż-Andrzejuk A, Berak H, Krygier R, Jaroszewicz J, Citko J, Piekarska A, Dobracka B, Socha Ł, Deroń Z, Laurans Ł, Białkowska-Warzecha J, Tronina O, Adamek B, Tomasiewicz K, Simon K, Pawłowska M, Halota W, Flisiak R*



**Retrospective Study**

- 2193** Totally laparoscopic total gastrectomy using the modified overlap method and conventional open total gastrectomy: A comparative study

*Ko CS, Choi NR, Kim BS, Yook JH, Kim MJ, Kim BS*

- 2205** Radiofrequency ablation *vs* surgical resection in elderly patients with hepatocellular carcinoma in Milan criteria

*Conticchio M, Inchingolo R, Delvecchio A, Laera L, Ratti F, Gelli M, Anelli F, Laurent A, Vitali G, Magistri P, Assirati G, Felli E, Wakabayashi T, Pessaux P, Piardi T, di Benedetto F, de'Angelis N, Briceño J, Rampoldi A, Adam R, Cherqui D, Aldrighetti LA, Memeo R*

**Clinical Trials Study**

- 2219** Responses to faecal microbiota transplantation in female and male patients with irritable bowel syndrome

*El-Salhy M, Casen C, Valeur J, Hausken T, Hatlebakk JG*

**Observational Study**

- 2238** Standard *vs* magnifying narrow-band imaging endoscopy for diagnosis of *Helicobacter pylori* infection and gastric precancerous conditions

*Cho JH, Jeon SR, Jin SY, Park S*

**ABOUT COVER**

Editorial Board Member of *World Journal of Gastroenterology*, Ferenc Sipos, MD, PhD, Senior Lecturer, Head of Department, Department of Internal Medicine and Haematology, Semmelweis University, Szentkirályi Street 46, Budapest H-1088, Hungary. sipos.ferenc@med.semmelweis-univ.hu

**AIMS AND SCOPE**

The primary aim of *World Journal of Gastroenterology* (WJG, *World J Gastroenterol*) is to provide scholars and readers from various fields of gastroenterology and hepatology with a platform to publish high-quality basic and clinical research articles and communicate their research findings online. WJG mainly publishes articles reporting research results and findings obtained in the field of gastroenterology and hepatology and covering a wide range of topics including gastroenterology, hepatology, gastrointestinal endoscopy, gastrointestinal surgery, gastrointestinal oncology, and pediatric gastroenterology.

**INDEXING/ABSTRACTING**

The WJG is now indexed in Current Contents®/Clinical Medicine, Science Citation Index Expanded (also known as SciSearch®), Journal Citation Reports®, Index Medicus, MEDLINE, PubMed, PubMed Central, and Scopus. The 2020 edition of Journal Citation Report® cites the 2019 impact factor (IF) for WJG as 3.665; IF without journal self cites: 3.534; 5-year IF: 4.048; Ranking: 35 among 88 journals in gastroenterology and hepatology; and Quartile category: Q2. The WJG's CiteScore for 2019 is 7.1 and Scopus CiteScore rank 2019: Gastroenterology is 17/137.

**RESPONSIBLE EDITORS FOR THIS ISSUE**

Production Editor: Ji-Hong Lin; Production Department Director: Yun-Xiaoqian Wu; Editorial Office Director: Ze-Mao Gong.

**NAME OF JOURNAL**

*World Journal of Gastroenterology*

**ISSN**

ISSN 1007-9327 (print) ISSN 2219-2840 (online)

**LAUNCH DATE**

October 1, 1995

**FREQUENCY**

Weekly

**EDITORS-IN-CHIEF**

Andrzej S Tarnawski, Subrata Ghosh

**EDITORIAL BOARD MEMBERS**

<http://www.wjgnet.com/1007-9327/editorialboard.htm>

**PUBLICATION DATE**

May 14, 2021

**COPYRIGHT**

© 2021 Baishideng Publishing Group Inc

**INSTRUCTIONS TO AUTHORS**

<https://www.wjgnet.com/bpg/gerinfo/204>

**GUIDELINES FOR ETHICS DOCUMENTS**

<https://www.wjgnet.com/bpg/gerinfo/287>

**GUIDELINES FOR NON-NATIVE SPEAKERS OF ENGLISH**

<https://www.wjgnet.com/bpg/gerinfo/240>

**PUBLICATION ETHICS**

<https://www.wjgnet.com/bpg/gerinfo/288>

**PUBLICATION MISCONDUCT**

<https://www.wjgnet.com/bpg/gerinfo/208>

**ARTICLE PROCESSING CHARGE**

<https://www.wjgnet.com/bpg/gerinfo/242>

**STEPS FOR SUBMITTING MANUSCRIPTS**

<https://www.wjgnet.com/bpg/gerinfo/239>

**ONLINE SUBMISSION**

<https://www.f6publishing.com>



## Role of microbial dysbiosis in the pathogenesis of esophageal mucosal disease: A paradigm shift from acid to bacteria?

Steve M D'Souza, Kevin Houston, Lauren Keenan, Byung Soo Yoo, Parth J Parekh, David A Johnson

**ORCID number:** Steve M D'Souza 0000-0003-3772-2616; Kevin Houston 0000-0002-8441-0132; Lauren Keenan 0000-0001-8807-0043; Byung Soo Yoo 0000-0002-8501-7922; Parth J Parekh 0000-0003-4750-775X; David A Johnson 0000-0002-8737-0711.

**Author contributions:** Johnson DA, Parekh PJ, D'Souza SM and Yoo BS contributed construction of project; all authors wrote and edited the manuscript.

**Conflict-of-interest statement:** The authors have no conflicts of interests or financial disclosures relevant to this manuscript.

**Open-Access:** This article is an open-access article that was selected by an in-house editor and fully peer-reviewed by external reviewers. It is distributed in accordance with the Creative Commons Attribution NonCommercial (CC BY-NC 4.0) license, which permits others to distribute, remix, adapt, build upon this work non-commercially, and license their derivative works on different terms, provided the original work is properly cited and the use is non-commercial. See: <http://creativecommons.org/licenses/by-nc/4.0/>

**Manuscript source:** Invited manuscript

**Steve M D'Souza, Kevin Houston, Lauren Keenan, Byung Soo Yoo, Parth J Parekh, David A Johnson,** Department of Internal Medicine, Division of Gastroenterology, Eastern Virginia Medical School, Norfolk, VA 23502, United States

**Corresponding author:** David A Johnson, MD, MACG, FASGE, FACP, MACP, Doctor, Professor, Department of Internal Medicine, Division of Gastroenterology, Eastern Virginia Medical School, 885 Kempsville Rd, Suite 114, Norfolk, VA 23502, United States. [dajevms@aol.com](mailto:dajevms@aol.com)

### Abstract

Genomic sequencing, bioinformatics, and initial speciation (*e.g.*, relative abundance) of the commensal microbiome have revolutionized the way we think about the “human” body in health and disease. The interactions between the gut bacteria and the immune system of the host play a key role in the pathogenesis of gastrointestinal diseases, including those impacting the esophagus. Although relatively stable, there are a number of factors that may disrupt the delicate balance between the luminal esophageal microbiome (EM) and the host. These changes are thought to be a product of age, diet, antibiotic and other medication use, oral hygiene, smoking, and/or expression of antibiotic products (bacteriocins) by other flora. These effects may lead to persistent dysbiosis which in turn increases the risk of local inflammation, systemic inflammation, and ultimately disease progression. Research has suggested that the etiology of gastroesophageal reflux disease-related esophagitis includes a cytokine-mediated inflammatory component and is, therefore, not merely the result of esophageal mucosal exposure to corrosives (*i.e.*, acid). Emerging evidence also suggests that the EM plays a major role in the pathogenesis of disease by inciting an immunogenic response which ultimately propagates the inflammatory cascade. Here, we discuss the potential role for manipulating the EM as a therapeutic option for treating the root cause of various esophageal disease rather than just providing symptomatic relief (*i.e.*, acid suppression).

**Key Words:** Microbiome; Gastroesophageal reflux disease; Probiotics; Prebiotics; Bacteriocins; Dysbiosis; Barrett's esophagus; Esophageal cancer; Esophagitis; Eosinophilic esophagitis

©The Author(s) 2021. Published by Baishideng Publishing Group Inc. All rights reserved.

**Specialty type:** Gastroenterology and hepatology

**Country/Territory of origin:** United States

**Peer-review report's scientific quality classification**

Grade A (Excellent): 0  
Grade B (Very good): B, B  
Grade C (Good): 0  
Grade D (Fair): 0  
Grade E (Poor): 0

**Received:** February 2, 2021

**Peer-review started:** February 2, 2021

**First decision:** February 27, 2021

**Revised:** March 6, 2021

**Accepted:** April 14, 2021

**Article in press:** April 14, 2021

**Published online:** May 14, 2021

**P-Reviewer:** Haruma K, Urabe M

**S-Editor:** Gao CC

**L-Editor:** A

**P-Editor:** Liu JH



**Core Tip:** The interactions between the gut bacteria and the immune system of the host play a key role in the pathogenesis of gastrointestinal diseases, including those impacting the esophagus. This evidence-based review brings forward the emerging data on the microbial changes related to esophageal disease. Better understanding of these data will lead to mitigation strategies for intervention and innovation.

**Citation:** D'Souza SM, Houston K, Keenan L, Yoo BS, Parekh PJ, Johnson DA. Role of microbial dysbiosis in the pathogenesis of esophageal mucosal disease: A paradigm shift from acid to bacteria? *World J Gastroenterol* 2021; 27(18): 2054-2072

**URL:** <https://www.wjgnet.com/1007-9327/full/v27/i18/2054.htm>

**DOI:** <https://dx.doi.org/10.3748/wjg.v27.i18.2054>

## INTRODUCTION

Investigation of the gut microbiome has progressively changed the understanding of esophageal disease. During the past two decades, 16S rRNA gene sequencing was used to characterize and compare the esophageal microbiomes (EMs) of healthy individuals with those in patients with esophageal diseases including gastroesophageal reflux disease (GERD), Barrett's esophagus (BE), esophageal adenocarcinoma (EAC), eosinophilic esophagitis (EoE), and esophageal motility disorders[1,2]. Analyzing the compositional differences between healthy and dysbiotic microbiomes in the esophagus has provided further insight into the pathogenesis of GERD and related sequelae along with other associated pathology (Table 1). In particular, it is noted that the diseased esophagus, relative to healthy controls, is colonized by a bacterial population that is unusually rich in gram-negative species. Furthermore, the aberrant bacteria conform, to a great extent, with pro-inflammatory oral pathogens. This insight into the EM can help guide further investigation into new therapeutic tools that target these mechanisms.

## NORMAL GASTROESOPHAGEAL MICROFLORA

### Characterizing the 'normal' vs 'abnormal' esophageal luminal flora

Metagenomic sequencing of the human population revealed that the gastroesophageal (GE) microbiome is predominated roughly in order of prevalence by six major phyla: Firmicutes, Bacteroidetes, Actinobacteria, Proteobacteria, Fusobacteria, and Saccharibacteria[3]. Typically, Bacteroidetes and Firmicutes often predominate primarily in response to abundance of either *Bacteroides* or *Clostridium* spp.[4]. Here, phylum-level classification is an oversimplification that does not account for the diversity that exists in a relatively simple microbiome like that found in the distal esophagus. Considerable variation of both the identity and relative abundance of specific bacteria exists, especially when the taxa are characterized with greater resolution by elucidation of taxa to species or strain-level. In 2009, one group identified two distinct types of GE microbiomes[5]. Comparing the results from individuals with GERD to healthy controls[5], they characterized the control population, which is predominated by gram-positive organisms, *Streptococcus* spp., as a type I microbiome. The type II microbiome was largely associated with pathological states, such as GERD and BE, and demonstrated a relative increase in abundance of gram-negative anaerobes[5].

Further work delineated the taxa and observed that three distinct clusters of esophageal microbiotas were predominant in biopsies of human esophageal tissue. Each is characterized by their relative abundance of *Streptococcus* and *Prevotella* spp.[6]. Cluster 1 is intermediate, with an approximately equal proportion of both genera with an increased presence of *Haemophilus* and *Rothia* spp. Cluster 2 consists predominantly of *Streptococcus* spp. Cluster 3 is primarily represented by *Prevotella* spp.[6].

In addition to inter-individual variation, the composition of luminal microbiota also varies in the esophagus from the mouth to the stomach both in health and disease. Specifically, the commensal flora of the proximal, mid-, and distal esophagus varies both in makeup, and relative abundance. In a study of 12 patients under routine

**Table 1 Changes in local flora that occur with particular esophageal disease states**

Disease states	Changes in microbiome
GERD	Non-erosive reflux disease: A shift towards Proteobacteria ( <i>Neisseria oralis</i> , <i>Moraxella spp.</i> ) and Bacteroidetes ( <i>Bacteroides uniformis</i> , <i>Capnocytophaga spp.</i> , and <i>Prevotella pallens</i> ); A shift away from Fusobacteria ( <i>Leptotrichia</i> ) and Actinobacteria ( <i>Rothia spp.</i> ); Increased abundance of <i>Dorea spp.</i>  Reflux esophagitis: Decreased Firmicutes ( <i>Mogibacterium spp.</i> , <i>Streptococcus infantis</i> , <i>Solobacterium moorei</i> ) and increased Fusobacteria ( <i>Leptotrichia spp.</i> ) and Proteobacteria ( <i>Marivita spp.</i> , <i>Nisaea spp.</i> , <i>Mesorhizobium spp.</i> )
Barrett's esophagus	Increased Fusobacteria, and Proteobacteria ( <i>Neisseria spp.</i> , and <i>Campylobacter spp.</i> ); Decreased alpha diversity as well as <i>Bacteroidetes</i> and <i>Prevotella</i>
Esophageal adenocarcinoma	Increased abundance of Proteobacteria and decreased Firmicutes; Relatively unchanged <i>Streptococci</i> abundance
Eosinophilic esophagitis	Increased Proteobacteria ( <i>Neisseria</i> and <i>Haemophilus</i> ) and <i>Corynebacterium</i> ; Decrease in <i>Clostridia spp.</i>

GERD: Gastroesophageal reflux disease.

surveillance for BE, the proximal esophagus was more similar to the oropharynx in that it had higher concentrations of gram-positive organisms than the distal esophagus[7]. *Streptococcus spp.* were found throughout the entirety of the esophagus, increasing in relative abundance from the proximal to mid-esophagus and markedly decreasing thereafter in the distal esophagus[7]. Gram-negative organisms included *Prevotella* and *Delftia spp.*, which overall were more concentrated in the distal esophagus[7]. This is not surprising, because the lipopolysaccharide (LPS) “shell” around gram-negative organisms hardens them to variation in pH, bile salt concentration, proteases, and to some extent, temperature[8-15]. This is why most enteric pathogens are gram negative—they can survive the selection and potentially adverse effects related to proximity to gastric contents. It would be thereby expected that the microbiome becomes much less diverse and increasingly enriched in gram-negative species. Diversity is greatest in the region nearest to the source (oronasal cavity) and with mildest conditions, e.g., saliva/mucous, luminal physiological pH, and moderate physiological temperatures[16,17]. It would be expected to see a gradient toward facultative and obligate anaerobes (probably from the subgingival space) in the esophageal lumen distally towards the stomach. Notably, many bacteria also have increased abundance because of the protective nature of sporulation (e.g., *Clostridia spp.*) within the harsh surrounding environment[18,19]. Accordingly, the underlying GE pathology appears to be associated with alterations in the composition of this gram positive/gram negative continuum and balance[7].

The biomic differences for esophageal disease is notable. Patients with BE had overall higher levels of *Streptococcus spp.* in tissue biopsies throughout the entirety of the tract compared to those without the disease. While this appears to be in contrast with the gram-positive/gram-negative imbalance discussed previously, this may be an indirect effect of persistent local irritation caused by immunogenic gram-negative species that facilitates bacterial proliferation and the infiltration of underlying tissue with gram-positive bacteria—of which streptococci are a major part. Whether this is a cause of BE metaplasia or a consequence is unknown. Furthermore, the sharper decrease in overall abundance of *Streptococcus spp.* from mid- to distal-esophagus is greater in individuals with BE compared to those without metaplasia, which suggests that the overall effect on relative composition of *Streptococcus spp.* is negative despite an increased tissue prevalence[7].

These findings suggest that an increase in relative abundance of gram-negative flora in the distal esophagus leads to a local inflammatory response which negatively impacts the barrier function. This ultimately leads to tissue proliferation of all flora, including commensal *Streptococcus spp.* The proximal-distal variation in specific flora changes from healthy to diseased states, in conjunction with the previous GE microbiome subtyping, illustrate the pathological potential of dysbiosis. The emerging data may offer insight into new treatment paradigms focused on microbial alteration which could supplement, and even possibly replace, the need for acid suppression in these disease states.

### Factors affecting the composition of the microbiota

The GE microbiome is shaped by the oral cavity, oropharynx, and stomach due to migration of oral bacteria to the esophagus and reflux of gastric microbiota[20].



Recognizably, this varies considerably from person to person, even in the apparently healthy population. In addition to anatomic location, factors that have been noted to alter the EM composition include age, diet, proton pump inhibitor (PPI) use, oral hygiene, and smoking. Studies of these factors have helped provide a framework for understanding the GE microbiota.

Contrary to the philosophy that, for example, the colon is a discrete microbiome that stands alone, we view the whole of the gastrointestinal tract as a contiguous system separated by “gates” imposed by selection pressure driven by factors related to function (pH, osmolarity, proteases, indigenous flora, *etc.*). That is, a series of discrete “neighborhoods” connected by means of a tube and the assumption that the oronasal cavity is the sole source of inoculum. Prior to weaning, infants do not have established “gates,” and an evolving colonization with what will ultimately become the adult microbiome takes place until the age of approximately three[21]. Thereafter, barring unnatural perturbation, the gastrointestinal neighborhoods are established, stable, and at equilibrium with the host. Unfortunately, humans are pioneers of the unnatural, and a number of behaviors, many now considered essential, systematically undermine the balance. Recognizably, there may be sequential changes associated with age, medication exposures, diet, hygiene, sleep efficiency, and environmental exposures.

**Age:** Age has an effect on the GE microbiome, although the full significance has not yet been determined[22-25]. During early life, the human colonic microbiome varies greatly. Analysis of the microbial composition of the human colonic microbiome in patients ranging from newborns to 80 years old, and across three distinct geographic locations (United States, Venezuela, and Malawi) has found that the phylogenetic composition fluctuates dramatically during the first 3 years of life before stabilizing into a more stable adult-like composition, regardless of geographic location[26]. Conceivably, a similar dynamic microbial shift exists for the esophagus given the same multifactorial environmental factors in early life, based on mode of delivery (vaginal birth or cesarean section), the type of dietary feeding (breast or formula feeding), as well as the timing of adult food introduction[27,28].

With aging, humans seem to have a less dramatic, but still notable shift in the GE microbiome. Evaluation of the EM of adults of ages 30 years to 60 years, using 16S rRNA-, 18S rRNA-amplicon sequencing, and shotgun sequencing, has found age to be a significant factor driving microbiome composition. Notably, they indicated a positive correlation with age and the relative abundance of Firmicutes such as some *Streptococcus spp.*, including *Streptococcus parasanguinis* with increasing age[6]. Furthermore, increasing age was inversely correlated with prevalence of Bacteroidetes including *Prevotella melaninogenica*[6]. To better place this in the context of our current understanding of the GE microbiome and the previously demonstrated community clusters (*Streptococcus* predominant, *Prevotella* predominant, and intermediate predominant), this study showed that regardless of disease state, with increased age, there is a more robust microbiome composition and a higher number of gram-positive (*Streptococcus parasanguinis*) species and a lower number of gram-negative (*Prevotella melaninogenica*) species[6]. Thus, age may contribute to the different esophageal microbial community types. Despite this, gram-negative proliferation is associated with progression of esophageal disease at all ages[6]. It may be that age may affect and predict a ‘baseline’ microbiome that is incrementally altered by microbial imbalance.

Notably, there is a degenerative effect of aging on esophageal motor function which may play a role in the differences seen in the GE microbiome of the elderly population as esophageal function naturally deteriorates after the age of 40[29]. The presence of GERD has a significant impact on esophageal contraction wave amplitude but not on peristalsis[30]. Accordingly and hypothetically, the mechanistic and functional changes of the esophagus influence the microbiota as a direct or indirect consequence of the aging process.

**Diet:** Dietary factors influence the colonic microbiome both as an infant (breast *vs* formula feeding) and as an adult (affecting the colonic microbiome with short-term macronutrient changes)[31-33]. With specific focus on the GE microbiome, dietary intake has been associated with the development of esophageal diseases such as BE, EAC, and esophageal squamous cell carcinoma (ESCC)[34,35]. In particular, consumption of leafy and cruciferous vegetables, as well as raw fruits is associated with decreased risk of BE and EAC, while red meat intake is associated with increased risk[35].

In early life, breastfeeding, formula feeding and the introduction of solid foods, play a large role in development of the gastrointestinal microbiome[36]. While more specific investigation is needed to evaluate the specific effects on the EM, it is likely

that similarities exist in the progression due to the same factors. Human breast milk is predominantly composed of the microbes *Corynebacterium*, *Ralstonia*, *Staphylococcus*, *Streptococcus*, *Serratia*, *Pseudomonas*, *Propionibacterium*, *Sphingomonas*, and *Bradyrhizobiaceae* in addition to milk oligosaccharides[37-39].

The impact of breastfeeding on the infant gastrointestinal microbiome was highlighted in two studies that found formula-fed infants to have a lower proportion of *Bifidobacterium* and *Lactobacillus spp.* and a higher proportion of Clostridiales and Proteobacteria when compared with breast-fed infants[40]. Furthermore, formula fed infants have lower microbial diversity after the first year of life when compared to breast-fed infants[41]. Several other epidemiologic studies have suggested breastfeeding to have a protective role against asthma, autism, and type 1 diabetes, while also showing a lower association of inflammatory and autoimmune diseases[37,42]. As stated earlier, the phylogenetic composition fluctuates dramatically during the first 3 years of life before evolving into a more mature and stable adult-like configuration[26]. This shift is likely to allow infants to be better equipped to handle processing of a more robust diet.

In adults, the GE microbiome and the relationship to diet is still under investigation. Our focus here will be on diet and its relationship to esophageal disease as a foundation for possible future studies into the GE microbiome role. There are several difficulties, particularly with confounding and study-design issues, when correlating dietary factors in adults with esophageal disease[34]. Thus, most of the existing literature on diet and BE or EAC is based on case-control studies in which minor to moderate inverse associations have been reported with a diet low in fruits and vegetables (green, leafy, and cruciferous vegetables). It has been theorized that fruits and vegetables, which are high in antioxidants, phytochemicals, and other substances, may inhibit carcinogenesis by free-radical reduction or by blocking the formation of N-nitroso compounds in the alimentary and respiratory tract[43,44]. Other case-control studies have shown an association with a diet high in red and processed meats and an increased risk of esophageal cancers, likely due to processed meats being a major source of nitrites and nitrosamines[35,45]. Given the potential for multiple interactions between specific macronutrients, other studies have turned to looking at diet-regimens for easier study design. They found that the Mediterranean diet is inversely associated with both BE and EAC, whereas the “Western diet”, high in meat consumption and low in fruits and vegetables, appears to increase the risk of these diseases[46,47]. Although this relationship between dietary intake of fruits, vegetables, as well as red and processed meats, has been more recently implicated, further evaluation is needed in regard to the interaction of these diets and the GE microbiome composition.

A study specifically looking at the relationship of diet with the GE microbiome evaluated patients with high overall fiber *vs* high fat intake and found that dietary fiber, but not fat intake was associated with a distinct EM[48]. In particular, increasing fiber intake was significantly associated with increasing relative abundance of Firmicutes, including *Streptococcus spp.*, and decreasing relative abundance of gram-negative bacteria overall[48]. Low fiber intake was associated with increased relative abundance of several gram-negative flora, including *Prevotella*, *Neisseria*, and *Eikenella spp.*[48]. These findings offer a potential dietary therapeutic option for prevention or slowing the progression of esophageal disease by decreasing exposure to a higher abundance of gram-negative influence, and thereby reducing the induction of a gram-negative-LPS induced inflammatory cascade.

**PPIs:** PPIs are the therapeutic first-line treatment for many esophageal disorders such as GERD, erosive esophagitis, and BE. The main mechanistic action of PPIs is to lower acid production at the level of the stomach by inhibiting the hydrogen-potassium ATPase pump, a transmembrane protein responsible for releasing hydrochloric acid into the stomach lumen. PPIs inhibit acid secretion by binding within this domain, promoting a higher gastric pH, and thus increasing the pH of the refluxate[49].

The use of PPIs has been demonstrated to alter both GE and colonic microbiomes, although the full extent is yet unknown. The clearest defined role is reduction of gastric acid, thereby allowing survival of orally ingested organisms to repopulate the more distal esophagus. This pH-related microflora change may allow propagation of bacterial species that would otherwise not flourish under more acidic conditions. For example, a significant increase in oral microbiome species such as *Rothia dentocariosa*, *Rothia mucilaginosa*, *Scardovia spp.*, and *Actinomyces spp.* in the gut microbiome has been noted following PPI use[50-52].

In the distal esophagus, the effect of PPIs may be more likely to be due to microbial related inflammatory changes, whereas previously attributed to direct acid contact mucosal injury. A study of patients with non-erosive reflux disease (NERD), erosive



GERD, and BE compared PPI use *vs* no use within each respective group and found no change in  $\alpha$  diversity or  $\beta$  diversity between PPI and non-PPI users of each group was reported, but composition of specific bacteria taxa at the phylum level was noted[53]. In particular, PPI use was associated with an increase in Firmicutes and Proteobacteria in BE, and a decrease in Bacteroidetes in NERD and reflux esophagitis (RE)[53]. In another study, biopsies taken before and after 8 wk of PPI treatment (lansoprazole 30 mg twice daily) revealed a significant decrease in the gram-negative *Comamonadaceae* spp. and increased gram-positive Clostridia (*Clostridiaceae* and *Lachnospiraceae* spp.) and Actinomycetales (*Micrococcaceae* and *Actinomycetaceae* spp.)[54].

These studies offer evidence that PPI use may have effects beyond that of acid suppression. This supports a possible mechanistic role for PPIs altering the GE microbiome, favoring gram-positive bacteria that prefer environments with higher pH. This effect would reduce induction of the Toll-like-receptor (TLR)/inflammatory cascade by gram-negative LPS producing bacteria.

Although their association with GERD is unknown, acid-producing bacteria are found in the esophagus and oral cavity. The use of PPIs may directly target the proton pumps (P-type ATPase enzymes) of these bacteria (notably *Streptococcus pneumoniae* and *Helicobacter pylori*)[55]. Further studies are warranted to determine if these bacteria are a causal factor of GERD by directly producing acid, which are in turn inhibited by PPIs. In addition, PPI use may indirectly change the natural bacterial flora in non-gastric tissues that express  $H^+/K^+$ -ATPases by shutting down proton pumps[55,56].

PPIs may also reduce inflammation apart from direct acid suppression. In esophageal squamous epithelial cells, omeprazole has been shown to inhibit interleukin (IL)-8 expression by blocking the nuclear translocation of a nuclear factor-kappa beta (NF- $\kappa$ B) subunit and the binding of AP-1 subunits to the IL-8 promoter[56]. IL-8 is an inflammatory mediator that has been implicated in the GERD, BE, and EAC pathways. Increased expression of LPS from gram-negative bacteria, and subsequent activation of the TLR-4-NF- $\kappa$ B pathway are associated with expression of downstream mediators such as IL-8 and cyclooxygenase (COX)-2[57]. The levels of both are directly correlated with transition from metaplasia to dysplasia in BE[57]. Thus, if PPI therapy has an effect on IL-8 expression by blocking NF- $\kappa$ B and AP-1, there may be a role for therapeutic use outside of direct acid suppression.

**Oral hygiene:** Oral hygiene is thought to play a vital role in the GE microbiome. Bacteria found in the oral cavity can migrate distally *via* deglutition[20]. The role of oral microbiota in colonizing the esophagus, and becoming part of the commensal GE microbiota, remains uncertain.

Maintained oral hygiene is associated with a higher proportion of gram-positive cocci and rods, mostly comprised of *Streptococcus* spp., which contrasts with those with poor oral hygiene showing shifts to a higher proportion of anaerobic gram-negative bacteria such as *Prevotella* spp.[58]. The oral microbiome shift to a more gram-negative dominant flora may have distal effects of LPS-inducing TLRs and activation of an inflammatory cascade in the esophagus as described previously. It is also unclear whether antibiotic mouthwashes damage an otherwise healthy microbiome. Further research is needed to better define the relationship between oral hygiene and the GE microbiome.

One recent population-based, case-control study reported that poor oral health was associated with an increased risk of ESCC[59]. More specifically, they found that tooth loss was associated with a moderately significant increased risk of esophageal cancer and that brushing once per day or less was associated with an 80% increased risk of developing ESCC in this population. They propose that tooth brushing influences the balance of microorganisms by directly removing plaque, food residue, and carcinogenic products of tobacco and alcohol. Accordingly, this affects the levels of inflammation and/or production of the carcinogenic by-products of nitrosamines and acetaldehyde. While this is currently theoretical, given the proximity of the oral cavity to the distal esophagus, it is reasonable that oral hygiene would have downstream effects on the GE microbiome and esophageal disease as well as perhaps on intestinal microbial mediated disease as well.

**Smoking:** Up to 20% of United States adults use a tobacco product, and tobacco's effect on the GE microbiome is uncertain[60]. Esophageal balloon procured cytology found that current smoking was associated with an increase in both  $\alpha$  and  $\beta$  diversity of the esophagus[61]. It is suspected that the increase is due to smoking-related immunosuppression, permitting novel bacteria to colonize the upper gastrointestinal tract[61]. The study also found two anaerobic bacteria, *Dialister invisus* and *Megasphaera micronuciformis*, are more commonly detected in current smokers[61].

Increased  $\alpha$  and  $\beta$  diversity after smoking exposure may also be a result of biofilm formation[62]. There is some evidence that cigarette smoking induces staphylococcal biofilm formation in an oxidant-dependent manner by increasing fibronectin binding protein-A. This leads to increased binding of staphylococci to fibronectin and increased adherence to human cells[62].

Smoking exposure can affect a wide range of human physiologic processes by inducing a proinflammatory state, increasing cytokines such as tumor necrosis factor (TNF)- $\alpha$ , IL-1, IL-6, IL-8 all while decreasing anti-inflammatory cytokines such as IL-10[63]. Further investigation into the EM and its relationship to smoking and the development of disease are needed.

### **Bacteriocins**

Bacteriocins are ribosomal derived peptides produced by microorganisms colonizing the gastrointestinal tract that are thought to inhibit competitive flora, thereby out-competing other pathogens. Additionally, in humans, bacteriocins are thought to maintain barrier function, partake in immune modulation, have direct antimicrobial activity, and also exhibit anti-neoplastic activity[64]. Bacteriocins' diverse functional role is reflected in their wide-ranging bactericidal properties, amino acid sequence and peptide structures, bacteriocin operon type, and different molecular weights and charges[65,66].

In a normal, healthy individual, the gut-blood barrier is responsible for maintaining homeostasis between the bloodstream and the gastrointestinal tract, which ultimately regulates water and nutrient absorption[67]. Along with a growing interest of the GE microbiome and its relationship with the intestinal barrier, recent *in vitro* studies have reported that the size and properties of bacteriocins allow them to cross this gut-blood barrier[64,68]. The size and charge contribute to bacteriocin movement across membranes and barriers and account for the large role in different physiologic mechanisms[64].

The bacteriocins in the gastrointestinal tract also have specific, potent antimicrobial properties[69,70]. This antibacterial property makes it essential in maintaining and affecting the composition of the local microbiome. The anti-neoplastic role of bacteriocins is still an area warranting further investigation. *In vitro* studies evaluating the effect of nisin have shown that bacteriocin may trigger apoptosis in head, neck, and squamous cell carcinoma, effectively reducing the size of tumor xenografts[71,72].

### **Defensins**

Defensins are small host-derived polypeptide molecules of host-origin that play a role in innate immunity with both direct and indirect bactericidal effects. They serve a similar purpose to bacteriocins, but are eukaryote derived[73]. Human defensins are typically classified into  $\alpha$ -defensins, which are mainly neutrophil-derived, and  $\beta$ -defensins, which are mainly epithelial cell-derived. Defensin expression is typically inducible through cellular exposure to bacterial products such as LPS or cytokines, which include TNF and IL-1[73]. Binding of defensins can lead to direct bacterial cell membrane disruption. The positive charge of some defensins is attracted to the negative components of bacterial capsules, leading to oligomerization and pore formation[74]. Alternately, defensin binding can stimulate recruitment of the adaptive immune response[73].

Defensins have been demonstrated to play a role in normal gut-microbe interactions. Loss of human  $\beta$ -defensin (hBD) 1 and hBD3 is associated with progression of EoE, and this may be a result of unmitigated microbe-immune interactions[75]. Uncontrolled defensin production may also negatively impact gut health. The production of hBD5 by metaplastic Paneth cells, can lead to a loss of E-cadherin, and thus inhibit cell adhesion[76]. This loss of structural integrity has been associated with progression of BE[76].

Similar to bacteriocins, modification of defensin expression or structure may provide a therapeutic venue for alteration of the commensal microbiome. Chimeric variants of defensins have been explored as possible antimicrobial agents, but this potential treatment modality is still in early stages of exploration, and further work is needed to evaluate their therapeutic safety and efficacy[77].

## MECHANISMS OF DYSBIOSIS

### *Initial paradigms for dysbiosis*

Dysbiosis is a term that encompasses a change in the composition of commensal microbiome relative to that found in healthy individuals[78]. When distinguishing the biome of a normal healthy esophagus to dysbiotic disease states such as GERD, EE, BE, or EAC, it is evident that dysbiosis may precede inflammation. Thus, the composition of the microbiota may play a large role in the downstream events[79]. Gram-negative bacterial products activate TLRs that are present on the esophageal endothelial cells causing an inflammatory cascade which leads to downstream LES relaxation[79]. *Prevotella*, which are found in greater abundance in the dysbiotic distal esophagus, have been shown to be a key producer of LPS that contributes to TLR activation[6]. The activation results in chemokine-induced production of nitric oxide and COX-2, which may promote LES relaxation and decrease gastric emptying[80].

## DYSBIOSIS IN DISEASE STATES

### **GERD**

GERD is an inflammatory disease state that is most commonly caused by inappropriate transient relaxation or secondly, by a chronically decreased tonicity of the lower esophageal sphincter[81]. It is further classified into two large phenotypes: RE and NERD, as determined by endoscopy. Additionally, there is a category of uninvestigated GERD wherein treatment is initiated without direction from an endoscopic evaluation[82].

**Inflammatory pathogenesis of GERD:** Classically, GERD has been described as the result of reflux of gastric acid and/or duodenal bile salts, causing direct chemical mediated mucosal injury and inflammation[83]. The majority of patients that present with clinical symptoms of GERD have no endoscopic evidence of reflux, suggesting alternative pathophysiologic pathways. An animal study demonstrated that RE does not develop as a chemical injury starting at the epithelial surface but rather, begins with a submucosal infiltration by lymphocytes that later progresses upward to the epithelial surface[84]. Subsequent work analyzed human esophageal squamous cell lines exposed to acidified bile salts and found evidence that reflux did not directly damage the mucosal esophagus, but instead stimulated epithelial cells and led to subepithelial cytokine-mediated and *retrograde* directed mucosal damage of the tissue[85].

Acid exposure is believed to contribute to mucosal expression of inflammatory markers, including IL-8, as well as several other chemokines, that promote local migration of leukocytes, mainly neutrophils[85]. This is done through activation of transient receptor potential cation channel subfamily V member 1 on epithelial cells and neurons, which results in calcitonin gene-related peptide (CGRP) and substance P expression[86]. Both CGRP and neutrophil activation initiate a cascade of cytokine expression, leading to local submucosal inflammation as well as hydrogen peroxide production as well as further immune cell, including lymphocytic proliferation into the mucosa (Figure 1). Peroxide-mediated smooth muscle relaxation of the lower esophageal sphincter further contributes to reflux[87].

**Role of the microbiome in GERD:** Gram-negative bacterial products, mainly LPS, bind to TLR-4, which stimulates IL-18 production, and initiates a cascade of IL and TNF production. This leads to downstream effects including lower esophageal sphincter relaxation as well as decreased gastric motility[1].

It has been theorized that the bacterial biofilm may be involved in the pathogenesis of GERD[88]. Biofilm is an organized community of microbes that produce protective factors and adhesion molecules which enhance the survival of the local microbial community. Biofilm has been implicated in the pathogenesis of a variety of disease states elsewhere in the gastrointestinal tract, notably in the oral cavity and colon, while the extent of contribution to esophageal disease is still unclear[89-91].

Compositional variation in the localized microbiome may help explain the mechanistic and clinical difference between the two phenotypes of GERD. A recent study found distinct microbiota in patients with NERD when compared with controls and RE subjects. The NERD microbiota composition shifted towards Proteobacteria (*Neisseria oralis* and *Moraxella spp.*) and Bacteroidetes (*Bacteroides uniformis*, *Capnocytophaga spp.*, and *Prevotella pallens*), and away from Fusobacteria (*Leptotrichia*) and

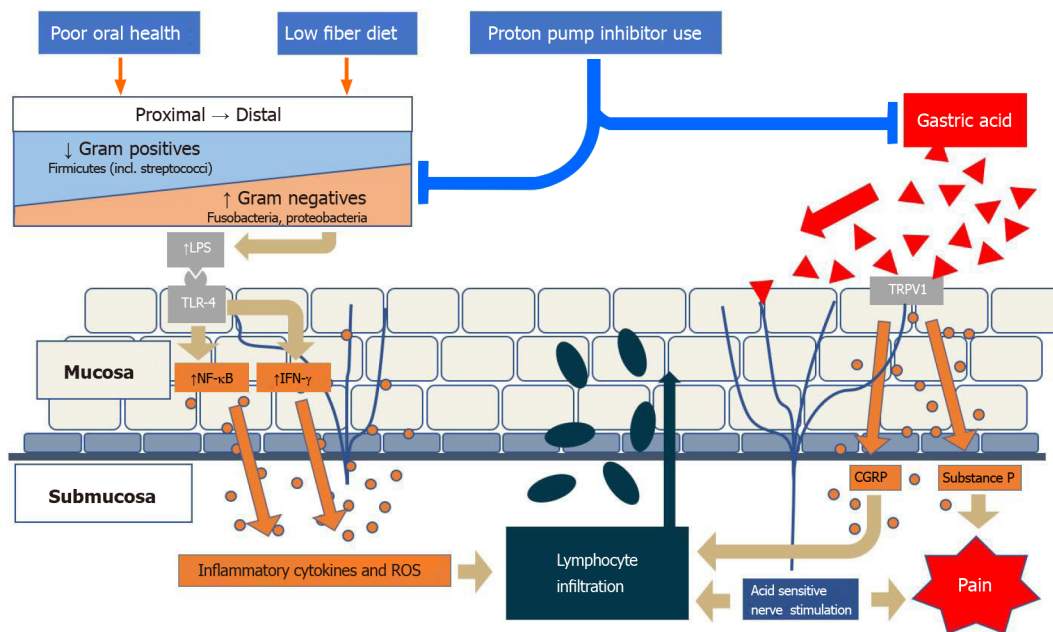


**Figure 1** Environmental factors alter the local esophageal microbiome, which normally has a gram-positive to gram-negative gradient, towards increased proportion of gram-negatives. Activation of Toll-like-receptor-4 by gram-negative lipopolysaccharide leads towards an inflammatory cascade that results in lymphocyte infiltration. In addition, gastric acid activates transient receptor potential cation channel subfamily V member 1 on local nerve fibers and results in calcitonin gene-related peptide and substance P expression, which contributes to the local inflammatory response as well as pain. LPS: Lipopolysaccharide; TLR: Toll-like-receptor; NF-κB: nuclear factor-kappa beta; IFN: Interferon; ROS: Reactive oxygen species; TRPV1: Transient receptor potential cation channel subfamily V member 1; CGRP: Calcitonin gene-related peptide.

Actinobacteria (*Rothia*)[53]. Several Firmicutes genera were reduced in NERD (*Peptococcus* and *Moryella*). An increased abundance of *Dorea spp.*, however, resulted in an overall higher Firmicutes composition compared with controls[53]. The same study speculated that the increase in sulfate-reducing *Proteobacteria spp.* and *Bacteroidetes spp.* along with hydrogen producing *Dorea spp.* is associated with a mechanistic role in visceral hypersensitivity present in NERD[53]. Alternatively, patients with RE have a decrease in Firmicutes (*Mogibacterium spp.*, *Streptococcus infantis*, *Solobacterium moorei*) and increase in gram-negative *Fusobacteria (Leptotrichia spp.)* and *Proteobacteria (Marivita, Neisseria, and Mesorhizobium spp.)*[53].

The compositional changes in esophageal flora can also occur as a response to environmental factors. High-fat diet has been heavily associated with localized mucosal inflammatory changes in murine models[92]. It is theorized that alterations in the luminal microenvironment seen with high-fat diet leads to increased gut-epithelial interactions and drives progression of the inflammatory response. In addition, these dietary changes have been demonstrated to contribute to colonic increased colonic Firmicutes/*Bacteroidetes* ratio, which is associated with obesity and an inflammatory response characterized by expression of chemokine IL-8[92]. Other dietary factors, including consumption of insoluble carbohydrates, can contribute to reflux through effect on gastric and esophageal tone. Colonic bacterial metabolism of carbohydrates into short-chain fatty acids (SCFAs) is associated with increase in peptide YY and oxyntomodulin, which inhibit gastric motility and LES function[93].

## BE

BE is a disease state characterized by stratified squamous to columnar metaplasia of the distal esophageal epithelium, and is typically associated with longstanding GERD[94,95]. The incidence of BE has increased since the mid-20<sup>th</sup> century, which is thought to be related to population-level changes in EM composition following the introduction of antibiotics[96]. The activation of the LPS-TLR4-NF-κB pathway through dysbiotic changes may contribute to inflammation and malignant transformation[3].

**Inflammatory pathogenesis of BE:** The inflammatory-mediated model of reflux-related inflammation seen in GERD is also present in BE[97]. There are, however, several specific dysbiotic changes that contribute to inflammatory mediated metaplasia as well. Murine models of BE demonstrated localized cytokine expression,



especially in the distal esophagus, which can lead to an inflammatory response in gastric stem cells, ultimately promoting columnar epithelial formation[98]. Additionally, the same pro-inflammatory response associated with LPS and TLR-4 binding may be more notable in the distal esophagus with increased gram negative presence, and specifically contributes to metaplastic transformation[80].

Pro-inflammatory cytokine IL-1b, has been shown to be highly expressed in BE. The precursor for IL-1b necessitates proteolytic cleavage by caspase-1[98]. Caspase-1 also allows apoptosis of cells which can elicit further inflammation[99]. The functional role of caspase-1 is activated by inflammasomes which contain pattern-recognition receptors (PRRs). The PRR captures particular pathogen-associated molecular patterns (PAMPs) from microbes and damage-associated molecular patterns (DAMPs) from injured cells[100]. Once the PRR recognizes a certain PAMP or DAMP, a large complex of inflammasomes activates caspase-1 which initiates the inflammatory response pathway. One study demonstrated that LPS in Barrett's epithelial cells was shown to prime and activate NOD-like receptor protein 3 inflammasomes and caused a cascade of pro-inflammatory responses and induced apoptosis[101]. These data suggest that BE is perpetuated through a chronic inflammatory response from localized cytokine release which is initiated at the molecular level of the microbiome and related mucosal cell responses.

**Role of the microbiome in BE:** Patients with BE have been found to have both similarities and distinct features in EM profile when compared to those with GERD[102]. Using the original clustering model, Type I to Type II microbiome transition likely contributes to local inflammation[103,104]. More recently, it has been demonstrated that specific flora plays a contributing role in its pathogenesis. *Fusobacteria*, *Neisseria spp.*, and *Campylobacter spp.* have been linked to BE when compared to controls[105]. Additionally, comparison of metaplastic tissue to adjacent normal areas demonstrates decreased  $\alpha$  diversity and decreased prevalence of Bacteroidetes including *Prevotella spp.*[106]. Distinct compositional differences in specific phyla occur along the NERD, BE, and EAC pathway. While Proteobacteria are massively over-represented in NERD (Bacteroidetes to a lesser extent), microbiota in in BE and RE demonstrate increase in *Fusobacteria* and Proteobacteria. The transition to the EAC microbiome demonstrates an increase in Firmicutes, which are decreased in NERD and BE[53]. This increase may mirror the increase in Firmicutes/Bacteroidetes ratio that is seen in obesity and colorectal adenocarcinoma, as impaired fermentation by *Bacteroidetes spp.* of fiber to anti-inflammatory SCFAs may contribute to the local inflammatory cascade.

## EAC

**Inflammatory pathogenesis:** The pathogenesis of EAC has been attributed to a combination of genetic predisposition as well as environmental factors[107]. The majority of cases are associated with environmental triggers such as smoking, obesity, and GERD/BE[108]. The incidence of EAC in BE has been clearly established, albeit more recent data suggests lower rates, more in the range of 0.1-0.2%[109].

**Role of the microbiome in EAC:** All stages in the GERD-BE-EAC pathway have commonalities in composition of local flora. The change from type I to type II EM is generally associated with the initiation of reflux-associated inflammatory processes that are present in GERD and BE, and persist in EAC. The subsequent activation of the LPS-TLR4 cascade leads to NF-kB activation, which further increases COX-2 production[3]. COX-2 elevation is associated with the progression of BE to high-grade dysplasia[80]. More recent data, however, has identified specific floral changes in relative abundance that are associated with the progression from BE high-grade dysplasia and EAC. Patients with dysplastic disease have increased abundance of Proteobacteria and decreased Firmicutes[110]. Notably, *Streptococcus spp.* abundance is reportedly unchanged between non-dysplastic BE and high-grade dysplasia/EAC, suggesting that variation in *Streptococcus spp.* may not play a role in carcinogenesis[110].

The composition of the EM in EAC is closely linked to that of the oral cavity, with aboral movement of flora being theorized as one mechanism for compositional changes[111]. Specifically, oral flora such as *Treponema denticola*, *Streptococcus mitis*, and *Streptococcus anginosus* are associated with esophageal carcinogenesis[112]. While the overall abundance of *Streptococci* appears unchanged in between non-dysplastic BE and EAC, it is possible that individual species may have varied abundance.

In addition to pathogenic linkage between the oral and esophageal flora, compositional changes that are associated with decreased adenocarcinoma risk are also shared. Notably, the abundance of *Bifidobacteria spp.*, *Bacteroides spp.*, *Fusobacteria spp.*, *Veillonella spp.*, *Lactobacillus spp.*, and *Staphylococcus spp.* is associated with adenocarcinoma risk[88,106]. *Leptotrichia spp.* have been demonstrated to be a specific genus linked to EAC. In addition, reduction in some species, including *Neisseria* and *Streptococcus pneumoniae* decreased risk of progression to cancer[113,114].

## ESCC

**Inflammatory pathogenesis:** ESCC is more common than EAC in regions such as Asia and South America[115]. Classically, ESCC has been associated with environmental exposures, including tobacco, alcohol, and hot-drink consumption, as well as genetic predisposition[116]. Other risk factors, such as poor oral health, have been linked to esophageal squamous dysplasia, a precursor for ESCC[117]. Exposure to various environmental triggers may directly stimulate epithelial expression of inflammatory markers, or may indirectly lead to proinflammatory state through changes in the microbiome[118].

**Role of the microbiome in ESCC:** Evaluation of microbiomes of patient's with ESCC demonstrates specific changes when compared to healthy controls, notably increased in proportion of *Actinomyces spp.* and *Atopobium spp.*, and decrease in *Fusobacterium spp.*, and *Porphyromonas spp.*[118]. Generally, there is also a decrease in bacterial diversity, and increase in interpersonal compositional variation, suggestive that the dysbiotic state is not stable[118,119]. As with EAC, there is a close association with oral cavity disease/dysbiosis and ESCC. Decrease diversity of oral flora is associated with ESCC, as aboral movement of microbes likely disrupts the normal esophageal microbial composition and contributes to dysbiosis[119].

Specific environmental agents may directly contribute to dysbiosis through nutrient availability. Tobacco smoking is associated with many oral microbiome changes that have some overlap with dysbiosis in ESCC. Particularly, increases in flora within phylum Actinobacteria and genera *Atopobium* and *Prevotella*, and decreases in *Fusobacteria spp.* have been reported[120]. Alcohol consumption may negatively affect epithelial barrier function that normally modulates epithelium-microbe interaction[121]. It may additionally contribute to local dysbiosis through metabolism by local flora into toxic metabolites such as acetaldehyde. Alcohol consumption is associated with colonic microbial changes that are reversible with probiotics, suggesting plasticity of the microbiome[122]. A combination of dysbiosis and epithelial dysfunction may contribute to endotoxemia and systemic inflammatory response[123], which may play a role in carcinogenesis.

Microbiome changes may also play a prognostic role in ESCC. Increases in phyla Firmicutes, Bacteroidetes, and Spirochaetes, and decrease in Proteobacteria are associated with lymph node spread, with *Streptococcus spp.* and *Prevotella spp.* being specifically indicated[124].

## EoE

**Inflammatory pathogenesis:** EoE is a chronic immune mediated disease of the esophagus characterized by marked eosinophilic infiltration in response to T helper type 2 (Th2) cells[125]. Factors such as genetics, environment, allergens, and microbiome have been identified as triggers of the chronic disease[126]. Several genes have been identified as contributors to EoE, which include thymic stromal lymphopoietin (TSLP), calpain 14 (CAPN14), EMSY, LRRC32, STAT6, and ANKRD27[126]. Among the identified genes, TSLP appears to be the major contributor as it is activated by epithelial cells and induces Th2 differentiation[127]. Different allergens also induce an inflammatory cascade which increases inflammatory markers such as IL-5 and IL-13, which introduce a potential inflammatory path of EoE[126]. In addition to the genetics and environmental exposure, the microbiome of the esophagus has recently emerged as a potentially key mediator in the pathogenesis of EoE.

**Role of the microbiome:** Analysis of the microbiome in EoE has reported an increase of proteobacteria, specifically *Neisseria spp.* and *Corynebacterium spp.*, in children with active EoE[128]. This study, in conjunction with the evidence of altered gut microbiome with infantile antibiotic use and Cesarean section delivery, further supports that dysbiosis in the human microbiome has a role in EoE[129,130]. Analysis by an esophageal string test to evaluate the microbiome of children and adults with active EoE found a greater abundance of *Haemophilus spp.* in active EoE[131]. Notably,

there was also a decrease in specific taxa of Clostridia that had been observed in patients with active EoE[132]. In antibiotic treated mice, the addition of Clostridia-containing microbiota prevents sensitization to a specific food allergen. Induction of IL-22 by RAR-related orphan receptor innate lymphoid cells and T cells in the intestinal lamina propria are proposed as the mechanism of blocking sensitization to a food allergen[133]. The recent evidence suggests that the EM may be involved in the pathogenesis of EoE, and may represent new treatment approaches.

## IMPLICATIONS FOR THERAPY

As previously discussed with modification of other environmental exposures, additional therapeutic options such as prebiotics, probiotics, and antibiotics have been investigated to reduce dysbiosis by directly or indirectly improving the gram-positive to gram-negative ratio for esophageal diseases. Although there is increasing evidence of altering dysbiosis utilizing these therapies in other gastrointestinal diseases, further research is needed in specific esophageal diseases.

### Prebiotics

Supplements which increase the concentration of beneficial flora have been investigated. *Lactobacillus spp.*, which are found in the esophagus, metabolize maltosyl-isomaltooligosaccharides (MIMO), thereby enhancing the populations of favorable gram-positive organisms. Daily ingestion of MIMO has been reported to improve or eliminate symptoms in chronic GERD patients[134]. An expanded comprehensive evaluation of this promising approach is needed. A tolerability study is underway (NCT04491734), and a comprehensive multicenter randomized placebo-controlled study will begin in early 2021. Sugarcane flour has also been evaluated as a prebiotic with some benefit seen on one study[135]. The proposed mechanism for benefit is slower fermentation and thus greater luminal availability compared to traditional fiber-containing products[135].

### Probiotics

Probiotics add bacterial strains as dietary supplementation, attempting to improve the gut flora composition to a preferential state. Probiotics containing *Lactobacilli spp.* and *Bifidobacteria spp.* have been evaluated and demonstrated relief of GERD symptoms[136-140]. However, long term effects and histological benefit have not been studied, and more recent guidelines have suggested no evidence based recommendation for routine use[141]. Further investigation is needed to evaluate potential efficacy of probiotics in esophageal diseases.

### Antibiotics

Antibiotics are a potential therapeutic option for direct modification of the EM, and are widely used in the treatment of gastrointestinal infectious diseases. Antibiotics with focused intraluminal bioavailability have been used in treating small-intestinal bacterial overgrowth, hepatic encephalopathy, and *Clostridium difficile* infections[142-144]. There is, however, no evidence of the effectiveness of antibiotic use for esophageal dysbiosis in GERD, BE, or EAC.

### Bacteriocins

Bacteriocins facilitate competition between local and foreign microbes, direct microbial properties, have potential for crossing the gut-blood barrier, and have antineoplastic properties[64]. Bacteriocin-based drug therapy, whether in the form of targeted drug therapy *via* encapsulation or attachment of bacteriocins to macromolecules, metals, or polymer-based nanoparticles, remains an area of ongoing investigation[145].

## CONCLUSION

The EM plays a major role in the pathogenesis of esophageal disease. Various factors can affect the composition of the commensal flora, which may lead to dysbiosis and ultimately result in esophageal diseases. The dysbiosis likely contributes to a pro-inflammatory, cytokine-mediated state that starts in the submucosa. The pathogenic consequence, affecting the esophageal mucosa, has previously been attributed to



caustic acid mucosal injury, but now appears to be multifactorial, with the EM playing a major role. Specific flora has been more recently identified that may play a pathogenic role in this process. Several potential methods for therapeutic alteration of microbiome exist, including prebiotics, probiotics, antibiotics, and bacteriocin based therapies. The prebiotic treatment data is particularly promising as directed EM modification for effective disease treatment.

## REFERENCES

- 1 **D'Souza SM**, Cundra LB, Yoo BS, Parekh PJ, Johnson DA. Microbiome and Gastroesophageal Disease: Pathogenesis and Implications for Therapy. *Ann Clin Gastroenterol Hepatol* 2020; **4**: 20-33 [DOI: [10.29328/journal.acgh.1001018](https://doi.org/10.29328/journal.acgh.1001018)]
- 2 **Corning B**, Copland AP, Frye JW. The Esophageal Microbiome in Health and Disease. *Curr Gastroenterol Rep* 2018; **20**: 39 [PMID: [30069679](https://pubmed.ncbi.nlm.nih.gov/30069679/) DOI: [10.1007/s11894-018-0642-9](https://doi.org/10.1007/s11894-018-0642-9)]
- 3 **Lv J**, Guo L, Liu JJ, Zhao HP, Zhang J, Wang JH. Alteration of the esophageal microbiota in Barrett's esophagus and esophageal adenocarcinoma. *World J Gastroenterol* 2019; **25**: 2149-2161 [PMID: [31143067](https://pubmed.ncbi.nlm.nih.gov/31143067/) DOI: [10.3748/wjg.v25.i18.2149](https://doi.org/10.3748/wjg.v25.i18.2149)]
- 4 **Rinninella E**, Raoul P, Cintoni M, Franceschi F, Miggiano GAD, Gasbarrini A, Mele MC. What is the Healthy Gut Microbiota Composition? *Microorganisms* 2019; **7** [PMID: [30634578](https://pubmed.ncbi.nlm.nih.gov/30634578/) DOI: [10.3390/microorganisms7010014](https://doi.org/10.3390/microorganisms7010014)]
- 5 **Yang L**, Lu X, Nossa CW, Francois F, Peek RM, Pei Z. Inflammation and intestinal metaplasia of the distal esophagus are associated with alterations in the microbiome. *Gastroenterology* 2009; **137**: 588-597 [PMID: [19394334](https://pubmed.ncbi.nlm.nih.gov/19394334/) DOI: [10.1053/j.gastro.2009.04.046](https://doi.org/10.1053/j.gastro.2009.04.046)]
- 6 **Deshpande NP**, Riordan SM, Castaño-Rodríguez N, Wilkins MR, Kaakoush NO. Signatures within the esophageal microbiome are associated with host genetics, age, and disease. *Microbiome* 2018; **6**: 227 [PMID: [30558669](https://pubmed.ncbi.nlm.nih.gov/30558669/) DOI: [10.1186/s40168-018-0611-4](https://doi.org/10.1186/s40168-018-0611-4)]
- 7 **Okereke I**, Hamilton C, Reep G, Krill T, Booth A, Ghouri Y, Jala V, Andersen C, Pyles R. Microflora composition in the gastrointestinal tract in patients with Barrett's esophagus. *J Thorac Dis* 2019; **11**: S1581-S1587 [PMID: [31489224](https://pubmed.ncbi.nlm.nih.gov/31489224/) DOI: [10.21037/jtd.2019.06.15](https://doi.org/10.21037/jtd.2019.06.15)]
- 8 **Li Y**, Powell DA, Shaffer SA, Rasko DA, Pelletier MR, Leszyk JD, Scott AJ, Masoudi A, Goodlett DR, Wang X, Raetz CR, Ernst RK. LPS remodeling is an evolved survival strategy for bacteria. *Proc Natl Acad Sci USA* 2012; **109**: 8716-8721 [PMID: [22586119](https://pubmed.ncbi.nlm.nih.gov/22586119/) DOI: [10.1073/pnas.1202908109](https://doi.org/10.1073/pnas.1202908109)]
- 9 **Audia JP**, Webb CC, Foster JW. Breaking through the acid barrier: an orchestrated response to proton stress by enteric bacteria. *Int J Med Microbiol* 2001; **291**: 97-106 [PMID: [11437344](https://pubmed.ncbi.nlm.nih.gov/11437344/) DOI: [10.1078/1438-4221-00106](https://doi.org/10.1078/1438-4221-00106)]
- 10 **Lund P**, Tramonti A, De Biase D. Coping with low pH: molecular strategies in neutralophilic bacteria. *FEMS Microbiol Rev* 2014; **38**: 1091-1125 [PMID: [24898062](https://pubmed.ncbi.nlm.nih.gov/24898062/) DOI: [10.1111/1574-6976.12076](https://doi.org/10.1111/1574-6976.12076)]
- 11 **Begley M**, Gahan CG, Hill C. The interaction between bacteria and bile. *FEMS Microbiol Rev* 2005; **29**: 625-651 [PMID: [16102595](https://pubmed.ncbi.nlm.nih.gov/16102595/) DOI: [10.1016/j.femsre.2004.09.003](https://doi.org/10.1016/j.femsre.2004.09.003)]
- 12 **Brown AD**, Turner HP. Membrane stability and salt tolerance in gram-negative bacteria. *Nature* 1963; **199**: 301-302 [PMID: [14076708](https://pubmed.ncbi.nlm.nih.gov/14076708/) DOI: [10.1038/199301a0](https://doi.org/10.1038/199301a0)]
- 13 **CHRISTIAN JH**, WALTHO JA. The sodium and potassium content of non-halophilic bacteria in relation to salt tolerance. *J Gen Microbiol* 1961; **25**: 97-102 [PMID: [13693390](https://pubmed.ncbi.nlm.nih.gov/13693390/) DOI: [10.1099/00221287-25-1-97](https://doi.org/10.1099/00221287-25-1-97)]
- 14 **Joo HS**, Fu CI, Otto M. Bacterial strategies of resistance to antimicrobial peptides. *Philos Trans R Soc Lond B Biol Sci* 2016; **371** [PMID: [27160595](https://pubmed.ncbi.nlm.nih.gov/27160595/) DOI: [10.1098/rstb.2015.0292](https://doi.org/10.1098/rstb.2015.0292)]
- 15 **Breijyeh Z**, Jubeh B, Karaman R. Resistance of Gram-Negative Bacteria to Current Antibacterial Agents and Approaches to Resolve It. *Molecules* 2020; **25** [PMID: [32187986](https://pubmed.ncbi.nlm.nih.gov/32187986/) DOI: [10.3390/molecules25061340](https://doi.org/10.3390/molecules25061340)]
- 16 **Dong L**, Yin J, Zhao J, Ma SR, Wang HR, Wang M, Chen W, Wei WQ. Microbial Similarity and Preference for Specific Sites in Healthy Oral Cavity and Esophagus. *Front Microbiol* 2018; **9**: 1603 [PMID: [30065718](https://pubmed.ncbi.nlm.nih.gov/30065718/) DOI: [10.3389/fmicb.2018.01603](https://doi.org/10.3389/fmicb.2018.01603)]
- 17 **Schwab F**, Gastmeier P, Meyer E. The warmer the weather, the more gram-negative bacteria - impact of temperature on clinical isolates in intensive care units. *PLoS One* 2014; **9**: e91105 [PMID: [24599500](https://pubmed.ncbi.nlm.nih.gov/24599500/) DOI: [10.1371/journal.pone.0091105](https://doi.org/10.1371/journal.pone.0091105)]
- 18 **Tetz G**, Tetz V. Introducing the sporobiota and sporobiome. *Gut Pathog* 2017; **9**: 38 [PMID: [28680484](https://pubmed.ncbi.nlm.nih.gov/28680484/) DOI: [10.1186/s13099-017-0187-8](https://doi.org/10.1186/s13099-017-0187-8)]
- 19 **Nicholson WL**, Munakata N, Horneck G, Melosh HJ, Setlow P. Resistance of Bacillus endospores to extreme terrestrial and extraterrestrial environments. *Microbiol Mol Biol Rev* 2000; **64**: 548-572 [PMID: [10974126](https://pubmed.ncbi.nlm.nih.gov/10974126/) DOI: [10.1128/mmbr.64.3.548-572.2000](https://doi.org/10.1128/mmbr.64.3.548-572.2000)]
- 20 **Bassis CM**, Erb-Downward JR, Dickson RP, Freeman CM, Schmidt TM, Young VB, Beck JM, Curtis JL, Huffnagle GB. Analysis of the upper respiratory tract microbiotas as the source of the lung and gastric microbiotas in healthy individuals. *mBio* 2015; **6**: e00037 [PMID: [25736890](https://pubmed.ncbi.nlm.nih.gov/25736890/) DOI: [10.1128/mBio.00037-15](https://doi.org/10.1128/mBio.00037-15)]
- 21 **Tanaka M**, Nakayama J. Development of the gut microbiota in infancy and its impact on health in later life. *Allergol Int* 2017; **66**: 515-522 [PMID: [28826938](https://pubmed.ncbi.nlm.nih.gov/28826938/) DOI: [10.1016/j.alit.2017.07.010](https://doi.org/10.1016/j.alit.2017.07.010)]

- 22 **Claesson MJ**, Cusack S, O'Sullivan O, Greene-Diniz R, de Weerd H, Flannery E, Marchesi JR, Falush D, Dinan T, Fitzgerald G, Stanton C, van Sinderen D, O'Connor M, Harnedy N, O'Connor K, Henry C, O'Mahony D, Fitzgerald AP, Shanahan F, Twomey C, Hill C, Ross RP, O'Toole PW. Composition, variability, and temporal stability of the intestinal microbiota of the elderly. *Proc Natl Acad Sci USA* 2011; **108** Suppl 1: 4586-4591 [PMID: [20571116](#) DOI: [10.1073/pnas.1000097107](#)]
- 23 **Feres M**, Teles F, Teles R, Figueiredo LC, Faveri M. The subgingival periodontal microbiota of the aging mouth. *Periodontol* 2000 2016; **72**: 30-53 [PMID: [27501490](#) DOI: [10.1111/prd.12136](#)]
- 24 **Odamaki T**, Kato K, Sugahara H, Hashikura N, Takahashi S, Xiao JZ, Abe F, Osawa R. Age-related changes in gut microbiota composition from newborn to centenarian: a cross-sectional study. *BMC Microbiol* 2016; **16**: 90 [PMID: [27220822](#) DOI: [10.1186/s12866-016-0708-5](#)]
- 25 **Conlon MA**, Bird AR. The impact of diet and lifestyle on gut microbiota and human health. *Nutrients* 2014; **7**: 17-44 [PMID: [25545101](#) DOI: [10.3390/nu7010017](#)]
- 26 **Yatsunenkov T**, Rey FE, Manary MJ, Trehan I, Dominguez-Bello MG, Contreras M, Magris M, Hidalgo G, Baldassano RN, Anokhin AP, Heath AC, Warner B, Reeder J, Kuczynski J, Caporaso JG, Lozupone CA, Lauber C, Clemente JC, Knights D, Knight R, Gordon JI. Human gut microbiome viewed across age and geography. *Nature* 2012; **486**: 222-227 [PMID: [22699611](#) DOI: [10.1038/nature11053](#)]
- 27 **Dominguez-Bello MG**, Costello EK, Contreras M, Magris M, Hidalgo G, Fierer N, Knight R. Delivery mode shapes the acquisition and structure of the initial microbiota across multiple body habitats in newborns. *Proc Natl Acad Sci USA* 2010; **107**: 11971-11975 [PMID: [20566857](#) DOI: [10.1073/pnas.1002601107](#)]
- 28 **Holgerson PL**, Vestman NR, Claesson R, Ohman C, Domellöf M, Tanner AC, Hernell O, Johansson I. Oral microbial profile discriminates breast-fed from formula-fed infants. *J Pediatr Gastroenterol Nutr* 2013; **56**: 127-136 [PMID: [22955450](#) DOI: [10.1097/MPG.0b013e31826f2bc6](#)]
- 29 **Gregersen H**, Pedersen J, Drewes AM. Deterioration of muscle function in the human esophagus with age. *Dig Dis Sci* 2008; **53**: 3065-3070 [PMID: [18461452](#) DOI: [10.1007/s10620-008-0278-y](#)]
- 30 **Gutschow CA**, Leers JM, Schröder W, Prenzel KL, Fuchs H, Bollschweiler E, Bludau M, Hölscher AH. Effect of aging on esophageal motility in patients with and without GERD. *Ger Med Sci* 2011; **9**: Doc22 [PMID: [21863136](#) DOI: [10.3205/000145](#)]
- 31 **Yoshioka H**, Iseki K, Fujita K. Development and differences of intestinal flora in the neonatal period in breast-fed and bottle-fed infants. *Pediatrics* 1983; **72**: 317-321 [PMID: [6412205](#)]
- 32 **Le Huërou-Luron I**, Blat S, Boudry G. Breast- v. formula-feeding: impacts on the digestive tract and immediate and long-term health effects. *Nutr Res Rev* 2010; **23**: 23-36 [PMID: [20450531](#) DOI: [10.1017/S0954422410000065](#)]
- 33 **David LA**, Maurice CF, Carmody RN, Gootenberg DB, Button JE, Wolfe BE, Ling AV, Devlin AS, Varma Y, Fischbach MA, Biddinger SB, Dutton RJ, Turnbaugh PJ. Diet rapidly and reproducibly alters the human gut microbiome. *Nature* 2014; **505**: 559-563 [PMID: [24336217](#) DOI: [10.1038/nature12820](#)]
- 34 **Dawsey SM**, Fagundes RB, Jacobson BC, Kresty LA, Mallery SR, Paski S, van den Brandt PA. Diet and esophageal disease. *Ann N Y Acad Sci* 2014; **1325**: 127-137 [PMID: [25266021](#) DOI: [10.1111/nyas.12528](#)]
- 35 **Kubo A**, Corley DA, Jensen CD, Kaur R. Dietary factors and the risks of oesophageal adenocarcinoma and Barrett's oesophagus. *Nutr Res Rev* 2010; **23**: 230-246 [PMID: [20624335](#) DOI: [10.1017/S0954422410000132](#)]
- 36 **Dong TS**, Gupta A. Influence of Early Life, Diet, and the Environment on the Microbiome. *Clin Gastroenterol Hepatol* 2019; **17**: 231-242 [PMID: [30196160](#) DOI: [10.1016/j.cgh.2018.08.067](#)]
- 37 **Pannaraj PS**, Li F, Cerini C, Bender JM, Yang S, Rollie A, Adisetiyo H, Zabih S, Lincez PJ, Bittinger K, Bailey A, Bushman FD, Sleasman JW, Aldrovandi GM. Association Between Breast Milk Bacterial Communities and Establishment and Development of the Infant Gut Microbiome. *JAMA Pediatr* 2017; **171**: 647-654 [PMID: [28492938](#) DOI: [10.1001/jamapediatrics.2017.0378](#)]
- 38 **Rudloff S**, Kunz C. Milk oligosaccharides and metabolism in infants. *Adv Nutr* 2012; **3**: 398S-405S [PMID: [22585918](#) DOI: [10.3945/an.111.001594](#)]
- 39 **Kim SY**, Yi DY. Analysis of the human breast milk microbiome and bacterial extracellular vesicles in healthy mothers. *Exp Mol Med* 2020; **52**: 1288-1297 [PMID: [32747701](#) DOI: [10.1038/s12276-020-0470-5](#)]
- 40 **Bezirtzoglou E**, Tsiotsias A, Welling GW. Microbiota profile in feces of breast- and formula-fed newborns by using fluorescence in situ hybridization (FISH). *Anaerobe* 2011; **17**: 478-482 [PMID: [21497661](#) DOI: [10.1016/j.anaerobe.2011.03.009](#)]
- 41 **Bokulich NA**, Chung J, Battaglia T, Henderson N, Jay M, Li H, D Lieber A, Wu F, Perez-Perez GI, Chen Y, Schweizer W, Zheng X, Contreras M, Dominguez-Bello MG, Blaser MJ. Antibiotics, birth mode, and diet shape microbiome maturation during early life. *Sci Transl Med* 2016; **8**: 343ra82 [PMID: [27306664](#) DOI: [10.1126/scitranslmed.aad7121](#)]
- 42 **Brugman S**, Visser JT, Hillebrands JL, Bos NA, Rosing J. Prolonged exclusive breastfeeding reduces autoimmune diabetes incidence and increases regulatory T-cell frequency in bio-breeding diabetes-prone rats. *Diabetes Metab Res Rev* 2009; **25**: 380-387 [PMID: [19334008](#) DOI: [10.1002/dmrr.953](#)]
- 43 **Steinmetz KA**, Potter JD. Vegetables, fruit, and cancer. II. Mechanisms. *Cancer Causes Control* 1991; **2**: 427-442 [PMID: [1764568](#) DOI: [10.1007/BF00054304](#)]
- 44 **Mirvish SS**, Wallcave L, Eagen M, Shubik P. Ascorbate-nitrite reaction: possible means of blocking

- the formation of carcinogenic N-nitroso compounds. *Science* 1972; **177**: 65-68 [PMID: [5041776](#) DOI: [10.1126/science.177.4043.65](#)]
- 45 **Jakszyn P**, Gonzalez CA. Nitrosamine and related food intake and gastric and oesophageal cancer risk: a systematic review of the epidemiological evidence. *World J Gastroenterol* 2006; **12**: 4296-4303 [PMID: [16865769](#) DOI: [10.3748/wjg.v12.i27.4296](#)]
  - 46 **Chen H**, Ward MH, Graubard BI, Heineman EF, Markin RM, Potischman NA, Russell RM, Weisenburger DD, Tucker KL. Dietary patterns and adenocarcinoma of the esophagus and distal stomach. *Am J Clin Nutr* 2002; **75**: 137-144 [PMID: [11756071](#) DOI: [10.1093/ajcn/75.1.137](#)]
  - 47 **Kubo A**, Levin TR, Block G, Rumore GJ, Quesenberry CP Jr, Buffler P, Corley DA. Dietary patterns and the risk of Barrett's esophagus. *Am J Epidemiol* 2008; **167**: 839-846 [PMID: [18218607](#) DOI: [10.1093/aje/kwm381](#)]
  - 48 **Nobel YR**, Snider EJ, Compres G, Freedberg DE, Khiabanian H, Lightdale CJ, Toussaint NC, Abrams JA. Increasing Dietary Fiber Intake Is Associated with a Distinct Esophageal Microbiome. *Clin Transl Gastroenterol* 2018; **9**: 199 [PMID: [30356041](#) DOI: [10.1038/s41424-018-0067-7](#)]
  - 49 **Katelaris PH**. Proton pump inhibitors. *Med J Aust* 1998; **169**: 208-211 [PMID: [9734580](#) DOI: [10.5694/j.1326-5377.1998.tb140224.x](#)]
  - 50 **Imhann F**, Bonder MJ, Vich Vila A, Fu J, Mujagic Z, Vork L, Tigchelaar EF, Jankipersadsing SA, Cenit MC, Harmsen HJ, Dijkstra G, Franke L, Xavier RJ, Jonkers D, Wijmenga C, Weersma RK, Zhernakova A. Proton pump inhibitors affect the gut microbiome. *Gut* 2016; **65**: 740-748 [PMID: [26657899](#) DOI: [10.1136/gutjnl-2015-310376](#)]
  - 51 **Jackson MA**, Goodrich JK, Maxan ME, Freedberg DE, Abrams JA, Poole AC, Sutter JL, Welter D, Ley RE, Bell JT, Spector TD, Steves CJ. Proton pump inhibitors alter the composition of the gut microbiota. *Gut* 2016; **65**: 749-756 [PMID: [26719299](#) DOI: [10.1136/gutjnl-2015-310861](#)]
  - 52 **Macke L**, Schulz C, Koletzko L, Malfertheiner P. Systematic review: the effects of proton pump inhibitors on the microbiome of the digestive tract-evidence from next-generation sequencing studies. *Aliment Pharmacol Ther* 2020; **51**: 505-526 [PMID: [31990420](#) DOI: [10.1111/apt.15604](#)]
  - 53 **Zhou J**, Shrestha P, Qiu Z, Harman DG, Teoh WC, Al-Sohaily S, Liem H, Turner I, Ho V. Distinct Microbiota Dysbiosis in Patients with Non-Erosive Reflux Disease and Esophageal Adenocarcinoma. *J Clin Med* 2020; **9** [PMID: [32650561](#) DOI: [10.3390/jcm9072162](#)]
  - 54 **Amir I**, Konikoff FM, Oppenheim M, Gophna U, Half EE. Gastric microbiota is altered in oesophagitis and Barrett's oesophagus and further modified by proton pump inhibitors. *Environ Microbiol* 2014; **16**: 2905-2914 [PMID: [24112768](#) DOI: [10.1111/1462-2920.12285](#)]
  - 55 **Vesper BJ**, Jawdi A, Altman KW, Haines GK 3rd, Tao L, Radosevich JA. The effect of proton pump inhibitors on the human microbiota. *Curr Drug Metab* 2009; **10**: 84-89 [PMID: [19149516](#) DOI: [10.2174/138920009787048392](#)]
  - 56 **Huo X**, Zhang X, Yu C, Zhang Q, Cheng E, Wang DH, Pham TH, Spechler SJ, Souza RF. In oesophageal squamous cells exposed to acidic bile salt medium, omeprazole inhibits IL-8 expression through effects on nuclear factor- $\kappa$ B and activator protein-1. *Gut* 2014; **63**: 1042-1052 [PMID: [24048734](#) DOI: [10.1136/gutjnl-2013-305533](#)]
  - 57 **Konturek PC**, Nikiforuk A, Kania J, Raithel M, Hahn EG, Mühldorfer S. Activation of NF $\kappa$ B represents the central event in the neoplastic progression associated with Barrett's esophagus: a possible link to the inflammation and overexpression of COX-2, PPAR $\gamma$  and growth factors. *Dig Dis Sci* 2004; **49**: 1075-1083 [PMID: [15387324](#) DOI: [10.1023/B:DDAS.0000037790.11724.70](#)]
  - 58 **Socransky SS**, Haffajee AD. Periodontal microbial ecology. *Periodontol 2000* 2005; **38**: 135-187 [PMID: [15853940](#) DOI: [10.1111/j.1600-0757.2005.00107.x](#)]
  - 59 **Chen X**, Yuan Z, Lu M, Zhang Y, Jin L, Ye W. Poor oral health is associated with an increased risk of esophageal squamous cell carcinoma - a population-based case-control study in China. *Int J Cancer* 2017; **140**: 626-635 [PMID: [27778330](#) DOI: [10.1002/ijc.30484](#)]
  - 60 **Wang TW**, Asman K, Gentzke AS, Cullen KA, Holder-Hayes E, Reyes-Guzman C, Jamal A, Neff L, King BA. Tobacco Product Use Among Adults - United States, 2017. *MMWR Morb Mortal Wkly Rep* 2018; **67**: 1225-1232 [PMID: [30408019](#) DOI: [10.15585/mmwr.mm6744a2](#)]
  - 61 **Vogtmann E**, Flores R, Yu G, Freedman ND, Shi J, Gail MH, Dye BA, Wang GQ, Klepac-Ceraj V, Paster BJ, Wei WQ, Guo HQ, Dawsey SM, Qiao YL, Abnet CC. Association between tobacco use and the upper gastrointestinal microbiome among Chinese men. *Cancer Causes Control* 2015; **26**: 581-588 [PMID: [25701246](#) DOI: [10.1007/s10552-015-0535-2](#)]
  - 62 **Kulkarni R**, Antala S, Wang A, Amaral FE, Rampersaud R, Larussa SJ, Planet PJ, Ratner AJ. Cigarette smoke increases *Staphylococcus aureus* biofilm formation via oxidative stress. *Infect Immun* 2012; **80**: 3804-3811 [PMID: [22890993](#) DOI: [10.1128/IAI.00689-12](#)]
  - 63 **Arnson Y**, Shoenfeld Y, Amital H. Effects of tobacco smoke on immunity, inflammation and autoimmunity. *J Autoimmun* 2010; **34**: J258-J265 [PMID: [20042314](#) DOI: [10.1016/j.jaut.2009.12.003](#)]
  - 64 **Dicks LMT**, Dreyer L, Smith C, van Staden AD. A Review: The Fate of Bacteriocins in the Human Gastro-Intestinal Tract: Do They Cross the Gut-Blood Barrier? *Front Microbiol* 2018; **9**: 2297 [PMID: [30323796](#) DOI: [10.3389/fmicb.2018.02297](#)]
  - 65 **Kumariya R**, Garsa AK, Rajput YS, Sood SK, Akhtar N, Patel S. Bacteriocins: Classification, synthesis, mechanism of action and resistance development in food spoilage causing bacteria. *Microb Pathog* 2019; **128**: 171-177 [PMID: [30610901](#) DOI: [10.1016/j.micpath.2019.01.002](#)]
  - 66 **Mathiesen G**, Huehne K, Kroeckel L, Axelsson L, Eijssink VG. Characterization of a new bacteriocin operon in sakacin P-producing *Lactobacillus sakei*, showing strong translational coupling

- between the bacteriocin and immunity genes. *Appl Environ Microbiol* 2005; **71**: 3565-3574 [PMID: 16000763 DOI: 10.1128/AEM.71.7.3565-3574.2005]
- 67 **Kelly JR**, Kennedy PJ, Cryan JF, Dinan TG, Clarke G, Hyland NP. Breaking down the barriers: the gut microbiome, intestinal permeability and stress-related psychiatric disorders. *Front Cell Neurosci* 2015; **9**: 392 [PMID: 26528128 DOI: 10.3389/fncel.2015.00392]
  - 68 **Spadoni I**, Zagato E, Bertocchi A, Paolinelli R, Hot E, Di Sabatino A, Caprioli F, Bottiglieri L, Oldani A, Viale G, Penna G, Dejana E, Rescigno M. A gut-vascular barrier controls the systemic dissemination of bacteria. *Science* 2015; **350**: 830-834 [PMID: 26564856 DOI: 10.1126/science.aad0135]
  - 69 **Okuda K**, Zendo T, Sugimoto S, Iwase T, Tajima A, Yamada S, Sonomoto K, Mizunoe Y. Effects of bacteriocins on methicillin-resistant *Staphylococcus aureus* biofilm. *Antimicrob Agents Chemother* 2013; **57**: 5572-5579 [PMID: 23979748 DOI: 10.1128/AAC.00888-13]
  - 70 **Corr SC**, Li Y, Riedel CU, O'Toole PW, Hill C, Gahan CG. Bacteriocin production as a mechanism for the antiinfective activity of *Lactobacillus salivarius* UCC118. *Proc Natl Acad Sci USA* 2007; **104**: 7617-7621 [PMID: 17456596 DOI: 10.1073/pnas.0700440104]
  - 71 **Joo NE**, Ritchie K, Kamarajan P, Miao D, Kapila YL. Nisin, an apoptogenic bacteriocin and food preservative, attenuates HNSCC tumorigenesis via CHAC1. *Cancer Med* 2012; **1**: 295-305 [PMID: 23342279 DOI: 10.1002/cam4.35]
  - 72 **Kamarajan P**, Hayami T, Matte B, Liu Y, Danciu T, Ramamoorthy A, Worden F, Kapila S, Kapila Y. Nisin ZP, a Bacteriocin and Food Preservative, Inhibits Head and Neck Cancer Tumorigenesis and Prolongs Survival. *PLoS One* 2015; **10**: e0131008 [PMID: 26132406 DOI: 10.1371/journal.pone.0131008]
  - 73 **Machado LR**, Ottolini B. An evolutionary history of defensins: a role for copy number variation in maximizing host innate and adaptive immune responses. *Front Immunol* 2015; **6**: 115 [PMID: 25852686 DOI: 10.3389/fimmu.2015.00115]
  - 74 **Raschig J**, Mailänder-Sánchez D, Berscheid A, Berger J, Strömmstedt AA, Courth LF, Malek NP, Brötz-Oesterhelt H, Wehkamp J. Ubiquitously expressed Human Beta Defensin 1 (hBD1) forms bacteria-entrapping nets in a redox dependent mode of action. *PLoS Pathog* 2017; **13**: e1006261 [PMID: 28323883 DOI: 10.1371/journal.ppat.1006261]
  - 75 **Schroeder S**, Robinson ZD, Masterson JC, Hosford L, Moore W, Pan Z, Harris R, Souza RF, Spechler SJ, Fillon SA, Furuta GT. Esophageal human  $\beta$ -defensin expression in eosinophilic esophagitis. *Pediatr Res* 2013; **73**: 647-654 [PMID: 23385963 DOI: 10.1038/pr.2013.23]
  - 76 **Nomura Y**, Tanabe H, Moriichi K, Igawa S, Ando K, Ueno N, Kashima S, Tominaga M, Goto T, Inaba Y, Ito T, Ishida-Yamamoto A, Fujiya M, Kohgo Y. Reduction of E-cadherin by human defensin-5 in esophageal squamous cells. *Biochem Biophys Res Commun* 2013; **439**: 71-77 [PMID: 23958301 DOI: 10.1016/j.bbrc.2013.08.026]
  - 77 **Jung S**, Mysliwy J, Spudy B, Lorenzen I, Reiss K, Gelhaus C, Podschun R, Leippe M, Grötzing J. Human beta-defensin 2 and beta-defensin 3 chimeric peptides reveal the structural basis of the pathogen specificity of their parent molecules. *Antimicrob Agents Chemother* 2011; **55**: 954-960 [PMID: 21189349 DOI: 10.1128/AAC.00872-10]
  - 78 **Petersen C**, Round JL. Defining dysbiosis and its influence on host immunity and disease. *Cell Microbiol* 2014; **16**: 1024-1033 [PMID: 24798552 DOI: 10.1111/cmi.12308]
  - 79 **Ajayi TA**, Cantrell S, Spann A, Garman KS. Barrett's esophagus and esophageal cancer: Links to microbes and the microbiome. *PLoS Pathog* 2018; **14**: e1007384 [PMID: 30571768 DOI: 10.1371/journal.ppat.1007384]
  - 80 **Yang L**, Francois F, Pei Z. Molecular pathways: pathogenesis and clinical implications of microbiome alteration in esophagitis and Barrett esophagus. *Clin Cancer Res* 2012; **18**: 2138-2144 [PMID: 22344232 DOI: 10.1158/1078-0432.CCR-11-0934]
  - 81 **Orlando RC**. The integrity of the esophageal mucosa. Balance between offensive and defensive mechanisms. *Best Pract Res Clin Gastroenterol* 2010; **24**: 873-882 [PMID: 21126700 DOI: 10.1016/j.bpg.2010.08.008]
  - 82 **Hershovici T**, Fass R. Nonerosive Reflux Disease (NERD) - An Update. *J Neurogastroenterol Motil* 2010; **16**: 8-21 [PMID: 20535321 DOI: 10.5056/jnm.2010.16.1.8]
  - 83 **Winkelstein A**. Peptic esophagitis. *J Am Med Assoc* 1935; **104**: 906-909 [DOI: 10.1001/jama.1935.02760110034008]
  - 84 **Dunbar KB**, Agoston AT, Odze RD, Huo X, Pham TH, CIPHER DJ, Castell DO, Genta RM, Souza RF, Spechler SJ. Association of Acute Gastroesophageal Reflux Disease With Esophageal Histologic Changes. *JAMA* 2016; **315**: 2104-2112 [PMID: 27187303 DOI: 10.1001/jama.2016.5657]
  - 85 **Souza RF**, Huo X, Mittal V, Schuler CM, Carmack SW, Zhang HY, Zhang X, Yu C, Hormi-Carver K, Genta RM, Spechler SJ. Gastroesophageal reflux might cause esophagitis through a cytokine-mediated mechanism rather than caustic acid injury. *Gastroenterology* 2009; **137**: 1776-1784 [PMID: 19660463 DOI: 10.1053/j.gastro.2009.07.055]
  - 86 **Ustaoglu A**, Nguyen A, Spechler S, Sifrim D, Souza R, Woodland P. Mucosal pathogenesis in gastro-esophageal reflux disease. *Neurogastroenterol Motil* 2020; **32**: e14022 [PMID: 33118247 DOI: 10.1111/nmo.14022]
  - 87 **Cheng L**, Harnett KM, Cao W, Liu F, Behar J, Fiocchi C, Biancani P. Hydrogen peroxide reduces lower esophageal sphincter tone in human esophagitis. *Gastroenterology* 2005; **129**: 1675-1685 [PMID: 16285965 DOI: 10.1053/j.gastro.2005.09.008]
  - 88 **Blackett KL**, Siddhi SS, Cleary S, Steed H, Miller MH, Macfarlane S, Macfarlane GT, Dillon JF.



- Oesophageal bacterial biofilm changes in gastro-oesophageal reflux disease, Barrett's and oesophageal carcinoma: association or causality? *Aliment Pharmacol Ther* 2013; **37**: 1084-1092 [PMID: [23600758](#) DOI: [10.1111/apt.12317](#)]
- 89 **Marsh PD.** Dental plaque as a biofilm and a microbial community - implications for health and disease. *BMC Oral Health* 2006; **6** Suppl 1: S14 [PMID: [16934115](#) DOI: [10.1186/1472-6831-6-S1-S14](#)]
  - 90 **Dejea CM,** Fathi P, Craig JM, Boleij A, Taddese R, Geis AL, Wu X, DeStefano Shields CE, Hechenbleikner EM, Huso DL, Anders RA, Giardiello FM, Wick EC, Wang H, Wu S, Pardoll DM, Housseau F, Sears CL. Patients with familial adenomatous polyposis harbor colonic biofilms containing tumorigenic bacteria. *Science* 2018; **359**: 592-597 [PMID: [29420293](#) DOI: [10.1126/science.aah3648](#)]
  - 91 **D'Souza SM,** Levitan O, Tieu AH. Bio-Geographic Variation of Colonic Biome and Biofilm Consequences on Disease: An Update for Clinicians. *World J Gastroenterol Hepatol Endosc Research* 2020; **1**: 1-11
  - 92 **Münch NS,** Fang HY, Ingermann J, Maurer HC, Anand A, Kellner V, Sahm V, Wiethaler M, Baumeister T, Wein F, Einwächter H, Bolze F, Klingenspor M, Haller D, Kavanagh M, Lysaght J, Friedman R, Dannenberg AJ, Pollak M, Holt PR, Muthupalani S, Fox JG, Whary MT, Lee Y, Ren TY, Elliot R, Fitzgerald R, Steiger K, Schmid RM, Wang TC, Quante M. High-Fat Diet Accelerates Carcinogenesis in a Mouse Model of Barrett's Esophagus *via* Interleukin 8 and Alterations to the Gut Microbiome. *Gastroenterology* 2019; **157**: 492-506. e2 [PMID: [30998992](#) DOI: [10.1053/j.gastro.2019.04.013](#)]
  - 93 **Ropert A,** Cherbut C, Rozé C, Le Quellec A, Holst JJ, Fu-Cheng X, Bruley des Varannes S, Galmiche JP. Colonic fermentation and proximal gastric tone in humans. *Gastroenterology* 1996; **111**: 289-296 [PMID: [8690193](#) DOI: [10.1053/gast.1996.v111.pm8690193](#)]
  - 94 **Shaheen NJ,** Falk GW, Iyer PG, Gerson LB; American College of Gastroenterology. ACG Clinical Guideline: Diagnosis and Management of Barrett's Esophagus. *Am J Gastroenterol* 2016; **111**: 30-50; quiz 51 [PMID: [26526079](#) DOI: [10.1038/ajg.2015.322](#)]
  - 95 **Naini BV,** Souza RF, Odze RD. Barrett's Esophagus: A Comprehensive and Contemporary Review for Pathologists. *Am J Surg Pathol* 2016; **40**: e45-e66 [PMID: [26813745](#) DOI: [10.1097/PAS.0000000000000598](#)]
  - 96 **May M,** Abrams JA. Emerging Insights into the Esophageal Microbiome. *Curr Treat Options Gastroenterol* 2018; **16**: 72-85 [PMID: [29350339](#) DOI: [10.1007/s11938-018-0171-5](#)]
  - 97 **Souza RF.** Reflux esophagitis and its role in the pathogenesis of Barrett's metaplasia. *J Gastroenterol* 2017; **52**: 767-776 [PMID: [28451845](#) DOI: [10.1007/s00535-017-1342-1](#)]
  - 98 **Quante M,** Bhagat G, Abrams JA, Marache F, Good P, Lee MD, Lee Y, Friedman R, Asfaha S, Dubeykovskaya Z, Mahmood U, Figueiredo JL, Kitajewski J, Shawber C, Lightdale CJ, Rustgi AK, Wang TC. Bile acid and inflammation activate gastric cardia stem cells in a mouse model of Barrett-like metaplasia. *Cancer Cell* 2012; **21**: 36-51 [PMID: [22264787](#) DOI: [10.1016/j.ccr.2011.12.004](#)]
  - 99 **Sollberger G,** Strittmatter GE, Garstkievicz M, Sand J, Beer HD. Caspase-1: the inflammasome and beyond. *Innate Immun* 2014; **20**: 115-125 [PMID: [23676582](#) DOI: [10.1177/1753425913484374](#)]
  - 100 **Guo H,** Callaway JB, Ting JP. Inflammasomes: mechanism of action, role in disease, and therapeutics. *Nat Med* 2015; **21**: 677-687 [PMID: [26121197](#) DOI: [10.1038/nm.3893](#)]
  - 101 **Nadatani Y,** Huo X, Zhang X, Yu C, Cheng E, Zhang Q, Dunbar KB, Theiss A, Pham TH, Wang DH, Watanabe T, Fujiwara Y, Arakawa T, Spechler SJ, Souza RF. NOD-Like Receptor Protein 3 Inflammasome Priming and Activation in Barrett's Epithelial Cells. *Cell Mol Gastroenterol Hepatol* 2016; **2**: 439-453 [PMID: [27777967](#) DOI: [10.1016/j.jcmgh.2016.03.006](#)]
  - 102 **Snider EJ,** Compres G, Freedberg DE, Giddins MJ, Khiabani H, Lightdale CJ, Nobel YR, Toussaint NC, Uhlemann AC, Abrams JA. Barrett's esophagus is associated with a distinct oral microbiome. *Clin Transl Gastroenterol* 2018; **9**: 135 [PMID: [29491399](#) DOI: [10.1038/s41424-018-0005-8](#)]
  - 103 **Yang L,** Chaudhary N, Baghdadi J, Pei Z. Microbiome in reflux disorders and esophageal adenocarcinoma. *Cancer J* 2014; **20**: 207-210 [PMID: [24855009](#) DOI: [10.1097/PPO.0000000000000044](#)]
  - 104 **Liu N,** Ando T, Ishiguro K, Maeda O, Watanabe O, Funasaka K, Nakamura M, Miyahara R, Ohmiya N, Goto H. Characterization of bacterial biota in the distal esophagus of Japanese patients with reflux esophagitis and Barrett's esophagus. *BMC Infect Dis* 2013; **13**: 130 [PMID: [23496929](#) DOI: [10.1186/1471-2334-13-130](#)]
  - 105 **Macfarlane S,** Furrie E, Macfarlane GT, Dillon JF. Microbial colonization of the upper gastrointestinal tract in patients with Barrett's esophagus. *Clin Infect Dis* 2007; **45**: 29-38 [PMID: [17554697](#) DOI: [10.1086/518578](#)]
  - 106 **Lopetuso LR,** Severgnini M, Pecere S, Ponziani FR, Boskoski I, Larghi A, Quaranta G, Masucci L, Ianiro G, Camboni T, Gasbarrini A, Costamagna G, Consolandi C, Cammarota G. Esophageal microbiome signature in patients with Barrett's esophagus and esophageal adenocarcinoma. *PLoS One* 2020; **15**: e0231789 [PMID: [32369505](#) DOI: [10.1371/journal.pone.0231789](#)]
  - 107 **Kamangar F,** Chow WH, Abnet CC, Dawsey SM. Environmental causes of esophageal cancer. *Gastroenterol Clin North Am* 2009; **38**: 27-57, vii [PMID: [19327566](#) DOI: [10.1016/j.gtc.2009.01.004](#)]
  - 108 **Engel LS,** Chow WH, Vaughan TL, Gammon MD, Risch HA, Stanford JL, Schoenberg JB, Mayne ST, Dubrow R, Rotterdam H, West AB, Blaser M, Blot WJ, Gail MH, Fraumeni JF Jr. Population

- attributable risks of esophageal and gastric cancers. *J Natl Cancer Inst* 2003; **95**: 1404-1413 [PMID: 13130116 DOI: 10.1093/jnci/djg047]
- 109 **Bhat S**, Coleman HG, Yousef F, Johnston BT, McManus DT, Gavin AT, Murray LJ. Risk of malignant progression in Barrett's esophagus patients: results from a large population-based study. *J Natl Cancer Inst* 2011; **103**: 1049-1057 [PMID: 21680910 DOI: 10.1093/jnci/djr203]
  - 110 **Snider EJ**, Compres G, Freedberg DE, Khiabani H, Nobel YR, Stump S, Uhlemann AC, Lightdale CJ, Abrams JA. Alterations to the Esophageal Microbiome Associated with Progression from Barrett's Esophagus to Esophageal Adenocarcinoma. *Cancer Epidemiol Biomarkers Prev* 2019; **28**: 1687-1693 [PMID: 31466948 DOI: 10.1158/1055-9965.EPI-19-0008]
  - 111 **Snider EJ**, Freedberg DE, Abrams JA. Potential Role of the Microbiome in Barrett's Esophagus and Esophageal Adenocarcinoma. *Dig Dis Sci* 2016; **61**: 2217-2225 [PMID: 27068172 DOI: 10.1007/s10620-016-4155-9]
  - 112 **Narikiyo M**, Tanabe C, Yamada Y, Igaki H, Tachimori Y, Kato H, Muto M, Montesano R, Sakamoto H, Nakajima Y, Sasaki H. Frequent and preferential infection of *Treponema denticola*, *Streptococcus mitis*, and *Streptococcus anginosus* in esophageal cancers. *Cancer Sci* 2004; **95**: 569-574 [PMID: 15245592 DOI: 10.1111/j.1349-7006.2004.tb02488.x]
  - 113 **Peters BA**, Wu J, Pei Z, Yang L, Purdue MP, Freedman ND, Jacobs EJ, Gapstur SM, Hayes RB, Ahn J. Oral Microbiome Composition Reflects Prospective Risk for Esophageal Cancers. *Cancer Res* 2017; **77**: 6777-6787 [PMID: 29196415 DOI: 10.1158/0008-5472.CAN-17-1296]
  - 114 **Zaidi AH**, Kelly LA, Kreft RE, Barlek M, Omstead AN, Matsui D, Boyd NH, Gazarik KE, Heit MI, Nistico L, Kasi PM, Spirk TL, Byers B, Lloyd EJ, Landreneau RJ, Jobe BA. Associations of microbiota and toll-like receptor signaling pathway in esophageal adenocarcinoma. *BMC Cancer* 2016; **16**: 52 [PMID: 26841926 DOI: 10.1186/s12885-016-2093-8]
  - 115 **Abnet CC**, Arnold M, Wei WQ. Epidemiology of Esophageal Squamous Cell Carcinoma. *Gastroenterology* 2018; **154**: 360-373 [PMID: 28823862 DOI: 10.1053/j.gastro.2017.08.023]
  - 116 **Lu CL**, Lang HC, Luo JC, Liu CC, Lin HC, Chang FY, Lee SD. Increasing trend of the incidence of esophageal squamous cell carcinoma, but not adenocarcinoma, in Taiwan. *Cancer Causes Control* 2010; **21**: 269-274 [PMID: 19866363 DOI: 10.1007/s10552-009-9458-0]
  - 117 **Sepehr A**, Kamangar F, Fahimi S, Saidi F, Abnet CC, Dawsey SM. Poor oral health as a risk factor for esophageal squamous dysplasia in northeastern Iran. *Anticancer Res* 2005; **25**: 543-546 [PMID: 15816626]
  - 118 **Wang Q**, Rao Y, Guo X, Liu N, Liu S, Wen P, Li S, Li Y. Oral Microbiome in Patients with Oesophageal Squamous Cell Carcinoma. *Sci Rep* 2019; **9**: 19055 [PMID: 31836795 DOI: 10.1038/s41598-019-55667-w]
  - 119 **Chen X**, Winckler B, Lu M, Cheng H, Yuan Z, Yang Y, Jin L, Ye W. Oral Microbiota and Risk for Esophageal Squamous Cell Carcinoma in a High-Risk Area of China. *PLoS One* 2015; **10**: e0143603 [PMID: 26641451 DOI: 10.1371/journal.pone.0143603]
  - 120 **Huang C**, Shi G. Smoking and microbiome in oral, airway, gut and some systemic diseases. *J Transl Med* 2019; **17**: 225 [PMID: 31307469 DOI: 10.1186/s12967-019-1971-7]
  - 121 **Bishehsari F**, Magno E, Swanson G, Desai V, Voigt RM, Forsyth CB, Keshavarzian A. Alcohol and Gut-Derived Inflammation. *Alcohol Res* 2017; **38**: 163-171 [PMID: 28988571]
  - 122 **Bull-Otterson L**, Feng W, Kirpich I, Wang Y, Qin X, Liu Y, Gobejishvili L, Joshi-Barve S, Ayvaz T, Petrosino J, Kong M, Barker D, McClain C, Barve S. Metagenomic analyses of alcohol induced pathogenic alterations in the intestinal microbiome and the effect of *Lactobacillus rhamnosus* GG treatment. *PLoS One* 2013; **8**: e53028 [PMID: 23326376 DOI: 10.1371/journal.pone.0053028]
  - 123 **Mutlu E**, Keshavarzian A, Engen P, Forsyth CB, Sikaroodi M, Gillevet P. Intestinal dysbiosis: a possible mechanism of alcohol-induced endotoxemia and alcoholic steatohepatitis in rats. *Alcohol Clin Exp Res* 2009; **33**: 1836-1846 [PMID: 19645728 DOI: 10.1111/j.1530-0277.2009.01022.x]
  - 124 **Liu Y**, Lin Z, Lin Y, Chen Y, Peng XE, He F, Liu S, Yan S, Huang L, Lu W, Xiang Z, Hu Z. *Streptococcus* and *Prevotella* are associated with the prognosis of oesophageal squamous cell carcinoma. *J Med Microbiol* 2018; **67**: 1058-1068 [PMID: 29923815 DOI: 10.1099/jmm.0.000754]
  - 125 **Dellon ES**, Gonsalves N, Hirano I, Furuta GT, Liacouras CA, Katzka DA; American College of Gastroenterology. ACG clinical guideline: Evidence based approach to the diagnosis and management of esophageal eosinophilia and eosinophilic esophagitis (EoE). *Am J Gastroenterol* 2013; **108**: 679-92; quiz 693 [PMID: 23567357 DOI: 10.1038/ajg.2013.71]
  - 126 **O'Shea KM**, Aceves SS, Dellon ES, Gupta SK, Spergel JM, Furuta GT, Rothenberg ME. Pathophysiology of Eosinophilic Esophagitis. *Gastroenterology* 2018; **154**: 333-345 [PMID: 28757265 DOI: 10.1053/j.gastro.2017.06.065]
  - 127 **Kitajima M**, Lee HC, Nakayama T, Ziegler SF. TSLP enhances the function of helper type 2 cells. *Eur J Immunol* 2011; **41**: 1862-1871 [PMID: 21484783 DOI: 10.1002/eji.201041195]
  - 128 **Benitez AJ**, Hoffmann C, Muir AB, Dods KK, Spergel JM, Bushman FD, Wang ML. Inflammation-associated microbiota in pediatric eosinophilic esophagitis. *Microbiome* 2015; **3**: 23 [PMID: 26034601 DOI: 10.1186/s40168-015-0085-6]
  - 129 **Jensen ET**, Kuhl JT, Martin LJ, Langefeld CD, Dellon ES, Rothenberg ME. Early-life environmental exposures interact with genetic susceptibility variants in pediatric patients with eosinophilic esophagitis. *J Allergy Clin Immunol* 2018; **141**: 632-637. e5 [PMID: 29029802 DOI: 10.1016/j.jaci.2017.07.010]
  - 130 **Radano MC**, Yuan Q, Katz A, Fleming JT, Kubala S, Shreffler W, Keet CA. Cesarean section and antibiotic use found to be associated with eosinophilic esophagitis. *J Allergy Clin Immunol Pract*

- 2014; **2**: 475-477. e1 [PMID: [25017541](#) DOI: [10.1016/j.jaip.2014.02.018](#)]
- 131 **Harris JK**, Fang R, Wagner BD, Choe HN, Kelly CJ, Schroeder S, Moore W, Stevens MJ, Yeckes A, Amsden K, Kagalwalla AF, Zalewski A, Hirano I, Gonsalves N, Henry LN, Masterson JC, Robertson CE, Leung DY, Pace NR, Ackerman SJ, Furuta GT, Fillon SA. Esophageal microbiome in eosinophilic esophagitis. *PLoS One* 2015; **10**: e0128346 [PMID: [26020633](#) DOI: [10.1371/journal.pone.0128346](#)]
- 132 **Kashyap PC**, Johnson S, Geno DM, Lekatiz HR, Lavey C, Alexander JA, Chen J, Katzka DA. A decreased abundance of clostridia characterizes the gut microbiota in eosinophilic esophagitis. *Physiol Rep* 2019; **7**: e14261 [PMID: [31650712](#) DOI: [10.14814/phy2.14261](#)]
- 133 **Stefka AT**, Feehley T, Tripathi P, Qiu J, McCoy K, Mazmanian SK, Tjota MY, Seo GY, Cao S, Theriault BR, Antonopoulos DA, Zhou L, Chang EB, Fu YX, Nagler CR. Commensal bacteria protect against food allergen sensitization. *Proc Natl Acad Sci USA* 2014; **111**: 13145-13150 [PMID: [25157157](#) DOI: [10.1073/pnas.1412008111](#)]
- 134 **Selling J**, Swann P, Madsen LR 2nd, Oswald J. Improvement in Gastroesophageal Reflux Symptoms From a Food-grade Maltosyl-isomaltooligosaccharide Soluble Fiber Supplement: A Case Series. *Integr Med (Encinitas)* 2018; **17**: 40-42 [PMID: [31043918](#)]
- 135 **Beckett JM**, Singh NK, Phillips J, Kalpurath K, Taylor K, Stanley RA, Eri RD. Anti-Heartburn Effects of Sugar Cane Flour: A Double-Blind, Randomized, Placebo-Controlled Study. *Nutrients* 2020; **12** [PMID: [32570710](#) DOI: [10.3390/nu12061813](#)]
- 136 **Cheng J**, Ouwehand AC. Gastroesophageal Reflux Disease and Probiotics: A Systematic Review. *Nutrients* 2020; **12** [PMID: [31906573](#) DOI: [10.3390/nu12010132](#)]
- 137 **Gomi A**, Yamaji K, Watanabe O, Yoshioka M, Miyazaki K, Iwama Y, Urita Y. Bifidobacterium bifidum YIT 10347 fermented milk exerts beneficial effects on gastrointestinal discomfort and symptoms in healthy adults: A double-blind, randomized, placebo-controlled study. *J Dairy Sci* 2018; **101**: 4830-4841 [PMID: [29573807](#) DOI: [10.3168/jds.2017-13803](#)]
- 138 **Waller PA**, Gopal PK, Leyer GJ, Ouwehand AC, Reifer C, Stewart ME, Miller LE. Dose-response effect of Bifidobacterium lactis HN019 on whole gut transit time and functional gastrointestinal symptoms in adults. *Scand J Gastroenterol* 2011; **46**: 1057-1064 [PMID: [21663486](#) DOI: [10.3109/00365521.2011.584895](#)]
- 139 **Nakae H**, Tsuda A, Matsuoka T, Mine T, Koga Y. Gastric microbiota in the functional dyspepsia patients treated with probiotic yogurt. *BMJ Open Gastroenterol* 2016; **3**: e000109 [PMID: [27752337](#) DOI: [10.1136/bmjgast-2016-000109](#)]
- 140 **Ohtsu T**, Takagi A, Uemura N, Inoue K, Sekino H, Kawashima A, Uchida M, Koga Y. The Ameliorating Effect of Lactobacillus gasseri OLL2716 on Functional Dyspepsia in Helicobacter pylori-Uninfected Individuals: A Randomized Controlled Study. *Digestion* 2017; **96**: 92-102 [PMID: [28768250](#) DOI: [10.1159/000479000](#)]
- 141 **Su GL**, Ko CW, Bercik P, Falck-Ytter Y, Sultan S, Weizman AV, Morgan RL. AGA Clinical Practice Guidelines on the Role of Probiotics in the Management of Gastrointestinal Disorders. *Gastroenterology* 2020; **159**: 697-705 [PMID: [32531291](#) DOI: [10.1053/j.gastro.2020.05.059](#)]
- 142 **Rao SSC**, Bhagatwala J. Small Intestinal Bacterial Overgrowth: Clinical Features and Therapeutic Management. *Clin Transl Gastroenterol* 2019; **10**: e00078 [PMID: [31584459](#) DOI: [10.14309/ctg.0000000000000078](#)]
- 143 **Acharya C**, Bajaj JS. Current Management of Hepatic Encephalopathy. *Am J Gastroenterol* 2018; **113**: 1600-1612 [PMID: [30002466](#) DOI: [10.1038/s41395-018-0179-4](#)]
- 144 **McDonald LC**, Gerding DN, Johnson S, Bakken JS, Carroll KC, Coffin SE, Dubberke ER, Garey KW, Gould CV, Kelly C, Loo V, Shaklee Sammons J, Sandora TJ, Wilcox MH. Clinical Practice Guidelines for Clostridium difficile Infection in Adults and Children: 2017 Update by the Infectious Diseases Society of America (IDSA) and Society for Healthcare Epidemiology of America (SHEA). *Clin Infect Dis* 2018; **66**: e1-e48 [PMID: [29462280](#) DOI: [10.1093/cid/cix1085](#)]
- 145 **Fahim HA**, Khairalla AS, El-Gendy AO. Nanotechnology: A Valuable Strategy to Improve Bacteriocin Formulations. *Front Microbiol* 2016; **7**: 1385 [PMID: [27695440](#) DOI: [10.3389/fmicb.2016.01385](#)]





## Immune disorders and rheumatologic manifestations of viral hepatitis

Roman Maslennikov, Vladimir Ivashkin, Irina Efremova, Elena Shirokova

**ORCID number:** Roman Maslennikov 0000-0001-7513-1636; Vladimir Ivashkin 0000-0002-6815-6015; Irina Efremova 0000-0002-4112-0426; Elena Shirokova 0000-0002-6819-0889.

**Author contributions:** Ivashkin V and Maslennikov R thought idea of the review; all authors searched original publications; Maslennikov R written the draft; all authors made the draft editing.

**Conflict-of-interest statement:** No conflict of interest for declaration.

**Open-Access:** This article is an open-access article that was selected by an in-house editor and fully peer-reviewed by external reviewers. It is distributed in accordance with the Creative Commons Attribution NonCommercial (CC BY-NC 4.0) license, which permits others to distribute, remix, adapt, build upon this work non-commercially, and license their derivative works on different terms, provided the original work is properly cited and the use is non-commercial. See: <http://creativecommons.org/licenses/by-nc/4.0/>

**Manuscript source:** Invited manuscript

**Specialty type:** Gastroenterology and hepatology

**Roman Maslennikov, Vladimir Ivashkin, Irina Efremova, Elena Shirokova,** Department of Internal Medicine, Gastroenterology and Hepatology, Sechenov University, Moscow 119435, Russia

**Roman Maslennikov,** The Interregional Public Organization “Scientific Community for the Promotion of the Clinical Study of the Human Microbiome”, Moscow 119435, Russia

**Roman Maslennikov,** Department of Internal Medicine 1, Consultative and Diagnostic Center 2 of the Moscow City Health Department, Moscow 107564, Russia

**Corresponding author:** Roman Maslennikov, MD, PhD, Assistant Professor, Professor, Department of Internal Medicine, Gastroenterology and Hepatology, Sechenov University, Pogodinskaya Street, 1, bld. 1, Moscow 119435, Russia. [mmmm00@yandex.ru](mailto:mmmm00@yandex.ru)

### Abstract

Infection with hepatotropic viruses is not limited to the liver and can lead to the development of various immunological disorders (the formation of cryoglobulins, rheumatoid factor, antinuclear antibodies, autoantibodies specific for autoimmune hepatitis and primary biliary cholangitis, and others), which can manifest as glomerulonephritis, arthritis, uveitis, vasculitis (cryoglobulinemic vasculitis, polyarteritis nodosa, Henoch-Schonlein purpura, isolated cutaneous necrotizing vasculitis), and other rheumatologic disorders, and be a trigger for the subsequent development of autoimmune hepatitis and primary biliary cholangitis. A further study of the association between autoimmune liver diseases and hepatotropic virus infection would be useful to assess the results of treatment of these associated diseases with antiviral drugs. The relationship of these immune disorders and their manifestations with hepatotropic viruses is best studied for chronic hepatitis B and C. Only isolated cases of these associations are described for hepatitis A. These links are least studied, and are often controversial for hepatitis E, possibly due to their relatively rare diagnoses. Patients with uveitis, glomerulonephritis, arthritis, vasculitis, autoimmune liver diseases should be tested for biomarkers of viral hepatitis, and if present, these patients should be treated with antiviral drugs.

**Key Words:** Hepatitis A; Hepatitis B; Hepatitis C; Hepatitis E; Vasculitis; Rheumatoid factor

©The Author(s) 2021. Published by Baishideng Publishing Group Inc. All rights reserved.

**Country/Territory of origin:** Russia**Peer-review report's scientific quality classification**

Grade A (Excellent): 0

Grade B (Very good): B, B

Grade C (Good): 0

Grade D (Fair): 0

Grade E (Poor): 0

**Received:** January 16, 2021**Peer-review started:** January 16, 2021**First decision:** February 28, 2021**Revised:** February 28, 2021**Accepted:** April 22, 2021**Article in press:** April 22, 2021**Published online:** May 14, 2021**P-Reviewer:** Fteiha B, Mohamed GA**S-Editor:** Zhang L**L-Editor:** A**P-Editor:** Liu JH

**Core Tip:** Infection with hepatotropic viruses is not limited to the liver and can lead to the development of various immunological disorders, which can manifest itself as glomerulonephritis, arthritis, uveitis, vasculitis, and other rheumatologic disorders, and be a trigger for the subsequent development of autoimmune hepatitis and primary biliary cholangitis. These associations are best studied for chronic hepatitis B and C. Only isolated cases of these are described for hepatitis A. These links are least studied, and are often controversial for hepatitis E. Patients with uveitis, glomerulonephritis, arthritis, vasculitis, autoimmune liver diseases should be tested for biomarkers of viral hepatitis.

**Citation:** Maslennikov R, Ivashkin V, Efremova I, Shirokova E. Immune disorders and rheumatologic manifestations of viral hepatitis. *World J Gastroenterol* 2021; 27(18): 2073-2089

**URL:** <https://www.wjgnet.com/1007-9327/full/v27/i18/2073.htm>

**DOI:** <https://dx.doi.org/10.3748/wjg.v27.i18.2073>

## INTRODUCTION

Viruses, unlike bacteria and fungi, cannot reproduce on their own and need the resources of a host cell as they are obligate intracellular parasites[1]. The viral proteins produced by the cell undergo partial proteolysis in the proteosomes, after which their fragments in conjunction with the molecules of the major histocompatibility complex type 1, are exposed on the cell surface to stimulate the immune system[2]. The partial proteolytic products of the cell's own proteins are exposed in a similar way. If these peptides have sufficient similarity to the partial proteolytic peptides of viral proteins, it is possible to develop an autoimmune cross-reaction in response to a viral infection[3]. Antiviral immunity is directed not only and not so much against the virus itself, but against the host cell infected with it, which serves as another predictor for the development of autoimmune aggression[4,5]. Among the autoantibodies produced in response to a viral infection, rheumatoid factor [(RF) an autoantibody against IgG], and cryoglobulins (antibodies that precipitate in the cold), are of utmost importance. The release of viral antigens into the bloodstream also plays a major role. Damage to the tissues, both directly by viruses and as a result of immune aggression against infected cells, also results in the release of a large number of tissue antigens. Tissue and viral antigens interact with antibodies to form immune complexes, which are fixed in the synovial membrane of the joints, glomerular membrane, and vascular wall, including the choroid. This leads to the development of arthritis, glomerulonephritis, vasculitis, and uveitis. Thus, viral infections can be triggers for autoimmune reactions and other immune disorders, which predispose to the development of rheumatologic and immunological complications of viral infections (Figure 1). However, the exact mechanisms of the development of autoimmune reactions in viral infections are yet to be established.

Many viruses can infect the liver, but only for five of them it is the main target organ: hepatitis A viruses (HAV), hepatitis B viruses (HBV), hepatitis C viruses (HCV), hepatitis D viruses (HDV) and hepatitis E viruses (HEV)[6]. HDV is a defective virus and can only replicate when co-infected with HBV[7].

Our review is devoted to describe the development of the aforementioned immunological disorders and caused by them rheumatologic and other extrahepatic manifestations in viral hepatitis. Knowing these complications is very important as infection with hepatotropic viruses can manifest only in the form of these disorders, leading to misdiagnosis and inadequate treatment.

## HEPATITIS A

Hepatitis A occurs only in an acute form[8]. Perhaps due to the short-term contact of the macroorganism with the virus, immune and rheumatologic disorders rarely develop.

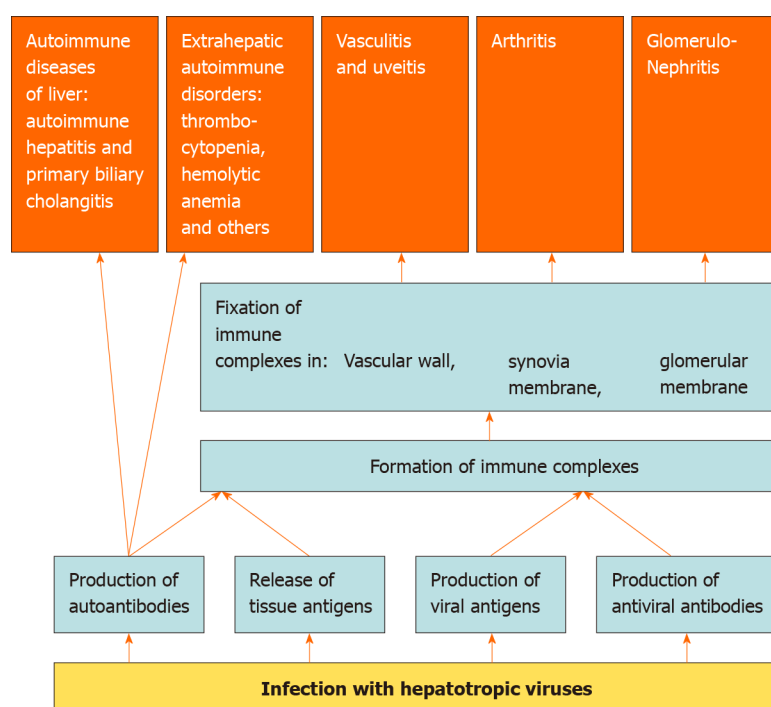


**Figure 1** Scheme of the development of immunological disorders and caused by them rheumatologic and other extrahepatic manifestations of viral hepatitis.

Joint pain without arthritis occurs on average in 10%-20% of patients with hepatitis A[9-11]. True arthritis in hepatitis A develops within vasculitis (see below).

RF was found in only two patients with hepatitis A who had cryoglobulinemic vasculitis[12].

Cryoglobulinemia is observed in 95% of patients with hepatitis A in one study. Cryoprecipitate was represented by IgM, including antibodies against HAV. IgA and/or IgG were also represented in the cryoprecipitate of 15% of patients. After recovery, the cryoglobulin content decreased to normal. Interestingly, the cryoglobulin level in hepatitis A was higher than in acute hepatitis B[13].

Mesangioproliferative glomerulonephritis with deposits of IgM and complement components was found in a 7-year-old boy with hepatitis A. This was accompanied by the development of severe nephrotic syndrome, neutrophilic leukocytosis, and a decrease in the blood complement (components C3 and C4) levels. The disease ended in complete recovery[14].

In another case, mesangioproliferative glomerulonephritis in a young woman led to deposits of all three types of immunoglobulins and complement component C1q, and was accompanied by the development of acute renal failure, but not nephrotic syndrome; blood complement levels were normal. Complete recovery was observed here also[15].

The development of IgA nephropathy in hepatitis A has also been reported[16,17].

Polymyositis with myoglobulinuria, increased creatine kinase activity and electromyographic changes was verified by muscle biopsy in a patient with hepatitis A[18].

A 23-year-old man with hepatitis A developed adult-onset Still's syndrome: Fever, maculopapular rash on the trunk and legs, generalized arthralgia, severe neutrophilic leukocytosis, and hyperferritinemia. The disease was successfully controlled by glucocorticoids[19].

A case of unilateral autoimmune parotitis with left-sided pain and swelling in the face, generalized arthralgia, and rash was reported. Biopsy revealed mononuclear infiltration of the affected parotid gland. The disease was resistant to antibiotics, but was quickly treated with prednisolone[20].

We found 13 published cases of hepatitis A-associated vasculitis (Tables 1 and 2) [12,21-30]. These were Henoch-Schonlein purpura (HSP) (53.8%), cryoglobulinemic vasculitis (CGV) (30.8%), and isolated cutaneous necrotizing vasculitis (15.4%). Most of them (76.9%) occurred in children. The pathological process involved the skin (92.3%), joints (69.2%), intestines (46.2%) and kidneys (7.7%). Arthralgia without synovitis was observed in 15.4% of cases and arthritis in 54.8% of cases (mainly in the knees and

**Table 1 Cases of vasculitis in hepatitis A**

Case	Dan <i>et al</i> [21]	Press <i>et al</i> [22]	Nassih <i>et al</i> [23]	Chemli <i>et al</i> [24]	Mohan <i>et al</i> [25]	Altinkaynak <i>et al</i> [26]
Age, yr	30	2	8	10	< 1	10
Sex	Female	Female	Female	Male	Female	Male
Diagnosis	CNV	CNV	CGV	HSP	HSP	HSP
Body temperature	N	N/A	N	N/A	Mild fever	N
Time of the onset after the onset of hepatitis	2 wk	N/A	8 wk	3 d after admission to hospital	During the first month of illness	2 wk
Second wave of hepatitis	-	N/A	-	-	-	-
Pruritus	+	N/A	+	+	-	-
Jaundice	+	N/A	+	N/A	+	+
Rash	EPR over the hips, but also involving the buttocks and arms, and rare petechiae	Ecchymotic lesions	PP on the legs, forearms, and the back	PP on the declivous regions	Bluish PP on both lower limbs, swelling over dorsum of hands and feet	PP on the legs and on the gluteal regions.
Joints	N	N/A	Arthritis in the knees	Arthralgia	Arthritis in the right knee	Arthralgia
GN	No	N/A	Dipstick test was positive to proteins (2+) and blood (3+)	No	No	No
Gut	N	N/A	N	Abdominal pain	Small amount of blood in stool	Abdominal pain
RF	N/A	N/A	Negative	N/A	Negative	Negative
ANA	N/A	N/A	Negative	N/A	Negative	Negative
WBC, 10 <sup>9</sup> /L	6.3	N/A	7.2	N/A	↑	9.9
CRP, mg/L	N/A	N/A	38	N/A	N/A	N
Platelets, 10 <sup>9</sup> /L	408	N/A	N/A	N/A	N	416
ESR, mm/h	80	N/A	80	N/A	N/A	N/A
Cryoglobulins	N/A	N/A	IgM, IgA, and IgG	N/A	N/A	N/A
Transaminases	↑	N/A	↑	↑	↑	↑
Complement	N	N/A	N/A	N/A	N/A	N
Skin biopsy	LCV with deposition of IgM and C3	Necrotizing vasculitis with fibrin thrombi	LCV	N/A	LCV	N/A
Treatment	N/A	GC	GC	N/A	Analgetics	N/A

ANA: Antinuclear antibodies; CNV: Cutaneous necrotizing vasculitis; CRP: C-reactive protein; CGV: Cryoglobulinemic vasculitis; EPR: Erythematous papular rash; ESR: Erythrocyte sedimentation rate; GN: Glomerulonephritis; GC: Glucocorticoids; HSP: Henoch-Schonlein purpura; LCV: Leukocytoclastic vasculitis; N: Normal; N/A: No available; PP: Palpable purpura; RF: Rheumatoid factor.

ankles). Vasculitis developed about 5wk after the onset of the disease, and was accompanied by a second wave of hepatitis in 30.8% of cases and a protracted course (more than one month) of hepatitis in 23.1% of cases. All patients experienced complete recovery.

Experimental infection of monkeys marmosets with HAV led to the development of proliferative glomerulonephritis with deposits of IgM, component C3 (less often other immunoglobulins), and vasculitis[31].

Isolated cases of uveitis associated with hepatitis A have also been described[32,33]. Moreover, uveitis appeared before the symptoms of hepatitis[32].

One patient with hepatitis A developed lupus-like syndrome: symmetrical arthralgia in the wrists, metacarpophalangeal and proximal interphalangeal joints, left-sided pleurisy, Lupus cells, and antinuclear antibodies (ANA), antibodies against

Table 2 Cases of vasculitis in hepatitis A

Case	Garty <i>et al</i> [27]	Sasan <i>et al</i> [28]	Islek <i>et al</i> [29]	Islek <i>et al</i> [29]	Bozaykut <i>et al</i> [30]	Inman <i>et al</i> [12]	Inman <i>et al</i> [12]
Age, yr	8	8	13	11	< 1	26	26
Sex	Male	Male	Male	Female	Female	Female	Female
Diagnosis	HSP	HSP	HSP	HSP	CGV	CGV	CGV
Body temperature	N/A	37.2	N	N	N	N	N
Time of the onset after the onset of hepatitis	5 wk	5 wk	13 wk	5 wk	N/A	20 wk	19 wk
Second wave of hepatitis	-	-	+	+	N/A	+	+
Pruritus	-	-	-	+	-	-	-
Jaundice	-	-	-	+	-	+	-
Rash	PP on on the buttocks, penis and legs, which began with darkening of the right half of the scrotum	Non blanching red-brown papules over both thighs and legs	PP on the legs	PP on the legs	Oedema and ecchymosis on the dorsum of the hands and from feet to the knees	PP on on the legs, buttocks, arms, which began with ankles	No rash
Joint	N	Arthritis in the knees and ankles	Arthritis in the right knee and ankle	Arthritis in unspecified joints	N	Arthritis in the knees and ankles	Arthritis in the ankles, right fourth and fifth right metatarsophalangeal joints
GN	No	No	No	No	No	No	No
Gut	N	Abdominal pain	Abdominal pain	Abdominal pain	N	N	N
RF	N/A	N/A	Negative	Negative	N/A	1:160	1:320
ANA	N/A	N/A	Negative	Negative	N/A	N/A	N/A
WBC, 10 <sup>9</sup> /L	N/A	10.1	4.6	7.2	12	N/A	N/A
CRP, mg/L	N/A	N/A	N	N/A	N/A	N/A	N/A
Platelets, 10 <sup>9</sup> /L	N/A	516	250	407	300	N/A	N/A
ESR, mm/h	N/A	34	22	42	N/A	N/A	N/A
Cryoglobulins	N/A	N/A	N/A	N/A	Positive	Anti-HAV IgG	Anti-HAV IgG
Transaminases	↑	N	↑	↑	N	↑	↑
Complement	N/A	N/A	N	C3↑, C4 - N	N	N/A	N/A
Skin biopsy	N/A	N/A	LCV with deposition of IgM in the dermo-epidermal junction	LCV	LCV	LCV	N/A
Treatment	N/A	GC	Symptomatically	N/A	No	No	NSAID

ANA: Antinuclear antibodies; CRP: C-reactive protein; CGV: Cryoglobulinemic vasculitis; ESR: Erythrocyte sedimentation rate; GN: Glomerulonephritis; GC: Glucocorticoids; HSP: Henoch-schonlein purpura; LCV: Leukocytoclastic vasculitis; N: Normal; N/A: No available; NSAID: Nonsteroidal anti-inflammatory drugs; PP: Palpable purpura; RF: Rheumatoid factor.

double-stranded deoxyribonucleic acid (DNA) and cardiolipin, which disappeared within a few months[34].

Autoimmune hepatitis (AIH) was triggered by hepatitis A in 11 published cases[35-44]. In some of these patients, this was accompanied by the appearance of ANA. A case of a 24-year-old woman with an autoimmune hepatitis/primary biliary cirrhosis overlap syndrome triggered by an acute hepatitis A infection was

reported[45]. No case of isolated primary biliary cholangitis (PBC) associated with HAV was found.

Thus, immunological disorders and rheumatologic manifestations in hepatitis A are rare, have a favorable prognosis, and run their course without treatment or after treatment with glucocorticoids or non-steroidal anti-inflammatory drugs.

## HEPATITIS B

Hepatitis B is characterized by lifelong infection, which predisposes to more frequent immunological disorders and caused by them rheumatologic and other extrahepatic manifestations.

Among patients with chronic hepatitis B, Raynaud's phenomenon occurs in 2%, arthralgia or arthritis in 3%, myalgia in 3%, Sjogren's syndrome in 3%, glomerulonephritis in 3%, uveitis in 2%, cryoglobulins in 2%[46].

RF is detected more often in asymptomatic carriers of HBV surface antigen (HBsAg) than in healthy individuals (11.8% *vs* 3.4%). RF positive rate was not significantly associated with the level of alanine aminotransferase or C-reactive protein in individuals with HBsAg[47]. HBV DNA levels significantly correlated with the titers of RF[48]. Antibodies against cyclic citrullated peptide (anti-CCP), a more specific marker of rheumatoid arthritis, were detected in individuals with HBsAg less often than was RF (4.6% *vs* 11.8%). Among patients with HBsAg, RF is found in 46% of patients with arthritis, 5% of patients with arthralgia, and in 8% of patients without rheumatologic complaints. Anti-CCP is found in 36%, 0% and less than 1% of these patients, respectively. Joint disorders and biochemical changes classified as rheumatoid arthritis were observed in 4.1% of patients with HBsAg. These patients accounted for 32.1% of HBV infected individuals with RF, 81.8% of those with anti-CCP and 90% of them have both RF and anti-CCP[49].

Patients with HBV infection accounted for 6.3% of patients with complaints of pain in joints and/or muscles. Moreover, only 26.3% of them had true arthritis[50].

HBV-associate non-rheumatoid arthritis can develop simultaneously in all affected joints, be migratory, or have an additive pattern. Synovitis develops abruptly and is severe. Arthritis develops within 12 wk after the onset of the disease, but in some cases, it is the first manifestation of hepatitis B. The age of patients with arthritis is 14-35 years in 82.8% of cases. Monoarthritis of a large joint is observed in about 40% of cases, polyarthritis of the small joints of the fingers in 10%, and a combined lesion of large and small joints in 50%. Among the large joints, the knee joints are most often affected, followed by the wrist, ankle, elbow, shoulder and hip joints. The metacarpophalangeal and proximal interphalangeal joints of the hands are affected as often as the knee joints, whereas the small joints of the feet are less frequently affected. Synovitis is usually symmetrical. The cervical and lumbar intervertebral joints are involved in about 10% of cases, usually together with other joints. ANA is determined in approximately 10% of such patients, and RF in approximately 25%, anti-CCP in approximately 5%. Complement is reduced in almost half of these patients. In all cases, arthritis resolved spontaneously or after treatment with non-steroidal anti-inflammatory drugs within 3-7 d. No development of chronic arthritis or recurrence of arthritis has been observed[49,51].

On average, 3% of glomerulonephritis is associated with the presence of HBsAg. It is membranous glomerulonephritis in 40% of cases, membranoproliferative glomerulonephritis in 20%, focal segmental glomerulosclerosis in 20%, IgA nephropathy in 10%; the remaining 10% account for the other forms. There are nephrotic syndrome in 60% of cases of HBV-associated glomerulonephritis, and nephritic syndrome or isolated changes in urine analysis in other cases[52].

Fibromyalgia is more often detected in patients with hepatitis B than in those without infection (32% *vs* 5%). Moreover, there was no difference in the incidence of this disease between patients with untreated active chronic hepatitis B, an inactive hepatitis B virus infection, and patients receiving treatment for this infection[53].

Autoantibodies are detected on average in 60% of patients with chronic hepatitis B. Most often, these are ANA (approximately 25%), anti-Ro52 (approximately 30%), anti-gp210 and anti-PML (approximately 10%), AMA-M2 (approximately 7%), anti-Sp100, anti-SMA, anti-LC-1 and anti-SLA/LP (all constituting approximately 3%), and anti-LKM-1 (< 1%). The frequency of detection of ANA was higher in the pre-cirrhotic stage than in cirrhosis (30% *vs* 20%). The frequency of detection of other autoantibodies did not differ significantly between these stages of the disease[54].



The high percentage of autoantibodies that are specific for PBC (anti-gp210, anti-PML, and AMA-M2) in HBV infection may indicate that HBV could be trigger for the development of this disease. Thus, in one study, signs of silent HBV infection (anti-HBc without HBsAg) were found in 40% of patients with PBC. Bilirubin level is higher and the degree of fibrosis is greater in these patients than in those with idiopathic PBC[55]. PBC will be diagnosed in 2%-3% of patients with hepatitis B over the next 15 years[56].

Specific biomarkers of AIH (anti-SMA, anti-LC-1, anti-SLA/LP, and anti-LKM-1) have been identified in 1%-3% of patients with hepatitis B[54]. Among patients with AIH, HBV DNA was detected in almost 25%, and serological biomarkers of HBV infection without signs of viral replication were found in another 30%[57].

About 35% of polyarteritis nodosa (PAN) cases are associated with hepatitis B. For this variant of the disease, neuropathies (approximately 85% *vs* 65%), arterial hypertension (49% *vs* 27%), abdominal pain (50% *vs* 28%), testicular involvement (24% *vs* 13%), cardiomyopathy (13% *vs* 4%) were more characteristic than for idiopathic PAN unlike livedo (10% *vs* 20%). The prognosis in patients with HBV-associated PAN was worse than in idiopathic PAN: 60% of patients from the first group and 74% from the second were alive after 10 years[58]. Hepatitis B was diagnosed before the development of PAN in approximately 30% of these patients. Vasculitis developed before the end of the clinical manifestations of hepatitis or in the next few days after this in half of these cases, and within the first 6 mo after this in the others. Transaminases are normal in 33%-50% of patients at the time of the onset of PAN[59,60].

Biomarkers of hepatitis B are detected in 2%-6% of cases with mixed cryoglobulinemia[61-63] and in almost 10% of cases with non-HCV CGV[64]. Manifestations of HBV-associated CGV are: Purpura (100%), arthralgias (71%), peripheral neuropathy (29%), glomerulonephritis (18%), Raynaud phenomenon (18%), and leg ulcer (6%)[65]. Cryoglobulins disappear in the serum leading to the regression of vasculitis in the majority of patients treated with entecavir, adefovir, and lamivudine. Corticosteroid therapy is effective for clinical symptoms of vasculitis, but ineffective for suppression of HBV and immunological features. Immunosuppressive agents are not recommended because of possible flare-up of viral replication. The use of interferons in these cases does not always lead to a positive effect[66].

There are only a few published cases of the association of HSP with hepatitis B[67-71].

Interestingly, according to a meta-analysis, biomarkers of hepatitis B are less common in systemic lupus erythematosus than in the general population: Odds ratio of HBsAg was 0.24 [95% confidence interval (CI): 0.17-0.33] and odds ratio of anti-HBc was 0.4 (95%CI: 0.31 - 0.50)[72].

## HEPATITIS C

HCV (like HBV) persists for a long time in the body; therefore, the frequency of immunological disorders and rheumatologic manifestations is also quite high[73].

Patients with HCV infection accounted for 5.3% of patients with complaints of pain in the joints and/or muscles. Moreover, 40% of them had true arthritis, 50% had arthralgia, and 10% had no joint disorders[50].

Pain in the joints and/or muscles are noted in 70% of patients with chronic hepatitis C if the medical history was collected carefully. Backache is the most common complaint (54%), followed by early morning stiffness (45%), arthralgia (42%), myalgia (38%), neck pain (33%), generalized pain (21%), and subjective joint swelling (20%). Diffuse pain was present in 23% of patients, non-diffuse regional plus axial pain in 18%, axial pain in 17%, and regional pain in 12%[74].

Among patients with HCV having no rheumatologic complaints, RF is detected more than in the general population (15% *vs* 5%), unlike anti-CCP with the same incidence (about 5%)[75]. Patients with HCV and joint involvement have RF in 60% of cases, cryoglobulins in almost 50%, and both in 40%. Anti-CCP was detected only in patients without RF and cryoglobulins[76].

Cryoglobulins are found in almost 65% of a general population of HCV patients, but they clinically manifest only in 5% of them. The achievement of a stable viral response leads to a decrease in the detection rate of cryoglobulins from 57% to 33%, whereas the detection rate remains unchanged among those in whom it was not achieved. In approximately 20% of patients with cryoglobulinemia, it persists for 8 years after achieving a stable viral response. Moreover, 80% of these patients with persisted cryoglobulinemia have its clinical manifestations during this time[77]. The high



incidence of cryoglobulinemia in chronic hepatitis C can be explained by the fact that HCV can replicate in lymphocytes, protecting them from apoptosis and resulting in polyclonal proliferation, including clones that produce cryoglobulins[78].

Anti-HCV antibodies are detected in 92%-95% of patients with mixed cryoglobulinemia, and HCV RNA in 90%[61,63].

Arthritis in HCV infection develops in 5%-10% of cases[79]: Symmetric polyarthritis in 2/3 of cases, and oligo- or monoarthritis in the rest 1/3 of cases. Morning stiffness for more than 1 h occurs in 70% of HCV infected patients with arthritis, whereas erosion in the joints and subcutaneous nodules are not observed. Cryoglobulins, RF and ANA are detected in 43%, 60% and 20% of these cases, respectively. The level of complement C3 is reduced in 15% of these patients, and C4 in 30% of these patients. In addition, 86% of them had elevated transaminases. The use of anti-inflammatory or disease-modifying drugs is not effective[80], but the use of direct-acting antivirals (DAA) drugs is the most promising[81]. This arthritis is very similar to rheumatoid arthritis, and anti-CCP (unlike RF) should be used to differentiate between these diseases[82,83].

Autoantibodies are detected in 66% of patients with chronic hepatitis C. These are ANA (20%-32%), anti-LKM-1 (1%-22%), anti-Ro52 (about 15%), anti-SMA (3%-8%), AMA-M2 (approximately 3%), and anti-LC-1 (approximately 1%)[54,84].

Furthermore, 8%-12% of patients with PBC had biomarkers of HCV-infection (anti-HCV antibodies or RNA HCV)[85-87]. Despite the frequent detection of AIH-specific antibodies, it is very rarely diagnosed in HCV-infection[88]. HCV biomarkers are also rarely detected in AIH[89]. However, AIH was successfully treated with DAA in a patient with concomitant HCV infection[90].

Antibodies against HCV are detected in 40% of patients with glomerulonephritis[91]. Occult HCV infection (presence of HCV RNA by an ultrasensitive method in the absence of antibodies against HCV) is detected in 40% of the rest part of these patients: in 40% with membranous glomerulonephritis, 30% with membranoproliferative glomerulonephritis, 50% with IgA nephropathy, 30% with idiopathic nephrotic syndrome (including minimal change disease, focal segmental glomerulosclerosis, and IgM nephropathy), 50% with lupus nephropathy, and 40% with anti-neutrophil cytoplasmic antibody (ANCA) positive glomerulonephritis and 4% in the control group (hereditary glomerular nephropathy)[92]. The most common form of HCV-nephropathy is membranoproliferative glomerulonephritis, followed by focal segmental glomerulosclerosis, mesangioproliferative, and membranous glomerulonephritis[91]. Anti-HCV is detected in 98% of cases of glomerulonephritis with mixed cryoglobulinemia and in 2% glomerulonephritis without cryoglobulinemia[93]. Autopsies of patients with hepatitis C revealed glomerulopathies: Mesangioproliferative glomerulonephritis (18%), membranoproliferative glomerulonephritis (11%), membranous glomerulonephritis (3%), and mesangial expansion without hypercellularity (23%). No glomerular pathology was observed in 45% of autopsies in hepatitis C[94].

The HCV antigen is detected in the glomeruli in almost 30% glomerulonephritis with antibodies against HCV in the blood and in almost 60% in glomerulonephritis with HCV RNA in the blood[95].

Extrarenal manifestations of HCV-glomerulopathy were absent in 80% of patients even though 54% had cryoglobulinemia. Electron microscopy revealed virus-like particles in 50% of renal biopsies[91].

There are publications showing the effectiveness of DAA in the treatment of HCV-nephropathy[96-98].

Among rheumatologic diseases in patients with HCV infection, Sjogren's syndrome is most often detected (almost 50% of cases) followed by rheumatoid arthritis (15%), systemic lupus erythematosus (11%), PAN (8%), antiphospholipid syndrome (6%), inflammatory myopathies (4%), systemic sclerosis (1%). The rest of rheumatic diseases, including HSP, accounted for less than 1%[99]. A meta-analysis showed that in patients with HCV infection, cryoglobulinemia [30% *vs* 2%, odd ratio (OR) is 11.5], CGV (5%), Sjogren's syndrome (12% *vs* 0.7%, odd ratio is 2.3) and arthritis (1% *vs* 0.1%, OR is 2.4) are significantly more often detected than in the general population[100]. Raynaud phenomenon was found in 8% of patients with HCV[101].

Vasculitis associated with HCV-infection are CGV in approximately 80% of cases and PAN in approximately 20% of cases[102]. Other vasculitis, including HSP, are rare[99].

Among patients with PAN, antibodies against HCV were detected in 20%, and HCV RNA in 5%[103]. PAN was diagnosed on average 2 years after the diagnosis of HCV infection. These patients had purpura (68%), livedo reticularis (20%-60%), arthralgia (61%), weight loss (60%), multiplex mononeuritis (70%), myalgias or weakness (58%),

altered arteriography (49%), hypertension (37%-55%), abdominal pain (30%), raised creatinine (26%), fever (20%), polyneuropathy (16%), proteinuria (16%), hematuria (16%), intestinal bleeding (16%), diarrhea (13%), orchitis (0%-7%)[99,102].

CGV was also diagnosed on average 2 years after the diagnosis of HCV infection. The most common manifestations of HCV-associated CGV are purpura (67%), polyneuropathy (65%), arthralgia (50%), proteinuria (30%), hematuria (22%), and arterial hypertension (22%). Myalgia (9%), multiplex mononeuritis (9%), livedo reticularis (3%), weight loss (4%), and abdominal pain (1.5%) are less common. Fever, intestinal bleeding, diarrhea, and orchitis are usually absent[102].

The differential diagnoses of vasculitis in HCV infection are presented in Table 3.

Rituximab allows to achieve remission in HCV-associated CGV in 87% of cases[104]. The effectiveness of DAA in the treatment of CGV in HCV-infection is under study. Experts currently recommend DAAs as first line treatment for mild to moderate CGV and rituximab with or without apheresis for severe cases[105].

Patients with HCV-associated Sjogren's syndrome present with xerophthalmia (97%), xerostomia (97%), positive Schirmer test (98%), altered salivary flow (81%), ANA (68%), RF (53%), and anti-Ro/La (25%)[99].

Very few cases of uveitis in HCV-infection were noted[106].

## HEPATITIS E

Hepatitis E, as a rule, is an acute infection but it can become chronic in persons with immunodeficiency[107].

Joint or/and muscle pain without arthritis and myositis is present in approximately 60% of patients with acute hepatitis E[108]. Arthralgias were observed in 5% of patients with chronic hepatitis E[109].

Two cases of arthritis development in acute hepatitis E have been described (Table 4)[110,111].

ANA were found in 9% of patients with acute hepatitis E and in 24% of patients with chronic hepatitis E. Cryoglobulins were found in 7% and 27%, respectively. Cryoglobulinemia persisted for a median of 4 mo (range 3-15 mo). Patients with cryoglobulins had higher levels of creatinine, IgM, and HEV RNA in the blood. There were no clinical manifestations of cryoglobulinemia in all patients in this study except for a patient with neuralgic amyotrophy[112]. In another study, ANA was detected in 37% of patients with acute hepatitis E, and anti-SMA test was positive in 23% of them. These antibodies remained in the blood for more than 1 year in 37% of these cases. Moreover, no patients developed AIH during this follow-up period[113]. Similar results were published in the third study[114]. Seroprevalence of HEV in patients with AIH did not differ from that of the general population[115,116]. Another study showed that antibodies against HEV were detected slightly more often in AIH than the average for the population, but the detection rate was significantly lower than in the previous study[117]. In general, the relationship between HEV and AIH remains unclear.

Antibodies against HEV were not found in any of the 25 patients with PBC; thus, the relationship between these diseases is extremely unlikely[118].

ANCA was positive in 15% of patients with acute hepatitis E[114].

Most cases of glomerulonephritis and manifested cryoglobulinemia in hepatitis E have been described after transplantation[119,120]. Therefore, the exact cause of their development is unclear: HEV infection, the consequences of transplantation, or their combination. In any case, testing for HEV biomarkers should be performed in these patients. A cure for cryoglobulinemic membranoproliferative glomerulonephritis has been described in such a patient after treatment with ribavirin[121].

Thus far, only one case of HEV-associated cryoglobulinemic membranoproliferative glomerulonephritis in a non-transplanted person has been published. The condition appeared a month after the onset of acute hepatitis E. The activity of the inflammatory process in the liver remained elevated. This patient had RF in the blood and was successfully treated with plasmapheresis and pulse glucocorticoids[122].

The only case of HSP triggered by acute hepatitis E virus infection has been described[123].

There are no published studies on the frequency of detection of HEV biomarkers in patients with uveitis or PAN.

**Table 3 Differential diagnosis of vasculitis in hepatitis C viruses-infection (modification from[102])**

	Cryoglobulinemic vasculitis	Polyarteritis nodosa
Weight loss	+/-	+++
Fever	-	++
Myalgia	+	++
Polyneuropathy	+++	++
Mononeuritis multiplex	+	+++
Livedo	+/-	++
Arterial hypertension	++	+++
Orchitis	-	+
Abdominal pain	+/-	++
Diarrhea	-	+
Intestinal bleeding	-	+
Microaneurysms or stenosis	-	+++
C-reactive protein level	Normal	↑

**Table 4 Cases of arthritis in hepatitis E**

Case	Al-Shukri <i>et al</i> [110]	Serratrice <i>et al</i> [111]
Age	52	51
Sex	Female	Female
Joints	Shoulders, elbows, hips, knees, ankles, left second and third metacarpophalangeal	Ankles and knees followed by the wrists and fingers
Duration of arthritis	No data	3 mo
Rash	Maculopapular, non-itchy rash all over her body	No
Fever	No	No
Jaundice	No	No
Pruritus	No	No
Other symptoms and signs	Retroorbital pain, eye discharge, headache, and loss of appetite	No
Rheumatoid factor	No	No
Antinuclear antibodies	No	No
White blood cells, 10 <sup>9</sup> /L	Normal	2.8
Erythrocyte sedimentation rate, mm/h	35	24
C-reactive protein, mg/L	25	3
Transaminases	↑	↑
Complement	C3 - ↑; C4 -Normal	No data
Treatment	No data	No specific treatment

## CONCLUSION

There is a wide array of extrahepatic manifestations potentially associated with hepatitis viruses. These viruses can lead to the development of various immunological disorders (the formation of autoantibodies and cryoglobulins), which can manifest as glomerulonephritis, arthritis, uveitis, vasculitis, and other rheumatologic disorders. In addition, it is quite possible that this infection could be a trigger for the subsequent development of AIH and PBC.

**Table 5 A summary of the main immunological and rheumatologic manifestation in viral hepatitis**

	Hepatitis A	Hepatitis B	Hepatitis C	Hepatitis E
Rheumatoid factor	Only 2 cases	Approximately 12% of patients	15% of patients	1 case in a patient without transplant
Antinuclear antibodies	In a case of lupus-like reaction and some cases of AIH triggered by HAV infection	Approximately 25% of patients	20%-30% of patients	9%-37% (acute) and 24% (chronic) of patients
Cryoglobulins	95% of patients in 1 study	2% of patients	65% of patients	7% (acute) and 27% (chronic) of patients
Arthralgia	10%-20% of patients	3% of patients	42% of patients	Approximately 60% of patients
Arthritis	Only in patients with vasculitis (7 cases)	About a quarter of patients with pain in joints	5%-10% of patients	2 cases
GN	4 cases of mesangio-proliferative GN	3% of GN: membranous GN (40%); membrano-proliferative GN (20%); focal segmental glomerulo-sclerosis (20%); mesangio-proliferative GN (10%), others (10%)	Approximately 50% of GN: membranous GN (5%); membrano-proliferative GN (55%); focal segmental glomerulo-sclerosis (25%); mesangio-proliferative GN (20%), others (5%)	1 case of membrano-proliferative GN; some cases of GN after transplantation
Henoch-Schonlein purpura	7 cases	Some cases	Some cases	1 case
CGV	4 cases	10% of non-HCV CGV cases	90%-95% of CGV cases	Some cases
PAN	No cases	35% of PAN cases	20% of PAN cases	No cases
Uveitis	Some cases	2% of patients	Some cases	No cases
AIH	11 cases	55% of AIH cases	Very rare	No cases
PBC	1 case of overlap syndrome	40% of PBC cases	Approximately 10% of PBC cases	No cases

AIH: Autoimmune hepatitis; CGV: Cryoglobulinemic vasculitis; GN: Glomerulonephritis; HCV: Hepatitis C viruses; PAN: Polyarteritis nodosa; PBC: Primary biliary cholangitis.

The relationship between autoimmune liver diseases and hepatotropic virus infection is very interesting, especially when treated with antiviral drugs. A further study of this field would be useful to test for biomarkers of hepatotropic viruses in these diseases and to analyze the results of their treatment with antiviral drugs.

In addition to the manifestations described above, immunological disorders due to infection with hepatotropic viruses can lead to the development of many other autoimmune diseases (autoimmune thyroiditis, thrombocytopenia, hemolytic anemia, diabetes mellitus, pulmonary fibrosis, and others), the consideration of which is beyond the scope of this review.

These associations are best shown for chronic viral hepatitis B and C. Only isolated cases of these are described for hepatitis A. These links are least studied, and often controversial for hepatitis E, possibly due to its relatively rare diagnoses.

We have summarized the data presented in the review in [Table 5](#).

To date, few studies have been published on the effectiveness of modern DAA in the treatment of patients with rheumatologic and autoimmune manifestations of hepatotropic virus infection, which represents a large field for future research.

Nevertheless, patients with uveitis, glomerulonephritis, arthritis, vasculitis, autoimmune liver diseases should be tested for biomarkers of viral hepatitis, and if these infections are present, they should be treated.

## REFERENCES

- 1 **Yin J**, Redovich J. Kinetic Modeling of Virus Growth in Cells. *Microbiol Mol Biol Rev* 2018; **82**: e00066-17 [PMID: 29592895 DOI: 10.1128/MMBR.00066-17]
- 2 **Hewitt EW**. The MHC class I antigen presentation pathway: strategies for viral immune evasion. *Immunology* 2003; **110**: 163-169 [PMID: 14511229 DOI: 10.1046/j.1365-2567.2003.01738.x]
- 3 **Getts DR**, Chastain EM, Terry RL, Miller SD. Virus infection, antiviral immunity, and

- autoimmunity. *Immunol Rev* 2013; **255**: 197-209 [PMID: [23947356](#) DOI: [10.1111/imr.12091](#)]
- 4 **Panoutsakopoulou V**, Cantor H. On the relationship between viral infection and autoimmunity. *J Autoimmun* 2001; **16**: 341-345 [PMID: [11334502](#) DOI: [10.1006/jaut.2000.0480](#)]
- 5 **Jara LJ**, Medina G, Saavedra MA. Autoimmune manifestations of infections. *Curr Opin Rheumatol* 2018; **30**: 373-379 [PMID: [29528865](#) DOI: [10.1097/BOR.0000000000000505](#)]
- 6 **Gallegos-Orozco JF**, Rakela-Brödnér J. Hepatitis viruses: not always what it seems to be. *Rev Med Chil* 2010; **138**: 1302-1311 [PMID: [21279280](#)]
- 7 **Abbas Z**, Afzal R. Life cycle and pathogenesis of hepatitis D virus: A review. *World J Hepatol* 2013; **5**: 666-675 [PMID: [24409335](#) DOI: [10.4254/wjh.v5.i12.666](#)]
- 8 **Jeong SH**, Lee HS. Hepatitis A: clinical manifestations and management. *Intervirology* 2010; **53**: 15-19 [PMID: [20068336](#) DOI: [10.1159/000252779](#)]
- 9 **Routenberg JA**, Dienstag JL, Harrison WO, Kilpatrick ME, Hooper RR, Chisari FV, Purcell RH, Fornes MF. Foodborne outbreak of hepatitis A: clinical and laboratory features of acute and protracted illness. *Am J Med Sci* 1979; **278**: 123-137 [PMID: [517565](#) DOI: [10.1097/00000441-197909000-00003](#)]
- 10 **Tong MJ**, el-Farra NS, Grew MI. Clinical manifestations of hepatitis A: recent experience in a community teaching hospital. *J Infect Dis* 1995; **171** Suppl 1: S15-S18 [PMID: [7876641](#) DOI: [10.1093/infdis/171.supplement\\_1.s15](#)]
- 11 **Koff RS**. Clinical manifestations and diagnosis of hepatitis A virus infection. *Vaccine* 1992; **10** Suppl 1: S15-S17 [PMID: [1335649](#) DOI: [10.1016/0264-410x\(92\)90533-p](#)]
- 12 **Inman RD**, Hodge M, Johnston ME, Wright J, Heathcote J. Arthritis, vasculitis, and cryoglobulinemia associated with relapsing hepatitis A virus infection. *Ann Intern Med* 1986; **105**: 700-703 [PMID: [3021038](#) DOI: [10.7326/0003-4819-105-5-700](#)]
- 13 **Shalit M**, Wollner S, Levo Y. Cryoglobulinemia in acute type-A hepatitis. *Clin Exp Immunol* 1982; **47**: 613-616 [PMID: [7083634](#)]
- 14 **Mathur RC**, Mathur NC. Mesangial proliferative glomerulonephritis and nephrotic syndrome with hepatitis A virus infection. *Indian Pediatr* 1996; **33**: 1051-1053 [PMID: [9141810](#)]
- 15 **McCann UG 2nd**, Rabito F, Shah M, Nolan CR 3rd, Lee M. Acute renal failure complicating nonfulminant hepatitis A. *West J Med* 1996; **165**: 308-310 [PMID: [8993209](#)]
- 16 **al-Homrany M**. Immunoglobulin A nephropathy associated with hepatitis A virus infection. *J Nephrol* 2001; **14**: 115-119 [PMID: [11411012](#)]
- 17 **Cheema SR**, Arif F, Charney D, Meisels IS. IgA-dominant glomerulonephritis associated with hepatitis A. *Clin Nephrol* 2004; **62**: 138-143 [PMID: [15356971](#) DOI: [10.5414/cnp62138](#)]
- 18 **Aggarwal SP**, Khurana SB, Sabharwal BD. Hepatitis A associated with myoglobinuria. *Indian J Gastroenterol* 1996; **15**: 107 [PMID: [8840643](#)]
- 19 **Seo SR**, Kim SS, Lee SJ, Kim TJ, Park YW, Lee SS. Adult-onset Still disease in a patient with acute hepatitis A. *J Clin Rheumatol* 2011; **17**: 444-445 [PMID: [22089987](#) DOI: [10.1097/RHU.0b013e31823ac4ac](#)]
- 20 **Bhatt G**, Sandhu VS, Mitchell CK. A rare presentation of hepatitis a infection with extrahepatic manifestations. *Case Rep Gastrointest Med* 2014; **2014**: 286914 [PMID: [25295197](#) DOI: [10.1155/2014/286914](#)]
- 21 **Dan M**, Yaniv R. Cholestatic hepatitis, cutaneous vasculitis, and vascular deposits of immunoglobulin M and complement associated with hepatitis A virus infection. *Am J Med* 1990; **89**: 103-104 [PMID: [2368780](#) DOI: [10.1016/0002-9343\(90\)90107-o](#)]
- 22 **Press J**, Maslovitz S, Avinoach I. Cutaneous necrotizing vasculitis associated with hepatitis A virus infection. *J Rheumatol* 1997; **24**: 965-967 [PMID: [9150090](#)]
- 23 **Nassih H**, Bourrahout A, Sab IA. Hepatitis A Virus Infection Associated with Cryoglobulinemic Vasculitis. *Indian Pediatr* 2020; **57**: 71-72 [PMID: [31937705](#) DOI: [10.1007/s13312-020-1709-x](#)]
- 24 **Chemli J**, Zouari N, Belkadi A, Abroug S, Harbi A. [Hepatitis A infection and Henoch-Schonlein purpura: a rare association]. *Arch Pediatr* 2004; **11**: 1202-1204 [PMID: [15475276](#) DOI: [10.1016/j.arcped.2004.06.014](#)]
- 25 **Mohan N**, Karkra S. Henoch schonlein purpura as an extra hepatic manifestation of hepatitis A. *Indian Pediatr* 2010; **47**: 448 [PMID: [20519793](#)]
- 26 **Altinkaynak S**, Ertekin V, Selimoglu MA. Association of Henoch-Schonlein purpura and hepatitis A. *J Emerg Med* 2006; **30**: 219-220 [PMID: [16567262](#) DOI: [10.1016/j.jemermed.2005.12.011](#)]
- 27 **Garty BZ**, Danon YL, Nitzan M. Schoenlein-Henoch purpura associated with hepatitis A infection. *Am J Dis Child* 1985; **139**: 547 [PMID: [4003354](#) DOI: [10.1001/archpedi.1985.02140080017017](#)]
- 28 **Sasan MS**, Doghaee MA. Association of henoch-schoenlein purpura with hepatitis a. *Iran J Pediatr* 2012; **22**: 571-572 [PMID: [23429757](#)]
- 29 **Islek I**, Kalayci AG, Gok F, Muslu A. Henoch-Schönlein purpura associated with hepatitis A infection. *Pediatr Int* 2003; **45**: 114-116 [PMID: [12654084](#) DOI: [10.1046/j.1442-200x.2003.01657.x](#)]
- 30 **Bozaykut A**, Atay E, Atay Z, Ipek IO, Akin M, Dursun E. Acute infantile haemorrhagic oedema associated with hepatitis A. *Ann Trop Paediatr* 2002; **22**: 59-61 [PMID: [11926052](#) DOI: [10.1179/027249302125000175](#)]
- 31 **Morita M**, Kitajima K, Yoshizawa H, Itoh Y, Iwakiri S, Shibata C, Mayumi M. Glomerulonephritis associated with arteritis in marmosets infected with hepatitis A virus. *Br J Exp Pathol* 1981; **62**: 103-113 [PMID: [6452891](#)]
- 32 **Azimi A**, Shirvani M, Hosseini S, Bazojoo V, Masihpoor N, Mohaghegh S, Sadeghi SM. Acute



- bilateral granulomatous anterior uveitis as an extra-hepatic manifestation of hepatitis A virus (HAV) infection: a case report. *J Ophthalmic Inflamm Infect* 2020; **10**: 18 [PMID: [32851489](#) DOI: [10.1186/s12348-020-00210-6](#)]
- 33 **Tien PT**, Lin CJ, Tsai YY, Chen HS, Hwang DK, Muo CH, Lin JM, Chen WL. Relationship Between Uveitis, Different Types Of Viral Hepatitis, And Liver Cirrhosis: A 12-Year Nationwide Population-Based Cohort Study. *Retina* 2016; **36**: 2391-2398 [PMID: [27870801](#) DOI: [10.1097/IAE.0000000000001103](#)]
  - 34 **Segev A**, Hadari R, Zehavi T, Schneider M, Hershkovich R, Mekori YA. Lupus-like syndrome with submassive hepatic necrosis associated with hepatitis A. *J Gastroenterol Hepatol* 2001; **16**: 112-114 [PMID: [11206308](#) DOI: [10.1046/j.1440-1746.2001.02314.x](#)]
  - 35 **S-Are V**, Yoder L, Samala N, Nephew L, Lammert C, Vuppalanchi R. An Outbreak Presents An Opportunity to Learn About A Rare Phenotype: Autoimmune Hepatitis After Acute Hepatitis A. *Ann Hepatol* 2020; **19**: 694-696 [PMID: [32927125](#) DOI: [10.1016/j.aohp.2020.08.069](#)]
  - 36 **Subramanian SK**, Patel JM, Younes M, Nevah Rubin MI. Postinfectious Autoimmune Hepatitis-Induced Liver Failure: A Consequence of Hepatitis A Virus Infection. *ACG Case Rep J* 2020; **7**: e00441 [PMID: [32821769](#) DOI: [10.14309/crj.0000000000000441](#)]
  - 37 **Grave A**, Juel J, Vyberg M, Olesen SS, Hansen JB. [Autoimmune hepatitis preceded by hepatitis A]. *Ugeskr Laeger* 2015; **177**: V12140669 [PMID: [25822815](#)]
  - 38 **Tanaka H**, Tujioaka H, Ueda H, Hamagami H, Kida Y, Ichinose M. Autoimmune hepatitis triggered by acute hepatitis A. *World J Gastroenterol* 2005; **11**: 6069-6071 [PMID: [16273628](#) DOI: [10.3748/wjg.v11.i38.6069](#)]
  - 39 **Kim YD**, Kim KA, Rou WS, Lee JS, Song TJ, Bae WK, Kim NH. [A case of autoimmune hepatitis following acute hepatitis A]. *Korean J Gastroenterol* 2011; **57**: 315-318 [PMID: [21623141](#) DOI: [10.4166/kjg.2011.57.5.315](#)]
  - 40 **Mikata R**, Yokosuka O, Imazeki F, Fukai K, Kanda T, Saisho H. Prolonged acute hepatitis A mimicking autoimmune hepatitis. *World J Gastroenterol* 2005; **11**: 3791-3793 [PMID: [15968741](#) DOI: [10.3748/wjg.v11.i24.3791](#)]
  - 41 **Huppertz HI**, Treichel U, Gassel AM, Jeschke R, Meyer zum Büschenfelde KH. Autoimmune hepatitis following hepatitis A virus infection. *J Hepatol* 1995; **23**: 204-208 [PMID: [7499793](#) DOI: [10.1016/0168-8278\(95\)80336-x](#)]
  - 42 **Singh G**, Palaniappan S, Rotimi O, Hamlin PJ. Autoimmune hepatitis triggered by hepatitis A. *Gut* 2007; **56**: 304 [PMID: [17303607](#) DOI: [10.1136/gut.2006.111864](#)]
  - 43 **Bouyahia O**, Naija O, Matoussi N, Khemiri M, Ben Mansour F, Khaldi F. [Autoimmune hepatitis following acute hepatitis A: a care report]. *Tunis Med* 2008; **86**: 87-88 [PMID: [19472711](#)]
  - 44 **Skoog SM**, Rivard RE, Batts KP, Smith CI. Autoimmune hepatitis preceded by acute hepatitis A infection. *Am J Gastroenterol* 2002; **97**: 1568-1569 [PMID: [12094893](#) DOI: [10.1111/j.1572-0241.2002.05751.x](#)]
  - 45 **Heurgué A**, Bernard-Chabert B, Picot R, Cadiot G, Thiéfin G. Overlap syndrome triggered by acute viral hepatitis A. *Eur J Gastroenterol Hepatol* 2009; **21**: 708-709 [PMID: [19282766](#) DOI: [10.1097/MEG.0b013e3282ffda23](#)]
  - 46 **Cacoub P**, Saadoun D, Bourlière M, Khiri H, Martineau A, Benhamou Y, Varastet M, Pol S, Thibault V, Rotily M, Halfon P. Hepatitis B virus genotypes and extrahepatic manifestations. *J Hepatol* 2005; **43**: 764-770 [PMID: [16087273](#) DOI: [10.1016/j.jhep.2005.05.029](#)]
  - 47 **Shim CN**, Hwang JW, Lee J, Koh EM, Cha HS, Ahn JK. Prevalence of rheumatoid factor and parameters associated with rheumatoid factor positivity in Korean health screening subjects and subjects with hepatitis B surface antigen. *Mod Rheumatol* 2012; **22**: 885-891 [PMID: [22327743](#) DOI: [10.1007/s10165-012-0603-3](#)]
  - 48 **Choi ST**, Lee HW, Song JS, Lee SK, Park YB. Analysis of rheumatoid factor according to various hepatitis B virus infectious statuses. *Clin Exp Rheumatol* 2014; **32**: 168-173 [PMID: [24143967](#)]
  - 49 **Lim MK**, Sheen DH, Lee YJ, Mun YR, Park M, Shim SC. Anti-cyclic citrullinated peptide antibodies distinguish hepatitis B virus (HBV)-associated arthropathy from concomitant rheumatoid arthritis in patients with chronic HBV infection. *J Rheumatol* 2009; **36**: 712-716 [PMID: [19286846](#) DOI: [10.3899/jrheum.080653](#)]
  - 50 **Oliveira ÍMX**, Silva RDSUD. Rheumatological Manifestations Associated with Viral Hepatitis B or C. *Rev Soc Bras Med Trop* 2019; **52**: e20180407 [PMID: [31800917](#) DOI: [10.1590/0037-8682-0407-2018](#)]
  - 51 **Duffy J**, Lidsky MD, Sharp JT, Davis JS, Person DA, Hollinger FB, Min KW. Polyarthritides, polyarteritis and hepatitis B. *Medicine (Baltimore)* 1976; **55**: 19-37 [PMID: [1629](#) DOI: [10.1097/00005792-197601000-00002](#)]
  - 52 **Raveendran N**, Beniwal P, D'Souza AV, Tanwar RS, Kimmatkar P, Agarwal D, Malhotra V. Profile of glomerular diseases associated with hepatitis B and C: A single-center experience from India. *Saudi J Kidney Dis Transpl* 2017; **28**: 355-361 [PMID: [28352020](#) DOI: [10.4103/1319-2442.202761](#)]
  - 53 **Yazmalar L**, Deveci Ö, Batmaz İ, İpek D, Çelepkolu T, Alpaycı M, Hattapoğlu E, Akdeniz D, Saryıldız MA. Fibromyalgia incidence among patients with hepatitis B infection. *Int J Rheum Dis* 2016; **19**: 637-643 [PMID: [26133007](#) DOI: [10.1111/1756-185X.12593](#)]
  - 54 **Li BA**, Liu J, Hou J, Tang J, Zhang J, Xu J, Song YJ, Liu AX, Zhao J, Guo JX, Chen L, Wang H, Yang LH, Lu J, Mao YL. Autoantibodies in Chinese patients with chronic hepatitis B: prevalence and clinical associations. *World J Gastroenterol* 2015; **21**: 283-291 [PMID: [25574103](#) DOI: [10.3748/wjg.v21.i1.283](#)]

- 55 **Zhang Y**, Shi Y, Wu R, Wang X, Gao X, Niu J. Primary biliary cholangitis is more severe in previous hepatitis B virus infection patients. *Eur J Gastroenterol Hepatol* 2018; **30**: 682-686 [PMID: 29462025 DOI: 10.1097/MEG.0000000000001100]
- 56 **Rigopoulou EI**, Zachou K, Gatselis NK, Papadamou G, Koukoulis GK, Dalekos GN. Primary biliary cirrhosis in HBV and HCV patients: Clinical characteristics and outcome. *World J Hepatol* 2013; **5**: 577-583 [PMID: 24179617 DOI: 10.4254/wjh.v5.i10.577]
- 57 **Chen XX**, Xiang KH, Zhang HP, Kong XS, Huang CY, Liu YM, Lou JL, Gao ZH, Yan HP. Occult HBV infection in patients with autoimmune hepatitis: A virological and clinical study. *J Microbiol Immunol Infect* 2020; **53**: 946-954 [PMID: 31153830 DOI: 10.1016/j.jmii.2019.04.009]
- 58 **Pagnoux C**, Seror R, Henegar C, Mahr A, Cohen P, Le Guern V, Bienvenu B, Mouthon L, Guillevin L; French Vasculitis Study Group. Clinical features and outcomes in 348 patients with polyarteritis nodosa: a systematic retrospective study of patients diagnosed between 1963 and 2005 and entered into the French Vasculitis Study Group Database. *Arthritis Rheum* 2010; **62**: 616-626 [PMID: 20112401 DOI: 10.1002/art.27240]
- 59 **Guillevin L**, Mahr A, Callard P, Godmer P, Pagnoux C, Leray E, Cohen P; French Vasculitis Study Group. Hepatitis B virus-associated polyarteritis nodosa: clinical characteristics, outcome, and impact of treatment in 115 patients. *Medicine (Baltimore)* 2005; **84**: 313-322 [PMID: 16148731 DOI: 10.1097/01.md.0000180792.80212.5e]
- 60 **Guillevin L**, Lhote F, Jarrousse B, Bironne P, Barrier J, Deny P, Trepo C, Kahn MF, Godeau P. Polyarteritis nodosa related to hepatitis B virus. A retrospective study of 66 patients. *Ann Med Interne (Paris)* 1992; **143** Suppl 1: 63-74 [PMID: 1363769]
- 61 **Ferri C**, Sebastiani M, Giuggioli D, Cazzato M, Longombardo G, Antonelli A, Puccini R, Michelassi C, Zignego AL. Mixed cryoglobulinemia: demographic, clinical, and serologic features and survival in 231 patients. *Semin Arthritis Rheum* 2004; **33**: 355-374 [PMID: 15190522 DOI: 10.1016/j.semarthrit.2003.10.001]
- 62 **Monti G**, Galli M, Invernizzi F, Pioltelli P, Saccardo F, Monteverde A, Pietrogrande M, Renoldi P, Bombardieri S, Bordin G. Cryoglobulinaemias: a multi-centre study of the early clinical and laboratory manifestations of primary and secondary disease. GISC. Italian Group for the Study of Cryoglobulinaemias. *QJM* 1995; **88**: 115-126 [PMID: 7704562]
- 63 **Mazzaro C**, Maso LD, Mauro E, Gattei V, Ghersetti M, Bulian P, Moratelli G, Grassi G, Zorat F, Pozzato G. Survival and Prognostic Factors in Mixed Cryoglobulinemia: Data from 246 Cases. *Diseases* 2018; **6** [PMID: 29751499 DOI: 10.3390/diseases6020035]
- 64 **Galli M**, Oreni L, Saccardo F, Castelnovo L, Filippini D, Marson P, Mascia MT, Mazzaro C, Origgi L, Ossi E, Pietrogrande M, Pioltelli P, Quartuccio L, Scarpato S, Sollima S, Riva A, Fraticelli P, Zani R, Giuggioli D, Sebastiani M, Sarzi Puttini P, Gabrielli A, Zignego AL, Scaini P, Ferri C, De Vita S, Monti G. HCV-unrelated cryoglobulinaemic vasculitis: the results of a prospective observational study by the Italian Group for the Study of Cryoglobulinaemias (GISC). *Clin Exp Rheumatol* 2017; **35** Suppl 103: 67-76 [PMID: 28466806]
- 65 **Mazzaro C**, Dal Maso L, Urraro T, Mauro E, Castelnovo L, Casarin P, Monti G, Gattei V, Zignego AL, Pozzato G. Hepatitis B virus related cryoglobulinemic vasculitis: A multicentre open label study from the Gruppo Italiano di Studio delle Crioglobulinemie - GISC. *Dig Liver Dis* 2016; **48**: 780-784 [PMID: 27106525 DOI: 10.1016/j.dld.2016.03.018]
- 66 **Mazzaro C**, Dal Maso L, Visentini M, Gitto S, Andreone P, Toffolutti F, Gattei V. Hepatitis B virus-related cryoglobulinemic vasculitis. The role of antiviral nucleot(s)ide analogues: a review. *J Intern Med* 2019; **286**: 290-298 [PMID: 31124596 DOI: 10.1111/joim.12913]
- 67 **Kurokawa M**, Hisano S, Ueda K. Hepatitis B virus and Schönlein-Henoch purpura. *Am J Dis Child* 1985; **139**: 861-862 [PMID: 4036912 DOI: 10.1001/archpedi.1985.02140110015013]
- 68 **Maggiore G**, Martini A, Grifeo S, De Giacomo C, Scotta MS. Hepatitis B virus infection and Schönlein-Henoch purpura. *Am J Dis Child* 1984; **138**: 681-682 [PMID: 6731386 DOI: 10.1001/archpedi.1984.02140450063019]
- 69 **Ergin S**, Sanli Erdoğan B, Turgut H, Evliyaoğlu D, Yalçın AN. Relapsing Henoch-Schönlein purpura in an adult patient associated with hepatitis B virus infection. *J Dermatol* 2005; **32**: 839-842 [PMID: 16361739 DOI: 10.1111/j.1346-8138.2005.tb00856.x]
- 70 **Stemerowicz R**, Möller B, Lobeck H, Oertel J, Hopf U. [Schoenlein-Henoch purpura in chronic HBsAG-positive hepatitis]. *Immun Infekt* 1988; **16**: 12-15 [PMID: 3360462]
- 71 **Shin JI**, Lee JS. Hepatitis B virus infection and Henoch-Schönlein purpura. *J Dermatol* 2007; **34**: 156; author reply 157 [PMID: 17239160 DOI: 10.1111/j.1346-8138.2006.00240.x]
- 72 **Wang S**, Chen Y, Xu X, Hu W, Shen H, Chen J. Prevalence of hepatitis B virus and hepatitis C virus infection in patients with systemic lupus erythematosus: a systematic review and meta-analysis. *Oncotarget* 2017; **8**: 102437-102445 [PMID: 29254259 DOI: 10.18632/oncotarget.22261]
- 73 **Kuna L**, Jakab J, Smolic R, Wu GY, Smolic M. HCV Extrahepatic Manifestations. *J Clin Transl Hepatol* 2019; **7**: 172-182 [PMID: 31293918 DOI: 10.14218/JCTH.2018.00049]
- 74 **Barkhuizen A**, Rosen HR, Wolf S, Flora K, Benner K, Bennett RM. Musculoskeletal pain and fatigue are associated with chronic hepatitis C: a report of 239 hepatology clinic patients. *Am J Gastroenterol* 1999; **94**: 1355-1360 [PMID: 10235218 DOI: 10.1111/j.1572-0241.1999.01087.x]
- 75 **Orge E**, Cefle A, Yazici A, Gürel-Polat N, Hulagu S. The positivity of rheumatoid factor and anti-cyclic citrullinated peptide antibody in nonarthritic patients with chronic hepatitis C infection. *Rheumatol Int* 2010; **30**: 485-488 [PMID: 19547976 DOI: 10.1007/s00296-009-0997-1]
- 76 **Liu FC**, Chao YC, Hou TY, Chen HC, Shyu RY, Hsieh TY, Chen CH, Chang DM, Lai JH.

- Usefulness of anti-CCP antibodies in patients with hepatitis C virus infection with or without arthritis, rheumatoid factor, or cryoglobulinemia. *Clin Rheumatol* 2008; **27**: 463-467 [PMID: 17876647 DOI: 10.1007/s10067-007-0729-4]
- 77 **Cheng YT**, Cheng JS, Lin CH, Chen TH, Lee KC, Chang ML. Rheumatoid factor and immunoglobulin M mark hepatitis C-associated mixed cryoglobulinaemia: an 8-year prospective study. *Clin Microbiol Infect* 2020; **26**: 366-372 [PMID: 31229596 DOI: 10.1016/j.cmi.2019.06.018]
  - 78 **Fuentes A**, Mardones C, Burgos PI. Understanding the Cryoglobulinemias. *Curr Rheumatol Rep* 2019; **21**: 60 [PMID: 31741077 DOI: 10.1007/s11926-019-0859-0]
  - 79 **Ferucci ED**, Choromanski TL, Varney DT, Ryan HS, Townshend-Bulson LJ, McMahon BJ, Wener MH. Prevalence and correlates of hepatitis C virus-associated inflammatory arthritis in a population-based cohort. *Semin Arthritis Rheum* 2017; **47**: 445-450 [PMID: 28532574 DOI: 10.1016/j.semarthrit.2017.04.004]
  - 80 **Zuckerman E**, Keren D, Rozenbaum M, Toubi E, Slobodin G, Tamir A, Naschitz JE, Yeshurun D, Rosner I. Hepatitis C virus-related arthritis: characteristics and response to therapy with interferon alpha. *Clin Exp Rheumatol* 2000; **18**: 579-584 [PMID: 11072597]
  - 81 **Koga T**, Kawashiri SY, Nakao K, Kawakami A. Successful ledipasvir + sofosbuvir treatment of active synovitis in a rheumatoid arthritis patient with hepatitis C virus-related mixed cryoglobulinemia. *Mod Rheumatol* 2017; **27**: 917-918 [PMID: 27848256 DOI: 10.1080/14397595.2016.1253814]
  - 82 **Siloşi I**, Boldeanu L, Biciuşcă V, Bogdan M, Avramescu C, Taisescu C, Padureanu V, Boldeanu MV, Dricu A, Siloşi CA. Serum Biomarkers for Discrimination between Hepatitis C-Related Arthropathy and Early Rheumatoid Arthritis. *Int J Mol Sci* 2017; **18** [PMID: 28629188 DOI: 10.3390/ijms18061304]
  - 83 **Ezzat WM**, Raslan HM, Aly AA, Emara NA, El Menyawi MM, Edrees A. Anti-cyclic citrullinated peptide antibodies as a discriminating marker between rheumatoid arthritis and chronic hepatitis C-related polyarthropathy. *Rheumatol Int* 2011; **31**: 65-69 [PMID: 19882340 DOI: 10.1007/s00296-009-1225-8]
  - 84 **Amin K**, Rasool AH, Hattem A, Al-Karboly TA, Taher TE, Bystrom J. Autoantibody profiles in autoimmune hepatitis and chronic hepatitis C identifies similarities in patients with severe disease. *World J Gastroenterol* 2017; **23**: 1345-1352 [PMID: 28293081 DOI: 10.3748/wjg.v23.i8.1345]
  - 85 **Chen HW**, Huang HH, Lai CH, Chang WE, Shih YL, Chang WK, Hsieh TY, Chu HC. Hepatitis C virus infection in patients with primary biliary cirrhosis. *Ann Hepatol* 2013; **12**: 78-84 [PMID: 23293197 DOI: 10.1016/S1665-2681(19)31388-2]
  - 86 **Floreani A**, Baragiotta A, Leone MG, Baldo V, Naccarato R. Primary biliary cirrhosis and hepatitis C virus infection. *Am J Gastroenterol* 2003; **98**: 2757-2762 [PMID: 14687829 DOI: 10.1111/j.1572-0241.2003.08717.x]
  - 87 **Bertolini E**, Battezzati PM, Zermiani P, Bruno S, Moroni GA, Marelli F, Villa E, Manenti F, Zuin M, Crosignani A. Hepatitis C virus testing in primary biliary cirrhosis. *J Hepatol* 1992; **15**: 207-210 [PMID: 1324271 DOI: 10.1016/0168-8278(92)90037-p]
  - 88 **Badiani RG**, Becker V, Perez RM, Matos CA, Lemos LB, Lanzoni VP, Andrade LE, Dellavance A, Silva AE, Ferraz ML. Is autoimmune hepatitis a frequent finding among HCV patients with intense interface hepatitis? *World J Gastroenterol* 2010; **16**: 3704-3708 [PMID: 20677344 DOI: 10.3748/wjg.v16.i29.3704]
  - 89 **Dvir R**, Sautto GA, Mancini N, Racca S, Diotti RA, Clementi M, Memoli M. Autoimmune hepatitis and occult HCV infection: A prospective single-centre clinical study. *Autoimmun Rev* 2017; **16**: 323-325 [PMID: 28161557 DOI: 10.1016/j.autrev.2017.01.015]
  - 90 **López Couceiro L**, Gómez Domínguez E, Muñoz Gómez R, Castellano Tortajada G, Ibarrola de Andrés C, Fernández Vázquez I. Healing of autoimmune hepatitis associated with hepatitis C virus infection treated with direct-acting antivirals. *Rev Esp Enferm Dig* 2019; **111**: 159-161 [PMID: 30449122 DOI: 10.17235/reed.2018.5528/2018]
  - 91 **Sabry AA**, Sobh MA, Irving WL, Grabowska A, Wagner BE, Fox S, Kudesia G, El Nahas AM. A comprehensive study of the association between hepatitis C virus and glomerulopathy. *Nephrol Dial Transplant* 2002; **17**: 239-245 [PMID: 11812873 DOI: 10.1093/ndt/17.2.239]
  - 92 **Castillo I**, Martínez-Ara J, Olea T, Bartolomé J, Madero R, Hernández E, Bernis C, Aguilar A, Quiroga JA, Carreño V, Selgas R. High prevalence of occult hepatitis C virus infection in patients with primary and secondary glomerular nephropathies. *Kidney Int* 2014; **86**: 619-624 [PMID: 24646855 DOI: 10.1038/ki.2014.68]
  - 93 **Misiani R**, Bellavita P, Fenili D, Borelli G, Marchesi D, Massazza M, Vendramin G, Comotti B, Tanzi E, Scudeller G. Hepatitis C virus infection in patients with essential mixed cryoglobulinemia. *Ann Intern Med* 1992; **117**: 573-577 [PMID: 1326246 DOI: 10.7326/0003-4819-117-7-573]
  - 94 **Arase Y**, Ikeda K, Murashima N, Chayama K, Tsubota A, Koida I, Suzuki Y, Saitoh S, Kobayashi M, Kumada H. Glomerulonephritis in autopsy cases with hepatitis C virus infection. *Intern Med* 1998; **37**: 836-840 [PMID: 9840704 DOI: 10.2169/internalmedicine.37.836]
  - 95 **Cao Y**, Zhang Y, Wang S, Zou W. Detection of the hepatitis C virus antigen in kidney tissue from infected patients with various glomerulonephritis. *Nephrol Dial Transplant* 2009; **24**: 2745-2751 [PMID: 19377056 DOI: 10.1093/ndt/gfp167]
  - 96 **Nayak S**, Kataria A, Sharma MK, Rastogi A, Gupta E, Singh A, Tiwari SC. Hepatitis C Virus-associated Membranoproliferative Glomerulonephritis Treated with Directly Acting Antiviral Therapy. *Indian J Nephrol* 2018; **28**: 462-464 [PMID: 30647501 DOI: 10.4103/ijn.IJN\_235\_17]

- 97 **Shimada M**, Nakamura N, Endo T, Yamabe H, Nakamura M, Murakami R, Narita I, Tomita H. Daclatasvir/asunaprevir based direct-acting antiviral therapy ameliorate hepatitis C virus-associated cryoglobulinemic membranoproliferative glomerulonephritis: a case report. *BMC Nephrol* 2017; **18**: 109 [PMID: [28356063](#) DOI: [10.1186/s12882-017-0534-5](#)]
- 98 **Obata F**, Murakami T, Miyagi J, Ueda S, Inagaki T, Minato M, Ono H, Nishimura K, Shibata E, Tamaki M, Yoshimoto S, Kishi F, Kishi S, Matsuura M, Nagai K, Abe H, Doi T. A case of rapid amelioration of hepatitis C virus-associated cryoglobulinemic membranoproliferative glomerulonephritis treated by interferon-free directly acting antivirals for HCV in the absence of immunosuppressant. *CEN Case Rep* 2017; **6**: 55-60 [PMID: [28509128](#) DOI: [10.1007/s13730-016-0244-z](#)]
- 99 **Ramos-Casals M**, Muñoz S, Medina F, Jara LJ, Rosas J, Calvo-Alen J, Brito-Zerón P, Forns X, Sánchez-Tapias JM; HISPAMEC Study Group. Systemic autoimmune diseases in patients with hepatitis C virus infection: characterization of 1020 cases (The HISPAMEC Registry). *J Rheumatol* 2009; **36**: 1442-1448 [PMID: [19369460](#) DOI: [10.3899/jrheum.080874](#)]
- 100 **Younossi Z**, Park H, Henry L, Adeyemi A, Stepanova M. Extrahepatic Manifestations of Hepatitis C: A Meta-analysis of Prevalence, Quality of Life, and Economic Burden. *Gastroenterology* 2016; **150**: 1599-1608 [PMID: [26924097](#) DOI: [10.1053/j.gastro.2016.02.039](#)]
- 101 **Lee YH**, Ji JD, Yeon JE, Byun KS, Lee CH, Song GG. Cryoglobulinaemia and rheumatic manifestations in patients with hepatitis C virus infection. *Ann Rheum Dis* 1998; **57**: 728-731 [PMID: [10070272](#) DOI: [10.1136/ard.57.12.728](#)]
- 102 **Saadoun D**, Terrier B, Semoun O, Sene D, Maisonnobe T, Musset L, Amoura Z, Rignon MR, Cacoub P. Hepatitis C virus-associated polyarteritis nodosa. *Arthritis Care Res (Hoboken)* 2011; **63**: 427-435 [PMID: [20981809](#) DOI: [10.1002/acr.20381](#)]
- 103 **Carson CW**, Conn DL, Czaja AJ, Wright TL, Brecher ME. Frequency and significance of antibodies to hepatitis C virus in polyarteritis nodosa. *J Rheumatol* 1993; **20**: 304-309 [PMID: [8097250](#)]
- 104 **Sneller MC**, Hu Z, Langford CA. A randomized controlled trial of rituximab following failure of antiviral therapy for hepatitis C virus-associated cryoglobulinemic vasculitis. *Arthritis Rheum* 2012; **64**: 835-842 [PMID: [22147444](#) DOI: [10.1002/art.34322](#)]
- 105 **Mazzaro C**, Mauro E, Ermacora A, Doretto P, Fumagalli S, Tonizzo M, Toffolutti F, Gattei V. Hepatitis C virus-related cryoglobulinemic vasculitis. *Minerva Med* 2020 [PMID: [33198444](#) DOI: [10.23736/S0026-4806.20.07120-7](#)]
- 106 **Disdier P**, Bolla G, Veit V, Ridings B, Gambarelli-Mouillac N, Harle JR, Weiller PJ. [Association of uveitis and hepatitis C. 5 cases]. *Presse Med* 1994; **23**: 541 [PMID: [8022745](#)]
- 107 **European Association for the Study of the Liver**. ; European Association for the Study of the Liver. EASL Clinical Practice Guidelines on hepatitis E virus infection. *J Hepatol* 2018; **68**: 1256-1271 [PMID: [29609832](#) DOI: [10.1016/j.jhep.2018.03.005](#)]
- 108 **Shinde N**, Patil T, Deshpande A, Gulhane R, Patil M, Bansod Y. Clinical profile, maternal and fetal outcomes of acute hepatitis e in pregnancy. *Ann Med Health Sci Res* 2014; **4**: S133-S139 [PMID: [25184080](#) DOI: [10.4103/2141-9248.138033](#)]
- 109 **Kamar N**, Garrouste C, Haagsma EB, Garrigue V, Pischke S, Chauvet C, Dumortier J, Cannesson A, Cassuto-Viguier E, Thervet E, Conti F, Lebray P, Dalton HR, Santella R, Kanaan N, Essig M, Mousson C, Radenne S, Roque-Afonso AM, Izopet J, Rostaing L. Factors associated with chronic hepatitis in patients with hepatitis E virus infection who have received solid organ transplants. *Gastroenterology* 2011; **140**: 1481-1489 [PMID: [21354150](#) DOI: [10.1053/j.gastro.2011.02.050](#)]
- 110 **Al-Shukri I**, Davidson E, Tan A, Smith DB, Wellington L, Johannessen I, Ramalingam S. Rash and arthralgia caused by hepatitis E. *Lancet* 2013; **382**: 1856 [PMID: [24290589](#) DOI: [10.1016/S0140-6736\(13\)62074-7](#)]
- 111 **Serratrice J**, Disdier P, Colson P, Ene N, de Roux CS, Weiller PJ. Acute polyarthritis revealing hepatitis E. *Clin Rheumatol* 2007; **26**: 1973-1975 [PMID: [17340044](#) DOI: [10.1007/s10067-007-0595-0](#)]
- 112 **Horvatits T**, Schulze Zur Wiesch J, Polywka S, Buescher G, Lütgehetmann M, Hussey E, Horvatits K, Peine S, Haag F, Addo MM, Lohse AW, Weiler-Normann C, Pischke S. Significance of Anti-Nuclear Antibodies and Cryoglobulins in Patients with Acute and Chronic HEV Infection. *Pathogens* 2020; **9** [PMID: [32947995](#) DOI: [10.3390/pathogens9090755](#)]
- 113 **Wu J**, Guo N, Zhu L, Zhang X, Xiong C, Liu J, Xu Y, Fan J, Yu J, Pan Q, Yang J, Liang H, Jin X, Ye S, Wang W, Liu C, Zhang J, Li G, Jiang B, Cao H, Li L. Seroprevalence of AIH-related autoantibodies in patients with acute hepatitis E viral infection: a prospective case-control study in China. *Emerg Microbes Infect* 2020; **9**: 332-340 [PMID: [32037983](#) DOI: [10.1080/22221751.2020.1722759](#)]
- 114 **Terziroli Beretta-Piccoli B**, Ripellino P, Gobbi C, Cerny A, Baserga A, Di Bartolomeo C, Bihl F, Deleonardi G, Melidona L, Grondona AG, Mieli-Vergani G, Vergani D, Muratori L; Swiss Autoimmune Hepatitis Cohort Study Group. Autoimmune liver disease serology in acute hepatitis E virus infection. *J Autoimmun* 2018; **94**: 1-6 [PMID: [30336842](#) DOI: [10.1016/j.jaut.2018.07.006](#)]
- 115 **Llovet LP**, Gratacós-Ginés J, Ortiz O, Rodríguez-Tajes S, Lens S, Reverter E, Ruiz-Ortiz E, Costa J, Viñas O, Forns X, Parés A, Londoño MC. Higher seroprevalence of hepatitis E virus in autoimmune hepatitis: Role of false-positive antibodies. *Liver Int* 2020; **40**: 558-564 [PMID: [31863722](#) DOI: [10.1111/Liv.14332](#)]
- 116 **van Gerven NM**, van der Eijk AA, Pas SD, Zaaier HL, de Boer YS, Witte BI, van Nieuwkerk CM,

- Mulder CJ, Bouma G, de Man RA; Dutch Autoimmune Hepatitis Study Group. Seroprevalence of Hepatitis E Virus in Autoimmune Hepatitis Patients in the Netherlands. *J Gastrointest Liver Dis* 2016; **25**: 9-13 [PMID: 27014749 DOI: 10.15403/jgld.2014.1121.251.hpe]
- 117 **Pischke S**, Gisa A, Suneetha PV, Wiegand SB, Taubert R, Schlue J, Wursthorn K, Bantel H, Raupach R, Bremer B, Zacher BJ, Schmidt RE, Manns MP, Rifai K, Witte T, Wedemeyer H. Increased HEV seroprevalence in patients with autoimmune hepatitis. *PLoS One* 2014; **9**: e85330 [PMID: 24465537 DOI: 10.1371/journal.pone.0085330]
- 118 **Le Cann P**, Tong MJ, Werneke J, Coursaget P. Detection of antibodies to hepatitis E virus in patients with autoimmune chronic active hepatitis and primary biliary cirrhosis. *Scand J Gastroenterol* 1997; **32**: 387-389 [PMID: 9140163 DOI: 10.3109/00365529709007689]
- 119 **Bazerbachi F**, Leise MD, Watt KD, Murad MH, Prokop LJ, Haffar S. Systematic review of mixed cryoglobulinemia associated with hepatitis E virus infection: association or causation? *Gastroenterol Rep (Oxf)* 2017; **5**: 178-184 [PMID: 28852522 DOI: 10.1093/gastro/gox021]
- 120 **Fousekis FS**, Mitselos IV, Christodoulou DK. Extrahepatic manifestations of hepatitis E virus: An overview. *Clin Mol Hepatol* 2020; **26**: 16-23 [PMID: 31601068 DOI: 10.3350/cmh.2019.0082]
- 121 **Del Bello A**, Guilbeau-Frugier C, Josse AG, Rostaing L, Izopet J, Kamar N. Successful treatment of hepatitis E virus-associated cryoglobulinemic membranoproliferative glomerulonephritis with ribavirin. *Transpl Infect Dis* 2015; **17**: 279-283 [PMID: 25708383 DOI: 10.1111/tid.12353]
- 122 **Guinault D**, Ribes D, Delas A, Milongo D, Abravanel F, Puissant-Lubrano B, Izopet J, Kamar N. Hepatitis E Virus-Induced Cryoglobulinemic Glomerulonephritis in a Nonimmunocompromised Person. *Am J Kidney Dis* 2016; **67**: 660-663 [PMID: 26682764 DOI: 10.1053/j.ajkd.2015.10.022]
- 123 **Thapa R**, Biswas B, Mallick D. Henoch-Schönlein purpura triggered by acute hepatitis E virus infection. *J Emerg Med* 2010; **39**: 218-219 [PMID: 19201130 DOI: 10.1016/j.jemermed.2008.10.004]





## Neurological manifestations of hepatitis E virus infection: An overview

Ashish Kumar Jha, Gaurav Kumar, Vishwa Mohan Dayal, Abhay Ranjan, Arya Suchismita

**ORCID number:** Ashish Kumar Jha 0000-0002-1208-8922; Gaurav Kumar 0000-0002-1220-7274; Vishwa Mohan Dayal 0000-0002-5511-3534; Abhay Ranjan 0000-0003-3616-742X; Arya Suchismita 0000-0002-6531-3249.

**Author contributions:** Jha AK wrote the manuscript, and prepared the figures and tables; Kumar G performed the data acquisition; Dayal VM, Ranjan A, and Suchismita A provided input to the writing of this paper.

### Conflict-of-interest statement:

There is no conflict of interest associated with any of the senior author or other coauthors contributed their efforts in this manuscript.

**Open-Access:** This article is an open-access article that was selected by an in-house editor and fully peer-reviewed by external reviewers. It is distributed in accordance with the Creative Commons Attribution NonCommercial (CC BY-NC 4.0) license, which permits others to distribute, remix, adapt, build upon this work non-commercially, and license their derivative works on different terms, provided the original work is properly cited and the use is non-commercial. See: <http://creativecommons.org/licenses/by-nc/4.0/>

**Ashish Kumar Jha, Gaurav Kumar, Vishwa Mohan Dayal,** Department of Gastroenterology, Indira Gandhi Institute of Medical Sciences, Patna 800014, India

**Abhay Ranjan,** Department of Neurology, Indira Gandhi Institute of Medical Sciences, Patna 800014, India

**Arya Suchismita,** Department of Pediatric Hepatology, Institute of Liver and Biliary Sciences, Basant Kunj 110070, New Delhi, India

**Corresponding author:** Ashish Kumar Jha, MBBS, MD, DM, Associate Professor, Department of Gastroenterology, Indira Gandhi Institute of Medical Sciences, Sheikhpura, Patna 800014, India. [ashishjhabn@yahoo.co.in](mailto:ashishjhabn@yahoo.co.in)

### Abstract

Hepatitis E virus (HEV) is an important cause of repeated waterborne outbreaks of acute hepatitis. Recently, several extrahepatic manifestations (EHMs) have been described in patients with HEV infection. Of these, neurological disorders are the most common EHM associated with HEV. The involvement of both the peripheral nervous system and central nervous system can occur together or in isolation. Patients can present with normal liver function tests, which can often be misleading for physicians. There is a paucity of data on HEV-related neurological manifestations; and these data are mostly described as case reports and case series. In this review, we analyzed data of 163 reported cases of HEV-related neurological disorders. The mechanisms of pathogenesis, clinico-demographic profile, and outcomes of the HEV-related neurological disorders are described in this article. Nerve root and plexus disorder were found to be the most commonly reported disease, followed by meningoencephalitis.

**Key Words:** Hepatitis E virus; Acute hepatitis E; Extrahepatic manifestations; Neurological manifestations; Neuralgic amyotrophy; Guillain-Barré syndrome

©The Author(s) 2021. Published by Baishideng Publishing Group Inc. All rights reserved.

**Core Tip:** Neurological involvement in patients with hepatitis E virus (HEV) infection is rare. There is a paucity of data on HEV-related neurological manifestations. This

**Manuscript source:** Invited manuscript

**Specialty type:** Gastroenterology and hepatology

**Country/Territory of origin:** India

**Peer-review report's scientific quality classification**

Grade A (Excellent): 0

Grade B (Very good): B, B, B, B

Grade C (Good): 0

Grade D (Fair): 0

Grade E (Poor): 0

**Received:** January 3, 2021

**Peer-review started:** January 3, 2021

**First decision:** January 23, 2021

**Revised:** February 27, 2021

**Accepted:** April 5, 2021

**Article in press:** April 5, 2021

**Published online:** May 14, 2021

**P-Reviewer:** Chawla S, Granito A, Shimizu Y

**S-Editor:** Gao CC

**L-Editor:** Filipodia

**P-Editor:** Liu JH



review comprehensively describes the mechanisms of pathogenesis, clinico-demographic profile, and outcomes of HEV-related neurological disorders. Nerve root and plexus disorder were the most commonly reported diseases followed by meningo-encephalitis. These patients can present with normal liver function tests, which can often be misleading for physicians.

**Citation:** Jha AK, Kumar G, Dayal VM, Ranjan A, Suchismita A. Neurological manifestations of hepatitis E virus infection: An overview. *World J Gastroenterol* 2021; 27(18): 2090-2104

**URL:** <https://www.wjgnet.com/1007-9327/full/v27/i18/2090.htm>

**DOI:** <https://dx.doi.org/10.3748/wjg.v27.i18.2090>

## INTRODUCTION

The hepatitis E virus (HEV) is a non-enveloped, positive-sense, single-stranded ribonucleic acid (RNA) virus. It belongs to the *Hepeviridae* family and is one of the most common causes of acute hepatitis globally. Currently, HEV is represented by one serotype and eight genotypes (GTs)[1]; of these, four GTs (GT1-4) are mainly responsible for human infection. Epidemiological characteristics of GT1-4 of HEV have been summarized in Table 1.

HEV is an important cause of repeated waterborne outbreaks of acute hepatitis. While HEV outbreaks have mainly been reported in Asia and Africa, it has recently been identified as an emerging issue in public health in Western countries. However, the global burden of HEV infection remains unclear. The recent meta-analysis estimated that approximately 939 million of the global population have experienced HEV infection once, and 15-110 million individuals have had a recent or have an ongoing infection. The seroprevalence rates of HEV infection in Africa, Asia, Europe, and America are 21.76%, 15.80%, 9.31%, and 7%-8% respectively[2]. The World Health Organization (WHO) estimated 14 million symptomatic cases of HEV infection, with 0.3 million deaths and 5.2 thousand stillbirths each year worldwide[3]. More than 50% of global HEV deaths were recorded in the WHO South-East Asia Region (SEAR), which includes India, Bangladesh, Thailand, the Democratic People's Republic of Korea, Myanmar, Nepal, Bhutan, Sri Lanka, Indonesia, Maldives, and Timor-Leste. In the WHO SEAR countries, annual symptomatic cases of HEV are estimated to be 6.5 million, with 0.16 million deaths and 2.7 thousand stillbirths[3].

Symptomatic HEV infection can present with anicteric or icteric acute hepatitis. It can also rarely lead to fulminant liver failure, and HEV infection further carries high mortality (25%) in pregnancy. While most cases of HEV-related acute hepatitis spontaneously resolve within 4-8 wk, HEV sometimes causes chronic infection, especially in immunosuppressed patients[4]. Chronic HEV infection has been defined as the persistence of HEV replication for more than 6 mo[5]. GT3 and GT4 (mainly GT3) can cause chronic infection, resulting in liver fibrosis and cirrhosis. HEV infection is also an important cause of acute-on-chronic liver failure (ACLF), especially in South-East Asian countries. In our prospective study, we observed that the hepatitis virus infection is the most common acute insult identified in patients with ACLF. Overall, the most common hepatitis virus superinfection was HEV (23% cases)[6]. In another study, Kumar *et al*[7] demonstrated a 44% HEV superinfection rate in a sample of patients with chronic liver disease.

Recently, several extrahepatic manifestations (EHMs) were described in patients with HEV infection (Table 2). These EHMs were reported as case-control studies and case series or reports during the last decades. In a recent systemic review, Rawla *et al*[8] analyzed data of 324 reported cases of EHM patients with HEV infection. The most common EHMs were neurological (55%), cardiovascular or hematological (35%), and gastrointestinal manifestations (7%). Rare manifestations included renal (1.24%), endocrine (0.31%), and skin disease (0.31%), as well as manifestations in the respiratory (0.31%), muscular (0.31%), and immune system (0.31%).

This review summarizes the available evidence regarding neurological manifestations in patients with HEV infection. To this end, we analyzed the literature related to the neurological manifestations associated with HEV. These reported manifestations were classified as central nervous system (CNS) disorders, nerve root and plexus disorders, neuropathy, cranial neuropathy, neuromuscular junction disorders, muscle

**Table 1 Hepatitis E virus: Epidemiological features**

Genotype	Hosts/reservoir	Mode of transmission	Geographic distribution	Remarks	Reported neurological manifestations <sup>1</sup>
GT1	Only humans	Fecal-oral transmission	Mostly Asia and Africa	Large outbreaks; Self-limiting; High mortality in pregnancy	Yes (2 cases)
GT2	Only humans	Fecal-oral transmission	Africa and Mexico	Large outbreaks; Self-limiting; High mortality in pregnancy	None
GT3	Human, swine, wild boar, goat, cattle, deer, camel and yak	Zoonotic infections in humans; Blood transfusion	Worldwide including Europe and America	Can cause chronic infection in organ transplant patients	Yes (56 cases)
GT4	Human, swine, wild boar, goat, cattle, deer, camel and yak	Zoonotic infections in humans; Blood transfusion	China, Japan, South-east Asia	Can cause chronic infection in organ transplant patients	Yes (4 cases)

<sup>1</sup>See Table 3 for reported neurological manifestations. GT: Genotype.

**Table 2 Relationship of hepatitis E virus infection with extrahepatic manifestations**

Extrahepatic manifestations	Likelihood of causal relationship, Hill criteria <sup>[9,97]</sup>	Evidence to support a casual role
<b>Neurological disorders</b>		
Neuralgic amyotrophy	Very probable	Good
Guillain-Barré syndrome	Very probable	Good
Meningoencephalitis	Very probable	Good
Others <sup>1</sup>	Possible/under debate	Remains to be established
<b>Kidney disorders</b>		
Membranoproliferative glomerulonephritis	Very probable	Good
Membranous glomerulonephritis	Very probable	Good
IgA nephropathy	Very probable	Good
<b>Gastrointestinal disorder</b>		
Acute pancreatitis	Very probable	Remains to be established
<b>Hematological diseases</b>		
Thrombocytopenia, monoclonal gammopathy of uncertain significance, Cryoglobulinemia, hemolytic anemia, aplastic anemia	Possible	Remains to be established
<b>Miscellaneous</b>		
Autoimmune hepatitis, myocarditis, thyroiditis	Doubtful/under debate	Remains to be established

<sup>1</sup>See Table 3 for other neurological disorders. IgA: Immunoglobulin A.

disorders, and other miscellaneous manifestations.

## RELATIONSHIP OF HEV INFECTION WITH EHMs

Various EHMs have a temporal relationship with HEV infections; however, whether it is a coincidence or an actual causal relationship remains unclear. A causal relationship between HEV and neurological has been proposed on the basis of a few well-described case-control studies, which showed a significantly higher seroprevalence of HEV-associated neuralgic amyotrophy (NA) and Guillain-Barré syndrome (GBS) compared to non-HEV-associated cases. Moreover, several case studies have documented the presence of HEV RNA in the cerebrospinal fluid (CSF). Although the authors

explained this association on the basis of existing evidence, the pathophysiological basis of a causal relationship remains unknown. There is good evidence to support a causal role of HEV in associated conditions such as NA, GBS, meningoencephalitis, membranoproliferative glomerulonephritis, membranous glomerulonephritis, and immunoglobulin (Ig) A nephropathy[5,9]. Relationships between other EHMs and HEV are based on case reports only; therefore, causality has yet to be established (Table 2).

## MECHANISMS OF PATHOGENESIS

The pathogenesis of EHMs in HEV infection is unclear. The mechanisms by which HEV can induce EHM may be caused by either direct or indirect mechanisms. Direct mechanisms involve HEV replication in affected tissues, resulting in cellular damage, whereas indirect mechanisms are caused by cross-reactive immune triggers, the formation of immune complexes, or by secondary infection[10]. Direct mechanisms are supported by *in vitro* studies. HEV can infect neuronal cells *in vitro* and human neuronal-derived cells support the full-length replication of viral RNA and translation of viral capsid protein[11,12]. Indirect immune trigger-mediated mechanisms appear to be more relevant in pathogenesis. Both humoral and cellular immune responses are likely to be involved in the pathogenesis of hepatic and EHMs. Furthermore, the prevalence of EHM is more common in immunocompetent patients than immunocompromised patients. In a study, the neurological manifestations were found to be significantly more common (22.6% as against 3.2%) in immunocompetent patients ( $n = 137$ ) compared to immunocompromised patients ( $n = 63$ ). The higher frequency of neurological disorders in immunocompetent patients suggests immune-mediated mechanisms causing EHMs[13]. In another study, all patients with NA were immunocompetent[14]. A schematic diagram of the potential mechanisms of EHM is shown in Figure 1.

## NEUROLOGICAL MANIFESTATIONS

The neurologic manifestations of HEV infection are being increasingly recognized. Retrospective studies from Europe revealed 5.5%-7.5% of neurological manifestations in HEV-infected patients[15,16]. Furthermore, two recent European prospective studies showed an even higher prevalence of neurological symptoms (16.5%-31%) in HEV-infected patients. Ripellino *et al*[14] indicated 31% prevalence of neurological symptoms in HEV-infected patients. However, two-third of patients had myalgia only, and none of these patients underwent brachial plexus MRI or muscle biopsy. In another recent prospective case-control study, out of 200 HEV-infected patients, 33 (16.5%) showed neurological symptoms. The most frequent manifestation was neuropathic pain (42%), which suggests small fiber neuropathy. However, the results of their neurological examination were normal, and extensive investigations were not performed to detect small fiber neuropathy[13]. The prevalence of HEV infection in patients with non-traumatic neurological injury ranges from 2.4% to 6.9%. In a multicentric European study, 2.4% of 464 patients with non-traumatic neurological injury showed evidence of recent HEV infection. Symptoms of hepatitis were mild or absent and all patients were anicteric[17]. Another study from France demonstrated a high seroprevalence (6.9%) of positive anti-HEV IgM in a cohort ( $n = 159$ ) of patients with acute non-traumatic, non-vascular neurological injuries as compared to seroprevalence in blood donors (0.4%) at the same period of time[18,19]. However, a recent study from China showed a similar HEV seroprevalence in patients with acute non-traumatic neuropathy ( $n = 1117$ ) and healthy controls ( $n = 1415$ ) (0.54% *vs* 0.68%;  $P = 0.65$ )[20].

Involvement of both the peripheral nervous system and CNS can occur together or in isolation. The various neurologic syndromes that have been reported in patients with HEV infection are shown in Table 3. Approximately 163 cases have been described to date, wherein the mean age of patients was 53.9 years with a male to female ratio (M:F) of 2.84:1. Neurological disorders are most commonly reported in Europe (74%) and SEAR nations (15%), mainly France, India, and Bangladesh. Nerve root and plexus disorders [NA (39%) and GBS (37%)] were the most commonly reported HEV-related neurological disorders, followed by CNS disorder [meningoencephalitis (4%)]. The majority of patients (88%) had normal bilirubin levels. Alanine aminotransferase (ALT) levels were widely variable [median (range): 345.5 (16-4502)

**Table 3** Hepatitis E virus-related neurological manifestations

Diseases	<i>n</i> (%)	Geographic distribution	Mean age in yr	M:F ratio	Serological diagnosis	Serum HEV-RNA	Genotype	CSF HEV- RNA	Elevated bilirubin, <i>n</i>	Median (range) ALT in IU/L	Use of anti-viral	Recovery
<b>Nerve root and plexus disorders</b>												
Neuralgic amyotrophy[13,15-17,28-56]	64 (39)	Europe: 62; SEAR: 1; United States: 1	45.7	6.5:1	51	44	GT3: 28	0	4	1007 (22-2579)	9	CR: 9; PR: 47; NM: 8
Guillain-Barré syndrome[13,15,16,20,36,58-85]	61 (37)	SEAR: 21; Europe: 30; China/Hong Kong: 5; Japan: 4; Iraq: 1	51.16	2.42:1	46	20	GT3: 10; GT4: 1; GT1: 2	3	11	1950 (57-4502)	1	CR: 23; PR: 14; Died: 1; NM: 23
<b>Central nervous system disorder</b>												
Meningoencephalitis[17,20,35,86,87]	6 (4)	Europe: 2; China: 2; SEAR: 1; United States: 1	44	1:1	6	5	GT 3: 2	2	0	142 (20-479)	1	CR: 5; NM: 1
Cerebral ischemia[17,20]	5 (3)	Europe: 3; China: 2	66	4:1	5	4	GT3: 2	0	0	18 (8-28)	0	CR: 3; PR: 2
Seizures[17]	2 (1)	Europe	71	1:1	2	1	GT3: 1	0	0	19 (10-28)	0	CR: 2
Transverse myelitis[88]	1 (0.6)	Europe	62	0:1	1	1	GT3: 1	1	0	1152	0	PR: 1
<b>Neuropathy</b>												
Mononeuritis multiplex[36]	6 (4)	Europe	53.16	1:1	6	4	GT3: 3	0	1	188 (118-3641)	1	CR: 5; PR: 1
Peripheral neuropathy[16,20,89]	5 (3)	Europe: 4; China: 1	57.4	3:2	5	5	GT3: 2	2	1	285 (30-1606)	1	CR: 2; PR: 3
<b>Cranial neuropathy</b>												
Cranial neuropathy[16,17,90-92]	5 (3)	SEAR: 2; Europe: 2; Japan: 1	53	4:1	2	2	GT3: 1; GT4: 3; ND	0	0	1200 (60-3866)	0	CR: 5
<b>Neuromuscular junction and muscle disorders</b>												
Myositis[93]	1 (0.6)	Europe	57	1:0	1	1	ND	0	1	1030	1	CR:1
Myasthenia gravis[18]	1 (0.6)	Europe	33	0:1	1	1	GT3: 1	0	0	190	1	NM: 1
<b>Others neurological disorders</b>												
Meningoradiculitis[36,94,95]	6 (4)	Europe	53.33	1:1	6	6	GT3: 5	4	1	406 (40-822)	1	CR: 5; Died: 1
<b>Total cases, <i>n</i> (%)</b>												
Total	163	Europe: 120 (74); WHO SEAR: 25 (15);	53.9	2.84:1	132 (81)	94 (58)	GT3: 56 (90);	12 (7)	19 (12)	345.5 (16-4502)	Ribavirin:	CR: 60 (46); PR: 68



China/Hong Kong: 10 (6), Japan: 4; United States: 2; Iraq: 1

GT4: 4; GT1: 2

16 (10)

(53) Died; 2; NM 33 (20)

ALT: Alanine aminotransferase; CR: Complete recovery; CSF: Cerebrospinal fluid; GT: Genotype; HEV: Hepatitis E virus; M:F ratio: Male to female ratio; NM: Not mention; PR: Partial recovery; SEAR: South-East Asia Region; WHO: World Health Organization.

IU/L]. HEV RNA was detected in serum in 94 (58%) cases. Genotyping was performed in 62 (38%) cases, which revealed that GT3 is the main GT (90%) associated with neurological disorders. HEV RNA was identified in CSF in 12 (7%) cases. Patients were mainly treated with supportive measures, intravenous Ig (IVIG), plasmapheresis, steroids, and physiotherapy. Antiviral treatment (ribavirin) was given to 16 (10%) patients only. Of the 163 patients, the follow-up details of 130 patients were available. Complete recovery was observed in 60 (46%) patients, while partial recovery or long-term disability and death were noted in 68 (53%) and 2 patients respectively.

Neurological disorders have also been described in cases of viral hepatitis A, B, and C[21-26]. Hepatitis C virus infection is often associated with neuropsychiatric disorders including peripheral neuropathy (mainly sensory), cognitive impairment, and cerebrovascular accidents. Encephalitis, myelitis, encephalomyelitis, and GBS are rarely described in patients with hepatitis C virus infection[21,22]. Hepatitis A virus infection is rarely associated with neurological disorders, especially GBS and encephalitis. Other hepatitis A-related neurological disorders include meningo-encephalitis, meningitis, transverse myelitis, peripheral neuropathy, optic neuritis, and neuromuscular junction and muscular disorders[23-25]. Hepatitis B virus infection is rarely associated with neurological disorders, especially GBS and peripheral neuropathy[26]. GBS and peripheral neuropathy have been reported with viral hepatitis A, B, C, and E. It is interesting to note that NA is described in HEV infection alone.

The causal association of HEV infection with GBS, NA, and meningoencephalitis is supported by good evidence, including well-described case cohorts and a large number of case reports. However, the association of HEV infection with other neurological diseases is primarily based on a small number of case reports without sufficient evidence to establish a causal relationship.

## NERVE ROOT AND PLEXUS DISORDERS

### NA

NA — also known as Parsonage-Turner syndrome or brachial plexus neuritis—is a distinct disorder, with core features that include episodes of severe shoulder and arm pain at symptom onset, rapid multifocal paresis, and atrophy of the upper extremity muscles, and a slow recovery, requiring a few months to several years. The disease is

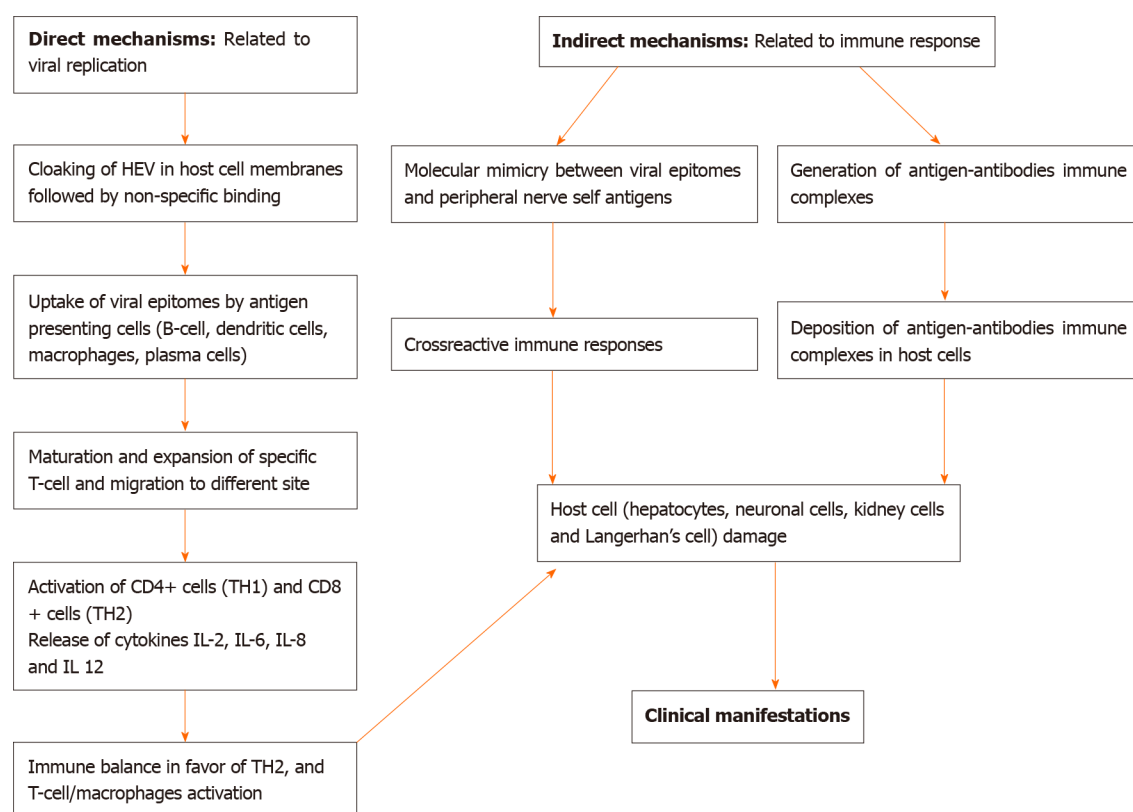


**Figure 1** Schematic diagram demonstrating the potential mechanisms of extrahepatic manifestations of hepatitis E virus infection. HEV: Hepatitis E virus; IL: Interleukin.

characterized by the patchy distribution of motor, sensory, and autonomic symptoms. Any part of the brachial plexus and the lumbosacral plexus can be involved, with any combination of motor and sensory impairment. Involvement of nerves from regions other than the brachial plexus is noted in about one-fourth of patients. The pathogenesis of NA is unknown, but it may share its pathogenesis mechanism with post-infectious GBS. No currently available tests can unequivocally confirm or exclude NA, although needle electromyography (EMG) can help in estimating axonal damage and reinnervation. Exclusion of other disorders such as cervical disc herniation and neoplasms of the superior sulcus region are usually required[27].

NA is likely to be causally associated with HEV infection. In a study, acute HEV infection was identified in 10.6% of NA patients ( $n = 47$ )[28]. Another study demonstrated a high seroprevalence (6.9%) of acute HEV infection in a cohort of patients with acute non-traumatic, non-vascular neurological injuries ( $n = 159$ ). Notably, more than half of the NA patients (57%) showed positive anti-HEV IgM assays[18]. Recently, a multi-center retrospective data analysis was performed for the comparison of HEV-associated NA ( $n = 57$ ) and NA without HEV infection ( $n = 61$ ). HEV-NA patients were found to have significantly more bilateral involvement (80% *vs* 9%), damage outside the brachial plexus (59% *vs* 11%), including phrenic nerve and lumbosacral plexus injury (25% *vs* 4% and 26% *vs* 7.0% respectively), sensory symptoms, and reduced reflexes. Despite more extensive damage to the brachial plexus in HEV-associated NA, the outcome was similar in the two groups. About 90% of patients with HEV-associated NA were anicteric[29].

Approximately 64 cases of HEV-associated NA have been reported to date[13,15-17,28-56]. The salient clinico-demographic features of NA are summarized in Tables 3 and 4. HEV-associated NA is predominantly seen in middle-aged males (mean age: 45.7 years; M:F = 6.5:1). Genotyping was conducted in 28 cases; all were found to be GT3. All patients were immunocompetent. All patients, except two, were from European countries. About 90% of the cases had bilateral involvement (89% *vs* 11% unilateral). Predominantly right-sided involvement was observed in 60% of the patients with bilateral involvement, whereas right-sided involvement was seen in 83% of the patients with unilateral involvement. An EMG was performed in 34 of the 64 cases and revealed denervation and/or damage of brachial plexus in 31 cases. Almost all patients (94%) had normal bilirubin levels and ALT levels were variable [median

**Table 4 Clinical description of nerve root and plexus disorders, *n* = 125**

Nerve root and plexus disorders	Source of infection	Hepatitis-neurological involvement interval	Type of involvement, <i>n</i> (%)	Specific remarks, <i>n</i> (%)
Neuralgic amyotrophy ( <i>n</i> = 64)	Described in 9. Sausage figatelli: 3; Vegetables: 2; Uncooked pork: 1; Manipulation of horse manure: 1; Travel history: 2	Described in 29. Mean delay: 8.4 d	Described in 54. Brachial plexus involvement: Bilateral 48 (89) [right > left: 15 (60); left > right: 10 (40); not described: 23]; Unilateral 6 (11) [right: 5 (83); left: 1]	94% had normal bilirubin levels. EMG findings mentioned: 34; Denervation and/or damage of brachial plexus: 31 (91)
Guillain-Barré syndrome ( <i>n</i> = 61)	Described in 5. Sausage figatelli: 2; Uncooked pork: 1; Dear meat: 1; Contact with farm animals: 1	Described in 51. Mean delay: 15 d; Concomitant: 6 patients	Described in 38. Acute inflammatory demyelinating polyneuropathy: 28 (74); Acute motor-sensory axonal neuropathy: 5 (13); Acute motor axonal neuropathy: 4 (11); Miller Fisher syndrome: 1 (3)	82% had normal bilirubin levels; Anti-ganglioside GM1 antibodies: 4; Anti-ganglioside GM 2 antibodies: 4; Anti-GQ1b ganglioside antibody: 1

EMG: Electromyography.

(range): 1007 (22-2579) IU/L]. HEV RNA was detected in serum in 44 cases but not detected in CSF. Patients were primarily treated with supportive measures, including physiotherapy. A total of nine patients were treated with ribavirin and IVIG. Complete recovery was seen in six patients only. Partial recovery and long-term disability was noted in 40 and 7 patients respectively.

### GBS

GBS is an inflammatory disease of the nerve root and plexus and is the most common cause of acute flaccid paralysis. It should be considered a diagnosis in patients who have experienced rapidly progressive bilateral weakness of the legs and/or arms, in the absence of CNS involvement or other obvious causes. Patients with the classic sensorimotor form of GBS present with distal paresthesia or sensory loss, accompanied or followed by weakness that starts in the legs and progresses to the arms and cranial muscles. Reflexes are decreased or absent in most patients at presentation and in almost all patients at nadir. GBS is a clinical diagnosis, but additional investigations are mostly performed for confirmation. The diagnosis of GBS can be supported by a CSF examination finding of classical cytoalbuminologic dissociation—the combination of a normal cell count and increased protein level. Nerve conduction studies can be helpful but are generally not required to diagnose GBS[57].

Prior respiratory or gastrointestinal tract infection has been reported in approximately two-thirds of GBS patients. A specific pathogen can be identified in about 50% of cases of GBS with a suspected infectious precipitant. Epidemiological studies have shown that *Campylobacter jejuni*, *Mycoplasma pneumoniae*, *Haemophilus influenzae*, *Cytomegalovirus*, and Epstein-Barr virus infections are strongly associated with GBS. These pathogens appear to act as potential triggers of a postinfectious immune-mediated process leading to GBS. Molecular mimicry and cross-reactive immune triggers play an important role in the immunopathogenesis of GBS. Antibodies to gangliosides following infection with *C. jejuni* have been demonstrated in patients with GBS.

Recently, case-control studies and several case reports reported an association between acute HEV infection and GBS. The seroprevalence of acute HEV infection in patients with GBS has been found to range from 5% to 11%[57-61]. In a retrospective cohort study, 8% of patients (*n* = 73) with GBS showed positive IgM assays for HEV[58]. The association of HEV infection with GBS has been described in at least three well-described case-control studies. A study conducted in the Netherlands indicated a significantly higher frequency of acute HEV infection in GBS patients (5%) compared to healthy controls (0.5%)[59]. Another study from Japan demonstrated that 4.8% of the patients (*n* = 63) with GBS showed an association with acute HEV infection[60]. A study in Bangladesh documented that 11% of GBS patients (*n* = 100) were associated with acute HEV infection and seroprevalence was significantly higher for this group compared to patients with other neurological disorders as well as healthy controls[61]. In all studies, no clinical differences were observed between HEV-associated GBS and other GBS cases[58-61].

We found 61 cases of HEV-associated GBS reported in the medical literature[13,15,16,20,36,58-85]. Salient clinico-demographic features of GBS are

summarized in Tables 3 and 4. The mean age of the patients was 51.16 years with an M:F of 2.42:1. Genotyping was performed in 13 cases. All patients, except three, were GT3. HEV-associated GBS is most commonly reported in Europe and Southeast Asia, followed by East Asia and China. The patients most commonly presented with acute inflammatory demyelinating polyneuropathy. The majority of patients (82%) had normal bilirubin levels, and ALT levels widely varied (median [range]: 1950 [57-4502] IU/L). HEV RNA was detected in serum in 20 cases, while HEV RNA was detected in CSF in 3 cases. Further, anti-ganglioside antibodies were documented in nine patients. Patients were mainly treated with supportive measures, including IVIG and physiotherapy. The follow-up details of 38 of 61 patients were available. Complete recovery was seen in only 23 patients. Partial recovery was noted in 14 patients and 1 patient died.

## CNS DISORDERS

The association between HEV infection and CNS disorders, including meningoencephalitis, cerebral ischemia, seizure, and transverse myelitis was reported in a few case reports. Meningoencephalitis was reported in six cases with acute HEV infection (mean age: 44 years; M:F = 1:1)[17,20,35,86,87]. Genotyping done in two cases revealed GT3, and all patients were anicteric. The median (range) ALT was 142 (20-479) IU/L. HEV RNA was detected in serum in all patients, except one. CSF examination for HEV RNA performed in four cases revealed the presence of HEV RNA in two cases. Of the six cases, complete recovery was seen in five.

Cerebral ischemia was reported in six cases[17,20], and all patients were anicteric. Serum HEV RNA was detected in four patients with cerebral ischemia. However, HEV RNA was not detected in CSF. Seizures were reported in two cases with HEV infection[17]. Transverse myelitis was reported in an anicteric patient with acute HEV (GT3) infection, and HEV RNA was detected in both serum and CSF[88].

## NEUROPATHIES

The association between HEV infection and neuropathy was reported in case series and reports. Mononeuritis multiplex, defined by asymmetric, asynchronous involvement of the noncontiguous nerve trunks has been documented in six patients with acute HEV infection (GT3) from France (mean age: 53.16 years; M:F = 1:1)[36]. All patients presented with neuropathic pain and paresthesia in multiple sites with hyporeflexia or areflexia, and all patients, except one, were anicteric. The median (range) ALT was 188 (118-3641) IU/L. HEV RNA was detected in serum in four cases. All patients, except one, had a complete recovery.

Peripheral neuropathy and small fiber neuropathy were reported in five cases, mostly from Europe (4/5; mean age: 57.4 years; M:F = 3:2)[16,20,89]. Genotyping done in two cases revealed GT3. Patients presented with neuropathic pain, paresthesia and weakness of limbs. All patients, except one, were anicteric. Median (range) ALT was 285 (30-1606) IU/L. HEV RNA was detected in serum in all five cases. HEV RNA was detected in CSF in two cases. Out of five, complete recovery was seen in two-cases only.

## CRANIAL NEUROPATHIES

Cranial nerve involvement was seen in five patients with acute HEV infection (mean age: 53 years; M:F = 4:1)[16,17,90-92]. Cases were reported from Europe ( $n = 2$ ), India ( $n = 2$ ), and Japan ( $n = 1$ ) respectively. Isolated facial nerve palsy (Bell's palsy) and vestibular nerve involvement were seen in three and one patient respectively. Combined facial nerve and vestibular nerve involvement was noted in one patient. All patients were anicteric. Median (range) ALT was 1200 (60-3866) IU/L. HEV RNA was detected in serum in two cases. Genotyping was done in two cases and revealed GT3 and GT4 (Europe: GT1; Japan: GT4). CSF examination for HEV RNA was performed in none of the patients, and complete recovery was observed in all.

## NEUROMUSCULAR JUNCTION AND MUSCLE DISORDERS

Cases of myasthenia gravis ( $n = 1$ ) and myositis ( $n = 1$ ) were also reported in serum HEV RNA positive patients[18,93]. However, HEV RNA was not detected in CSF.

## OTHER NEUROLOGICAL DISORDERS

Meningoradiculitis refers to the combined involvement of meninges and nerve roots, and the lumbosacral region is the most common site of involvement. Etiology includes inflammatory, infectious, and neoplastic disorders. Recently, meningoradiculitis was reported in six patients with acute HEV infection from Europe[36,94,95]. The mean age of patients was 53.33 years with M:F of 1:1. Genotyping was done in five cases and showed GT3. Patients mainly presented with arthromyalgia and asthenia. All patients, except one, were anicteric. Median (range) ALT was 406 (40-822) IU/L. HEV RNA was detected in serum in all six cases. HEV RNA was detected in CSF in four cases. Of the six, complete recovery was noted in five cases.

## DIAGNOSIS OF HEV INFECTION

Acute HEV infection is diagnosed through the detection of serum and/or stool HEV RNA by polymerase chain reaction (PCR), serum anti-HEV immunoglobulin M, HEV antigen, and rising anti-HEV immunoglobulin G titer. A negative PCR does not exclude acute infection, and serology sometimes gives false negatives in the case of immunocompromised patients. Therefore, serology and PCR testing are best used in combination. Testing for HEV should be conducted in all patients with suspicion of acute hepatitis, immunosuppressed patients with unexplained deranged liver function tests (LFTs), and in patients with NA and GBS. Testing is also suggested in patients with unexplained ACLF, and encephalitis or myelitis. Moreover, testing for proteinuria is suggested in HEV-infected patients[5].

## TREATMENT

The HEV is spontaneously cleared in almost all patients with acute infection. Therefore, acute hepatitis does not require antiviral therapy. In a few case studies, ribavirin treatment of severe acute HEV infection showed rapid normalization of liver enzymes and viremia. Therefore, ribavirin treatment may be considered in cases of severe acute hepatitis E or ACLF[5,96]. Antiviral treatment is also suggested for patients with chronic HEV infection, and HEV-associated glomerular disease. There is no sufficient evidence of ribavirin use in HEV-associated neurological disorders.

## PREVENTION

Several epidemiological factors associated with HEV infection are described in Table 1. HEV is principally transmitted *via* the fecal-oral route due to fecal contamination of drinking water. As such, it has been detected in sewage water, rivers, pork liver sausages, shellfish, cattle milk, unpeeled fruit, strawberries, berries, salads, and leafy green vegetables. Poor hygiene, exposure to contaminated environments, consumption of raw meat, exposure to soil, travel to endemic areas, contact with farm animals and pets, living in rural areas, and receiving lower levels of education were identified as risk factors for HEV infection. Transmission from infected blood products and vertical transmission are other modes of transmission[13]. The spread of HEV can be reduced by maintaining quality standards for public water supplies, ensuring proper disposal of human feces, maintaining individual hygienic practices, and avoiding consumption of foods of unknown purity. A recombinant subunit vaccine demonstrated efficacy against HEV infection. However, no vaccine is commercially available yet for this infection, except in China.



## CONCLUSION

The neurologic manifestations of HEV infection are increasingly recognized worldwide, especially in Europe and Southeast Asia. Nerve root and plexus disorder (NA and GBS) are the most commonly reported diseases followed by meningo-encephalitis. NA, GBS, and meningoencephalitis appear to be causally associated with HEV-infection. Further, GT3 is the most common GT identified in these patients. The majority of patients present without jaundice. However, the absence of jaundice and normal LFTs can mislead the physician. Thus, detailed neurological evaluation is warranted in patients with HEV infection and neurological symptoms. Patients with neurological disorders and deranged LFTs require further investigation to diagnose HEV infection. Testing for HEV in patients with neurological disorders and unexplained etiology can also be rewarding. Finally, there is no sufficient evidence of routine use of an anti-viral agent in HEV-related neurological disorders.

## REFERENCES

- 1 **Purdy MA**, Harrison TJ, Jameel S, Meng XJ, Okamoto H, Van der Poel WHM, Smith DB; Ictv Report Consortium. ICTV Virus Taxonomy Profile: Hepeviridae. *J Gen Virol* 2017; **98**: 2645-2646 [PMID: 29022866 DOI: 10.1099/jgv.0.000940]
- 2 **Li P**, Liu J, Li Y, Su J, Ma Z, Bramer WM, Cao W, de Man RA, Peppelenbosch MP, Pan Q. The global epidemiology of hepatitis E virus infection: A systematic review and meta-analysis. *Liver Int* 2020; **40**: 1516-1528 [PMID: 32281721 DOI: 10.1111/liv.14468]
- 3 **World Health Organization**. Viral hepatitis in the WHO South-East Asia Region. [cited 15 November 2020]. In: World Health Organization [Internet]. Available from: <https://apps.who.int/iris/handle/10665/206521>
- 4 **Kamar N**, Selves J, Mansuy JM, Ouezzani L, Péron JM, Guitard J, Cointault O, Esposito L, Abravanel F, Danjoux M, Durand D, Vinel JP, Izopet J, Rostaing L. Hepatitis E virus and chronic hepatitis in organ-transplant recipients. *N Engl J Med* 2008; **358**: 811-817 [PMID: 18287603 DOI: 10.1056/NEJMoa0706992]
- 5 **European Association for the Study of the Liver**. EASL Clinical Practice Guidelines on hepatitis E virus infection. *J Hepatol* 2018; **68**: 1256-1271 [PMID: 29609832 DOI: 10.1016/j.jhep.2018.03.005]
- 6 **Jha AK**, Nijhawan S, Rai RR, Nepalia S, Jain P, Suchismita A. Etiology, clinical profile, and inhospital mortality of acute-on-chronic liver failure: a prospective study. *Indian J Gastroenterol* 2013; **32**: 108-114 [PMID: 23526372 DOI: 10.1007/s12664-012-0295-9]
- 7 **Kumar A**, Aggarwal R, Naik SR, Saraswat V, Ghoshal UC, Naik S. Hepatitis E virus is responsible for decompensation of chronic liver disease in an endemic region. *Indian J Gastroenterol* 2004; **23**: 59-62 [PMID: 15176538]
- 8 **Rawla P**, Raj JP, Kannemkuzhiyil AJ, Aluru JS, Thandra KC, Gajendran M. A Systematic Review of the Extra-Hepatic Manifestations of Hepatitis E Virus Infection. *Med Sci (Basel)* 2020; **8** [PMID: 32033102 DOI: 10.3390/medsci8010009]
- 9 **Pischke S**, Hartl J, Pas SD, Lohse AW, Jacobs BC, Van der Eijk AA. Hepatitis E virus: Infection beyond the liver? *J Hepatol* 2017; **66**: 1082-1095 [PMID: 27913223 DOI: 10.1016/j.jhep.2016.11.016]
- 10 **Feng Z**. Causation by HEV of extrahepatic manifestations remains unproven. *Liver Int* 2016; **36**: 477-479 [PMID: 27005694 DOI: 10.1111/liv.13085]
- 11 **Zhou X**, Huang F, Xu L, Lin Z, de Vrij FMS, Ayo-Martin AC, van der Kroeg M, Zhao M, Yin Y, Wang W, Cao W, Wang Y, Kushner SA, Marie Peron J, Alric L, de Man RA, Jacobs BC, van Eijk JJ, Aronica EMA, Sprengers D, Metselaar HJ, de Zeeuw CI, Dalton HR, Kamar N, Peppelenbosch MP, Pan Q. Hepatitis E Virus Infects Neurons and Brains. *J Infect Dis* 2017; **215**: 1197-1206 [PMID: 28199701 DOI: 10.1093/infdis/jix079]
- 12 **Drave SA**, Debing Y, Walter S, Todt D, Engelmann M, Friesland M, Wedemeyer H, Neyts J, Behrendt P, Steinmann E. Extra-hepatic replication and infection of hepatitis E virus in neuronal-derived cells. *J Viral Hepat* 2016; **23**: 512-521 [PMID: 26891712 DOI: 10.1111/jvh.12515]
- 13 **Abravanel F**, Pique J, Couturier E, Nicot F, Dimeglio C, Lhomme S, Chiabrando J, Saune K, Péron JM, Kamar N, Evrard S, de Valk H, Cintas P, Izopet J; HEV study group. Acute hepatitis E in French patients and neurological manifestations. *J Infect* 2018; **77**: 220-226 [PMID: 29966614 DOI: 10.1016/j.jinf.2018.06.007]
- 14 **Ripellino P**, Pasi E, Melli G, Staedler C, Fraga M, Moradpour D, Sahli R, Aubert V, Martinetti G, Bihl F, Bernasconi E, Terziroli Beretta-Piccoli B, Cerny A, Dalton HR, Zehnder C, Mathis B, Zecca C, Disanto G, Kaelin-Lang A, Gobbi C. Neurologic complications of acute hepatitis E virus infection. *Neurol Neuroimmunol Neuroinflamm* 2020; **7** [PMID: 31806684 DOI: 10.1212/NXI.0000000000000643]
- 15 **Kamar N**, Bendall RP, Peron JM, Cintas P, Prudhomme L, Mansuy JM, Rostaing L, Keane F, Ijaz S, Izopet J, Dalton HR. Hepatitis E virus and neurologic disorders. *Emerg Infect Dis* 2011; **17**: 173-179 [PMID: 21291585 DOI: 10.3201/eid1702.100856]

- 16 **Woolson KL**, Forbes A, Vine L, Beynon L, McElhinney L, Panayi V, Hunter JG, Madden RG, Glasgow T, Kotecha A, Dalton HC, Mihailescu L, Warshow U, Hussaini HS, Palmer J, Mclean BN, Haywood B, Bendall RP, Dalton HR. Extra-hepatic manifestations of autochthonous hepatitis E infection. *Aliment Pharmacol Ther* 2014; **40**: 1282-1291 [PMID: [25303615](#) DOI: [10.1111/apt.12986](#)]
- 17 **Dalton HR**, van Eijk JJJ, Cintas P, Madden RG, Jones C, Webb GW, Norton B, Pique J, Lutgens S, Devooght-Johnson N, Woolson K, Baker J, Saunders M, Househam L, Griffiths J, Abravanel F, Izopet J, Kamar N, van Alfen N, van Engelen BGM, Hunter JG, van der Eijk AA, Bendall RP, Mclean BN, Jacobs BC. Hepatitis E virus infection and acute non-traumatic neurological injury: A prospective multicentre study. *J Hepatol* 2017; **67**: 925-932 [PMID: [28734938](#) DOI: [10.1016/j.jhep.2017.07.010](#)]
- 18 **Belbézier A**, Deroux A, Sarrot-Reynaud F, Colombe B, Bosseray A, Wintenberger C, Dumanoir P, Lugosi M, Boccon-Gibod I, Leroy V, Maignan M, Collomb-Muret R, Viglino D, Vaillant M, Minotti L, Lagrange E, Epaulard O, Dumestre-Perard C, Lhomme S, Lupo J, Larrat S, Morand P, Schwebel C, Vilotitch A, Bosson JL, Bouillet L. Screening of hepatitis E in patients presenting for acute neurological disorders. *J Infect Public Health* 2020; **13**: 1047-1050 [PMID: [32224109](#) DOI: [10.1016/j.jiph.2019.12.012](#)]
- 19 **Mansuy JM**, Gallian P, Dimeglio C, Saune K, Arnaud C, Pelletier B, Morel P, Legrand D, Tiberghien P, Izopet J. A nationwide survey of hepatitis E viral infection in French blood donors. *Hepatology* 2016; **63**: 1145-1154 [PMID: [27008201](#) DOI: [10.1002/hep.28436](#)]
- 20 **Wang Y**, Wang S, Wu J, Jiang Y, Zhang H, Li S, Liu H, Yang C, Tang H, Guo N, Peppelenbosch MP, Wei L, Pan Q, Zhao J. Hepatitis E virus infection in acute non-traumatic neuropathy: A large prospective case-control study in China. *EBioMedicine* 2018; **36**: 122-130 [PMID: [30190208](#) DOI: [10.1016/j.ebiom.2018.08.053](#)]
- 21 **Adinolfi LE**, Nevola R, Lus G, Restivo L, Guerrera B, Romano C, Zampino R, Rinaldi L, Sellitto A, Giordano M, Marrone A. Chronic hepatitis C virus infection and neurological and psychiatric disorders: an overview. *World J Gastroenterol* 2015; **21**: 2269-2280 [PMID: [25741133](#) DOI: [10.3748/wjg.v21.i8.2269](#)]
- 22 **Mapoure NY**, Budzi MN, Eloumou SAFB, Malongue A, Okalla C, Luma HN. Neurological manifestations in chronic hepatitis C patients receiving care in a reference hospital in sub-Saharan Africa: A cross-sectional study. *PLoS One* 2018; **13**: e0192406 [PMID: [29513678](#) DOI: [10.1371/journal.pone.0192406](#)]
- 23 **Menon D**, Jagtap SA, Nair MD. Guillain-Barré syndrome following acute viral hepatitis A. *J Neurosci Rural Pract* 2014; **5**: 204-205 [PMID: [24966576](#) DOI: [10.4103/0976-3147.131695](#)]
- 24 **Lee JJ**, Kang K, Park JM, Kwon O, Kim BK. Encephalitis associated with acute hepatitis a. *J Epilepsy Res* 2011; **1**: 27-28 [PMID: [24649441](#) DOI: [10.14581/jer.11005](#)]
- 25 **Chonmaitree P**, Methawasiri K. Transverse Myelitis in Acute Hepatitis A Infection: The Rare Co-Occurrence of Hepatology and Neurology. *Case Rep Gastroenterol* 2016; **10**: 44-49 [PMID: [27403101](#) DOI: [10.1159/000444013](#)]
- 26 **Kappus MR**, Sterling RK. Extrahepatic manifestations of acute hepatitis B virus infection. *Gastroenterol Hepatol (N Y)* 2013; **9**: 123-126 [PMID: [23983659](#)]
- 27 **van Alfen N**, van Engelen BG. The clinical spectrum of neuralgic amyotrophy in 246 cases. *Brain* 2006; **129**: 438-450 [PMID: [16371410](#) DOI: [10.1093/brain/awh722](#)]
- 28 **van Eijk JJ**, Madden RG, van der Eijk AA, Hunter JG, Reimerink JH, Bendall RP, Pas SD, Ellis V, van Alfen N, Beynon L, Southwell L, McLean B, Jacobs BC, van Engelen BG, Dalton HR. Neuralgic amyotrophy and hepatitis E virus infection. *Neurology* 2014; **82**: 498-503 [PMID: [24401685](#) DOI: [10.1212/WNL.0000000000000112](#)]
- 29 **van Eijk JJJ**, Dalton HR, Ripellino P, Madden RG, Jones C, Fritz M, Gobbi C, Melli G, Pasi E, Herrod J, Lissmann RF, Ashraf HH, Abdelrahim M, Masri OABAL, Fraga M, Benninger D, Kuntzer T, Aubert V, Sahli R, Moradpour D, Blasco-Perrin H, Attarian S, Gérolami R, Colson P, Giordani MT, Hartl J, Pischke S, Lin NX, Mclean BN, Bendall RP, Panning M, Peron JM, Kamar N, Izopet J, Jacobs BC, van Alfen N, van Engelen BGM. Clinical phenotype and outcome of hepatitis E virus-associated neuralgic amyotrophy. *Neurology* 2017; **89**: 909-917 [PMID: [28768846](#) DOI: [10.1212/WNL.0000000000004297](#)]
- 30 **Fong F**, Illahi M. Neuralgic amyotrophy associated with hepatitis E virus. *Clin Neurol Neurosurg* 2009; **111**: 193-195 [PMID: [18986757](#) DOI: [10.1016/j.clineuro.2008.09.005](#)]
- 31 **Rianthavorn P**, Thongmee C, Limpaphayom N, Komolmit P, Theamboonlers A, Poovorawan Y. The entire genome sequence of hepatitis E virus genotype 3 isolated from a patient with neuralgic amyotrophy. *Scand J Infect Dis* 2010; **42**: 395-400 [PMID: [20100114](#) DOI: [10.3109/00365540903496551](#)]
- 32 **Carli P**, Landais C, Poisnel E, Cournac JM, Aletti M, Paris JF, Martinez V. [Shoulder pain in a 30-year-old man]. *Rev Med Interne* 2012; **33**: 111-114 [PMID: [22192515](#) DOI: [10.1016/j.revmed.2011.11.004](#)]
- 33 **Moisset X**, Vitello N, Bicilli E, Courtin R, Ferrier A, Taithe F, Lahaye C, Hssain AA, Garrouste C, Pierre C. Severe bilateral amyotrophic neuralgia associated with major dysphagia secondary to acute hepatitis E. *F1000Res* 2013; **2**: 259 [PMID: [24555112](#) DOI: [10.12688/f1000research.2-259.v2](#)]
- 34 **Motte A**, Franques J, Weitten T, Colson P. Hepatitis E-associated Parsonage-Turner syndrome, France. *Clin Res Hepatol Gastroenterol* 2014; **38**: e11-e14 [PMID: [24246798](#) DOI: [10.1016/j.clinre.2013.08.011](#)]
- 35 **Deroux A**, Brion JP, Hyerle L, Belbezier A, Vaillant M, Mosnier E, Larrat S, Morand P, Pavese P.

- Association between hepatitis E and neurological disorders: two case studies and literature review. *J Clin Virol* 2014; **60**: 60-62 [PMID: 24583064 DOI: 10.1016/j.jcv.2014.01.026]
- 36 **Perrin HB**, Cintas P, Abravanel F, G  rolami R, d'Altoche L, Raynal JN, Alric L, Dupuis E, Prudhomme L, Vaucher E, Couzigou P, Liversain JM, Bureau C, Vinel JP, Kamar N, Izopet J, Peron JM. Neurologic Disorders in Immunocompetent Patients with Autochthonous Acute Hepatitis E. *Emerg Infect Dis* 2015; **21**: 1928-1934 [PMID: 26490255 DOI: 10.3201/eid2111.141789]
- 37 **D  card BF**, Grimm A, Andelova M, Deman A, Banderet B, Garcia M, Fuhr P. Hepatitis-E virus associated neuralgic amyotrophy with sustained plexus brachialis swelling visualized by high-resolution ultrasound. *J Neurol Sci* 2015; **351**: 208-210 [PMID: 25769655 DOI: 10.1016/j.jns.2015.03.003]
- 38 **Theochari E**, Vincent-Smith L, Ellis C. Neuralgic amyotrophy complicating acute hepatitis E infection: a rare association. *BMJ Case Rep* 2015; **2015** [PMID: 25739795 DOI: 10.1136/bcr-2014-207669]
- 39 **Mart  nez Rodr  guez L**, Carvajal P, Mor  s G. [Neuralgic amyotrophy associated to hepatitis E virus infection]. *Med Clin (Barc)* 2015; **145**: 462-463 [PMID: 25817452 DOI: 10.1016/j.medcli.2015.01.021]
- 40 **Dartevel A**, Colombe B, Bosseray A, Larrat S, Sarrot-Reynauld F, Belbezier A, Lagrange E, Bouillet L. Hepatitis E and neuralgic amyotrophy: Five cases and review of literature. *J Clin Virol* 2015; **69**: 156-164 [PMID: 26209399 DOI: 10.1016/j.jcv.2015.06.091]
- 41 **Avila JD**, Lacomis D, Lam EM. Neuralgic Amyotrophy Associated With Hepatitis E Virus Infection: First Case in the United States. *J Clin Neuromuscul Dis* 2016; **18**: 96-100 [PMID: 27861224 DOI: 10.1097/CND.0000000000000137]
- 42 **Silva M**, Wicki B, Tsouni P, Cunningham S, Doerig C, Zanetti G, Aubert V, Sahli R, Moradpour D, Kuntzer T. Hepatitis E virus infection as a direct cause of neuralgic amyotrophy. *Muscle Nerve* 2016; **54**: 325-327 [PMID: 26939568 DOI: 10.1002/mus.25096]
- 43 **Altuna-Azkargorta M**, Torne-Hernandez L, Aznar-Gomez P, Ibricu-Yanguas MA, Ducouret A. [Infection by the hepatitis E virus as a precipitating factor of Parsonage-Turner syndrome]. *Rev Neurol* 2016; **62**: 572-574 [PMID: 27270680]
- 44 **Pischke S**, Ryll U, De Weerth A, Ufer F, Gelderblom M. [Neuralgic amyotrophy: an extrahepatic manifestation of hepatitis E]. *Dtsch Med Wochenschr* 2016; **141**: 1239-1242 [PMID: 27557071 DOI: 10.1055/s-0042-102289]
- 45 **Bisciglia M**, Van den Bergh P, Duprez T, Kabamba BM, Ivanoiu A. Neuralgic amyotrophy associated with hepatitis E virus (HEV) infection: a case report. *Acta Neurol Belg* 2017; **117**: 555-557 [PMID: 27095100 DOI: 10.1007/s13760-016-0642-1]
- 46 **Velay A**, Kack-Kack W, Abravanel F, Lhomme S, Leyendecker P, Kremer L, Chamouard P, Izopet J, Fafi-Kremer S, Barth H. Parsonage-Turner syndrome due to autochthonous acute genotype 3f hepatitis E virus infection in a nonimmunocompromised 55-year-old patient. *J Neurovirol* 2017; **23**: 615-620 [PMID: 28439773 DOI: 10.1007/s13365-017-0525-0]
- 47 **Scanvion Q**, Perez T, Cassim F, Outterryck O, Lanteri A, Hatron PY, Lambert M, Morell-Dubois S. Neuralgic amyotrophy triggered by hepatitis E virus: a particular phenotype. *J Neurol* 2017; **264**: 770-780 [PMID: 28247042 DOI: 10.1007/s00415-017-8433-z]
- 48 **Fraga M**, Doerig C, Moulin H, Bihl F, Brunner F, M  llhaupt B, Ripellino P, Semela D, Stickel F, Terziroli Beretta-Piccoli B, Aubert V, Telenti A, Greub G, Sahli R, Moradpour D. Hepatitis E virus as a cause of acute hepatitis acquired in Switzerland. *Liver Int* 2018; **38**: 619-626 [PMID: 28834649 DOI: 10.1111/liv.13557]
- 49 **Fritz M**, Berger B, Schemmerer M, Endres D, Wenzel JJ, Stich O, Panning M. Pathological Cerebrospinal Fluid Findings in Patients With Neuralgic Amyotrophy and Acute Hepatitis E Virus Infection. *J Infect Dis* 2018; **217**: 1897-1901 [PMID: 29547884 DOI: 10.1093/infdis/jiy128]
- 50 **S  nchez Azofra M**, Romero Portales M, Tortajada Laureiro L, Garc  a-Samaniego J, Mora Sanz P. Hepatitis E virus in neurological disorders: a case of Parsonage-Turner syndrome. *Rev Esp Enferm Dig* 2018; **110**: 402-403 [PMID: 29685043 DOI: 10.17235/reed.2018.5506/2018]
- 51 **Njabom CN**, Gilbert A, Brasseur E, Zandona R, Ghuysen A, D'Orio V. Parsonage-Turner Syndrome as a Rare Extrahepatic Complication of Hepatitis E Infection. *Eur J Case Rep Intern Med* 2019; **6**: 001208 [PMID: 31508389 DOI: 10.12890/2019\_001208]
- 52 **Ar  nyi Z**, Szpisjak L, Sz  ke K. Multiphasic presentation of neuralgic amyotrophy associated with hepatitis E virus infection. *Muscle Nerve* 2020; **61**: 108-110 [PMID: 31573093 DOI: 10.1002/mus.26722]
- 53 **Mendoza-Lopez C**, Lopez-Lopez P, Atienza-Ayala S, Rivero-Juarez A, Benito R. Parsonage-Turner syndrome associated with hepatitis E infection in immunocompetent patients. *Virus Res* 2020; **290**: 198165 [PMID: 33007343 DOI: 10.1016/j.virusres.2020.198165]
- 54 **Inghilleri ML**, Grini Mazouzi M, Juntas Morales R. [Neuralgic amyotrophy as a manifestation of hepatitis E infection]. *Rev Neurol (Paris)* 2012; **168**: 383-384 [PMID: 22398219 DOI: 10.1016/j.neurol.2011.07.014]
- 55 **Diebold M**, Fischer-Barnicol B, Tsagkas C, Kuhle J, Kappos L, Derfuss T, D  card BF. Hepatitis E virus infections in patients with MS on oral disease-modifying treatment. *Neurol Neuroimmunol Neuroinflamm* 2019; **6** [PMID: 31454772 DOI: 10.1212/NXI.0000000000000594]
- 56 **Cheung MC**, Maguire J, Carey I, Wendon J, Agarwal K. Review of the neurological manifestations of hepatitis E infection. *Ann Hepatol* 2012; **11**: 618-622 [PMID: 22947521]
- 57 **van den Berg B**, Walgaard C, Drenthen J, Fokke C, Jacobs BC, van Doorn PA. Guillain-Barr  

- syndrome: pathogenesis, diagnosis, treatment and prognosis. *Nat Rev Neurol* 2014; **10**: 469-482 [PMID: 25023340 DOI: 10.1038/nrneurol.2014.121]
- 58 **Stevens O**, Claeys KG, Poesen K, Saegeman V, Van Damme P. Diagnostic Challenges and Clinical Characteristics of Hepatitis E Virus-Associated Guillain-Barré Syndrome. *JAMA Neurol* 2017; **74**: 26-33 [PMID: 27820624 DOI: 10.1001/jamaneurol.2016.3541]
  - 59 **van den Berg B**, van der Eijk AA, Pas SD, Hunter JG, Madden RG, Tio-Gillen AP, Dalton HR, Jacobs BC. Guillain-Barré syndrome associated with preceding hepatitis E virus infection. *Neurology* 2014; **82**: 491-497 [PMID: 24415572 DOI: 10.1212/WNL.0000000000000111]
  - 60 **Fukae J**, Tsugawa J, Ouma S, Umezu T, Kusunoki S, Tsuboi Y. Guillain-Barré and Miller Fisher syndromes in patients with anti-hepatitis E virus antibody: a hospital-based survey in Japan. *Neurol Sci* 2016; **37**: 1849-1851 [PMID: 27389141 DOI: 10.1007/s10072-016-2644-4]
  - 61 **Geurtsvankessel CH**, Islam Z, Mohammad QD, Jacobs BC, Endtz HP, Osterhaus AD. Hepatitis E and Guillain-Barre syndrome. *Clin Infect Dis* 2013; **57**: 1369-1370 [PMID: 23899686 DOI: 10.1093/cid/cit512]
  - 62 **Sood A**, Midha V, Sood N. Guillain-Barré syndrome with acute hepatitis E. *Am J Gastroenterol* 2000; **95**: 3667-3668 [PMID: 11151929 DOI: 10.1111/j.1572-0241.2000.03409.x]
  - 63 **Kamani P**, Baijal R, Amarapurkar D, Gupte P, Patel N, Kumar P, Agal S. Guillain-Barre syndrome associated with acute hepatitis E. *Indian J Gastroenterol* 2005; **24**: 216 [PMID: 16361768]
  - 64 **Khanam R**, Faruq M, Basunia R, Ahsan A. Guillain-Barré Syndrome Associated with Acute HEV Hepatitis. *IMCJ* 2008; **2**: 32-34 [DOI: 10.3329/imcj.v2i1.2930]
  - 65 **Loly JP**, Rikir E, Seivert M, Legros E, Defrance P, Belaiche J, Moonen G, Delwaide J. Guillain-Barré syndrome following hepatitis E. *World J Gastroenterol* 2009; **15**: 1645-1647 [PMID: 19340910 DOI: 10.3748/wjg.15.1645]
  - 66 **Cronin S**, McNicholas R, Kavanagh E, Reid V, O'Rourke K. Anti-glycolipid GM2-positive Guillain-Barre syndrome due to hepatitis E infection. *Ir J Med Sci* 2011; **180**: 255-257 [PMID: 21063804 DOI: 10.1007/s11845-010-0635-7]
  - 67 **Maurissen I**, Jeurissen A, Strauven T, Sprengers D, De Schepper B. First case of anti-ganglioside GM1-positive Guillain-Barré syndrome due to hepatitis E virus infection. *Infection* 2012; **40**: 323-326 [PMID: 21877179 DOI: 10.1007/s15010-011-0185-6]
  - 68 **Del Bello A**, Arné-Bes MC, Lavayssière L, Kamar N. Hepatitis E virus-induced severe myositis. *J Hepatol* 2012; **57**: 1152-1153 [PMID: 22641093 DOI: 10.1016/j.jhep.2012.05.010]
  - 69 **Tse AC**, Cheung RT, Ho SL, Chan KH. Guillain-Barré syndrome associated with acute hepatitis E infection. *J Clin Neurosci* 2012; **19**: 607-608 [PMID: 22285113 DOI: 10.1016/j.jocn.2011.06.024]
  - 70 **Santos L**, Mesquita JR, Rocha Pereira N, Lima-Alves C, Serrão R, Figueiredo P, Reis J, Simões J, Nascimento M, Sarmento A. Acute hepatitis E complicated by Guillain-Barre syndrome in Portugal, December 2012--a case report. *Euro Surveill* 2013; **18** [PMID: 23987830 DOI: 10.2807/1560-7917.es2013.18.34.20563]
  - 71 **Sharma B**, Nagpal K, Bakki Sannegowda R, Prakash S. Hepatitis E with Gullain-Barré syndrome: still a rare association. *J Neurovirol* 2013; **19**: 186-187 [PMID: 23471727 DOI: 10.1007/s13365-013-0156-z]
  - 72 **Chen XD**, Zhou YT, Zhou JJ, Wang YW, Tong DM. Guillain-Barré syndrome and encephalitis/encephalopathy of a rare case of Northern China acute severe hepatitis E infection. *Neurol Sci* 2014; **35**: 1461-1463 [PMID: 24700050 DOI: 10.1007/s10072-014-1731-7]
  - 73 **Scharn N**, Ganzenmueller T, Wenzel JJ, Dengler R, Heim A, Wegner F. Guillain-Barré syndrome associated with autochthonous infection by hepatitis E virus subgenotype 3c. *Infection* 2014; **42**: 171-173 [PMID: 23512540 DOI: 10.1007/s15010-013-0448-5]
  - 74 **Comont T**, Bonnet D, Sigur N, Gerdelat A, Legrand-Abravanel F, Kamar N, Alric L. [Acute hepatitis E infection associated with Guillain-Barré syndrome in an immunocompetent patient]. *Rev Med Interne* 2014; **35**: 333-336 [PMID: 24080239 DOI: 10.1016/j.revmed.2013.05.005]
  - 75 **Bandyopadhyay D**, Ganesan V, Choudhury C, Kar SS, Karmakar P, Choudhary V, Banerjee P, Bhar D, Hajra A, Layek M, Mukhopadhyay S. Two Uncommon Causes of Guillain-Barré Syndrome: Hepatitis E and Japanese Encephalitis. *Case Rep Neurol Med* 2015; **2015**: 759495 [PMID: 26798531 DOI: 10.1155/2015/759495]
  - 76 **Higuchi MA**, Fukae J, Tsugawa J, Ouma S, Takahashi K, Mishihiro S, Tsuboi Y. Dysgeusia in a Patient with Guillain-Barré Syndrome Associated with Acute Hepatitis E: A Case Report and Literature Review. *Intern Med* 2015; **54**: 1543-1546 [PMID: 26073247 DOI: 10.2169/internalmedicine.54.3506]
  - 77 **Ji SB**, Lee SS, Jung HC, Kim HJ, Kim TH, Jung WT, Lee OJ, Song DH. A Korean patient with Guillain-Barré syndrome following acute hepatitis E whose cholestasis resolved with steroid therapy. *Clin Mol Hepatol* 2016; **22**: 396-399 [PMID: 27572076 DOI: 10.3350/cmh.2015.0039]
  - 78 **Lei JH**, Tian Y, Luo HY, Chen Z, Peng F. Guillain-Barré syndrome following acute co-super-infection of hepatitis E virus and cytomegalovirus in a chronic hepatitis B virus carrier. *J Med Virol* 2017; **89**: 368-372 [PMID: 27358107 DOI: 10.1002/jmv.24620]
  - 79 **Salim OJ**, Davidson A, Li K, Leach JP, Heath C. Brainstem encephalitis and acute polyneuropathy associated with hepatitis E infection. *BMJ Case Rep* 2017; **2017** [PMID: 28899886 DOI: 10.1136/bcr-2017-220799]
  - 80 **Troussière AC**, Sudaveschi V, Collardelle P, Marque Juliette S, Servan J, Pico F. Guillain-Barré syndrome due to hepatitis E. *Rev Neurol (Paris)* 2018; **174**: 72-74 [PMID: 29132643 DOI: 10.1016/j.neurol.2017.06.018]



- 81 **Zheng X**, Yu L, Xu Q, Gu S, Tang L. Guillain-Barre syndrome caused by hepatitis E infection: case report and literature review. *BMC Infect Dis* 2018; **18**: 50 [PMID: [29357816](#) DOI: [10.1186/s12879-018-2959-2](#)]
- 82 **Choudhary MC**, Bajpai V, Anand L, Gupta E. Guillain-Barré syndrome in a patient of acute Hepatitis E virus infection associated with genotype 1: Case report and literature review. *Intractable Rare Dis Res* 2019; **8**: 43-47 [PMID: [30881857](#) DOI: [10.5582/irdr.2018.01099](#)]
- 83 **Kumar R**, Bhoi S, Kumar M, Sharma B, Singh BM, Gupta BB. Guillain-Barré syndrome and acute hepatitis E: A rare association. *JLACM* 2002; **4**: 389-391
- 84 **Oh HW**, Cha RR, Lee SS, Lee CM, Kim WS, Jo YW, Kim JJ, Lee JM, Kim HJ, Ha CY, Kim TH, Jung WT, Lee OJ. Comparing the Clinical Features and Outcomes of Acute Hepatitis E Viral Infections with Those of Acute Hepatitis A, B, and C Infections in Korea. *Intervirology* 2017; **60**: 109-117 [PMID: [29145204](#) DOI: [10.1159/000480506](#)]
- 85 **Al-Saffar A**, Al-Fatly B. Acute Motor Axonal Neuropathy in Association with Hepatitis E. *Front Neurol* 2018; **9**: 62 [PMID: [29479336](#) DOI: [10.3389/fneur.2018.00062](#)]
- 86 **Pasha SA**, Pasha SA, Suhasini T, Rao DA. Hepatitis E Virus-Associated Acute Encephalitic Parkinsonism. *J Assoc Physicians India* 2018; **66**: 92-93 [PMID: [30341882](#)]
- 87 **Murkey JA**, Chew KW, Carlson M, Shannon CL, Sirohi D, Sample HA, Wilson MR, Vespa P, Humphries RM, Miller S, Klausner JD, Chiu CY. Hepatitis E Virus-Associated Meningoencephalitis in a Lung Transplant Recipient Diagnosed by Clinical Metagenomic Sequencing. *Open Forum Infect Dis* 2017; **4**: ofx121 [PMID: [28721353](#) DOI: [10.1093/ofid/ofx121](#)]
- 88 **Sarkar P**, Morgan C, Ijaz S. Transverse myelitis caused by hepatitis E: previously undescribed in adults. *BMJ Case Rep* 2015; **2015** [PMID: [26150621](#) DOI: [10.1136/bcr-2014-209031](#)]
- 89 **Bennett S**, Li K, Gunson RN. Hepatitis E virus infection presenting with paraesthesia. *Scott Med J* 2015; **60**: e27-e29 [PMID: [25663032](#) DOI: [10.1177/0036933015572093](#)]
- 90 **Dixit VK**, Abhilash VB, Kate MP, Jain AK. Hepatitis E infection with Bell's palsy. *J Assoc Physicians India* 2006; **54**: 418 [PMID: [16909746](#)]
- 91 **Jha AK**, Nijhawan S, Nepalia S, Suchismita A. Association of Bell's Palsy with Hepatitis E Virus Infection: A Rare Entity. *J Clin Exp Hepatol* 2012; **2**: 88-90 [PMID: [25755411](#) DOI: [10.1016/S0973-6883\(12\)60082-6](#)]
- 92 **Yazaki Y**, Sugawara K, Honda M, Ohnishi H, Nagashima S, Takahashi M, Okamoto H. Characteristics of 20 Patients with Autochthonous Acute Hepatitis E in Hokkaido, Japan: First Report of Bilateral Facial Palsy Following the Infection with Genotype 4 Hepatitis E Virus. *Tohoku J Exp Med* 2015; **236**: 263-271 [PMID: [26228039](#) DOI: [10.1620/tjem.236.263](#)]
- 93 **Mengel AM**, Stenzel W, Meisel A, Büning C. Hepatitis E-induced severe myositis. *Muscle Nerve* 2016; **53**: 317-320 [PMID: [26514272](#) DOI: [10.1002/mus.24959](#)]
- 94 **Despieres LA**, Kaphan E, Attarian S, Cohen-Bacrie S, Pelletier J, Pouget J, Motte A, Charrel R, Gerolami R, Colson P. Neurologic disorders and hepatitis E, France, 2010. *Emerg Infect Dis* 2011; **17**: 1510-1512 [PMID: [21801637](#) DOI: [10.3201/eid1708.102028](#)]
- 95 **Belliere J**, Abravanel F, Nogier MB, Martinez S, Cintas P, Lhomme S, Lavayssière L, Cointault O, Faguer S, Izopet J, Kamar N. Transfusion-acquired hepatitis E infection misdiagnosed as severe critical illness polyneuropathy in a heart transplant patient. *Transpl Infect Dis* 2017; **19** [PMID: [28963742](#) DOI: [10.1111/tid.12784](#)]
- 96 **Péron JM**, Dalton H, Izopet J, Kamar N. Acute autochthonous hepatitis E in western patients with underlying chronic liver disease: a role for ribavirin? *J Hepatol* 2011; **54**: 1323-4; author reply 1324 [PMID: [21281681](#) DOI: [10.1016/j.jhep.2011.01.009](#)]
- 97 **Hill AB**. The environment and disease: Association or causation? *Proc R Soc Med* 1965; **58**: 295-300 [PMID: [14283879](#)]





## Stroma-targeting strategies in pancreatic cancer: Past lessons, challenges and prospects

Faran Polani, Patrick M Grierson, Kian-Huat Lim

**ORCID number:** Faran Polani 0000-0002-7663-4793; Patrick M Grierson 0000-0002-0624-6699; Kian-Huat Lim 0000-0002-2766-200X.

**Author contributions:** Polani F, Grierson P and Lim KH contributed to the concepts, performed literature review, drafted the manuscript, and approved the final manuscript; Polani F and Lim KH drew the figure using BioRender.

**Supported by** National Institutes of Health/National Cancer Institute, No. 5R37CA219697-01 (to Lim KH); American Cancer Society, No. RSG-17-203-01-TBG (to Lim KH); and Alvin J. Siteman Cancer Center Siteman Investment Program (from Barnard Trust and The Foundation for Barnes-Jewish Hospital) (to Lim KH); and Emerson Collective Grant (to Grierson PM).

**Conflict-of-interest statement:** The authors have declared no conflict of interests.

**Open-Access:** This article is an open-access article that was selected by an in-house editor and fully peer-reviewed by external reviewers. It is distributed in accordance with the Creative Commons Attribution NonCommercial (CC BY-NC 4.0) license, which permits others to distribute, remix, adapt, build

**Faran Polani, Patrick M Grierson, Kian-Huat Lim**, Division of Oncology, Department of Internal Medicine, Barnes-Jewish Hospital and The Alvin J. Siteman Comprehensive Cancer Center, Washington University School of Medicine, Saint Louis, MO 63110, United States

**Corresponding author:** Kian-Huat Lim, MD, PhD, Associate Professor, Division of Oncology, Department of Internal Medicine, Barnes-Jewish Hospital and The Alvin J. Siteman Comprehensive Cancer Center, Washington University School of Medicine, 660 South Euclid Avenue, Saint Louis, MO 63110, United States. [klim@dom.wustl.edu](mailto:klim@dom.wustl.edu)

### Abstract

Pancreatic ductal adenocarcinoma (PDAC) is projected to emerge as the second leading cause of cancer-related death after 2030. Extreme treatment resistance is perhaps the most significant factor that underlies the poor prognosis of PDAC. To date, combination chemotherapy remains the mainstay of treatment for most PDAC patients. Compared to other cancer types, treatment response of PDAC tumors to similar chemotherapy regimens is clearly much lower and shorter-lived. Aside from typically harboring genetic alterations that to date remain undruggable and are drivers of treatment resistance, PDAC tumors are uniquely characterized by a densely fibrotic stroma that has well-established roles in promoting cancer progression and treatment resistance. However, emerging evidence also suggests that indiscriminate targeting and near complete depletion of stroma may promote PDAC aggressiveness and lead to detrimental outcomes. These conflicting results undoubtedly warrant the need for a more in-depth understanding of the heterogeneity of tumor stroma in order to develop modulatory strategies in favor of tumor suppression. The advent of novel techniques including single cell RNA sequencing and multiplex immunohistochemistry have further illuminated the complex heterogeneity of tumor cells, stromal fibroblasts, and immune cells. This new knowledge is instrumental for development of more refined therapeutic strategies that can ultimately defeat this disease. Here, we provide a concise review on lessons learned from past stroma-targeting strategies, new challenges revealed from recent preclinical and clinical studies, as well as new prospects in the treatment of PDAC.

**Key Words:** Stroma; Pancreatic cancer; Treatment resistance; Cancer-associated fibroblasts; Clinical trials

©The Author(s) 2021. Published by Baishideng Publishing Group Inc. All rights reserved.

upon this work non-commercially, and license their derivative works on different terms, provided the original work is properly cited and the use is non-commercial. See: <http://creativecommons.org/licenses/by-nc/4.0/>

**Manuscript source:** Invited manuscript

**Specialty type:** Gastroenterology and hepatology

**Country/Territory of origin:** United States

**Peer-review report's scientific quality classification**

Grade A (Excellent): 0  
Grade B (Very good): B, B  
Grade C (Good): 0  
Grade D (Fair): 0  
Grade E (Poor): 0

**Received:** January 8, 2021

**Peer-review started:** January 8, 2021

**First decision:** February 23, 2021

**Revised:** March 9, 2021

**Accepted:** April 21, 2021

**Article in press:** April 21, 2021

**Published online:** May 14, 2021

**P-Reviewer:** Chen I, Yamada T

**S-Editor:** Gao CC

**L-Editor:** A

**P-Editor:** Liu JH



**Core Tip:** Stromal desmoplasia is not only a prominent histological hallmark of pancreatic cancer, but also a biological barrier to therapies. Various strategies aimed at targeting the stroma to improve therapeutic outcomes have been largely unsuccessful. Here we comprehensively reviewed the rationales and lessons learned from various stromal-targeting strategies and provide prospects on improving these approaches in future clinical trials.

**Citation:** Polani F, Grierson PM, Lim KH. Stroma-targeting strategies in pancreatic cancer: Past lessons, challenges and prospects. *World J Gastroenterol* 2021; 27(18): 2105-2121

**URL:** <https://www.wjgnet.com/1007-9327/full/v27/i18/2105.htm>

**DOI:** <https://dx.doi.org/10.3748/wjg.v27.i18.2105>

## INTRODUCTION

Pancreatic ductal adenocarcinoma (PDAC) is currently the seventh leading cause of cancer related death in the industrialized world[1]. In the United States, PDAC is projected to be the second leading cause of cancer death by 2030[2]. The current 5-year survival rate of PDAC is 9%, making it one of the deadliest cancers[3].

There are several factors that contribute to the poor outcomes of PDAC. First, non-specific symptoms and lack of PDAC specific markers and screening lead to late detection[4]. Less than 10% of PDAC is resectable at the time of diagnosis. Second, PDAC cells are highly metastatic, evidenced by the fact that most patients develop local or distal recurrences even after seemingly successful surgical resection. Third, PDAC is extremely resistant to chemotherapy and radiation. For example, the triple therapy of folinic acid, 5-fluorouracil (5-FU), irinotecan, oxaliplatin (as FOLFIRINOX or FOLFOXIRI) has been used as a first line regimen in the treatment of various gastrointestinal malignancies. A phase III trial conducted by The Groupo Oncologico Nord Ovest used FOLFOXIRI as a first line treatment in patients with metastatic colorectal cancer. The objective response rate (ORR) to FOLFOXIRI in these patients was 60%[5]. A phase II trial of FOLFIRINOX in patients with advanced gastro-esophageal cancer showed an ORR of 61%[6]. This is in contrast to a response rate of only 31.6% in patients with metastatic PDAC receiving FOLFIRINOX[7]. For patients with localized PDAC who have undergone R0 or R1 surgical resection upfront and have postoperative CA19-9 of less than 180 U/mL, treatment with FOLFIRINOX resulted in a 3-year disease free survival rate of 39.7% as opposed to 21.4% with gemcitabine[8]. While these results demonstrate that strong combination chemotherapy can potentially cure additional patients, it is also worth noting that a significant subset (approximately 60%) of patients will still succumb to disease relapse despite having received adjuvant FOLFIRINOX, clearly demonstrating that PDAC tumors are highly chemo-resistant even at the micro-metastatic stage. Another regimen that is commonly used in patients with advanced inoperable PDAC is gemcitabine plus nab-paclitaxel (GnP). A phase III trial including 842 patients with metastatic PDAC (MPACT trial) in 2013 showed the benefit of GnP over gemcitabine alone [median overall survival (OS) 8.5 vs 6.7 mo; 95% confidence interval (CI) 0.62-0.83;  $P < 0.001$ ], and response rate to GnP was 23%[9]. For patients with locally advanced PDAC, the response rate to FOLFIRINOX was 19% and to GnP was as low as 6%[10]. However, these two regimens are associated with significant toxicities, therefore escalation of these regimens by adding additional cytotoxic agents is expected to be clinically challenging and prohibitive.

PDAC is driven by mutations of multiple genes including *KRAS*, *TP53*, *CDKN2A* and *SMAD4*[11], which are also present in other cancer types such as non-small cell lung and colorectal cancers. However, PDAC tumors are characterized by a profound desmoplastic tumor microenvironment (TME), which accounts for 80%-90% of the tumor architecture[12]. Major components of the TME include a dense fibrotic matrix deposited by cancer-associated fibroblasts (CAFs), and significant infiltration of various subsets of immunosuppressive myeloid cells, vascular cells, and nerve cells[13-15]. The dense stroma plays an important role in tumor growth, proliferation, epithelial-mesenchymal transition (EMT), immune evasion and resistance to various therapies[16]. The low vascularity combined with elevated interstitial pressure dramatically limits vascular delivery and diffusion of therapeutic agents to tumor

cells[17-19]. Therefore, targeting the stroma to improve therapeutic response has been fervently pursued in recent years, albeit with limited success. Importantly, the role of stroma in PDAC progression and treatment resistance has become increasingly controversial. Preclinical mouse models suggest that depletion of stromal fibroblasts alone carries a risk of reverting PDAC cells to a more progenitor-like and aggressive state, with corresponding inferior outcomes[20,21]. These observations underscore the critical need to delineate the diverse interplay between different components of the tumor stroma in order to develop therapies that can modify the tumor stroma in favor of tumor suppression[22]. Herein, we focus specifically on stroma-targeting clinical trials, discuss the outcomes and provide future prospects of this strategy.

## COMPONENTS OF THE PANCREATIC TME

Pancreatic stellate cells (PSCs) are star-shaped cells that resemble their hepatic counterparts and were first discovered in 1998[23]. PSCs are found in the exocrine component of healthy pancreas, which when in their quiescent state are characterized by the presence of desmin intermediary filaments, vitamin A and fat droplets. During neoplastic progression, PSCs become activated, acquire a myofibroblast-like phenotype, express  $\alpha$ -SMA and secrete extracellular matrix (ECM) proteins (collagen I, collagen III, collagen IV and fibronectin)[24]. These activated PSC are termed CAFs. The ECM proteins secreted/deposited by CAF form a three-dimensional stiff mesh which, along with high molecular weight glycosaminoglycans such as hyaluronan (HA), raises the interstitial pressure that leads to vascular collapse, forming a hypoxic and nutrient poor TME[25,26].

Transcriptomic profiling shows that CAFs consist of at least three distinct subpopulations: Myofibroblast-like (myCAF), inflammatory (iCAF) and antigen-presenting (apCAF, Figure 1)[27,28]. The myCAFs are the most abundant subtype, characterized by high  $\alpha$ -SMA expression and hypothesized to have a favorable tumor-restrictive role, potentially explaining paradoxical PDAC progression in genetically engineered mouse models (GEMM) when CAFs are globally depleted[29]. The iCAFs are rich in expression of multiple inflammatory chemokines including interleukin (IL)-6 and proposed to be pro-tumorigenic. The least abundant apCAFs are characterized by abundant expression of MHC class II and therefore may be able to bind and present antigens to CD4<sup>+</sup> cytotoxic T-cells. However, due to a lack of co-stimulatory molecules on apCAFs, apCAFs actually dampen, instead of activating the interacting CD4<sup>+</sup> T cells[30]. Importantly, it appears that these subtypes are interchangeable, providing an avenue to reprogram these CAFs for therapeutic purposes.

The other predominant cellular components of the pancreatic tumor stroma include endothelial cells, inflammatory cells and nerve cells which have complex interactions with CAFs. Angiogenesis in PDAC is regulated by CAFs, PDAC cells, inflammatory cells and endothelial cells. The hypoxic microenvironment of PDAC acts as a trigger for the transcription factor hypoxia induced factor 1 expression which leads to increased vascular endothelial growth factor (VEGF) production and angiogenesis[31]. VEGF has been identified as an important negative prognostic marker in PDAC which has led to multiple preclinical and clinical studies targeting this pathway[32]. In addition, PDAC stroma is rife with various types of immune cells of myeloid lineages, T cells, B cells that are collectively rendered pro-tumorigenic by various environmental clues[33,34]. Targeting the immune compartment of PDAC, especially the suppressive myeloid cells including macrophages and monocytes, is a rapidly emerging therapeutic strategy, and is outside the scope of this review.

The acellular ECM proteins include collagen I, II, IV, XI-A, fibronectin, laminin, tenascin C and HA. While the dense ECM may physically restrict PDAC progression, ECM proteins have been shown to be protective to PDAC cells. PDAC cells detached from ECM proteins, especially laminin and fibronectin, are prone to apoptosis and necrosis as a result of mitochondrial depolarization and release of cytochrome c and Smac/DIABLO[35]. Various ECM proteins are also capable of promoting EMT and hence therapeutic resistance of PDAC cells[16]. These studies provide solid rationale for targeting these acellular ECM proteins as a therapeutic strategy. The ECM also contains a group of enzymes known as matrix metalloproteinases (MMP), which play a role in degradation of ECM components. The turnover of ECM is a dynamic process and is regulated by tissue MMP inhibitors secreted by stromal cellular structures[36].

Therapies targeting PDAC cells such as chemotherapy, radiation and surgery when used alone or in combination have only provided limited benefit in patients with advanced/metastatic PDAC, rarely improving survival beyond one year. This shifts

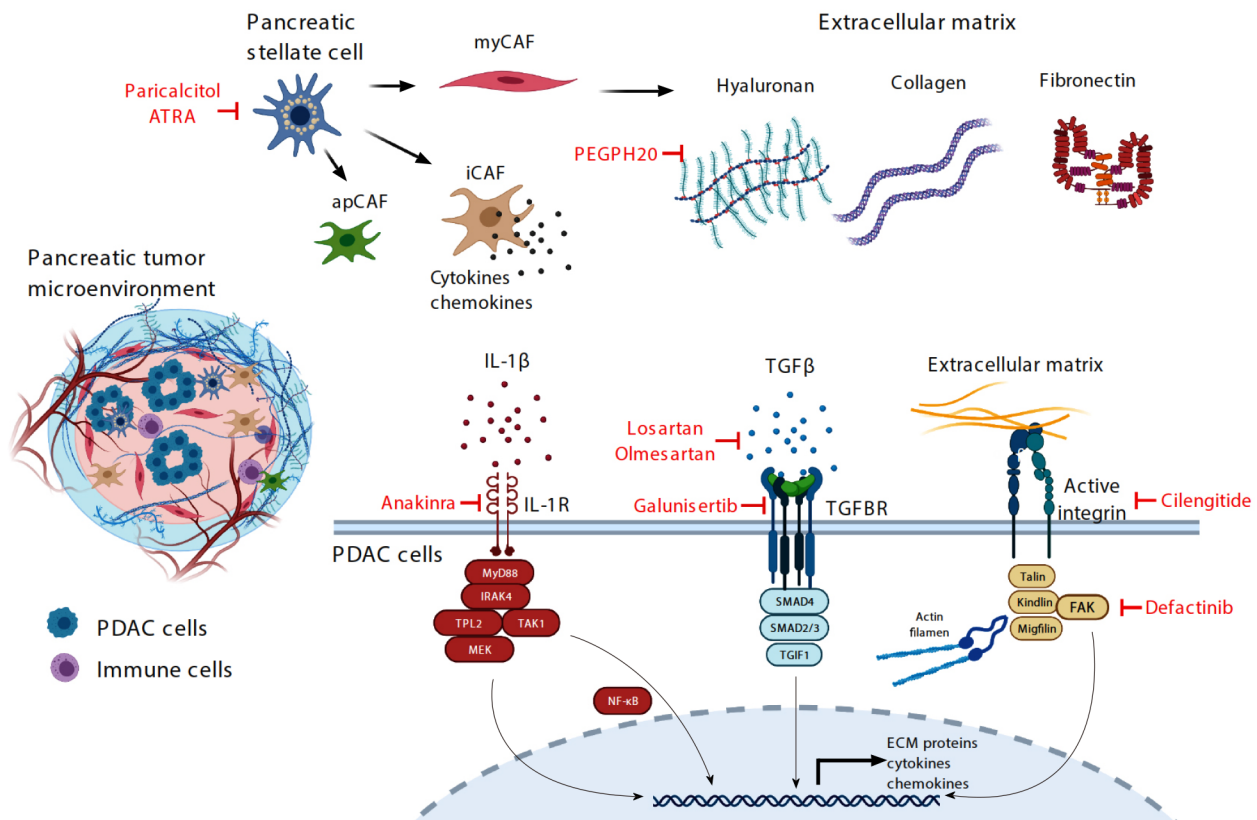


**Figure 1** Illustration of the complex pancreatic ductal adenocarcinoma tumor microenvironment that consists of various cell types and acellular extracellular matrix proteins and proteoglycans. Therapeutic strategies that have recently been tested or are being tested in clinical trials are highlighted in red. PDAC: Pancreatic ductal adenocarcinoma; ATRA: All trans retinoic acid; apCAF: Antigen-presenting cancer-associated fibroblasts; iCAF: Inflammatory cancer-associated fibroblasts; myCAF: Myofibroblast-like cancer-associated fibroblasts; IL: Interleukin; TGF: Transforming growth factor; TGFBR: Transforming growth factor  $\beta$  receptor; PEGPH20: Pegylated PH20; NF- $\kappa$ B: Nuclear factor-kappa  $\beta$ ; ECM: Extracellular matrix; FAK: Focal adhesion kinase.

the focus to the TME which plays a crucial role in inhibiting the effectiveness of cytotoxic therapies, making them less effective by providing a drug free sanctuary enabling them to thrive and proliferate[37]. A number of preclinical studies involving GEMM targeted the tumor stroma showing a beneficial effect toward better drug delivery and overall disease progression. A number of novel therapeutic strategies targeting the complex interaction of various cellular and acellular components of the PDAC microenvironment were first studied in the pre-clinical setting. The promising results of these in-vitro and in-vivo experiments resulted in clinical translation in an effort to alter the tumor micro-environment to improve outcomes of PDAC patients. Herein we review the effectiveness of these therapies and lessons learned from them, which provides guidance towards future treatments.

## TARGETING STROMA-PROMOTING PATHWAYS IN PDAC CELLS

### Sonic hedgehog pathway

Cancer stem cells (CSCs) are a small population of cancer cells responsible for tumor initiation, recurrence, growth and metastasis. Like normal stem cells, pancreatic CSCs are regulated by several common signaling pathways, one of which is the Sonic hedgehog (SHH) pathway. The SHH signaling pathway is regulated by a few critical nodes: the HH ligand, the Patched (PTCH) transmembrane receptor, the integral smoothened (SMO) protein and the Glioma Associated Oncogene (GLI) transcription factors. In the absence of SHH, PTCH binds and destabilizes SMO, leading to its degradation. Binding of SHH ligand to PTCH results in internalization and lysosomal degradation of both SHH and PTCH, thereby relieving SMO and allowing it to contribute to the activation of the GLI transcription factors. The GLI factors control several genes that participate in developmental patterning and also production of more SHH[38]. Compared to normal pancreatic stem cells, expression of SHH is upregulated in PDAC CSCs[39]. Olive *et al*[39] showed that targeting SMO with



sarigedib (or IPI-926) depletes the stromal tissue and transiently improves the delivery and therapeutic effect of gemcitabine in an orthotopic transplantable mouse model, suggesting that the SHH pathway may contribute to stromal fibrosis and hindrance of therapeutics in PDAC. In January 2012, a phase II trial involving the SHH pathway inhibitor saridegib (IPI-926) was halted due to detrimental outcomes of patients in the gemcitabine plus saridegib arm compared to the gemcitabine plus placebo arm (NCT01130142). This also resulted in early closure of another trial evaluating the efficacy of saridegib with modified FOLFIRINOX (NCT01383538)[40]. Vismodegib (or GDC-0449) is a competitive SMO inhibitor that is FDA-approved for treatment of advanced or metastatic basal cell carcinoma, in which loss-of-function mutations of *PTCH1* gene are common. A pilot study involving 25 patients showed downregulation of GLI and *PTCH1* expression in patients receiving combination of gemcitabine and vismodegib (NCT01195415)[41]. However, a larger phase IB/II trial evaluating 106 patients showed no improvement in response rate, OS or progression free survival (PFS). Importantly, contrary to the results reported by Olive *et al*[39] (NCT01064622), vismodegib did not improve intratumoral delivery of gemcitabine, and when combined with gemcitabine also did not statistically improve the survival of autochthonous PDAC mice[42]. A later Phase II trial (NCT01088815) evaluating 67 patients with untreated metastatic PDAC showed that addition of vismodegib to GnP did not improve PFS or OS compared to historical data of chemotherapy alone[43]. Sonidegib is another orally bioavailable SMO receptor antagonist approved for the treatment of recurrent locally advanced basal cell carcinoma[44]. This drug was studied in patients with PDAC in combination with both gemcitabine and GnP. Two small phase I trials showed good tolerance but no improvement in OS or PFS compared to standard chemotherapy (NCT01487785), (NCT02358161)[45,46]. These clinical studies show that targeting the SHH pathway in combination with standard chemotherapy is ineffective in PDAC. Furthermore, these studies underscore the need to obtain on-treatment correlative data to allow investigation into mechanisms of resistance and treatment failure.

### **Transforming growth factor $\beta$ pathway**

Enhanced intratumoral transforming growth factor  $\beta$  (TGF- $\beta$ ) signaling promotes tumor fibrosis, progression and poor patient survival in PDAC[47,48]. Importantly, more than half of PDAC cases carry inactivating mutations of *SMAD4*, which encodes a growth-inhibitory transcription factor downstream of the TGF receptor. Unlike other cellular components in the PDAC stroma, pancreatic cancer cells are often deficient in *SMAD4*. This leads to upregulation of TGF- $\beta$  ligand and has far reaching effects on other cellular components of PDAC that remain *SMAD4* proficient in the stroma. In these cells, TGF- $\beta$  acts as a driver for desmoplasia. Galunisertib is a small molecule serine/threonine kinase inhibitor of the TGF- $\beta$  receptor. A phase Ib/II study comparing galunisertib plus gemcitabine *vs* placebo plus gemcitabine was carried out in patients with advanced PDAC including 104 patients in the treatment arm and 52 patients in the placebo arm. There was a modest survival benefit in the treatment group. The median OS was 8.9 mo (95%CI: 7.3-11.1) for the galunisertib group and 7.1 mo (95%CI: 5.8-9.0) for the placebo group. The overall response rate was numerically superior in the galunisertib group, however, the differences were not statistically significant. No significant difference in PFS was observed in the two groups. Patients in the galunisertib group did not experience increased toxicity (NCT01373164)[49]. This modest but encouraging benefit of TGF- $\beta$  receptor inhibition has led to further clinical trials evaluating the effect of galunisertib with the anti PD-L1 (programmed death ligand 1) monoclonal antibody durvalumab (NCT02734160). To date, the results of this trial are pending.

The angiotensin II receptor blockers losartan and olmesartan have been evaluated in animal models based on their TGF- $\beta$  pathway inhibitor effects[50,51]. A retrospective study was carried out at Massachusetts General Hospital evaluating PDAC patients taking or not taking angiotensin pathway inhibitors. These investigators found that patients chronically taking angiotensin pathway inhibitors with non-metastatic PDAC had superior OS independent of chemotherapy[52]. A single arm phase II trial enrolled patients with locally advanced pancreatic cancer (LAPC) and treated with total neoadjuvant therapy of FOLFIRINOX and losartan followed by individualized chemoradiotherapy (NCT01821729). This study showed a high rate of R0 resection (69%) as well as prolonged OS among all patients (31.4 mo) including those who underwent resection (33 mo)[53]. This led to a large multicenter trial using losartan with FOLFIRINOX followed by SBRT and nivolumab in LAPC (NCT03563248). To date, the results of this clinical trial are pending.



### **Focal adhesion kinase**

Enhanced focal adhesion kinase (FAK) activity is commonly found in PDAC cells and CAFs and is a determinant of stromal fibrosis and immune evasion[54,55]. Targeting FAK using small molecule inhibitors dramatically attenuated stromal fibrosis, greatly potentiated chemotherapy and immune checkpoint blockade in several preclinical mouse models including the highly aggressive autochthonous KPC (*p48-Cre/p53<sup>fl</sup>/LSL-KRAS<sup>G12D</sup>*) mouse model[54]. These findings provided a solid rationale for combining a FAK inhibitor (defactinib) with gemcitabine and anti-PD-1 (programmed death 1) in a clinical trial of patients with PDAC after progression on frontline 5FU-based chemotherapy (NCT02546531). Results of this study are pending.

### **IL-1 receptor pathway**

Constitutive activation of the canonical nuclear factor-kappa  $\beta$  (NF- $\kappa$ B) pathway is a major mechanism that contributes to stromal fibrosis, chemoresistance and poor prognosis in PDAC[56]. In PDAC, activation of the canonical NF- $\kappa$ B cascade is driven both by KRAS-MAPK cascades and reciprocal IL-1 $\beta$  signaling, which drives IRAK4-TPL2 and IKK kinases[56-58]. Targeting IKK kinases has proven to be clinically challenging due to lack of safe and effective agents, but other strategies are being developed to target this pathway. For instance, targeting IRAK4 using small molecule kinase inhibitors was shown to reduce stromal fibrosis and potentiate the efficacy of chemotherapy in preclinical mouse models[56,58]. Currently, the IL-1 receptor antagonist Anakinra is being tested in combination with nab-paclitaxel, gemcitabine and cisplatin in patients with resectable or potentially resectable PDAC (NCT 02550327). To date, the results for this clinical trial are pending.

### **Connective tissue growth factor**

The PDAC TME is rife with a myriad of pro-tumorigenic and pro-fibrotic growth factors. One of these is connective tissue growth factor (CTGF). Interestingly, in preclinical models, treatment with pamrevlumab (or FG-3019), a humanized monoclonal antibody targeting CTGF, potentiates the effect of gemcitabine by downregulating X-linked inhibitor of apoptosis protein, rather than promoting delivery of gemcitabine[59]. In other PDAC pre-clinical studies pamrevlumab was shown to attenuate tumor growth, metastasis and angiogenesis[60]. These studies collectively suggest that the therapeutic effect of pamrevlumab is predominantly through targeting tumor cells. A phase I/II study evaluated pamrevlumab with gemcitabine and nab-paclitaxel in patients with LAPC. After 6 cycles/months of therapy, more patients treated with pamrevlumab and chemotherapy underwent resection compared to patients receiving chemotherapy only (33.3% *vs* 7.7%). The higher resection rate translated into improved OS (non-estimable *vs* 18.56 mo,  $P = 0.0141$ ). However, it was unclear whether the higher resectability among patients treated with pamrevlumab and chemotherapy was due to higher response rates or lower incidence of disease progression during the six cycles of treatment. Importantly, addition of pamrevlumab did not increase perioperative adverse events or delay in surgical wound healing[61]. A phase III trial is currently underway evaluating the safety and efficacy of pamrevlumab in combination with gemcitabine and nab-paclitaxel for patients with locally advanced PDAC (NCT03941093).

---

## **TARGETING STROMA-PROMOTING PATHWAYS IN CAFs**

---

### **Vitamin D receptor**

The role of vitamin D in the risk of developing pancreatic cancer is highly controversial, with studies showing high serum vitamin D levels to be protective, detrimental or have no impact on pancreatic cancer development[62-64]. However, the role of vitamin D repletion in PDAC patients after initial diagnosis and during treatment is actively being pursued in clinical studies. This is based on observational studies showing that higher pre-diagnostic serum vitamin D levels were shown to be associated with better survival in PDAC patients[65], and overwhelming preclinical studies demonstrating protective effects of vitamin D. Specifically, in mouse models ligation of vitamin D receptor with the vitamin D receptor ligand calcipotriol markedly impeded PSC activation, leading to stromal remodeling that augmented intratumoral gemcitabine, reduced tumor volume and prolonged the survival of KPC mice by 57% compared to mice treated with gemcitabine alone[66]. However, it is critical to emphasize that although calcipotriol impedes activation of PSCs, it fails to

block  $\alpha$ -SMA expression or collagen I production of fully activated PSCs[67], raising the concern for the modest efficacy of stromal effect of vitamin D receptor ligands. However, vitamin D receptor ligands could have tumor-intrinsic effects. In PDAC cells, calcipotriol lowered the expression of low-density lipoprotein receptor-related protein 6 and inhibits autocrine Wnt signaling[68]. Paricalcitol was also shown to impede PDAC cell proliferation by upregulating cell cycle inhibitors p21 (Waf1/CIP1) and p27 (Kip1)[69]. On these premises, multiple phase I or II studies testing the impact of paricalcitol are currently opened. These include in combination with cisplatin, gemcitabine and nab-paclitaxel for patients with treatment-naïve metastatic PDAC (NCT04054362); in combination with hydroxychloroquine, gemcitabine and nab-paclitaxel for patients with treatment-naïve metastatic PDAC (NCT04524702); in combination with 5-FU/Liposomal irinotecan for patients who have progressed through frontline gemcitabine-based therapies (NCT03883919); and in combination with anti-PD-1 (pembrolizumab) as maintenance treatment for patients who have achieved partial response or stable disease for at least two months on chemotherapy (NCT03331562).

### **All-trans retinoic acid**

There is an association with lower levels of fat-soluble vitamin A and risk of pancreatic cancer, theorized to be due to impaired absorption of fat-soluble vitamins[70]. Preclinical data has shown that vitamin A deficiency leads to activation of PSC, while repletion of vitamin A in culture media converts the PSCs from an activated to a quiescent state. Using the KPC model of human PDAC, treatment with all-trans retinoic acid (ATRA) induced quiescence of PSC, reduced proliferation of PDAC cells and led to increased apoptosis of PDAC cells in part by down-regulating Wnt signaling[71]. Based on this data, a phase I clinical trial was conducted enrolling 27 patients with unresectable PDAC, treated with GnP in combination with ATRA using the established dose for acute promyelocytic leukemia. This study demonstrated the safety and tolerability of the regimen, and diffusion weighted-magnetic resonance imaging identified signals of stromal modulation. This has led to the possibility of repurposing ATRA as a stromal targeting agent in PDAC. Based on these data, the combination of ATRA along with GnP is currently being studied in the Phase II randomized STAR\_PAC trial (NCT03307148) enrolling patients with locally advanced or metastatic disease[72].

### **Other agents targeting PSCs**

Pirfenidone is an anti-inflammatory and anti-fibrotic agent that is clinically used for treatment of idiopathic pulmonary fibrosis, however with an unknown mechanism of action. In primary human lung fibroblasts, pirfenidone inhibits proliferation, TGF- $\beta$ -induced myofibroblast differentiation and pro-collagen expression[73]. Pirfenidone also blocks proliferation, production of collagen, fibronectin and periostin by PSCs *in vitro* and *in vivo*, and potentiates the anti-tumor effect of gemcitabine by reducing stromal fibrosis[74].

Halofunginone (HF) is another anti-fibrotic drug that is of interest in pre-clinical studies. The exact mechanism of action of this agent is unclear however it has shown to cause resolution of pathologic liver fibrosis. In animal models, HF works by inhibiting the activation of PSC's which in-turn decreases the deposition of ECM proteins such as collagen and HA. HF inhibits the downstream signaling of TGF- $\beta$  by inhibiting SMAD2 and SMAD3 receptors. HF not only improves drug delivery by decreasing fibrosis, but it also fosters favorable immune response by augmenting cytotoxic T-cells and stimulatory myeloid cells in the tumor stroma[75]. To date, no clinical trials are opened yet incorporating these two agents for PDAC patients.

---

## **TARGETING ECM**

---

### **HA**

HA is a high molecular weight glycosaminoglycan that is synthesized by HA synthases (HAS1, HAS2, and HAS3) in PDAC cells and CAFs and deposited into the ECM framework[76]. Intratumoral HA undergoes constant turnover *via* degradation by hyaluronidases (HYAL1-4, HYALP1, and PH20). Excessive HA deposition, which is common in PDAC tumors, causes elevated water retention and consequently high interstitial pressure that collapses tumor vasculature and limits delivery of therapeutics[19]. High expression of HA in tumors has been associated with shorter survival post-surgical resection in patients with PDAC[77]. Importantly, aside from

being an important structural component of the ECM, HA has an active signaling function. CD44 is a well-established cellular receptor for HA. Engagement of CD44 on PDAC cells enhances invasion, metastasis, angiogenesis and survival[78]. In PDAC mouse models, addition of hyaluronidase such as pegylated PH20 (PEGPH20) reduces intratumoral HA content and interstitial pressure, thereby permitting re-expansion of the microvasculature. In mouse models, this results in improved delivery of chemotherapy into the PDAC TME and prolongation of survival[19,79].

The above promising preclinical data led to incorporation of PEGPH20 with gemcitabine in a phase Ib clinical trial. Patients with high intratumoral HA content had improved PFS (7.2 mo *vs* 3.5 mo) and OS (13 mo *vs* 5.7 mo) compared to patients with low HA[80]. This encouraging data led to a larger randomized placebo-controlled phase II study (HALO 202) comparing gemcitabine/nab-paclitaxel plus either PEGPH20 (PAG arm) or placebo (AG arm). Again, patients with high HA level (defined as HA staining of > 50% of tumor surface at any intensity) had improved PFS [9.2 mo *vs* 5.2 mo, hazard ratio (HR), 0.51; 95%CI: 0.26-1.00;  $P = 0.048$ ] and OS (11.5 mo *vs* 8.5 mo, HR, 0.96; 95%CI: 0.57-1.61) compared to patients with low HA tumors[81]. Unfortunately, these promising results failed to be recapitulated in a subsequent larger randomized phase III study (HALO 109-301). In this study, only patients with high HA tumors were enrolled, and 492 patients were included in intention-to-treat analysis. Median OS for PAG *vs* AG was 11.2 mo *vs* 11.5 mo (HR, 1.00, 95%CI: 0.80-1.27;  $P = 0.97$ ); median PFS was 7.1 *vs* 7.1 mo (HR, 0.97, 95%CI: 0.75-1.26); confirmed ORR was 34% *vs* 27% (NCT02715804)[82]. In this study, all patients treated with PEGPH20 were anticoagulated with low molecular weight heparin to prevent venous thromboembolism. In another phase Ib/II study (SWOG S1313), PEGPH20 was tested in combination with modified FOLFIRINOX *vs* modified FOLFIRINOX alone for treatment naïve PDAC patients. This study had to be halted after interim futility analysis showing inferior outcomes in the PEGPH20 group. Median OS and PFS was strikingly inferior in the PEGPH20 group with a HR of 2.07 (7.7 mo *vs* 14.4 mo, 95%CI: 1.28-3.34,  $P < 0.01$ ) and 1.74 (4.3 mo *vs* 6.2 mo, 95%CI: 1.14-2.66,  $P = 0.01$ ). ORR in PEGPH20 group was also lower, although this difference did not reach statistical significance (33% *vs* 45%,  $P = 0.2$ ) (NCT01959139)[83]. A critical factor leading to the poor outcome of PEGPH20 group was the unexpectedly increased gastrointestinal toxicity and thromboembolic events, which likely resulted in dose reduction of chemotherapy or treatment interruptions[84]. These setbacks led to the cessation of further development of PEGPH20 in cancer clinical trials.

### **ECM-remodeling enzyme lysyl oxidase-like 2**

The ECM-remodeling enzyme lysyl oxidase-like 2 (LOXL2) is a secreted enzyme that maintains the stromal microenvironment in PDAC. Preclinical data identified LOXL2 to be upregulated in cell lines with high invasive potential, and furthermore in human tissue, elevated LOXL2 expression correlates with greater depth of tumor invasion, lymph node involvement, and inferior OS[85]. Simtuzumab, an immunoglobulin G4 monoclonal antibody against LOXL2, was studied in a phase II randomized double-blind placebo-controlled study in combination with gemcitabine in metastatic PDAC patients (NCT01472198). The 240 patients were divided into three groups and received simtuzumab 700 mg, simtuzumab 200 mg or placebo along with gemcitabine. Unfortunately, despite encouraging preclinical and correlative clinical data, when prospectively evaluated, the addition of simtuzumab to gemcitabine did not prolong OS in either cohort of patients with metastatic PDAC compared to gemcitabine alone[86].

### **Integrins**

Integrins are cell surface receptors that mediate surface adhesion of various components of ECM including fibronectin, laminin, collagen and fibrinogen[87]. They play an important role in tumor angiogenesis and lymphangiogenesis, and hence are attractive therapeutic targets[88]. Cilengitide is a low molecular weight anti-angiogenic molecule that acts by inhibiting the integrin surface receptors of endothelial cells[89]. A randomized multi-center phase II trial enrolled patients with unresectable PDAC and treated them with cilengitide and gemcitabine *vs* gemcitabine alone. There were no signs of efficacy, including a median OS of 6.7 mo for those receiving cilengitide and gemcitabine *vs* 7.7 mo for those receiving gemcitabine alone (ISRCTN13413322)[90].

### **Drugs targeting MMPs**

The MMPs are proteolytic enzymes that play an important role in remodeling of ECM

proteins and modifying the tumor stroma in favor of tumor proliferation, invasion and metastasis. MMP inhibitors have been evaluated in multiple solid tumors based on their fundamental role in modulating tumor stroma, with encouraging preclinical data[91]. However, clinical outcomes have been disappointing in PDAC. Specifically, the MMP inhibitors marimastat and BAY12-9566 were studied in comparison to gemcitabine as first line therapy in advanced PDAC patients. These studies both demonstrated superior outcomes with gemcitabine compared to the MMP inhibitors[92,93].

## LESSONS AND PROSPECTS

The histologic predominance and tumor-modulating role of stroma continues to propel preclinical and clinical research into stromal-targeting strategies for PDAC (Figure 1). However, clinical success remains limited (Table 1). Until the present time, clinical progress in PDAC has been the result of increasingly aggressive combination chemotherapies, demonstrating that targeting PDAC cells with cytotoxic agents remains a viable strategy, although not ideal, as it is no longer clinically feasible to add further cytotoxic agents to current regimens considering treatment-limiting toxicity. For this reason, stroma-targeting approaches are gaining significant attention. The excitement surrounding stromal targeting is well deserved, given that in preclinical models these approaches permit effective immunotherapy and durable tumor control. As described above, these mechanisms include re-activating T cell and myeloid compartments with or without directly altering the physical immunosuppressive stroma. In contrast to many other solid tumors, clinical efficacy has not yet been realized in PDAC. Studies to date have taught us that PDAC is a very unique tumor type, such that findings in other solid tumors cannot be extrapolated to PDAC. Thus, a more in depth understanding of the different cellular and acellular components of the pancreatic stroma is needed, in order for subsets of cellular or acellular components to be targeted. We have learned that oversimplified preclinical models, especially the widely used GEMM such as KPC mice, which consists of merely two mutations (*KRAS* and *TP53*), are clearly inadequate in PDAC, with findings that do not faithfully translate to patients.

Numerous challenges remain ahead in pancreatic cancer. In the design of future clinical trials, several factors should be taken into consideration. First, the robustness of preclinical data needs to be evaluated carefully before proceeding into the clinical setting. The most pertinent questions to ask are, what type of models were used (patient-derived xenograft, organoid, GEMM)? How many different models were studied to confirm results? How predictive is the current model, in light of prior investigations? What endpoints were considered as significant and meaningful anti-tumor activities (survival, tumor shrinkage)? How was suppressed tumor growth or tumor shrinkage in the animal models defined? Was any synergistic effect seen between the agent of interest and cytotoxic agents? How dramatic is the effect that was seen preclinically? Given that the effect seen in patients is nearly always more modest than that seen in preclinical studies, only those combinations with profound preclinical efficacy, rather than those that meet statistically significant *P* values, should be advanced into the clinic. Despite all of these considerations, the apparent discrepancies between preclinical and clinical success in PDAC research should remind us of the fact that none of the current experimental models are by themselves adequate. Multiple models, both human and mouse-based, must be tested, and ultimately better preclinical models need to be developed.

The phase I trial is a great opportunity for pharmacokinetic and pharmacodynamic (PD) investigation; however, a recent trend has arisen that shifts the focus of the phase I trial to identifying an early efficacy signal, such that subsequent investigations can directly move into the phase III setting. Tissue biopsy collection is essential for PDAC trials for two important reasons. First, rigorous collection of tissues or surrogate biospecimens for the purpose of in-human verification of PD target effects is critical. This will verify *in vivo* on-target activity of the agent being evaluated, which is necessary to confirm relative dose sufficiency and appropriate frame treatment failures. Second, tissue collection will allow an initial assessment of *in vivo* mechanisms of resistance and correlative analyses. Finally, every effort should be made to enroll PDAC patients in appropriate clinical trials to allow patient access to the most advanced therapeutics, optimizing their outcome to the greatest extent possible. Recent failed clinical trials based on impressive preclinical data have provided us with an undesired but valuable opportunity to reexamine the challenges

**Table 1 Summary of stromal-targeting clinical trials in pancreatic cancer**

Drug	Mechanism of action	Backbone therapy	Outcome
<b>Targeting stroma-promoting pathways in PDAC cells</b>			
Saridegib (IPI-926)	SHH pathway inhibitor	Gemcitabine; mFOLFIRINOX	No improvement in OS or PFS (NCT01130142); No improvement in OS or PFS (NCT01383538)
Vismodegib	SHH pathway inhibitor	Gemcitabine; Gemcitabine + nab-paclitaxel	No improvement in OS or PFS (NCT01064622); No improvement in OS or PFS (NCT01088815)
Sonidegib	SHH pathway inhibitor (SMO receptor antagonist)	Gemcitabine; Gemcitabine + nab-Paclitaxel	No improvement in OS or PFS (NCT01487785); No improvement in OS or PFS (NCT02358161)
Galunisertib	TGF- $\beta$ receptor inhibitor	Gemcitabine; Gemcitabine + Durvalumab	Ongoing trial (NCT01373164); Ongoing trial (NCT02734160)
Losartan	TGF- $\beta$ ligand inhibitor	FOLFIRINOX; Nivolumab + FOLFIRINOX	Ongoing trial (NCT01821729); Ongoing trial (NCT03563248)
Defactinib	Focal Adhesion Kinase inhibitor	Gemcitabine + Pembrolizumab	Ongoing trial (NCT02546531)
Anakinra	IL-1 receptor inhibitor	GnP + Cisplatin	Ongoing trial (NCT02550327)
<b>Targeting stroma-promoting pathways in CAFs</b>			
Pamrevlumab	Antibody against CTGF	Gemcitabine + nab-paclitaxel	Ongoing trial (NCT03941093)
Paricalcitol	Vitamin D agonist; Inactivation of PSC	GnP + Cisplatin; GnP + Hydroxychloroquine; 5FU/Leucovorin/liposomal Irinotecan; Pembrolizumab (2 <sup>nd</sup> line)	Ongoing trial (NCT04054362); Ongoing trial (NCT04524702); Ongoing trial (NCT03883919); Ongoing trial (NCT03331562)
ATRA	Inactivation of PSC	Gemcitabine + nab-paclitaxel	Ongoing trial (NCT03307148)
<b>Targeting ECM</b>			
PEGPH20	Hyaluronan degradation	Gemcitabine + nab-paclitaxel; mFOLFIRINOX	No improvement in OS or PFS (NCT02715804); Poor OS due to poor tolerance (NCT01959139)
Simtuzumab	Antibody against LOXL2	Gemcitabine	No improvement in OS (NCT01472198)
Cilengitide	Integrin inhibitor	Gemcitabine	No improvement in OS (ISRCTN13413322)
Marimastat	MMP inhibitor	Gemcitabine	No improvement in OS
Bay-12-9566	MMP inhibitor	Gemcitabine	No improvement in OS
<b>Others</b>			
Halofuginone	PSC/CAF and SMAD2,3 inhibitor	-	Positive pre-clinical outcomes
Pirfenidone	Cell cycle inhibitor of CAF	-	Positive pre-clinical outcomes

SHH: Sonic hedgehog; OS: Overall survival; PFS: Progression free survival; SMO: Smoothened; TGF: Transforming growth factor; IL: Interleukin; GnP: Gemcitabine plus nab-paclitaxel; CTGF: Connective tissue growth factor; CAF: Cancer-associated fibroblasts; PSC: Pancreatic stellate cell; ECM: Extracellular matrix; LOXL2: Lysyl oxidase-like 2; MMP: Matrix metalloproteinases.

of PDAC and re-iterate the importance of more rigorously designed and scientifically-based clinical investigations. In summary, much progress has been made in recent years understanding the pancreatic tumor stroma, however, lack of subsequent clinical success is evidence that much work remains to be done.

## CONCLUSION

The poor response of PDAC to standard cytotoxic regimens has directed attention towards the dense fibrous stroma. The stroma is thought to be a fortress that protects PDAC cells from immune invasion, leads to chemotherapeutic resistance, and thereby provides a sanctuary for these cells to proliferate[16]. There are multiple pre-clinical and *in vitro* studies wherein stroma depletion led to decreased progression and improved survival among animal models. Based on these a variety of novel approaches have been adapted in human trials for clinical translation[35,37,79]. Some of these approaches were initially promising, however, most if not all have led to negative outcomes, financial waste and frustration in the clinic. This has made stromal



targeting in PDAC a much controversial subject. It has been established time and again that indiscriminate targeting and near complete depletion of tumor stroma can cause more harm than good[40,94]. However, these attempts have enhanced our understanding of the tumor micro-environment. There is increased need for caution when targeting these matrix components as we have discovered cellular and acellular components of the stroma that in fact restrain tumor growth and progression[95].

A better understanding of plasticity of the stroma will lead to development of therapeutics that can accurately modulate the tumor micro-environment in favor of tumor suppression. The discovery of heterogeneity among CAF and their paradoxical role in tumor growth further delineates the importance of development of targeted therapies that downregulate subsets of CAF (such as iCAF or possibly apCAF) by selectively modifying the stroma[27,30]. Furthermore, vigorous evaluation of pre-clinical data, comparison of its effectiveness in multiple models and assessment of synergistic response of these novel therapeutics with existing cytotoxic therapy in both human and mouse models is vital to avoid detrimental clinical outcomes. There is a need for development of more standardized pre-clinical models and critical analysis of the data in relation to tumor response in these models before we can translate preclinical findings into clinical success. Such agents once developed may synergistically improve the efficacy of currently available cytotoxic and immune modulating therapies.

## ACKNOWLEDGEMENTS

We thank the researchers whose related work was not cited in this review.

## REFERENCES

- 1 **Bray F**, Ferlay J, Soerjomataram I, Siegel RL, Torre LA, Jemal A. Global cancer statistics 2018: GLOBOCAN estimates of incidence and mortality worldwide for 36 cancers in 185 countries. *CA Cancer J Clin* 2018; **68**: 394-424 [PMID: 30207593 DOI: 10.3322/caac.21492]
- 2 **Rahib L**, Smith BD, Aizenberg R, Rosenzweig AB, Fleshman JM, Matrisian LM. Projecting cancer incidence and deaths to 2030: the unexpected burden of thyroid, liver, and pancreas cancers in the United States. *Cancer Res* 2014; **74**: 2913-2921 [PMID: 24840647 DOI: 10.1158/0008-5472.CAN-14-0155]
- 3 **Siegel RL**, Miller KD, Jemal A. Cancer statistics, 2020. *CA Cancer J Clin* 2020; **70**: 7-30 [PMID: 31912902 DOI: 10.3322/caac.21590]
- 4 **Hasan S**, Jacob R, Manne U, Paluri R. Advances in pancreatic cancer biomarkers. *Oncol Rev* 2019; **13**: 410 [PMID: 31044028 DOI: 10.4081/oncol.2019.410]
- 5 **Falcone A**, Ricci S, Brunetti I, Pfanner E, Allegrini G, Barbara C, Crinò L, Benedetti G, Evangelista W, Fanchini L, Cortesi E, Picone V, Vitello S, Chiara S, Granetto C, Porcile G, Fioretto L, Orlandini C, Andreuccetti M, Masi G; Gruppo Oncologico Nord Ovest. Phase III trial of infusional fluorouracil, leucovorin, oxaliplatin, and irinotecan (FOLFOXIRI) compared with infusional fluorouracil, leucovorin, and irinotecan (FOLFIRI) as first-line treatment for metastatic colorectal cancer: the Gruppo Oncologico Nord Ovest. *J Clin Oncol* 2007; **25**: 1670-1676 [PMID: 17470860 DOI: 10.1200/jco.2006.09.0928]
- 6 **Park H**, Jin RU, Wang-Gillam A, Suresh R, Rigden C, Amin M, Tan BR, Pedersen KS, Lim KH, Trikalinos NA, Acharya A, Copsey ML, Navo KA, Morton AE, Gao F, Lockhart AC. FOLFIRINOX for the Treatment of Advanced Gastroesophageal Cancers: A Phase 2 Nonrandomized Clinical Trial. *JAMA Oncol* 2020; **6**: 1231-1240 [PMID: 32469386 DOI: 10.1001/jamaoncol.2020.2020]
- 7 **Conroy T**, Desseigne F, Ychou M, Bouché O, Guimbaud R, Bécaud Y, Adenis A, Raoul JL, Gourgou-Bourgade S, de la Fouchardière C, Bannoun J, Bachet JB, Khemissa-Akouz F, Péré-Vergé D, Delbaldo C, Assenat E, Chauffert B, Michel P, Montoto-Grillot C, Ducreux M; Groupe Tumeurs Digestives of Unicancer; PRODIGE Intergroup. FOLFIRINOX vs gemcitabine for metastatic pancreatic cancer. *N Engl J Med* 2011; **364**: 1817-1825 [PMID: 21561347 DOI: 10.1056/NEJMoa1011923]
- 8 **Conroy T**, Hammel P, Hebbar M, Ben Abdelghani M, Wei AC, Raoul JL, Choné L, Francois E, Artru P, Biagi JJ, Lecomte T, Assenat E, Faroux R, Ychou M, Volet J, Sauvanet A, Breysacher G, Di Fiore F, Cripps C, Kavan P, Texereau P, Bouhier-Leporrier K, Khemissa-Akouz F, Legoux JL, Juzyna B, Gourgou S, O'Callaghan CJ, Jouffroy-Zeller C, Rat P, Malka D, Castan F, Bachet JB; Canadian Cancer Trials Group and the Unicancer-GI-PRODIGE Group. FOLFIRINOX or Gemcitabine as Adjuvant Therapy for Pancreatic Cancer. *N Engl J Med* 2018; **379**: 2395-2406 [PMID: 30575490 DOI: 10.1056/NEJMoa1809775]
- 9 **Von Hoff DD**, Ervin T, Arena FP, Chiorean EG, Infante J, Moore M, Seay T, Tjuland SA, Ma WW, Saleh MN, Harris M, Reni M, Dowden S, Laheru D, Bahary N, Ramanathan RK, Tabernero J,

- Hidalgo M, Goldstein D, Van Cutsem E, Wei X, Iglesias J, Renschler MF. Increased survival in pancreatic cancer with nab-paclitaxel plus gemcitabine. *N Engl J Med* 2013; **369**: 1691-1703 [PMID: 24131140 DOI: 10.1056/NEJMoa1304369]
- 10 Perri G, Prakash L, Qiao W, Varadhachary GR, Wolff R, Fogelman D, Overman M, Pant S, Javle M, Koay EJ, Herman J, Kim M, Ikoma N, Tzeng CW, Lee JE, Katz MHG. Response and Survival Associated With First-line FOLFIRINOX vs Gemcitabine and nab-Paclitaxel Chemotherapy for Localized Pancreatic Ductal Adenocarcinoma. *JAMA Surg* 2020; **155**: 832-839 [PMID: 32667641 DOI: 10.1001/jamasurg.2020.2286]
- 11 Bardeesy N, DePinho RA. Pancreatic cancer biology and genetics. *Nat Rev Cancer* 2002; **2**: 897-909 [PMID: 12459728 DOI: 10.1038/nrc949]
- 12 Feig C, Gopinathan A, Neesse A, Chan DS, Cook N, Tuveson DA. The pancreas cancer microenvironment. *Clin Cancer Res* 2012; **18**: 4266-4276 [PMID: 22896693 DOI: 10.1158/1078-0432.CCR-11-3114]
- 13 Mitchem JB, Brennan DJ, Knolhoff BL, Belt BA, Zhu Y, Sanford DE, Belaygorod L, Carpenter D, Collins L, Piwnica-Worms D, Hewitt S, Udupi GM, Gallagher WM, Wegner C, West BL, Wang-Gillam A, Goedegebuure P, Linehan DC, DeNardo DG. Targeting tumor-infiltrating macrophages decreases tumor-initiating cells, relieves immunosuppression, and improves chemotherapeutic responses. *Cancer Res* 2013; **73**: 1128-1141 [PMID: 23221383 DOI: 10.1158/0008-5472.CAN-12-2731]
- 14 Goedegebuure P, Mitchem JB, Porembka MR, Tan MC, Belt BA, Wang-Gillam A, Gillanders WE, Hawkins WG, Linehan DC. Myeloid-derived suppressor cells: general characteristics and relevance to clinical management of pancreatic cancer. *Curr Cancer Drug Targets* 2011; **11**: 734-751 [PMID: 21599634 DOI: 10.2174/156800911796191024]
- 15 Bayne LJ, Beatty GL, Jhala N, Clark CE, Rhim AD, Stanger BZ, Vonderheide RH. Tumor-derived granulocyte-macrophage colony-stimulating factor regulates myeloid inflammation and T cell immunity in pancreatic cancer. *Cancer Cell* 2012; **21**: 822-835 [PMID: 22698406 DOI: 10.1016/j.ccr.2012.04.025]
- 16 Bulle A, Lim KH. Beyond just a tight fortress: contribution of stroma to epithelial-mesenchymal transition in pancreatic cancer. *Signal Transduct Target Ther* 2020; **5**: 249 [PMID: 33122631 DOI: 10.1038/s41392-020-00341-1]
- 17 Kong X, Li L, Li Z, Xie K. Targeted destruction of the orchestration of the pancreatic stroma and tumor cells in pancreatic cancer cases: molecular basis for therapeutic implications. *Cytokine Growth Factor Rev* 2012; **23**: 343-356 [PMID: 22749856 DOI: 10.1016/j.cytogfr.2012.06.006]
- 18 Hidalgo M. Pancreatic cancer. *N Engl J Med* 2010; **362**: 1605-1617 [PMID: 20427809 DOI: 10.1056/NEJMra0901557]
- 19 Jacobetz MA, Chan DS, Neesse A, Bapiro TE, Cook N, Frese KK, Feig C, Nakagawa T, Caldwell ME, Zecchini HI, Lolkema MP, Jiang P, Kultti A, Thompson CB, Maneval DC, Jodrell DI, Frost GI, Shepard HM, Skepper JN, Tuveson DA. Hyaluronan impairs vascular function and drug delivery in a mouse model of pancreatic cancer. *Gut* 2013; **62**: 112-120 [PMID: 22466618 DOI: 10.1136/gutjnl-2012-302529]
- 20 Rhim AD, Oberstein PE, Thomas DH, Mirek ET, Palermo CF, Sastra SA, Dekleva EN, Saunders T, Becerra CP, Tattersall IW, Westphalen CB, Kitajewski J, Fernandez-Barrena MG, Fernandez-Zapico ME, Iacobuzio-Donahue C, Olive KP, Stanger BZ. Stromal elements act to restrain, rather than support, pancreatic ductal adenocarcinoma. *Cancer Cell* 2014; **25**: 735-747 [PMID: 24856585 DOI: 10.1016/j.ccr.2014.04.021]
- 21 Özdemir BC, Pentcheva-Hoang T, Carstens JL, Zheng X, Wu CC, Simpson TR, Laklai H, Sugimoto H, Kahlert C, Novitskiy SV, De Jesus-Acosta A, Sharma P, Heidari P, Mahmood U, Chin L, Moses HL, Weaver VM, Maitra A, Allison JP, LeBleu VS, Kalluri R. Depletion of carcinoma-associated fibroblasts and fibrosis induces immunosuppression and accelerates pancreas cancer with reduced survival. *Cancer Cell* 2014; **25**: 719-734 [PMID: 24856586 DOI: 10.1016/j.ccr.2014.04.005]
- 22 Wang Z, Li J, Chen X, Duan W, Ma Q, Li X. Disrupting the balance between tumor epithelia and stroma is a possible therapeutic approach for pancreatic cancer. *Med Sci Monit* 2014; **20**: 2002-2006 [PMID: 25327552 DOI: 10.12659/MSM.892523]
- 23 Apte MV, Haber PS, Applegate TL, Norton ID, McCaughan GW, Korsten MA, Pirola RC, Wilson JS. Periacinar stellate shaped cells in rat pancreas: identification, isolation, and culture. *Gut* 1998; **43**: 128-133 [PMID: 9771417 DOI: 10.1136/gut.43.1.128]
- 24 Bachem MG, Schneider E, Gross H, Weidenbach H, Schmid RM, Menke A, Siech M, Beger H, Grünert A, Adler G. Identification, culture, and characterization of pancreatic stellate cells in rats and humans. *Gastroenterology* 1998; **115**: 421-432 [PMID: 9679048 DOI: 10.1016/s0016-5085(98)70209-4]
- 25 DuFort CC, DelGiorno KE, Carlson MA, Osgood RJ, Zhao C, Huang Z, Thompson CB, Connor RJ, Thanos CD, Scott Brockenbrough J, Provenzano PP, Frost GI, Michael Shepard H, Hingorani SR. Interstitial Pressure in Pancreatic Ductal Adenocarcinoma Is Dominated by a Gel-Fluid Phase. *Biophys J* 2016; **110**: 2106-2119 [PMID: 27166818 DOI: 10.1016/j.bpj.2016.03.040]
- 26 DuFort CC, DelGiorno KE, Hingorani SR. Mounting Pressure in the Microenvironment: Fluids, Solids, and Cells in Pancreatic Ductal Adenocarcinoma. *Gastroenterology* 2016; **150**: 1545-1557. e2 [PMID: 27072672 DOI: 10.1053/j.gastro.2016.03.040]
- 27 Öhlund D, Handly-Santana A, Biffi G, Elyada E, Almeida AS, Ponz-Sarvise M, Corbo V, Oni TE, Hearn SA, Lee EJ, Chio II, Hwang CI, Tiriack H, Baker LA, Engle DD, Feig C, Kultti A, Egeblad M,

- Fearon DT, Crawford JM, Clevers H, Park Y, Tuveson DA. Distinct populations of inflammatory fibroblasts and myofibroblasts in pancreatic cancer. *J Exp Med* 2017; **214**: 579-596 [PMID: [28232471](#) DOI: [10.1084/jem.20162024](#)]
- 28 **Elyada E**, Bolisetty M, Laise P, Flynn WF, Courtois ET, Burkhart RA, Teinor JA, Belleau P, Biffi G, Lucito MS, Sivajothi S, Armstrong TD, Engle DD, Yu KH, Hao Y, Wolfgang CL, Park Y, Preall J, Jaffee EM, Califano A, Robson P, Tuveson DA. Cross-Species Single-Cell Analysis of Pancreatic Ductal Adenocarcinoma Reveals Antigen-Presenting Cancer-Associated Fibroblasts. *Cancer Discov* 2019; **9**: 1102-1123 [PMID: [31197017](#) DOI: [10.1158/2159-8290.CD-19-0094](#)]
- 29 **Hwang RF**, Moore T, Arumugam T, Ramachandran V, Amos KD, Rivera A, Ji B, Evans DB, Logsdon CD. Cancer-associated stromal fibroblasts promote pancreatic tumor progression. *Cancer Res* 2008; **68**: 918-926 [PMID: [18245495](#) DOI: [10.1158/0008-5472.CAN-07-5714](#)]
- 30 **Djurec M**, Graña O, Lee A, Troulé K, Espinet E, Cabras L, Navas C, Blasco MT, Martín-Díaz L, Burdiel M, Li J, Liu Z, Vallespinós M, Sanchez-Bueno F, Sprick MR, Trumpp A, Sainz B Jr, Al-Shahrour F, Rabadan R, Guerra C, Barbacid M. Saa3 is a key mediator of the protumorigenic properties of cancer-associated fibroblasts in pancreatic tumors. *Proc Natl Acad Sci USA* 2018; **115**: E1147-E1156 [PMID: [29351990](#) DOI: [10.1073/pnas.1717802115](#)]
- 31 **Masamune A**, Kikuta K, Watanabe T, Satoh K, Hirota M, Shimosegawa T. Hypoxia stimulates pancreatic stellate cells to induce fibrosis and angiogenesis in pancreatic cancer. *Am J Physiol Gastrointest Liver Physiol* 2008; **295**: G709-G717 [PMID: [18669622](#) DOI: [10.1152/ajpgi.90356.2008](#)]
- 32 **Ikeda N**, Adachi M, Taki T, Huang C, Hashida H, Takabayashi A, Sho M, Nakajima Y, Kanehiro H, Hisanaga M, Nakano H, Miyake M. Prognostic significance of angiogenesis in human pancreatic cancer. *Br J Cancer* 1999; **79**: 1553-1563 [PMID: [10188906](#) DOI: [10.1038/sj.bjc.6690248](#)]
- 33 **Wahab ZA**, Metzgar RS. Human cytotoxic lymphocytes reactive with pancreatic adenocarcinoma cells. *Pancreas* 1991; **6**: 307-317 [PMID: [1862066](#) DOI: [10.1097/00006676-199105000-00008](#)]
- 34 **Thomas SK**, Lee J, Beatty GL. Paracrine and cell autonomous signalling in pancreatic cancer progression and metastasis. *EBioMedicine* 2020; **53**: 102662 [PMID: [32139180](#) DOI: [10.1016/j.ebiom.2020.102662](#)]
- 35 **Vaquero EC**, Edderkaoui M, Nam KJ, Gukovsky I, Pandol SJ, Gukovskaya AS. Extracellular matrix proteins protect pancreatic cancer cells from death via mitochondrial and nonmitochondrial pathways. *Gastroenterology* 2003; **125**: 1188-1202 [PMID: [14517801](#) DOI: [10.1016/s0016-5085\(03\)01203-4](#)]
- 36 **Stetler-Stevenson WG**, Liotta LA, Kleiner DE Jr. Extracellular matrix 6: role of matrix metalloproteinases in tumor invasion and metastasis. *FASEB J* 1993; **7**: 1434-1441 [PMID: [8262328](#) DOI: [10.1096/fasebj.7.15.8262328](#)]
- 37 **Apte MV**, Xu Z, Pothula S, Goldstein D, Pirola RC, Wilson JS. Pancreatic cancer: The microenvironment needs attention too! *Pancreatol* 2015; **15**: S32-S38 [PMID: [25845856](#) DOI: [10.1016/j.pan.2015.02.013](#)]
- 38 **Sari IN**, Phi LTH, Jun N, Wijaya YT, Lee S, Kwon HY. Hedgehog Signaling in Cancer: A Prospective Therapeutic Target for Eradicating Cancer Stem Cells. *Cells* 2018; **7** [PMID: [30423843](#) DOI: [10.3390/cells7110208](#)]
- 39 **Olive KP**, Jacobetz MA, Davidson CJ, Gopinathan A, McIntyre D, Honess D, Madhu B, Goldgraben MA, Caldwell ME, Allard D, Frese KK, Denicola G, Feig C, Combs C, Winter SP, Ireland-Zecchini H, Reichelt S, Howat WJ, Chang A, Dhara M, Wang L, Rückert F, Grützmann R, Pilarsky C, Izeradjene K, Hingorani SR, Huang P, Davies SE, Plunkett W, Egorin M, Hruban RH, Whitebread N, McGovern K, Adams J, Iacobuzio-Donahue C, Griffiths J, Tuveson DA. Inhibition of Hedgehog signaling enhances delivery of chemotherapy in a mouse model of pancreatic cancer. *Science* 2009; **324**: 1457-1461 [PMID: [19460966](#) DOI: [10.1126/science.1171362](#)]
- 40 **Ko AH**, LoConte N, Tempero MA, Walker EJ, Kate Kelley R, Lewis S, Chang WC, Kantoff E, Vannier MW, Catenacci DV, Venook AP, Kindler HL. A Phase I Study of FOLFIRINOX Plus IPI-926, a Hedgehog Pathway Inhibitor, for Advanced Pancreatic Adenocarcinoma. *Pancreas* 2016; **45**: 370-375 [PMID: [26390428](#) DOI: [10.1097/MPA.0000000000000458](#)]
- 41 **Kim EJ**, Sahai V, Abel EV, Griffith KA, Greenson JK, Takebe N, Khan GN, Blau JL, Craig R, Balis UG, Zalupski MM, Simeone DM. Pilot clinical trial of hedgehog pathway inhibitor GDC-0449 (vismodegib) in combination with gemcitabine in patients with metastatic pancreatic adenocarcinoma. *Clin Cancer Res* 2014; **20**: 5937-5945 [PMID: [25278454](#) DOI: [10.1158/1078-0432.CCR-14-1269](#)]
- 42 **Catenacci DV**, Junttila MR, Karrison T, Bahary N, Horiba MN, Nattam SR, Marsh R, Wallace J, Kozloff M, Rajdev L, Cohen D, Wade J, Sleekman B, Lenz HJ, Stiff P, Kumar P, Xu P, Henderson L, Takebe N, Salgia R, Wang X, Stadler WM, de Sauvage FJ, Kindler HL. Randomized Phase Ib/II Study of Gemcitabine Plus Placebo or Vismodegib, a Hedgehog Pathway Inhibitor, in Patients With Metastatic Pancreatic Cancer. *J Clin Oncol* 2015; **33**: 4284-4292 [PMID: [26527777](#) DOI: [10.1200/JCO.2015.62.8719](#)]
- 43 **De Jesus-Acosta A**, Sugar EA, O'Dwyer PJ, Ramanathan RK, Von Hoff DD, Rasheed Z, Zheng L, Begum A, Anders R, Maitra A, McAllister F, Rajeshkumar NV, Yabuuchi S, de Wilde RF, Batukbhai B, Sahin I, Laheru DA. Phase 2 study of vismodegib, a hedgehog inhibitor, combined with gemcitabine and nab-paclitaxel in patients with untreated metastatic pancreatic adenocarcinoma. *Br J Cancer* 2020; **122**: 498-505 [PMID: [31857726](#) DOI: [10.1038/s41416-019-0683-3](#)]
- 44 **Burness CB**. Sonidegib: First Global Approval. *Drugs* 2015; **75**: 1559-1566 [PMID: [26323341](#) DOI: [10.1007/s40265-015-0458-y](#)]
- 45 **Macarulla T**, Tabernero J, Palmer DH, Sharma S, Yu KH, Sellami DB, Zhou J, Yi W, Boss H, Kwak

- EL. A phase Ib dose escalation, safety, and tolerability study of sonidegib in combination with gemcitabine in patients with locally advanced or metastatic pancreatic adenocarcinoma. *J Clin Oncol* 2016; **34**: 371-371 [DOI: [10.1200/jco.2016.34.4\\_suppl.371](https://doi.org/10.1200/jco.2016.34.4_suppl.371)]
- 46 **Lee K**, Molenaar RJ, Klaassen R, Bijlsma MF, Weterman MJ, Richel DJ, Wymenga M, van Laarhoven HWM, Wilmink JW. A Phase I study of LDE225 in combination with gemcitabine and nab-paclitaxel in patients with metastasized pancreatic cancer. *Ann Oncol* 2017; **28**: v260 [DOI: [10.1093/annonc/mdx369.143](https://doi.org/10.1093/annonc/mdx369.143)]
  - 47 **Principe DR**, DeCant B, Mascariñas E, Wayne EA, Diaz AM, Akagi N, Hwang R, Pasche B, Dawson DW, Fang D, Bentrem DJ, Munshi HG, Jung B, Grippo PJ. TGFβ Signaling in the Pancreatic Tumor Microenvironment Promotes Fibrosis and Immune Evasion to Facilitate Tumorigenesis. *Cancer Res* 2016; **76**: 2525-2539 [PMID: [26980767](https://pubmed.ncbi.nlm.nih.gov/26980767/) DOI: [10.1158/0008-5472.CAN-15-1293](https://doi.org/10.1158/0008-5472.CAN-15-1293)]
  - 48 **Friess H**, Yamanaka Y, Büchler M, Ebert M, Beger HG, Gold LI, Korc M. Enhanced expression of transforming growth factor beta isoforms in pancreatic cancer correlates with decreased survival. *Gastroenterology* 1993; **105**: 1846-1856 [PMID: [8253361](https://pubmed.ncbi.nlm.nih.gov/8253361/) DOI: [10.1016/0016-5085\(93\)91084-u](https://doi.org/10.1016/0016-5085(93)91084-u)]
  - 49 **Melisi D**, Garcia-Carbonero R, Macarulla T, Pezet D, Deplanque G, Fuchs M, Trojan J, Oettle H, Kozloff M, Cleverly A, Smith C, Estrem ST, Gueorguieva I, Lahn MMF, Blunt A, Benhadji KA, Tabernero J. Galunisertib plus gemcitabine vs. gemcitabine for first-line treatment of patients with unresectable pancreatic cancer. *Br J Cancer* 2018; **119**: 1208-1214 [PMID: [30318515](https://pubmed.ncbi.nlm.nih.gov/30318515/) DOI: [10.1038/s41416-018-0246-z](https://doi.org/10.1038/s41416-018-0246-z)]
  - 50 **Masamune A**, Hamada S, Kikuta K, Takikawa T, Miura S, Nakano E, Shimosegawa T. The angiotensin II type I receptor blocker olmesartan inhibits the growth of pancreatic cancer by targeting stellate cell activities in mice. *Scand J Gastroenterol* 2013; **48**: 602-609 [PMID: [23477656](https://pubmed.ncbi.nlm.nih.gov/23477656/) DOI: [10.3109/00365521.2013.777776](https://doi.org/10.3109/00365521.2013.777776)]
  - 51 **Arnold SA**, Rivera LB, Carbon JG, Toombs JE, Chang CL, Bradshaw AD, Brekken RA. Losartan slows pancreatic tumor progression and extends survival of SPARC-null mice by abrogating aberrant TGFβ activation. *PLoS One* 2012; **7**: e31384 [PMID: [22348081](https://pubmed.ncbi.nlm.nih.gov/22348081/) DOI: [10.1371/journal.pone.0031384](https://doi.org/10.1371/journal.pone.0031384)]
  - 52 **Liu H**, Naxerova K, Pinter M, Incio J, Lee H, Shigeta K, Ho WW, Crain JA, Jacobson A, Michelakos T, Dias-Santos D, Zanonato A, Hong TS, Clark JW, Murphy JE, Ryan DP, Deshpande V, Lillemoe KD, Fernandez-Del Castillo C, Downes M, Evans RM, Michaelson J, Ferrone CR, Boucher Y, Jain RK. Use of Angiotensin System Inhibitors Is Associated with Immune Activation and Longer Survival in Nonmetastatic Pancreatic Ductal Adenocarcinoma. *Clin Cancer Res* 2017; **23**: 5959-5969 [PMID: [28600474](https://pubmed.ncbi.nlm.nih.gov/28600474/) DOI: [10.1158/1078-0432.CCR-17-0256](https://doi.org/10.1158/1078-0432.CCR-17-0256)]
  - 53 **Murphy JE**, Wo JY, Ryan DP, Clark JW, Jiang W, Yeap BY, Drapek LC, Ly L, Baglini CV, Blaszkowsky LS, Ferrone CR, Parikh AR, Weekes CD, Nipp RD, Kwak EL, Allen JN, Corcoran RB, Ting DT, Faris JE, Zhu AX, Goyal L, Berger DL, Qadan M, Lillemoe KD, Talele N, Jain RK, DeLaney TF, Duda DG, Boucher Y, Fernández-Del Castillo C, Hong TS. Total Neoadjuvant Therapy With FOLFIRINOX in Combination With Losartan Followed by Chemoradiotherapy for Locally Advanced Pancreatic Cancer: A Phase 2 Clinical Trial. *JAMA Oncol* 2019; **5**: 1020-1027 [PMID: [31145418](https://pubmed.ncbi.nlm.nih.gov/31145418/) DOI: [10.1001/jamaoncol.2019.0892](https://doi.org/10.1001/jamaoncol.2019.0892)]
  - 54 **Jiang H**, Hegde S, Knolhoff BL, Zhu Y, Herndon JM, Meyer MA, Nywening TM, Hawkins WG, Shapiro IM, Weaver DT, Pachter JA, Wang-Gillam A, DeNardo DG. Targeting focal adhesion kinase renders pancreatic cancers responsive to checkpoint immunotherapy. *Nat Med* 2016; **22**: 851-860 [PMID: [27376576](https://pubmed.ncbi.nlm.nih.gov/27376576/) DOI: [10.1038/nm.4123](https://doi.org/10.1038/nm.4123)]
  - 55 **Zaghdoudi S**, Decaup E, Belhabib I, Samain R, Cassant-Sourdy S, Rochotte J, Brunel A, Schlaepfer D, Cros J, Neuzillet C, Strehaiano M, Alard A, Tomasini R, Rajeev V, Perraud A, Mathonnet M, Pearce OM, Martineau Y, Pyronnet S, Bousquet C, Jean C. FAK activity in cancer-associated fibroblasts is a prognostic marker and a druggable key metastatic player in pancreatic cancer. *EMBO Mol Med* 2020; **12**: e12010 [PMID: [33025708](https://pubmed.ncbi.nlm.nih.gov/33025708/) DOI: [10.15252/emmm.202012010](https://doi.org/10.15252/emmm.202012010)]
  - 56 **Zhang D**, Li L, Jiang H, Knolhoff BL, Lockhart AC, Wang-Gillam A, DeNardo DG, Ruzinova MB, Lim KH. Constitutive IRAK4 Activation Underlies Poor Prognosis and Chemoresistance in Pancreatic Ductal Adenocarcinoma. *Clin Cancer Res* 2017; **23**: 1748-1759 [PMID: [27702822](https://pubmed.ncbi.nlm.nih.gov/27702822/) DOI: [10.1158/1078-0432.CCR-16-1121](https://doi.org/10.1158/1078-0432.CCR-16-1121)]
  - 57 **Dodhiwala PB**, Khurana N, Zhang D, Cheng Y, Li L, Wei Q, Seehra K, Jiang H, Grierson PM, Wang-Gillam A, Lim KH. TPL2 enforces RAS-induced inflammatory signaling and is activated by point mutations. *J Clin Invest* 2020; **130**: 4771-4790 [PMID: [32573499](https://pubmed.ncbi.nlm.nih.gov/32573499/) DOI: [10.1172/JCI137660](https://doi.org/10.1172/JCI137660)]
  - 58 **Zhang D**, Li L, Jiang H, Li Q, Wang-Gillam A, Yu J, Head R, Liu J, Ruzinova MB, Lim KH. Tumor-Stroma IL1β-IRAK4 Feedforward Circuitry Drives Tumor Fibrosis, Chemoresistance, and Poor Prognosis in Pancreatic Cancer. *Cancer Res* 2018; **78**: 1700-1712 [PMID: [29363544](https://pubmed.ncbi.nlm.nih.gov/29363544/) DOI: [10.1158/0008-5472.CAN-17-1366](https://doi.org/10.1158/0008-5472.CAN-17-1366)]
  - 59 **Neesse A**, Frese KK, Bapiro TE, Nakagawa T, Sternlicht MD, Seeley TW, Pilarsky C, Jodrell DI, Spong SM, Tuveson DA. CTGF antagonism with mAb FG-3019 enhances chemotherapy response without increasing drug delivery in murine ductal pancreas cancer. *Proc Natl Acad Sci U S A* 2013; **110**: 12325-12330 [PMID: [23836645](https://pubmed.ncbi.nlm.nih.gov/23836645/) DOI: [10.1073/pnas.1300415110](https://doi.org/10.1073/pnas.1300415110)]
  - 60 **Aikawa T**, Gunn J, Spong SM, Klaus SJ, Korc M. Connective tissue growth factor-specific antibody attenuates tumor growth, metastasis, and angiogenesis in an orthotopic mouse model of pancreatic cancer. *Mol Cancer Ther* 2006; **5**: 1108-1116 [PMID: [16731742](https://pubmed.ncbi.nlm.nih.gov/16731742/) DOI: [10.1158/1535-7163.Mct-05-0516](https://doi.org/10.1158/1535-7163.Mct-05-0516)]
  - 61 **Picozzi VJ**, Pishvaian MJ, Mody K, Winter JM, Glaspy JA, Larson T, Matrana MR, Saikali K, Carney M, Porter S, Yu P, Kouchakji E, Carrier E. Effect of anti-CTGF human recombinant



- monoclonal antibody pamrevlumab on resectability and resection rate when combined with gemcitabine/nab-paclitaxel in phase 1/2 clinical study for the treatment of locally advanced pancreatic cancer patients. *J Clin Oncol* 2018; **36**: 4016-4016 [DOI: [10.1200/JCO.2018.36.15\\_suppl.4016](https://doi.org/10.1200/JCO.2018.36.15_suppl.4016)]
- 62 **van Duijnhoven FJB**, Jenab M, Hveem K, Siersema PD, Fedirko V, Duell EJ, Kampman E, Halfweeg A, van Kranen HJ, van den Ouweland JMW, Weiderpass E, Murphy N, Langhammer A, Ness-Jensen E, Olsen A, Tjønneland A, Overvad K, Cadeau C, Kvaskoff M, Boutron-Ruault MC, Katzke VA, Kühn T, Boeing H, Trichopoulou A, Kotanidou A, Kritikou M, Palli D, Agnoli C, Tumino R, Panico S, Matullo G, Peeters P, Brustad M, Olsen KS, Lasheras C, Obón-Santacana M, Sánchez MJ, Dorronsoro M, Chirlaque MD, Barricarte A, Manjer J, Almquist M, Renström F, Ye W, Wareham N, Khaw KT, Bradbury KE, Freisling H, Aune D, Norat T, Riboli E, Bueno-de-Mesquita HBA. Circulating concentrations of vitamin D in relation to pancreatic cancer risk in European populations. *Int J Cancer* 2018; **142**: 1189-1201 [PMID: [29114875](https://pubmed.ncbi.nlm.nih.gov/29114875/) DOI: [10.1002/ijc.31146](https://doi.org/10.1002/ijc.31146)]
- 63 **Waterhouse M**, Risch HA, Bosetti C, Anderson KE, Petersen GM, Bamlet WR, Cotterchio M, Cleary SP, Ibiebele TI, La Vecchia C, Skinner HG, Strayer L, Bracci PM, Maisonneuve P, Bueno-de-Mesquita HB, Zaton Ski W, Lu L, Yu H, Janik-Konieczny K, Polesel J, Serraino D, Neale RE; Pancreatic Cancer Case-Control Consortium (PanC4). Vitamin D and pancreatic cancer: a pooled analysis from the Pancreatic Cancer Case-Control Consortium. *Ann Oncol* 2015; **26**: 1776-1783 [PMID: [25977560](https://pubmed.ncbi.nlm.nih.gov/25977560/) DOI: [10.1093/annonc/mdv236](https://doi.org/10.1093/annonc/mdv236)]
- 64 **Weinstein SJ**, Stolzenberg-Solomon RZ, Kopp W, Rager H, Virtamo J, Albanes D. Impact of circulating vitamin D binding protein levels on the association between 25-hydroxyvitamin D and pancreatic cancer risk: a nested case-control study. *Cancer Res* 2012; **72**: 1190-1198 [PMID: [22232734](https://pubmed.ncbi.nlm.nih.gov/22232734/) DOI: [10.1158/0008-5472.CAN-11-2950](https://doi.org/10.1158/0008-5472.CAN-11-2950)]
- 65 **Yuan C**, Qian ZR, Babic A, Morales-Oyarvide V, Rubinson DA, Kraft P, Ng K, Bao Y, Giovannucci EL, Ogino S, Stampfer MJ, Gaziano JM, Sesso HD, Buring JE, Cochrane BB, Chlebowski RT, Snetselaar LG, Manson JE, Fuchs CS, Wolpin BM. Prediagnostic Plasma 25-Hydroxyvitamin D and Pancreatic Cancer Survival. *J Clin Oncol* 2016; **34**: 2899-2905 [PMID: [27325858](https://pubmed.ncbi.nlm.nih.gov/27325858/) DOI: [10.1200/JCO.2015.66.3005](https://doi.org/10.1200/JCO.2015.66.3005)]
- 66 **Sherman MH**, Yu RT, Engle DD, Ding N, Atkins AR, Tiriach H, Collisson EA, Connor F, Van Dyke T, Kozlov S, Martin P, Tseng TW, Dawson DW, Donahue TR, Masamune A, Shimosegawa T, Apte MV, Wilson JS, Ng B, Lau SL, Gunton JE, Wahl GM, Hunter T, Drebin JA, O'Dwyer PJ, Liddle C, Tuveson DA, Downes M, Evans RM. Vitamin D receptor-mediated stromal reprogramming suppresses pancreatitis and enhances pancreatic cancer therapy. *Cell* 2014; **159**: 80-93 [PMID: [25259922](https://pubmed.ncbi.nlm.nih.gov/25259922/) DOI: [10.1016/j.cell.2014.08.007](https://doi.org/10.1016/j.cell.2014.08.007)]
- 67 **Wallbaum P**, Rohde S, Ehlers L, Lange F, Hohn A, Bergner C, Schwarzenböck SM, Krause BJ, Jaster R. Antifibrogenic effects of vitamin D derivatives on mouse pancreatic stellate cells. *World J Gastroenterol* 2018; **24**: 170-178 [PMID: [29375203](https://pubmed.ncbi.nlm.nih.gov/29375203/) DOI: [10.3748/wjg.v24.i2.170](https://doi.org/10.3748/wjg.v24.i2.170)]
- 68 **Arensman MD**, Nguyen P, Kershaw KM, Lay AR, Ostertag-Hill CA, Sherman MH, Downes M, Liddle C, Evans RM, Dawson DW. Calcipotriol Targets LRP6 to Inhibit Wnt Signaling in Pancreatic Cancer. *Mol Cancer Res* 2015; **13**: 1509-1519 [PMID: [26224368](https://pubmed.ncbi.nlm.nih.gov/26224368/) DOI: [10.1158/1541-7786.MCR-15-0204](https://doi.org/10.1158/1541-7786.MCR-15-0204)]
- 69 **Schwartz GG**, Eads D, Naczki C, Northrup S, Chen T, Koumenis C. 19-nor-1 alpha,25-dihydroxyvitamin D2 (paricalcitol) inhibits the proliferation of human pancreatic cancer cells *in vitro* and *in vivo*. *Cancer Biol Ther* 2008; **7**: 430-436 [PMID: [18094617](https://pubmed.ncbi.nlm.nih.gov/18094617/) DOI: [10.4161/cbt.7.3.5418](https://doi.org/10.4161/cbt.7.3.5418)]
- 70 **Huang X**, Gao Y, Zhi X, Ta N, Jiang H, Zheng J. Association between vitamin A, retinol and carotenoid intake and pancreatic cancer risk: Evidence from epidemiologic studies. *Sci Rep* 2016; **6**: 38936 [PMID: [27941847](https://pubmed.ncbi.nlm.nih.gov/27941847/) DOI: [10.1038/srep38936](https://doi.org/10.1038/srep38936)]
- 71 **Froeling FE**, Feig C, Chelala C, Dobson R, Mein CE, Tuveson DA, Clevers H, Hart IR, Kocher HM. Retinoic acid-induced pancreatic stellate cell quiescence reduces paracrine Wnt- $\beta$ -catenin signaling to slow tumor progression. *Gastroenterology* 2011; **141**: 1486-1497, 1497.e1-1497. 14 [PMID: [21704588](https://pubmed.ncbi.nlm.nih.gov/21704588/) DOI: [10.1053/j.gastro.2011.06.047](https://doi.org/10.1053/j.gastro.2011.06.047)]
- 72 **Kocher HM**, Basu B, Froeling FEM, Sarker D, Slater S, Carlin D, deSouza NM, De Paep KN, Goulart MR, Hughes C, Imrali A, Roberts R, Pawula M, Houghton R, Lawrence C, Yogeswaran Y, Mousa K, Coetzee C, Sasieni P, Prendergast A, Propper DJ. Phase I clinical trial repurposing all-trans retinoic acid as a stromal targeting agent for pancreatic cancer. *Nat Commun* 2020; **11**: 4841 [PMID: [32973176](https://pubmed.ncbi.nlm.nih.gov/32973176/) DOI: [10.1038/s41467-020-18636-w](https://doi.org/10.1038/s41467-020-18636-w)]
- 73 **Conte E**, Gili E, Fagone E, Fruciano M, Iemmolo M, Vancheri C. Effect of pirfenidone on proliferation, TGF- $\beta$ -induced myofibroblast differentiation and fibrogenic activity of primary human lung fibroblasts. *Eur J Pharm Sci* 2014; **58**: 13-19 [PMID: [24613900](https://pubmed.ncbi.nlm.nih.gov/24613900/) DOI: [10.1016/j.ejps.2014.02.014](https://doi.org/10.1016/j.ejps.2014.02.014)]
- 74 **Kozono S**, Ohuchida K, Eguchi D, Ikenaga N, Fujiwara K, Cui L, Mizumoto K, Tanaka M. Pirfenidone inhibits pancreatic cancer desmoplasia by regulating stellate cells. *Cancer Res* 2013; **73**: 2345-2356 [PMID: [23348422](https://pubmed.ncbi.nlm.nih.gov/23348422/) DOI: [10.1158/0008-5472.CAN-12-3180](https://doi.org/10.1158/0008-5472.CAN-12-3180)]
- 75 **Elahi-Gedwillo KY**, Carlson M, Zettervall J, Provenzano PP. Antifibrotic Therapy Disrupts Stromal Barriers and Modulates the Immune Landscape in Pancreatic Ductal Adenocarcinoma. *Cancer Res* 2019; **79**: 372-386 [PMID: [30401713](https://pubmed.ncbi.nlm.nih.gov/30401713/) DOI: [10.1158/0008-5472.CAN-18-1334](https://doi.org/10.1158/0008-5472.CAN-18-1334)]
- 76 **Toole BP**. Hyaluronan: from extracellular glue to pericellular cue. *Nat Rev Cancer* 2004; **4**: 528-539 [PMID: [15229478](https://pubmed.ncbi.nlm.nih.gov/15229478/) DOI: [10.1038/nrc1391](https://doi.org/10.1038/nrc1391)]
- 77 **Cheng XB**, Sato N, Kohi S, Yamaguchi K. Prognostic impact of hyaluronan and its regulators in pancreatic ductal adenocarcinoma. *PLoS One* 2013; **8**: e80765 [PMID: [24244714](https://pubmed.ncbi.nlm.nih.gov/24244714/) DOI: [10.1371/journal.pone.0080765](https://doi.org/10.1371/journal.pone.0080765)]



- 10.1371/journal.pone.0080765]
- 78 **Toole BP**, Slomiany MG. Hyaluronan: a constitutive regulator of chemoresistance and malignancy in cancer cells. *Semin Cancer Biol* 2008; **18**: 244-250 [PMID: [18534864](#) DOI: [10.1016/j.semcancer.2008.03.009](#)]
- 79 **Provenzano PP**, Cuevas C, Chang AE, Goel VK, Von Hoff DD, Hingorani SR. Enzymatic targeting of the stroma ablates physical barriers to treatment of pancreatic ductal adenocarcinoma. *Cancer Cell* 2012; **21**: 418-429 [PMID: [22439937](#) DOI: [10.1016/j.ccr.2012.01.007](#)]
- 80 **Hingorani SR**, Harris WP, Beck JT, Berdov BA, Wagner SA, Pshevlovsky EM, Tjulandin SA, Gladkov OA, Holcombe RF, Korn R, Raghunand N, Dychter S, Jiang P, Shepard HM, Devoe CE. Phase Ib Study of PEGylated Recombinant Human Hyaluronidase and Gemcitabine in Patients with Advanced Pancreatic Cancer. *Clin Cancer Res* 2016; **22**: 2848-2854 [PMID: [26813359](#) DOI: [10.1158/1078-0432.CCR-15-2010](#)]
- 81 **Hingorani SR**, Zheng L, Bullock AJ, Seery TE, Harris WP, Sigal DS, Braiteh F, Ritch PS, Zalupski MM, Bahary N, Oberstein PE, Wang-Gillam A, Wu W, Chondros D, Jiang P, Khelifa S, Pu J, Aldrich C, Hendifar AE. HALO 202: Randomized Phase II Study of PEGPH20 Plus Nab-Paclitaxel/Gemcitabine Versus Nab-Paclitaxel/Gemcitabine in Patients With Untreated, Metastatic Pancreatic Ductal Adenocarcinoma. *J Clin Oncol* 2018; **36**: 359-366 [PMID: [29232172](#) DOI: [10.1200/JCO.2017.74.9564](#)]
- 82 **Tempero MA**, Cutsem EV, Sigal D, Oh D-Y, Fazio N, Macarulla T, Hitre E, Hammel P, Hendifar AE, Bates SE, Li C-P, Fouchardiere CDL, Heinemann V, Maraveyas A, Bahary N, Layos L, Sahai V, Zheng L, Lacy J, Bullock AJ, Investigators H-. HALO 109-301: A randomized, double-blind, placebo-controlled, phase 3 study of pegvorhyaluronidase alfa (PEGPH20) + nab-paclitaxel/gemcitabine (AG) in patients (pts) with previously untreated hyaluronan (HA)-high metastatic pancreatic ductal adenocarcinoma (mPDA). *J Clin Oncol* 2020; **38**: 638-638 [DOI: [10.1200/JCO.2020.38.4\\_suppl.638](#)]
- 83 **Ramanathan RK**, McDonough SL, Philip PA, Hingorani SR, Lacy J, Kortmansky JS, Thumar J, Chiorean EG, Shields AF, Behl D, Mehan PT, Gaur R, Seery T, Guthrie KA, Hochster HS. Phase IB/II Randomized Study of FOLFIRINOX Plus Pegylated Recombinant Human Hyaluronidase Versus FOLFIRINOX Alone in Patients With Metastatic Pancreatic Adenocarcinoma: SWOG S1313. *J Clin Oncol* 2019; **37**: 1062-1069 [PMID: [30817250](#) DOI: [10.1200/JCO.18.01295](#)]
- 84 **Wang-Gillam A**. Targeting Stroma: A Tale of Caution. *J Clin Oncol* 2019; **37**: 1041-1043 [PMID: [30860950](#) DOI: [10.1200/JCO.19.00056](#)]
- 85 **Peng L**, Ran YL, Hu H, Yu L, Liu Q, Zhou Z, Sun YM, Sun LC, Pan J, Sun LX, Zhao P, Yang ZH. Secreted LOXL2 is a novel therapeutic target that promotes gastric cancer metastasis via the Src/FAK pathway. *Carcinogenesis* 2009; **30**: 1660-1669 [PMID: [19625348](#) DOI: [10.1093/carcin/bgp178](#)]
- 86 **Benson AB 3rd**, Wainberg ZA, Hecht JR, Vyushkov D, Dong H, Bendell J, Kudrik F. A Phase II Randomized, Double-Blind, Placebo-Controlled Study of Simtuzumab or Placebo in Combination with Gemcitabine for the First-Line Treatment of Pancreatic Adenocarcinoma. *Oncologist* 2017; **22**: 241-e15 [PMID: [28246206](#) DOI: [10.1634/theoncologist.2017-0024](#)]
- 87 **Brooks PC**. Role of integrins in angiogenesis. *Eur J Cancer* 1996; **32A**: 2423-2429 [PMID: [9059330](#) DOI: [10.1016/s0959-8049\(96\)00381-4](#)]
- 88 **Garay-Susini B**, Varner JA. Roles of integrins in tumor angiogenesis and lymphangiogenesis. *Lymphat Res Biol* 2008; **6**: 155-163 [PMID: [19093788](#) DOI: [10.1089/lrb.2008.1011](#)]
- 89 **Eskens FA**, Dumez H, Hoekstra R, Perschl A, Brindley C, Böttcher S, Wynendaal W, Dreys J, Verweij J, van Oosterom AT. Phase I and pharmacokinetic study of continuous twice weekly intravenous administration of Cilengitide (EMD 121974), a novel inhibitor of the integrins  $\alpha$ 5 $\beta$ 1 and  $\alpha$ 5 $\beta$ 3 in patients with advanced solid tumours. *Eur J Cancer* 2003; **39**: 917-926 [PMID: [12706360](#) DOI: [10.1016/s0959-8049\(03\)00057-1](#)]
- 90 **Friess H**, Langrehr JM, Oettle H, Raedle J, Niedergethmann M, Dittich C, Hossfeld DK, Stöger H, Neyns B, Herzog P, Piedbois P, Dobrowolski F, Scheithauer W, Hawkins R, Katz F, Balcke P, Vermorken J, van Belle S, Davidson N, Esteve AA, Castellano D, Kleeff J, Tempia-Caliera AA, Kovar A, Nippgen J. A randomized multi-center phase II trial of the angiogenesis inhibitor Cilengitide (EMD 121974) and gemcitabine compared with gemcitabine alone in advanced unresectable pancreatic cancer. *BMC Cancer* 2006; **6**: 285 [PMID: [17156477](#) DOI: [10.1186/1471-2407-6-285](#)]
- 91 **Winer A**, Adams S, Mignatti P. Matrix Metalloproteinase Inhibitors in Cancer Therapy: Turning Past Failures Into Future Successes. *Mol Cancer Ther* 2018; **17**: 1147-1155 [PMID: [29735645](#) DOI: [10.1158/1535-7163.MCT-17-0646](#)]
- 92 **Moore MJ**, Hamm J, Dancey J, Eisenberg PD, Dagenais M, Fields A, Hagan K, Greenberg B, Colwell B, Zee B, Tu D, Ottaway J, Humphrey R, Seymour L; National Cancer Institute of Canada Clinical Trials Group. Comparison of gemcitabine vs the matrix metalloproteinase inhibitor BAY 12-9566 in patients with advanced or metastatic adenocarcinoma of the pancreas: a phase III trial of the National Cancer Institute of Canada Clinical Trials Group. *J Clin Oncol* 2003; **21**: 3296-3302 [PMID: [12947065](#) DOI: [10.1200/jco.2003.02.098](#)]
- 93 **Evans JD**, Stark A, Johnson CD, Daniel F, Carmichael J, Buckels J, Imrie CW, Brown P, Neoptolemos JP. A phase II trial of marimastat in advanced pancreatic cancer. *Br J Cancer* 2001; **85**: 1865-1870 [PMID: [11747327](#) DOI: [10.1054/bjoc.2001.2168](#)]
- 94 **van Mackelenbergh MG**, Stroes CI, Spijker R, van Eijck CHJ, Wilmink JW, Bijlsma MF, van Laarhoven HWM. Clinical Trials Targeting the Stroma in Pancreatic Cancer: A Systematic Review

- and Meta-Analysis. *Cancers (Basel)* 2019; **11** [PMID: 31035512 DOI: 10.3390/cancers11050588]
- 95 **Jiang H**, Torphy RJ, Steiger K, Hongo H, Ritchie AJ, Kriegsmann M, Horst D, Umetsu SE, Joseph NM, McGregor K, Pishvaian MJ, Blais EM, Lu B, Li M, Hollingsworth M, Stashko C, Volmar K, Yeh JJ, Weaver VM, Wang ZJ, Tempero MA, Weichert W, Collisson EA. Pancreatic ductal adenocarcinoma progression is restrained by stromal matrix. *J Clin Invest* 2020; **130**: 4704-4709 [PMID: 32749238 DOI: 10.1172/JCI136760]



## Magnetic resonance imaging-based artificial intelligence model in rectal cancer

Pei-Pei Wang, Chao-Lin Deng, Bin Wu

**ORCID number:** Pei-Pei Wang 0000-0002-2648-5283; Chao-Lin Deng 0000-0003-2314-5934; Bin Wu 0000-0003-0413-6987.

**Author contributions:** Wu B designed and revised the review; Wang PP collected the literature for recent advances in the field and wrote the manuscript; Deng CL modified the article format; all authors have read and approved the final version to be published.

**Conflict-of-interest statement:** The authors have nothing to declare.

**Open-Access:** This article is an open-access article that was selected by an in-house editor and fully peer-reviewed by external reviewers. It is distributed in accordance with the Creative Commons Attribution NonCommercial (CC BY-NC 4.0) license, which permits others to distribute, remix, adapt, build upon this work non-commercially, and license their derivative works on different terms, provided the original work is properly cited and the use is non-commercial. See: <http://creativecommons.org/licenses/by-nc/4.0/>

**Manuscript source:** Invited manuscript

**Specialty type:** Gastroenterology and hepatology

**Pei-Pei Wang, Chao-Lin Deng, Bin Wu,** Department of General Surgery, Peking Union Medical College Hospital, Chinese Academy of Medical Sciences and Peking Union Medical College, Beijing 100730, China

**Corresponding author:** Bin Wu, MD, Professor, Department of General Surgery, Peking Union Medical College Hospital, Chinese Academy of Medical Sciences and Peking Union Medical College, No. 1 Shuaifu Yuan, Dongcheng District, Beijing 100730, China.  
[wubin0279@hotmail.com](mailto:wubin0279@hotmail.com)

### Abstract

Rectal magnetic resonance imaging (MRI) is the preferred method for the diagnosis of rectal cancer as recommended by the guidelines. Rectal MRI can accurately evaluate the tumor location, tumor stage, invasion depth, extramural vascular invasion, and circumferential resection margin. We summarize the progress of research on the use of artificial intelligence (AI) in rectal cancer in recent years. AI, represented by machine learning, is being increasingly used in the medical field. The application of AI models based on high-resolution MRI in rectal cancer has been increasingly reported. In addition to staging the diagnosis and localizing radiotherapy, an increasing number of studies have reported that AI models based on high-resolution MRI can be used to predict the response to chemotherapy and prognosis of patients.

**Key Words:** Artificial intelligence; Deep learning; Colorectal cancer; Magnetic resonance imaging; Radiomics

©The Author(s) 2021. Published by Baishideng Publishing Group Inc. All rights reserved.

**Core Tip:** Recently, there has been an increase in the use of artificial intelligence (AI) models based on magnetic resonance (MR) images in locally advanced rectal cancer. MR imaging based on big datasets helps in the provision of systematic and precise medical services to patients with rectal cancer in the treatment process. This review summarizes recent research progress on the application of AI based on MR images in rectal cancer.

**Citation:** Wang PP, Deng CL, Wu B. Magnetic resonance imaging-based artificial intelligence

**Country/Territory of origin:** China**Peer-review report's scientific quality classification**

Grade A (Excellent): 0

Grade B (Very good): B, B

Grade C (Good): 0

Grade D (Fair): 0

Grade E (Poor): 0

**Received:** January 10, 2021**Peer-review started:** January 10, 2021**First decision:** February 11, 2021**Revised:** February 23, 2021**Accepted:** March 16, 2021**Article in press:** March 16, 2021**Published online:** May 14, 2021**P-Reviewer:** Boscá L, Tanabe S**S-Editor:** Zhang H**L-Editor:** Wang TQ**P-Editor:** Ma YJmodel in rectal cancer. *World J Gastroenterol* 2021; 27(18): 2122-2130**URL:** <https://www.wjgnet.com/1007-9327/full/v27/i18/2122.htm>**DOI:** <https://dx.doi.org/10.3748/wjg.v27.i18.2122>

## INTRODUCTION

Over 1 million people die from colorectal cancer (CRC) every year worldwide. According to the statistics by the United States National Cancer Institute, CRC is the third most common cancer in both men and women[1]. The risk of lymph node metastasis in patients with rectal cancer is 29%-52%[2-4]. Lymph node metastasis has predictive value for postoperative local recurrence and distant metastasis. High-resolution magnetic resonance imaging (MRI) is the preferred clinical imaging method to evaluate lymph node metastasis of rectal cancer[5]. Rectal MRI can accurately evaluate the tumor location, tumor stage, invasion depth, extramural vascular invasion (EMVI), and circumferential resection margin[6-8]. Accurate MRI assessment is of great significance to patients with rectal cancer, as it is related to the patients' prognosis[9]. It can be used to make a reasonable clinical treatment plan.

Nowadays, with the rapid development of advanced technology, artificial intelligence (AI) is being used in many fields. AI, represented by machine learning, is being increasingly used in the medical field too[10-12]. Machine learning-based AI uses big data collection and analysis to make effective decisions and predictions about new situations. In terms of algorithm application, artificial neural networks, support vector machines (SVM), and kernel methods are what are mainly being used[13-18] (Figure 1). With the increasing application of AI in the medical field, MRI based on big datasets helps in the provision of systematic and precise medical services to patients with rectal cancer in the treatment process.

## MRI-BASED AI MODEL IMPROVES THE ACCURACY OF STAGING RECTAL CANCER

Lymphatic spread is an important metastatic route of rectal cancer, and many studies have reported that lymph node metastasis increases the risk of local recurrence in patients. Only 10% of the patients with stage T1 rectal cancer had lymph node metastasis. More than 40% of rectal cancer patients with lymph node metastasis did not have distant metastasis when local recurrence occurred[19,20]. If a metastatic lymph node can be identified before surgery, it is necessary and reasonable to perform radical surgery involving regional lymph node dissection for these patients. According to the National Comprehensive Cancer Network guidelines and clinical practice, neoadjuvant chemoradiotherapy is recommended for patients with locally advanced rectal cancer. Therefore, accurate evaluation by using MRI to stage the disease is crucial for clinical decision-making.

High-resolution MRI has many advantages for clinically staging rectal cancer[21]. The images are reviewed by two radiologists who are experts in clinical work. It is time-consuming to make an accurate diagnosis. There is an inevitable subjective bias among different physicians[22]. Girshick *et al* [23] put forward faster region-based convolutional neural network ("Faster R-CNN") in 2016, which was widely used in the simulation of medical image diagnosis. Ding *et al*[24] developed an AI model based on the "Faster R-CNN" algorithm to detect the lymph nodes of patients with rectal cancer. The accuracy of the model was verified by multicenter clinical practice. The MRI data of 414 CRC patients with pelvic lymph node metastasis were first identified using the R-CNN system, and the results were compared to those of radiologists and pathologists. The consistency between radiologists and the AI model was 0.912. The consistency of the AI model and pathology diagnosis was 0.448. The consistency between radiologists and pathologists was only 0.134. The conclusion was that the AI model based on "Faster R-CNN" was superior to the radiologists in predicting pelvic lymph node metastasis in rectal cancer patients, but its accuracy was inferior to that of the pathologists.

Lymph node detection is more complicated due to obvious individual differences in lymph node locations and sizes. He *et al*[25] proposed the "Mask R-CNN" that has excellent data processing ability. Multiparametric MRI (mpMRI) includes images such as T2WI and DWI. Zhao *et al*[26] attempted to combine mpMRI and "Mask R-CNN"

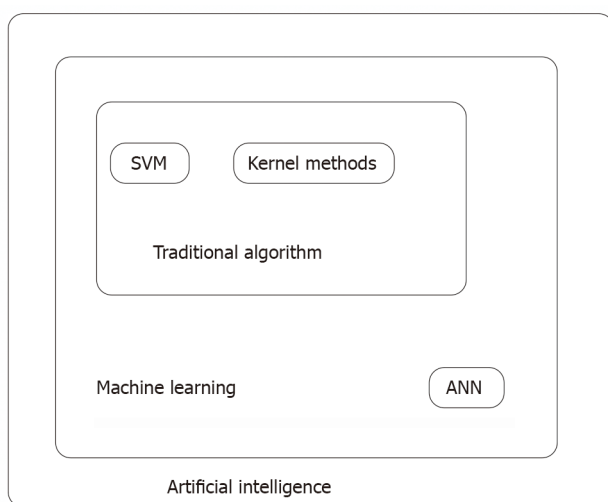


**Figure 1 Relationship between artificial neural networks and support vector machines in artificial intelligence.** ANN: Artificial neural networks; SVM: Support vector machines.

into an automatic lymph node detection system. The sensitivity for lymph node detection in this model was 80%. The results are similar to those of Barbu *et al* (80%) and Feuersteins *et al* (82.1%), which were higher than those of Kitasaka *et al* (57%) and Feulner *et al* (65.4%)[27-29]. The positive predictive value of the AI model for lymph node detection was 73.5%, which was significantly higher than that of the other four studies. The average time required by the AI model to detect a patient was 1.43 s. The average time required for a radiologist with nine years of experience at the center was 134.4 s. The AI model reduces the time cost to some extent. The conclusion is that the AI detection system can improve the efficiency of lymph node detection, especially for lymph nodes  $\geq 3$  mm. Based on this study, we can infer that R-CNN combined with multi-parameter MRI can better improve the efficiency of lymph node detection.

A single-center retrospective study reported that high-resolution MRI based on an AI model can be used to evaluate the involvement of circumferential resection margins in rectal cancer[30]. A total of 240 CRC patients with positive circumferential resection margins were included, and image training was carried out based on the regional convolutional neural network AI model. In the training set, the ratio of positive to negative images was 1:2. The diagnosis results of the AI platform were compared with those of a senior radiologist. The accuracy, sensitivity, and specificity of the model were 0.932, 0.838, and 0.956, respectively. The area under the curve (AUC) was 0.953. This study suggested high-resolution MRI based on an AI model has a good prospect of application in evaluation for the involvement of circumferential resection margins in rectal cancer.

Concurrent peritoneal metastasis (PM) may occur in 5%–15% of CRC patients, and heterochronous peritoneal metastasis may occur in approximately 20% of CRC patients. The sensitivity of computed tomography (CT) to PM was positively correlated with lesion size, especially for lesions  $< 0.5$  cm. The sensitivity was between 11% and 70%[31]. It is difficult for radiologists to detect simultaneous peritoneal metastasis in CRC. Yuan *et al*[32] constructed an AI model based on an SVM classifier using the RESnet-3D algorithm to evaluate simultaneous peritoneal metastatic carcinoma of CRC. In this model, CT images of 54 patients with peritoneal metastatic cancer and 76 patients with CRC without peritoneal metastatic cancer were included in the training set. The RESnet-3D features were combined with 12 specific signs of peritoneal metastatic cancer in order to construct an SVM classifier. The sensitivity, specificity, and accuracy of the AI model for PM detection were 93.75%, 94.44%, and 94.11%, respectively. It is therefore much better than conventional enhanced CT. It is believed that there will be a more developed image diagnosis system based on the AI model in the future that will make staging diagnosis in MR images more efficient, accurate, and stable, and reduce the judgment error caused by the differences in radiologists' diagnostic abilities to a certain extent.



## APPLICATION OF AN MRI-BASED AI MODEL IN RADIOTHERAPY

It is a very important yet time-consuming process to manually draw tumor volume contours in rectal cancer radiotherapy. Wang *et al*[33] aimed to develop an automatic tumor segmentation algorithm based on deep learning to segment rectal tumors using T2-weighted MRI images. This study included 93 patients with locally advanced rectal cancer (cT3-4 and/or cN1-2) who underwent surgical treatment following neoadjuvant chemoradiotherapy (nCRT). The model was trained in two stages: Tumor recognition and tumor segmentation. The data sets were randomly divided into training sets (90%) and validation sets (10%). Four indices, namely, the Hausdorff distance (HD), average surface distance (ASD), Dice index (DSC), and Jaccard index (JSC), were calculated to evaluate the advantages and disadvantages of automatic and manual segmentation. The DSC, JSC, HD, and ASD results of the AI model and those of radiologists (manual segmentation) were compared as follows: DSC [(0.74 ± 0.14) *vs* (0.71 ± 0.13)] (*P* = 0.42), JSC [0.60 ± 0.16 *vs* 0.57 ± 0.15] (*P* = 0.35), HD [20.44 ± 13.35 *vs* 14.91 ± 7.62] (*P* = 0.35), and ASD [3.25 ± 1.69 mm *vs* 2.67 ± 1.46] (*P* = 0.16), which showed no statistically significant difference between the automatic segmentation group and the manual segmentation group. A total of 140 patients with locally advanced rectal cancer were included in another study[34]. The multi-parameter MRI images of patients were identified using an AI model based on a deep learning algorithm. Its deep learning algorithm was mainly based on a convolutional neural network. The model was used to segment the tumor after recognition of the MRI image. In this study, the results of the AI model were compared with those of two senior radiologists, and the AUC was 0.99. The AI model can be accurate in tumor location and tumor segmentation in CRC patients.

CNNs are an advanced algorithm applied at present. However, repeated pooling and undersampling can reduce the resolution of the features and may result in the loss of detailed information. Men *et al*[35] combined cascaded atrous convolution (CAC) and spatial pyramid pooling module (SPP), and developed a new-type CNN (CAC-SPP) that could further improve the accuracy of tumor segmentation. The detection efficiency of the CAC-SPP model was superior to that of the algorithm models U-NET and RESnet-101 (*P* < 0.05). The detection speed of the CAC-SPP model was similar to that of RESnet-101, which was faster than that of U-NET. In short, the CAC-SPP model with high-resolution MRI can improve the accuracy of rectal tumor segmentation by obtaining more tumor features.

## APPLICATION OF AN MRI-BASED AI MODEL IN THE EVALUATION OF STAGE AFTER NEOADJUVANT THERAPY FOR RECTAL CANCER

Currently, total mesorectal excision has become the standard treatment for locally advanced rectal cancer[36]. In clinical practice, there are often patients with rectal cancer of the same stage for whom nCRT has different curative effects. Some patients achieved a pathological complete response (PCR) after nCRT, while others did not respond to treatment and some even had progressive disease. Over 30% of the patients could not benefit from nCRT[37]. For the patients who had a PCR after neoadjuvant therapy, the risk of local recurrence was relatively low. For these patients, minimally invasive and anal sphincter sparing surgery, or even the "watch and see" strategy is the mainstream opinion at present. However, due to the limitations of the current diagnostic methods, clinical complete response is not equivalent to PCR. Clinicians should focus on improving the accuracy of MRI by using high-resolution MRI and selecting a more effective MR contrast agent. The increase in the MR sequence increases the workload of the radiologists and leads to the consumption of imaging examination time. In addition, different hospitals have different clinical diagnostic abilities and different radiologists are inconsistent in making imaging diagnoses. Combined with radiomics and convolutional neural networks, increasing research has been conducted on construction of image recognition models based on AI in order to solve these problems. The use of MR images based on AI models to evaluate the response to neoadjuvant therapy in patients with locally advanced rectal cancer and identify patients with a complete pathological response in the early stages will be of great significance for the realization of individualized precision therapy for CRC in the future.

Ferrari *et al*[38] developed an AI model based on high-resolution MRI, hoping that this model can help identify patients with a complete pathological response after neoadjuvant therapy in locally advanced rectal cancer, and can identify the non-

responders after neoadjuvant therapy in the early stages. This study included 55 patients with locally advanced rectal cancer who received surgical treatment after neoadjuvant therapy. The patients were randomly divided into two groups, one for the training cohort and the other for the validation cohort. In the training cohort, the MRI images of patients were combined with the histopathological results using the algorithm, and the model performance was verified in the validation cohort. The AUC for identifying complete reaction in the validation set was 0.86 (95%CI: 0.70, 0.94), and the AUC for identifying the non-responders was 0.83 (95%CI: 0.71, 0.92). In conclusion, the AI model based on high-resolution MR images has achieved good results, which is helpful in identifying patients with complete remission after neoadjuvant therapy and patients with no response to neoadjuvant therapy in the early stages.

Zhang *et al*[39] developed a deep learning algorithm model based on T2 weighting and diffusion kurtosis MR images. A prospective study was carried out based on this model, involving 383 patients with 308 as the training set and 104 as the verification set. The model aimed to evaluate PCR, tumor regression grade, and down-staging of locally advanced rectal cancer after neoadjuvant therapy. The study results showed that the AUC of the validation set in predicting PCR was 0.99. The AUC for T-cell receptor gamma and T staging assessments was 0.70 and 0.79, respectively. With the assistance of the deep learning algorithm model, the error rate of radiology physicians in reading films was significantly reduced. A deep learning model based on diffusion kurtosis MR can evaluate the PCR of patients after nCRT and assist radiologists in evaluating the chemotherapy responses after neoadjuvant therapy in locally advanced rectal cancer.

Shi *et al*[40] developed an AI model based on a deep learning algorithm using MRI images before and during neoadjuvant therapy. The study aimed to evaluate and predict the patient's response to neoadjuvant therapy. It was found that the AI image recognition model based solely on MR images before nCRT or MRI images during neoadjuvant therapy was less effective than that combining two MR images in terms of PCR or good response after neoadjuvant therapy.

## APPLICATION OF AN MRI-BASED AI MODEL IN PREDICTING CHEMORADIOTHERAPY RESPONSE IN PATIENTS WITH RECTAL CANCER

Fu *et al*[41] designed a study using experienced radiation oncologists and a deep learning algorithm model to map tumor volume contours on DWI images after neoadjuvant therapy in patients with locally advanced rectal cancer. In this study, a least absolute shrinkage and selection operator-logistic regression model was used to predict treatment response. The results of the two models were verified and compared with regard to the AUC. The AUC of the manual drawing group was 0.64, and that of the deep learning group was 0.73 ( $P < 0.05$ ). On analysis of the findings from this study, the performance of the deep learning model was found to be better than that of manual mapping in predicting the response of rectal cancer to neoadjuvant therapy. A similar retrospective study was recently published by Yi *et al*[42]. A total of 134 patients were included, and T2-weighted MRI images were extracted using machine learning models to predict the patients' chemotherapeutic response and tumor downstaging. The results were verified using the subject work curve. The AUC of the PCR group was 0.91 (95%CI: 0.83-0.98), that of the good response group was 0.90 (95%CI: 0.83-0.97), and the tumor downstage AUC was 0.93 (95%CI: 0.87-0.98). The results suggest that radiomics based on machine learning has promising application prospects in predicting the response of patients to chemotherapy. A study compared a Bayesian network algorithm model with a model combining SVM, Bayesian networks, convolutional neural networks, and the K-nearest algorithm in predicting CRC patients' responses to neoadjuvant therapy[43]. The shape feature set, texture feature set, intensity feature set, and the other information of the MR images were extracted by the two models for comprehensive evaluation. The AUC and accuracy of the Bayesian network algorithm model in the validation queue were 74% and 79%, respectively, while the AUC and accuracy of the combined model were 95% and 90%, respectively. The deep learning model integrated with multiple algorithms showed better performance in predicting neoadjuvant therapy responsiveness in rectal cancer patients.

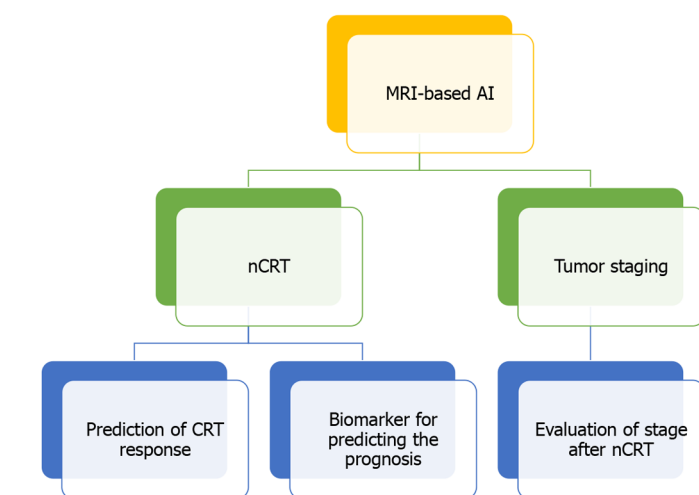


**Figure 2 Application of artificial intelligence based on magnetic resonance images in rectal cancer.** MRI: Magnetic resonance imaging; AI: Artificial intelligence; nCRT: Neoadjuvant chemoradiotherapy.

## MRI-BASED AI MODEL MAY BE AN EFFECTIVE BIOMARKER FOR PREDICTING THE PROGNOSIS OF PATIENTS

Many scholars have realized the role of radiological characteristics in predicting the mutation status of the *KRAS* gene in patients. Recently, Cui *et al*[44] used an AI model based on MR images to predict individuals with *KRAS* gene mutations among CRC patients. In this study, 304 patients were included, and the model predicted performance with an AUC of 0.722 (95%CI, 0.654-0.790) in the training set and 0.714 (95%CI, 0.602-0.827) in the validation set.

Radiomics features based on T2-weighted images are effective in predicting the *KRAS* status in patients with rectal cancer to determine the expression of *KRAS* in patients with rectal cancer, which may be helpful in supplementing genomic analysis of patients. In the future, more MR images should be included, analyzed, and trained to improve the predictive efficiency of this model.

MrT staging, mrN staging, positive EMVI, and peritoneal reflection invasion were all associated with heterochronic distant metastasis after surgery. It has been confirmed that histological invasion of the vessels around the intestinal wall is an independent predictor of distant metastasis for rectal cancer[45]. Clinically, if the high-risk population of postoperative local recurrence and distant metastasis of rectal cancer can be identified and screened in the early stages, targeted systematic treatment can be administered to high-risk populations before surgery to adjust the treatment strategy and improve the prognosis of patients. It has been reported that the radiomics model based on MRI can be used to predict lymph node metastasis of bladder cancer and breast cancer[46,47]. The results suggest that the radiological information contained in MRI images may serve as an effective biomarker for predicting the prognosis of patients. In other words, the MR-based AI models use automated, high-throughput technologies to extract image information and features to capture intra-tumor heterogeneity in a non-invasive manner to guide personalized medicine and precision therapy.

## CONCLUSION

AI is a new technical science. AI methods represented by machine learning have been applied more and more widely in the field of medicine (Figure 2). Rectal MRI is considered the preferred method for the diagnosis of rectal cancer as recommended by national guidelines. Therefore, its importance is self-evident. Recently, there has been an increase in the use of AI models based on MR images in locally advanced rectal cancer. MRI combined with AI can not only improve the accuracy of staging and the efficiency of lymph node detection but also effectively evaluate the patients' response to neoadjuvant chemoradiotherapy. Through continuous optimization of the deep learning algorithm, MRI combined with a deep learning image recognition system can effectively predict the prognosis and treatment response of patients. It is believed that

in the near future, AI models based on MRI will be vital in the provision of systematic and precise medical services for the treatment of CRC patients.

## REFERENCES

- 1 Siegel RL, Miller KD, Jemal A. Cancer statistics, 2020. *CA Cancer J Clin* 2020; **70**: 7-30 [PMID: 31912902 DOI: 10.3322/caac.21590]
- 2 Ogura A, Konishi T, Cunningham C, Garcia-Aguilar J, Iversen H, Toda S, Lee IK, Lee HX, Uehara K, Lee P, Putter H, van de Velde CJH, Beets GL, Rutten HJT, Kusters M; Lateral Node Study Consortium. Neoadjuvant (Chemo)radiotherapy With Total Mesorectal Excision Only Is Not Sufficient to Prevent Lateral Local Recurrence in Enlarged Nodes: Results of the Multicenter Lateral Node Study of Patients With Low cT3/4 Rectal Cancer. *J Clin Oncol* 2019; **37**: 33-43 [PMID: 30403572 DOI: 10.1200/JCO.18.00032]
- 3 Ngamruengphong S, Kamal A, Akshintala V, Hajiyeve G, Hanada Y, Chen YI, Sanaei O, Fluxa D, Haito Chavez Y, Kumbhari V, Singh VK, Lennon AM, Canto MI, Khashab MA. Prevalence of metastasis and survival of 788 patients with T1 rectal carcinoid tumors. *Gastrointest Endosc* 2019; **89**: 602-606 [PMID: 30447216 DOI: 10.1016/j.gie.2018.11.010]
- 4 Cordero-Gallardo F, Lee Burnett O 3rd, McNamara MM, Weber TM, Zarzour J, Bae S, Jang S, Barrett OC, McDonald A, Kim RY. Incidence of mesorectal node metastasis in locally advanced cervical cancer: its therapeutic implications. *Int J Gynecol Cancer* 2019; **29**: 48-52 [PMID: 30640683 DOI: 10.1136/ijgc-2018-000031]
- 5 Taylor FG, Quirke P, Heald RJ, Moran B, Blomqvist L, Swift I, Sebag-Montefiore DJ, Tekkis P, Brown G; MERCURY study group. Preoperative high-resolution magnetic resonance imaging can identify good prognosis stage I, II, and III rectal cancer best managed by surgery alone: a prospective, multicenter, European study. *Ann Surg* 2011; **253**: 711-719 [PMID: 21475011 DOI: 10.1097/SLA.0b013e31820b8d52]
- 6 Dieguez A. Rectal cancer staging: focus on the prognostic significance of the findings described by high-resolution magnetic resonance imaging. *Cancer Imaging* 2013; **13**: 277-297 [PMID: 23876415 DOI: 10.1102/1470-7330.2013.0028]
- 7 Horvat N, Veeraraghavan H, Khan M, Blazic I, Zheng J, Capanu M, Sala E, Garcia-Aguilar J, Gollub MJ, Petkovska I. MR Imaging of Rectal Cancer: Radiomics Analysis to Assess Treatment Response after Neoadjuvant Therapy. *Radiology* 2018; **287**: 833-843 [PMID: 29514017 DOI: 10.1148/radiol.2018172300]
- 8 Chen Y, Yang X, Wen Z, Liu Y, Lu B, Yu S, Xiao X. Association between high-resolution MRI-detected extramural vascular invasion and tumour microcirculation estimated by dynamic contrast-enhanced MRI in rectal cancer: preliminary results. *BMC Cancer* 2019; **19**: 498 [PMID: 31133005 DOI: 10.1186/s12885-019-5732-z]
- 9 Lambregts DM, Beets GL, Maas M, Kessels AG, Bakkers FC, Cappendijk VC, Engelen SM, Lahaye MJ, de Bruïne AP, Lammering G, Leiner T, Verwoerd JL, Wildberger JE, Beets-Tan RG. Accuracy of gadofosveset-enhanced MRI for nodal staging and restaging in rectal cancer. *Ann Surg* 2011; **253**: 539-545 [PMID: 21239980 DOI: 10.1097/SLA.0b013e31820b01f1]
- 10 Thrall JH, Li X, Li Q, Cruz C, Do S, Dreyer K, Brink J. Artificial Intelligence and Machine Learning in Radiology: Opportunities, Challenges, Pitfalls, and Criteria for Success. *J Am Coll Radiol* 2018; **15**: 504-508 [PMID: 29402533 DOI: 10.1016/j.jacr.2017.12.026]
- 11 Hecht J. Managing expectations of artificial intelligence. *Nature* 2018; **563**: S141-S143 [PMID: 30487629 DOI: 10.1038/d41586-018-07504-9]
- 12 Kohli M, Geis R. Ethics, Artificial Intelligence, and Radiology. *J Am Coll Radiol* 2018; **15**: 1317-1319 [PMID: 30017625 DOI: 10.1016/j.jacr.2018.05.020]
- 13 Ahmed FE. Artificial neural networks for diagnosis and survival prediction in colon cancer. *Mol Cancer* 2005; **4**: 29 [PMID: 16083507 DOI: 10.1186/1476-4598-4-29]
- 14 Nartowt BJ, Hart GR, Roffman DA, Llor X, Ali I, Muhammad W, Liang Y, Deng J. Scoring colorectal cancer risk with an artificial neural network based on self-reportable personal health data. *PLoS One* 2019; **14**: e0221421 [PMID: 31437221 DOI: 10.1371/journal.pone.0221421]
- 15 Zhao D, Liu H, Zheng Y, He Y, Lu D, Lyu C. Whale optimized mixed kernel function of support vector machine for colorectal cancer diagnosis. *J Biomed Inform* 2019; **92**: 103124 [PMID: 30796977 DOI: 10.1016/j.jbi.2019.103124]
- 16 Zhi J, Sun J, Wang Z, Ding W. Support vector machine classifier for prediction of the metastasis of colorectal cancer. *Int J Mol Med* 2018; **41**: 1419-1426 [PMID: 29328363 DOI: 10.3892/ijmm.2018.3359]
- 17 Yang K, Zhou B, Yi F, Chen Y. Colorectal Cancer Diagnostic Algorithm Based on Sub-Patch Weight Color Histogram in Combination of Improved Least Squares Support Vector Machine for Pathological Image. *J Med Syst* 2019; **43**: 306 [PMID: 31410693 DOI: 10.1007/s10916-019-1429-8]
- 18 Alam MA, Shahjaman M, Rahman MF, Hossain F, Deng HW. Gene shaving using a sensitivity analysis of kernel based machine learning approach, with applications to cancer data. *PLoS One* 2019; **14**: e0217027 [PMID: 31120939 DOI: 10.1371/journal.pone.0217027]
- 19 Ishihara S, Kawai K, Tanaka T, Kiyomatsu T, Hata K, Nozawa H, Morikawa T, Watanabe T. Oncological Outcomes of Lateral Pelvic Lymph Node Metastasis in Rectal Cancer Treated With

- Preoperative Chemoradiotherapy. *Dis Colon Rectum* 2017; **60**: 469-476 [PMID: 28383446 DOI: 10.1097/DCR.0000000000000752]
- 20 **Sato H**, Maeda K, Maruta M, Masumori K, Koide Y. Who can get the beneficial effect from lateral lymph node dissection for Dukes C rectal carcinoma below the peritoneal reflection? *Dis Colon Rectum* 2006; **49**: S3-12 [PMID: 17106812 DOI: 10.1007/s10350-006-0699-7]
  - 21 **Kennedy ED**, Simunovic M, Jhaveri K, Kirsch R, Brierley J, Drolet S, Brown C, Vos PM, Xiong W, MacLean T, Kanthan S, Stotland P, Raphael S, Chow G, O'Brien CA, Cho C, Streutker C, Wong R, Schmocker S, Liberman S, Reinhold C, Kopek N, Marcus V, Bouchard A, Lavoie C, Morin S, Périgny M, Wright A, Neumann K, Clarke S, Patil NG, Arnason T, Williams L, McLeod R, Brown G, Mathieson A, Pooni A, Baxter NN. Safety and Feasibility of Using Magnetic Resonance Imaging Criteria to Identify Patients With "Good Prognosis" Rectal Cancer Eligible for Primary Surgery: The Phase 2 Nonrandomized QuickSilver Clinical Trial. *JAMA Oncol* 2019; **5**: 961-966 [PMID: 30973610 DOI: 10.1001/jamaoncol.2019.0186]
  - 22 **Ogawa S**, Hida J, Ike H, Kinugasa T, Ota M, Shinto E, Itabashi M, Kameoka S, Sugihara K. Selection of Lymph Node-Positive Cases Based on Perirectal and Lateral Pelvic Lymph Nodes Using Magnetic Resonance Imaging: Study of the Japanese Society for Cancer of the Colon and Rectum. *Ann Surg Oncol* 2016; **23**: 1187-1194 [PMID: 26671038 DOI: 10.1245/s10434-015-5021-2]
  - 23 **Ren S**, He K, Girshick R, Sun J. Faster R-CNN: Towards Real-Time Object Detection with Region Proposal Networks. *IEEE Trans Pattern Anal Mach Intell* 2017; **39**: 1137-1149 [PMID: 27295650 DOI: 10.1109/TPAMI.2016.2577031]
  - 24 **Ding L**, Liu GW, Zhao BC, Zhou YP, Li S, Zhang ZD, Guo YT, Li AQ, Lu Y, Yao HW, Yuan WT, Wang GY, Zhang DL, Wang L. Artificial intelligence system of faster region-based convolutional neural network surpassing senior radiologists in evaluation of metastatic lymph nodes of rectal cancer. *Chin Med J (Engl)* 2019; **132**: 379-387 [PMID: 30707177 DOI: 10.1097/CM9.0000000000000095]
  - 25 **He K**, Gkioxari G, Dollar P, Girshick R. Mask R-CNN. *IEEE Trans Pattern Anal Mach Intell* 2020; **42**: 386-397 [PMID: 29994331 DOI: 10.1109/TPAMI.2018.2844175]
  - 26 **Zhao X**, Xie P, Wang M, Li W, Pickhardt PJ, Xia W, Xiong F, Zhang R, Xie Y, Jian J, Bai H, Ni C, Gu J, Yu T, Tang Y, Gao X, Meng X. Deep learning-based fully automated detection and segmentation of lymph nodes on multiparametric-mri for rectal cancer: A multicentre study. *EBioMedicine* 2020; **56**: 102780 [PMID: 32512507 DOI: 10.1016/j.ebiom.2020.102780]
  - 27 **Barbu A**, Suehling M, Xu X, Liu D, Zhou SK, Comaniciu D. Automatic detection and segmentation of lymph nodes from CT data. *IEEE Trans Med Imaging* 2012; **31**: 240-250 [PMID: 21968722 DOI: 10.1109/TMI.2011.2168234]
  - 28 **Kitasaka T**, Tsujimura Y, Nakamura Y, Mori K, Suenaga Y, Ito M, Nawano S. Automated extraction of lymph nodes from 3-D abdominal CT images using 3-D minimum directional difference filter. *Med Image Comput Comput Assist Interv* 2007; **10**: 336-343 [PMID: 18044586 DOI: 10.1007/978-3-540-75759-7\_41]
  - 29 **Feulner J**, Zhou SK, Hammon M, Horneegger J, Comaniciu D. Lymph node detection and segmentation in chest CT data using discriminative learning and a spatial prior. *Med Image Anal* 2013; **17**: 254-270 [PMID: 23246185 DOI: 10.1016/j.media.2012.11.001]
  - 30 **Wang D**, Xu J, Zhang Z, Li S, Zhang X, Zhou Y, Lu Y. Evaluation of Rectal Cancer Circumferential Resection Margin Using Faster Region-Based Convolutional Neural Network in High-Resolution Magnetic Resonance Images. *Dis Colon Rectum* 2020; **63**: 143-151 [PMID: 31842158 DOI: 10.1097/DCR.0000000000001519]
  - 31 **Koumpa FS**, Xylas D, Konopka M, Galea D, Veselkov K, Antoniou A, Mehta A, Mirnezami R. Colorectal Peritoneal Metastases: A Systematic Review of Current and Emerging Trends in Clinical and Translational Research. *Gastroenterol Res Pract* 2019; **2019**: 5180895 [PMID: 31065262 DOI: 10.1155/2019/5180895]
  - 32 **Yuan Z**, Xu T, Cai J, Zhao Y, Cao W, Fichera A, Liu X, Yao J, Wang H. Development and Validation of an Image-based Deep Learning Algorithm for Detection of Synchronous Peritoneal Carcinomatosis in Colorectal Cancer. *Ann Surg* 2020 [PMID: 32694449 DOI: 10.1097/SLA.0000000000004229]
  - 33 **Wang J**, Lu J, Qin G, Shen L, Sun Y, Ying H, Zhang Z, Hu W. Technical Note: A deep learning-based autosegmentation of rectal tumors in MR images. *Med Phys* 2018; **45**: 2560-2564 [PMID: 29663417 DOI: 10.1002/mp.12918]
  - 34 **Trebeschi S**, van Griethuysen JJM, Lambregts DMJ, Lahaye MJ, Parmar C, Bakers FCH, Peters NHGM, Beets-Tan RGH, Aerts HJWL. Deep Learning for Fully-Automated Localization and Segmentation of Rectal Cancer on Multiparametric MR. *Sci Rep* 2017; **7**: 5301 [PMID: 28706185 DOI: 10.1038/s41598-017-05728-9]
  - 35 **Men K**, Boimel P, Janopaul-Naylor J, Zhong H, Huang M, Geng H, Cheng C, Fan Y, Plastaras JP, Ben-Josef E, Xiao Y. Cascaded atrous convolution and spatial pyramid pooling for more accurate tumor target segmentation for rectal cancer radiotherapy. *Phys Med Biol* 2018; **63**: 185016 [PMID: 30109986 DOI: 10.1088/1361-6560/aada6c]
  - 36 **Kapiteijn E**, Marijnen CA, Nagtegaal ID, Putter H, Steup WH, Wiggers T, Rutten HJ, Pahlman L, Glimelius B, van Krieken JH, Leer JW, van de Velde CJ; Dutch Colorectal Cancer Group. Preoperative radiotherapy combined with total mesorectal excision for resectable rectal cancer. *N Engl J Med* 2001; **345**: 638-646 [PMID: 11547717 DOI: 10.1056/NEJMoa010580]
  - 37 **O'Neill BD**, Brown G, Heald RJ, Cunningham D, Tait DM. Non-operative treatment after neoadjuvant chemoradiotherapy for rectal cancer. *Lancet Oncol* 2007; **8**: 625-633 [PMID: 17613424]



DOI: [10.1016/S1470-2045\(07\)70202-4](https://doi.org/10.1016/S1470-2045(07)70202-4)

- 38 **Ferrari R**, Mancini-Terracciano C, Voena C, Rengo M, Zerunian M, Ciardiello A, Grasso S, Mare' V, Paramatti R, Russomando A, Santacesaria R, Satta A, Solfaroli Camillocci E, Faccini R, Laghi A. MR-based artificial intelligence model to assess response to therapy in locally advanced rectal cancer. *Eur J Radiol* 2019; **118**: 1-9 [PMID: [31439226](https://pubmed.ncbi.nlm.nih.gov/31439226/) DOI: [10.1016/j.ejrad.2019.06.013](https://doi.org/10.1016/j.ejrad.2019.06.013)]
- 39 **Zhang XY**, Wang L, Zhu HT, Li ZW, Ye M, Li XT, Shi YJ, Zhu HC, Sun YS. Predicting Rectal Cancer Response to Neoadjuvant Chemoradiotherapy Using Deep Learning of Diffusion Kurtosis MRI. *Radiology* 2020; **296**: 56-64 [PMID: [32315264](https://pubmed.ncbi.nlm.nih.gov/32315264/) DOI: [10.1148/radiol.2020190936](https://doi.org/10.1148/radiol.2020190936)]
- 40 **Shi L**, Zhang Y, Nie K, Sun X, Niu T, Yue N, Kwong T, Chang P, Chow D, Chen JH, Su MY. Machine learning for prediction of chemoradiation therapy response in rectal cancer using pre-treatment and mid-radiation multi-parametric MRI. *Magn Reson Imaging* 2019; **61**: 33-40 [PMID: [31059768](https://pubmed.ncbi.nlm.nih.gov/31059768/) DOI: [10.1016/j.mri.2019.05.003](https://doi.org/10.1016/j.mri.2019.05.003)]
- 41 **Fu J**, Zhong X, Li N, Van Dams R, Lewis J, Sung K, Raldow AC, Jin J, Qi XS. Deep learning-based radiomic features for improving neoadjuvant chemoradiation response prediction in locally advanced rectal cancer. *Phys Med Biol* 2020; **65**: 075001 [PMID: [32092710](https://pubmed.ncbi.nlm.nih.gov/32092710/) DOI: [10.1088/1361-6560/ab7970](https://doi.org/10.1088/1361-6560/ab7970)]
- 42 **Yi X**, Pei Q, Zhang Y, Zhu H, Wang Z, Chen C, Li Q, Long X, Tan F, Zhou Z, Liu W, Li C, Zhou Y, Song X, Li Y, Liao W, Li X, Sun L, Pei H, Zee C, Chen BT. MRI-Based Radiomics Predicts Tumor Response to Neoadjuvant Chemoradiotherapy in Locally Advanced Rectal Cancer. *Front Oncol* 2019; **9**: 552 [PMID: [31293979](https://pubmed.ncbi.nlm.nih.gov/31293979/) DOI: [10.3389/fonc.2019.00552](https://doi.org/10.3389/fonc.2019.00552)]
- 43 **Shayesteh SP**, Alikhasshi A, Fard Esfahani A, Miraie M, Geramifard P, Bitarafan-Rajabi A, Haddad P. Neo-adjuvant chemoradiotherapy response prediction using MRI based ensemble learning method in rectal cancer patients. *Phys Med* 2019; **62**: 111-119 [PMID: [31153390](https://pubmed.ncbi.nlm.nih.gov/31153390/) DOI: [10.1016/j.ejmp.2019.03.013](https://doi.org/10.1016/j.ejmp.2019.03.013)]
- 44 **Cui Y**, Liu H, Ren J, Du X, Xin L, Li D, Yang X, Wang D. Development and validation of a MRI-based radiomics signature for prediction of KRAS mutation in rectal cancer. *Eur Radiol* 2020; **30**: 1948-1958 [PMID: [31942672](https://pubmed.ncbi.nlm.nih.gov/31942672/) DOI: [10.1007/s00330-019-06572-3](https://doi.org/10.1007/s00330-019-06572-3)]
- 45 **Chand M**, Swift RI, Tekkis PP, Chau I, Brown G. Extramural venous invasion is a potential imaging predictive biomarker of neoadjuvant treatment in rectal cancer. *Br J Cancer* 2014; **110**: 19-25 [PMID: [24300971](https://pubmed.ncbi.nlm.nih.gov/24300971/) DOI: [10.1038/bjc.2013.603](https://doi.org/10.1038/bjc.2013.603)]
- 46 **Wu S**, Zheng J, Li Y, Yu H, Shi S, Xie W, Liu H, Su Y, Huang J, Lin T. A Radiomics Nomogram for the Preoperative Prediction of Lymph Node Metastasis in Bladder Cancer. *Clin Cancer Res* 2017; **23**: 6904-6911 [PMID: [28874414](https://pubmed.ncbi.nlm.nih.gov/28874414/) DOI: [10.1158/1078-0432.CCR-17-1510](https://doi.org/10.1158/1078-0432.CCR-17-1510)]
- 47 **Dong Y**, Feng Q, Yang W, Lu Z, Deng C, Zhang L, Lian Z, Liu J, Luo X, Pei S, Mo X, Huang W, Liang C, Zhang B, Zhang S. Preoperative prediction of sentinel lymph node metastasis in breast cancer based on radiomics of T2-weighted fat-suppression and diffusion-weighted MRI. *Eur Radiol* 2018; **28**: 582-591 [PMID: [28828635](https://pubmed.ncbi.nlm.nih.gov/28828635/) DOI: [10.1007/s00330-017-5005-7](https://doi.org/10.1007/s00330-017-5005-7)]



## Remaining issues of recommended management in current guidelines for asymptomatic common bile duct stones

Hirokazu Saito, Yoshihiro Kadono, Takashi Shono, Kentaro Kamikawa, Atsushi Urata, Jiro Nasu, Haruo Imamura, Ikuo Matsushita, Shuji Tada

**ORCID number:** Hirokazu Saito 0000-0001-8729-9604; Yoshihiro Kadono 0000-0003-2358-120X; Takashi Shono 0000-0002-7577-2991; Kentaro Kamikawa 0000-0002-7783-7584; Atsushi Urata 0000-0001-8232-0988; Jiro Nasu 0000-0001-8555-7454; Haruo Imamura 0000-0001-6825-3758; Ikuo Matsushita 0000-0001-5160-8823; Shuji Tada 0000-0001-9087-5457.

**Author contributions:** Saito H, Kadono Y, Shono T, Kamikawa K, Urata A, Nasu J, Imamura H, Matsushita I and Tada S have been involved equally and have read and approved the final manuscript; Saito H, Kadono Y, Shono T, Kamikawa K, Urata A, Nasu J, Imamura H, Matsushita I and Tada S meet the criteria for authorship established by the International Committee of Medical Journal Editors and verify the validity of the results reported.

**Conflict-of-interest statement:** There are no conflicts of interest to declare in relation to this article.

**Open-Access:** This article is an open-access article that was selected by an in-house editor and fully peer-reviewed by external reviewers. It is distributed in accordance with the Creative Commons Attribution NonCommercial (CC BY-NC 4.0)

**Hirokazu Saito, Shuji Tada,** Department of Gastroenterology, Kumamoto City Hospital, Kumamoto City 862-8505, Japan

**Yoshihiro Kadono,** Department of Gastroenterology, Tsuruta Hospital, Kumamoto City 862-0925, Japan

**Takashi Shono, Ikuo Matsushita,** Department of Gastroenterology, Kumamoto Chuo Hospital, Kumamoto City 862-0965, Japan

**Kentaro Kamikawa, Atsushi Urata, Haruo Imamura,** Department of Gastroenterology, Saiseikai Kumamoto Hospital, Kumamoto City 861-4193, Japan

**Jiro Nasu,** Department of Gastroenterological Surgery, Kumamoto Chuo Hospital, Kumamoto City 862-0965, Japan

**Corresponding author:** Hirokazu Saito, MD, Doctor, Department of Gastroenterology, Kumamoto City Hospital, 4-1-60, Higashimachi, Higashi-ku, Kumamoto City 862-8505, Japan. [arnestwest@yahoo.co.jp](mailto:arnestwest@yahoo.co.jp)

### Abstract

Current guidelines for treating asymptomatic common bile duct stones (CBDS) recommend stone removal, with endoscopic retrograde cholangiopancreatography (ERCP) being the first treatment choice. When deciding on ERCP treatment for asymptomatic CBDS, the risk of ERCP-related complications and outcome of natural history of asymptomatic CBDS should be compared. The incidence rate of ERCP-related complications, particularly of post-ERCP pancreatitis for asymptomatic CBDS, was reportedly higher than that of symptomatic CBDS, increasing the risk of ERCP-related complications for asymptomatic CBDS compared with that previously reported for biliopancreatic diseases. Although studies have reported short- to middle-term outcomes of natural history of asymptomatic CBDS, its long-term natural history is not well known. Till date, there are no prospective studies that determined whether ERCP has a better outcome than no treatment in patients with asymptomatic CBDS or not. No randomized controlled trial has evaluated the risk of early and late ERCP-related complications *vs* the risk of biliary complications in the wait-and-see approach, suggesting that a change is needed in our perspective on endoscopic treatment for asymptomatic CBDS. Further studies examining long-term complication risks of ERCP and wait-and-see groups for asymptomatic CBDS are warranted to discuss

license, which permits others to distribute, remix, adapt, build upon this work non-commercially, and license their derivative works on different terms, provided the original work is properly cited and the use is non-commercial. See: <http://creativecommons.org/licenses/by-nc/4.0/>

**Manuscript source:** Invited manuscript

**Specialty type:** Gastroenterology and hepatology

**Country/Territory of origin:** Japan

**Peer-review report's scientific quality classification**

Grade A (Excellent): 0  
Grade B (Very good): B, B  
Grade C (Good): 0  
Grade D (Fair): 0  
Grade E (Poor): 0

**Received:** February 12, 2021

**Peer-review started:** February 12, 2021

**First decision:** March 28, 2021

**Revised:** April 1, 2021

**Accepted:** April 21, 2021

**Article in press:** April 21, 2021

**Published online:** May 14, 2021

**P-Reviewer:** Pan W

**S-Editor:** Gong ZM

**L-Editor:** A

**P-Editor:** Ma YJ



whether routine endoscopic treatment for asymptomatic CBDS is justified or not.

**Key Words:** Asymptomatic common bile duct stone; Endoscopic retrograde cholangiopancreatography; Complication; Natural history of asymptomatic common bile duct stone; Guideline; Recommendation

©The Author(s) 2021. Published by Baishideng Publishing Group Inc. All rights reserved.

**Core Tip:** Current guidelines recommend endoscopic stone removal for asymptomatic common bile duct stones (CBDS). However, the risks of endoscopic retrograde cholangiopancreatography (ERCP)-related complication and natural history outcome of asymptomatic CBDS should be compared to decide on endoscopic treatment by ERCP. ERCP for asymptomatic CBDS reportedly has a high risk of ERCP-related complications; post-ERCP pancreatitis risk being the most common. The long-term natural history of asymptomatic CBDS is not well known. Further studies examining long-term complication risks of ERCP and wait-and-see groups for asymptomatic CBDS are warranted to evaluate whether routine endoscopic stone removal for asymptomatic CBDS is justified or not.

**Citation:** Saito H, Kadono Y, Shono T, Kamikawa K, Urata A, Nasu J, Imamura H, Matsushita I, Tada S. Remaining issues of recommended management in current guidelines for asymptomatic common bile duct stones. *World J Gastroenterol* 2021; 27(18): 2131-2140

**URL:** <https://www.wjgnet.com/1007-9327/full/v27/i18/2131.htm>

**DOI:** <https://dx.doi.org/10.3748/wjg.v27.i18.2131>

## INTRODUCTION

Common bile duct stones (CBDS) are a common biliary tract disease worldwide with secondary CBDS migrated from gallbladder into CBD, being one of major causes of CBDS[1]. The prevalence of gallstones has increased in the elderly population[2], and for this reason, the number of patients with CBDS is likely to increase in the future as the world's population ages. Owing to diagnostic modalities, such as computed tomography (CT), endoscopic ultrasonography (EUS) or magnetic resonance cholangiopancreatography (MRCP) recently developed, there is greater probability for asymptomatic CBDS to be discovered incidentally.

Endoscopic management by endoscopic retrograde cholangiopancreatography (ERCP) is widely accepted as a first choice of treatment for CBDS[3]. For asymptomatic CBDS, endoscopic treatment is consistently recommended in current guidelines[1,3-5], and removal of asymptomatic CBDS is a common practice as asymptomatic CBDS have a potential risk of causing obstructive jaundice, acute cholangitis, and biliary pancreatitis.

ERCP is however an endoscopic procedure with high risk of procedure-related complications. In general, an overall incidence of ERCP-related complications, including post-ERCP pancreatitis (PEP), cholangitis, bleeding, and perforation has been reported in 4.0%-15.9% of patients[6,7], PEP being the most common. A systematic review of randomized controlled trials revealed an overall PEP incidence of 9.7%[8].

When determining the indication of ERCP for asymptomatic CBDS, the risk of ERCP-related complications should be focused on asymptomatic CBDS rather than on average risk of ERCP-related complications of biliopancreatic diseases.

Some investigators recently reported the risk of ERCP-related complications focusing on asymptomatic CBDS. An overall incidence rate of ERCP-related complication for asymptomatic CBDS was reported to be approximately 15%-25%, with a PEP incidence of approximately 12%-20%[9-13]. The risk of ERCP-related complications, in particular the risk of PEP, for asymptomatic CBDS appeared to be higher than that previously reported. The risk of ERCP-related complications for asymptomatic common bile duct (CBD) should therefore not be the same as the previously reported risk of ERCP-related complications for biliopancreatic diseases.

When determining the indication of ERCP for asymptomatic CBDS, the risk of biliary complications in wait-and-see approach should be considered. Previous studies on the natural history of CBDS reported the biliary complication rates of wait-and-see approach for asymptomatic CBDS to vary between 0-25.3% during a follow-up period of 30 d to 4.8 years[14-18]. Endoscopic sphincterotomy, endoscopic papillary balloon dilation, or endoscopic large papillary balloon dilation was performed for endoscopic stone removal bearing in mind the risk of stone recurrence as these procedures can cause papillary dysfunction[19,20].

We clarified the remaining issues of recommended management in current guidelines for asymptomatic CBDS by reviewing the current guidelines for asymptomatic CBDS and previous studies on the risk of ERCP-related complications and natural history of asymptomatic CBDS.

## EPIDEMIOLOGY OF CBDS

The origin of CBDS is different in Asian populations and Western population. Primary CBDS, which are more common in Asian populations, form *de novo* in the intra- and extrahepatic ducts. Primary CBDS are associated with biliary infection and cholestasis[21-24]. Secondary CBDS, which are more prevalent in Western populations, typically originate in the gallbladder and migrate into CBD[1].

The prevalence of CBDS in patients with symptomatic gallstones is estimated to be 10%-20%[25-29]. In patients without jaundice and dilated CBD on trans-abdominal ultrasound, the prevalence of CBDS during cholecystectomy is reported to be < 5%[15]. It has been reported that the rate of coexisting CBDS was increased in elderly populations with symptomatic gallstones[2].

However, to best of our knowledge, there are no studies focusing on the prevalence of CBDS in patients with asymptomatic gallstones, as most studies are based on intraoperative cholangiography during cholecystectomy for symptomatic gallstones. Although the prevalence of CBDS is expected to increase due to the aging of world population, the prevalence of CBDS is still unknown.

Further studies are warranted to clarify the prevalence of asymptomatic CBDS for a better understanding of the natural history of asymptomatic CBDS.

## DIAGNOSTIC MODALITIES OF CBDS

Recent guidelines recommend the use of either EUS or MRCP to diagnose CBDS in patients with suspected CBDS. A recent meta-analysis of five head-to-head studies revealed that the sensitivity and specificity of EUS and MRCP are 97% *vs* 90%, and specificity 87% *vs* 92%, respectively. However, the overall diagnostic odds ratio of EUS was significantly higher than that of MRCP because EUS had a higher detection rate of small CBDS compared with that of MRCP, while the specificity showed no significant differences between the two modalities[30]. Another meta-analysis demonstrated high diagnostic accuracy for EUS and MRCP. This meta-analysis reported that the sensitivity and specificity for EUS were 95% and 97%, and 93% and 96% for MRCP[31].

Although CT is a diagnostic modality for CBDS, routine CT scanning for suspected CBDS is not recommended in current guidelines because of some disadvantages, such as radiation exposure, side effects of contrast agent, and lower diagnostic ability for CBDS compared with MRCP and EUS[3,32]. Several studies examining the diagnostic ability of multi-slice CT scanner for CBDS showed that conventional CT scanning had reasonable sensitivity (69%-87%) and specificity (68%-96%) for diagnostic CBDS[33-36]. Recently, dual-energy CT scanner and dual-layer spectral CT (DLCT) scanner, which can perform a multiparameter approach, are commercially available. These CT scanners can detect noncalcified stones, which cannot be detected in conventional CT. A recent retrospective study comparing the diagnostic ability between DLCT and modern MRCP suggested that the diagnostic ability of DLCT for biliary stones was comparable to that of modern MRCP[37]; the detection of noncalcified small stones < 9 mm in diameter seem to be a limitation of dual-energy CT and DLCT scanners[37-39].

Diagnostic modalities for CBDS, such as EUS, MRCP, and CT have recently been developed increasing the chance of detecting incidentally discovered asymptomatic CBD.

## RECOMMENDED MANAGEMENT IN CURRENT GUIDELINES FOR ASYMPTOMATIC CBDS

Recommended management of current guidelines is presented in Table 1. Current guidelines published by European Society of Gastrointestinal Endoscopy, The British Society of Gastroenterology, American Society for Gastrointestinal Endoscopy, and The Japanese Society of Gastroenterology strongly recommend bile duct stone removal[1,3-5], with ERCP as the first choice of treatment for asymptomatic CBDS removal.

Although the lifetime risk of untreated CBDS is unknown, complication of CBDS, such as pain, obstructive jaundice, acute cholangitis, hepatic abscesses, biliary pancreatitis, secondary biliary cirrhosis, and portal hypertension due to biliary obstruction are potentially life threatening. Available guidelines recommend treatment for asymptomatic CBDS. A conservative approach can only be considered in patients in whom the risks of CBDS removal are higher than the risks of leaving CBDS in situ[1,3,4].

Current guidelines strongly recommended stone removal for asymptomatic CBDS even though the evidence quality is low.

## RISK OF ERCP-RELATED COMPLICATIONS FOR ASYMPTOMATIC CBDS

It has been recognized that the risk of ERCP-related complications of CBDS was 6%-15%[6,7]. However, the risk of ERCP focusing on asymptomatic CBDS is important to determine the indication of ERCP for asymptomatic CBDS.

Recently, several reports revealed that the risk of ERCP-related complications for patients with asymptomatic CBDS was higher than that for symptomatic patients (Table 2). A multicenter retrospective study including 164 patients with asymptomatic CBDS and 949 patients with symptomatic CBDS reported that the incidence rate of ERCP-related complications was 19.5% in asymptomatic patients and 6.2% in symptomatic patients. In particular, PEP was significantly higher in asymptomatic patients than symptomatic patients (14.6% *vs* 3.0%)[11]. A prospective study including 53 asymptomatic patients and 274 symptomatic patients reported the similar results. The rate of ERCP-related complications in asymptomatic patients and symptomatic patients were 26.4% *vs* 11.7%, respectively, and the rate of PEP was 20.8% *vs* 6.9%, respectively[12]. The possible explanation for a higher incidence of PEP in asymptomatic patients is that the number of asymptomatic patients with normal serum bilirubin, nondilated CBD, and difficult cannulation, which are patient- and procedure-related risk factors of PEP, was higher than that of symptomatic patients because of no cholestasis in patients with asymptomatic CBDS. Furthermore, asymptomatic CBDS itself may be an important clinical risk factor of PEP[11].

Although a single-center retrospective study, in which ERCP was performed by skilled endoscopists, reported that the incidence of both overall ERCP-related complications and PEP in asymptomatic patients were comparable with those of symptomatic patients[13], other studies reported that the incidence rate of overall ERCP-related complication was approximately 15%-25% in asymptomatic patients and 4%-12% in symptomatic patients, and the incidence of PEP was approximately 12%-20% in asymptomatic patients and 2%-7% in symptomatic patients[9-12]. Therefore, the risk of ERCP-related complications, in particular the risk of PEP, in asymptomatic patients with CBDS is possibly higher than that of symptomatic patients.

## NATURAL HISTORY OF ASYMPTOMATIC CBDS

About 2%-4% of patients with asymptomatic gallstones becomes symptomatic over the years. Multiple gallstones, negative cholecystography findings, and young age are the risk factors for transition from asymptomatic to symptomatic[40-43]. The potential risk of intraoperative and postoperative complications related to surgery explains why current guidelines are against laparoscopic cholecystectomy for patients with asymptomatic gallstones in a normal gallbladder[4,32].

Although the long-term natural history of CBDS is less understood than that of gallstones, several studies have examined the short- to middle-term natural history of asymptomatic CBDS[14-18] (Table 3).



**Table 1 Recommended management and evidence level in current guidelines for asymptomatic common bile duct stones**

Guideline	Recommendation
ESGE[1]	ESGE recommends stone extraction in all patients with CBDS, regardless of being symptomatic or not, who are fit enough to tolerate the intervention. (Strong recommendation, low quality evidence)
BSG[3]	Stone extraction is recommended in patients diagnosed with CBDS if possible. Evidence of benefit of stone extraction is greatest for symptomatic patients (Low quality evidence; strong recommendation)
JGES[4]	Asymptomatic choledocholithiasis should be treated because of a risk of developing biliary complications. [Evidence level: A; Strength of recommendation (agreement rate): 2 (100%)]
ASGE[5]	CBDS should be treated if detected regardless of the presence or absence of significant mitigating clinical circumstances (Moderate quality)

CBDS: Common bile duct stones; ESGE: European Society of Gastrointestinal Endoscopy; BSG: The British Society of Gastroenterology; ASGE: American Society for Gastrointestinal Endoscopy; JSGE: The Japanese Society of Gastroenterology.

**Table 2 Summary of studies comparing the risks of endoscopic retrograde cholangiopancreatography-related complications for asymptomatic and symptomatic patients with common bile duct stones**

Ref.	Study design	Patients, <i>n</i>		Overall, complications (%)		PEP (%)	
		Asymptomatic group	Symptomatic group	Asymptomatic group	Symptomatic group	Asymptomatic group	Symptomatic group
Kim <i>et al</i> [9], 2016	Single-center retrospective	32	536	15.6	10.4	12.5 <sup>a</sup>	3.9
Saito <i>et al</i> [10], 2017	Multicenter retrospective	67	536	26.9 <sup>a</sup>	3.9	16.4 <sup>a</sup>	2.2
Saito <i>et al</i> [11], 2019	Multicenter retrospective	164	949	19.5 <sup>a</sup>	6.2	14.6 <sup>a</sup>	3.0
Xu <i>et al</i> [12], 2019	Single-center prospective	53	274	26.4 <sup>a</sup>	11.7	20.8 <sup>a</sup>	6.9
Xiao <i>et al</i> [13], 2021	Single-center retrospective	79	795	13.3	9.7	7.6	6.9

<sup>a</sup>Statistically significant difference. ERCP: Endoscopic retrograde cholangiopancreatography; PEP: Postendoscopic retrograde cholangiopancreatography pancreatitis.

**Table 3 Summary of studies reporting natural history of asymptomatic common bile duct stones**

Ref.	Study design	Patients, <i>n</i>	Median follow-up period	Cumulative incidence of biliary complications, <i>n</i> (%)
Ammori <i>et al</i> [14], 2000	Prospective	14	1.4 yr	4 (29)
Collins <i>et al</i> [15], 2004	Prospective	46	6 wk	0
Caddy <i>et al</i> [16], 2005	Retrospective	59	4.8 yr	0
Moller <i>et al</i> [17], 2014	Retrospective	594	30 d	150 (25)
Hakuta <i>et al</i> [18], 2020	Retrospective	114	3.2 yr	20 (18)

Data from the GallRiks study, including 594 patients who had CBDS incidentally discovered by intraoperative cholangiography and were untreated, suggest that 25.3% (150/594) of patients developed unfavorable outcomes defined as incomplete clearance of CBDS and/or complications within 30 d post cholecystectomy. Among the 3234 patients who underwent any procedure of CBDS removal, including post- or intraoperative ERCP, laparoscopic or open choledochotomy, transcystic stone extraction, or flushing/manipulation, 12.7% (411/3234) developed unfavorable

outcomes. This led to conclusion that if CBDS are detected, they should be removed to reduce the risk of CBDS-related complications over time[17].

However, there are several noteworthy aspects in the results of GallRiks study. First, long-term outcomes of patients in the untreated asymptomatic CBDS group and treated asymptomatic CBDS group were unclear. Second, patients who underwent postoperative ERCP had a high unfavorable outcome rate of 18% (103/572), suggesting that ERCP for asymptomatic CBDS had a high risk of ERCP-related complications. Third, although the unfavorable outcome rate of no treatment for CBDS also included post-ERCP complications in patients who became symptomatic and underwent ERCP within 30 d post cholecystectomy, this unfavorable outcome should also be included in the unfavorable outcomes of treatment strategies. Therefore, the risk of ERCP-related complications for CBDS removal may be underestimated in the GallRiks study.

Hakuta *et al*[18] recently reported that out of the 114 patients with asymptomatic CBDS who underwent wait-and-see approach, 18% developed CBDS-related complications, which were cholangitis in 16 patients (14%), cholecystitis in 1 patient (0.9%), and cholestasis in 4 patients (3.5%), and no biliary pancreatitis during the average follow-up period of 3.2 years.

In some patients with asymptomatic small CBDS, the stones can be drained into duodenum spontaneously without the need for an intervention[44-48]. Collins *et al*[15] demonstrated the spontaneous passage of small CBDS without serious complications in 24 of 46 patients with a filling defect observed by intraoperative cholangiography during cholecystectomy within 6 wk of surgery. Asymptomatic spontaneous passage of small CBDS less than 8 mm in size has also been found in approximately 20% CBDS in the interval between diagnosis at EUS and ERCP[49].

Clarifying the long-term natural history of asymptomatic CBDS is essential to determine whether intervention by ERCP or wait-and-see approach for asymptomatic CBDS has a better outcome. A large-scale prospective study examining long-term natural history of asymptomatic CBDS is therefore warranted.

## RECCURENCE OF CBDS AFTER ENDOSCOPIC STONE REMOVAL

The Korean nationwide study including 46181 patients with CBDS demonstrated that 5228 (11.3%) patients experienced first CBDS recurrence at mean follow-up of 4.3 years. The cumulative second and third recurrence rates after the initial CBD recurrence were 23.4% and 33.4%. Therefore, the higher the frequency of recurrence of stones, the higher the recurrence rate of the stones[19]. Another retrospective study revealed that CBDS recurrence was observed in 121 patients (12.4%) out of 976 patients. Multiple recurrence after first recurrence was observed in 26 patients (21.5%) of 121 patients with stone recurrence during a median follow-up period of 5.1 years. The risk factors for single recurrence were CBD size, gallbladder left in situ with gallstones, and pneumobilia after ERCP, and the risk factor for multiple recurrence was the number of CBDS at the first recurrence[20].

Stone recurrence should be considered when balancing stone removal by ERCP *vs* wait-and-see approach for asymptomatic CBDS.

## REMAINING ISSUES IN CURRENT GUIDELINES FOR ASYMPTOMATIC CBDS

When determining the indication of ERCP for patient with asymptomatic CBDS, the risk of early and late ERCP-related complications and long-term natural history of asymptomatic CBDS should be considered.

Recently, the risk of ERCP-related complications for asymptomatic CBDS and the short- to middle-term natural history of this disease have been reported as above[9-18].

Based on the previous reports, the risk of early ERCP-related complications, including PEP, cholangitis, bleeding, and perforation can be estimated to approximately 15%-25% with the incidence of PEP of 12%-20% in patients with asymptomatic CBDS[9-14]. The risk of late ERCP-related complications including stone recurrence and cholangitis can be estimated to approximately 10%[18-20], with the risk of early and late ERCP-related complications for asymptomatic CBDS being approximately 25%-35%. The risk of biliary complications in wait-and-see approach during median follow-up period of 30 d to 4.9 years was estimated to be approximately 0%-

25%[14-18]; ERCP for asymptomatic CBDS may therefore have poorer outcomes than that of wait-and-see approach. A retrospective longitudinal cohort study revealed that out of 77 who underwent ERCP, 16 patients (21%) experienced PEP and 25 patients (32%) experienced early ERCP-related complications and late biliary complications, such as cholangitis and cholecystitis; further, recurrence of CBDS was observed in 7 patients (9.6%) out of 73 patients during a median follow-up period of 1.9 years. They reported that out of the 114 patients with asymptomatic CBDS who underwent wait-and-see approach, 18% developed CBDS-related complications, among which 16 patients (14%) developed cholangitis, 1 patient (0.9%) developed cholecystitis, 4 patients (3.5%) developed cholestasis, and no patients developed biliary pancreatitis during an average follow-up period of 3.2 years. The outcome of intervention group by ERCP was poorer than that of wait-and-see group for patients with asymptomatic CBDS[18].

The fact that there are no randomized prospective studies to compare the risk of ERCP and wait-and-see approach for asymptomatic CBDS is a serious issue as it is important to determine the indication of ERCP for asymptomatic CBDS. Although current guidelines for asymptomatic CBDS recommend stone removal for asymptomatic CBDS, the risk of ERCP and the risk of wait-and-see approach for patients with asymptomatic CBDS cannot be balanced currently because of the absence of randomized controlled studies. Patients should be told that current guidelines' recommendation is to undergo stone extraction in patients with asymptomatic CBDS based on the evidence from the symptomatic patients and expert opinion[1,3].

Further large-scale prospective studies comparing the risk of ERCP and the risk of wait-and-see approach for patients with asymptomatic CBDS are warranted. The indication for preoperative or postoperative ERCP for cholelithiasis should equally be discussed after clarifying the risk and benefit of ERCP for asymptomatic CBDS.

## STRATEGY OF ERCP FOR ASYMPTOMATIC CBDS TO REDUCE ERCP-RELATED COMPLICATIONS

Because asymptomatic CBDS are a benign disease with no noticeable symptoms, endoscopists must try to reduce ERCP-related complications particularly when performing ERCP for asymptomatic CBDS. A previous study reported that precut sphincterotomy, biliary sphincter dilation, and involvement of trainees were significant risk factors for developing PEP in asymptomatic CBDS[50]. A propensity-score matched study reported that ERCP for asymptomatic CBDS conducted by experienced endoscopists was of comparable safety as ERCP for symptomatic CBDS[13]. ERCP for asymptomatic CBDS should therefore be performed by experienced endoscopists. Prophylactic procedure such as prophylactic pancreatic stent placement should be considered in asymptomatic patients with risk factors of PEP including precut sphincterotomy and biliary sphincter dilation[50].

Single-stage CBDS removal following endoscopic sphincterotomy at first ERCP session in patients with mild-to-moderate cholangitis is accepted in the revised Tokyo guidelines for the management of acute cholangitis and cholecystitis[51], making patients with asymptomatic CBDS a candidate for single-stage CBDS removal. A retrospective study revealed that single-stage CBDS removal with difficult biliary cannulation requiring > 15 min is a significant risk factor of PEP. It may be preferable to remove CBDS at second session ERCP in asymptomatic patients requiring > 15 min for biliary cannulation in order to reduce the development of PEP[52].

## CONCLUSION

Although current guidelines for asymptomatic CBDS recommend stone removal for asymptomatic CBDS, there is need for a change in perspective on ERCP for asymptomatic CBDS. To best of our knowledge, no prospective studies exist as to whether ERCP has a better outcome than no treatment in patients with asymptomatic CBDS. The risk of inducing early and late ERCP-related complications *vs* the risk of complication related to the natural history of asymptomatic CBDS cannot be balanced currently.

Further studies examining long-term complication risks of ERCP group and wait-and-see group is warranted to discuss whether routine treatment of asymptomatic CBDS is justified or not.

## REFERENCES

- 1 **Manes G**, Paspatis G, Aabakken L, Anderloni A, Arvanitakis M, Ah-Soune P, Barthet M, Domagk D, Dumonceau JM, Gigot JF, Hritz I, Karamanolis G, Laghi A, Mariani A, Parakeva K, Pohl J, Ponchon T, Swahn F, Ter Steege RWF, Tringali A, Vezakis A, Williams EJ, van Hooft JE. Endoscopic management of common bile duct stones: European Society of Gastrointestinal Endoscopy (ESGE) guideline. *Endoscopy* 2019; **51**: 472-491 [PMID: 30943551 DOI: 10.1055/a-0862-0346]
- 2 **Siegel JH**, Kasmin FE. Biliary tract diseases in the elderly: management and outcomes. *Gut* 1997; **41**: 433-435 [PMID: 9391238 DOI: 10.1136/gut.41.4.433]
- 3 **Williams E**, Beekingham I, El Sayed G, Gurusamy K, Sturgess R, Webster G, Young T. Updated guideline on the management of common bile duct stones (CBDS). *Gut* 2017; **66**: 765-782 [PMID: 28122906 DOI: 10.1136/gutjnl-2016-312317]
- 4 **Tazuma S**, Unno M, Igarashi Y, Inui K, Uchiyama K, Kai M, Tsuyuguchi T, Maguchi H, Mori T, Yamaguchi K, Ryoza S, Nimura Y, Fujita N, Kubota K, Shoda J, Tabata M, Mine T, Sugano K, Watanabe M, Shimosegawa T. Evidence-based clinical practice guidelines for cholelithiasis 2016. *J Gastroenterol* 2017; **52**: 276-300 [PMID: 27942871 DOI: 10.1007/s00535-016-1289-7]
- 5 **ASGE Standards of Practice Committee**, Maple JT, Ikenberry SO, Anderson MA, Appalaneni V, Decker GA, Early D, Evans JA, Fanelli RD, Fisher D, Fisher L, Fukami N, Hwang JH, Jain R, Jue T, Khan K, Krinsky ML, Malpas P, Ben-Menachem T, Sharaf RN, Dominitz JA. The role of endoscopy in the management of choledocholithiasis. *Gastrointest Endosc* 2011; **74**: 731-744 [PMID: 21951472 DOI: 10.1016/j.gie.2011.04.012]
- 6 **Andriulli A**, Loperfido S, Napolitano G, Niro G, Valvano MR, Spirito F, Pilotto A, Forlano R. Incidence rates of post-ERCP complications: a systematic survey of prospective studies. *Am J Gastroenterol* 2007; **102**: 1781-1788 [PMID: 17509029 DOI: 10.1111/j.1572-0241.2007.01279.x]
- 7 **Freeman ML**, Nelson DB, Sherman S, Haber GB, Herman ME, Dorsher PJ, Moore JP, Fennerty MB, Ryan ME, Shaw MJ, Lande JD, Pheley AM. Complications of endoscopic biliary sphincterotomy. *N Engl J Med* 1996; **335**: 909-918 [PMID: 8782497 DOI: 10.1056/NEJM199609263351301]
- 8 **Kochar B**, Akshintala VS, Afghani E, Elmunzer BJ, Kim KJ, Lennon AM, Khashab MA, Kalloo AN, Singh VK. Incidence, severity, and mortality of post-ERCP pancreatitis: a systematic review by using randomized, controlled trials. *Gastrointest Endosc* 2015; **81**: 143-149. e9 [PMID: 25088919 DOI: 10.1016/j.gie.2014.06.045]
- 9 **Kim SB**, Kim KH, Kim TN. Comparison of Outcomes and Complications of Endoscopic Common Bile Duct Stone Removal Between Asymptomatic and Symptomatic Patients. *Dig Dis Sci* 2016; **61**: 1172-1177 [PMID: 26589817 DOI: 10.1007/s10620-015-3965-5]
- 10 **Saito H**, Kakuma T, Kadono Y, Urata A, Kamikawa K, Imamura H, Tada S. Increased risk and severity of ERCP-related complications associated with asymptomatic common bile duct stones. *Endosc Int Open* 2017; **5**: E809-E817 [PMID: 28879226 DOI: 10.1055/s-0043-107615]
- 11 **Saito H**, Koga T, Sakaguchi M, Kadono Y, Kamikawa K, Urata A, Imamura H, Tada S, Kakuma T, Matsushita I. Post-endoscopic retrograde cholangiopancreatography pancreatitis in patients with asymptomatic common bile duct stones. *J Gastroenterol Hepatol* 2019; **34**: 1153-1159 [PMID: 30650203 DOI: 10.1111/jgh.14604]
- 12 **Xu XD**, Qian JQ, Dai JJ, Sun ZX. Endoscopic treatment for choledocholithiasis in asymptomatic patients. *J Gastroenterol Hepatol* 2020; **35**: 165-169 [PMID: 31334888 DOI: 10.1111/jgh.14790]
- 13 **Xiao L**, Geng C, Li X, Li Y, Wang C. Comparable safety of ERCP in symptomatic and asymptomatic patients with common bile duct stones: a propensity-matched analysis. *Scand J Gastroenterol* 2021; **56**: 111-117 [PMID: 33295209 DOI: 10.1080/00365521.2020.1853222]
- 14 **Ammori BJ**, Birbas K, Davides D, Vezakis A, Larvin M, McMahon MJ. Routine vs "on demand" postoperative ERCP for small bile duct calculi detected at intraoperative cholangiography. Clinical evaluation and cost analysis. *Surg Endosc* 2000; **14**: 1123-1126 [PMID: 11148780 DOI: 10.1007/s004640000146]
- 15 **Collins C**, Maguire D, Ireland A, Fitzgerald E, O'Sullivan GC. A prospective study of common bile duct calculi in patients undergoing laparoscopic cholecystectomy: natural history of choledocholithiasis revisited. *Ann Surg* 2004; **239**: 28-33 [PMID: 14685097 DOI: 10.1097/01.sla.0000103069.00170.9c]
- 16 **Caddy GR**, Kirby J, Kirk SJ, Allen MJ, Moorehead RJ, Tham TC. Natural history of asymptomatic bile duct stones at time of cholecystectomy. *Ulster Med J* 2005; **74**: 108-112 [PMID: 16235763]
- 17 **Möller M**, Gustafsson U, Rasmussen F, Persson G, Thorell A. Natural course vs interventions to clear common bile duct stones: data from the Swedish Registry for Gallstone Surgery and Endoscopic Retrograde Cholangiopancreatography (GallRiks). *JAMA Surg* 2014; **149**: 1008-1013 [PMID: 25133326 DOI: 10.1001/jamasurg.2014.249]
- 18 **Hakuta R**, Hamada T, Nakai Y, Oyama H, Kanai S, Suzuki T, Sato T, Ishigaki K, Saito K, Saito T, Takahara N, Mizuno S, Kogure H, Watadani T, Tsujino T, Tada M, Abe O, Isayama H, Koike K. Natural history of asymptomatic bile duct stones and association of endoscopic treatment with clinical outcomes. *J Gastroenterol* 2020; **55**: 78-85 [PMID: 31473828 DOI: 10.1007/s00535-019-01612-7]
- 19 **Park BK**, Seo JH, Jeon HH, Choi JW, Won SY, Cho YS, Lee CK, Park H, Kim DW. A nationwide population-based study of common bile duct stone recurrence after endoscopic stone removal in Korea. *J Gastroenterol* 2018; **53**: 670-678 [PMID: 29192348 DOI: 10.1007/s00535-017-1419-x]
- 20 **Kawaji Y**, Isayama H, Nakai Y, Saito K, Sato T, Hakuta R, Saito T, Takahara N, Mizuno S, Kogure H, Matsubara S, Tada M, Kitano M, Koike K. Multiple recurrences after endoscopic removal of

- common bile duct stones: A retrospective analysis of 976 cases. *J Gastroenterol Hepatol* 2019; **34**: 1460-1466 [PMID: [30761603](#) DOI: [10.1111/jgh.14630](#)]
- 21 **Kaufman HS**, Magnuson TH, Lillemo KD, Frasca P, Pitt HA. The role of bacteria in gallbladder and common duct stone formation. *Ann Surg* 1989; **209**: 584-91; discussion 591 [PMID: [2705823](#) DOI: [10.1097/0000658-198905000-00011](#)]
  - 22 **Cetta FM**. Bile infection documented as initial event in the pathogenesis of brown pigment biliary stones. *Hepatology* 1986; **6**: 482-489 [PMID: [3519417](#) DOI: [10.1002/hep.1840060327](#)]
  - 23 **Tazuma S**. Gallstone disease: Epidemiology, pathogenesis, and classification of biliary stones (common bile duct and intrahepatic). *Best Pract Res Clin Gastroenterol* 2006; **20**: 1075-1083 [PMID: [17127189](#) DOI: [10.1016/j.bpg.2006.05.009](#)]
  - 24 **Tsui WM**, Lam PW, Lee WK, Chan YK. Primary hepatolithiasis, recurrent pyogenic cholangitis, and oriental cholangiohepatitis: a tale of 3 countries. *Adv Anat Pathol* 2011; **18**: 318-328 [PMID: [21654363](#) DOI: [10.1097/PAP.0b013e318220fb75](#)]
  - 25 **Neuhaus H**, Feussner H, Ungeheuer A, Hoffmann W, Siewert JR, Classen M. Prospective evaluation of the use of endoscopic retrograde cholangiography prior to laparoscopic cholecystectomy. *Endoscopy* 1992; **24**: 745-749 [PMID: [1468389](#) DOI: [10.1055/s-2007-1010576](#)]
  - 26 **Saltstein EC**, Peacock JB, Thomas MD. Preoperative bilirubin, alkaline phosphatase and amylase levels as predictors of common duct stones. *Surg Gynecol Obstet* 1982; **154**: 381-384 [PMID: [6175028](#)]
  - 27 **Lacaine F**, Corlette MB, Bismuth H. Preoperative evaluation of the risk of common bile duct stones. *Arch Surg* 1980; **115**: 1114-1116 [PMID: [7416958](#) DOI: [10.1001/archsurg.1980.01380090080019](#)]
  - 28 **Houdart R**, Perniceni T, Darne B, Salmeron M, Simon JF. Predicting common bile duct lithiasis: determination and prospective validation of a model predicting low risk. *Am J Surg* 1995; **170**: 38-43 [PMID: [7793492](#) DOI: [10.1016/s0002-9610\(99\)80249-9](#)]
  - 29 **Welbourn CR**, Mehta D, Armstrong CP, Gear MW, Eyre-Brook IA. Selective preoperative endoscopic retrograde cholangiography with sphincterotomy avoids bile duct exploration during laparoscopic cholecystectomy. *Gut* 1995; **37**: 576-579 [PMID: [7489949](#) DOI: [10.1136/gut.37.4.576](#)]
  - 30 **Meeralam Y**, Al-Shammari K, Yaghoobi M. Diagnostic accuracy of EUS compared with MRCP in detecting choledocholithiasis: a meta-analysis of diagnostic test accuracy in head-to-head studies. *Gastrointest Endosc* 2017; **86**: 986-993 [PMID: [28645544](#) DOI: [10.1016/j.gie.2017.06.009](#)]
  - 31 **Giljaca V**, Gurusamy KS, Takwoingi Y, Higgie D, Poropat G, Štimac D, Davidson BR. Endoscopic ultrasound versus magnetic resonance cholangiopancreatography for common bile duct stones. *Cochrane Database Syst Rev* 2015; CD011549 [PMID: [25719224](#) DOI: [10.1002/14651858.CD011549](#)]
  - 32 **Internal Clinical Guidelines Team (UK)**. Gallstone Disease: Diagnosis and Management of Cholelithiasis, Cholecystitis and Choledocholithiasis. London: National Institute for Health and Care Excellence (UK); 2014 [PMID: [25473723](#)]
  - 33 **Anderson SW**, Lucey BC, Varghese JC, Soto JA. Accuracy of MDCT in the diagnosis of choledocholithiasis. *AJR Am J Roentgenol* 2006; **187**: 174-180 [PMID: [16794173](#) DOI: [10.2214/AJR.05.0459](#)]
  - 34 **Anderson SW**, Rho E, Soto JA. Detection of biliary duct narrowing and choledocholithiasis: accuracy of portal venous phase multidetector CT. *Radiology* 2008; **247**: 418-427 [PMID: [18372450](#) DOI: [10.1148/radiol.2472070473](#)]
  - 35 **Kim CW**, Chang JH, Lim YS, Kim TH, Lee IS, Han SW. Common bile duct stones on multidetector computed tomography: attenuation patterns and detectability. *World J Gastroenterol* 2013; **19**: 1788-1796 [PMID: [23555167](#) DOI: [10.3748/wjg.v19.i11.1788](#)]
  - 36 **Tseng CW**, Chen CC, Chen TS, Chang FY, Lin HC, Lee SD. Can computed tomography with coronal reconstruction improve the diagnosis of choledocholithiasis? *J Gastroenterol Hepatol* 2008; **23**: 1586-1589 [PMID: [18713297](#) DOI: [10.1111/j.1440-1746.2008.05547.x](#)]
  - 37 **Saito H**, Iwagoi Y, Noda K, Atsugi S, Takaoka H, Kajihara H, Shono T, Nasu J, Obara H, Kakuma T, Tada S, Morishita S, Matsushita I, Katahira K. Dual-layer spectral detector computed tomography versus magnetic resonance cholangiopancreatography for biliary stones. *Eur J Gastroenterol Hepatol* 2021; **33**: 32-39 [PMID: [32639415](#) DOI: [10.1097/MEG.0000000000001832](#)]
  - 38 **Kim JE**, Lee JM, Baek JH, Han JK, Choi BI. Initial assessment of dual-energy CT in patients with gallstones or bile duct stones: can virtual nonenhanced images replace true nonenhanced images? *AJR Am J Roentgenol* 2012; **198**: 817-824 [PMID: [22451546](#) DOI: [10.2214/AJR.11.6972](#)]
  - 39 **Uyeda JW**, Richardson IJ, Sodickson AD. Making the invisible visible: improving conspicuity of noncalcified gallstones using dual-energy CT. *Abdom Radiol (NY)* 2017; **42**: 2933-2939 [PMID: [28660332](#) DOI: [10.1007/s00261-017-1229-x](#)]
  - 40 **Wittenburg H**. Hereditary liver disease: gallstones. *Best Pract Res Clin Gastroenterol* 2010; **24**: 747-756 [PMID: [20955975](#) DOI: [10.1016/j.bpg.2010.07.004](#)]
  - 41 **Ransohoff DF**, Gracie WA. Treatment of gallstones. *Ann Intern Med* 1993; **119**: 606-619 [PMID: [8363172](#) DOI: [10.7326/0003-4819-119-7\\_part\\_1-199310010-00010](#)]
  - 42 **Haldestam I**, Enell EL, Kullman E, Borch K. Development of symptoms and complications in individuals with asymptomatic gallstones. *Br J Surg* 2004; **91**: 734-738 [PMID: [15164444](#) DOI: [10.1002/bjs.4547](#)]
  - 43 **Attili AF**, De Santis A, Capri R, Repice AM, Maselli S. The natural history of gallstones: the GREPCO experience. The GREPCO Group. *Hepatology* 1995; **21**: 655-660 [PMID: [7875663](#) DOI: [10.1002/hep.1840210309](#)]



- 44 **Murison MS**, Gartell PC, McGinn FP. Does selective peroperative cholangiography result in missed common bile duct stones? *J R Coll Surg Edinb* 1993; **38**: 220-224 [PMID: [7693932](#)]
- 45 **Soper NJ**, Dunnegan DL. Routine versus selective intra-operative cholangiography during laparoscopic cholecystectomy. *World J Surg* 1992; **16**: 1133-1140 [PMID: [1455885](#) DOI: [10.1007/BF02067079](#)]
- 46 **Nies C**, Bauknecht F, Groth C, Clerici T, Bartsch D, Lange J, Rothmund M. [Intraoperative cholangiography as a routine method? *Chirurg* 1997; **68**: 892-897 [PMID: [9410677](#) DOI: [10.1007/s001040050290](#)]
- 47 **Khan OA**, Balaji S, Branagan G, Bennett DH, Davies N. Randomized clinical trial of routine on-table cholangiography during laparoscopic cholecystectomy. *Br J Surg* 2011; **98**: 362-367 [PMID: [21254008](#) DOI: [10.1002/bjs.7356](#)]
- 48 **Hauer-Jensen M**, Karesen R, Nygaard K, Solheim K, Amlie EJ, Havig O, Rosseland AR. Prospective randomized study of routine intraoperative cholangiography during open cholecystectomy: long-term follow-up and multivariate analysis of predictors of choledocholithiasis. *Surgery* 1993; **113**: 318-323 [PMID: [8441966](#)]
- 49 **Frossard JL**, Hadengue A, Amouyal G, Choury A, Marty O, Giostra E, Sivignon F, Sosa L, Amouyal P. Choledocholithiasis: a prospective study of spontaneous common bile duct stone migration. *Gastrointest Endosc* 2000; **51**: 175-179 [PMID: [10650260](#) DOI: [10.1016/s0016-5107\(00\)70414-7](#)]
- 50 **Saito H**, Kakuma T, Matsushita I. Risk factors for the development of post-endoscopic retrograde cholangiopancreatography pancreatitis in patients with asymptomatic common bile duct stones. *World J Gastrointest Endosc* 2019; **11**: 515-522 [PMID: [31798772](#) DOI: [10.4253/wjge.v11.i10.515](#)]
- 51 **Miura F**, Okamoto K, Takada T, Strasberg SM, Asbun HJ, Pitt HA, Gomi H, Solomkin JS, Schlossberg D, Han HS, Kim MH, Hwang TL, Chen MF, Huang WS, Kiriya S, Itoi T, Garden OJ, Liao KH, Horiguchi A, Liu KH, Su CH, Gouma DJ, Belli G, Dervenis C, Jagannath P, Chan ACW, Lau WY, Endo I, Suzuki K, Yoon YS, de Santibañes E, Giménez ME, Jonas E, Singh H, Honda G, Asai K, Mori Y, Wada K, Higuchi R, Watanabe M, Rikiyama T, Sata N, Kano N, Umezawa A, Mukai S, Tokumura H, Hata J, Kozaka K, Iwashita Y, Hibi T, Yokoe M, Kimura T, Kitano S, Inomata M, Hirata K, Sumiyama Y, Inui K, Yamamoto M. Tokyo Guidelines 2018: initial management of acute biliary infection and flowchart for acute cholangitis. *J Hepatobiliary Pancreat Sci* 2018; **25**: 31-40 [PMID: [28941329](#) DOI: [10.1002/jhbp.509](#)]
- 52 **Saito H**, Koga T, Sakaguchi M, Kadono Y, Kamikawa K, Urata A, Imamura H, Tada S, Kakuma T, Matsushita I. Post-endoscopic retrograde cholangiopancreatography pancreatitis in single-stage endoscopic common bile duct stone removal. *JGH Open* 2020; **4**: 394-399 [PMID: [32514443](#) DOI: [10.1002/jgh3.12263](#)]



## Basic Study

# Alleviation of acute pancreatitis-associated lung injury by inhibiting the p38 mitogen-activated protein kinase pathway in pulmonary microvascular endothelial cells

Xiao-Xin Zhang, Hao-Yang Wang, Xue-Fei Yang, Zi-Qi Lin, Na Shi, Chan-Juan Chen, Lin-Bo Yao, Xin-Min Yang, Jia Guo, Qing Xia, Ping Xue

**ORCID number:** Xiao-Xin Zhang 0000-0002-3196-6532; Hao-Yang Wang 0000-0003-2878-3548; Xue-Fei Yang 0000-0003-1514-3234; Zi-Qi Lin 0000-0002-0445-9607; Na Shi 0000-0001-6395-3122; Chan-Juan Chen 0000-0002-9853-2632; Lin-Bo Yao 0000-0001-9087-7030; Xin-Min Yang 0000-0002-9441-7119; Jia Guo 0000-0001-8221-5459; Qing Xia 0000-0003-4373-2722; Ping Xue 0000-0003-3935-4845.

**Author contributions:** Zhang XX, Guo J and Xue P obtained funding and designed the experiments; Zhang XX, Wang HY, Yang XF and Lin ZQ performed the experiments and literature search; Shi N, Chen CJ, Yao LB and Yang XM evaluated histological images and carried out a biochemical analysis; Zhang XX, Xia Q and Xue P wrote and revised the manuscript; All authors have read and approved the final manuscript.

**Supported by** National Natural Science Foundation of China, No. 81873107, No. 82004154 and No. 81573766; and Science and Technology Planning Program of Sichuan, No. 2019YFS0259.

**Institutional animal care and use committee statement:** The study

Xiao-Xin Zhang, Hao-Yang Wang, Xue-Fei Yang, Zi-Qi Lin, Na Shi, Chan-Juan Chen, Lin-Bo Yao, Xin-Min Yang, Jia Guo, Qing Xia, Ping Xue, Department of Integrated Traditional Chinese and Western Medicine, West China Hospital of Sichuan University, Chengdu 610041, Sichuan Province, China

**Corresponding author:** Ping Xue, MD, PhD, Professor, Department of Integrated Traditional Chinese and Western Medicine, West China Hospital of Sichuan University, No. 37 Guoxue Lane, Chengdu 610041, Sichuan Province, China. [xueping@wchscu.cn](mailto:xueping@wchscu.cn)

## Abstract

### BACKGROUND

Previous reports have suggested that the p38 mitogen-activated protein kinase signaling pathway is involved in the development of severe acute pancreatitis (SAP)-related acute lung injury (ALI). Inhibition of p38 by SB203580 blocked the inflammatory responses in SAP-ALI. However, the precise mechanism associated with p38 is unclear, particularly in pulmonary microvascular endothelial cell (PMVEC) injury.

### AIM

To determine its role in the tumor necrosis factor- $\alpha$  (TNF- $\alpha$ )-induced inflammation and apoptosis of PMVECs *in vitro*. We then conducted *in vivo* experiments to confirm the effect of SB203580-mediated p38 inhibition on SAP-ALI.

### METHODS

*In vitro*, PMVEC were transfected with mitogen-activated protein kinase kinase 6 (Glu), which constitutively activates p38, and then stimulated with TNF- $\alpha$ . Flow cytometry and western blotting were performed to detect the cell apoptosis and inflammatory cytokine levels, respectively. *In vivo*, SAP-ALI was induced by 5% sodium taurocholate and three different doses of SB203580 (2.5, 5.0 or 10.0 mg/kg) were intraperitoneally injected prior to SAP induction. SAP-ALI was assessed by performing pulmonary histopathology assays, measuring myeloperoxidase activity, conducting arterial blood gas analyses and measuring TNF- $\alpha$ , interleukin (IL)-1 $\beta$  and IL-6 levels. Lung microvascular permeability was measured by determining bronchoalveolar lavage fluid protein concentration, Evans blue

was performed according to the Guidelines of Animal Care and Use Committee of West China Hospital of Sichuan University (protocol number, 2017082A).

**Conflict-of-interest statement:** The authors declare that they have no conflict of interest.

**Data sharing statement:** No additional data are available.

**ARRIVE guidelines statement:** The manuscript has been prepared and revised according to the ARRIVE guidelines.

**Open-Access:** This article is an open-access article that was selected by an in-house editor and fully peer-reviewed by external reviewers. It is distributed in accordance with the Creative Commons Attribution NonCommercial (CC BY-NC 4.0) license, which permits others to distribute, remix, adapt, build upon this work non-commercially, and license their derivative works on different terms, provided the original work is properly cited and the use is non-commercial. See: <http://creativecommons.org/licenses/by-nc/4.0/>

**Manuscript source:** Unsolicited manuscript

**Specialty type:** Gastroenterology and hepatology

**Country/Territory of origin:** China

**Peer-review report's scientific quality classification**

Grade A (Excellent): A  
Grade B (Very good): 0  
Grade C (Good): 0  
Grade D (Fair): 0  
Grade E (Poor): 0

**Received:** December 25, 2020

**Peer-review started:** December 26, 2020

**First decision:** January 29, 2021

**Revised:** February 6, 2021

**Accepted:** March 29, 2021

**Article in press:** March 29, 2021

**Published online:** May 14, 2021

**P-Reviewer:** Kozarek R

**S-Editor:** Zhang L

extravasation and ultrastructural changes in PMVECs. The apoptotic death of pulmonary cells was confirmed by performing a terminal deoxynucleotidyl transferase-mediated dUTP nick end labeling analysis and examining the Bcl2, Bax, Bim and cle-caspase3 levels. The proteins levels of P-p38, NFκB, IκB, P-signal transducer and activator of transcription-3, nuclear factor erythroid 2-related factor 2, HO-1 and Myd88 were detected in the lungs to further evaluate the potential mechanism underlying the protective effect of SB203580.

## RESULTS

*In vitro*, mitogen-activated protein kinase (Glu) transfection resulted in higher apoptotic rates and cytokine (IL-1β and IL-6) levels in TNF-α-treated PMVECs. *In vivo*, SB203580 attenuated lung histopathological injury, decreased inflammatory activity (TNF-α, IL-1β, IL-6 and myeloperoxidase) and preserved pulmonary function. Furthermore, SB203580 significantly reversed changes in the bronchoalveolar lavage fluid protein concentration, Evans blue accumulation, terminal deoxynucleotidyl transferase-mediated dUTP nick end labeling-positive cell numbers, apoptosis-related proteins (cle-caspase3, Bim and Bax) and endothelial microstructure. Moreover, SB203580 significantly reduced the pulmonary P-p38, NFκB, P-signal transducer and activator of transcription-3 and Myd88 levels but increased the IκB and HO-1 levels.

## CONCLUSION

p38 inhibition may protect against SAP-ALI by alleviating inflammation and the apoptotic death of PMVECs.

**Key Words:** Acute pancreatitis; Acute lung injury; Pulmonary microvascular endothelial cells; P38; SB203580; Apoptosis

©The Author(s) 2021. Published by Baishideng Publishing Group Inc. All rights reserved.

**Core Tip:** We explored the role of the p38 mitogen-activated protein kinase pathway in the tumor necrosis factor-α-induced inflammation and apoptosis of pulmonary microvascular endothelial cells *in vitro* and verified the effect of SB203580-mediated p38 inhibition on severe acute pancreatitis-related acute lung injury in rats. p38 mitogen-activated protein kinase overactivation promoted tumor necrosis factor-α-induced inflammatory cytokine expression and pulmonary microvascular endothelial cell apoptosis *in vitro*. SB203580 improved severe acute pancreatitis-related acute lung injury by downregulating P-p38, NFκB, P-SATA3 and Myd88 and upregulating IκB and HO-1, which alleviated inflammation and apoptotic cell death in rats.

**Citation:** Zhang XX, Wang HY, Yang XF, Lin ZQ, Shi N, Chen CJ, Yao LB, Yang XM, Guo J, Xia Q, Xue P. Alleviation of acute pancreatitis-associated lung injury by inhibiting the p38 mitogen-activated protein kinase pathway in pulmonary microvascular endothelial cells. *World J Gastroenterol* 2021; 27(18): 2141-2159

**URL:** <https://www.wjgnet.com/1007-9327/full/v27/i18/2141.htm>

**DOI:** <https://dx.doi.org/10.3748/wjg.v27.i18.2141>

## INTRODUCTION

Acute pancreatitis (AP), a common gastrointestinal disease, ranges from a self-limiting disease to a severe condition with high mortality. The overall mortality rate is approximately 2%[1], while the mortality rate of severe AP (SAP) with distant organ dysfunction increases to 37%-50%[2]. To date, the pathogenesis of SAP has not been completely clarified, and no specific pharmacological therapies for SAP or its associated organ failure are available. The management of AP is mainly limited to supportive care. The lung is the most vulnerable organ in patients with SAP. Acute lung injury (ALI) or its more severe form, acute respiratory distress syndrome, is reported to occur in 10%-25% of patients with AP and accounts for up to 60% of AP-associated deaths[3,4]. Therefore, the identification of an effective therapy for AP-

L-Editor: Filipodia

P-Editor: Ma YJ



associated ALI is still urgently needed to decrease AP mortality.

ALI secondary to SAP is clinically and histologically indistinguishable from other indirect (sepsis, trauma or burns) or direct (*e.g.*, toxins or infection) insults to the lungs[5]. ALI is characterized by disruption of the alveolar capillary barrier, which increases endothelial and epithelial permeability, decreases lung compliance and impairs gas exchange[6]. Multiple biological processes are involved in the mechanisms of endothelial permeability, such as cytoskeletal rearrangements, assembly/disassembly of cell junctions and survival/death[7-9]. Pulmonary microvascular endothelial cells (PMVECs) line the interior of blood vessels and are an essential part of the blood and tissue microenvironment. They are major actors responding to insults related to ALI[10,11]. PMVECs are the main targets of humoral and cellular mediators during injury[12] and actively produce proinflammatory cytokines, increase the levels of adhesion molecules and secrete prothrombotic substances, promoting injury by transforming to a prothrombotic and proinflammatory phenotype to further activate the immune and hemostatic systems[4,8]. PMVECs are likely to be the first-line responders in efforts to prevent the development of SAP-associated ALI. Therefore, modulation of pulmonary vascular homeostasis is crucial for the successful treatment of AP-associated ALI.

p38 mitogen-activated protein kinase (p38 MAPK), a member of the serine/threonine kinase family, is ubiquitously expressed. It plays an important role in diverse processes including endocytosis, gene transcription, cell proliferation, cytokine production, apoptosis and cytoskeletal redistribution[8]. Therefore, unsurprisingly, p38 MAPK is involved in many cascades that result in the development of mild AP with limited pancreatic injury to SAP with ALI. In an experimental AP model, p38 MAPK activation was observed in the lungs as early as 2 h after model establishment[13], while p38 MAPK inhibitors (SB203580 or CN1-1493) alleviated pancreatic and pulmonary injury, limited cytokine increases and improved survival[14-16]. Currently, the precise mechanism by which the p38 MAPK signaling pathway regulates SAP-related ALI is unclear, particularly PMVEC injury. In this study, we overactivated p38 MAPK to define its role in the tumor necrosis factor- $\alpha$  (TNF- $\alpha$ )-induced inflammation and apoptosis of rat PMVECs *in vitro* and then investigated the effect of SB203580, a specific p38 MAPK inhibitor, on SAP rats with ALI *in vivo*.

## MATERIALS AND METHODS

### Cell culture

Rat PMVECs were obtained from the BeNa Culture Collection (338210, Beijing, China). Cells were identified according to staining with rat anti-factor VIII and binding of FITC-labeled lectin (Sigma, United States)[17]. The cells were cultured in DMEM (Thermo Fisher, United States) supplemented with 100 mL/L fetal bovine serum (BI, Australia), 50 U/mL penicillin and 50  $\mu$ g/mL streptomycin (Thermo Fisher, United States). PMVECs were maintained at 37 °C in a humidified atmosphere with 95 mL/L O<sub>2</sub> and 5 mL/L CO<sub>2</sub>.

### Mitogen-activated protein kinase kinase 6 (Glu) recombinant adenovirus construction and transduction

The MAPK pathway is comprised of three sequential dual-specificity kinases, and MAPK kinase (MKK) 6 is highly selective for p38 activation. Overexpression of activated MKK 6 (Glu) constitutively activates p38 MAPK[18,19]. Lentiviruses carrying either no inserted sequence (null) or the MKK 6 (Glu) gene were constructed by Wuhan PeptBio company limited China. PMVECs were infected with the lentivirus at a multiplicity of infection of 10 in the presence of 5  $\mu$ g/mL polybrene (Sigma, United States). After lentivirus infection, MKK 6 (Glu)-overexpressing cells and control cells were obtained *via* puromycin (2  $\mu$ g/mL) screening and analyzed using western blotting. When the cells reached 70%–80% confluence, they were treated with TNF- $\alpha$  (20 ng/mL) for the indicated times and then used for the subsequent analyses.

### Flow cytometry

PMVEC apoptosis was assessed using an Annexin V-FITC/PI kit (4A Biotech, China). Briefly, PMVECs were detached using trypsin, washed with cold PBS, pelleted and resuspended in binding buffer. Then, 10  $\mu$ L of Annexin V was added, and they were incubated for 5 min in the dark. After mixing with 5  $\mu$ L of propidium iodide, the cells were analyzed using a flow cytometer (BD Biosciences, United States).

### Animals

Adult male Sprague-Dawley rats ( $n = 25$ , 210-230 g) were purchased from the Experimental Animal Center of Sichuan University (Chengdu, China). The animals were housed at 22-25 °C on a 12 h day-night cycle and fed standard rodent chow and tap water *ad libitum* for 1 wk of acclimation. The animal experiments performed in this study were conducted in accordance with the National Institutes of Health Guide for the Care and Use of Laboratory Animals. The protocol was designed to minimize pain or discomfort to the animals and approved by the Animal Ethics Committee of West China Hospital of Sichuan University.

### Induction of the SAP model and experimental groups

After fasting for 12 h, the SAP model was established by biliary-pancreatic duct injection of 50 g/L sodium taurocholate (Sigma, United States, 1 mL/kg) using a micropump at a speed of 0.2 mL/min[20]. In the sham group, the rats received the same volume of saline instead of sodium taurocholate. All rats received a saline injection subcutaneously to compensate for fluid loss during the surgery (20 mL/kg body weight). The rats were randomly divided into the SO group, SAP group and SAP + SB203580 group. The SAP + SB203580 group was further divided into low-dose (SB2.5 group), middle-dose (SB5 group) and high-dose (SB10 group) subgroups according to the dose of SB203580 (2.5 mg/kg, 5.0 mg/kg and 10.0 mg/kg, respectively,  $n = 5$ ). SB203580 (Selleck, United States) was intraperitoneally administered before model establishment. The rats were sacrificed 12 h after model induction, and samples were harvested rapidly for subsequent analysis.

### Arterial blood gas analysis

At the end of the experiment, arterial blood samples were collected by cardiac puncture. A blood gas analysis was performed to detect the partial pressure of oxygen ( $\text{PaO}_2$ ) and oxygen saturation ( $\text{SaO}_2$ , Cobas b 123 Analyzer, Roche, Switzerland).

### Bronchoalveolar lavage fluid collection

After opening the chest, the right lung was ligated. Bronchoalveolar lavage fluid (BALF) was collected through slow and careful lavage of the left lung with 2 mL of 4 °C PBS. Then, the fluid was centrifuged at 500 g for 5 min. The supernatant was collected and stored at -80 °C until the analyses of the protein concentration and cytokine levels.

### Histological examination and terminal deoxynucleotidyl transferase-mediated dUTP nick end labeling staining

The pancreas and lung were fixed with 40 g/L formaldehyde for 24 h. The tissues were then embedded in paraffin, and continuously sliced at a 5 mm thickness for staining with hematoxylin and eosin. The pancreatic and pulmonary histological assessment was performed and scored by two pathologists using a microscope at 200 × magnification[21,22]. For the assessment of the apoptosis of lung tissue, terminal deoxynucleotidyl transferase-mediated dUTP nick end labeling (TUNEL) staining was performed with a commercially available In Situ Cell Death Detection Kit (Roche, Mannheim, Germany) according to the manufacturer's instructions.

### Measurements of cytokines and BALF protein concentrations

Concentrations of TNF- $\alpha$ , interleukin (IL)-1 $\beta$  and IL-6 in the serum and BALF were evaluated using ELISA kits according to the manufacturer's instructions (R and D Systems, United States). The BALF protein concentration was determined using a BCA kit (Thermo, United States).

### Lung microvascular permeability analysis

Evans blue extravasation was used to quantify the capillary permeability in the lungs. A 10 g/L Evans Blue solution (20 mg/kg, Sigma-Aldrich, United States) was injected into the tail vein 1 h before exsanguination. PBS was used to flush the remaining Evans blue from the pulmonary vascular system. After the complete removal of blood, the left lung was removed, weighed, homogenized in formamide and incubated at 37 °C for 24 h. Finally, the supernatant was quantified spectrophotometrically at 620 nm.

### Myeloperoxidase activity

Pulmonary myeloperoxidase (MPO) activity was measured using the method described by Dawra *et al*[23]. Briefly, lung tissue was homogenized in phosphate



buffer (100 mmol/L, pH 7.4) at 4 °C and centrifuged to pellet the tissues. The samples were then resuspended in phosphate buffer (100 mmol/L, pH 5.4) containing protease inhibitors, 5 g/L hexadecyl trimethyl ammonium bromide and 10 mmol/L EDTA and subjected to three rapid freeze-thaw cycles. The suspension was sonicated and centrifuged to obtain the supernatant. Twenty microliters of the supernatant were incubated with 200 µL of phosphate buffer (pH 5.4) containing 5 g/L hexadecyl trimethyl ammonium bromide and 2 mmol/L 3,3',5,5'-tetramethylbenzidine for 3 min at room temperature followed by the addition of 50 µL H<sub>2</sub>O<sub>2</sub>. The difference in the absorbance of this assay solution between 0 min and 3 min was measured at 655 nm at 37 °C with a microplate reader (BMG LABTECH, Germany). MPO activity was calculated from a human MPO standard curve, normalized to the protein concentration and reported as mU/mg protein.

### Western blotting

Lysates from PMVECs or lung tissues were extracted with RIPA lysis buffer (Abcam, United Kingdom) supplemented with protease inhibitors (Roche, Germany). The total protein concentration was quantified using a BCA kit (Thermo, United States). The same amounts of protein were separated on 10% or 12% SDS-PAGE gels and transferred to a polyvinylidene fluoride membrane. Membranes were blocked with 50 g/L nonfat milk for 2 h at room temperature and subsequently incubated with the following primary antibodies overnight at 4 °C: P-p38 (1:2000), NFκB (1:1000), IκB (1:1000), cleaved caspase-3 (cle-casp3, 1:1000), P-signal transducer and activator of transcription-3 (P-STAT3, 1:1000), myeloid differentiation factor 88 (Myd88, 1:1000), nuclear factor erythroid 2-related factor 2 (Nrf2, 1:1000), Bax (1:1000) and Bim (1:1000) from CST, United States; IL-1β (1:1000), heme oxygenase-1 (HO-1, 1:1000) and Bcl2 (1:1000) from Abcam, United States; and TNF-α (1:1000), IL-6 (1:1000) and β-actin (1:1000) from Proteintech, China. After rinsing with Tris-buffered saline containing Tween 20 (10 min, × 3), the membranes were incubated with a secondary goat anti-rabbit (1:5000, Proteintech, China) or a goat anti-mouse IgG-HRP antibody (1:10000, Proteintech, China) for 1-2 h at room temperature. Finally, after washing, the membranes were imaged using a chemiluminescence detection system (Bio-Rad, United States) and analyzed with Image Lab software.

### Transmission electron microscopy

A 2 mm<sup>3</sup> peripheral specimen was fixed with 25 mL/L glutaraldehyde for 2 h and then washed with 0.1 mol/L phosphate buffer (pH 7.4, 10 min × 3). After fixing the samples with 10 mL/L osmium tetroxide for 2 h, the specimens were dehydrated through a graded series of ethanol solutions and acetone and embedded in Epon 812 (Sigma, United States). Ultrathin sections were cut with an ultramicrotome (Leica, Germany). Finally, the sections were stained with uranyl acetate and lead citrate and examined using a JEM-1230 transmission electron microscope (JEOL, Japan).

### Statistical analysis

All statistical tests were performed using SPSS 20.0 (SPSS, United States) by a biomedical statistician. Data are presented as the mean ± SE for continuous variables or frequencies and percentages for categorical variables. Data were analyzed using one-way analysis of variance or the Kruskal-Wallis test. A *P* value of < 0.05 was considered statistically significant.

## RESULTS

### *Overactivation of p38 MAPK aggravates TNF-α-induced apoptosis and inflammatory cytokine expression in PMVECs*

We overexpressed a constitutively activated MKK6 (Glu) in PMVECs, which was confirmed to over activate p38 MAPK (Figure 1A). Then, the cells were incubated in the absence or presence of TNF-α. Flow cytometry analysis showed TNF-α induced apoptosis in both null and MKK (Glu) cells. Compared with the null groups, the apoptotic rate was significantly higher in the MKK (Glu) group treated with TNF-α (Figure 1B and 1C). Meanwhile, the levels of inflammatory cytokines (IL-6 and IL-1β) were also significantly upregulated in the MKK (Glu) cells (Figure 1D and 1E).

### *SB203580 attenuates pancreatic damage in SAP rats*

Representative images of hematoxylin and eosin staining of the pancreas were shown

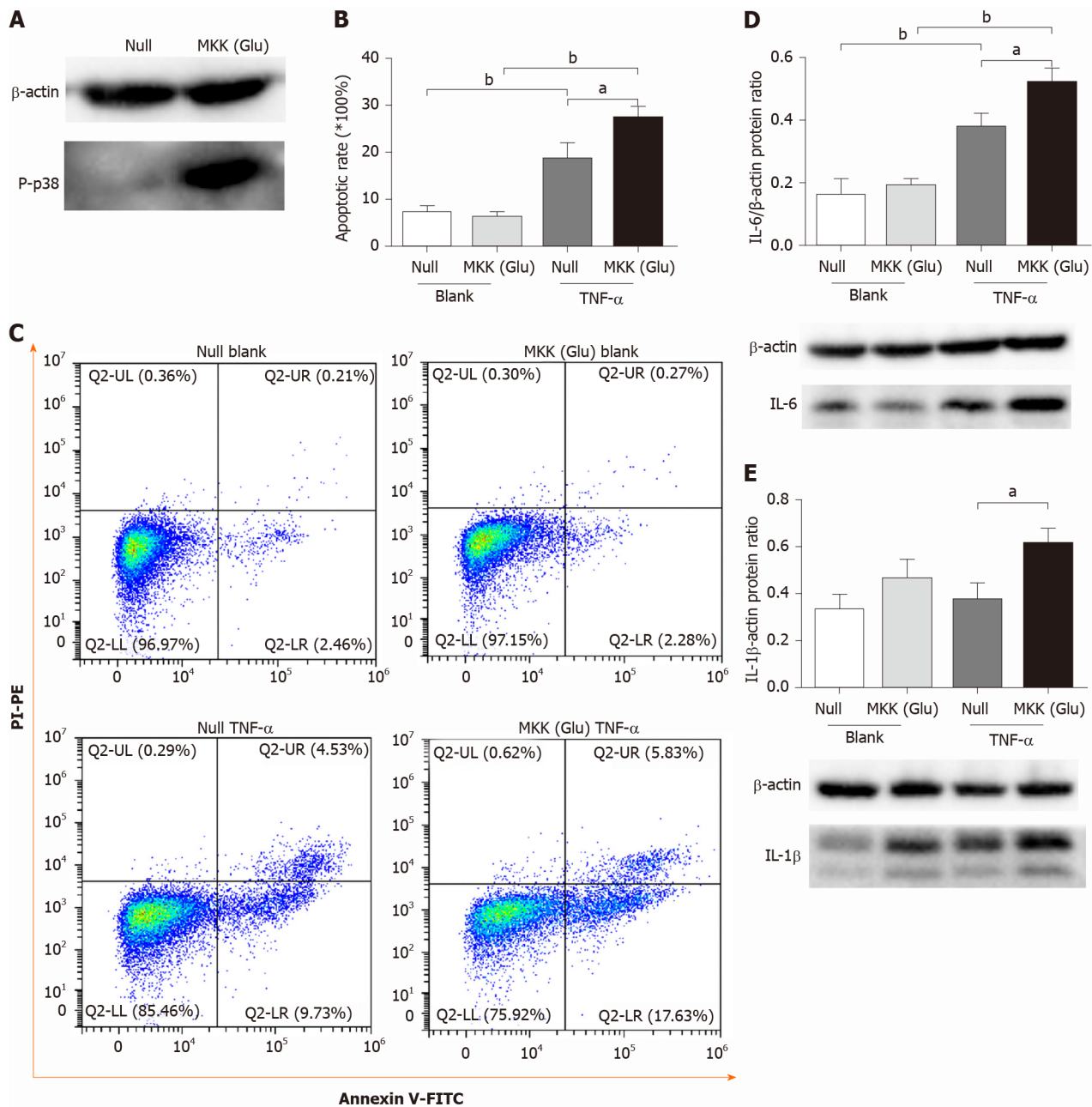


**Figure 1** p38 mitogen-activated protein kinase overactivation aggravates tumor necrosis factor- $\alpha$ -induced apoptosis and inflammatory cytokine expression in pulmonary microvascular endothelial cells. **A:** Western blotting confirmed that mitogen-activated protein kinase (Glu) transfection constitutively activated p38 mitogen-activated protein kinase in pulmonary microvascular endothelial cells; **B:** Apoptotic rate in null and mitogen-activated protein kinase kinase (Glu) pulmonary microvascular endothelial cells stimulated with or without tumor necrosis factor- $\alpha$  for 24 h; **C:** Representative images of flow cytometry analysis for apoptosis; **D:** The expression level of interleukin-6 in each group; **E:** The expression level of interleukin-1 $\beta$  in each group. Data are expressed as mean  $\pm$  SE of 3-4 samples per group;  $^aP < 0.05$ ;  $^bP < 0.01$ . IL: Interleukin; MKK: Mitogen-activated protein kinase kinase; TNF- $\alpha$ : Tumor necrosis factor- $\alpha$ .

in Figure 2A. Except for slight pancreatic edema, no obvious changes indicative of AP were observed in sham-operated animals. Sodium taurocholate induced typical histopathological changes associated with AP, including diffuse edema, marked neutrophil infiltration, intrapancreatic hemorrhage and acinar cell necrosis. The histopathological scores were all significantly increased (Figure 2B-F). All three tested doses of SB203580 (2.5, 5.0 and 10.0 mg/kg) alleviated injury to the pancreatic tissues (all  $P < 0.05$ ). We explored the difference in the therapeutic effect among the three different doses; compared to the SB2.5 group, 10.0 mg/kg SB203580 further significantly decreased the histopathological inflammatory infiltration, necrosis and total scores (Figure 2B, 2D and 2F).

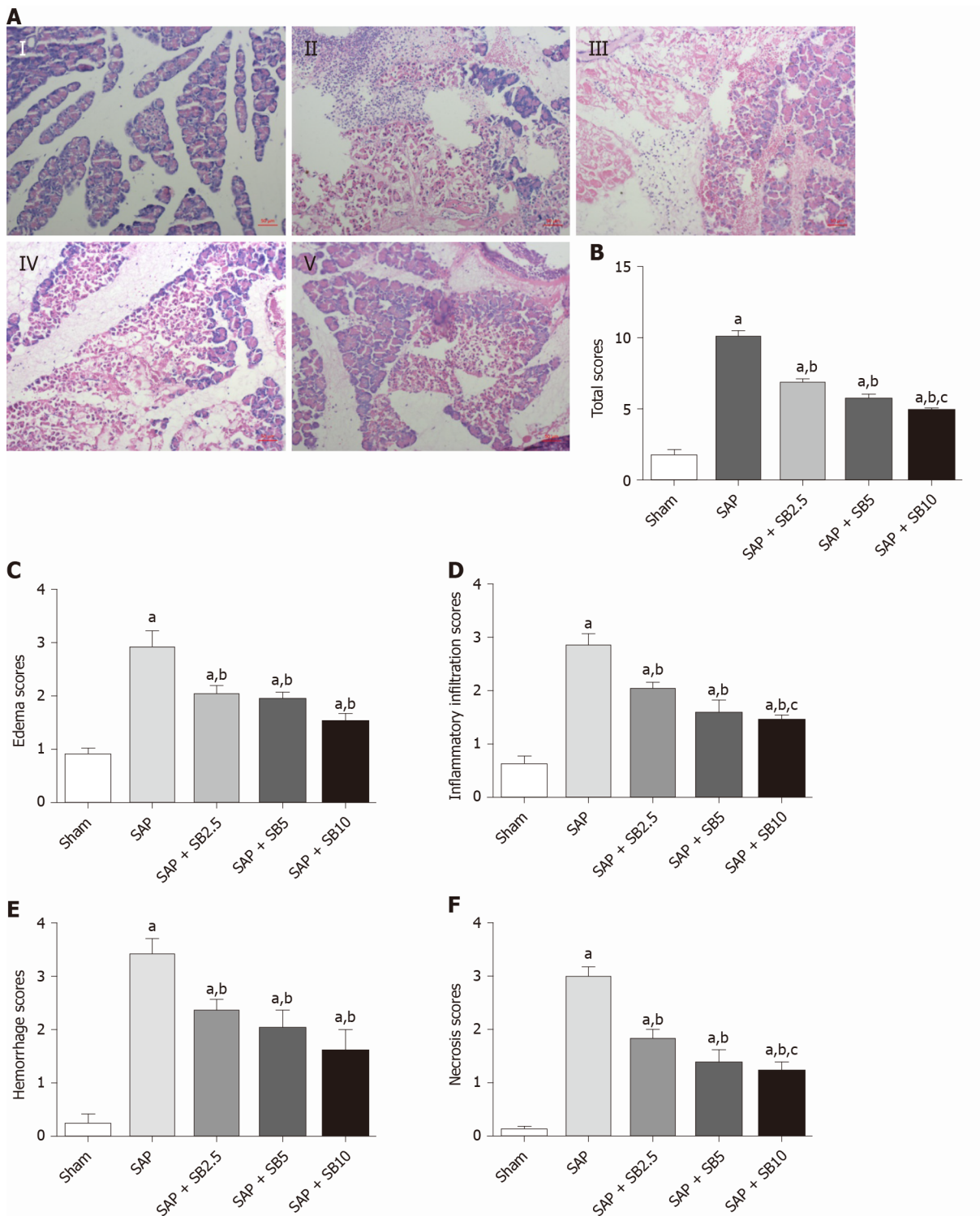
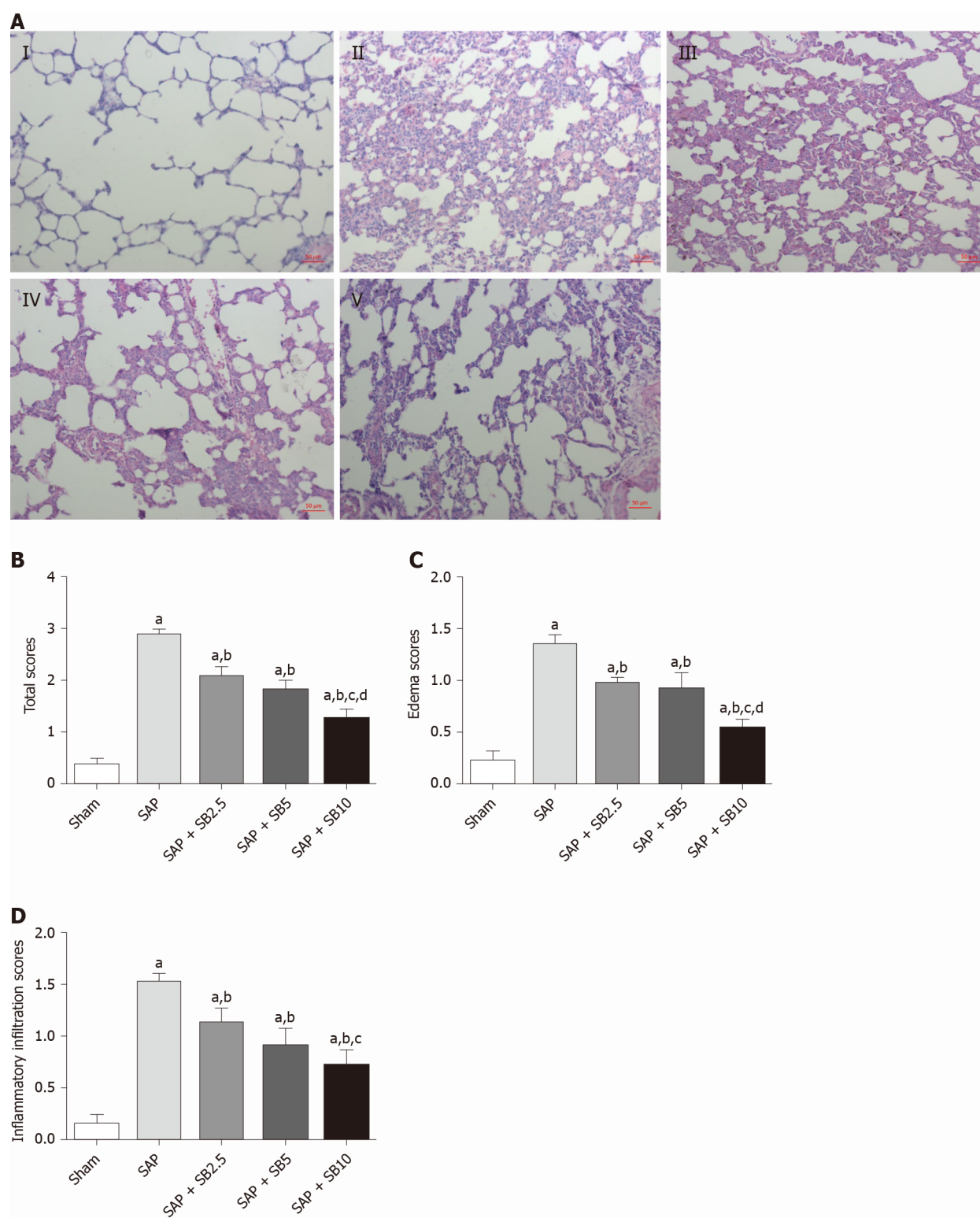


**Figure 2** Effects of SB203580 on pancreatic histopathological changes and histopathological severity scores. A: Representative hematoxylin and eosin images of pancreatic sections (magnification 200 ×); I: Sham group; II: Severe acute pancreatitis (SAP) group; III: SAP + SB2.5 group; IV: SAP + SB5 group; V: SAP + SB10 group; B: Total scores; C: Edema scores; D: Inflammatory infiltration scores; E: Hemorrhage scores; F: Necrosis scores. B-F: Pancreatic histopathology scores in different groups; Data were expressed as mean ± SE; <sup>a</sup> $P < 0.05$  vs sham group; <sup>b</sup> $P < 0.05$  vs SAP group; <sup>c</sup> $P < 0.05$  vs SAP + SB2.5 group. SAP: Severe acute pancreatitis.

### SB203580 alleviates lung injury in SAP rats

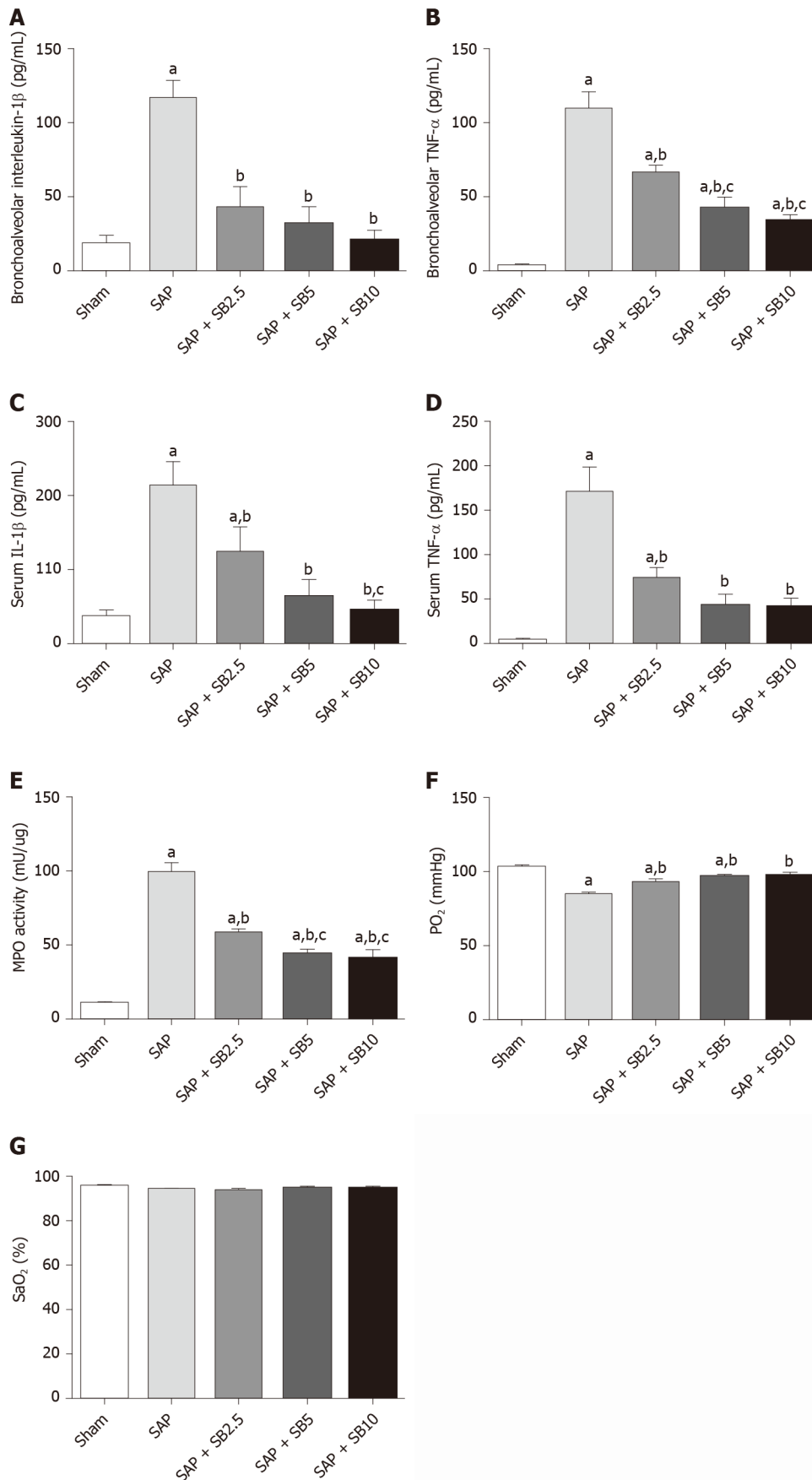
The histopathological changes in the pulmonary tissues were shown in **Figure 3A**. In SAP rats, lung damage was characterized by neutrophil infiltration, thickened alveolar walls, intra-alveolar hemorrhaging and alveolar collapse. The histopathological scores were also significantly increased (**Figure 3B-D**). These changes were accompanied by significantly increased IL-1 and TNF- $\alpha$  levels in the BALF and serum (**Figure 4A-D**).





**Figure 3** Effects of SB203580 on pulmonary histopathological changes and histopathological severity scores. A: Representative hematoxylin and eosin images of pulmonary sections (magnification 200 ×); I: Sham group; II: Severe acute pancreatitis (SAP) group; III: SAP + SB2.5 group; IV: SAP + SB5 group; V: SAP + SB10 group; B: Total scores; C: Edema scores; D: Inflammatory infiltration scores. B-D: Pulmonary histopathology scores in different groups; Data are expressed as mean  $\pm$  SE of the mean; <sup>a</sup> $P < 0.05$  vs sham group; <sup>b</sup> $P < 0.05$  vs SAP group; <sup>c</sup> $P < 0.05$  vs SAP + SB2.5 group; <sup>d</sup> $P < 0.05$  vs SAP + SB5 group. SAP: Severe acute pancreatitis.

and pulmonary MPO activity (Figure 4E) and a decreased  $\text{PaO}_2$  (Figure 4F). There was no change of  $\text{SO}_2$  in the SAP rats (Figure 4G). At the same time, western blotting analysis also confirmed increased levels of inflammatory cytokines (IL-1, TNF- $\alpha$ , IL-6) in the SAP group compared with the sham group (Figure 4H-J). SB203580 treatment alleviated the histopathological injuries and scores, decreased the levels of inflam-





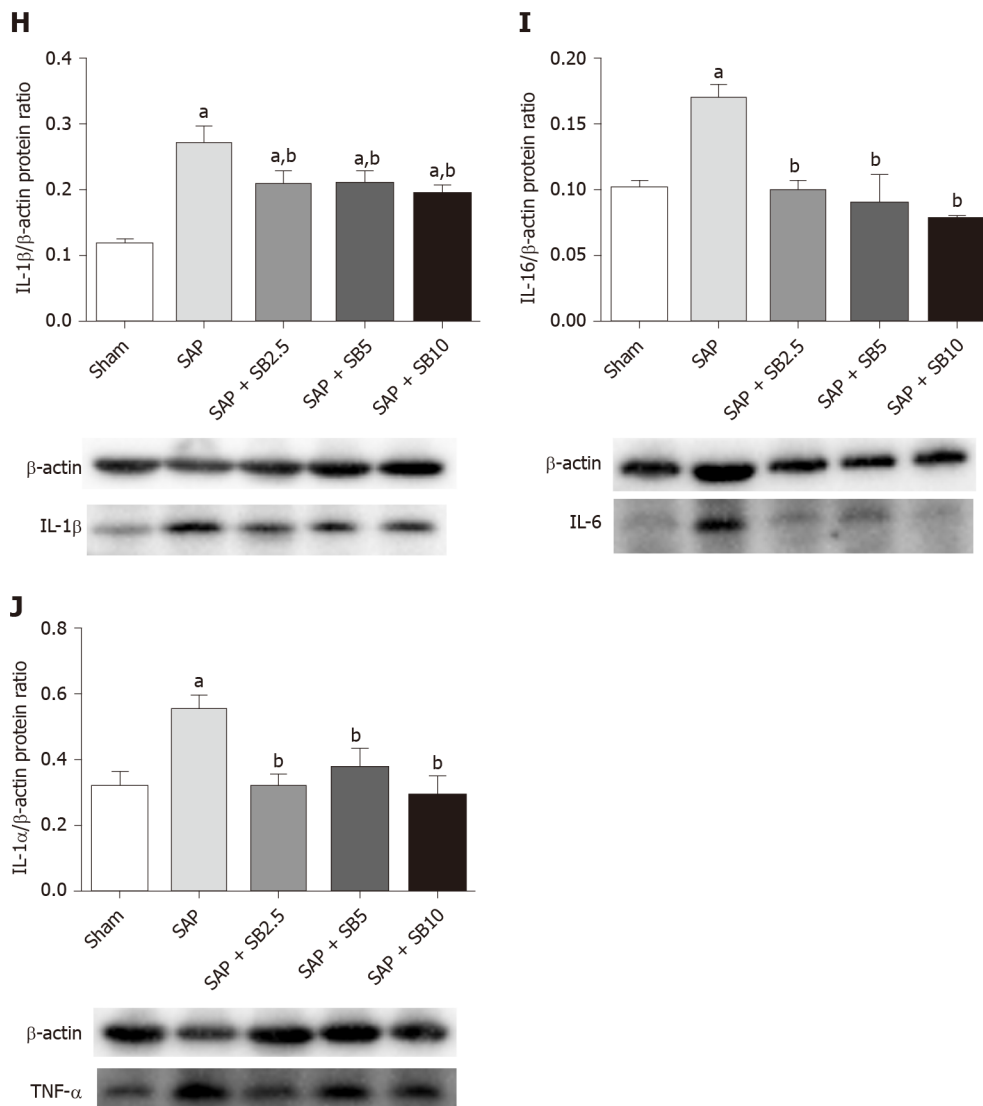


**Figure 4** Effects of SB203580 on pulmonary severity indices of severe acute pancreatitis in rats. A: Bronchoalveolar interleukin-1β (IL-1β); B: Bronchoalveolar tumor necrosis factor alpha (TNF-α); C: Serum IL-1β; D: Serum TNF-α; E: Lung myeloperoxidase activity; F: Partial pressure of oxygen; G: Oxygen saturation; H: Representative western blotting analysis results for IL-1β in lung tissues; I: Representative western blotting analysis results for IL-6 in lung tissues; J: Representative western blotting analysis results for TNF-α in lung tissues. Data are expressed as mean ± SE of the mean; <sup>a</sup>*P* < 0.05 vs sham group; <sup>b</sup>*P* < 0.05 vs severe acute pancreatitis group; <sup>c</sup>*P* < 0.05 vs severe acute pancreatitis + SB2.5 group. IL: Interleukin; MPO: Myeloperoxidase; PaO<sub>2</sub>: Pressure of oxygen; SaO<sub>2</sub>: Oxygen saturation; SAP: Severe acute pancreatitis; TNF-α: Tumor necrosis factor-alpha.

matory factors (IL-1, TNF-α, IL-6 and MPO) and preserved PaO<sub>2</sub>. Among the three doses tested, SB203580 at 10.0 mg/kg consistently and significantly reduced all histopathological and biochemical severity indices with the highest efficiency.

#### Protective effects of SB203580 on capillary injury

The permeability of the PMVECs was evaluated *in vivo* by measuring the BALF protein concentration and Evans blue accumulation in the lung tissue. Quantitative analysis showed a significant increase in these two parameters in SAP rats, which were suppressed by SB203580 cotreatment (Figure 5A and 5B). They further decreased after treatment with increasing SB203580 doses. The microstructure and integrity of the endothelium were evaluated using transmission electron microscopy. In the sham group, the lung tissues showed a normal capillary endothelium, as evidenced by an intact capillary basal membrane, dense endothelial cell-cell junctions and continuous and clear delineation between cells (Figure 5C). In the SAP group, capillary endothelial dissolution and rupture were noted. In addition, low electron density clouds with an irregular thickness indicating basal membrane edema, increased vacuolization, loose cellular junctions, swollen cellular organelles and nuclear degeneration were often observed. In contrast, the swelling and injury of endothelial cells were partially alleviated in lungs from SB203580-treated rats. After treatment with 10.0 mg/kg

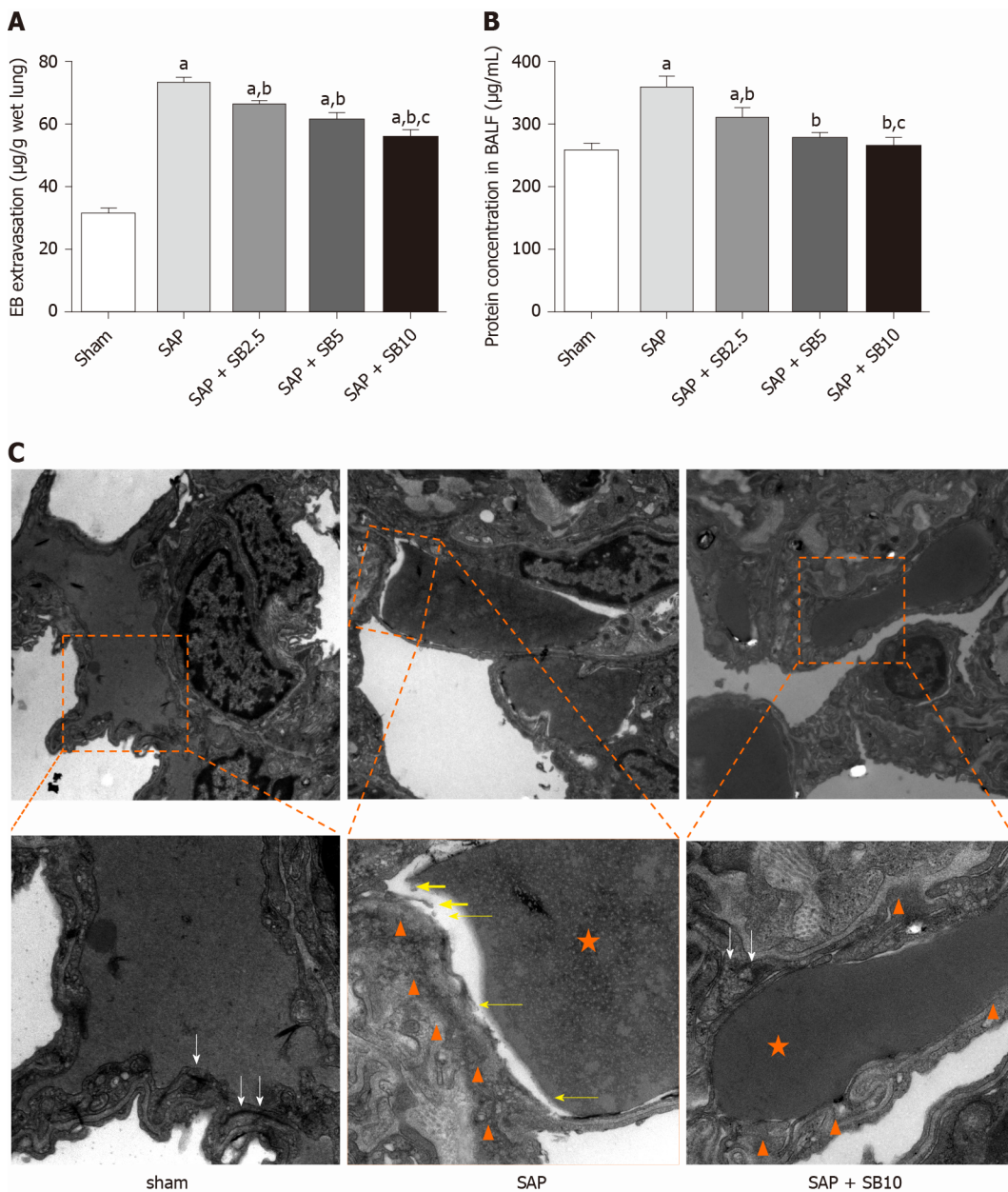
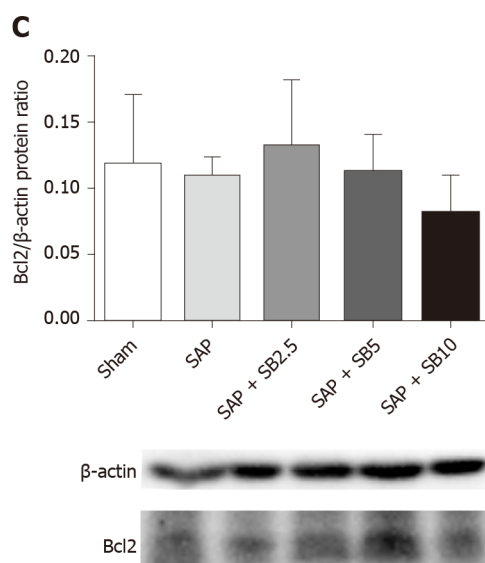
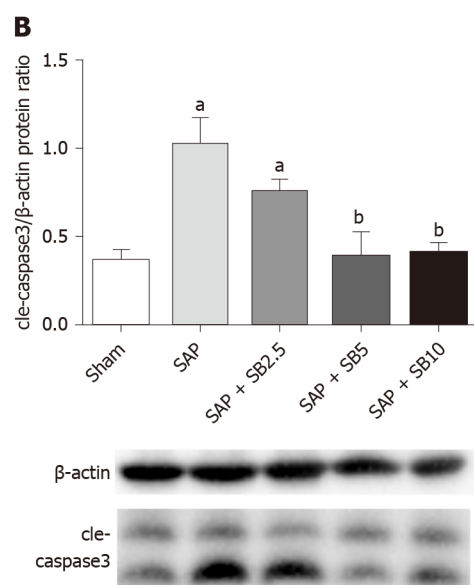
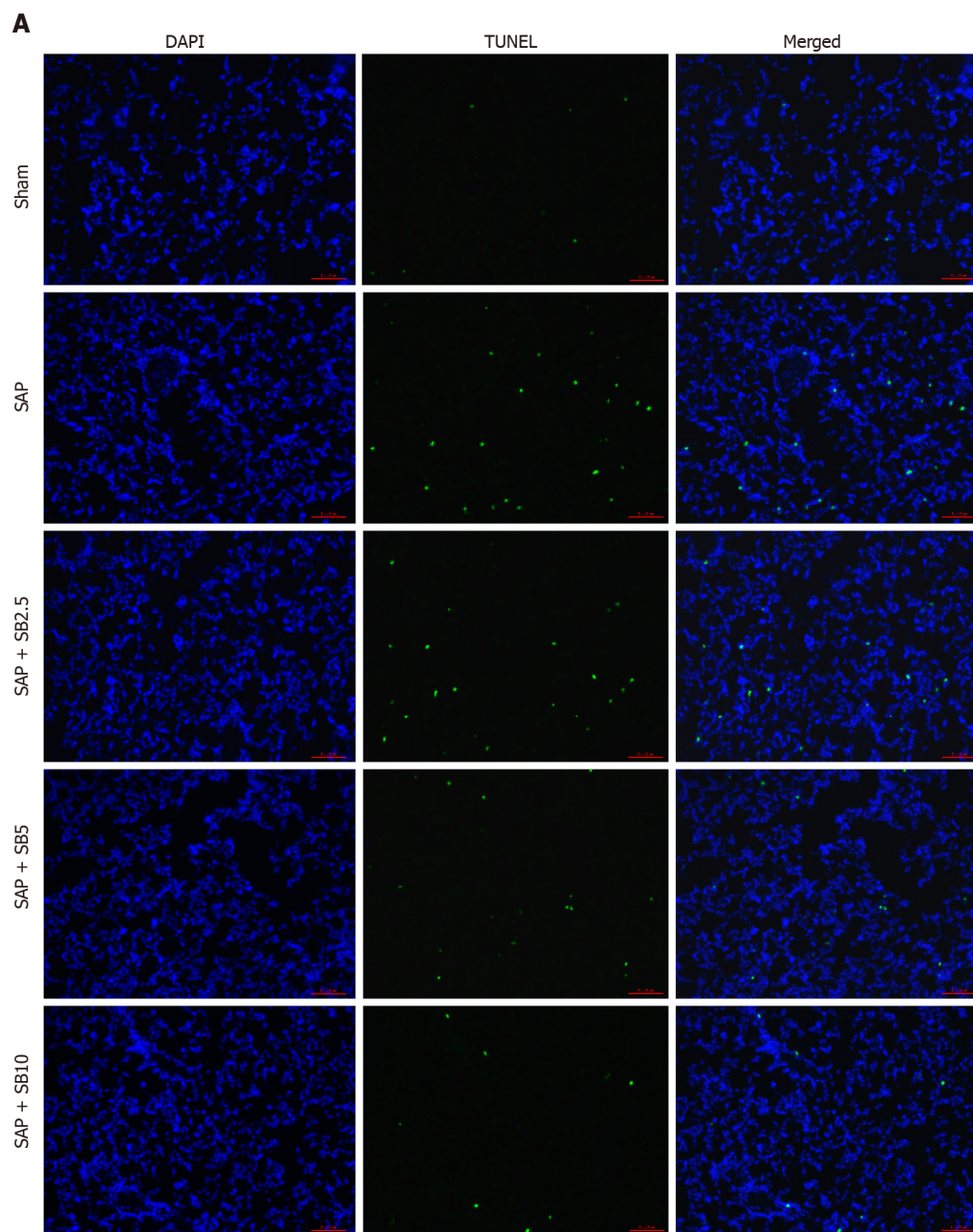


**Figure 5 Effects of SB203580 on pulmonary capillary injury of severe acute pancreatitis rats.** A: Evans blue extravasation in lung tissues; B: Bronchoalveolar protein concentration; C: Representative electron microscope photomicrographs of pulmonary microvascular endothelial cells in lung tissues; Sham group: Magnification 1500 × and 4000 ×, respectively; Severe acute pancreatitis (SAP) group: Magnification 1500 × and 5000 ×, respectively; SAP + SB10 group: Magnification 1500 × and 5000 ×, respectively; White arrows: Dense endothelial cell-cell junctions; White arrowheads: Low electron density clouds with an irregular thickness indicating basal membrane edema; Yellow arrows: Dissolution, rupture and debris of capillary endothelial; Orange star: Red blood cell. Data were expressed as mean ± SE; <sup>a</sup>*P* < 0.05 vs sham group; <sup>b</sup>*P* < 0.05 vs SAP group; <sup>c</sup>*P* < 0.05 vs SAP + SB2.5 group. SAP: Severe acute pancreatitis.

SB203580, no obvious rupture of endothelial cells or red cells extravasating from the vessels were observed.

#### **SB203580 inhibits apoptosis in the lungs of SAP rats**

TUNEL staining was used to examine cell death in lung tissues. Cell apoptosis in the lung tissues was assessed by the colocalization of TUNEL-green and DAPI-blue staining. A prominent increase in the number of positively stained cells was observed in the SAP group compared to the sham group, indicating a higher apoptotic rate (Figure 6A). Treatment of SAP rats with SB203580 significantly decreased the number of apoptotic cells, and the greatest inhibitory effect was observed in rats treated with 10.0 mg/kg SB203580. Proteins regulating the apoptotic signaling pathways were examined using western blotting to further confirm the cell death pathway. As shown in Figure 6B-E, although no change in the antiapoptotic protein Bcl2 was observed, the levels of the proapoptotic proteins Bax, Bim and cle-caspase3 were upregulated in the





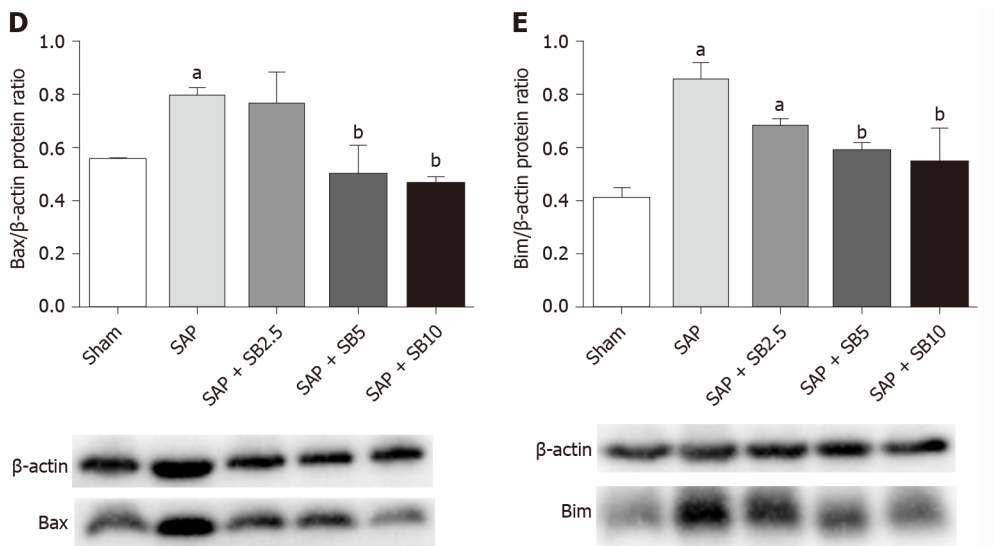


**Figure 6 Effect of SB203580 on apoptosis of lung tissues in severe acute pancreatitis.** A: Representative terminal deoxynucleotidyl transferase-mediated dUTP nick end labeling images of pulmonary sections (200 ×); B: Cle-caspase3; C: Bcl2; D: Bax; E: Bim. B-E: Representative western blotting analysis results for apoptosis-related proteins in lung tissues; Data were expressed as mean ± SE; <sup>a</sup>*P* < 0.05 vs sham group; <sup>b</sup>*P* < 0.05 vs severe acute pancreatitis group. SAP: Severe acute pancreatitis.

SAP group compared to the sham group. SB203580 treatment reversed the changes in the levels of these proteins in the SAP group in a dose-dependent manner.

### **SB203580 protects against ALI by regulating proinflammatory and proapoptotic signaling pathways**

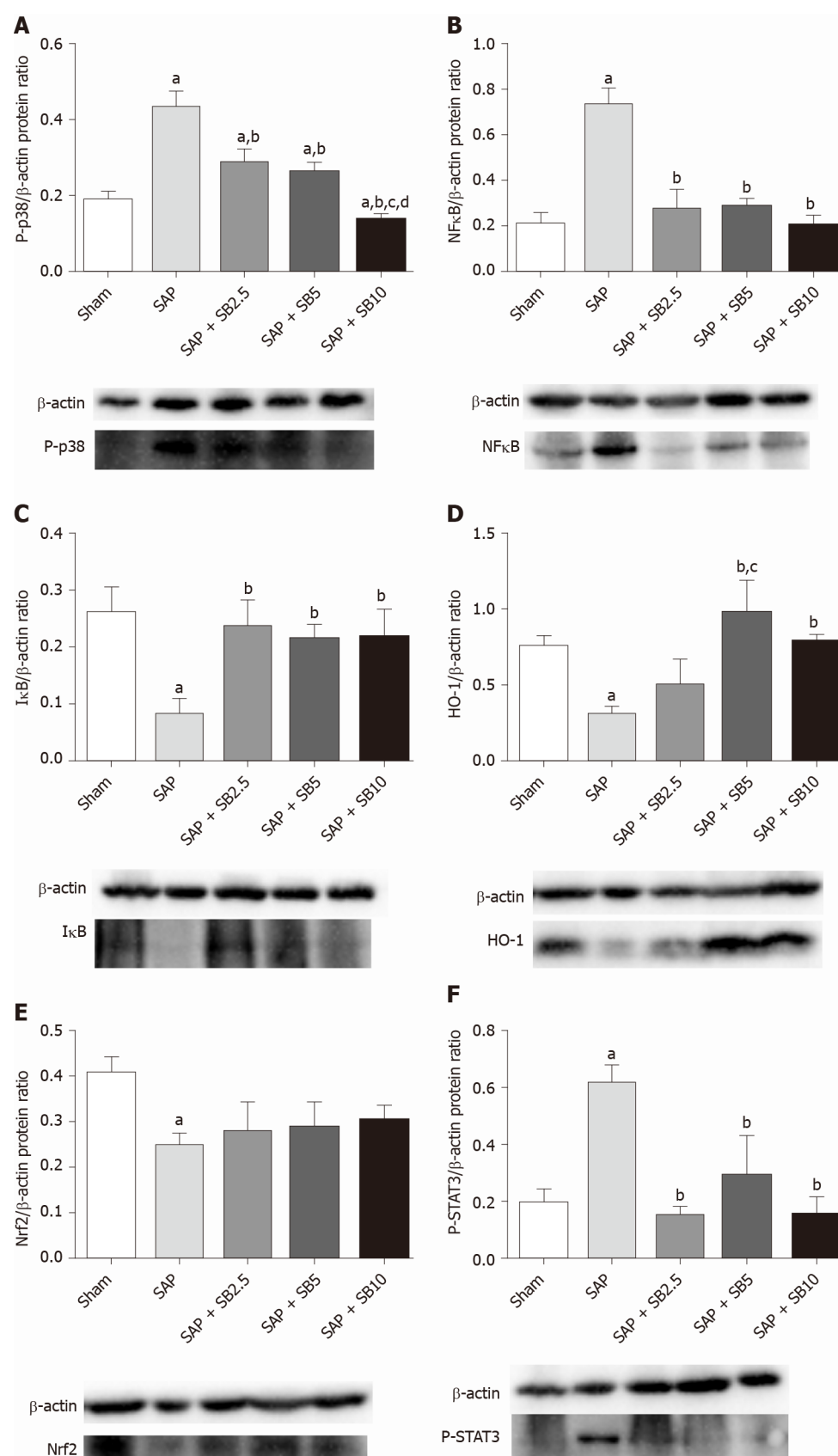
Levels of the P-p38, NFκB, IκB, Nrf2, HO-1, P-SATA3 and Myd88 proteins were detected in the lungs for further evaluation of the protective mechanism of SB203580. Figure 7 showed increased levels of P-p38, NFκB, P-SATA3 and Myd88 but decreased levels of IκB, Nrf2 and HO-1 in the SAP group compared with the sham group. Intriguingly, SB203580 reversed the changes in the levels of these proteins, reducing P-p38, NFκB, P-SATA3 and Myd88 levels but increasing IκB and HO-1 levels compared with the SAP group. However, except for P-p38 and HO-1, the improvement of these parameters was not positively related to the dose of SB203580. In addition, SB203580 slightly increased the level of Nrf2, but the difference was not statistically significant (Figure 7E).

## **DISCUSSION**

Although the mechanisms of ALI/acute respiratory distress syndrome following SAP have not been completely elucidated, an increasing number of studies have described PMVEC injury and dysfunction as prerequisites for ALI[24]. The PMVECs are activated, participate in host defenses and result in increased microvascular permeability and damaged lung function[8,25]. Regardless of the etiology, an exaggerated inflammatory response is widely accepted to play a vital role in the transition of AP into a systemic disease[26]. Various inflammatory mediators have been related to AP severity and they induce their own or other mediators' secretion through a positive feedback mechanism, leading to amplification of the inflammatory cascade[27]. TNF-α was discovered to play a role in the early phase and cause the activation and injury of endothelial cells, functioning as a key promoter of the development of SAP-ALI[28]. In the present study, TNF-α was used to mimic SAP-related PMVEC injury *in vitro*.

p38 is activated by various insults, including cytokines, while the activation of p38 MAPK inevitably induces the expression of proinflammatory cytokines[29]. In our study, TNF-α induced higher levels of inflammatory cytokines (IL-1β and IL-6) in PMVECs with p38 overactivation (Figure 1D and 1E). These results further confirmed a positive role for the p38 MAPK signaling pathway in regulating cytokine expression.

According to previous studies, p38 MAPK is involved in both survival and apoptosis pathways. It promotes anti- or proapoptotic effects in a cell type and





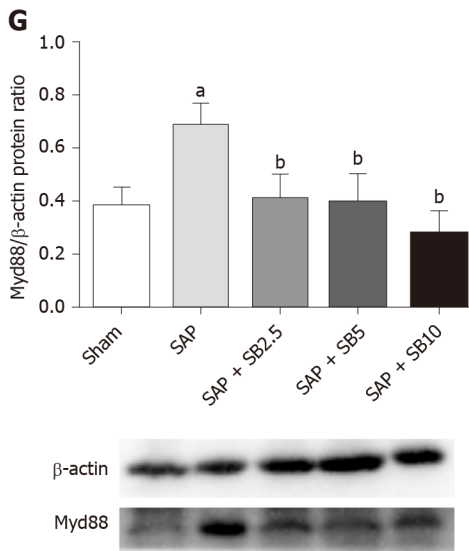


**Figure 7 Effect of SB203580 on proinflammatory and proapoptotic signaling pathways.** Representative Western blotting analysis results for protein expression in pulmonary tissue; A: P-p38; B: NFκB; C: IκB; D: HO-1; E: Nrf2; F: P-STAT3; G: Myd88. Data are expressed as mean ± SE; <sup>a</sup>P < 0.05 vs sham group; <sup>b</sup>P < 0.05 vs severe acute pancreatitis group; <sup>c</sup>P < 0.05 vs severe acute pancreatitis + SB2.5 group; <sup>d</sup>P < 0.05 vs severe acute pancreatitis + SB5 group. Nrf2: Nuclear factor erythroid 2-related factor 2; STAT3: Signal transducer and activator of transcription-3.

stimulus-specific manner in endothelial cells. For example, one group reported that SB203580 inhibited p38 MAPK and then decreased the endothelial cell apoptosis stimulated by TNF-α and cycloheximide[30], while another group illustrated that SB203580 enhanced endothelial cell apoptosis triggered by TNF-α alone[31]. It was reported that endothelial cells are relatively resistant to TNF-α, which induce only modest or no cell damage[31,32]. Then, we chose to overexpress activated MKK 6 (Glu) to constitutively activate p38 MAPK in PMVECs. Flow cytometry analysis revealed apoptotic cell death in null PMVECs stimulated with TNF-α, and MKK 6 (Glu) transfection resulted in a significantly higher apoptotic rate (Figure 1B). This finding indicated that persistent activation of p38 MAPK promotes TNF-α-induced PMVEC apoptosis. However, SB203580 pretreatment conversely aggravated PMVEC injury in this study (data not shown) and did not alleviate cell apoptosis. This discrepancy may be attributed to the extent or duration of p38 MAPK activation[33]. Rapid and transient p38 activation modulates inhibitors of the apoptosis protein family to prevent TNF-α-induced apoptosis[31], while sustained activation leads to apoptosis through the phosphorylation and downregulation of Bcl-x<sub>L</sub>[30]. Therefore, SB203580 may exert a beneficial effect to maintain an appropriate level of p38 MAPK activity.

Many small-molecule inhibitors targeting p38 MAPK, such as SB203850, CNI-1493[34], SB202190[35], RWJ-67657[36] and UM101[37], have been tested in various cell injury or disease models. In AP, the p38 MAPK signaling pathway is involved not only in pancreatic acinar injury[20,38] but also in injury to distant organs (lung, liver, kidney, gut and placenta)[39-43]. SB203850 is a pyridinyl imidazole derivative that competes for ATP binding, and the inhibition of p38 MAPK has been shown to attenuate the severity of AP and its related distant organ injury[14,15,39,44]. In the present study, we treated SAP rats with SB203580 to investigate its protective effect on SAP-associated lung injury and the potential underlying mechanisms. As shown in Figure 2, SB203580 significantly alleviated pancreatic histopathological damage in SAP rats. Furthermore, it alleviated lung histopathological injuries (Figure 3), decreased the levels of inflammatory factors (IL-1β, TNF-α, IL-6 and MPO, Figure 4) and preserved PaO<sub>2</sub>, consistent with previous reports[14,15]. Based on these results, SB203580 effectively decreased the inflammatory response in rats with SAP-ALI. In addition, by analyzing three different doses of SB203580, we observed a dose-dependent improvement in the therapeutic effects, as 10.0 mg/kg was the most effective.

Although apoptosis is regarded as a protective mechanism, excessive apoptosis is harmful to the alveolar capillary membrane and pulmonary function. As the first-line responder to systemic injurious factor insults, damage to endothelial cells is detected earlier than damage to epithelial cells[45]. PMVEC damage results in lung injury, which in turn promotes the secretion of inflammatory mediators to destroy PMVECs in individuals with SAP[46]. In the present study, increased Evans blue extravasation

and BALF protein concentrations revealed increased capillary permeability in SAP rats. Moreover, transmission electron microscopy analysis directly confirmed capillary endothelial dissolution and rupture in the lung (Figure 5). Finally, the results of the TUNEL and western blot analyses (Figure 6) suggested that an increased number of apoptotic cells was involved in the pathological process of SAP-ALI. However, SB203580 significantly reversed the changes in Evans blue accumulation, BALF protein concentration, TUNEL-positive cells, apoptosis-regulated proteins and endothelial microstructure, providing evidence for the underlying protective effects of p38 MAPK inhibitors on endothelial cell apoptosis.

Because p38 MAPK is a proximal initiator of signal transduction, various substrates are directly or indirectly activated by p38 MAPK, permitting it to perform a wide range of functions[29,47]. The biological consequences of p38 MAPK inhibition are complicated by interactions with other signaling pathways. p38 MAPK was reported to have a dual function in regulating Nrf2/HO-1 signaling[48,49]. HO-1 possesses cytoprotective properties, including anti-inflammatory, antioxidant and antiapoptotic activities. NFκB, which is downstream of p38 MAPK, represses Nrf2 transcriptional activity[50,51], while HO-1 inhibits proinflammatory mediators through the inactivation of NFκB[52]. STAT3 is activated by p38 MAPK, transferring signals to the nucleus and regulating gene expression[53,54]. MyD88 is considered a classical proinflammatory and proapoptotic upstream signaling adaptor molecule of p38 MAPK[55]. While the mechanism underlying the effects of SB203580 must be further elucidated, the levels of these key proteins involved in inflammatory, oxidative and apoptotic signaling pathways were measured. In the present study, SB203580 treatment reversed the increased levels of P-p38, NFκB, P-STAT3 and Myd88 and decreased levels of IκB and HO-1 in the SAP group (Figure 7). Therefore, the protective effects of p38 inhibition *via* SB203580 were likely partially attributed to the inhibition of pulmonary proinflammatory and proapoptotic signaling pathways.

## CONCLUSION

In conclusion, p38 MAPK overactivation promoted TNF-α-induced inflammatory cytokine expression and PMVEC apoptosis *in vitro*. The inhibition of p38 MAPK with SB203580 protected against SAP-ALI by alleviating inflammation and apoptotic cell death in rats. Therefore, SB203580 may alleviate SAP-ALI by inhibiting the proinflammatory and proapoptotic effects of the p38 MAPK pathway on PMVECs. These results suggest the possibility of applying p38 MAPK inhibitors as treatments for SAP-ALI in the clinical setting.

## ARTICLE HIGHLIGHTS

### Research background

Acute lung injury (ALI) is the main reason for the high mortality of patients with severe acute pancreatitis (SAP). Injury and dysfunction of pulmonary microvascular endothelial cells (PMVEC) are considered prerequisites for ALI. The p38 mitogen-activated protein kinase (p38 MAPK) signaling pathway is involved in the development of SAP-related ALI. However, the precise mechanism by which p38 MAPK regulates PMVEC injury in SAP-related ALI is unclear.

### Research motivation

To date, no specific pharmacological therapies for SAP associated ALI are available. Elucidating the mechanism of PMVEC injury regulated by p38 MAPK is expected to help identify new treatments for SAP-associated ALI.

### Research objectives

To determine the role of p38 MAPK in the tumor necrosis factor-α-induced injury of PMVECs *in vitro* and to explore the effect of SB203580-mediated p38 inhibition on SAP-ALI *in vivo*.

### Research methods

*In vitro*, PMVECs were transfected with MAPK kinase 6 (Glu) and stimulated with tumor necrosis factor-α to detect cell apoptosis and inflammatory cytokine levels.

*In vivo*, SAP-ALI rats were treated with three different doses of SB203580 (2.5, 5.0 or 10.0 mg/kg). Blood, bronchoalveolar lavage fluid and tissue samples were harvested to assess cytokine levels, blood gas analyses, histopathological changes, myeloperoxidase activity, bronchoalveolar protein concentration, Evans blue extravasation, apoptosis and ultrastructural changes of PMVECs. Then, the mechanism underlying the effects of SB203580 was also detected in the lungs.

### Research results

*In vitro*, MAPK kinase (Glu) transfection resulted in higher apoptotic rates and cytokine levels in TNF- $\alpha$ -treated PMVECs. *In vivo*, SB203580 attenuated lung histopathological injury, decreased inflammatory activity and preserved pulmonary function. Furthermore, SB203580 significantly reversed the microvascular permeability, the increase in the number of terminal deoxynucleotidyl transferase-mediated dUTP nick end labeling-positive cells, the increased expression of apoptosis-related proteins and the endothelial microstructure changes. Moreover, SB203580 significantly reduced pulmonary P-p38, NF $\kappa$ B, P-SATA3 and Myd88 levels but increased the I $\kappa$ B and HO-1 levels.

### Research conclusions

p38 inhibition may protect against SAP-ALI by alleviating inflammation and the apoptotic death of PMVECs.

### Research perspectives

In this study, p38 MAPK overactivation promoted PMVEC injury *in vitro*, while p38 inhibition protected against SAP-ALI *in vivo*. These results suggest the potential of applying p38 MAPK inhibitors as treatments for SAP-ALI in the clinical setting.

## REFERENCES

- 1 Forsmark CE, Vege SS, Wilcox CM. Acute Pancreatitis. *N Engl J Med* 2016; **375**: 1972-1981 [PMID: 27959604 DOI: 10.1056/NEJMr1505202]
- 2 Banks PA, Bollen TL, Dervenis C, Gooszen HG, Johnson CD, Sarr MG, Tsiotos GG, Vege SS; Acute Pancreatitis Classification Working Group. Classification of acute pancreatitis--2012: revision of the Atlanta classification and definitions by international consensus. *Gut* 2013; **62**: 102-111 [PMID: 23100216 DOI: 10.1136/gutjnl-2012-302779]
- 3 Elder AS, Saccone GT, Dixon DL. Lung injury in acute pancreatitis: mechanisms underlying augmented secondary injury. *Pancreatology* 2012; **12**: 49-56 [PMID: 22487475 DOI: 10.1016/j.pan.2011.12.012]
- 4 De Campos T, Deree J, Coimbra R. From acute pancreatitis to end-organ injury: mechanisms of acute lung injury. *Surg Infect (Larchmt)* 2007; **8**: 107-120 [PMID: 17381402 DOI: 10.1089/sur.2006.011]
- 5 Matthay MA, Zemans RL. The acute respiratory distress syndrome: pathogenesis and treatment. *Annu Rev Pathol* 2011; **6**: 147-163 [PMID: 20936936 DOI: 10.1146/annurev-pathol-011110-130158]
- 6 Aldridge AJ. Role of the neutrophil in septic shock and the adult respiratory distress syndrome. *Eur J Surg* 2002; **168**: 204-214 [PMID: 12440757 DOI: 10.1080/11024150260102807]
- 7 Fang M, Zhong WH, Song WL, Deng YY, Yang DM, Xiong B, Zeng HK, Wang HD. Ulinastatin Ameliorates Pulmonary Capillary Endothelial Permeability Induced by Sepsis Through Protection of Tight Junctions via Inhibition of TNF- $\alpha$  and Related Pathways. *Front Pharmacol* 2018; **9**: 823 [PMID: 30150933 DOI: 10.3389/fphar.2018.00823]
- 8 Maniatis NA, Kotanidou A, Catravas JD, Orfanos SE. Endothelial pathomechanisms in acute lung injury. *Vascul Pharmacol* 2008; **49**: 119-133 [PMID: 18722553 DOI: 10.1016/j.vph.2008.06.009]
- 9 Lum H, Malik AB. Mechanisms of increased endothelial permeability. *Can J Physiol Pharmacol* 1996; **74**: 787-800 [PMID: 8946065 DOI: 10.1139/y96-081]
- 10 Suzuki T, Sakata K, Mizuno N, Palikhe S, Yamashita S, Hattori K, Matsuda N, Hattori Y. Different involvement of the MAPK family in inflammatory regulation in human pulmonary microvascular endothelial cells stimulated with LPS and IFN- $\gamma$ . *Immunobiology* 2018; **223**: 777-785 [PMID: 30115376 DOI: 10.1016/j.imbio.2018.08.003]
- 11 Maniatis NA, Orfanos SE. The endothelium in acute lung injury/acute respiratory distress syndrome. *Curr Opin Crit Care* 2008; **14**: 22-30 [PMID: 18195622 DOI: 10.1097/MCC.0b013e3282f269b9]
- 12 Yang Y, Li Q, Deng Z, Zhang Z, Xu J, Qian G, Wang G. Protection from lipopolysaccharide-induced pulmonary microvascular endothelial cell injury by activation of hedgehog signaling pathway. *Mol Biol Rep* 2011; **38**: 3615-3622 [PMID: 21110116 DOI: 10.1007/s11033-010-0473-8]
- 13 de Campos T, Deree J, Martins JO, Loomis WH, Shenvi E, Putnam JG, Coimbra R. Pentoxifylline attenuates pulmonary inflammation and neutrophil activation in experimental acute pancreatitis. *Pancreas* 2008; **37**: 42-49 [PMID: 18580443 DOI: 10.1097/MPA.0b013e3181612d19]

- 14 **Zhou Y**, Xia H, Zhao L, Mei F, Li M, You Y, Zhao K, Wang W. SB203580 attenuates acute lung injury and inflammation in rats with acute pancreatitis in pregnancy. *Inflammopharmacology* 2019; **27**: 99-107 [PMID: 30094758 DOI: 10.1007/s10787-018-0522-9]
- 15 **Cao MH**, Xu J, Cai HD, Lv ZW, Feng YJ, Li K, Chen CQ, Li YY. p38 MAPK inhibition alleviates experimental acute pancreatitis in mice. *Hepatobiliary Pancreat Dis Int* 2015; **14**: 101-106 [PMID: 25655298 DOI: 10.1016/s1499-3872(15)60327-7]
- 16 **Yang J**, Denham W, Tracey KJ, Wang H, Kramer AA, Salhab KF, Norman J. The physiologic consequences of macrophage pacification during severe acute pancreatitis. *Shock* 1998; **10**: 169-175 [PMID: 9744644 DOI: 10.1097/00024382-199809000-00004]
- 17 **King J**, Hamil T, Creighton J, Wu S, Bhat P, McDonald F, Stevens T. Structural and functional characteristics of lung macro- and microvascular endothelial cell phenotypes. *Microvasc Res* 2004; **67**: 139-151 [PMID: 15020205 DOI: 10.1016/j.mvr.2003.11.006]
- 18 **Li L**, Hu J, He T, Zhang Q, Yang X, Lan X, Zhang D, Mei H, Chen B, Huang Y. P38/MAPK contributes to endothelial barrier dysfunction via MAP4 phosphorylation-dependent microtubule disassembly in inflammation-induced acute lung injury. *Sci Rep* 2015; **5**: 8895 [PMID: 25746230 DOI: 10.1038/srep08895]
- 19 **Hu JY**, Chu ZG, Han J, Dang YM, Yan H, Zhang Q, Liang GP, Huang YS. The p38/MAPK pathway regulates microtubule polymerization through phosphorylation of MAP4 and Op18 in hypoxic cells. *Cell Mol Life Sci* 2010; **67**: 321-333 [PMID: 19915797 DOI: 10.1007/s00018-009-0187-z]
- 20 **Ren HB**, Li ZS, Xu GM, Tu ZX, Shi XG, Jia YT, Gong YF. Dynamic changes of mitogen-activated protein kinase signal transduction in rats with severe acute pancreatitis. *Chin J Dig Dis* 2004; **5**: 123-125 [PMID: 15612248 DOI: 10.1111/j.1443-9573.2004.00162.x]
- 21 **Zemans RL**, Colgan SP, Downey GP. Transepithelial migration of neutrophils: mechanisms and implications for acute lung injury. *Am J Respir Cell Mol Biol* 2009; **40**: 519-535 [PMID: 18978300 DOI: 10.1165/rcmb.2008-0348TR]
- 22 **Schmidt J**, Rattner DW, Lewandrowski K, Compton CC, Mandavilli U, Knoefel WT, Warshaw AL. A better model of acute pancreatitis for evaluating therapy. *Ann Surg* 1992; **215**: 44-56 [PMID: 1731649 DOI: 10.1097/00000658-199201000-00007]
- 23 **Dawra R**, Ku YS, Sharif R, Dhaulakhandi D, Phillips P, Dudeja V, Saluja AK. An improved method for extracting myeloperoxidase and determining its activity in the pancreas and lungs during pancreatitis. *Pancreas* 2008; **37**: 62-68 [PMID: 18580446 DOI: 10.1097/MPA.0b013e3181607761]
- 24 **Ye W**, Zheng C, Yu D, Zhang F, Pan R, Ni X, Shi Z, Zhang Z, Xiang Y, Sun H, Shi K, Chen B, Zhang Q, Zhou M. Lipoxin A4 Ameliorates Acute Pancreatitis-Associated Acute Lung Injury through the Antioxidative and Anti-Inflammatory Effects of the Nrf2 Pathway. *Oxid Med Cell Longev* 2019; **2019**: 2197017 [PMID: 31781326 DOI: 10.1155/2019/2197017]
- 25 **Yi L**, Huang X, Guo F, Zhou Z, Chang M, Huan J. GSK-3 $\beta$ -Dependent Activation of GEF-H1/ROCK Signaling Promotes LPS-Induced Lung Vascular Endothelial Barrier Dysfunction and Acute Lung Injury. *Front Cell Infect Microbiol* 2017; **7**: 357 [PMID: 28824887 DOI: 10.3389/fcimb.2017.00357]
- 26 **Yang X**, Zhang X, Lin Z, Guo J, Yang X, Yao L, Wang H, Xue P, Xia Q. Chaiqin chengqi decoction alleviates severe acute pancreatitis associated acute kidney injury by inhibiting endoplasmic reticulum stress and subsequent apoptosis. *Biomed Pharmacother* 2020; **125**: 110024 [PMID: 32187959 DOI: 10.1016/j.biopha.2020.110024]
- 27 **Sandoval J**, Pereda J, Pérez S, Finamor I, Vallet-Sánchez A, Rodríguez JL, Franco L, Sastre J, López-Rodas G. Epigenetic Regulation of Early- and Late-Response Genes in Acute Pancreatitis. *J Immunol* 2016; **197**: 4137-4150 [PMID: 27798150 DOI: 10.4049/jimmunol.1502378]
- 28 **Yu S**, Xie J, Xiang Y, Dai S, Yu D, Sun H, Chen B, Zhou M. Downregulation of TNF- $\alpha$ /TNF-R1 Signals by AT-Lipoxin A4 May Be a Significant Mechanism of Attenuation in SAP-Associated Lung Injury. *Mediators Inflamm* 2019; **2019**: 9019404 [PMID: 31097921 DOI: 10.1155/2019/9019404]
- 29 **Viemann D**, Goebeler M, Schmid S, Klimmek K, Sorg C, Ludwig S, Roth J. Transcriptional profiling of IKK2/NF-kappa B- and p38 MAP kinase-dependent gene expression in TNF-alpha-stimulated primary human endothelial cells. *Blood* 2004; **103**: 3365-3373 [PMID: 14715628 DOI: 10.1182/blood-2003-09-3296]
- 30 **Grethe S**, Ares MP, Andersson T, Pörn-Ares ML. p38 MAPK mediates TNF-induced apoptosis in endothelial cells via phosphorylation and downregulation of Bcl-x(L). *Exp Cell Res* 2004; **298**: 632-642 [PMID: 15265709 DOI: 10.1016/j.yexcr.2004.05.007]
- 31 **Furusu A**, Nakayama K, Xu Q, Konta T, Kitamura M. MAP kinase-dependent, NF-kappaB-independent regulation of inhibitor of apoptosis protein genes by TNF-alpha. *J Cell Physiol* 2007; **210**: 703-710 [PMID: 17133355 DOI: 10.1002/jcp.20881]
- 32 **Roulston A**, Reinhard C, Amiri P, Williams LT. Early activation of c-Jun N-terminal kinase and p38 kinase regulate cell survival in response to tumor necrosis factor alpha. *J Biol Chem* 1998; **273**: 10232-10239 [PMID: 9553074 DOI: 10.1074/jbc.273.17.10232]
- 33 **Matsuzawa A**, Ichijo H. Stress-responsive protein kinases in redox-regulated apoptosis signaling. *Antioxid Redox Signal* 2005; **7**: 472-481 [PMID: 15706095 DOI: 10.1089/ars.2005.7.472]
- 34 **Yang J**, Murphy C, Denham W, Botchkina G, Tracey KJ, Norman J. Evidence of a central role for p38 map kinase induction of tumor necrosis factor alpha in pancreatitis-associated pulmonary injury. *Surgery* 1999; **126**: 216-222 [PMID: 10455887]
- 35 **Lüschen S**, Scherer G, Ussat S, Ungefroren H, Adam-Klages S. Inhibition of p38 mitogen-activated protein kinase reduces TNF-induced activation of NF-kappaB, elicits caspase activity, and enhances



- cytotoxicity. *Exp Cell Res* 2004; **293**: 196-206 [PMID: [14729457](#) DOI: [10.1016/j.yexcr.2003.10.009](#)]
- 36 **Kuldo JM**, Westra J, Asgeirsdóttir SA, Kok RJ, Oosterhuis K, Rots MG, Schouten JP, Limburg PC, Molema G. Differential effects of NF- $\kappa$ B and p38 MAPK inhibitors and combinations thereof on TNF- $\alpha$ - and IL-1 $\beta$ -induced proinflammatory status of endothelial cells in vitro. *Am J Physiol Cell Physiol* 2005; **289**: C1229-C1239 [PMID: [15972838](#) DOI: [10.1152/ajpcell.00620.2004](#)]
  - 37 **Shah NG**, Tulapurkar ME, Ramarathnam A, Brophy A, Martinez R 3rd, Hom K, Hodges T, Samadani R, Singh IS, MacKerell AD Jr, Shapiro P, Hasday JD. Novel Noncatalytic Substrate-Selective p38 $\alpha$ -Specific MAPK Inhibitors with Endothelial-Stabilizing and Anti-Inflammatory Activity. *J Immunol* 2017; **198**: 3296-3306 [PMID: [28298524](#) DOI: [10.4049/jimmunol.1602059](#)]
  - 38 **Twait E**, Williard DE, Samuel I. Dominant negative p38 mitogen-activated protein kinase expression inhibits NF- $\kappa$ B activation in AR42J cells. *Pancreatology* 2010; **10**: 119-128 [PMID: [20453549](#) DOI: [10.1159/000290656](#)]
  - 39 **Ouyang J**, Zhang ZH, Zhou YX, Niu WC, Zhou F, Shen CB, Chen RG, Li X. Up-regulation of Tight-Junction Proteins by p38 Mitogen-Activated Protein Kinase/p53 Inhibition Leads to a Reduction of Injury to the Intestinal Mucosal Barrier in Severe Acute Pancreatitis. *Pancreas* 2016; **45**: 1136-1144 [PMID: [27171513](#) DOI: [10.1097/MPA.0000000000000656](#)]
  - 40 **Fan HN**, Chen W, Fan LN, Wu JT, Zhu JS, Zhang J. Macrophages-derived p38 $\alpha$  promotes the experimental severe acute pancreatitis by regulating inflammation and autophagy. *Int Immunopharmacol* 2019; **77**: 105940 [PMID: [31655340](#) DOI: [10.1016/j.intimp.2019.105940](#)]
  - 41 **Wang B**, Zhao KL, Hu WJ, Zuo T, Ding YM, Wang WX. Macrophage Migration Inhibitor Promoted the Intrahepatic Bile Duct Injury in Rats with Severe Acute Pancreatitis. *Dig Dis Sci* 2019; **64**: 759-772 [PMID: [30465176](#) DOI: [10.1007/s10620-018-5379-7](#)]
  - 42 **Li M**, Yu J, Zhao L, Mei FC, Zhou Y, Hong YP, Zuo T, Wang WX. Inhibition of macrophage migration inhibitory factor attenuates inflammation and fetal kidney injury in a rat model of acute pancreatitis in pregnancy. *Int Immunopharmacol* 2019; **68**: 106-114 [PMID: [30622028](#) DOI: [10.1016/j.intimp.2018.12.068](#)]
  - 43 **Zuo T**, Yu J, Wang WX, Zhao KL, Chen C, Deng WH, He XB, Wang P, Shi Q, Guo WY. Mitogen-Activated Protein Kinases Are Activated in Placental Injury in Rat Model of Acute Pancreatitis in Pregnancy. *Pancreas* 2016; **45**: 850-857 [PMID: [26491907](#) DOI: [10.1097/MPA.0000000000000528](#)]
  - 44 **Wan YD**, Zhu RX, Bian ZZ, Pan XT. Improvement of Gut Microbiota by Inhibition of P38 Mitogen-Activated Protein Kinase (MAPK) Signaling Pathway in Rats with Severe Acute Pancreatitis. *Med Sci Monit* 2019; **25**: 4609-4616 [PMID: [31226101](#) DOI: [10.12659/MSM.914538](#)]
  - 45 **Wang F**, Lu F, Huang H, Huang M, Luo T. Ultrastructural changes in the pulmonary mechanical barriers in a rat model of severe acute pancreatitis-associated acute lung injury. *Ultrastruct Pathol* 2016; **40**: 33-42 [PMID: [26512751](#) DOI: [10.3109/01913123.2015.1088907](#)]
  - 46 **Han X**, Wang Y, Chen H, Zhang J, Xu C, Li J, Li M. Enhancement of ICAM-1 via the JAK2/STAT3 signaling pathway in a rat model of severe acute pancreatitis-associated lung injury. *Exp Ther Med* 2016; **11**: 788-796 [PMID: [26997994](#) DOI: [10.3892/etm.2016.2988](#)]
  - 47 **Hoefen RJ**, Berk BC. The role of MAP kinases in endothelial activation. *Vascul Pharmacol* 2002; **38**: 271-273 [PMID: [12487031](#) DOI: [10.1016/s1537-1891\(02\)00251-3](#)]
  - 48 **Naidu S**, Vijayan V, Santoso S, Kietzmann T, Immenschuh S. Inhibition and genetic deficiency of p38 MAPK up-regulates heme oxygenase-1 gene expression via Nrf2. *J Immunol* 2009; **182**: 7048-7057 [PMID: [19454702](#) DOI: [10.4049/jimmunol.0900006](#)]
  - 49 **Zhou MM**, Zhang WY, Li RJ, Guo C, Wei SS, Tian XM, Luo J, Kong LY. Anti-inflammatory activity of Khayandirobilide A from *Khaya senegalensis* via NF- $\kappa$ B, AP-1 and p38 MAPK/Nrf2/HO-1 signaling pathways in lipopolysaccharide-stimulated RAW 264.7 and BV-2 cells. *Phytomedicine* 2018; **42**: 152-163 [PMID: [29655681](#) DOI: [10.1016/j.phymed.2018.03.016](#)]
  - 50 **Reboll MR**, Schweda AT, Bartels M, Franke R, Frank R, Nourbakhsh M. Mapping of NRF binding motifs of NF- $\kappa$ B p65 subunit. *J Biochem* 2011; **150**: 553-562 [PMID: [21821668](#) DOI: [10.1093/jb/mvr099](#)]
  - 51 **Niedick I**, Froese N, Oumard A, Mueller PP, Nourbakhsh M, Hauser H, Köster M. Nucleolar localization and mobility analysis of the NF- $\kappa$ B repressing factor NRF. *J Cell Sci* 2004; **117**: 3447-3458 [PMID: [15226370](#) DOI: [10.1242/jcs.01129](#)]
  - 52 **Ha YM**, Kim MY, Park MK, Lee YS, Kim YM, Kim HJ, Lee JH, Chang KC. Higenamine reduces HMGB1 during hypoxia-induced brain injury by induction of heme oxygenase-1 through PI3K/Akt/Nrf-2 signal pathways. *Apoptosis* 2012; **17**: 463-474 [PMID: [22183510](#) DOI: [10.1007/s10495-011-0688-8](#)]
  - 53 **Stephanou A**, Latchman DS. Opposing actions of STAT-1 and STAT-3. *Growth Factors* 2005; **23**: 177-182 [PMID: [16243709](#) DOI: [10.1080/08977190500178745](#)]
  - 54 **Ng DC**, Long CS, Bogoyevitch MA. A role for the extracellular signal-regulated kinase and p38 mitogen-activated protein kinases in interleukin-1  $\beta$ -stimulated delayed signal transducer and activator of transcription 3 activation, atrial natriuretic factor expression, and cardiac myocyte morphology. *J Biol Chem* 2001; **276**: 29490-29498 [PMID: [11382751](#) DOI: [10.1074/jbc.M100699200](#)]
  - 55 **Shih JH**, Tsai YF, Li IH, Chen MH, Huang YS. Hp-s1 Ganglioside Suppresses Proinflammatory Responses by Inhibiting MyD88-Dependent NF- $\kappa$ B and JNK/p38 MAPK Pathways in Lipopolysaccharide-Stimulated Microglial Cells. *Mar Drugs* 2020; **18** [PMID: [33003399](#) DOI: [10.3390/md18100496](#)]





## Basic Study

# Partially hydrolyzed guar gum attenuates non-alcoholic fatty liver disease in mice through the gut-liver axis

Shun Takayama, Kazuhiro Katada, Tomohisa Takagi, Takaya Iida, Tomohiro Ueda, Katsura Mizushima, Yasuki Higashimura, Mayuko Morita, Tetsuya Okayama, Kazuhiro Kamada, Kazuhiko Uchiyama, Osamu Handa, Takeshi Ishikawa, Zenta Yasukawa, Tsutomu Okubo, Yoshito Itoh, Yuji Naito

**ORCID number:** Shun Takayama 0000-0001-7040-8632; Kazuhiro Katada 0000-0002-9629-9507; Tomohisa Takagi 0000-0002-6119-4828; Takaya Iida 0000-0002-0754-1067; Tomohiro Ueda 0000-0002-3017-4912; Katsura Mizushima 0000-0001-5481-7022; Yasuki Higashimura 0000-0003-0540-4306; Mayuko Morita 0000-0002-7968-8156; Tetsuya Okayama 0000-0001-5171-4079; Kazuhiro Kamada 0000-0001-5144-6625; Kazuhiko Uchiyama 0000-0001-5210-167X; Osamu Handa 0000-0003-2228-0405; Takeshi Ishikawa 0000-0002-5770-9710; Zenta Yasukawa 0000-0003-2219-9009; Tsutomu Okubo 0000-0003-0822-5442; Yoshito Itoh 0000-0001-9890-3635; Yuji Naito 0000-0001-5443-788X.

**Author contributions:** Takayama S performed the research, analyzed the data, and wrote the manuscript; Katada K designed the research study, and wrote the manuscript; Higashimura Y performed the biostatistical analysis, and critically reviewed the manuscript; Takagi T, Iida T, Ueda T, Mizushima K, Morita M, Okayama T, Kamada K, Uchiyama K, Handa O, Ishikawa T, Yasukawa Z, Okubo T, Itoh Y, and Naito Y contributed to data collection and interpretation, and critically reviewed the manuscript;

Shun Takayama, Kazuhiro Katada, Tomohisa Takagi, Takaya Iida, Tomohiro Ueda, Katsura Mizushima, Tetsuya Okayama, Kazuhiro Kamada, Kazuhiko Uchiyama, Takeshi Ishikawa, Yoshito Itoh, Yuji Naito, Department of Molecular Gastroenterology and Hepatology, Graduate School of Medical Science, Kyoto Prefectural University of Medicine, Kyoto 602-8566, Japan

Tomohisa Takagi, Department of Medical Innovation and Translational Medical Science, Graduate School of Medical Science, Kyoto Prefectural University of Medicine, Kyoto 602-8566, Japan

Yasuki Higashimura, Department of Food Science, Ishikawa Prefectural University, Nonoichi 921-8836, Japan

Mayuko Morita, Department of Health Care Nutrition, Showa Gakuin Junior College, Ichikawa 272-0823, Japan

Osamu Handa, Division of Gastroenterology, Department of Internal Medicine, Kawasaki Medical School, Kurashiki 701-0192, Japan

Zenta Yasukawa, Tsutomu Okubo, Department of Nutrition, Taiyo Kagaku Co. Ltd, Yokkaichi 510-0844, Japan

**Corresponding author:** Kazuhiro Katada, MD, PhD, Assistant Professor, Department of Molecular Gastroenterology and Hepatology, Graduate School of Medical Science, Kyoto Prefectural University of Medicine, 465 Kajii-cho, Kawaramachi-Hirokoji, Kamigyo-ku, Kyoto 602-8566, Japan. [katada@koto.kpu-m.ac.jp](mailto:katada@koto.kpu-m.ac.jp)

## Abstract

### BACKGROUND

The gut-liver axis has attracted much interest in the context of chronic liver disease pathogenesis. Prebiotics such as dietary fibers were shown to attenuate non-alcoholic fatty liver disease (NAFLD) by modulating gut microbiota. Partially hydrolyzed guar gum (PHGG), a water-soluble dietary fiber, has been reported to alleviate the symptoms of various intestinal diseases and metabolic syndromes. However, its effects on NAFLD remain to be fully elucidated.

### AIM

all authors approved the final version of the manuscript, and agree to be accountable for all aspects of the work in ensuring that questions related to the accuracy or integrity of any part of the work are appropriately investigated and resolved.

**Supported by** Scientific Research (KAKENHI) (C), No. 25460958; Japan Society for the Promotion of Science, No. 20K11513; and Adaptable and Seamless Technology Transfer Program through target driven R&D from the Japan Agency for Medical Research and Development.

#### **Institutional review board**

**statement:** At our institution, the attached "Institutional Animal Care and Use Committee Approval Form" also serves as the Institutional Review Board Approval Form. The study was reviewed and approved by the Institutional Review Board at Kyoto Prefectural University of Medicine.

#### **Institutional animal care and use**

**committee statement:** All procedures involving animal subject is approved by the Animal Care Committee of the Kyoto Prefectural University of Medicine, Kyoto, Japan, No. M2020-126.

**Conflict-of-interest statement:** All authors have nothing to disclose.

**Data sharing statement:** No additional data are available.

**ARRIVE guidelines statement:** The authors have read the ARRIVE guidelines, and the manuscript was prepared and revised according to the ARRIVE guidelines.

**Open-Access:** This article is an open-access article that was selected by an in-house editor and fully peer-reviewed by external reviewers. It is distributed in accordance with the Creative Commons Attribution NonCommercial (CC BY-NC 4.0) license, which permits others to distribute, remix, adapt, build

To determine whether treatment with PHGG attenuates NAFLD development in mice through the gut-liver axis.

## **METHODS**

Seven-week-old male C57BL/6J mice with increased intestinal permeability were fed a control or atherogenic (Ath) diet (a mouse model of NAFLD) for 8 wk, with or without 5% PHGG. Increased intestinal permeability was induced through chronic intermittent administration of low-dose dextran sulfate sodium. Body weight, liver weight, macroscopic findings in the liver, blood biochemistry [aspartate aminotransferase (AST) and alanine aminotransferase (ALT), total cholesterol, triglyceride, free fatty acids, and glucose levels], liver histology, myeloperoxidase activity in liver tissue, mRNA expression in the liver and intestine, serum endotoxin levels in the portal vein, intestinal permeability, and microbiota and short-chain fatty acid (SCFA) profiles in the cecal samples were investigated.

## **RESULTS**

Mice with increased intestinal permeability subjected to the Ath diet showed significantly increased serum AST and ALT levels, liver fat accumulation, liver inflammatory (tumor necrosis factor- $\alpha$  and monocyte chemoattractant protein-1) and fibrogenic (collagen 1 $\alpha$ 1 and  $\alpha$  smooth muscle actin) marker levels, and liver myeloperoxidase activity, which were significantly attenuated by PHGG treatment. Furthermore, the Ath diet combined with increased intestinal permeability resulted in elevated portal endotoxin levels and activated toll-like receptor (TLR) 4 and TLR9 expression, confirming that intestinal permeability was significantly elevated, as observed by evaluating the lumen-to-blood clearance of fluorescein isothiocyanate-conjugated dextran. PHGG treatment did not affect fatty acid metabolism in the liver. However, it decreased lipopolysaccharide signaling through the gut-liver axis. In addition, it significantly increased the abundance of cecal *Bacteroides* and *Clostridium* subcluster XIVa. Treatment with PHGG markedly increased the levels of SCFAs, particularly, butyric acid, acetic acid, propionic acid, and formic acid, in the cecal samples.

## **CONCLUSION**

PHGG partially prevented NAFLD development in mice through the gut-liver axis by modulating microbiota and downstream SCFA profiles.

**Key Words:** Non-alcoholic fatty liver disease; Partially hydrolyzed guar gum; Gut-liver axis; Intestinal barrier integrity; Microbiota; Short-chain fatty acids

©The Author(s) 2021. Published by Baishideng Publishing Group Inc. All rights reserved.

**Core Tip:** The gut-liver axis has attracted much interest in the context of chronic liver disease pathogenesis, including non-alcoholic fatty liver disease (NAFLD). Here, by using a mouse model of NAFLD induced by an atherogenic diet combined with increased intestinal permeability, we report that partially hydrolyzed guar gum (PHGG), a water-soluble dietary fiber, prevented NAFLD development in mice partially through the gut-liver axis by modulating the microbiota and downstream short-chain fatty acid profiles, highlighting that treatment with PHGG might show great promise as a therapeutic strategy for NAFLD.

**Citation:** Takayama S, Katada K, Takagi T, Iida T, Ueda T, Mizushima K, Higashimura Y, Morita M, Okayama T, Kamada K, Uchiyama K, Handa O, Ishikawa T, Yasukawa Z, Okubo T, Itoh Y, Naito Y. Partially hydrolyzed guar gum attenuates non-alcoholic fatty liver disease in mice through the gut-liver axis. *World J Gastroenterol* 2021; 27(18): 2160-2176

**URL:** <https://www.wjgnet.com/1007-9327/full/v27/i18/2160.htm>

**DOI:** <https://dx.doi.org/10.3748/wjg.v27.i18.2160>

upon this work non-commercially, and license their derivative works on different terms, provided the original work is properly cited and the use is non-commercial. See: <http://creativecommons.org/licenses/by-nc/4.0/>

**Manuscript source:** Unsolicited manuscript

**Specialty type:** Gastroenterology and hepatology

**Country/Territory of origin:** Japan

**Peer-review report's scientific quality classification**

Grade A (Excellent): 0  
Grade B (Very good): 0  
Grade C (Good): C, C  
Grade D (Fair): 0  
Grade E (Poor): 0

**Received:** February 6, 2021

**Peer-review started:** February 6, 2021

**First decision:** February 27, 2021

**Revised:** March 12, 2021

**Accepted:** April 21, 2021

**Article in press:** April 21, 2021

**Published online:** May 14, 2021

**P-Reviewer:** Tarantino G

**S-Editor:** Fan JR

**L-Editor:** A

**P-Editor:** Liu JH



## INTRODUCTION

The incidence of obesity is currently increasing owing to changing dietary habits, consequently resulting in the development of a fatty liver irrespective of alcohol consumption, a condition known as non-alcoholic fatty liver disease (NAFLD)[1]. NAFLD is an acquired metabolic stress-related liver disease that is strongly associated with obesity, dyslipidemia, hypertension, type 2 diabetes mellitus, and metabolic syndrome[2]. It was originally considered a benign disease. However, 37% of patients with NAFLD were recently reported to progress to non-alcoholic steatohepatitis (NASH) and consequent cirrhosis. Multiple studies have shown the pathogenesis and pathophysiology of NAFLD[3,4]. Various treatments such as vitamin E[5], anti-diabetic agents[6], farnesoid X receptor ligand[7], bile acid sequestrant, and apical sodium-dependent bile acid transporter inhibitors are under investigation[4], but there is no established standard treatment at present.

The mechanisms underlying NAFLD/NASH are far from being clarified and the supposed mechanisms that are at the basis of numerous attempts to cure NAFLD until now have ended, at best, in modest results[8]. The “gut-liver axis”, which is potentially involved in the pathogenesis of NAFLD, has attracted much interest in the context of chronic liver disease[9]. Serum levels of lipopolysaccharide (LPS), derived from gram-negative bacteria in the gut, are elevated in patients with NASH and in animal models of NASH[10,11]. Additionally, activation of toll-like receptor (TLR) 4 in the liver plays an important role in NASH development in mice[12]. Furthermore, increased intestinal permeability is highlighted as the primary cause of liver injury in NASH[13]. Gäbele *et al*[14] reported that increased intestinal permeability *via* dextran sulfate sodium (DSS) treatment induces colitis, increases portal LPS levels, and enhances hepatic inflammation and fibrogenesis in an experimental NASH model[14]. In addition to these studies, recent evidence strongly supports a close link between gut microbiota and NAFLD. The severity of NAFLD is reportedly associated with gut dysbiosis and a shift in the metabolic function of the gut microbiota[3]. Therefore, many NAFLD studies have focused on gut dysbiosis, microbiota composition, and on treatments targeting the gut-liver axis that include antibiotics, probiotics, prebiotics, and synbiotics[15].

Probiotic and prebiotic supplements, which are inexpensive and safe for humans, may be considered as possible interventions for NAFLD. Probiotics are live microbial food supplements or bacterial components that are suggested to improve liver function and reduce liver fat in NASH patients[16,17]. In contrast, prebiotics refer to a group of non-digestible carbohydrates that alter the composition and activity of the gut microbiota[18]. The beneficial effects of prebiotics on NAFLD have been demonstrated in a few human studies[19]. Furthermore, a recent review showed that clinical trials using prebiotics such as oligofructose, oat bran, and inulin might not be applicable[4]. Therefore, further studies are required to demonstrate the effect of prebiotics on NAFLD.

Partially hydrolyzed guar gum (PHGG) is a water-soluble dietary fiber prepared from guar gum, a galactomannan obtained from the seeds of *Cyamopsis tetragonoloba* through microbial endo- $\beta$ -mannanase activity to reduce its high viscosity[20]. PHGG treatment has been reported to improve the symptoms associated with both constipation- and diarrhea-predominant forms of irritable bowel syndrome[21]. The beneficial effects of dietary PHGG have also been demonstrated in the treatment of cholera[22], small intestinal bacterial overgrowth[23], pediatric functional gastrointestinal disorders[24], and metabolic syndrome-related functions such as aberrant lipid and glucose metabolism[25,26]. PHGG remains undigested in the upper gastrointestinal tract and is fermented by colonic bacteria, resulting in the production of short-chain fatty acids (SCFAs), particularly butyrate. It has recently been reported that PHGG increases butyrate-producing bacteria in the intestine[27]. More recently, PHGG treatment has been reported to alter the composition of the human microbiota, along with increasing the abundance of metabolites such as butyrate, acetate, and various amino acids[28]. To this end, PHGG should exert beneficial health effects on the host through alterations to the gut microbiota and SCFA production. However, the mechanisms by which PHGG prevents NAFLD development are yet to be elucidated. In this study, we used a murine model of NAFLD induced by an atherogenic (Ath) diet and an increase in intestinal permeability, and investigated the protective mechanisms by which PHGG modulates the gut microbiota.

## MATERIALS AND METHODS

### Experimental design

Seven-week-old male C57BL/6J mice were purchased from Shimizu Laboratory Supplies (Kyoto, Japan). The mice were caged individually in a room maintained at 18–24 °C with 40%–70% relative humidity and a 12-h light/dark cycle. The mice were allowed free access to drinking water and were fed with rodent diet CE-2 (Nihon Clea, Tokyo, Japan) during their 1-wk acclimatization period. Mouse maintenance and all subsequent experimental procedures were performed in accordance with the National Institutes of Health guidelines for the use of experimental animals. All the programs were approved by the Animal Care Committee of the Kyoto Prefectural University of Medicine (Kyoto, Japan, M2020-126). For NAFLD induction, mice were fed for 8 wk with an Ath diet as described by Matsuzawa *et al*[29], which resulted in hepatic steatosis and inflammation. The Ath diet was prepared by the addition of cocoa butter, cholesterol, and cholate to corticotropin-releasing factor-1 (CRF-1) (Oriental Yeast, Tokyo, Japan). Increased intestinal permeability was induced through the administration of 0.5% DSS (MW 36000–50000, MP Biomedicals, Illkirch, France) in drinking water as described previously[14]. DSS was administered in cycles, each consisting of 5-d DSS administration followed by a 9-d interval with normal drinking water. The cycles were repeated throughout the experimental period of 8 wk. Mice were randomly allocated to the following groups: (1) control mice fed standard chow (CRF-1; Control); (2) control mice fed a CRF-1 diet containing 5% PHGG (Control + PHGG); (3) NAFLD mice fed the Ath diet along with DSS induction (NAFLD); and (4) NAFLD mice supplemented with 5% PHGG (NAFLD + PHGG). Ingredient and fat contents of CRF-1 and the Ath diet are shown in Table 1. The commercial PHGG preparation (Sunfiber) used in this study was obtained from Taiyo Kagaku (Yokkaichi, Japan). The preparation was obtained by treating guar gum with  $\beta$ -endo-galactomannase from a strain of *Aspergillus niger*. Mice were sacrificed after being anesthetized with ketamine and xylazine. Blood samples were collected from the portal vein for serum endotoxin measurements through opposite cannulation with a 23-gauge needle or from the inferior vena cava for serum chemistry measurements followed by exsanguination, and the organs and cecal contents were harvested.

### Serum biochemistry and liver histology

Serum levels of aspartate aminotransferase (AST) and alanine aminotransferase (ALT) were measured using commercial assay kits (SRL, Tokyo, Japan) with an automated chemical analyzer (Olympus Automated Chemistry Analyzer AU5400, Tokyo, Japan). For hematoxylin and eosin (H&E) staining, liver samples were fixed in formalin, embedded in paraffin, sectioned at 5  $\mu$ m, and stained with H&E. Histopathological changes were evaluated under a light microscope (Olympus BX50, Tokyo, Japan) in a blinded manner.

### Measurement of myeloperoxidase activity

Tissue-associated myeloperoxidase (MPO) activity was measured in the liver tissue by a modified method reported by Grisham *et al*[30] as an index of neutrophil accumulation[30]. Liver tissue fragments were homogenized in 1 mL of 10 mmol/L potassium phosphate buffer (pH 7.8) containing 30 mmol/L KCl using a Teflon Potter-Elvehjem homogenizer. MPO activity was then determined. Briefly, liver homogenates were centrifuged at 20000  $\times$ g for 15 min at 4 °C. The resulting pellet was then rehomogenized in 0.3 mL of 50 mmol/L potassium phosphate buffer (pH 5.4) containing 0.5% hexadecyltrimethylammonium bromide. The mixture was then centrifuged at 20000  $\times$ g for 15 min at 4 °C, and the supernatants were collected. MPO activity was assessed by measuring the H<sub>2</sub>O<sub>2</sub>-dependent oxidation of 3,3',5,5'-tetramethylbenzidine. One unit of enzyme activity was defined as the amount of MPO that changed the absorbance by 1.0/min at 460 nm and 37 °C. Total protein in the tissue homogenates was measured using a Bio-Rad Protein Assay kit (Bio-Rad Laboratories, K. K., Tokyo, Japan) according to the manufacturer's protocol.

### Analysis of mRNA expression in the liver and intestine

Hepatic and intestinal mRNA expression was determined using real-time polymerase chain reaction (PCR). Total RNA was extracted using the acid-guanidinium-phenol chloroform method (Isogen kit; Nippon Gene, Tokyo, Japan). Extracted RNA was stored at –80 °C until use in real-time PCR. For the latter, 1  $\mu$ g of RNA was reverse-transcribed to first-strand complementary DNA (cDNA) using a high capacity cDNA Reverse Transcription Kit (Applied Biosystems, Foster City, CA, United States). Real-



**Table 1 Ingredients and fat content of the experimental diets**

Ingredients (g/kg)	CRF-1	Ath
Moisture (g/kg)	82	74.5
Protein (g/kg)	219	199
Fat (g/kg)	54	141.5
Crude ash (g/kg)	63	57
Crude fiber (g/kg)	29	26
Soluble nitrogen free extract (g/kg)	553	502
Total (g)	1000	1000
<b>Fat content</b>	<b>CRF-1</b>	<b>Ath</b>
Fatty acid (g/kg)	54	124
Cholesterol (g/kg)		12.5
Cholate (g/kg)		5

Ath: Atherogenic; CRF-1: Corticotropin-releasing factor-1.

time PCR was carried out on a 7300 real-time PCR system (Applied Biosystems, Foster City, CA, United States) using the DNA-binding dye SYBR Green to detect the PCR products with the primers shown in Table 2. Gene expression was normalized to that of *b-actin* as an internal control.

### **Serum endotoxin levels in the portal vein**

After the experimental period of 8 wk, blood samples were collected from the portal vein. The chromogenic Limulus Amebocyte Lysate (LAL) Endotoxin Assay kit (GenScript, Piscataway, NJ, United States) was used to measure serum endotoxin levels. In brief, the samples, blanks, or standards were incubated with reconstituted LAL at 37 °C for 45 min followed by incubation with a reconstituted chromogenic substrate solution at 37 °C for 6 min. After adding the stop solution, the absorbance of each reaction was recorded at 545 nm with a microplate reader (Spectramax M2; Molecular Devices, Sunnyvale, CA, United States). Distilled water was used as the blank.

### **Intestinal permeability assay**

Intestinal permeability was determined by measuring the lumen-to-blood clearance of fluorescein isothiocyanate (FITC)-conjugated dextran according to a previously published method, with some modifications[31,32]. In brief, after the experimental period of 8 wk, mice were anesthetized with ketamine and xylazine, and FITC-conjugated dextran (1 mg/mL; molecular mass, 4 kDa; Sigma Aldrich, St. Louis, MO, United States) in poly(butylene succinate) was administered from the proximal duodenum in a total volume of 0.5 mL. One hour after administration, blood samples were collected, centrifuged, and stored at -80 °C. The serum was then examined at the excitation/emission wavelengths of 490 nm/525 nm using a spectrofluorometer (Spectramax M2; Molecular Devices, Sunnyvale, CA, United States).

### **DNA extraction from mouse fecal samples**

After the experimental period of 8 wk, mouse fecal samples were collected from the cecum, suspended in lysis buffer [4 mol/L guanidinium thiocyanate, 100 mmol/L tris-HCl (pH 9.0), 40 mmol/L ethylenediaminetetraacetic acid, and 0.001% bromothymol blue], and shaken in the presence of zirconia beads. DNA was extracted from the resultant suspension (Magtration System 12GC and GC series MagDEA DNA 200; Precision System Science, Chiba, Japan).

### **PCR amplification and terminal restriction fragment length polymorphism analysis**

The 16S rRNA gene was amplified from fecal DNA using the 516F (5'-TGCCAGCAGCCGCGGTA-3'; *Escherichia coli* positions 516 to 532) and 1510R (5'-GGTTACCTTGTTACGACTT-3'; *Escherichia coli* positions 1510 to 1492) primers. The 5'-ends of the forward primers were labeled with 6'-carboxyfluorescein synthesized by



**Table 2 Primer sequences for the targeted mouse genes**

Gene	Forward primer	Reverse primer
<i>m_βactin</i>	TATCCACCTTCCAGCAGATGT	AGCTCAGTAACAGTCCGCCTA
<i>m_TNF-α</i>	ATCCGCGACGTGGAAC TG	ACCGCTGGAGTCTGGAA
<i>m_MCP-1</i>	CTTCCTCCACCACCATGCA	CCAGCCGGCAACTGTGA
<i>m_αSMA</i>	GTCCCAGACATCAGGGAGTAA	TCCGATACTTCAGCGTCAGGA
<i>m_collagen1a1</i>	GCTTCACCTACAGCACCTTGT	GATGACTGTCTTGCCCCAAGTT
<i>m_Acc</i>	CTGGCTGCATCCATTATGTCA	TGGTAGACTGCCCGTGTGAA
<i>m_Cpt2</i>	GGGCGAGCTTCAGCATATG	GGCCCATCGCTGCTTCTT
<i>m_PPARGα</i>	CGATGCTGTCTCCTTGATGA	CGCGTGTGATAAAGCCATTG
<i>m_PPARGγ</i>	CTTGCTGTGGGGATGTCTCA	ATCTCCGCCAACAGCTTCTC
<i>m_TLR4</i>	CCTCTGCCTTCACTACAGAGACTTT	CACAATAACCTTCCGGCTCTTG
<i>m_TLR9</i>	CCITTCGTGGTGTTCGATAAGG	CACCCGCAGCTCGTTATACA

TNF-α: Tumor necrosis factor-α; MCP-1: Monocyte chemotactic protein 1; αSMA: α smooth muscle actin; ACC: Acetyl-CoA carboxylase; CPT2: Carnitine O-palmitoyltransferase II; PPAR: Peroxisome proliferator-activated receptor; TLR: Toll-like receptor.

Applied Biosystems (Life Technologies, Thermo Fisher Scientific, Waltham, MA). PCR amplification of the DNA samples (10 ng of each DNA sample) was performed according to a previously described protocol[33]. The amplified 16S rDNA genes were purified (MultiScreen PCR micro96 Plate; Merck Millipore, Tokyo, Japan) and dissolved in 40 μL of distilled water. The restriction enzymes for restriction fragment length polymorphism (RFLP) were selected according to a previously described protocol[34]. Purified PCR products were digested for 3 h with 10 U of the restriction enzyme *Bs*I at 55 °C. The length of the terminal RF (T-RF) was determined using a genetic analyzer (ABI PRISM 3130xl; Applied Biosystems, Life Technologies, Thermo Fisher Scientific) and analysis software (GeneMapper; Applied Biosystems, Life Technologies, Thermo Fisher Scientific, Waltham, MA, United States). Standard-size markers were used (*e.g.*, MapMarker X-Rhodamine Labeled 50-1000 bp; BioVentures, Murfreesboro, TN, United States). An operational taxonomic unit (OTU) was used to describe the clusters of clone sequences that differed from the known species by approximately 2%, which was at least 98% similar to the members of their cluster[35]. As the apparent size of identical T-RFs can vary over a range of 1-3 bp, major T-RFs that were similar in size to within 1-3 bp, were grouped as OTUs[34]. The major T-RFs were identified using a computer simulation with a T-RFLP analysis program and a phylogenetic assignment database for the T-RFLP analysis of human colonic microbiota[36].

### **Determination of organic acid concentration in cecal contents**

A portion of the cecal contents (0.5 g) was suspended in 0.5 mL of 14% perchloric acid to remove proteins. After centrifugation at 10000 × g for 5 min at 4 °C, the supernatant was filtered through a cellulose acetate membrane filter with a pore size of 0.45 μm, and its organic acid content was then analyzed with ion-exclusion high performance liquid chromatography as described by Ushida and Sakata[37].

### **Statistical analyses**

Data are expressed as the mean ± SD. Overall differences between groups were determined by one-way analysis of variance (ANOVA). Differences between individual groups were determined using Tukey's multiple comparison tests when one-way ANOVA indicated a significant difference. Target gene copy numbers, estimated using real-time PCR, and the concentration of organic acids were analyzed using the Steel-Dwass method after the Friedman test. A *P* value < 0.05 was considered statistically significant. All analyses were performed using GraphPad Prism 7 (GraphPad Software, San Diego, CA, United States) for Macintosh.

## RESULTS

### **Effects of PHGG on body weight, liver weight, and biochemical parameters**

Mice with increased intestinal permeability exposed to the Ath diet showed significant increases in liver weight, liver/body ratios, AST, ALT, and total cholesterol levels, as well as a significant decrease in body weight and triglyceride levels, as shown in Table 3. Treatment with PHGG did not change the NAFLD model-induced change in body weight, liver weight, liver/body ratio, and total cholesterol levels but significantly improved the increase in AST and ALT levels.

### **Effects of PHGG on liver damage, inflammation, and fibrosis**

Macroscopic observation showed that livers from mice subjected to the Ath diet with increased intestinal permeability were visibly lighter and fatty compared to those from mice subjected to a control diet (Figure 1A). Treatment with PHGG did not induce a dramatic change, but partly reverted some morphological alterations. Histological analysis of the liver tissues indicated that the fat content in mice fed a control diet with or without PHGG treatment were normal without inflammatory infiltration (Figure 1B). In contrast, mice with increased intestinal permeability exposed to the Ath diet showed both increased fat content and inflammatory infiltration (Figure 1B). These alterations were prevented by PHGG treatment (Figure 1B). The observed inflammatory infiltration was supported by the MPO activity results, which confirmed that treatment with PHGG attenuated liver damage in the NAFLD model (Figure 1C). Histological analysis of intestine and colon tissues indicated that mice with increased intestinal permeability exposed to the Ath diet did not show any morphological changes compared to the control mice (data not shown). Figure 2 shows hepatic inflammation and fibrosis in the NAFLD model. *Tumor necrosis factor- $\alpha$*  (TNF- $\alpha$ ; Figure 2A) and *monocyte chemoattractant protein-1* (MCP-1; MCP-1; Figure 2B) mRNA expression was significantly higher in the liver tissue of mice with increased intestinal permeability exposed to the Ath diet than in that of control mice. This increase was significantly attenuated by treatment with PHGG. With respect to hepatic fibrosis, *collagen 1 $\alpha$ 1* (Figure 2C) and *smooth muscle actin* ( $\alpha$ SMA;  $\alpha$ SMA; Figure 2D) mRNA expression was significantly elevated in the liver tissue of mice with NAFLD compared to that in control mice. Treatment with PHGG clearly decreased *collagen 1 $\alpha$ 1* mRNA expression in the NAFLD model.

### **Effects of PHGG on lipid synthesis and degradation in the liver**

Enzymes of the lipid synthesis and degradation pathways in the liver were further assessed as shown in Figure 3. Mice with increased intestinal permeability exposed to the Ath diet showed upregulation of *acetyl-CoA carboxylase* and *peroxisome proliferator-activated receptor  $\gamma$*  (PPAR $\gamma$ ) and downregulation of *carnitine O-palmitoyltransferase II* and PPAR $\alpha$  mRNA expression. Treatment with PHGG did not change these effects. Moreover, enzymes related to lipid absorption, such as *acetyl-coenzyme A acetyltransferase 2*, *Niemann-Pick C1-like 1*, and *fatty acid binding protein*, were evaluated in the intestine. Ath diet combined with increased intestinal permeability, and treatment with PHGG, did not affect the levels of these enzymes (data not shown).

### **Effects of PHGG on regulation of the gut-liver axis**

The concept of the gut-liver axis has received considerable attention in recent years. In this study, chronic administration of 0.5% DSS did not result in morphological changes such as mucosal disruption. However, it induced some effects on the liver, thereby leading to NAFLD development. We therefore examined the expression of TLRs in the liver. The results showed that the Ath diet combined with increased intestinal permeability significantly increased the mRNA expression of *TLR4* and *TLR9* in the liver, and that treatment with PHGG significantly attenuated this upregulation (Figure 4A and B). These results are consistent with the endotoxin levels determined in the portal vein (Figure 4C). To determine whether our NAFLD model or PHGG treatment resulted in altered intestinal permeability, we evaluated the lumen-to-blood clearance of FITC-conjugated dextran (FD4 flux). As shown in Figure 5, the FD4 flux was significantly elevated in the NAFLD model mice, and this increase was significantly reduced by treatment with PHGG.

### **Effects of PHGG on SCFA profiles and cecal bacteria**

The SCFA profiles of the cecal contents were determined using ion-exclusion high performance liquid chromatography, the results of which are summarized in Table 4. Under normal conditions, treatment with PHGG significantly increased the acetic acid,

**Table 3 Characteristics of the experimental groups**

Characteristics	Control	Control + PHGG	NAFLD	NAFLD + PHGG
Body weight (g)	25.7 ± 0.5	25.2 ± 1.1	20.6 ± 0.8 <sup>a</sup>	20.8 ± 1.6 <sup>a</sup>
Liver weight (g)	1.17 ± 0.05	1.03 ± 0.08	1.47 ± 0.11 <sup>a</sup>	1.55 ± 0.13 <sup>a</sup>
Liver weight (% body)	4.45 ± 0.13	4.13 ± 0.32	7.13 ± 0.40 <sup>a</sup>	7.44 ± 0.61 <sup>a</sup>
Aspartate aminotransferase (IU/L)	72.0 ± 7.1	73.1 ± 11.9	133.1 ± 69.1 <sup>a</sup>	83.5 ± 24.1 <sup>a,b</sup>
Alanine aminotransferase (IU/L)	23.4 ± 2.9	20.0 ± 3.4	112.9 ± 77.0 <sup>a</sup>	46.3 ± 15.9 <sup>a,b</sup>
Total cholesterol (mg/dL)	97.7 ± 6.6	83.7 ± 10.8	359.7 ± 95.0 <sup>a</sup>	306.7 ± 26.5 <sup>a</sup>
Triglyceride (mg/dL)	88.9 ± 25.4	71.1 ± 25.1	16.6 ± 4.0 <sup>a</sup>	36.2 ± 25.7 <sup>a,b</sup>
Free fatty acids (mEQ/L)	1668 ± 257	1334 ± 254 <sup>a</sup>	1254 ± 201 <sup>a</sup>	1119 ± 310 <sup>a</sup>
Glucose (mg/dL)	70 ± 53	73 ± 16	73 ± 19	95 ± 32

Data are presented as the mean ± SD.

<sup>a</sup>*P* < 0.05 significant differences compared to the control group.

<sup>b</sup>*P* < 0.05 significant differences between the non-alcoholic fatty liver disease (NAFLD) group and the NAFLD + Partially hydrolyzed guar gum group. Non-alcoholic fatty liver disease group was induced by high fat diet with increased intestinal permeability. NAFLD: Non-alcoholic fatty liver disease; PHGG: Partially hydrolyzed guar gum.

**Table 4 Partially hydrolyzed guar gum-mediated profiles of short-chain fatty acids in cecal contents**

Short chain fatty acids (mmol/g)	Control	Control + PHGG	NAFLD	NAFLD + PHGG
Succinic acid	0.82 ± 0.34	0.85 ± 0.36	5.08 ± 2.27 <sup>a</sup>	5.28 ± 2.20 <sup>a</sup>
Lactic acid	0.05 ± 0.08	0.09 ± 0.13	0.40 ± 0.46 <sup>a</sup>	0.45 ± 0.39 <sup>a</sup>
Formic acid	0.89 ± 0.09	1.90 ± 0.06 <sup>a</sup>	0.72 ± 0.16 <sup>a</sup>	0.83 ± 0.28 <sup>b</sup>
Acetic acid	41.2 ± 6.0	47.9 ± 8.8 <sup>a</sup>	32.8 ± 5.3 <sup>a</sup>	33.1 ± 7.9 <sup>a</sup>
Propionic acid	8.18 ± 1.14	9.16 ± 1.04 <sup>a</sup>	9.76 ± 2.56 <sup>a</sup>	9.82 ± 3.39 <sup>a</sup>
Isobutyric acid	1.19 ± 0.11	1.04 ± 0.11	1.44 ± 0.20 <sup>a</sup>	1.06 ± 0.28 <sup>b</sup>
Butyric acid	8.86 ± 2.42	13.81 ± 5.14 <sup>a</sup>	3.91 ± 0.58 <sup>a</sup>	3.34 ± 1.09 <sup>a</sup>
Isovaleric acid	0.33 ± 0.14	0.12 ± 0.11 <sup>a</sup>	1.05 ± 0.40 <sup>a</sup>	0.38 ± 0.40 <sup>b</sup>
Valeric acid	0.49 ± 0.18	0.48 ± 0.14	0.50 ± 0.22	0.18 ± 0.17 <sup>a,b</sup>

Data are presented as the mean ± SD.

<sup>a</sup>*P* < 0.05 significant differences compared to the control group.

<sup>b</sup>*P* < 0.05 significant differences between the non-alcoholic fatty liver disease (NAFLD) group and the NAFLD + Partially hydrolyzed guar gum group. PHGG: Partially hydrolyzed guar gum; NAFLD: Non-alcoholic fatty liver disease.

formic acid, propionic acid, and butyric acid contents. In contrast, isovaleric acid content was significantly decreased after PHGG treatment. The Ath diet together with increased intestinal permeability significantly elevated succinic acid, lactic acid, propionic acid, isobutyric acid, and isovaleric acid contents and significantly reduced formic acid, acetic acid, and butyric acid contents. In the NAFLD model, PHGG treatment significantly upregulated formic acid levels and significantly downregulated isobutyric acid, isovaleric acid, and valeric acid contents.

To determine whether treatment with PHGG altered the cecal bacteria profiles, we examined the variation in eight representative bacterial groups using T-RFLP analysis. Chronic administration of 0.5% DSS caused a dramatic decrease in the number of cecal bacteria, and therefore, cecal bacterial profiles were only analyzed in the control and control + PHGG groups. As shown in Figure 6, the administration of PHGG altered the cecal bacteria profiles (Figure 6A) and significantly increased the cecal *Bacteroides* (Figure 6B) and *Clostridium* subcluster XIVa (Figure 6C) compared with that in the control mice. Conversely, PHGG treatment significantly reduced the cecal *Prevotella*, *Bifidobacterium* (Figure 6D), and *Clostridium* cluster XVIII (Figure 6E).



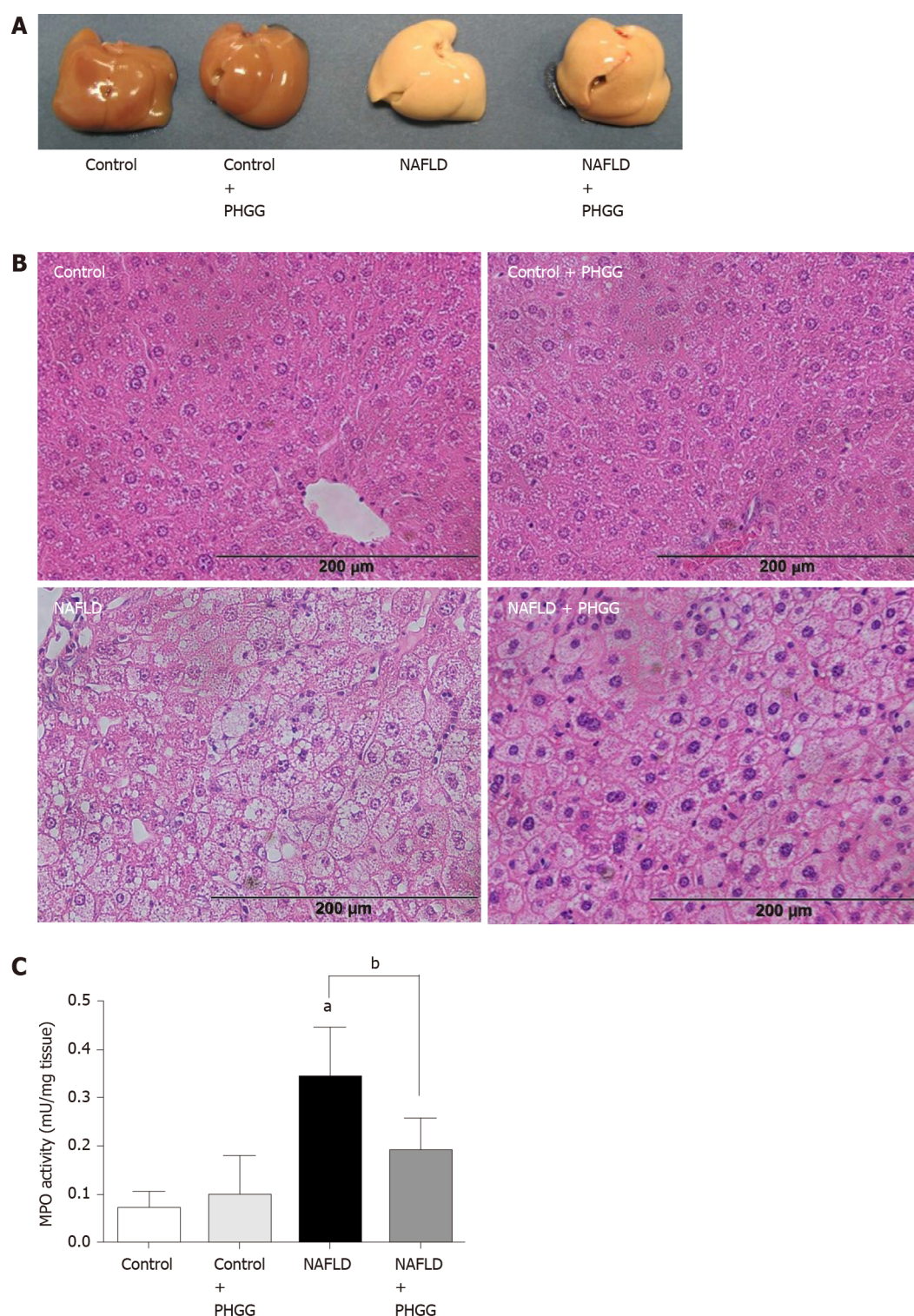


**Figure 1 Effects of partially hydrolyzed guar gum on the non-alcoholic fatty liver disease model.** A: Representative macroscopic findings in the liver. Non-alcoholic fatty liver disease was induced in mice subjected to the atherogenic diet with increased intestinal permeability for 8 wk; B: Representative histological findings in the liver. Magnification,  $\times 100$ . Hematoxylin and eosin staining; C: Myeloperoxidase (MPO) activity. The liver was homogenized and MPO activity was determined as an index of neutrophil accumulation in the liver. Data represent the mean  $\pm$  SD of seven mice. <sup>a</sup> $P < 0.05$  significant differences compared to the control group; <sup>b</sup> $P < 0.05$  significant differences between the 2 selected groups. NAFLD: Non-alcoholic fatty liver disease; PHGG: Partially hydrolyzed guar gum; MPO: Myeloperoxidase.

## DISCUSSION

Our results clearly indicate that increased intestinal permeability in combination with the administration of Ath diet resulted in NAFLD development through the gut-liver axis and that treatment with PHGG significantly attenuated NAFLD development in mice. The protective effects of PHGG might result in part from the modulation of

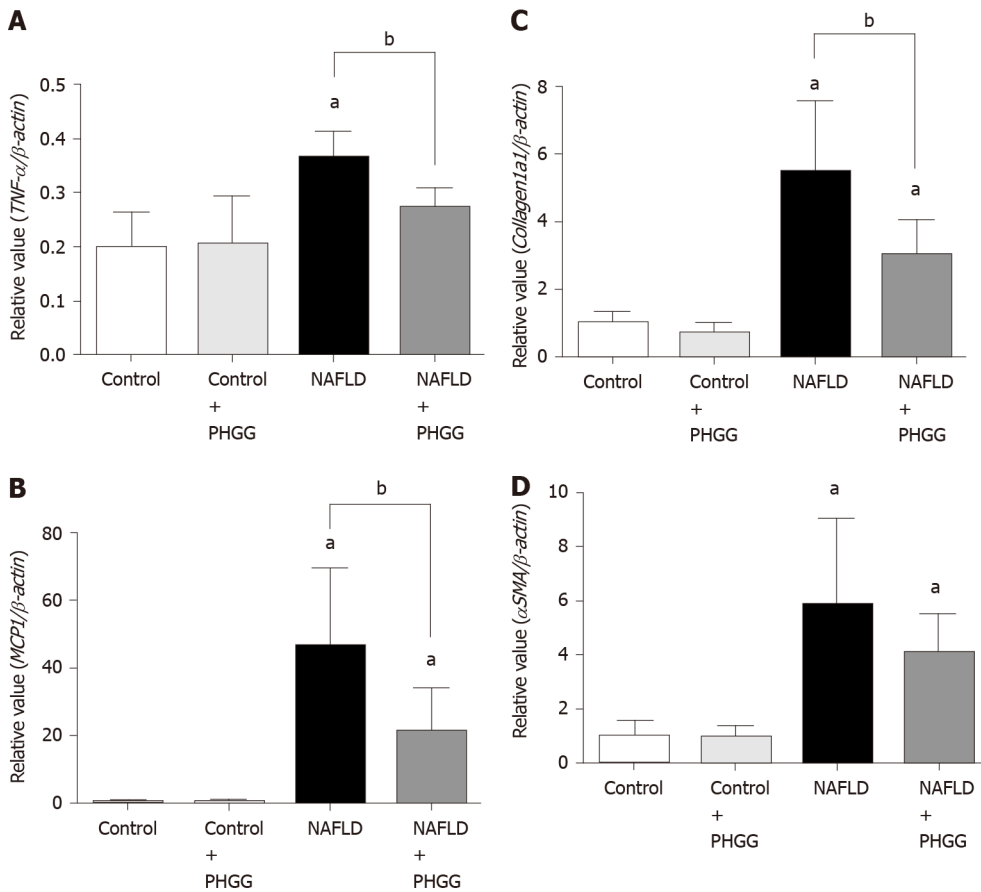


**Figure 2** Effects of partially hydrolyzed guar gum on hepatic inflammation and fibrosis in the non-alcoholic fatty liver disease model. A: Tumor necrosis factor- $\alpha$ ; B: Monocyte chemoattractant protein-1; C: Collagen 1 $\alpha$ 1; D:  $\alpha$  smooth muscle actin mRNA expression in the liver. mRNA expression was evaluated using real-time polymerase chain reaction. Data represent the mean  $\pm$  SD of seven mice. <sup>a</sup> $P < 0.05$  significant differences compared to the control group; <sup>b</sup>  $P < 0.05$  significant differences between the 2 selected groups. NAFLD: Non-alcoholic fatty liver disease; PHGG: Partially hydrolyzed guar gum; TNF- $\alpha$ : Tumor necrosis factor- $\alpha$ ; MCP-1: Monocyte chemoattractant protein-1;  $\alpha$ SMA:  $\alpha$  smooth muscle actin.

microbiota composition and SCFA profiles, leading to attenuation of the increased intestinal permeability. A variety of animal models for NAFLD and NASH, including models induced by high-fat, high-fructose, high-cholesterol, high-sucrose, Ath, choline- and L-amino acid-deficient, and methionine- and choline-deficient diets, have been used to investigate the pathophysiology of NAFLD and NASH, indicating the important role of diet in these clinical states. However, because of the complex, multidirectional pathophysiology involved in NAFLD, the perfect animal model representing the complete NAFLD spectrum in a workable time frame does not appear to exist[38]. Moreover, due to the substantial physiological differences between rodents and humans, animal models should be used with caution.

Accumulating evidence indicates the significance of alterations in intestinal permeability in NAFLD and NASH pathogenesis. An increase in intestinal epithelial cell permeability is reported to allow the translocation of microbial products into the portal vein, subsequently inducing hepatic inflammation[14,39]. Luther *et al*[31] demonstrated that an early phase of hepatic injury and inflammation contributes to altered intestinal permeability[31]. Furthermore, Mouries *et al*[40] demonstrated that disruption of the gut vascular barrier is an early event in NASH pathogenesis and is a consequence of diet-induced dysbiosis[40]. These data suggest that communication between the gut and liver plays an important role in NAFLD development. In this context, the murine NAFLD model described in the present study appears to be valuable for investigating the pathophysiology of this disease. Our study also clearly shows that increased intestinal permeability combined with the Ath diet resulted in increased liver weight, AST/ALT, total cholesterol levels, and lipid accumulation in the liver, as well as the upregulation of pro-inflammatory cytokines/chemokines such as TNF- $\alpha$  and MCP-1, neutrophil accumulation, lipid synthesis, and hepatic fibrogenesis. These results are consistent with those of a previous study[14]. Several cytokines, such as interleukin (IL)-6, IL-1b, and TNF- $\alpha$ , have been recently suggested to be involved in the so-called chronic low-grade inflammation or meta inflammation



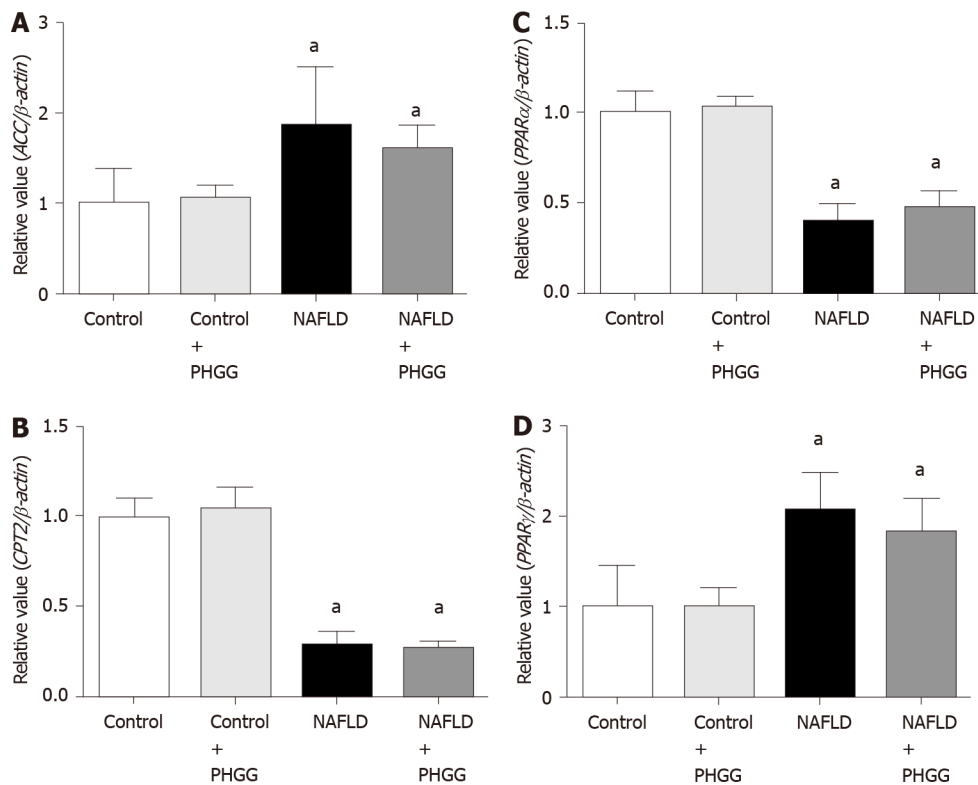


**Figure 3** Effects of partially hydrolyzed guar gum on lipid synthesis and degradation in the non-alcoholic fatty liver disease model. A: Acetyl-CoA carboxylase; B: Carnitine O-palmitoyltransferase II; C: Peroxisome proliferator-activated receptor (PPAR)  $\alpha$ ; D: PPAR $\gamma$  mRNA expression in the liver. mRNA expression was evaluated using real-time polymerase chain reaction. Data represent the mean  $\pm$  SD of seven mice. <sup>a</sup> $P < 0.05$  significant differences compared to the control group. NAFLD: Non-alcoholic fatty liver disease; PHGG: Partially hydrolyzed guar gum; ACC: Acetyl-CoA carboxylase; PPAR: Peroxisome proliferator-activated receptor; CPT2: Carnitine O-palmitoyltransferase II.

of NAFLD/NASH[41,42]. Our study further demonstrates that increased intestinal permeability in combination with the Ath diet resulted in elevated portal endotoxin levels and activated the expression of TLR4 and TLR9, confirming that intestinal permeability was significantly elevated in this NAFLD model. Indeed, the FD4 flux, a marker of lumen-to-serum permeability, was significantly increased in our NAFLD model. These findings are consistent with those of a recent review[4,15,43]. Interestingly, our study also shows that treatment with PHGG significantly attenuated the development of NAFLD by decreasing TLR signaling and its downstream molecules, such as pro-inflammatory cytokines, despite continued lipid synthesis and degradation, suggesting that treatment with PHGG might have therapeutic effects on NAFLD through the gut-liver axis. Another study has also shown that a prebiotic, fermentable, dietary fructo-oligosaccharide alleviates hepatic steatosis[44]. However, in this study, the protection appeared to be mediated by reduced fatty acid oxidation and cholesterol accumulation. Thus, the protective mechanisms by which various prebiotics modulate NAFLD remain to be fully elucidated.

Accumulating evidence suggests a relationship between the intestinal microbiota and NAFLD, and modification of the composition of the former could play a role in the development and progression of the latter[45]. Le Roy *et al*[46] have shown that in mice fed the Ath diet, the gut microbiota composition alters lipid metabolism in the liver[46]. De Minicis *et al*[47] also demonstrated that the Ath diet model subjected to bile duct ligation shows an increase in the abundance of gram-negative bacteria, a reduced Bacteroidetes/Firmicutes ratio, the complete disappearance of *Bifido-bacteriaceae*, and increased abundance of gram-negative *Proteobacteria* (especially *Enterobacteriaceae*)[47]. In our experiments, we quantified the *Clostridium* subcluster XIVa, *Clostridium* cluster IV, and *Bacteroides* as the SCFA-producing indigenous bacteria, *Prevotella* as resident microbiota, *Bifidobacterium* as a beneficial bacterium, Lactobacillales as the lactate-producing bacteria, *Clostridium* cluster XI as the harmful bacteria, including *Clostridium difficile*, and the *Clostridium* cluster XVIII as pathogenic bacteria such as *Escherichia coli* in regard to the cecal bacteria profiles. Additionally, the compositional alterations in intestinal bacteria might also change their metabolic capacity. Colonic fermentation of carbohydrates results in the generation of SCFAs.

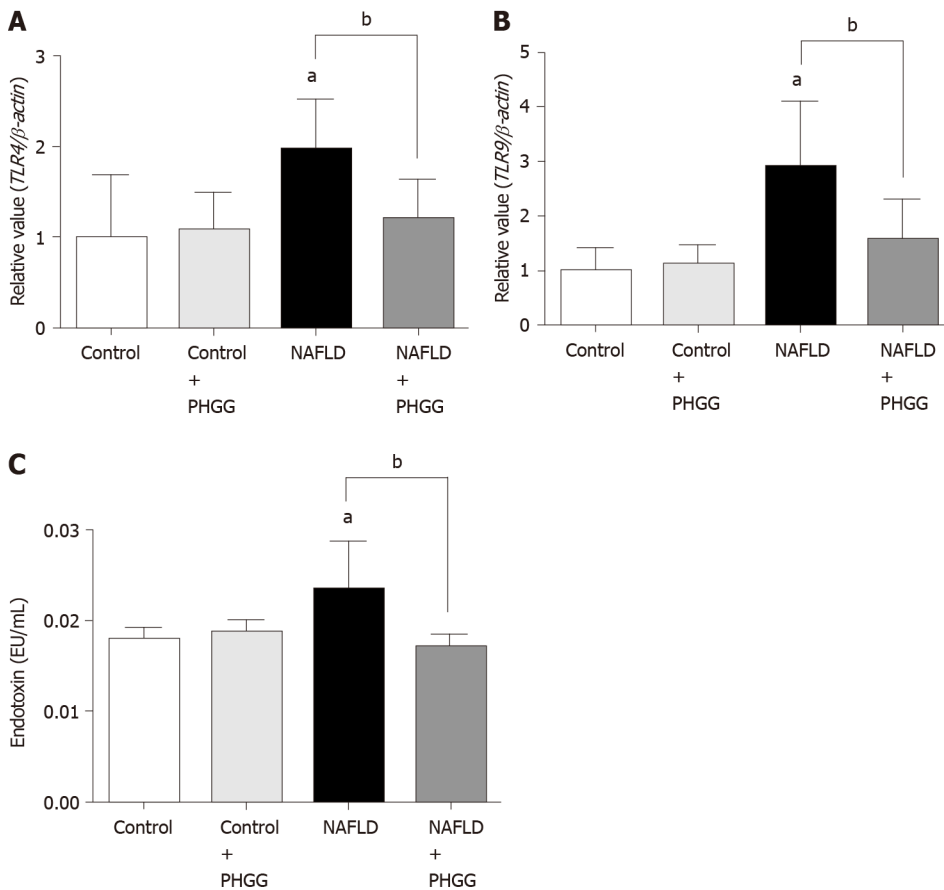


**Figure 4** Effects of partially hydrolyzed guar gum on toll-like receptor signaling through the gut-liver axis. A: Toll-like receptor (TLR) 4 mRNA expression; B: TLR9 mRNA expression in the liver. mRNA expression was evaluated using real-time polymerase chain reaction; C: Endotoxin levels in the portal vein. Endotoxin levels were measured using the chromogenic Limulus Amebocyte Lysate Endotoxin Assay kit. Data represent the mean  $\pm$  SD of seven mice. <sup>a</sup> $P < 0.05$  significant differences compared to the control group; <sup>b</sup> $P < 0.05$  significant differences between the 2 selected groups. NAFLD: Non-alcoholic fatty liver disease; PHGG: Partially hydrolyzed guar gum; TLR: Toll-like receptor.

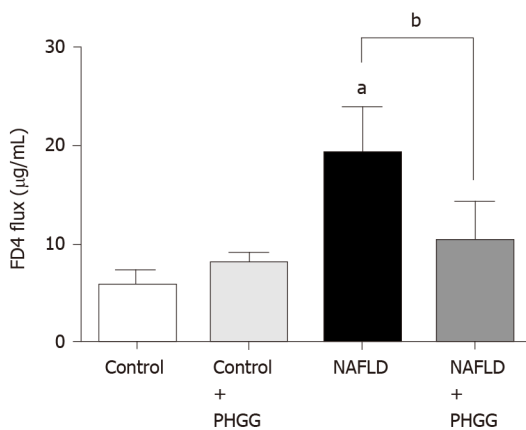


**Figure 5** Effects of partially hydrolyzed guar gum on intestinal permeability in the non-alcoholic fatty liver disease model. Lumen-to-blood clearance of fluorescein isothiocyanate-conjugated dextran was evaluated by injection into the duodenum and collection of blood after 60 min. Fluorescence intensity in the serum was measured with a spectrofluorometer. Data represent the mean  $\pm$  SD of seven mice. <sup>a</sup> $P < 0.05$  significant differences compared to the control group; <sup>b</sup> $P < 0.05$  significant differences between the 2 selected groups. NAFLD: Non-alcoholic fatty liver disease; PHGG: Partially hydrolyzed guar gum.

Recent evidence suggests that supplementation with sodium butyrate protects mice from NASH development[48]. Moreover, a recent review indicated the beneficial effects of commensal bacteria on the intestinal epithelial barrier and the importance of butyrate-producing bacteria for intestinal health[49]. A recent study also showed that SCFAs (acetate, propionate, and butyrate) stimulate and protect the intestinal barrier function[50].

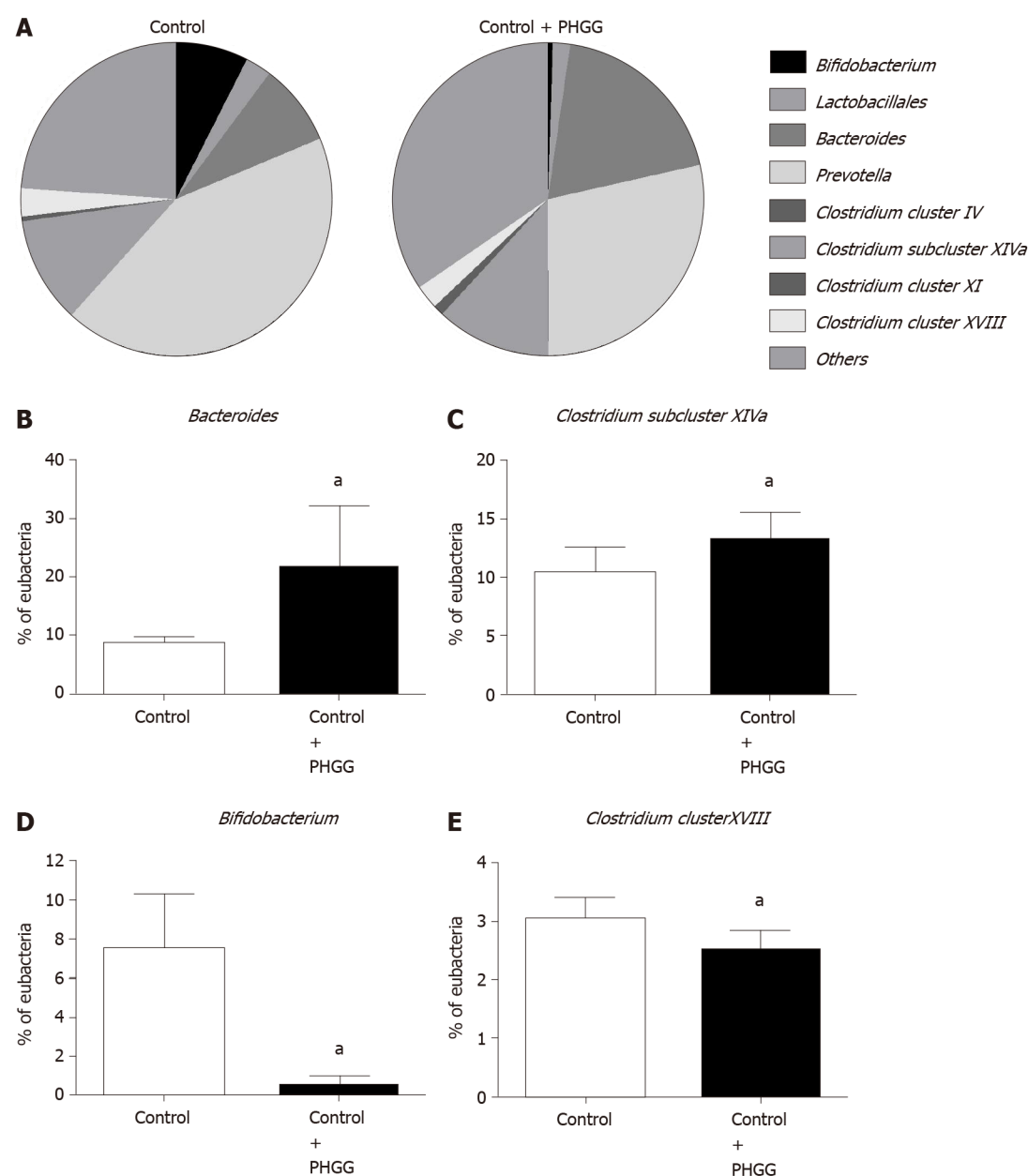


**Figure 6** Effects of partially hydrolyzed guar gum on cecal microbiota after administration. A: Percentage of the total identified sequences per group. Microbiota profiles in the cecal contents were analyzed using terminal restriction fragment-length polymorphism; B–E: Changes in the microbiota composition. Bars represent the mean  $\pm$  SD of seven mice. <sup>a</sup> $P < 0.05$  significant differences compared to the control group. PHGG: Partially hydrolyzed guar gum.

In our study, treatment with PHGG significantly increased the abundance of cecal *Bacteroides* and *Clostridium* subcluster XIVa. Our results are partially in agreement with previous human experiments showing that PHGG increases the abundance of butyrate-producing bacteria, including *Clostridium* subcluster XIVa, in the intestine[27]. Moreover, treatment with PHGG resulted in a significant increase in SCFA levels, particularly butyric acid, acetic acid, propionic acid, and formic acid, in the cecal content. These results are consistent with those of a previous study[27]. PHGG-mediated increases in SCFA levels might exert protective effects on the intestinal barrier function. These observations are supported by a recent study[50], although it lacked direct data.

Our study has the following limitations: (1) the dramatic changes in microbiota and SCFA profiles in the current NAFLD model resulting from the adverse effects of DSS administration; (2) the method of analysis of microbiota, T-RFLP analysis; (3) the lack of determination of IL-6 and IL-1b (other markers of low-grade inflammation of NAFLD/NASH); and (4) the modest sample size of each group associated with mean differences and SD in some experiments. Further investigations are therefore required.

## CONCLUSION

In summary, our data indicate that PHGG inhibits NAFLD development in mice, which is associated with decreased lipid accumulation, pro-inflammatory cytokine/chemokine production, and neutrophil infiltration in the liver. These findings might be related to the gut-liver axis, through the protection of intestinal barrier integrity, as well as cecal bacteria and SCFA profile alterations. Particularly, treatment with PHGG promotes an SCFA-producing bacterial group of *Clostridium* subcluster XIV and *Bacteroides*. Further studies are warranted to elucidate the detailed mechanisms involved in this phenomenon; however, treatment with PHGG in humans could show great promise as a therapeutic strategy for NAFLD.

## ARTICLE HIGHLIGHTS

### Research background

Non-alcoholic fatty liver disease (NAFLD) is caused by a variety of pathogenesis, and may involve the gut-liver axis, which has attracted much attention. Prebiotics such as dietary fibers were shown to attenuate NAFLD by modulating gut microbiota. Partially hydrolyzed guar gum (PHGG), a water-soluble dietary fiber, is associated with alteration of gut microbiota and the production of short-chain fatty acids (SCFAs), and has been reported to alleviate the symptoms of various intestinal diseases and metabolic syndrome.

### Research motivation

PHGG should exert beneficial health effects on the host through alterations to the gut microbiota and SCFA production. However, its effects on NAFLD remain to be fully elucidated.

### Research objectives

The present study aimed to determine whether treatment with PHGG attenuates NAFLD development in mice through the gut-liver axis.

### Research methods

Male C57BL/6J mice with increased intestinal permeability by chronic intermittent administration of low-dose dextran sulfate sodium were fed a control or atherogenic (Ath) diet (a mouse model of NAFLD) for 8 wk, with or without 5% PHGG. Body weight, liver weight, macroscopic findings in the liver, blood biochemistry, liver histology, myeloperoxidase activity in liver tissue, mRNA expression in the liver and intestine, serum endotoxin levels in the portal vein, intestinal permeability, and microbiota and SCFA profiles in the cecal samples were investigated.

### Research results

Mice subjected to a Ath diet with increased intestinal permeability showed significantly increased serum aspartate aminotransferase and alanine aminotransferase levels, liver fat accumulation, liver inflammatory (tumor necrosis factor- $\alpha$  and monocyte chemoattractant protein-1) and fibrogenic (collagen 1 $\alpha$ 1 and  $\alpha$  smooth muscle actin) marker levels, and liver myeloperoxidase activity, which were significantly attenuated by PHGG treatment. Moreover, increased intestinal permeability in combination with the Ath diet resulted in increased portal endotoxin levels and activated toll-like receptor (TLR) 4 and TLR9 expression. PHGG administration did not affect fatty acid metabolism in the liver, but decreased lipopolysaccharide signaling through the gut-liver axis. The administration of PHGG altered the cecal bacteria profiles and significantly increased the cecal *Bacteroides* and *Clostridium* subcluster XIVa. Treatment with PHGG markedly increased the levels of SCFAs, particularly, butyric acid, acetic acid, propionic acid, and formic acid, in the cecal samples.

### Research conclusions

Treatment with PHGG attenuated NAFLD development in mice through the gut-liver axis by modulating microbiota and downstream SCFA profiles.

### Research perspectives

By indicating that PHGG administration inhibits NAFLD development through the

gut-liver axis, the present study showed a possible treatment strategy of NAFLD in humans.

## REFERENCES

- 1 **Angulo P.** Nonalcoholic fatty liver disease. *N Engl J Med* 2002; **346**: 1221-1231 [PMID: [11961152](#) DOI: [10.1056/NEJMra011775](#)]
- 2 **Chalasani N**, Younossi Z, Lavine JE, Diehl AM, Brunt EM, Cusi K, Charlton M, Sanyal AJ; American Gastroenterological Association; American Association for the Study of Liver Diseases; American College of Gastroenterology. The diagnosis and management of non-alcoholic fatty liver disease: practice guideline by the American Gastroenterological Association, American Association for the Study of Liver Diseases, and American College of Gastroenterology. *Gastroenterology* 2012; **142**: 1592-1609 [PMID: [22656328](#) DOI: [10.1053/j.gastro.2012.04.001](#)]
- 3 **Boursier J**, Mueller O, Barret M, Machado M, Fizanne L, Araujo-Perez F, Guy CD, Seed PC, Rawls JF, David LA, Hunault G, Oberti F, Calès P, Diehl AM. The severity of nonalcoholic fatty liver disease is associated with gut dysbiosis and shift in the metabolic function of the gut microbiota. *Hepatology* 2016; **63**: 764-775 [PMID: [26600078](#) DOI: [10.1002/hep.28356](#)]
- 4 **Hu H**, Lin A, Kong M, Yao X, Yin M, Xia H, Ma J, Liu H. Intestinal microbiome and NAFLD: molecular insights and therapeutic perspectives. *J Gastroenterol* 2020; **55**: 142-158 [PMID: [31845054](#) DOI: [10.1007/s00535-019-01649-8](#)]
- 5 **Lavine JE**, Schwimmer JB, Van Natta ML, Molleston JP, Murray KF, Rosenthal P, Abrams SH, Scheimann AO, Sanyal AJ, Chalasani N, Tonascia J, Unalp A, Clark JM, Brunt EM, Kleiner DE, Hoofnagle JH, Robuck PR; Nonalcoholic Steatohepatitis Clinical Research Network. Effect of vitamin E or metformin for treatment of nonalcoholic fatty liver disease in children and adolescents: the TONIC randomized controlled trial. *JAMA* 2011; **305**: 1659-1668 [PMID: [21521847](#) DOI: [10.1001/jama.2011.520](#)]
- 6 **Sanyal AJ**, Chalasani N, Kowdley KV, McCullough A, Diehl AM, Bass NM, Neuschwander-Tetri BA, Lavine JE, Tonascia J, Unalp A, Van Natta M, Clark J, Brunt EM, Kleiner DE, Hoofnagle JH, Robuck PR; NASH CRN. Pioglitazone, vitamin E, or placebo for nonalcoholic steatohepatitis. *N Engl J Med* 2010; **362**: 1675-1685 [PMID: [20427778](#) DOI: [10.1056/NEJMoa0907929](#)]
- 7 **Neuschwander-Tetri BA**, Loomba R, Sanyal AJ, Lavine JE, Van Natta ML, Abdelmalek MF, Chalasani N, Dasarthy S, Diehl AM, Hameed B, Kowdley KV, McCullough A, Terrault N, Clark JM, Tonascia J, Brunt EM, Kleiner DE, Doo E; NASH Clinical Research Network. Farnesoid X nuclear receptor ligand obeticholic acid for non-cirrhotic, non-alcoholic steatohepatitis (FLINT): a multicentre, randomised, placebo-controlled trial. *Lancet* 2015; **385**: 956-965 [PMID: [25468160](#) DOI: [10.1016/S0140-6736\(14\)61933-4](#)]
- 8 **Tarantino G**, Citro V, Capone D. Nonalcoholic Fatty Liver Disease: A Challenge from Mechanisms to Therapy. *J Clin Med* 2019; **9** [PMID: [31861591](#) DOI: [10.3390/jcm9010015](#)]
- 9 **Zeuzem S.** Gut-liver axis. *Int J Colorectal Dis* 2000; **15**: 59-82 [PMID: [10855547](#)]
- 10 **Cani PD**, Amar J, Iglesias MA, Poggi M, Knauf C, Bastelica D, Neyrinck AM, Fava F, Tuohy KM, Chabo C, Waget A, Delmée E, Cousin B, Sulpice T, Chamontin B, Ferrières J, Tanti JF, Gibson GR, Casteilla L, Delzenne NM, Alessi MC, Burcelin R. Metabolic endotoxemia initiates obesity and insulin resistance. *Diabetes* 2007; **56**: 1761-1772 [PMID: [17456850](#) DOI: [10.2337/db06-1491](#)]
- 11 **Miele L**, Valenza V, La Torre G, Montalto M, Cammarota G, Ricci R, Mascianà R, Forgione A, Gabrieli ML, Perotti G, Vecchio FM, Rapaccini G, Gasbarrini G, Day CP, Grieco A. Increased intestinal permeability and tight junction alterations in nonalcoholic fatty liver disease. *Hepatology* 2009; **49**: 1877-1887 [PMID: [19291785](#) DOI: [10.1002/hep.22848](#)]
- 12 **Csak T**, Velayudham A, Hritz I, Petrasek J, Levin I, Lippai D, Catalano D, Mandrekar P, Dolganiuc A, Kurt-Jones E, Szabo G. Deficiency in myeloid differentiation factor-2 and toll-like receptor 4 expression attenuates nonalcoholic steatohepatitis and fibrosis in mice. *Am J Physiol Gastrointest Liver Physiol* 2011; **300**: G433-G441 [PMID: [21233280](#) DOI: [10.1152/ajpgi.00163.2009](#)]
- 13 **Seki E**, Schnabl B. Role of innate immunity and the microbiota in liver fibrosis: crosstalk between the liver and gut. *J Physiol* 2012; **590**: 447-458 [PMID: [22124143](#) DOI: [10.1113/jphysiol.2011.219691](#)]
- 14 **Gäbele E**, Dostert K, Hofmann C, Wiest R, Schölmerich J, Hellerbrand C, Obermeier F. DSS induced colitis increases portal LPS levels and enhances hepatic inflammation and fibrogenesis in experimental NASH. *J Hepatol* 2011; **55**: 1391-1399 [PMID: [21703208](#) DOI: [10.1016/j.jhep.2011.02.035](#)]
- 15 **Safari Z**, Gérard P. The links between the gut microbiome and non-alcoholic fatty liver disease (NAFLD). *Cell Mol Life Sci* 2019; **76**: 1541-1558 [PMID: [30683985](#) DOI: [10.1007/s00018-019-03011-w](#)]
- 16 **Aller R**, De Luis DA, Izaola O, Conde R, Gonzalez Sagrado M, Primo D, De La Fuente B, Gonzalez J. Effect of a probiotic on liver aminotransferases in nonalcoholic fatty liver disease patients: a double blind randomized clinical trial. *Eur Rev Med Pharmacol Sci* 2011; **15**: 1090-1095 [PMID: [22013734](#)]
- 17 **Malaguarnera M**, Vacante M, Antic T, Giordano M, Chisari G, Acquaviva R, Mastrojeni S, Malaguarnera G, Mistretta A, Li Volti G, Galvano F. Bifidobacterium longum with fructo-oligosaccharides in patients with non alcoholic steatohepatitis. *Dig Dis Sci* 2012; **57**: 545-553 [PMID: [21901256](#) DOI: [10.1007/s10620-011-1887-4](#)]



- 18 **Roberfroid M**, Gibson GR, Hoyles L, McCartney AL, Rastall R, Rowland I, Wolvers D, Watzl B, Szajewska H, Stahl B, Guarner F, Respondek F, Whelan K, Coxam V, Davicco MJ, Léotoing L, Wittrant Y, Delzenne NM, Cani PD, Neyrinck AM, Meheust A. Prebiotic effects: metabolic and health benefits. *Br J Nutr* 2010; **104** Suppl 2: S1-63 [PMID: [20920376](#) DOI: [10.1017/S0007114510003363](#)]
- 19 **Parnell JA**, Raman M, Rioux KP, Reimer RA. The potential role of prebiotic fibre for treatment and management of non-alcoholic fatty liver disease and associated obesity and insulin resistance. *Liver Int* 2012; **32**: 701-711 [PMID: [22221818](#) DOI: [10.1111/j.1478-3231.2011.02730.x](#)]
- 20 **Yoon SJ**, Chu DC, Raj Juneja L. Chemical and physical properties, safety and application of partially hydrolyzed guar gum as dietary fiber. *J Clin Biochem Nutr* 2008; **42**: 1-7 [PMID: [18231623](#) DOI: [10.3164/jcbs.2008001](#)]
- 21 **Giannini EG**, Mansi C, Dulbecco P, Savarino V. Role of partially hydrolyzed guar gum in the treatment of irritable bowel syndrome. *Nutrition* 2006; **22**: 334-342 [PMID: [16413751](#) DOI: [10.1016/j.nut.2005.10.003](#)]
- 22 **Alam NH**, Ashraf H, Sarker SA, Olesen M, Troup J, Salam MA, Gyr N, Meier R. Efficacy of partially hydrolyzed guar gum-added oral rehydration solution in the treatment of severe cholera in adults. *Digestion* 2008; **78**: 24-29 [PMID: [18769066](#) DOI: [10.1159/000152844](#)]
- 23 **Furnari M**, Parodi A, Gemignani L, Giannini EG, Marengo S, Savarino E, Assandri L, Fazio V, Bonfanti D, Inferriera S, Savarino V. Clinical trial: the combination of rifaximin with partially hydrolysed guar gum is more effective than rifaximin alone in eradicating small intestinal bacterial overgrowth. *Aliment Pharmacol Ther* 2010; **32**: 1000-1006 [PMID: [20937045](#) DOI: [10.1111/j.1365-2036.2010.04436.x](#)]
- 24 **Romano C**, Comito D, Famiani A, Calamarà S, Loddo I. Partially hydrolyzed guar gum in pediatric functional abdominal pain. *World J Gastroenterol* 2013; **19**: 235-240 [PMID: [23345946](#) DOI: [10.3748/wjg.v19.i2.235](#)]
- 25 **Dall'Alba V**, Silva FM, Antonio JP, Steemburgo T, Royer CP, Almeida JC, Gross JL, Azevedo MJ. Improvement of the metabolic syndrome profile by soluble fibre - guar gum - in patients with type 2 diabetes: a randomised clinical trial. *Br J Nutr* 2013; **110**: 1601-1610 [PMID: [23551992](#) DOI: [10.1017/S0007114513001025](#)]
- 26 **Yasukawa Z**, Naito Y, Takagi T, Mizushima K, Tokunaga M, Ishihara N, R Juneja L, Yoshikawa T. Partially hydrolyzed guar gum affects the expression of genes involved in host defense functions and cholesterol absorption in colonic mucosa of db/db male mice. *J Clin Biochem Nutr* 2012; **51**: 33-38 [PMID: [22798710](#) DOI: [10.3164/jcbs.11-104](#)]
- 27 **Ohashi Y**, Sumitani K, Tokunaga M, Ishihara N, Okubo T, Fujisawa T. Consumption of partially hydrolysed guar gum stimulates Bifidobacteria and butyrate-producing bacteria in the human large intestine. *Benef Microbes* 2015; **6**: 451-455 [PMID: [25519526](#) DOI: [10.3920/BM2014.0118](#)]
- 28 **Reider SJ**, Moosmang S, Tragust J, Trgovec-Greif L, Tragust S, Perschy L, Przysiecki N, Sturm S, Tilg H, Stuppner H, Rattei T, Moschen AR. Prebiotic Effects of Partially Hydrolyzed Guar Gum on the Composition and Function of the Human Microbiota-Results from the PAGODA Trial. *Nutrients* 2020; **12** [PMID: [32354152](#) DOI: [10.3390/nu12051257](#)]
- 29 **Matsuzawa N**, Takamura T, Kurita S, Misu H, Ota T, Ando H, Yokoyama M, Honda M, Zen Y, Nakanuma Y, Miyamoto K, Kaneko S. Lipid-induced oxidative stress causes steatohepatitis in mice fed an atherogenic diet. *Hepatology* 2007; **46**: 1392-1403 [PMID: [17929294](#) DOI: [10.1002/hep.21874](#)]
- 30 **Grisham MB**, Hernandez LA, Granger DN. Xanthine oxidase and neutrophil infiltration in intestinal ischemia. *Am J Physiol* 1986; **251**: G567-G574 [PMID: [3020994](#) DOI: [10.1152/ajpgi.1986.251.4.G567](#)]
- 31 **Luther J**, Garber JJ, Khalili H, Dave M, Bale SS, Jindal R, Motola DL, Luther S, Bohr S, Jeoung SW, Deshpande V, Singh G, Turner JR, Yarmush ML, Chung RT, Patel SJ. Hepatic Injury in Nonalcoholic Steatohepatitis Contributes to Altered Intestinal Permeability. *Cell Mol Gastroenterol Hepatol* 2015; **1**: 222-232 [PMID: [26405687](#) DOI: [10.1016/j.jcmgh.2015.01.001](#)]
- 32 **Nagahama S**, Korenaga D, Honda M, Inutsuka S, Sugimachi K. Assessment of the intestinal permeability after a gastrectomy and the oral administration of anticancer drugs in rats: nitric oxide release in response to gut injury. *Surgery* 2002; **131**: S92-S97 [PMID: [11821793](#)]
- 33 **Kish L**, Hotte N, Kaplan GG, Vincent R, Tso R, Gänzle M, Rioux KP, Thiesen A, Barkema HW, Wine E, Madsen KL. Environmental particulate matter induces murine intestinal inflammatory responses and alters the gut microbiome. *PLoS One* 2013; **8**: e62220 [PMID: [23638009](#) DOI: [10.1371/journal.pone.0062220](#)]
- 34 **Nagashima K**, Hisada T, Sato M, Mochizuki J. Application of new primer-enzyme combinations to terminal restriction fragment length polymorphism profiling of bacterial populations in human feces. *Appl Environ Microbiol* 2003; **69**: 1251-1262 [PMID: [12571054](#)]
- 35 **Suau A**, Bonnet R, Sutren M, Godon JJ, Gibson GR, Collins MD, Doré J. Direct analysis of genes encoding 16S rRNA from complex communities reveals many novel molecular species within the human gut. *Appl Environ Microbiol* 1999; **65**: 4799-4807 [PMID: [10543789](#)]
- 36 **Nagahama K**, Mochizuki J, Suzuki S, Shimomura K. Phylogenetic Analysis of 16S ribosomal RNA gene sequences from human fecal microbiota and improved utility of terminal restriction fragment length polymorphism profiling. *Biosci Microflora* 2006; **25**: 99-107 [DOI: [10.12938/bifidus.25.99](#)]
- 37 **Ushida K**, Sakata T. Effect of pH on oligosaccharide fermentation by porcine cecal digesta. *Animal Sci Technol* 1998; **69**: 100-107 [DOI: [10.2508/chikusan.69.100](#)]

- 38 **Van Herck MA**, Vonghia L, Francque SM. Animal Models of Nonalcoholic Fatty Liver Disease-A Starter's Guide. *Nutrients* 2017; **9**: 1072 [PMID: [28953222](#) DOI: [10.3390/nu9101072](#)]
- 39 **Henao-Mejia J**, Elinav E, Jin C, Hao L, Mehal WZ, Strowig T, Thaïss CA, Kau AL, Eisenbarth SC, Jurczak MJ, Camporez JP, Shulman GI, Gordon JI, Hoffman HM, Flavell RA. Inflammasome-mediated dysbiosis regulates progression of NAFLD and obesity. *Nature* 2012; **482**: 179-185 [PMID: [22297845](#) DOI: [10.1038/nature10809](#)]
- 40 **Mouries J**, Brescia P, Silvestri A, Spadoni I, Sorribas M, Wiest R, Mileti E, Galbiati M, Invernizzi P, Adorini L, Penna G, Rescigno M. Microbiota-driven gut vascular barrier disruption is a prerequisite for non-alcoholic steatohepatitis development. *J Hepatol* 2019; **71**: 1216-1228 [PMID: [31419514](#) DOI: [10.1016/j.jhep.2019.08.005](#)]
- 41 **Pessentheiner AR**, Ducasa GM, Gordts PLSM. Proteoglycans in Obesity-Associated Metabolic Dysfunction and Meta-Inflammation. *Front Immunol* 2020; **11**: 769 [PMID: [32508807](#) DOI: [10.3389/fimmu.2020.00769](#)]
- 42 **Power Guerra N**, Müller L, Pilz K, Glatzel A, Jenderny D, Janowitz D, Vollmar B, Kuhla A. Dietary-Induced Low-Grade Inflammation in the Liver. *Biomedicines* 2020; **8** [PMID: [33317065](#) DOI: [10.3390/biomedicines8120587](#)]
- 43 **Carotti S**, Guarino MP, Vespasiani-Gentilucci U, Morini S. Starring role of toll-like receptor-4 activation in the gut-liver axis. *World J Gastrointest Pathophysiol* 2015; **6**: 99-109 [PMID: [26600967](#) DOI: [10.4291/wjgp.v6.i4.99](#)]
- 44 **Pachikian BD**, Essaghir A, Demoulin JB, Catry E, Neyrinck AM, Dewulf EM, Sohet FM, Portois L, Clerbaux LA, Carpentier YA, Possemiers S, Bommer GT, Cani PD, Delzenne NM. Prebiotic approach alleviates hepatic steatosis: implication of fatty acid oxidative and cholesterol synthesis pathways. *Mol Nutr Food Res* 2013; **57**: 347-359 [PMID: [23203768](#) DOI: [10.1002/mnfr.201200364](#)]
- 45 **Abdou RM**, Zhu L, Baker RD, Baker SS. Gut Microbiota of Nonalcoholic Fatty Liver Disease. *Dig Dis Sci* 2016; **61**: 1268-1281 [PMID: [26898658](#) DOI: [10.1007/s10620-016-4045-1](#)]
- 46 **Le Roy T**, Llopis M, Lepage P, Bruneau A, Rabot S, Bevilacqua C, Martin P, Philippe C, Walker F, Bado A, Perlemuter G, Cassard-Doulcier AM, Gérard P. Intestinal microbiota determines development of non-alcoholic fatty liver disease in mice. *Gut* 2013; **62**: 1787-1794 [PMID: [23197411](#) DOI: [10.1136/gutjnl-2012-303816](#)]
- 47 **De Minicis S**, Rychlicki C, Agostinelli L, Saccomanno S, Candelaresi C, Trozzi L, Mingarelli E, Facinelli B, Magi G, Palmieri C, Marzoni M, Benedetti A, Svegliati-Baroni G. Dysbiosis contributes to fibrogenesis in the course of chronic liver injury in mice. *Hepatology* 2014; **59**: 1738-1749 [PMID: [23959503](#) DOI: [10.1002/hep.26695](#)]
- 48 **Jin CJ**, Sellmann C, Engstler AJ, Ziegenhardt D, Bergheim I. Supplementation of sodium butyrate protects mice from the development of non-alcoholic steatohepatitis (NASH). *Br J Nutr* 2015; **114**: 1745-1755 [PMID: [26450277](#) DOI: [10.1017/S0007114515003621](#)]
- 49 **Hiippala K**, Jouhten H, Ronkainen A, Hartikainen A, Kainulainen V, Jalanka J, Satokari R. The Potential of Gut Commensals in Reinforcing Intestinal Barrier Function and Alleviating Inflammation. *Nutrients* 2018; **10** [PMID: [30060606](#) DOI: [10.3390/nu10080988](#)]
- 50 **Feng Y**, Wang Y, Wang P, Huang Y, Wang F. Short-Chain Fatty Acids Manifest Stimulative and Protective Effects on Intestinal Barrier Function Through the Inhibition of NLRP3 Inflammasome and Autophagy. *Cell Physiol Biochem* 2018; **49**: 190-205 [PMID: [30138914](#) DOI: [10.1159/000492853](#)]



## Retrospective Cohort Study

# Factors influencing the failure of interferon-free therapy for chronic hepatitis C: Data from the Polish EpiTer-2 cohort study

Ewa Janczewska, Mateusz Franciszek Kołek, Beata Lorenc, Jakub Klapaczyński, Magdalena Tudrujek-Zdunek, Marek Sitko, Włodzimierz Mazur, Dorota Zarębska-Michaluk, Iwona Buczyńska, Dorota Dybowska, Agnieszka Czauż-Andrzejuk, Hanna Berak, Rafał Krygier, Jerzy Jaroszewicz, Jolanta Citko, Anna Piekarska, Beata Dobracka, Łukasz Socha, Zbigniew Deroń, Łukasz Laurans, Jolanta Białkowska-Warzecha, Olga Tronina, Brygida Adamek, Krzysztof Tomasiewicz, Krzysztof Simon, Małgorzata Pawłowska, Waldemar Halota, Robert Flisiak

**ORCID number:** Ewa Janczewska 0000-0002-5406-4603; Mateusz Franciszek Kołek 0000-0001-6470-4830; Beata Lorenc 0000-0002-6319-9278; Jakub Klapaczyński 0000-0003-0209-1930; Magdalena Tudrujek-Zdunek 0000-0002-5640-5432; Marek Sitko 0000-0003-3078-8604; Włodzimierz Mazur 0000-0001-9023-2670; Dorota Zarębska-Michaluk 0000-0003-0938-1084; Iwona Buczyńska 0000-0003-4446-9102; Dorota Dybowska 0000-0002-1961-8519; Agnieszka Czauż-Andrzejuk 0000-0002-5753-5589; Hanna Berak 0000-0002-0844-9158; Rafał Krygier 0000-0003-3821-6854; Jerzy Jaroszewicz 0000-0003-0139-4753; Jolanta Citko 0000-0003-0323-9466; Anna Piekarska 0000-0002-7188-4881; Beata Dobracka 0000-0003-3171-4711; Łukasz Socha 0000-0001-9871-5327; Zbigniew Deroń 0000-0002-5368-1845; Łukasz Laurans 0000-0001-5751-7308; Jolanta Białkowska-Warzecha 0000-0002-2728-3456; Olga Tronina 0000-0001-9446-5324; Brygida Adamek 0000-0002-3300-4935; Krzysztof Tomasiewicz 0000-0001-7868-2708; Krzysztof Simon 0000-0002-8040-0412; Małgorzata Pawłowska 0000-0002-6044-0425; Waldemar Halota 0000-0003-2952-2374; Robert Flisiak 0000-0003-3394-1635.

**Ewa Janczewska, Brygida Adamek**, Department of Basic Medical Sciences, The School of Health Sciences in Bytom, Medical University of Silesia, Bytom 41-902, Poland

**Mateusz Franciszek Kołek**, Department of Animal Physiology, Faculty of Biology, University of Warsaw, Warszawa 02-096, Poland

**Beata Lorenc**, Pomeranian Center of Infectious Diseases, Medical University Gdańsk, Gdańsk 80-214, Poland

**Jakub Klapaczyński**, Department of Internal Medicine and Hepatology, Central Clinical Hospital of the Ministry of Internal Affairs and Administration, Warszawa 02-507, Poland

**Magdalena Tudrujek-Zdunek, Krzysztof Tomasiewicz**, Department of Infectious Diseases, Medical University of Lublin, Lublin 20-081, Poland

**Marek Sitko**, Department of Infectious and Tropical Diseases, Jagiellonian University, Kraków 30-688, Poland

**Włodzimierz Mazur**, Clinical Department of Infectious Diseases, Medical University of Silesia in Katowice, Chorzów 41-500, Poland

**Dorota Zarębska-Michaluk**, Department of Infectious Diseases, Jan Kochanowski University Kielce, Kielce 25-369, Poland

**Iwona Buczyńska, Krzysztof Simon**, Department of Infectious Diseases and Hepatology, Medical University Wrocław, Wrocław 51-149, Poland

**Dorota Dybowska**, Department of Infectious Diseases and Hepatology, Ludwik Rydygier Collegium Medicum in Bydgoszcz Faculty of Medicine Nicolaus Copernicus University in Toruń, Bydgoszcz 85-030, Poland

**Agnieszka Czauż-Andrzejuk, Robert Flisiak**, Department of Infectious Diseases and Hepatology, Medical University of Białystok, Białystok 15-540, Poland

**Hanna Berak**, One-Day Department, Hospital for Infectious Diseases in Warsaw, Warszawa 01-

**Author contributions:** Janczewska E and Flisiak R conceived the study design; Janczewska E, Lorenc B, Klapaczyński J, Tudrujek-Zdunek M, Sitko M, Mazur W, Zarębska-Michaluk D, Buczyńska I, Dybowska D, Czauż-Andrzejuk A, Berak H, Krygier R, Jaroszewicz J, Citko J, Piekarska A, Dobracka B, Socha Ł, Deroń Z, Laurans Ł, Białkowska-Warzecha J, Tronina O, Adamek B, Tomaszewicz K, Simon K, Pawłowska M, Halota W and Flisiak R acquired the data; Janczewska E and Kołek MF analyzed and interpreted the data; Kołek MF performed statistical analysis, Janczewska E drafted the manuscript; Janczewska E, Kołek MF, Lorenc B, Klapaczyński J, Tudrujek-Zdunek M, Sitko M, Mazur W, Zarębska-Michaluk D, Buczyńska I, Dybowska D, Czauż-Andrzejuk A, Berak H, Krygier R, Jaroszewicz J, Citko J, Piekarska A, Dobracka B, Socha Ł, Deroń Z, Laurans Ł, Białkowska-Warzecha J, Tronina O, Adamek B, Tomaszewicz K, Simon K, Pawłowska M, Halota W and Flisiak R made critical revisions related to important intellectual content of the manuscript and approved the final version of the manuscript.

#### Institutional review board

**statement:** Patients participating in the study were not exposed to any experimental interventions, nor did the study intervene with the clinical management of the patient. The study only collected information from patient records. The data were originally collected to assess treatment efficacy and safety in individual patients, not for scientific purposes. Hence, the treating physicians did not obtain approval from the ethics committee. According to local law (Pharmaceutical Law of 6th September 2001, art. 37a), non-interventional studies do not require ethics committee approval.

**Informed consent statement:** All study participants provided informed consent for treatment and the processing of personal data.

201, Poland

**Rafał Krygier**, Outpatient Clinic, State University of Applied Sciences in Konin, Konin 62-510, Poland

**Jerzy Jaroszewicz**, Department of Infectious Diseases and Hepatology, Medical University of Silesia in Katowice, Bytom 41-902, Poland

**Jolanta Citko**, Department of Medical Practice of Infections, Regional Hospital, Olsztyn 10-561, Poland

**Anna Piekarska**, Department of Infectious Diseases and Hepatology, Medical University of Łódź, Łódź 90-419, Poland

**Beata Dobracka**, MedicalSpec Center, Wrocław 53-428, Poland

**Łukasz Socha, Łukasz Laurans**, Department of Infectious Diseases, Hepatology and Liver Transplantation, Pomeranian Medical University, Szczecin 71-455, Poland

**Zbigniew Deroń**, Ward of Infectious Diseases and Hepatology, Biegański Regional Specialist Hospital, Łódź 91-347, Poland

**Łukasz Laurans**, Infectious and Liver Diseases Clinic, Multidisciplinary Regional Hospital, Gorzów Wielkopolski 66-400, Poland

**Jolanta Białkowska-Warzecha**, Department of Infectious and Liver Diseases, Medical University of Łódź, Łódź 91-347, Poland

**Olga Tronina**, Department of Transplantation Medicine, Nephrology, and Internal Diseases, Medical University of Warsaw, Warszawa 02-091, Poland

**Malgorzata Pawłowska**, Department of Paediatric Infectious Diseases and Hepatology, Faculty of Medicine, Collegium Medicum Bydgoszcz, Nicolaus Copernicus University Toruń, Bydgoszcz 85-030, Poland

**Waldemar Halota**, Department of Infectious Diseases and Hepatology, Ludwik Rydygier Collegium Medicum in Bydgoszcz, Faculty of Medicine, Nicolaus Copernicus University in Toruń, Bydgoszcz 85-030, Poland

**Corresponding author:** Ewa Janczewska, DSc, MD, PhD, Adjunct Professor, Department of Basic Medical Sciences, The School of Health Sciences in Bytom, Medical University of Silesia, Piekarska 18, Bytom 41-902, Poland. [ejanczewska@sum.edu.pl](mailto:ejanczewska@sum.edu.pl)

## Abstract

### BACKGROUND

The introduction of direct-acting antiviral drugs into clinical practice has revolutionized the treatment of chronic hepatitis C, making it highly effective and safe for patients. However, few researchers have analyzed the factors causing therapy failure in some patients.

### AIM

To analyze factors influencing the failure of direct antiviral drugs in the large, multicenter EpiTer-2 cohort in a real-world setting.

### METHODS

The study cohort consisted of patients with chronic hepatitis C treated at 22 Polish centers from 2016-2020. Data collected from the online EpiTer-2 database included the following: hepatitis C virus (HCV) genotype, stage of fibrosis, hematology and liver function parameters, Child-Turcotte-Pugh and Model for End-stage Liver Disease scores, prior antiviral therapy, concomitant diseases, and drugs used in relation to hepatitis B virus (HBV) and/or human immunodeficiency virus (HIV) coinfections. Adverse events observed during the treatment and follow-up period were reported. Both standard and machine learning methods were used for statistical analysis.



**Conflict-of-interest statement:**

Janczewska E has acted as a speaker and/or advisor for AbbVie, Gilead, MSD, Ipsen, and has received funding for clinical trials from AbbVie, Allergan, BMS, Celgene, Cymabay, Dr Falk Pharma, Exelixis, GSK, and MSD. Jakub Klapaczynski has acted as a speaker for Gilead and AbbVie. Mazur W has acted as a speaker and/or advisor for AbbVie, Gilead, Merck, and has received funding for clinical trials from AbbVie, Gilead, and Janssen. Zarębska-Michaluk D has acted as a speaker for AbbVie and Gilead. Dybowska D has received funding for participation in the conference: from AbbVie. Czauż-Andrzejuk A has received funding for clinical trials from AbbVie and Merck. Berak H has acted as a speaker and/or advisor for Gilead, AbbVie, and MSD. Krygier R has acted as a consultant for AbbVie and Gilead. Jaroszewicz J has acted as a speaker and/or advisor for AbbVie, Gilead, Merck, Roche, AlfaSigma, MSD, Gilead and PRO.MED. CS. Piekarska A has acted as a speaker and/or advisor for AbbVie, Gilead, Merck, and Roche. Socha Ł has acted as a consultant for BMS. Brygida Adamek has acted as a speaker for AbbVie, Gilead, and MSD. Tomaszewicz K has acted as a speaker and/or advisor AbbVie, Alfa Wasserman, BMS, Gilead, Janssen, Merck, Roche, and has received funding for clinical trials from AbbVie, BMS, Gilead, Janssen, Merck, and Roche. Simon K has acted as a speaker and/or advisor: AbbVie, Gilead, Merck, Alfa-Wassermann, Novartis, Lilly, Bayer, and has received funding for clinical trials from: AbbVie, Allergan, Bayer, Eisai, Gilead, Intercept, Pfizer. Pawłowska M has acted as a speaker and/or advisor for AbbVie, Gilead, Merck, Roche and has received funding for clinical trials from AbbVie, Gilead, and Roche. Halota W has acted as a speaker and/or advisor for AbbVie, BMS, Gilead, Janssen, Merck, Roche, and has received funding for clinical trials from AbbVie, Gilead, and Roche. Flisiak

**RESULTS**

During analysis, 12614 patients with chronic hepatitis C were registered, of which 11938 (mean age: 52 years) had available sustained virologic response (SVR) data [11629 (97%) achieved SVR and 309 (3%) did not]. Most patients (78.1%) were infected with HCV genotype 1b. Liver cirrhosis was diagnosed in 2974 patients, while advanced fibrosis (F3) was diagnosed in 1717 patients. We included patients with features of hepatic failure at baseline [ascites in 142 (1.2%) and encephalopathy in 68 (0.6%) patients]. The most important host factors negatively influencing treatment efficacy were liver cirrhosis, clinical and laboratory features of liver failure, history of hepatocellular carcinoma, and higher body mass index. Among viral factors, genotype 3 and viral load also exerted an influence on treatment efficacy. Classical statistical analysis revealed that treatment ineffectiveness seemed to be influenced by the male sex, which was not confirmed by the multivariate analysis using the machine learning algorithm (random forest). Coinfection with HBV (including patients with on-treatment reactivation of HBV infection) or HIV, extrahepatic manifestations, and renal failure did not significantly affect the treatment efficacy.

**CONCLUSION**

In patients with advanced liver disease, individualized therapy (testing for resistance-associated variants and response-guided treatment) should be considered to maximize the chance of achieving SVR.

**Key Words:** Advanced liver disease; Chronic hepatitis C; Direct-acting antiviral drugs; Sustained virologic response; Interferon-free therapy; Antiviral therapy

©The Author(s) 2021. Published by Baishideng Publishing Group Inc. All rights reserved.

**Core Tip:** We analyzed factors influencing the failure of direct-acting antiviral drugs (DAAs) in a large, multicenter EpiTer-2 cohort of patients treated across 22 centers. Our findings demonstrate that failure of DAA treatment occurred mainly in patients with liver cirrhosis and deterioration of liver function. Our machine learning analysis further revealed that older age and creatinine and hemoglobin levels also influenced treatment failure, as did viral factors such as genotype 3 and viral load. Thus, in patients with advanced liver disease, individualized therapy (testing for resistance-associated variants, response-guided treatment) should be considered to maximize the chance of achieving a sustained virologic response.

**Citation:** Janczewska E, Kołek MF, Lorenc B, Klapaczynski J, Tudrujek-Zdunek M, Sitko M, Mazur W, Zarębska-Michaluk D, Buczyńska I, Dybowska D, Czauż-Andrzejuk A, Berak H, Krygier R, Jaroszewicz J, Citko J, Piekarska A, Dobracka B, Socha Ł, Deroń Z, Laurans Ł, Białkowska-Warzecha J, Tronina O, Adamek B, Tomaszewicz K, Simon K, Pawłowska M, Halota W, Flisiak R. Factors influencing the failure of interferon-free therapy for chronic hepatitis C: Data from the Polish EpiTer-2 cohort study. *World J Gastroenterol* 2021; 27(18): 2177-2192

**URL:** <https://www.wjgnet.com/1007-9327/full/v27/i18/2177.htm>

**DOI:** <https://dx.doi.org/10.3748/wjg.v27.i18.2177>

**INTRODUCTION**

The introduction of direct-acting antiviral drugs (DAAs) into clinical practice has revolutionized the treatment of chronic hepatitis C, making it highly effective and safe for patients. Interferon-free therapies with a short duration and the absence of significant adverse events (AEs) allow for a sustained virologic response (SVR) in over 90% of patients, both in randomized clinical trials[1-3] and in real-world settings[4,5]. Previous research has demonstrated that pangenotypic therapies significantly increase the effectiveness of treatment in patients infected with hepatitis C virus (HCV) genotype 3, which is considered more difficult to treat[6-9].



R has acted as a speaker and/or advisor, and has received funding for clinical trials from AbbVie, Gilead, Merck, and Roche. Lorenc B, Kolek MF, Tudrujek-Zdunek M, Sitko M, Buczyńska I, Citko J, Dobracka B, Deroń Z, Laurans Ł, Białkowska-Warzechka J and Tronina O have no conflict of interest to declare.

**Data sharing statement:** The original anonymous dataset is available on request from the corresponding author at [ejanczewska@sum.edu.pl](mailto:ejanczewska@sum.edu.pl).

**STROBE statement:** The authors have read the STROBE Statement-checklist of items, and the manuscript was prepared and revised according to the STROBE Statement-checklist of items.

**Open-Access:** This article is an open-access article that was selected by an in-house editor and fully peer-reviewed by external reviewers. It is distributed in accordance with the Creative Commons Attribution NonCommercial (CC BY-NC 4.0) license, which permits others to distribute, remix, adapt, build upon this work non-commercially, and license their derivative works on different terms, provided the original work is properly cited and the use is non-commercial. See: <http://creativecommons.org/licenses/by-nc/4.0/>

**Manuscript source:** Invited manuscript

**Specialty type:** Gastroenterology and hepatology

**Country/Territory of origin:** Poland

**Peer-review report's scientific quality classification**

Grade A (Excellent): 0  
Grade B (Very good): B, B, B, B  
Grade C (Good): C  
Grade D (Fair): 0  
Grade E (Poor): 0

**Received:** January 26, 2021

**Peer-review started:** January 26, 2021

**First decision:** February 27, 2021

Numerous studies have confirmed the high efficacy of treatment with DAAs in almost all groups of patients, including those with liver cirrhosis, renal failure, and organ transplants, regardless of age or concomitant diseases, including human immunodeficiency virus (HIV) or hepatitis B virus (HBV) coinfections[10,11].

Most of the publications evaluating interferon-free therapies are devoted to assessing their efficacy and safety. Few researchers, however, have analyzed the factors that cause the therapy to fail in some patients. Therefore, we aimed to analyze this issue in the large, multicenter EpiTer-2 cohort and to present the characteristics of patients in whom DAA treatment has failed in a real-world setting. Knowledge of these factors may aid in determining the qualifying criteria for antiviral therapy and the way it is conducted, which would further minimize the failure rate.

Achieving SVR does not completely exclude the development adverse consequences of chronic hepatitis C, but there are no better methods to prevent the progression of liver fibrosis, development of cirrhosis, liver failure, and hepatocellular carcinoma (HCC) than to eliminate the infection. Thus, all measures should be taken to maximize treatment efficacy.

## MATERIALS AND METHODS

### Study population

In 2016, on the initiative of investigators, a group of 22 Polish centers began collecting data on the efficacy and safety of drugs used in the treatment of patients with chronic hepatitis C. This study, called EpiTer-2, was supported by the Polish Association of Epidemiologists and Infectologists. The data were collected using a web-based questionnaire, in accordance with the National General Data Protection Regulation.

The therapies were financed by the National Health Fund under general health insurance. The parameters collected in the database were as follows: HCV genotype, stage of fibrosis, hematology and liver function parameters, Child-Turcotte-Pugh and Model for End-stage Liver Disease (MELD) scores, prior antiviral therapy, concomitant diseases and drugs used in relation to them, HBV and/or HIV coinfections.

Hepatic fibrosis was evaluated *via* a liver biopsy based on the METAVIR or Scheuer scoring system, transient elastography using the FibroScan (Echosens, Paris) device, or real-time shear wave elastography) using the Aixplorer (Supersonic, Aix-en-Provence) device.

HCV RNA was monitored prior to and after the treatment (end of treatment virologic response), and then after at least a 12-wk follow-up period (SVR). Two assays were used to measure HCV RNA, depending on local practices at the testing site: Roche COBAS TaqMan with a lower limit of quantification (LLOQ) of 15 IU/mL or Abbott RealTime with an LLOQ of 12 IU/mL.

Peripheral blood counts, liver function, and kidney function were evaluated to assess the safety of the therapy. The basic scope of tests and schedule of patients' visits were defined in the National Health Fund therapeutic program. For the safety of the patient, additional examinations were performed if necessary.

The drug used, the dosage and length of the treatment regimen, and the decision to add ribavirin were determined by treating physicians based on the applicable product characteristics and recommendations of the Polish Group of Experts for HCV[12].

AEs observed during the treatment and follow-up periods were reported as well, with particular attention to events related to liver disease.

### Ethical considerations

This observational study was conducted in a real-world setting with approved drugs. Patients were not exposed to any experimental interventions, nor did the study intervene with the clinical management of the patient. The study only collected information from patient records. The analysis included routine examinations and tests performed in patients treated within the therapeutic program of the National Health Fund. The data were originally collected to assess treatment efficacy and safety in individual patients, not for scientific purposes. Hence, the treating physicians did not obtain approval from the ethics committee. According to local law (Pharmaceutical Law of 6<sup>th</sup> September 2001, art. 37a), non-interventional studies do not require ethics committee approval. Patients provided informed consent for treatment and the processing of personal data. Patient data were collected through an online system, and only physicians caring for patients had access to the patients' personal information. Planning, conduct, and reporting of the study were in line with the tenets outlined in

**Revised:** March 13, 2021**Accepted:** April 20, 2021**Article in press:** April 20, 2021**Published online:** May 14, 2021**P-Reviewer:** Anastasiou I, Derviş Hakim G, Feng QS, Grawish ME, Irato P**S-Editor:** Gao CC**L-Editor:** A**P-Editor:** Wang LL

the Declaration of Helsinki, as revised in 2013.

### Statistical analysis

To identify the best predictors of HCV detectability by at least the 12<sup>th</sup> week of follow-up, machine learning (ML) techniques were used to develop a statistical model. First, variables with more than 10% of missing observations were removed from the dataset.

Because the dataset was unbalanced for the dependent variable, an oversampling technique was used. The data were split into learning (75%) and testing (25%) sets. Four ML models were built using the following algorithm types: k-nearest neighbor, support vector machine, classification and regression tree, and random forest. The algorithm with the best accuracy was used for further analysis. Then, the selected parameters were optimized to boost the algorithm performance. Twelve variables with the highest predictive value were plotted.

Standard statistical methods were used to compare data between patients positive and negative for HCV at least 12 wk after the end of treatment.

Data are presented as the mean [95% confidence interval (CI)] for continuous variables and as counts (%) for categorical variables. Groups were compared with nonparametric Mann-Whitney *U*-tests and Pearson chi-square tests.

The parametric tests were not used because of the unequal sample size (SVR *n* = 11629; non-SVR *n* = 309).

Analysis was performed using the R programming language in RStudio (R Core Team, 2020) and IBM SPSS Statistics 25 (IBM Corp., 2017). The level of statistical significance was set at *P* < 0.05.

## RESULTS

Patients' disposition and treatment outcomes are presented in **Figure 1**. At the time of analysis, a total of 12614 patients with chronic hepatitis C were registered in the database, of which 11938 had available SVR data. Among them, 11629 (97%) achieved SVR, while 309 (3%) did not.

### Characteristics of the study group

The baseline characteristics of patients with SVR and their relationships to treatment efficacy are presented in Tables 1 and 2. As there were missing data for some parameters, the number of patients for a given parameter is not always equal to the total number of patients.

The studied population consisted of 5762 men (48.3%) and 6176 women (51.7%), with a mean age of 52 years. Most patients (78.1%) were infected with HCV genotype 1b, which is typical for the population of Polish patients with chronic hepatitis C. Liver cirrhosis was diagnosed in 2974 patients, while advanced fibrosis (F3) was diagnosed in 1717 patients. The study group also included patients with features of hepatic failure at baseline: ascites in 142 (1.2%) patients and encephalopathy in 68 (0.6%) patients. Esophageal varices were diagnosed in 989 (10.5%) patients.

A history of HCC was documented in 179 patients (1.5%), and 146 (1.2%) patients underwent liver transplantation prior to the antiviral treatment. HIV coinfection was diagnosed in 587 (5%) patients, while HBV coinfection was diagnosed in 1570 (13.5%) patients, among whom 124 patients were HBsAg-positive.

### Treatment regimens

Treatment regimens and the percentages of patients taking particular medications among patients who achieved or did not achieve SVR are presented in **Figure 2**. The most commonly used drugs during the study (2016-2020) were paritaprevir/ritonavir/ombitasvir +/- dasabuvir +/- ribavirin (RBV); ledipasvir/sofosbuvir (LDV/SOF) +/- RBV; grazoprevir/elbasvir +/- RBV, glecaprevir/pibrentasvir, and velpatasvir/SOF +/- RBV.

The remaining drugs, asunaprevir plus daclatasvir (ASV+DCV) or SOF + RBV, were used during the initial period of the EpiTer-2 study, and fewer patients were treated with these drugs.

The percentages of patients treated with VEL/SOF +/- RBV, ASV + DCV, and SOF + RBV were higher among patients without SVR than among those who achieved SVR.

The vast majority of patients received complete therapy as planned, although treatment was terminated prematurely in 86 (0.7%) and modified in 275 (2.2%). The modifications were mainly related to changes in the dose of RBV. The proportion of patients not completing full scheduled therapy was higher in the non-SVR group than

**Table 1** Baseline characteristics of patients with and without sustained virologic response and their relationship to treatment efficacy

Variable	Total, <i>n</i> = 11938	SVR, <i>n</i> = 11629	Non-SVR, <i>n</i> = 309	<i>P</i> value
Sex, <i>n</i> (%)				
Male	5762 (48.3)	5553 (47.8)	209 (67.6)	< 0.001
Female	6176 (51.7)	6076 (52.2)	100 (32.4)	
Age	52.24 (51.77-52.70)	52.24 (51.77-52.71)	52.16 (50.74-53.58)	0.869
BMI (kg/m <sup>2</sup> )	26.47 (26.29-26.64)	26.45 (26.26-26.62)	27.20 (26.68-27.72)	< 0.001
Fibrosis				
F0	277 (1.9)	225 (99.1)	2 (0.9)	
F1	4539 (38.8)	4469 (98.5)	70 (1.5)	
F2	2249 (19.2)	2204 (98.0)	45 (2.0)	< 0.001
F3	1717 (14.7)	1684 (98.1)	33 (1.9)	
F4	2974 (25.4)	2828 (95.1)	146 (4.9)	
Liver stiffness (kPa)	12.72 (12.45-12.99)	12.53 (12.29-12.76)	20.27 (14.78-25.76)	< 0.001
Child Pugh, <i>n</i> (%)				
A	11320 (96.9)	11050 (97.1)	270 (89.7)	
B	346 (3.0)	315 (2.8)	31 (10.3)	< 0.001
C	13 (0.1)	13 (0.1)	0 (0.0)	
MELD score	7.81 (7.76-7.85)	7.79 (7.74-7.84)	8.39 (8.11-8.67)	< 0.001
Esophageal varices, <i>n</i> (%)				
Yes	989 (10.5)	922 (10.1)	67 (27.1)	< 0.001
No	8413 (89.5)	8233 (89.9)	180 (72.9)	
Ascites at the start of the treatment, <i>n</i> (%)				
No	11742 (98.8)	11444 (98.9)	298 (96.4)	
Moderate	136 (1.2)	125 (1.1)	11 (3.6)	< 0.001
Tense	6 (0.0)	6 (0.0)	0 (0.0)	
Encephalopathy at the start of the treatment, <i>n</i> (%)				
No	11808 (99.4)	11507 (99.5)	301 (97.8)	
Grade 1-2	67 (0.6)	60 (0.5)	7 (2.2)	0.001
Grade 3-4	1 (0.0)	1 (0.0)	0 (0.0)	
History of hepatocellular carcinoma, <i>n</i> (%)				
Yes	179 (1.5)	167 (1.5)	12 (4.1)	< 0.001
No	11515 (98.5)	11231 (98.5)	284 (95.9)	
Extrahepatic manifestations, <i>n</i> (%)				
Yes	948 (8.3)	916 (8.2)	32 (10.8)	0.282
No	10513 (91.7)	10248 (91.8)	265 (89.2)	
HIV coinfection, <i>n</i> (%)				
Yes	587 (5.0)	564 (4.9)	23 (7.6)	0.098
No	11161 (95.0)	10881 (95.1)	280 (92.4)	
HBV coinfection, <i>n</i> (%)				
Yes	1570 (13.5)	1526 (13.4)	44 (14.6)	0.851
No	10098 (86.5)	9840 (86.6)	258 (85.4)	

HBsAg(+), <i>n</i> (%)	124 (8.0)	122 (8.1)	2 (4.5)	0.543
Reactivation of HBV infection, <i>n</i> (%)				
Yes	11 (0.1)	11 (0.1)	0 (0.0)	0.510
No	10707 (99.9)	10435 (99.9)	272 (100.0)	
History of liver transplantation, <i>n</i> (%)				
Yes	146 (1.2)	144 (1.3)	2 (0.7)	0.576
No	11555 (98.8)	11253 (98.7)	302 (99.3)	
Course of treatment, <i>n</i> (%)				
As planned	11516 (97.1)	11238 (97.3)	278 (90.2)	
Terminated early	86 (0.7)	71 (0.6)	15 (4.9)	< 0.001
Modified	257 (2.2)	242 (2.1)	15 (4.9)	
Ascites appearing while on treatment, <i>n</i> (%)				
Yes	64 (0.5)	57 (0.5)	7 (2.3)	< 0.001
No	11773 (99.5)	11473 (99.5)	300 (97.7)	
Encephalopathy appearing while on treatment, <i>n</i> (%)				
Yes	43 (0.4)	35 (0.3)	8 (2.6)	< 0.001
No	11773 (99.6)	11474 (99.7)	299 (97.4)	
Gastrointestinal bleeding while on treatment, <i>n</i> (%)				
Yes	16 (0.1)	14 (0.1)	2 (0.7)	0.044
No	11798 (99.9)	11494 (99.9)	304 (99.3)	

SVR: Sustained virologic response; BMI: Body mass index; MELD: Model for End-stage Liver Disease; HBV: Hepatitis B virus; INR: International normalized ratio; PLT: Platelets; ALT: Alanine aminotransferase; eGFR: Estimated glomerular filtration rate; HCV: Hepatitis C virus.

in the SVR group; however, overall, it was not high (4.9% for both terminated and modified treatments).

### **Factors influencing treatment efficacy assessed using “traditional” statistics**

**Host factors:** In the group of patients who did not achieve SVR, men predominated (67.7%). No age-related differences between the SVR and non-SVR groups were observed in the standard statistical analysis. However, body mass index (BMI) and mean liver stiffness (20.27 *vs* 12.35 kPa) were higher in the non-SVR group than in the SVR group.

DAA therapy was more often ineffective in patients with liver cirrhosis (F4 4.9% *vs* F3 1.9%; F2 2.0%; F1 1.5%; F0 0.9%), and with symptoms of liver failure (ascites, encephalopathy, esophageal varices, or higher Child-Pugh or MELD scores) at baseline. In addition, the occurrence of symptoms of liver failure during therapy decreased the probability of achieving SVR. Significant differences in laboratory markers of liver injury and function [alanine aminotransferase, albumin, bilirubin, international normalized ratio (INR), and platelet count] were also observed between the SVR and non-SVR groups ( $P < 0.001$ ). However, it is worth noting that all 13 patients classified into Child-Pugh class C at baseline achieved SVR.

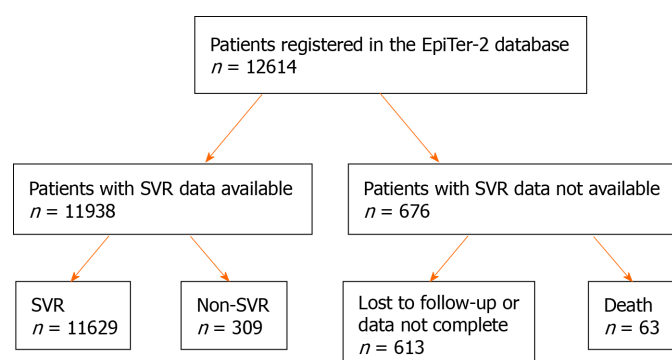
The percentage of patients with a history of HCC was significantly higher in the non-SVR group than in the SVR group (4.2% *vs* 1.5%,  $P < 0.001$ ). Coinfection with HBV (including patients with on-treatment reactivation of HBV infection) or HIV, extrahepatic manifestations, and renal failure did not significantly affect the efficacy of therapy.

**Viral factors:** Infection with the HCV genotype 3 was more common in the non-SVR group than in the SVR group (34.6% *vs* 10.5%). Viral load was also higher among those without SVR (6.36  $\log_{10}$  *vs* 6.39  $\log_{10}$ ).

**Table 2** Baseline characteristics of patients with and without sustained virologic response and their relationship to treatment efficacy-laboratory parameters

Variable	Total, <i>n</i> = 11938	SVR, <i>n</i> = 11629	Non-SVR, <i>n</i> = 309	<i>P</i> value
Albumin (g/dL)	4.37 (4.2-4.45)	4.38 (4.29-4.46)	4.02 (3.76-4.28)	< 0.001
Bilirubin (mg/dL)	0.80 (0.79-0.81)	0.79 (0.78-0.80)	1.06 (0.98-1.15)	< 0.001
INR	1.10 (1.07-1.12)	1.10 (1.07-1.12)	1.11 (1.08-1.13)	< 0.001
PLT (K/ $\mu$ L)	191.47 (190.07-192.85)	192.62 (191.22-194.02)	147.63 (139.07-156.19)	< 0.001
ALT (U/L)	78.39 (77.19-79.59)	77.92 (76.71-79.13)	96.07 (87.16-104.98)	< 0.001
Creatinine (mg/dL)	0.92 (0.89-0.96)	0.93 (0.89-0.96)	0.81 (0.79-0.83)	0.749
eGFR, <i>n</i> (%)				
< 30 mL/min	137 (29.2)	137 (29.7)	0 (0.0)	0.252
> 60 mL/min	160 (34.0)	157 (34.0)	3 (37.5)	
30-60 mL/min	173 (36.8)	168 (36.3)	5 (62.5)	
Hemoglobin (g/dL)	14.40 (14.37-14.43)	14.40 (14.37-14.44)	14.35 (14.15-14.55)	0.812
HCV genotype, <i>n</i> (%)				
1A	434 (3.6)	426 (3.7)	8 (2.6)	< 0.001
1B	9327 (78.1)	9147 (78.7)	180 (58.3)	
2	20 (0.2)	20 (0.2)	0 (0.0)	
3	1328 (11.1)	1221 (10.5)	107 (34.6)	
4	575 (4.8)	565 (4.9)	10 (3.2)	
5	1 (0.0)	1 (0.0)	0 (0.0)	
6	2 (0.0)	2 (0.0)	0 (0.0)	
HCV RNA (log <sub>10</sub> )	6.37 (6.34-6.39)	6.36 (6.34-6.39)	6.39 (6.31-6.46)	0.004

SVR: Sustained virologic response; INR: International normalized ratio; PLT: Platelets; ALT: Alanine aminotransferase; eGFR: Estimated glomerular filtration rate; HCV: Hepatitis C virus.

**Figure 1** Patient disposition and treatment outcomes. SVR: Sustained virologic response.

### Multivariate analysis using ML methods

ML techniques were used to develop a predictive model. The variables in which the missing data accounted for over 10% of all observations were extracted from the database and removed from the analysis. Although four models were constructed using ML algorithms, the random forest model was selected because it yielded the best prediction accuracy. The accuracy of the models is presented in [Figure 3](#). The area under the receiver operating characteristic curve for the random forest model was 0.999 ([Figure 4](#)).



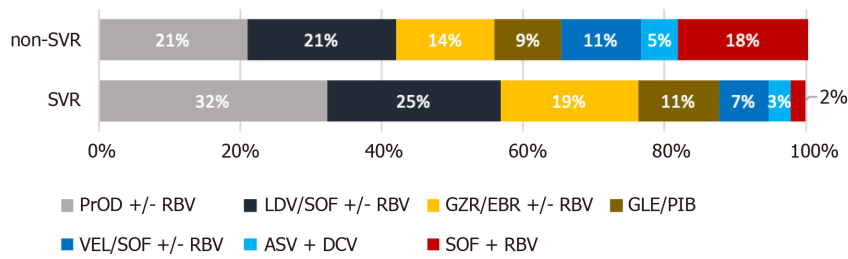


**Figure 2 Distribution of treatment regimens among patients who did and did not achieve sustained virologic response.** SVR: Sustained virologic response; RBV: Ribavirin; SOF: Sofosbuvir; PrOD: Paritaprevir/ritonavir +/- dasabuvir; LDV: Ledipasvir; GZR: Grazoprevir; EBR: Elbasvir; GLE: Glecaprevir; PIB: Pibrentasvir; VEL: Velpatasvir; ASV: Asunaprevir; DCV: Daclatasvir.

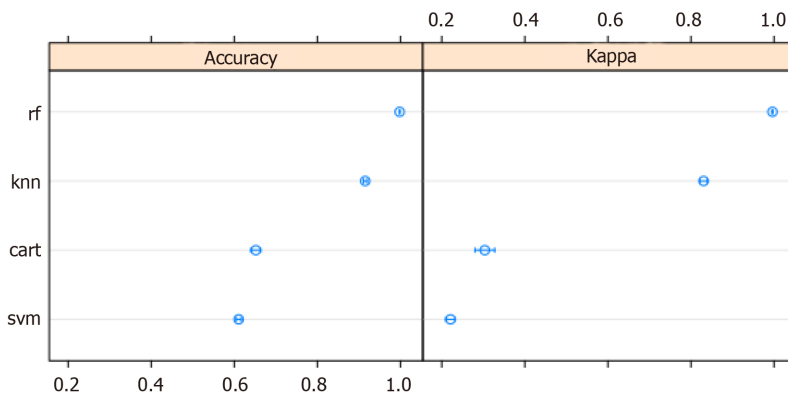


**Figure 3 Prediction accuracy and the value of Cohen's  $\kappa$  statistic for individual machine learning algorithms.** cart: Classification and regression tree; knn: K-nearest neighbors; svm: Support vector machine; rf: Random forest.

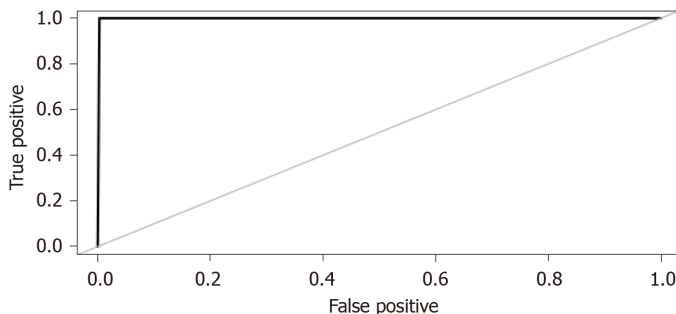


**Figure 4 The receiver operating characteristic curve showing the accuracy of the final model for the test data.**

The accuracy of the final model was checked using 10-fold cross-validation. The model was "taught" on the training data and then validated using the test data. The final model was built based on 14012 observations and 36 variables. Its accuracy was 0.9993 on the training set, and Cohen's  $\kappa$  statistic was 0.9985. When validating the model using the test set ( $n = 4670$ ), an accuracy of 0.9985 (95%CI: 0.9969-0.9994) and a Cohen  $\kappa$  statistic of 0.9970 were obtained.

Based on the constructed model, the weights of variables influencing HCV RNA detectability at least 12 wk after the end of treatment (non-SVR) were determined. Two measures were used for this purpose: the average loss of accuracy, which is determined by how much the accuracy of the model has decreased after the removal of a specific variable (Figure 5), and the average loss of the Gini coefficient (Figure 6), on which the random forest algorithm is based. The greater the value of the loss of the Gini coefficient, the more important the variable is, because it leads to a reduction in the entropy of the output variable.

Figures 5 and 6 show the top 12 factors contributing to treatment failure.

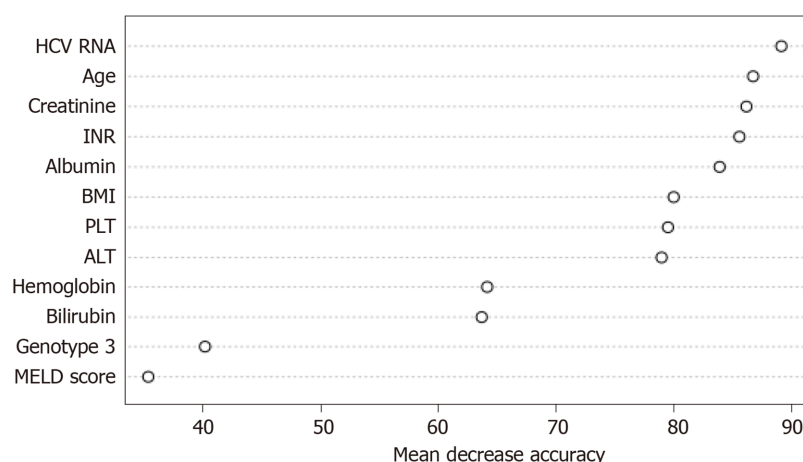


**Figure 5 The most important factors influencing treatment failure: mean accuracy decrease.** HCV: Hepatitis C virus; INR: International normalized ratio; BMI: Body mass index; PLT: Platelets; ALT: Alanine aminotransferase; MELD: Model for End-stage Liver Disease.

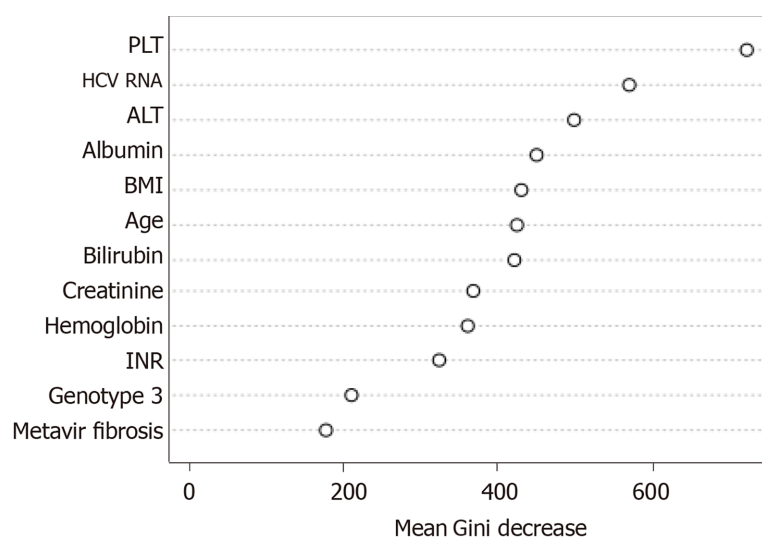


**Figure 6 The most important factors influencing treatment failure: mean Gini coefficient decrease.** HCV: Hepatitis C virus; INR: International normalized ratio; BMI: Body mass index; PLT: Platelets; ALT: Alanine aminotransferase; MELD: Model for End-stage Liver Disease.

In the case of the remaining variables, the degree of accuracy decrease indicated their minor importance in predicting therapy ineffectiveness.

Based on the statistical analysis of the factors influencing the failure of antiviral therapy performed with the use of the random forest algorithm, the following factors seem to be the most important: advancement of liver disease (platelets, albumin, INR, bilirubin, fibrosis), HCV characteristics (viral load, genotype 3), patient characteristics (age, BMI), hemoglobin levels, and creatinine levels. Conversely, the following factors seem to be of minor importance: HBV and HIV coinfections, extrahepatic manifestations of HCV infection, and coexistence of HCC.

Male sex was statistically significant in the conventional statistics. However, in the ML analysis, this parameter did not significantly affect treatment outcome (average accuracy decrease: 31<sup>st</sup> position, loss of the Gini coefficient: 14<sup>th</sup> position).

## DISCUSSION

Treatment of chronic hepatitis C with DAAs rarely does not eliminate HCV infection. In our group, 97% of patients achieved SVR, which is consistent with the results of clinical trials[1-3,8,9] and other cohort studies[13-17]. In the analysis of our large, multicenter cohort of over 11000 patients, we assessed the factors that may have contributed to the ineffectiveness of DAA therapy in the remaining 3%.

Due to the specifics of the collected data (a very large study group, a large number of variables, a large disproportion between the number of patients who achieved and did not achieve SVR), we utilized ML techniques in addition to the traditional statistical analysis. Both types of statistical analysis revealed that the factors that have the greatest negative impact on the efficacy of DAA treatment are those related to the advancement of liver disease and impairment of its function. These observations are in line with the results of other cohort studies[18-22]. Because of the very low treatment failure rate, the numbers of patients failing to achieve SVR in these studies were significantly smaller than that in the present study. Gathering a group of 309 patients who did not achieve SVR makes our analysis more reliable than those conducted for groups with only several dozen non-SVR patients and can only be comparable to a few large study cohorts, such as the Veterans cohort[18].

In the classical statistical analysis, male sex seemed to be of importance, which is consistent with the findings of previous studies[17,18]. However, in the ML analysis, this factor was not among those with the greatest impact on treatment efficacy. Another difference between conventional statistics and the ML algorithm is the significance of age, creatinine, and hemoglobin in relation to treatment failure. These factors appeared to be irrelevant in the conventional analysis; however, they were among the important determinants of treatment failure in the random forest algorithm. Higher BMI was also an unfavorable prognostic factor in both types of statistical analysis. Among the virological factors examined, genotype 3 and viral load appeared to influence the efficacy of DAA treatment as well. Different results were obtained by Ioannou *et al*[18] in a large cohort of Veterans, in which, using conventional statistical methods, viral load and age had no effect on the treatment efficacy.

Neither HBV nor HIV coinfection influenced the results of therapy in our group.

Rial-Crestelo *et al*[23] in their publication, describes a cohort of 316 patients with HCV/HIV coinfection treated with DAAs between 2014 and 2018 (including 43.9% cirrhotics), in which the SVR rate was 90.9%. The factors with the greatest impact on the therapy ineffectiveness in this group were alcohol abuse and higher bilirubin levels. In our cohort, patients co-infected with HIV accounted for 5%, and only patients without active addictions were eligible for treatment. Higher bilirubin levels in our study were also associated with less effective therapy, as demonstrated by both traditional statistics and ML.

Part of the analyzed parameters showed a significant impact on the treatment effect in both "traditional" statistics and ML. For other parameters, we observed differences in statistical significance between these methods.

Direct comparison of these methods is difficult, because they involve different aspects of data collected. "Traditional" statistics cannot assess the interaction between many continuous variables and many factors simultaneously. We used this method for univariate analysis only.

ML algorithms are a multivariate way to analyze the data. It takes into account interaction between all variables, and this is a reason for inconsistency between "traditional" and ML sections. In our opinion, ML algorithms perform better because of the following reasons – the large data frame with more than 11000 observations and a significant disproportion between patients who achieved and did not achieve SVR (97% *vs* 3%); ML counts interactions between all variables; the oversampling technique allows us to have equal groups of HCV RNA detectability (in standard statistics, oversampling does not work because multiplication of data may result in biased outcomes).

The percentages of patients treated with VEL/SOF +/- RBV, ASV + DCV, and SOF + RBV were higher among patients without SVR than among those who achieved SVR.

The lower efficacy of treatment with SOF + RBV or ASV + DCV has been observed in previous studies and in clinical practice[24-27].

The relatively high percentage of patients treated with VEL/SOF +/- RBV among therapy failures is somewhat surprising. However, patients with hepatic failure were treated with this drug because treatment with a regimen containing protease inhibitors is contraindicated in this group. Thus, higher treatment failure rates may be associated with more severe liver disease. On the other hand, no such effect was observed in patients treated with LDV/SOF +/- RBV in the earlier period of the EpiTer-2 study, when relatively more patients with advanced liver disease were included[28].

Resistance-associated variants (RASs) were not analyzed in this study because they are not routinely used in clinical practice and are determined only in a few cases at select centers. Pre-treatment RAS data were not available for all patients, although some who qualified had them assessed as part of a separate study[29]. A study carried out on a population partially overlapping our study group reported an increased frequency of baseline NS5A RASs (particularly Y93H) in patients with advanced

fibrosis and cirrhosis. Data from the study by Parczewski *et al*[29], which included 265 patients, some of whom were subsequently treated in the EpiTer-2 study, suggest that the incidence of NS5A RASs increases in patients with advanced fibrosis and cirrhosis in comparison to levels observed in those with mild fibrosis, even in those with no history of antiviral therapy.

The frequent occurrence of RASs was also observed in the Italian cohort of 87 patients after failing DAAs therapy, 79.5% of whom were patients with cirrhosis[30].

Considering the lower efficacy of treatment in patients with advanced liver disease and a greater tendency to develop RASs in these groups[29-31], sequencing tests should be considered in patients with cirrhosis, especially those with the features of deteriorating liver function (both with signs of overt failure and those meeting the Child-Pugh A criteria, but with decreased platelet count and albumin and/or elevated bilirubin). This would allow for the selection of personalized therapy with the maximum chance of eliminating HCV infection, which is important in this particular group of patients at risk of complications of liver cirrhosis and/or the development of HCC.

Recently, there has been a tendency to shorten therapy in patients with cirrhosis, making its duration equal to that utilized in patients with less advanced liver disease[32,33]. Our data suggest that longer treatment durations should be considered in patients with cirrhosis, especially those with borderline or overt liver failure and high HCV viral load, with monitoring of early responses during the treatment period (response-guided therapy). Although the percentage of patients not achieving SVR was statistically low, this applies mainly to patients with cirrhosis, in whom the elimination of HCV sometimes determines their further health and even life. Therefore, a special approach to the treatment of these patients should be considered[33,34]. Due to the serious prognosis in these patients, it is important to maximize the effectiveness of the therapy in order to eliminate HCV infection as soon as possible, to prevent the development of additional RASs that can limit the efficacy of possible re-therapy, and to start the process of liver regeneration.

It would be advisable to conduct a further study to verify our findings and, if necessary, to develop guidelines for personalized therapy of such patients.

The strength of our study lies primarily in the inclusion of a large group of non-SVR patients treated in the setting of everyday clinical practice, which allowed us to assess the effects of treatment in patients with more advanced liver injury and concomitant diseases, in contrast to most clinical trials. There are, however, several limitations in our study. This was a cohort study in which various drugs were used depending on their availability over the 4-year data collection period. At that time, manufacturers also made changes to the characteristics of medicinal products used (*e.g.*, shortening the treatment period, recommended treatment with or without RBV). However, it is known that these changes were introduced after evidence from clinical trials showed that they did not significantly reduce the efficacy of treatment and may improve the patient's safety[32].

In addition, some data were not entered for all patients, which is the case in such large, multicenter, real-world projects. However, despite the omitted data, the size of the group was large enough to draw reliable conclusions.

## CONCLUSION

In conclusion, our findings demonstrate that failure of treatment with DAAs occurs mainly in patients with liver cirrhosis and deterioration of liver function. Our ML analysis further revealed that older age, creatinine, and hemoglobin levels also influenced treatment failure, as did viral factors such as genotype 3 and viral load. In patients with advanced liver disease, individualization of therapy (RAS testing, response-guided treatment) should be considered to maximize the chance of achieving SVR.

## ARTICLE HIGHLIGHTS

### Research background

Treatment with direct-acting antiviral drugs (DAAs) is highly effective and safe. Interferon-free therapies allow for a sustained virologic response (SVR) in over 90% of patients, both in randomized clinical trials and in real-world settings.

### Research motivation

Treatment of chronic hepatitis C with DAAs rarely does not eliminate hepatitis C virus (HCV) infection. Numerous studies have confirmed the high efficacy of treatment with direct-acting antivirals. Most of the publications evaluating interferon-free therapies are devoted to assessing their efficacy and safety. Few researchers, however, have analyzed the factors that cause the therapy to fail in some patients.

### Research objectives

To analyze factors influencing the failure of direct antiviral drugs in the large, Polish multicenter EpiTer-2 cohort of 12614 patients in a real-world setting.

### Research methods

The study cohort consisted of patients treated at 22 centers from 2016-2020. Both standard and machine learning methods were used for statistical analysis.

### Research results

Among 11938 patients with SVR data available, 11629 (97%) achieved SVR and 309 (3%) did not. Most patients (78.1%) were infected with HCV genotype 1b. Liver cirrhosis was diagnosed in 2974 patients, advanced fibrosis (F3) in 1717 patients. The most important host factors negatively influencing treatment efficacy were liver cirrhosis, clinical and laboratory features of liver failure, history of hepatocellular carcinoma, and higher body mass index. Among viral factors, genotype 3 and viral load also exerted an influence on treatment efficacy.

### Research conclusions

In patients with advanced liver disease, individualized therapy (testing for resistance-associated variants and response-guided treatment) should be considered to maximize the chance of achieving SVR.

### Research perspectives

The EpiTer-2 is still an active study, and data on patients treated for HCV infection are still being collected. The obtained data will allow us to confirm the results of our research on a larger group of patients and to verify the validity of the hypothesis that individualization of therapy in patients with liver cirrhosis may improve the treatment efficacy.

## ACKNOWLEDGEMENTS

We would like to thank Polish Association of Epidemiologists and Infectiologists for the creation and maintenance of the database.

## REFERENCES

- 1 Ferenci P, Bernstein D, Lalezari J, Cohen D, Luo Y, Cooper C, Tam E, Marinho RT, Tsai N, Nyberg A, Box TD, Younes Z, Enayati P, Green S, Baruch Y, Bhandari BR, Caruntu FA, Sepe T, Chulanov V, Janczewska E, Rizzardini G, Gervain J, Planas R, Moreno C, Hassanein T, Xie W, King M, Podsadecki T, Reddy KR; PEARL-III Study; PEARL-IV Study. ABT-450/r-ombitasvir and dasabuvir with or without ribavirin for HCV. *N Engl J Med* 2014; **370**: 1983-1992 [PMID: 24795200 DOI: 10.1056/NEJMoa1402338]
- 2 Zeuzem S, Ghalib R, Reddy KR, Pockros PJ, Ben Ari Z, Zhao Y, Brown DD, Wan S, DiNubile MJ, Nguyen BY, Robertson MN, Wahl J, Barr E, Butters J. Grazoprevir-Elbasvir Combination Therapy for Treatment-Naive Cirrhotic and Noncirrhotic Patients With Chronic Hepatitis C Virus Genotype 1, 4, or 6 Infection: A Randomized Trial. *Ann Intern Med* 2015; **163**: 1-13 [PMID: 25909356 DOI: 10.7326/M15-0785]
- 3 Afdhal N, Zeuzem S, Kwo P, Chojkier M, Gitlin N, Puoti M, Romero-Gomez M, Zarski JP, Agarwal K, Buggisch P, Foster GR, Bräu N, Buti M, Jacobson IM, Subramanian GM, Ding X, Mo H, Yang JC, Pang PS, Symonds WT, McHutchison JG, Muir AJ, Mangia A, Marcellin P; ION-1 Investigators. Ledipasvir and sofosbuvir for untreated HCV genotype 1 infection. *N Engl J Med* 2014; **370**: 1889-1898 [PMID: 24725239 DOI: 10.1056/NEJMoa1402454]
- 4 Mangia A, Milligan S, Khalili M, Fagioli S, Shafran SD, Carrat F, Ouzan D, Papatheodoridis G, Ramji A, Borgia SM, Wedemeyer H, Losappio R, Pérez-Hernandez F, Wick N, Brown RS Jr, Lampertico P, Doucette K, Ntalla I, Ramroth H, Mertens M, Vanstraelen K, Turnes J. Global real-



- world evidence of sofosbuvir/velpatasvir as simple, effective HCV treatment: Analysis of 5552 patients from 12 cohorts. *Liver Int* 2020; **40**: 1841-1852 [PMID: 32449966 DOI: 10.1111/liv.14537]
- 5 **Puenpatom A**, Cao Y, Yu X, Kanwal F, El-Serag HB, Kramer JR. Effectiveness of Elbasvir/Grazoprevir in US Veterans with Chronic Hepatitis C Virus Genotype 1b Infection. *Infect Dis Ther* 2020; **9**: 355-365 [PMID: 32297307 DOI: 10.1007/s40121-020-00293-7]
  - 6 **Zuckerman E**, Gutierrez JA, Dylla DE, de Ledinghen V, Muir AJ, Gschwantsler M, Puoti M, Caruntu F, Slim J, Nevens F, Sigal S, Cohen S, Fredrick LM, Pires Dos Santos AG, Rodrigues L Jr, Dillon JF. Eight Weeks of Treatment With Glecaprevir/Pibrentasvir Is Safe and Efficacious in an Integrated Analysis of Treatment-Naïve Patients With Hepatitis C Virus Infection. *Clin Gastroenterol Hepatol* 2020; **18**: 2544-2553. e6 [PMID: 32621971 DOI: 10.1016/j.cgh.2020.06.044]
  - 7 **Boyle A**, Marra F, Peters E, Datta S, Ritchie T, Priest M, Heydtmann M, Barclay ST. Eight weeks of sofosbuvir/velpatasvir for genotype 3 hepatitis C in previously untreated patients with significant (F2/3) fibrosis. *J Viral Hepat* 2020; **27**: 371-375 [PMID: 31756019 DOI: 10.1111/jvh.13239]
  - 8 **Zoratti MJ**, Siddiqua A, Morassut RE, Zeraatkar D, Chou R, van Holten J, Xie F, Druyts E. Pangenotypic direct acting antivirals for the treatment of chronic hepatitis C virus infection: A systematic literature review and meta-analysis. *EClinicalMedicine* 2020; **18**: 100237 [PMID: 31922124 DOI: 10.1016/j.eclinm.2019.12.007]
  - 9 **Falade-Nwulia O**, Suarez-Cuervo C, Nelson DR, Fried MW, Segal JB, Sulkowski MS. Oral Direct-Acting Agent Therapy for Hepatitis C Virus Infection: A Systematic Review. *Ann Intern Med* 2017; **166**: 637-648 [PMID: 28319996 DOI: 10.7326/M16-2575]
  - 10 **Li T**, Qu Y, Guo Y, Wang Y, Wang L. Efficacy and safety of direct-acting antivirals-based antiviral therapies for hepatitis C virus patients with stage 4-5 chronic kidney disease: a meta-analysis. *Liver Int* 2017; **37**: 974-981 [PMID: 27943605 DOI: 10.1111/liv.13336]
  - 11 **Peters MG**, Kottlilil S, Terrault N, Amara D, Husson J, Huprikar S, Florman S, Sulkowski MS, Durand CM, Luetkemeyer AF, Rogers R, Grab J, Haydel B, Blumberg E, Dove L, Emond J, Olthoff K, Smith C, Fishbein T, Masur H, Stock PG. Retrospective-prospective study of safety and efficacy of sofosbuvir-based direct-acting antivirals in HIV/HCV-coinfected participants with decompensated liver disease pre- or post-liver transplant. *Am J Transplant* 2020 [PMID: 33277801 DOI: 10.1111/ajt.16427]
  - 12 **Polish Group of Experts for HCV**, Halota W, Flisiak R, Juszczak J, Małkowski P, Pawłowska M, Simon K, Tomaszewicz K. Recommendations for the treatment of hepatitis C in 2017. *Clin Exp Hepatol* 2017; **3**: 47-55 [PMID: 2885629 DOI: 10.5114/ceh.2017.67782]
  - 13 **Calleja JL**, Crespo J, Rincón D, Ruiz-Antorán B, Fernandez I, Perelló C, Gea F, Lens S, García-Samaniego J, Sacristán B, García-Eliz M, Llerena S, Pascasio JM, Turnes J, Torras X, Morillas RM, Llaneras J, Serra MA, Diago M, Rodríguez CF, Ampuero J, Jorquera F, Simon MA, Arenas J, Navascues CA, Bañares R, Muñoz R, Albillos A, Mariño Z; Spanish Group for the Study of the Use of Direct-acting Drugs Hepatitis C Collaborating Group. Effectiveness, safety and clinical outcomes of direct-acting antiviral therapy in HCV genotype 1 infection: Results from a Spanish real-world cohort. *J Hepatol* 2017; **66**: 1138-1148 [PMID: 28189751 DOI: 10.1016/j.jhep.2017.01.028]
  - 14 **Bischoff J**, Mauss S, Cordes C, Lutz T, Scholten S, Moll A, Jäger H, Cornberg M, Manns MP, Baumgarten A, Rockstroh JK. Rates of sustained virological response 12 weeks after the scheduled end of direct-acting antiviral (DAA)-based hepatitis C virus (HCV) therapy from the National German HCV registry: does HIV coinfection impair the response to DAA combination therapy? *HIV Med* 2018; **19**: 299-307 [PMID: 29368456 DOI: 10.1111/hiv.12579]
  - 15 **Huang CF**, Iio E, Jun DW, Ogawa E, Toyoda H, Hsu YC, Haga H, Iwane S, Enomoto M, Lee DH, Wong G, Liu CH, Tada T, Chuang WL, Cheung R, Hayashi J, Tseng CH, Yasuda S, Tran S, Kam L, Henry L, Jeong JY, Nomura H, Park SH, Nakamura M, Huang JF, Tai CM, Lo GH, Lee MH, Yang HL, Kao JH, Tamori A, Eguchi Y, Ueno Y, Furusyo N, Tanaka Y, Yu ML, Nguyen MH; REAL-C Investigators. Direct-acting antivirals in East Asian hepatitis C patients: real-world experience from the REAL-C Consortium. *Hepatol Int* 2019; **13**: 587-598 [PMID: 31463665 DOI: 10.1007/s12072-019-09974-z]
  - 16 **Salmon D**, Trimoulet P, Gilbert C, Solas C, Lafourcade E, Chas J, Piroth L, Lacombe K, Katlama C, Peytavin G, Aumaitre H, Alric L, Boué F, Morlat P, Poizot-Martin I, Billaud E, Rosenthal E, Naqvi A, Mialhes P, Bani-Sadr F, Esterle L, Carrieri P, Dabis F, Sogni P, Wittkop L; ANRS CO13 HepaviH study Group. Factors associated with DAA virological treatment failure and resistance-associated substitutions description in HIV/HCV coinfecting patients. *World J Hepatol* 2018; **10**: 856-866 [PMID: 30533186 DOI: 10.4254/wjh.v10.i11.856]
  - 17 **Dalgard O**, Weiland O, Norberg G, Karlén L, Heggelund L, Färkkilä M, Balslev U, Belard E, Øvrehus A, Skalshei Kjaer M, Krarup H, Thorup Røge B, Hallager S, Madsen LG, Lund Laursen A, Lagging M, Weis N. Sofosbuvir based treatment of chronic hepatitis C genotype 3 infections-A Scandinavian real-life study. *PLoS One* 2017; **12**: e0179764 [PMID: 28704381 DOI: 10.1371/journal.pone.0179764]
  - 18 **Ioannou GN**, Beste LA, Chang MF, Green PK, Lowy E, Tsui JJ, Su F, Berry K. Effectiveness of Sofosbuvir, Ledipasvir/Sofosbuvir, or Paritaprevir/Ritonavir/Ombitasvir and Dasabuvir Regimens for Treatment of Patients with Hepatitis C in the Veterans Affairs National Health Care System. *Gastroenterology* 2016; **151**: 457-471. e5 [PMID: 2726705]
  - 19 **Chang CY**, Nguyen P, Le A, Zhao C, Ahmed A, Daugherty T, Garcia G, Lutchman G, Kumari R, Nguyen MH. Real-world experience with interferon-free, direct acting antiviral therapies in Asian Americans with chronic hepatitis C and advanced liver disease. *Medicine (Baltimore)* 2017; **96**: e6128

- [PMID: 28178174 DOI: 10.1097/MD.00000000000006128]
- 20 **Ippolito AM**, Milella M, Messina V, Conti F, Cozzolongo R, Morisco F, Brancaccio G, Barone M, Santantonio T, Masetti C, Tundo P, Smedile A, Carretta V, Gatti P, Termite AP, Valvano MR, Bruno G, Fabrizio C, Andreone P, Zappimbulso M, Gaeta GB, Napoli N, Fontanella L, Lauletta G, Cuccorese G, Metrangola A, Francavilla R, Ciraci E, Rizzo S, Andriulli A. HCV clearance after direct-acting antivirals in patients with cirrhosis by stages of liver impairment: The ITAL-C network study. *Dig Liver Dis* 2017; **49**: 1022-1028 [PMID: 28487083 DOI: 10.1016/j.dld.2017.03.025]
  - 21 **Jiménez-Macías FM**, Cabanillas-Casafranca M, Maraver-Zamora M, Romero-Herrera G, García-García F, Correia-Varela-Almeida A, Cabello-Fernández A, Ramos-Lora M. Experience in real clinical practice with new direct acting antivirals in chronic hepatitis C. *Med Clin (Barc)* 2017; **149**: 375-382 [PMID: 28416232 DOI: 10.1016/j.medcli.2017.03.007]
  - 22 **Terrault NA**, Zeuzem S, Di Bisceglie AM, Lim JK, Pockros PJ, Frazier LM, Kuo A, Lok AS, Shiffman ML, Ben Ari Z, Akushevich L, Vainorius M, Sulkowski MS, Fried MW, Nelson DR; HCV-TARGET Study Group. Effectiveness of Ledipasvir-Sofosbuvir Combination in Patients With Hepatitis C Virus Infection and Factors Associated With Sustained Virologic Response. *Gastroenterology* 2016; **151**: 1131-1140. e5 [PMID: 27565882 DOI: 10.1053/j.gastro.2016.08.004]
  - 23 **Rial-Crestelo D**, Sepúlveda MA, González-Gasca FJ, Geijo-Martínez P, Martínez-Alfaro E, Barberá JR, Yzusqui M, Casallo S, García M, Muñoz Hornero C, Espinosa-Gimeno A, Torralba M; Grupo de Estudio de Castilla la Manche de enfermedades Infecciosas (GECMEI). Impact of interferon-free therapies in HIV/HCV co-infected patients on real clinical practice: results from a multicenter region-wide cohort study (2014-2018). *Eur J Gastroenterol Hepatol* 2021; **32**: 279-287 [PMID: 33252415 DOI: 10.1097/MEG.0000000000000212]
  - 24 **Suzuki F**, Hatanaka N, Bando E, Nakamura K, Komoto A. Safety and effectiveness of daclatasvir and asunaprevir dual therapy in patients with genotype 1 chronic hepatitis C: results from postmarketing surveillance in Japan. *Hepatol Int* 2018; **12**: 244-253 [PMID: 29900486 DOI: 10.1007/s12072-018-9872-z]
  - 25 **Kumada H**, Suzuki Y, Ikeda K, Toyota J, Karino Y, Chayama K, Kawakami Y, Ido A, Yamamoto K, Takaguchi K, Izumi N, Koike K, Takehara T, Kawada N, Sata M, Miyagoshi H, Eley T, McPhee F, Damokosh A, Ishikawa H, Hughes E. Daclatasvir plus asunaprevir for chronic HCV genotype 1b infection. *Hepatology* 2014; **59**: 2083-2091 [PMID: 24604476 DOI: 10.1002/hep.27113]
  - 26 **Gane EJ**, Stedman CA, Hyland RH, Ding X, Svarovskaia E, Symonds WT, Hinds RG, Berrey MM. Nucleotide polymerase inhibitor sofosbuvir plus ribavirin for hepatitis C. *N Engl J Med* 2013; **368**: 34-44 [PMID: 23281974 DOI: 10.1056/NEJMoa1208953]
  - 27 **Herbst DA Jr**, Reddy KR. Sofosbuvir, a nucleotide polymerase inhibitor, for the treatment of chronic hepatitis C virus infection. *Expert Opin Investig Drugs* 2013; **22**: 527-536 [PMID: 23448131 DOI: 10.1517/13543784.2013.775246]
  - 28 **Flisiak R**, Zarębska-Michaluk D, Janczewska E, Staniaszek A, Gietka A, Mazur W, Tudrujek M, Tomasiewicz K, Belica-Wdowik T, Baka-Ćwierz B, Dybowska D, Halota W, Lorenc B, Sitko M, Garlicki A, Berak H, Horban A, Orlowska I, Simon K, Socha Ł, Wawrzynowicz-Syczewska M, Jaroszewicz J, Deroń Z, Czauż-Andrzejuk A, Citko J, Krygier R, Piekarska A, Laurans Ł, Dobracki W, Białkowska J, Tronina O, Pawłowska M. Treatment of HCV infection in Poland at the beginning of the interferon-free era-the EpiTer-2 study. *J Viral Hepat* 2018; **25**: 661-669 [PMID: 29316039 DOI: 10.1111/jvh.12861]
  - 29 **Parczewski M**, Kordek J, Janczewska E, Pisula A, Łojewski W, Socha Ł, Wawrzynowicz-Syczewska M, Bociąga-Jasik M, Szymczak A, Cielniak I, Siwak E, Mularska E, Aksak-Wąs B, Urbańska A, Lübke N. Hepatitis C virus (HCV) genotype 1 NS5A resistance-associated variants are associated with advanced liver fibrosis independently of HCV-transmission clusters. *Clin Microbiol Infect* 2019; **25**: 513.e1-513. e6 [PMID: 29981869 DOI: 10.1016/j.cmi.2018.06.028]
  - 30 **Starace M**, Minichini C, De Pascalis S, Macera M, Occhiello L, Messina V, Sangiovanni V, Adinolfi LE, Claar E, Precone D, Stornaiuolo G, Stanzione M, Ascione T, Caroprese M, Zampino R, Parrilli G, Gentile I, Brancaccio G, Iovinella V, Martini S, Masarone M, Fontanella L, Masiello A, Sagnelli E, Punzi R, Salomone Megna A, Santoro R, Gaeta GB, Coppola N. Virological patterns of HCV patients with failure to interferon-free regimens. *J Med Virol* 2018; **90**: 942-950 [PMID: 29315640 DOI: 10.1002/jmv.25022]
  - 31 **Di Stefano M**, Faleo G, Farhan Mohamed AM, Morella S, Bruno SR, Tundo P, Fiore JR, Santantonio TA. Resistance Associated Mutations in HCV Patients Failing DAA Treatment. *New Microbiol* 2021; **44**: 12-18 [PMID: 33453702]
  - 32 **Brown RS Jr**, Buti M, Rodrigues L, Chulanov V, Chuang WL, Aguilar H, Horváth G, Zuckerman E, Carrion BR, Rodriguez-Perez F, Urbánek P, Abergel A, Cohen E, Lovell SS, Schnell G, Lin CW, Zha J, Wang S, Trinh R, Mensa FJ, Burroughs M, Felizarta F. Glecaprevir/pibrentasvir for 8 wk in treatment-naïve patients with chronic HCV genotypes 1-6 and compensated cirrhosis: The EXPEDITION-8 trial. *J Hepatol* 2020; **72**: 441-449 [PMID: 31682879 DOI: 10.1016/j.jhep.2019.10.020]
  - 33 **Lampertico P**, Mauss S, Persico M, Barclay ST, Marx S, Lohmann K, Bondin M, Zhang Z, Marra F, Belperio PS, Wedemeyer H, Flamm S Real-World Clinical Practice Use of 8-Week Glecaprevir/Pibrentasvir in Treatment-Naive Patients with Compensated Cirrhosis. *Lampertico P, Mauss S, Persico M, Barclay ST, Marx S, Lohmann K, Bondin M, Zhang Z, Marra F, Belperio PS, Wedemeyer H, Flamm S Real-World Clinical Practice Use of 8-Week Glecaprevir/Pibrentasvir in Treatment-Naive Patients with Adv Ther* 2020; **37**(9): 4033-4042 [PMID: 3275482 DOI: 10.1016/j.jhep.2019.10.020]

[10.1007/s12325-020-01449-0](https://doi.org/10.1007/s12325-020-01449-0)]

- 34 **Peiffer KH**, Vermehren J, Kuhnhen L, Susser S, Dietz J, Finkelmeier F, Weiler N, Welzel T, Grammatikos G, Zeuzem S, Sarrazin C. Interferon-free treatment choice according to baseline RASs leads to high SVR rates in HCV genotype 1 infected patients. *J Infect Chemother* 2018; **24**: 524-530 [PMID: [29628383](https://pubmed.ncbi.nlm.nih.gov/29628383/) DOI: [10.1016/j.jiac.2018.02.008](https://doi.org/10.1016/j.jiac.2018.02.008)]



## Retrospective Study

# Totally laparoscopic total gastrectomy using the modified overlap method and conventional open total gastrectomy: A comparative study

Chang Seok Ko, Nam Ryong Choi, Byung Sik Kim, Jeong Hwan Yook, Min-Ju Kim, Beom Su Kim

**ORCID number:** Chang Seok Ko 0000-0002-4155-4312; Nam Ryong Choi 0000-0002-7120-660X; Byung Sik Kim 0000-0001-9579-9211; Jeong Hwan Yook 0000-0002-7987-5808; Min-Ju Kim 0000-0003-4600-5352; Beom Su Kim 0000-0002-3656-2086.

**Author contributions:** Ko CS, Choi NR, Kim BS, Yook JH and Kim BS performed the literature search, conception and design, drafting of the article; Kim MJ performed the analysis and interpretation; all authors were involved in the critical revision and final approval of the article.

**Institutional review board statement:** This study was approved by the Institutional Review Board of the Asan Medical Center (approval No. 2019-0702).

**Informed consent statement:** Patients were not required to give informed consent for the study because the clinical data were obtained retrospectively after each patient agreed to treatment by written consent.

**Conflict-of-interest statement:** We have no financial relationships to disclose.

**Data sharing statement:** No

**Chang Seok Ko, Nam Ryong Choi, Byung Sik Kim, Jeong Hwan Yook, Beom Su Kim,** Department of Surgery, Asan Medical Center, University of Ulsan College of Medicine, Seoul 05505, South Korea

**Min-Ju Kim,** Department of Clinical Epidemiology and Biostatistics, Asan Medical Center, University of Ulsan College of Medicine, Seoul 05505, South Korea

**Corresponding author:** Beom Su Kim, MD, PhD, Professor, Surgeon, Department of Surgery, Asan Medical Center, University of Ulsan College of Medicine, 88, Olympic-ro 43-gil, Songpa-gu, Seoul 05505, South Korea. [bskim0251@naver.com](mailto:bskim0251@naver.com)

## Abstract

### BACKGROUND

Although several methods of totally laparoscopic total gastrectomy (TLTG) have been reported. The best anastomosis technique for LTG has not been established.

### AIM

To investigate the effectiveness and surgical outcomes of TLTG using the modified overlap method compared with open total gastrectomy (OTG) using the circular stapled method.

### METHODS

We performed 151 and 131 surgeries using TLTG with the modified overlap method and OTG for gastric cancer between March 2012 and December 2018. Surgical and oncological outcomes were compared between groups using propensity score matching. In addition, we analyzed the risk factors associated with postoperative complications.

### RESULTS

Patients who underwent TLTG were discharged earlier than those who underwent OTG [TLTG ( $9.62 \pm 5.32$ ) vs OTG ( $13.51 \pm 10.67$ ),  $P < 0.05$ ]. Time to first flatus and soft diet were significantly shorter in TLTG group. The pain scores at all postoperative periods and administration of opioids were significantly lower in the TLTG group than in the OTG group. No significant difference in early, late and esophagojejunostomy (EJ)-related complications or 5-year recurrence free and overall survival between groups. Multivariate analysis demonstrated that body

additional data are available.

**Open-Access:** This article is an open-access article that was selected by an in-house editor and fully peer-reviewed by external reviewers. It is distributed in accordance with the Creative Commons Attribution NonCommercial (CC BY-NC 4.0) license, which permits others to distribute, remix, adapt, build upon this work non-commercially, and license their derivative works on different terms, provided the original work is properly cited and the use is non-commercial. See: <http://creativecommons.org/licenses/by-nc/4.0/>

**Manuscript source:** Invited manuscript

**Specialty type:** Gastroenterology and hepatology

**Country/Territory of origin:** South Korea

**Peer-review report's scientific quality classification**

Grade A (Excellent): 0  
Grade B (Very good): B, B  
Grade C (Good): C, C, C, C  
Grade D (Fair): D, D  
Grade E (Poor): 0

**Received:** January 27, 2021

**Peer-review started:** January 27, 2021

**First decision:** March 7, 2021

**Revised:** March 21, 2021

**Accepted:** April 20, 2021

**Article in press:** April 20, 2021

**Published online:** May 14, 2021

**P-Reviewer:** Balducci G, Garbarino GM, Laracca GG, Zhou XP

**S-Editor:** Gao CC

**L-Editor:** A

**P-Editor:** Liu JH



mass index [odds ratio (OR), 1.824; 95% confidence interval (CI): 1.029-3.234,  $P = 0.040$ ] and American Society of Anaesthesiologists (ASA) score (OR, 3.154; 95%CI: 1.084-9.174,  $P = 0.035$ ) were independent risk factors of early complications. Additionally, age was associated with  $\geq 3$  Clavien-Dindo classification and EJ-related complications.

## CONCLUSION

Although TLTG with the modified overlap method showed similar complication rate and oncological outcome with OTG, it yields lower pain score, earlier bowel recovery, and discharge. Surgeons should perform total gastrectomy cautiously and delicately in patients with obesity, high ASA scores, and older ages.

**Key Words:** Laparoscopic surgery; Gastrectomy; Anastomosis; Stomach neoplasms; Totally laparoscopic total gastrectomy

©The Author(s) 2021. Published by Baishideng Publishing Group Inc. All rights reserved.

**Core Tip:** The aim of the present study was to investigate the effectiveness and surgical outcomes of totally laparoscopic total gastrectomy (TLTG) using the modified overlap method compared with open total gastrectomy (OTG) using the circular stapled method. Although TLTG with the modified overlap method demonstrated similar complication rate and oncological outcome with OTG, it resulted in lower pain scores, and earlier bowel recovery and hospital discharge.

**Citation:** Ko CS, Choi NR, Kim BS, Yook JH, Kim MJ, Kim BS. Totally laparoscopic total gastrectomy using the modified overlap method and conventional open total gastrectomy: A comparative study. *World J Gastroenterol* 2021; 27(18): 2193-2204

**URL:** <https://www.wjgnet.com/1007-9327/full/v27/i18/2193.htm>

**DOI:** <https://dx.doi.org/10.3748/wjg.v27.i18.2193>

## INTRODUCTION

Laparoscopic total gastrectomy (LTG) is becoming increasingly used to treat upper or middle third gastric cancer because it shows earlier recovery and is considered less invasive[1-3]. Of the entire procedure of LTG, esophagojejunal reconstruction is the most crucial process. This is because the failure of esophagojejunostomy (EJ) such as leakage and stricture could induce the patients to suffer[4]. When performing EJ, EJ using linear stapler method is widely adopted due to its simplicity in comparison to the circular stapled method, such as overlap and functional method[5-9]. Nonetheless, the linear stapled method has a fundamental problem that it requires larger space to dissect around the distal esophagus than does the circular stapled method because the linear stapler needs to be inserted in the abdominal hiatus.

Recently, we developed a modified overlap method for totally LTG (TLTG) for overcoming these disadvantages of linear stapled method[10]. This method is performed with an intracorporeal side to side esophagojejunal anastomosis using a 45-mm linear stapler at 45° from the longitudinal direction of the esophagus (Figure 1). This procedure requires less dissection around abdominal esophagus; therefore, it can create a secure esophagojejunal anastomosis with reduced tension as circular stapled method.

Several studies have investigated the surgical outcomes of the TLTG compared with open total gastrectomy (OTG), including EJ-related complications[11,12]. However, to the best of our knowledge, there are few studies which compared TLTG with the overlap method and OTG with circular stapled method including oncological outcome.

The aim of the present study was to investigate the technical feasibility and oncological outcome of TLTG with the modified overlap method when compared with OTG with circular stapled method in the treatment of upper or middle third gastric cancer.



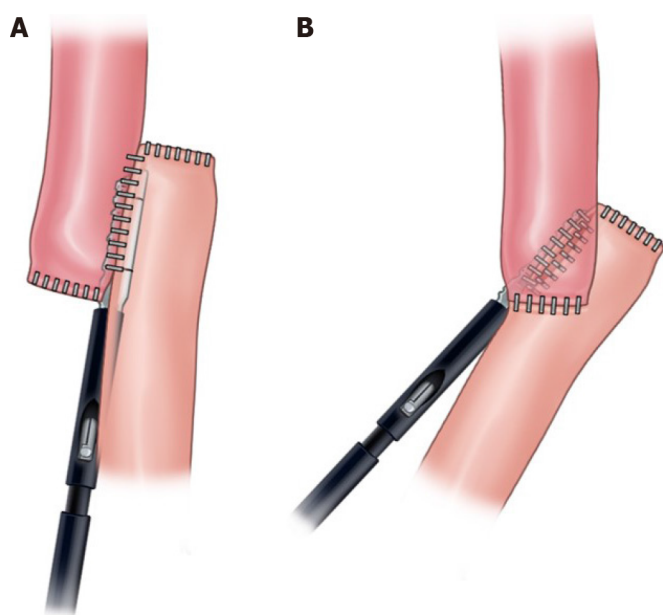


**Figure 1** Two types of intracorporeal esophagojejunostomy methods. A: The conventional overlap method; B: The modified overlap method.

## MATERIALS AND METHODS

### Patients

This study was approved by the institutional review board of the Asan Medical Center. We reviewed the retrospectively collected and analyzed data of 462 patients who underwent curative TLTG ( $n = 178$ ) and OTG ( $n = 284$ ) as a treatment for upper or middle third gastric cancer between March 2012 and December 2018 at Asan Medical Center. We excluded all patients who received neoadjuvant chemotherapy, were diagnosed with esophagogastric junction cancer, underwent resection additional organs except for gall bladder, and did not have a gastric cancer diagnosis. Finally, 151 and 131 patients who underwent TLTG and OTG, respectively, were enrolled. All TLTG procedures were performed as TLTG with the modified overlap method. We evaluated TNM (tumor-node-metastasis) stage using the American Joint Committee on Cancer (AJCC), 7<sup>th</sup> edition[13]. Clinical characteristics and pathologic data were compared between TLTG and OTG groups. Additionally, we evaluated surgical outcomes, including EJ-related complications, and oncologic outcomes, including recurrence free survival (RFS) and overall survival (OS). Early and late complications were defined as events occurring within or after 30 d postoperatively, respectively. EJ complications, including bleeding, leakage and stricture, were diagnosed *via* upper gastrointestinal series, esophagogastrroduodenoscopy, computed tomography, and clinical signs. These complications were reviewed and classified based on the Clavien-Dindo classification system (CDC)[14]. Patients were matched using propensity score matching (PSM) analysis and surgical and oncological outcomes were evaluated.

### Surgical technique of anastomosis

We performed TLTG with modified overlap method and OTG with circular stapled method, which was similar to our previous studies[3,10]. Both procedures were performed by a single experienced surgeon who conducts approximately 300 cases of gastrectomy annually.

### Statistical analysis

In the un-matched group, numerical variables were presented as the mean  $\pm$  SD using the Student's *t*-test or Kruskal-Wallis test. Categorical variables was performed using the Chi-square test. Univariate and multivariate analyses were performed for the entire patient cohort (un-matched group) using logistic regression. Variables were included in the multivariate analysis if their univariate significance was  $< 0.1$ .

To reduce the impact of treatment selection bias and potential confounding factors in this observational study, we performed rigorous adjustments for significant differences in the baseline characteristics of patients using the logistic regression models with generalized estimating equations (GEE) with a propensity score matched

set. When that technique was used, the propensity scores were estimated without considering the outcomes using multiple logistic regression analysis. A full non-parsimonious model was developed that included all the variables shown in Table 1. Model discrimination was assessed using the C statistic and model calibration was evaluated using Hosmer-Lemeshow statistics. Overall, the model was well calibrated (Hosmer-Lemeshow test;  $P = 0.368$ ) with reasonable discrimination (C statistic = 0.858). We matched the two groups (1:1 ratio) using a 'greedy nearest-neighbour' algorithm method. The Matching balance was measured based on the standardized mean differences. A  $> 10\%$  difference in the absolute value was considered significantly imbalanced.

In the matched group, numerical variables were reported as the means  $\pm$  SD using the paired *t*-test. Categorical variables were performed using McNemar's test or Marginal homogeneity test. To evaluate the association between type of surgery, and complication and survival (and recurrence), the propensity score adjusted model was applied. Finally, the logistic regression model with GEE was applied using propensity score-based matching. The Cox proportional hazards model was applied using propensity score-based matching with robust standard errors. All reported *P* values are two-sided; values  $< 0.05$  were considered statistically significant. Data manipulation and statistical analyses were performed using SAS® Version 9.4 (SAS Institute Inc., Cary, NC, United States).

## RESULTS

### *Clinicopathological characteristics*

The clinical variables are summarized in Table 1. There was a significant difference in body mass index (BMI), tumor size, and pathologic tumor stage before PSM between groups (all  $P < 0.05$ ); however, these differences disappeared after PSM. There were no statistically significant differences in all baseline variables included in the model between groups.

### *Surgical outcomes and postoperative complications in PSM*

All surgical outcomes and postoperative complications are shown in Table 2. There was no significant difference in operation time between groups ( $P = 0.351$ ). Patients who underwent TLTG had significantly lower pain scores on all postoperative days than patients who underwent OTG. Moreover, patients in the TLTG group required significantly less analgesic and opioid administration than in the OTG group. The TLTG group reported earlier time to first flatus ( $3.62 \pm 0.84$  d vs  $4.15 \pm 0.87$  d,  $P = 0.002$ ) and soft diet ( $4.62 \pm 2.67$  d vs  $7.47 \pm 7.92$  d,  $P = 0.001$ ). Furthermore, patients who underwent TLTG stayed statistically significantly fewer days at the hospital after surgery than patients who underwent OTG ( $9.62 \pm 5.32$  d vs  $13.51 \pm 10.67$  d;  $P < 0.001$ ). No significant differences in postoperative complications were noted between the two groups ( $P = 0.161$ ).

Postoperative complications, including EJ-related complications, are summarized in Table 3. There were no significant differences in the early and late postoperative overall complications between groups ( $P = 0.317$  and  $P = 0.257$ , respectively). In addition, there was no difference in the incidence of patients with  $\geq 3$  CDC complications in the early and late postoperative periods between groups ( $P = 0.428$  and  $P > 0.999$ , respectively). There was no significant differences in EJ-related complications. Table 4 shows the details of EJ-related complications. Five cases of EJ leakage were observed, and two cases of EJ bleeding were found. Four patients with CDC 3 complications required interventions such as endoscopic management and pigtail drainage, whereas 2 patients with CDC 2 complications fully recovered by conservative treatment. One postoperative mortality occurred due to EJ bleeding.

### *Oncologic outcomes of PSM*

There were no significant differences in the number of retrieved lymph nodes between groups ( $P = 0.713$ ). The 5-year RFS and OS are shown in Figure 2. There were no significant differences in pathologic tumor stage between groups after PSM. The 5-year RFS rates of patients who underwent TLTG and OTG were 87.7% and 92.3%, respectively; however, these differences were not significant ( $P = 0.653$ ). The 5-year OS rates of patients who underwent TLTG and OTG were 74.6% and 80.4%, respectively ( $P = 0.476$ ).

Table 1 Patient clinical characteristics

Variable	Total set (n = 282)		P value	SD	PSM set (1:1) (n = 122)		P value	SD
	TLTG (n = 151)	OTG (n = 131)			TLTG (n = 61)	OTG (n = 61)		
Age (yr)	60.74 ± 11.55	59.11 ± 11.02	0.231	0.144	58.30 ± 11.26	58.70 ± 10.65	0.841	0.037
Gender			0.257	0.136			0.847	0.035
Male	94 (62.25)	90 (68.70)			40 (65.57)	41 (67.21)		
Female	57 (37.75)	41 (31.30)			21 (34.43)	20 (32.79)		
BMI (kg/m <sup>2</sup> )	24.57 ± 3.25	23.69 ± 3.21	0.023	0.273	24.01 ± 2.98	23.98 ± 2.73	0.957	0.010
ASA score			0.859	0.044			0.885	0.073
I	30 (19.87)	26 (19.85)			13 (21.31)	14 (22.95)		
II	114 (75.50)	97 (74.05)			46 (75.41)	44 (72.13)		
III	7 (4.64)	8 (6.11)			2 (3.28)	3 (4.92)		
Number of comorbidities			0.068	0.222			0.655	0.083
0-2	137 (90.73)	126 (96.18)			59 (75.41)	44 (72.13)		
> 2	14 (9.27)	5 (3.82)			2 (3.28)	3 (4.92)		
Combined operation			0.176	0.161			> 0.999	0
No	136 (90.07)	111 (84.73)			55 (90.16)	55 (90.16)		
Yes	15 (9.93)	20 (15.27)			6 (9.84)	6 (9.84)		
History of abdominal surgery			0.061	0.254			0.846	0.103
No	120 (79.47)	102 (77.86)			50 (81.97)	48 (78.69)		
Minor surgery	24 (15.89)	14 (10.69)			6 (9.84)	6 (9.84)		
Major surgery	7 (4.64)	15 (11.45)			5 (8.20)	7 (11.48)		
Tumor size (mm, median)	31 (22, 46)	64 (36, 85)	< 0.001	0.841	39 (27, 62)	50 (28, 68)	0.865	0.028
Pathologic tumor stage			< 0.001	1.012			0.824	0.085
I	109 (72.19)	38 (29.01)			31 (50.82)	33 (54.10)		
II	28 (18.54)	41 (31.30)			19 (31.15)	19 (31.15)		
III	14 (9.27)	52 (39.69)			11 (18.03)	9 (14.75)		

Values are expressed as mean ± SD or n (%). PSM: Propensity score matching; BMI: Body mass index; ASA score: American Society of Anesthesiologists Physical Status Classification; TLTG: Totally laparoscopic gastrectomy; OTG: Open total gastrectomy.

### Risk factors for postoperative complications

Tables 5 and 6 demonstrate the risk factors for postoperative complications after TLTG and OTG. BMI and American Society of Anaesthesiologists (ASA) scores were significantly associated with the occurrence of early complications in the univariate analysis. In addition, ASA score and age were significantly associated with the incidence of ≥ 3 CDC and EJ-related complications, respectively. Multivariate analysis demonstrated that BMI [odds ratio (OR), 1.824; 95% confidence interval (CI): 1.029-3.234, *P* = 0.040] and ASA score (OR, 3.154; 95%CI: 1.084-9.174, *P* = 0.035) were independent risk factors of early complications. Furthermore, multivariate analysis revealed that age was associated with ≥ 3 CDC and EJ-related complications.

## DISCUSSION

To the best of our knowledge, this is the first study to compare feasibility and oncological outcomes between patients who underwent TLTG with the modified overlap method and OTG. This study demonstrated that TLTG with the modified overlap method is a technically safe procedure based on acceptable postoperative

**Table 2 Early surgical outcomes and pathologic data in patients undergoing the totally laparoscopic gastrectomy with the modified overlap method and open total gastrectomy**

Variable	Total set (n = 282)		P value	PSM set (1:1) (n = 122)		P value
	TLTG (n = 151)	OTG (n = 131)		TLTG (n = 61)	OTG (n = 61)	
Operative time (min)	147.68 ± 29.64	145.24 ± 35.48	0.282	147.11 ± 25.48	143.46 ± 38.09	0.351
Time to first flatus (d)	3.73 ± 0.90	4.14 ± 0.81	< 0.001	3.62 ± 0.84	4.15 ± 0.87	<b>0.002</b>
Time to soft diet (d)	4.99 ± 3.78	7.24 ± 6.29	< 0.001	4.62 ± 2.67	7.47 ± 7.92	<b>0.001</b>
Perioperative transfusion (n)			< 0.001			<b>0.035</b>
No	145 (96.03)	107 (81.68)		59 (96.72)	52 (85.25)	
Yes	6 (3.97)	24 (18.32)		2 (3.28)	9 (14.75)	
Hospital day after surgery (d)	9.96 ± 6.36	13.06 ± 11.09	< 0.001	9.62 ± 5.32	13.51 ± 10.67	<b>&lt; 0.001</b>
Pick of pain score (VAS)	4 (3.92)	5 (2.51)	0.494	3 (3.16)	1 (1.05)	0.317
Pain score at postoperative day	3.19 ± 1.04	3.83 ± 1.14	< 0.001	3.23 ± 1.09	4.07 ± 1.35	<b>&lt; 0.001</b>
Pain score at postoperative day 1	2.98 ± 1.07	3.76 ± 1.13	< 0.001	2.97 ± 0.87	3.77 ± 1.07	<b>&lt; 0.001</b>
Pain score at postoperative day 3	2.68 ± 1.17	3.10 ± 1.28	< 0.001	2.75 ± 1.31	3.16 ± 1.27	<b>&lt; 0.001</b>
Pain score at postoperative day 5	1.93 ± 1.13	2.61 ± 1.49	< 0.001	1.82 ± 1.13	2.64 ± 1.21	<b>&lt; 0.001</b>
Administration of analgesics (n)	9.74 ± 8.92	16.22 ± 18.06	< 0.001	10.61 ± 11.07	16.92 ± 13.72	<b>&lt; 0.001</b>
Administration of opioid (n)	2.89 ± 5.49	5.43 ± 11.51	< 0.001	3.21 ± 6.98	4.48 ± 5.15	<b>0.031</b>
Retrieved LN	39.53 ± 15.59	41.03 ± 15.31	0.265	38.67 ± 13.82	38.13 ± 14.52	0.713

Values are expressed as mean ± SD or n (%) or median (range). PSM: Propensity score matching; LN: Lymph node; PRM: Proximal resection margin; TLTG: Totally laparoscopic gastrectomy; OTG: Open total gastrectomy.

complications, including EJ-related complications.

The overlap method is a widely used EJ reconstruction method in TLTG, it which can lessen the tension in the anastomosis and reduce mesentery division. This secures additional jejunum length for anastomosis[15,16]. This method involves a linear stapler for anastomosis; therefore, the area around the abdominal esophagus requires sufficient dissection. Furthermore, and space in the hiatus and length of the esophagus in which the stapler will be placed should be secured. This may lead to tension in the esophagus after anastomosis and hiatal hernia caused by excessive hiatus dissection. We have devised a novel method to minimize these risks, named the modified overlap method. We use a linear stapler; however, compared with the existing side-to-side anastomosis, less esophageal dissection is required. Further, anastomosis is completed obliquely at 45°; therefore, the resulting anastomosis is similar to when a circular stapler is used because end to side anastomosis is possible. This study proved the TLTG with this modified overlap method showed no significant difference in EJ complications when compared with OTG.

A previous comparative study of LTG and OTG reported similar EJ anastomotic complications; however, a previous large multicenter cohort study in Japan has shown that open surgery is safer for EJ reconstruction[11,12,17]. This indicates that controversy remains regarding the superior method for EJ anastomosis between OTG and LTG. Furthermore, international treatment guidelines, including the Korean gastric cancer treatment and Japanese gastric cancer treatment guidelines, do not yet recognize LTG as a standard treatment[18,19]. Nonetheless, our data indicate that a randomized clinical trial assessing the surgical and oncological outcomes using the modified overlap method should be conducted to confirm its safety and efficacy.

In this study, we overcame operative time and lymphadenectomy issues using the TLTG with the modified overlap method. First, laparoscopic gastrectomy surgery is longer than open gastrectomy[2,20,21]. However, the institution in which this study was conducted is a high-volume center where more than a thousand laparoscopic gastrectomies are performed annually. The lead surgeon in this study performs > 300 gastric cancer operations per year. All surgical team members in this institution are skilled and experienced; therefore, we predicted a reduced operative time while maintaining acceptable surgical and oncological outcomes. However, it may be

Table 3 Postoperative complications

Variable	Total set (n = 282)		P value	PSM set (1:1) (n = 122)		P value
	TLTG (n = 151)	OTG (n = 131)		TLTG (n = 61)	OTG (n = 61)	
Early complications						
No	119 (78.81)	99 (75.57)	0.518	48 (78.69)	43 (70.49)	0.317
Yes	32 (21.19)	32 (24.43)		13 (21.31)	18 (29.51)	
Late complications						
No	142 (94.04)	125 (95.42)	0.607	56 (91.80)	59 (96.72)	0.257
Yes	9 (5.96)	6 (4.58)		5 (8.20)	2 (3.28)	
CDC			0.426			0.564
0-2	138 (91.39)	116 (88.55)		56 (91.80)	54 (88.52)	
≥ 3	13 (8.61)	15 (11.45)		5 (8.20)	7 (11.48)	
EJ related complications			0.090			0.270
No	148 (98.01)	123 (93.89)		59 (96.72)	56 (91.80)	
Yes	3 (1.99)	8 (6.11)		2 (3.28)	5 (8.20)	

Values are expressed as mean ± SD or *n* (%). PSM: Propensity score matching; TLTG: Totally laparoscopic gastrectomy; OTG: Open total gastrectomy; CDC: Clavien-Dindo classification; EJ: Esophagojejunostomy.

Table 4 Characteristics of the patients with esophagojejunostomy-related complications

Case	Sex	Age	Primary operation	TNMstage	Early or late	Type of complication	CDC	Treatment	Hospital day
1	F	79	TLTG	III	Early	Bleeding	5	Operation	8
2	M	65	TLTG	II	Early	Leakage	3A	Intervention	20
3	M	74	OTG	I	Early	Leakage	2	Conservative	14
4	M	74	OTG	I	Early	Bleeding	3A	Intervention	72
5	M	60	OTG	I	Early	Leakage	3A	Intervention	48
6	M	66	OTG	I	Early	Leakage	2	Conservative	25
7	M	63	OTG	I	Early	Leakage	3A	Intervention	32

TNM: Tumor-node-metastasis; CDC: Clavien-Dindo classification; F: Female; M: Male; TLTG: Totally laparoscopic gastrectomy; OTG: Open total gastrectomy.

difficult to apply the results of this study to low-volume centers or inexperienced surgeons.

Second, lymph node dissection is an important procedure in gastric cancer surgery because the oncologic outcome is dependent on a proper lymphadenectomy[22]. The AJCC recommends that ≥ 30 lymph nodes be removed for lymphadenectomy in gastric cancer[23]. In this study, there was no statistically significant difference in the number of retrieved lymph nodes between groups; ≥ 30 lymph nodes were removed in both groups. In addition, this study showed that the 5-year overall and RFS after PSM analysis did not differ between groups.

In general, the risk factors associated with surgical complications in laparoscopic gastrectomy are comorbidity, surgeon experience, age, malnutrition, gender, and chronic liver disease[24-26]. Most studies have included and analyzed patients who underwent total and distal gastrectomies. Fewer studies have analyzed total gastrectomy alone. Kosuga *et al*[25] and Martin *et al*[26] have classified total gastrectomy as a risk factor for complications (OR 1.63 and 3.13, respectively). This indicates that it is important to evaluate risk factors relative to limited total gastrectomy. Li *et al*[27] have shown that old age combined with splenectomy is a risk factor for overall complications after total gastrectomy. In this study, preoperative BMI and ASA scores were risk factors associated with early complications. Further, old age



**Table 5 Univariate analysis of risk factors for overall early, Clavien-Dindo classification  $\geq 3$ , and esophagojejunostomy-related complications**

Variables	Early complications		CDC $\geq 3$ complications		EJ-related complications	
	OR (95%CI)	P value	OR (95%CI)	P value	OR (95%CI)	P value
Type of surgery		0.518		0.428		0.090
TLTG	1		1		1	
OTG	1.202 (0.688-2.100)		1.373 (0.628-3.002)		3.209 (0.833-12.356)	
Age		0.289		0.051		<b>0.035</b>
< 60	1		1		1	
$\geq 60$	1.358 (0.772-2.390)		2.347 (0.997-5.525)		9.220 (1.164-73.022)	
BMI		<b>0.045</b>		0.380		0.402
< 25	1		1		1	
$\geq 25$	1.773 (1.012-3.109)		1.419 (0.649-3.101)		1.678 (0.500-5.633)	
ASA score		<b>0.030</b>		<b>0.036</b>		
1-2	1		1			
3	3.224 (1.122-9.265)		3.682 (1.088-12.456)			
Number of comorbidities		0.342				0.752
0-2	1				1	
> 2	1.631 (0.594-4.480)				1.406 (0.170-11.599)	
Combined operation		0.685		0.381		0.735
No	1		1		1	
Yes	0.833 (0.346-2.008)		0.515 (0.117-2.272)		0.697 (0.086-5.618)	
History of abdominal surgery		0.130		0.323		
No	1		1		1	
Yes	1.640 (0.864-3.111)		1.554 (0.648-3.726)		1.408 (0.362-5.478)	0.622
Tumor size		0.521		0.442		0.053
< 5 cm	1		1		1	
$\geq 5$ cm	0.830 (0.470-1.466)	0.521	0.727 (0.323-1.638)		3.786 (0.983-14.585)	
Operation time		0.225		0.605		0.805
< 150 min	1		1		1	
$\geq 150$ min	1.414 (0.808-2.477)		1.230 (0.562-2.692)		1.165 (0.347-3.912)	
Retrieved lymph node		0.714		0.662		0.246
< 30	1		1		1	
$\geq 30$	0.888 (0.471-1.676)		1.235 (0.480-3.181)		3.416 (0.429-27.170)	
Pathologic tumor stage		0.418		0.864		0.875
I	1		1		1	
II	0.666 (0.328-1.351)		1.246 (0.497-3.126)		0.701 (0.138-3.568)	
III	0.704 (0.346-1.431)		0.950 (0.348-2.592)		1.119 (0.27-4.617)	

Values are expressed as mean  $\pm$  SD or *n* (%). TLTG: Totally laparoscopic total gastrectomy; OTG: Open total gastrectomy; CDC: Clavien-Dindo classification; EJ: Esophagojejunostomy; CI: Confidence interval; OR: Odds ratio.

was a risk factor associated with EJ complications. Patients over 60-year-old with a BMI over 25 and ASA scores of  $\geq 3$  were more likely to have surgical complications; therefore, caution is required during surgery and careful perioperative management is necessary.

**Table 6** Multivariate analysis of risk factors for early, Clavien-Dindo classification  $\geq 3$ , and esophagojejunostomy-related complications

Variables	Early complications		CDC $\geq 3$ complications		EJ related complications	
	OR (95%CI)	P value	OR (95%CI)	P value	OR (95%CI)	P value
Type of surgery						
TLTG	1		1		1	
OTG	1.275 (0.719-2.262)	0.405	1.431 (0.650-3.153)	0.373	3.546 (0.908-13.854)	0.069
Age						
< 60			1		1	
$\geq 60$			2.391 (1.013-5.641)	0.047	9.925 (1.245-79.107)	0.030
BMI						
< 25	1					
$\geq 25$	1.824 (1.029-3.234)	0.040				
ASA score						
1-2	1					
3	3.154 (1.084-9.174)	0.035				

Values are expressed as mean  $\pm$  SD or *n* (%). TLTG: Totally laparoscopic total gastrectomy; OTG: Open total gastrectomy; CDC: Clavien-Dindo classification; EJ: Esophagojejunostomy; CI: Confidence interval; OR: Odds ratio; BMI: Body mass index; ASA score: American Society of Anesthesiologists Physical Status Classification.

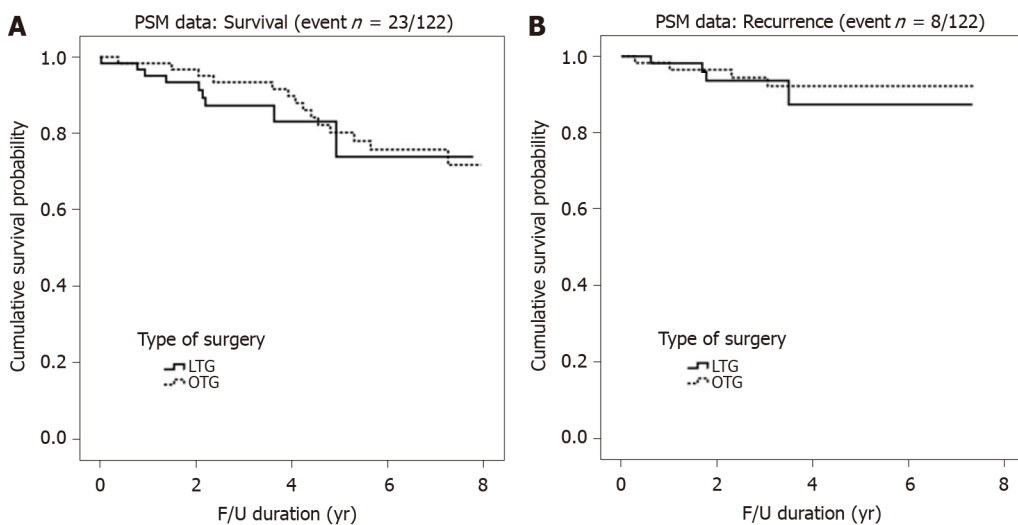


**Figure 2** Survival curves for matched patients. A: Overall survival; B: Recurrence free survival. PSM: Propensity score matching; TLTG: Laparoscopic total gastrectomy; OTG: Open total gastrectomy; F/U: Follow up.

This study has some limitations. First, it is a retrospective study performed by a single experienced surgeon at a high-volume center. Therefore, our method might not be appropriate for relatively inexperienced surgeons or small-volume institutes. Second, the number of enrolled patients is relatively small; therefore, subgroup analysis, such as distinguishing between early gastric cancer and advanced gastric cancer or grouping by stage, was not possible.

## CONCLUSION

In conclusion, we confirmed that TLTG with the modified overlap method had several advantages over OTG. These included a lower pain score, earlier bowel recovery, and discharge based on acceptable postoperative complications and oncological outcomes.

## ARTICLE HIGHLIGHTS

**Research background**

Although several methods of totally laparoscopic total gastrectomy (TLTG) have been reported, the best anastomosis technique of TLTG has not been conclusively established. Recently, we developed a modified overlap method for TLTG for overcoming these disadvantages of linear stapled method. This procedure requires less dissection around abdominal esophagus; therefore, it can create a secure esophagojejunal anastomosis with reduced tension as circular stapled method.

**Research motivation**

Whether is a more optimal anastomotic method of esophagojejunostomy in TLTG and open total gastrectomy (OTG) remains unclear. Especially, there was no report about comparing between TLTG with overlap method and OTG.

**Research objectives**

The aim of this study was to investigate the effectiveness and surgical outcomes including recurrence and survival of TLTG using the modified overlap method compared with OTG using the circular stapled method.

**Research methods**

We performed 151 TLTG with modified overlap method and 131 OTG for gastric cancer between March 2012 and December 2018 at Asan Medical Center. We evaluated surgical and oncological outcomes between the two groups using propensity score matching. In addition, we analyzed risk factors associated with postoperative complications for improvement of postoperative management of gastric cancer surgery.

**Research results**

The patients who underwent TLTG were discharged earlier than those who underwent OTG. Time to first flatus and soft diet were significantly shorter in TLTG group. Pain score at all postoperative period and administration of opioid were significantly lower after the TLTG. No statistically significant difference was found between the two groups in terms of early, late and esophagojejunostomy-related complications. Significant differences were observed not with respect to 5-year recurrence free survival and overall survival.

**Research conclusions**

TLTG with modified overlap method have favorable surgical and oncological outcomes compared with OTG. Furthermore, the surgeon should perform total gastrectomy cautiously and delicately especially with the patients with obese, high American Society of Anaesthesiologists score and old age.

**Research perspectives**

Based on our results, we confirmed that the TLTG with modified overlap method has several advantages over OTG. However, this study has certain limitations. It is a retrospective study performed by a single experienced surgeon at a high-volume center, and the number of enrolled patients is relatively small.

## REFERENCES

- 1 **Chen K**, Pan Y, Zhai ST, Yu WH, Pan JH, Zhu YP, Chen QL, Wang XF. Totally laparoscopic vs open total gastrectomy for gastric cancer: A case-matched study about short-term outcomes. *Medicine (Baltimore)* 2017; **96**: e8061 [PMID: 28930841 DOI: 10.1097/MD.0000000000008061]
- 2 **Haverkamp L**, Weijs TJ, van der Sluis PC, van der Tweel I, Ruurda JP, van Hillegersberg R. Laparoscopic total gastrectomy vs open total gastrectomy for cancer: a systematic review and meta-analysis. *Surg Endosc* 2013; **27**: 1509-1520 [PMID: 23263644 DOI: 10.1007/s00464-012-2661-1]
- 3 **Kim HS**, Kim BS, Lee IS, Lee S, Yook JH. Comparison of totally laparoscopic total gastrectomy and open total gastrectomy for gastric cancer. *J Laparoendosc Adv Surg Tech A* 2013; **23**: 323-331 [PMID: 23379920 DOI: 10.1089/lap.2012.0389]
- 4 **Gong W**, Li J. Combat with esophagojejunal anastomotic leakage after total gastrectomy for gastric cancer: A critical review of the literature. *Int J Surg* 2017; **47**: 18-24 [PMID: 28935529 DOI: 10.1016/j.ijsu.2017.09.019]
- 5 **Ebihara Y**, Okushiba S, Kawarada Y, Kitashiro S, Katoh H. Outcome of functional end-to-end

- esophagojejunostomy in totally laparoscopic total gastrectomy. *Langenbecks Arch Surg* 2013; **398**: 475-479 [PMID: 23354359 DOI: 10.1007/s00423-013-1051-z]
- 6 **Ito H**, Inoue H, Odaka N, Satodate H, Onimaru M, Ikeda H, Takayanagi D, Nakahara K, Kudo SE. Evaluation of the safety and efficacy of esophagojejunostomy after totally laparoscopic total gastrectomy using a trans-orally inserted anvil: a single-center comparative study. *Surg Endosc* 2014; **28**: 1929-1935 [PMID: 24488351 DOI: 10.1007/s00464-014-3417-x]
  - 7 **Jeong O**, Jung MR, Kim GY, Kim HS, Ryu SY, Park YK. Comparison of short-term surgical outcomes between laparoscopic and open total gastrectomy for gastric carcinoma: case-control study using propensity score matching method. *J Am Coll Surg* 2013; **216**: 184-191 [PMID: 23211117 DOI: 10.1016/j.jamcollsurg.2012.10.014]
  - 8 **Okabe H**, Obama K, Tanaka E, Nomura A, Kawamura J, Nagayama S, Itami A, Watanabe G, Kanaya S, Sakai Y. Intracorporeal esophagojejunal anastomosis after laparoscopic total gastrectomy for patients with gastric cancer. *Surg Endosc* 2009; **23**: 2167-2171 [PMID: 18553203 DOI: 10.1007/s00464-008-9987-8]
  - 9 **Shim JH**, Yoo HM, Oh SI, Nam MJ, Jeon HM, Park CH, Song KY. Various types of intracorporeal esophagojejunostomy after laparoscopic total gastrectomy for gastric cancer. *Gastric Cancer* 2013; **16**: 420-427 [PMID: 23097123 DOI: 10.1007/s10120-012-0207-9]
  - 10 **Choi M**, Ko CS, Yook JH, Kim BS. Comparative outcomes between totally laparoscopic total gastrectomy with the modified overlap method for early gastric cancer and advanced gastric cancer: review of 149 consecutive cases. *Wideochir Inne Tech Maloinwazyjne* 2020; **15**: 437-445 [PMID: 32904610 DOI: 10.5114/wiitm.2020.96098]
  - 11 **Inokuchi M**, Otsuki S, Fujimori Y, Sato Y, Nakagawa M, Kojima K. Systematic review of anastomotic complications of esophagojejunostomy after laparoscopic total gastrectomy. *World J Gastroenterol* 2015; **21**: 9656-9665 [PMID: 26327774 DOI: 10.3748/wjg.v21.i32.9656]
  - 12 **Lee JH**, Nam BH, Ryu KW, Ryu SY, Park YK, Kim S, Kim YW. Comparison of outcomes after laparoscopy-assisted and open total gastrectomy for early gastric cancer. *Br J Surg* 2015; **102**: 1500-1505 [PMID: 26398912 DOI: 10.1002/bjs.9902]
  - 13 **Union for International Cancer Control**. What is TNM cancer staging system? [cited 17 March 2021]. In: Union for International Cancer Control (UICC) homepage [Internet]. Available from: <https://www.uicc.org/resources/tnm>
  - 14 **Dindo D**, Demartines N, Clavien PA. Classification of surgical complications: a new proposal with evaluation in a cohort of 6336 patients and results of a survey. *Ann Surg* 2004; **240**: 205-213 [PMID: 15273542 DOI: 10.1097/01.sla.0000133083.54934.ae]
  - 15 **Kawamura H**, Ohno Y, Ichikawa N, Yoshida T, Homma S, Takahashi M, Taketomi A. Anastomotic complications after laparoscopic total gastrectomy with esophagojejunostomy constructed by circular stapler (OrVil™) vs linear stapler (overlap method). *Surg Endosc* 2017; **31**: 5175-5182 [PMID: 28488177 DOI: 10.1007/s00464-017-5584-z]
  - 16 **Son SY**, Cui LH, Shin HJ, Byun C, Hur H, Han SU, Cho YK. Modified overlap method using knotless barbed sutures (MOBS) for intracorporeal esophagojejunostomy after totally laparoscopic gastrectomy. *Surg Endosc* 2017; **31**: 2697-2704 [PMID: 27699517 DOI: 10.1007/s00464-016-5269-z]
  - 17 **Kodera Y**, Yoshida K, Kumamaru H, Kakeji Y, Hiki N, Etoh T, Honda M, Miyata H, Yamashita Y, Seto Y, Kitano S, Konno H. Introducing laparoscopic total gastrectomy for gastric cancer in general practice: a retrospective cohort study based on a nationwide registry database in Japan. *Gastric Cancer* 2019; **22**: 202-213 [PMID: 29427039 DOI: 10.1007/s10120-018-0795-0]
  - 18 **Guideline Committee of the Korean Gastric Cancer Association (KGCA)**; Development Working Group & Review Panel. Erratum: Korean Practice Guideline for Gastric Cancer 2018: an Evidence-based, Multi-disciplinary Approach. *J Gastric Cancer* 2019; **19**: 372-373 [PMID: 31598379 DOI: 10.5230/jgc.2019.19.e32]
  - 19 **Japanese Gastric Cancer Association**. Japanese gastric cancer treatment guidelines 2018 (5th edition). *Gastric Cancer* 2021; **24**: 1-21 [PMID: 32060757 DOI: 10.1007/s10120-020-01042-y]
  - 20 **Deng Y**, Zhang Y, Guo TK. Laparoscopy-assisted vs open distal gastrectomy for early gastric cancer: A meta-analysis based on seven randomized controlled trials. *Surg Oncol* 2015; **24**: 71-77 [PMID: 25791201 DOI: 10.1016/j.suronc.2015.02.003]
  - 21 **Zeng YK**, Yang ZL, Peng JS, Lin HS, Cai L. Laparoscopy-assisted vs open distal gastrectomy for early gastric cancer: evidence from randomized and nonrandomized clinical trials. *Ann Surg* 2012; **256**: 39-52 [PMID: 22664559 DOI: 10.1097/SLA.0b013e3182583e2e]
  - 22 **Schwarz RE**, Smith DD. Clinical impact of lymphadenectomy extent in resectable gastric cancer of advanced stage. *Ann Surg Oncol* 2007; **14**: 317-328 [PMID: 17094022 DOI: 10.1245/s10434-006-9218-2]
  - 23 **Edge SB**, Byrd DR, Compton CC, Fritz AG, Greene FL, Trotti AI; American Joint Committee of Cancer. AJCC cancer staging manual. 7th ed. New York: Springer, 2010
  - 24 **Kim MC**, Kim W, Kim HH, Ryu SW, Ryu SY, Song KY, Lee HJ, Cho GS, Han SU, Hyung WJ; Korean Laparoscopic Gastrointestinal Surgery Study (KLASS) Group. Risk factors associated with complication following laparoscopy-assisted gastrectomy for gastric cancer: a large-scale korean multicenter study. *Ann Surg Oncol* 2008; **15**: 2692-2700 [PMID: 18663532 DOI: 10.1245/s10434-008-0075-z]
  - 25 **Kosuga T**, Ichikawa D, Komatsu S, Kubota T, Okamoto K, Konishi H, Shiozaki A, Fujiwara H, Otsuji E. Clinical and surgical factors associated with organ/space surgical site infection after laparoscopic gastrectomy for gastric cancer. *Surg Endosc* 2017; **31**: 1667-1674 [PMID: 27506433]

DOI: [10.1007/s00464-016-5156-7](https://doi.org/10.1007/s00464-016-5156-7)

- 26 **Martin AN**, Das D, Turrentine FE, Bauer TW, Adams RB, Zaydfudim VM. Morbidity and Mortality After Gastrectomy: Identification of Modifiable Risk Factors. *J Gastrointest Surg* 2016; **20**: 1554-1564 [PMID: [27364726](https://pubmed.ncbi.nlm.nih.gov/27364726/) DOI: [10.1007/s11605-016-3195-y](https://doi.org/10.1007/s11605-016-3195-y)]
- 27 **Li Z**, Liu Y, Bai B, Yu D, Lian B, Zhao Q. Surgical and Long-Term Survival Outcomes After Laparoscopic and Open Total Gastrectomy for Locally Advanced Gastric Cancer: A Propensity Score-Matched Analysis. *World J Surg* 2019; **43**: 594-603 [PMID: [30229383](https://pubmed.ncbi.nlm.nih.gov/30229383/) DOI: [10.1007/s00268-018-4799-z](https://doi.org/10.1007/s00268-018-4799-z)]





## Retrospective Study

# Radiofrequency ablation vs surgical resection in elderly patients with hepatocellular carcinoma in Milan criteria

Maria Conticchio, Riccardo Inchingolo, Antonella Delvecchio, Letizia Laera, Francesca Ratti, Maximiliano Gelli, Ferdinando Anelli, Alexis Laurent, Giulio Vitali, Paolo Magistri, Giacomo Assirati, Emanuele Felli, Taiga Wakabayashi, Patrick Pessaux, Tullio Piardi, Fabrizio di Benedetto, Nicola de'Angelis, Javier Briceño, Antonio Rampoldi, Renè Adam, Daniel Cherqui, Luca Antonio Aldrighetti, Riccardo Memeo

**ORCID number:** Maria Conticchio 0000-0003-3177-5274; Riccardo Inchingolo 0000-0002-0253-5936; Antonella Delvecchio 0000-0002-7759-4340; Letizia Laera 0000-0003-2183-8817; Francesca Ratti 0000-0002-4710-6940; Maximiliano Gelli 0000-0001-9807-4021; Ferdinando Anelli 0000-0002-0916-1946; Alexis Laurent 0000-0003-1372-0843; Giulio Vitali 0000-0001-8956-0247; Paolo Magistri 0000-0001-8326-069X; Giacomo Assirati 0000-0001-8240-1497; Emanuele Felli 0000-0002-6510-1457; Taiga Wakabayashi 0000-0002-5074-0205; Patrick Pessaux 0000-0001-5635-7437; Tullio Piardi 0000-0001-6704-3206; Fabrizio di Benedetto 0000-0002-6718-8760; Nicola de'Angelis 0000-0002-1211-4916; Javier Briceño 0000-0001-7027-7898; Antonio Rampoldi 0000-0003-2494-5925; Renè Adam 0000-0003-2169-5449; Daniel Cherqui 0000-0001-5270-2731; Luca Antonio Aldrighetti 0000-0001-7729-2468; Riccardo Memeo 0000-0002-1668-932X.

**Author contributions:** All authors equally contributed to this paper with conception and design of the study, literature review and analysis, drafting and critical revision and editing, and final approval of the final version.

**Maria Conticchio**, Departement of Emergency and Trasplantation of Organs, General Surgery Unit "M. Rubino", Policlinico di Bari, Bari 70124, Italy

**Riccardo Inchingolo**, Interventional Radiology Unit, "F. Miulli" General Regional Hospital, Acquaviva delle Fonti 70021, Italy

**Antonella Delvecchio**, Department of Emergency and Organ Transplantation, General Surgery Unit "M. Rubino", University of Bari, Ceglie Messapica 70124, Italy

**Letizia Laera**, Department of Oncology, "F. Miulli" General Regional Hospital, Acquaviva delle Fonti 70021, Italy

**Francesca Ratti**, Department of Surgery, Univ Vita Salute San Raffaele, Milan 20132, Italy

**Maximiliano Gelli**, Department of Visceral and Oncological Surgery, Gustave Roussy Cancer Campus Grand Paris, Villejuif 94800, France

**Ferdinando Anelli**, Unit of Oncologic and Pancreatic Surgery, Hospital University Reina Sofia, Cordoba 14004, Spain

**Alexis Laurent**, Department of Digestive and Hepatobiliary Surgery, Henri Mondor University Hospital, Creteil 94000, France

**Giulio Vitali**, Department of Surgery, University of Geneva Hospitals, Geneva 44041, Switzerland

**Paolo Magistri, Giacomo Assirati, Fabrizio di Benedetto**, Hepato-Pancreato-Biliary Surgery and Liver Transplantation Unit, University of Modena and Reggio Emilia, Modena 41124, Italy

**Emanuele Felli**, Institut de Recherche Contre les Cancers de l'Appareil Digestif, Strasbourg 67000, France

**Taiga Wakabayashi**, Department of Surgery, Keio University School of Medicine, Shinjuku-ku 160-8582, Japan

**Patrick Pessaux**, Hepato-Biliary and Pancreatic Surgical Unit, Nouvel Hôpital Civil, Strasbourg cedex 67091, France

# Institutional review board

**statement:** This study was reviewed and approved by the Ethics Committee of "F. Miulli" General Regional Hospital.

# Informed consent statement:

Patients were not required to give informed consent to the study because the analysis used anonymous clinical data that were obtained after each patient agreed to treatment by written consent.

**Conflict-of-interest statement:** All the authors are aware of the content of the manuscript and have no conflict of interest.

**Data sharing statement:** No additional data are available.

**Open-Access:** This article is an open-access article that was selected by an in-house editor and fully peer-reviewed by external reviewers. It is distributed in accordance with the Creative Commons Attribution NonCommercial (CC BY-NC 4.0) license, which permits others to distribute, remix, adapt, build upon this work non-commercially, and license their derivative works on different terms, provided the original work is properly cited and the use is non-commercial. See: <http://creativecommons.org/licenses/by-nc/4.0/>

**Manuscript source:** Invited manuscript

**Specialty type:** Gastroenterology and hepatology

**Country/Territory of origin:** Italy

**Peer-review report's scientific quality classification**

Grade A (Excellent): 0  
Grade B (Very good): B, B, B  
Grade C (Good): C  
Grade D (Fair): 0  
Grade E (Poor): 0

**Received:** February 1, 2021

**Peer-review started:** February 1, 2021

**First decision:** February 27, 2021

**Revised:** March 13, 2021

**Accepted:** April 21, 2021

**Tullio Piardi**, Department of Hepatobiliary, Pancreatic and Digestive Surgery, University Hospital Robert Debré of Reims, Reims 51100, France

**Tullio Piardi**, Hepatobiliary and Pancreatic Surgery Unit, General Surgery Departement, Troyes Hospital, Troyes Zip or Postal Code, France

**Tullio Piardi**, University of Champagne - Ardenne, Reims 51100, France

**Nicola de'Angelis**, Unit of Minimally Invasive and Robotic Digestive Surgery, "F. Miulli" General Regional Hospital, Acquaviva delle Fonti 70021, Italy

**Javier Briceño**, Department of General and Digestive Surgery, Reina Sofia University Hospital, Cordoba 14004, Spain

**Antonio Rampoldi**, Interventional Radiology Unit, Niguarda Hospital, Milan 20132, Italy

**René Adam**, Department of Surgery, Hopital Paul Brousse, Villejuif 94800, France

**Daniel Cherqui**, Hepatobiliary Center, Hopital Paul Brousse, Villejuif 94800, France

**Luca Antonio Aldrighetti**, Unit of Hepato-Pancreatic-Biliary Surgery, Univ Vita Salute San Raffaele, Milan 20132, Italy

**Riccardo Memeo**, Unit of Hepato-Pancreatic-Biliary Surgery, "F. Miulli" General Regional Hospital, Acquaviva delle Fonti 70021, Italy

**Corresponding author:** Riccardo Inchingolo, MD, Chief Doctor, Director, Doctor, Interventional Radiology Unit, "F. Miulli" General Regional Hospital, Via di Santeramo, Acquaviva delle Fonti 70021, Italy. [riccardoin@hotmail.it](mailto:riccardoin@hotmail.it)

# Abstract

## BACKGROUND

Surgical resection and radiofrequency ablation (RFA) represent two possible strategy in treatment of hepatocellular carcinoma (HCC) in Milan criteria.

## AIM

To evaluate short- and long-term outcome in elderly patients (> 70 years) with HCC in Milan criteria, which underwent liver resection (LR) or RFA.

## METHODS

The study included 594 patients with HCC in Milan criteria (429 in LR group and 165 in RFA group) managed in 10 European centers. Statistical analysis was performed using the Kaplan-Meier method before and after propensity score matching (PSM) and Cox regression.

## RESULTS

After PSM, we compared 136 patients in the LR group with 136 patients in the RFA group. Overall survival at 1, 3, and 5 years was 91%, 80%, and 76% in the LR group and 97%, 67%, and 41% in the RFA group respectively ( $P = 0.001$ ). Disease-free survival at 1, 3, and 5 years was 84%, 60% and 44% for the LR group, and 63%, 36%, and 25% for the RFA group ( $P = 0.001$ ). Postoperative Clavien-Dindo III-IV complications were lower in the RFA group (1% *vs* 11%,  $P = 0.001$ ) in association with a shorter length of stay (2 d *vs* 7 d,  $P = 0.001$ ). In multivariate analysis, Model for End-stage Liver Disease (MELD) score (> 10) [odds ratio (OR) = 1.89], increased value of international normalized ratio (> 1.3) (OR = 1.60), treatment with radiofrequency (OR = 1.46), and multiple nodules (OR = 1.19) were independent predictors of a poor overall survival while a high MELD score (> 10) (OR = 1.51) and radiofrequency (OR = 1.37) were independent factors associated with a higher recurrence rate.

## CONCLUSION

Despite a longer length of stay and a higher rate of severe postoperative complications, surgery provided better results in long-term oncological outcomes as compared to ablation in elderly patients (> 70 years) with HCC in Milan criteria.

Article in press: April 21, 2021

Published online: May 14, 2021

P-Reviewer: Chen Z, Liao R, Zheng L

S-Editor: Gao CC

L-Editor: A

P-Editor: Liu JH



**Key Words:** Hepatocellular carcinoma; Milan criteria; Radiofrequency ablation; Surgical resection; Elderly patients; Propensity score matching

©The Author(s) 2021. Published by Baishideng Publishing Group Inc. All rights reserved.

**Core Tip:** Surgical resection and radiofrequency ablation represent two possible strategy in treatment of hepatocellular carcinoma in Milan criteria. In order to evaluate which of the two therapeutic options can provide better short-term and oncological outcomes, we compared data from 10 European centers before and after propensity score matching. Despite a longer length of stay and a higher rate of severe postoperative complications, surgery provided better results in long-term oncological outcomes as compared to ablation.

**Citation:** Conticchio M, Inchingolo R, Delvecchio A, Laera L, Ratti F, Gelli M, Anelli F, Laurent A, Vitali G, Magistri P, Assirati G, Felli E, Wakabayashi T, Pessaux P, Piardi T, di Benedetto F, de'Angelis N, Briceño J, Rampoldi A, Adam R, Cherqui D, Aldrighetti LA, Memeo R. Radiofrequency ablation vs surgical resection in elderly patients with hepatocellular carcinoma in Milan criteria. *World J Gastroenterol* 2021; 27(18): 2205-2218

**URL:** <https://www.wjgnet.com/1007-9327/full/v27/i18/2205.htm>

**DOI:** <https://dx.doi.org/10.3748/wjg.v27.i18.2205>

## INTRODUCTION

Hepatocellular carcinoma (HCC) is the sixth most common cancer and the third global cause of cancer-related death[1]. The therapeutic strategy for patients with HCC varies considerably, according to the Barcelona clinic liver cancer (BCLC) algorithm[2], from liver transplantation to resection or ablation, passing through a series of options (chemoembolization, systemic supportive therapy, and systemic chemotherapy), based on the stage of neoplasia and patient's general condition. The best radical treatment is still debated. For patients within Milan criteria, liver transplantation represents the treatment of choice, but unfortunately it is not suitable for all patients due to the scarcity of donors or due to an age limit[3-5].

For patients with very early and early-stage HCC (BCLC 0-A), liver resection (LR) represented the treatment of choice when liver function was well-preserved and when the remnant liver was sufficient. In elderly patients, these conditions were sometimes more precarious and required a more careful evaluation of the risk-benefit ratio in terms of treatment. In fact, the prognostic role of advanced age was not defined in patients with HCC subjected to resection nor was there any mention in official guidelines[6,7].

The aim of our work was to evaluate short-term and long-term outcomes in elderly HCC patients (> 70 years) within Milan criteria, undergoing LR or radiofrequency ablation (RFA).

## MATERIALS AND METHODS

### Patients

A multicentric retrospective study included 594 patients who were managed from January 2009 to January 2019 in the following centers: Centre Hépatobiliaire Paul Brousse, Villejuif, France; Hôpital Henry Mondor, Créteil, France; Hospital Universitario Reina Sofia, Cordoba, Spain; Hôpitaux Universitaires Genève, Switzerland; Ospedale Niguarda, Milan, Italy; Nouvel Hôpital Civil, Strasbourg, France; Ospedale San Raffaele, Milan, Italy; Ospedale Miulli, Bari, Italy; Policlinico di Modena, Italy; Centre Hospitalier Universitaire, Reims, France).

We included patients who underwent laparoscopic and open LR or RFA in the study. Inclusion criteria: ≥ 70 years old patients, with Child A-B disease, in BCLC 0/A stage, with tumor within Milan criteria (solitary HCC < 5 cm in diameter, or multiple HCC < 3 lesions, each < 3 cm in diameter). Exclusion criteria: patients with tumor

beyond Milan criteria, with radiological evidence of major portal/hepatic vein branch invasion, with evidence of extrahepatic disease.

The diagnosis of HCC was based on non-invasive findings [ultrasonography, computed tomography (CT) scan, magnetic resonance imaging] or histopathology (with biopsy), according to the European Association for Study of Liver (EASL) consensus criteria[2]. The type of treatment was planned in multidisciplinary team discussions including surgeons, hepatologists, oncologists, interventional radiologists, and pathologists.

### **RFA procedure**

RFA was performed using an internally cooled electrode. Depending on tumor size and position, either a single or clustered electrode was used for ablation under ultrasound guidance percutaneously or using a laparoscopic or open approach. The procedure was performed under local anesthesia and intravenous sedation for percutaneous ablation, and under general anesthesia for laparoscopic and open ablations. A control liver ultrasound was performed on the first postoperative day to assess the quality of the ablation in term of necrotic area.

### **LR procedure**

The surgical strategy was tailored based on tumor size, position, and liver function. The type of LR was defined according to the Brisbane classification[8]. Anatomical resection, wedge resection, minor and major resections were performed under general anesthesia, with an open or laparoscopic approach. Minor resection was defined as the resection of two or fewer Couinaud's liver segments, and major resection was defined as the resection of three or more liver segments. Intraoperative ultrasonography was used routinely. A Pringle's maneuver was used during hepatectomy to control intraoperative bleeding.

### **Follow-up**

Short-term outcomes included operative time, blood transfusion, complications based on the Clavien-Dindo classification[9], length of hospital stay and mortality within 90 d. Long-term outcomes evaluated rates of overall survival (OS) and disease free survival. Liver function (complete blood count, liver test, and coagulation profile) were assessed on postoperative days 1, 3, and 5. Follow-up was performed with CT-scan and blood tests (including liver function and oncological markers) once every 3 mo during the first year and every 4 mo thereafter. For patients undergoing to RFA, a CT-scan at 1 mo after ablation was performed, in order to assess results of treatment according mRECIST (modified Response Evaluation Criteria in Solid Tumors) criteria[10]. Recurrence treatment included repeat resection, ablation, trans-arterial chemo-embolization, liver transplantation, percutaneous ethanol injection, sorafenib chemotherapy, or supportive care according to the EASL-EORTC (European Organisation for Research and Treatment of Cancer) clinical practice guidelines[2].

### **Statistical analysis**

Statistical analysis was performed using the IBM SPSS 20 software. Continuous variables were compared using an independent sample t-test and Mann-Whitney U test. Categorical variables were compared using the chi-square test and Kruskal-Wallis test respectively. Recurrence-free survival (RFS) and OS curves were constructed using the Kaplan-Meier method and compared using the log-rank test. The Cox proportional hazards model was used in a stepwise manner (entry criterion  $P = 0.05$  and removal criterion  $P = 0.1$ ) to explore independent prognostic RFS and OS factors. We performed a propensity score matching (PSM) analysis to decrease selection bias by building a matched group of patients to compare perioperative characteristics, short-term and long-term outcomes in resection and ablation groups. Variables entered in our propensity model were co-morbidities, American Society of Anaesthesiologists (ASA) score, Child and MELD scores, number of lesions, and tumor size. We calculated propensity scores by applying these variables to a logistic regression model and calculated C-statistics to evaluate the goodness of fit. One-to-one PSM was performed with a caliper width ranging from the  $< 0.2$  pooled standard deviation of estimated propensity scores. A total of 136 patients out of 429 in the resection group and a total of 136 patients out of 165 in the ablation group were matched for further analyses. The relative prognostic significance of the variables in predicting OS and overall recurrence was established using univariate and multivariate Cox proportional hazards regression models. All variables with a  $P$  value  $< 0.05$  in the univariate analysis were subjected to the multivariate comparison. Results of the multivariate

analysis were presented as relative risk with a corresponding 95% confidence interval.

## RESULTS

### Before PSM

We identified 594 patients within the Milan criteria. A total of 429 patients underwent LR and 165 RFA. Perioperative data are described in [Table 1](#). The RFA group presented more co-morbidities than the LR group (64% *vs* 33%,  $P = 0.001$ ). The RFA group also had a higher percentage of patients with ASA score III-IV than the LR group (73% *vs* 60%,  $P = 0.001$ ), and a greater MELD score value (8 *vs* 6,  $P = 0.001$ ). The LR group was associated with a larger tumor size than the RFA group (30 mm *vs* 24 mm,  $P = 0.001$ ). Perioperative and postoperative data are described in [Table 2](#). Operative time was significantly increased in the resection group as compared to the RFA group (205 min *vs* 25 min,  $P = 0.0001$ ). Additionally, the perioperative blood transfusion rate was markedly higher in the LR group than in the RFA group (15% *vs* 8%,  $P = 0.001$ ).

The RFA postoperative course was burdened by a lower rate of serious complications (Clavien-Dindo III-IV) than the LR group (1% *vs* 9%,  $P = 0.001$ ). The RFA group had also significantly shorter postoperative hospital stays than the LR group (2 d *vs* 6 d,  $P = 0.001$ ).

The estimated 1-, 3-, and 5-year OS rates were 91.9%, 84%, and 75.5% for the LR group and 92%, 66.4%, and 37.8% for the RFA group ( $P = 0.001$ , [Figure 1](#)). The estimated 1-, 3-, and 5-year disease-free survival rates were 85.7%, 63.7%, and 50.3% for the LR group, and 66.7%, 37.8%, and 27.7% for the RFA group ( $P = 0.001$ , [Figure 2](#)).

### After PSM

After matching, we obtained a comparable population for both groups ([Table 1](#)). The variables included in the PSM are comorbidities, ASA and MELD score, tumor size and number of lesions. The use of these parameters for the PSM allowed us to obtain two samples to be compared more homogeneous, and therefore to have short- and long-term results between the two groups less burdened by other variables, although the number of patients in the two groups are smaller after pairing. Perioperative and postoperative results are described in [Table 2](#). The postoperative course of the RFA group was burdened by a lower rate of serious complications (Clavien-Dindo III-IV) as compared to the LR group (1% *vs* 11%,  $P = 0.001$ ). The RFA group had also significantly shorter postoperative hospital stays than the LR group (2 d *vs* 7 d,  $P = 0.001$ ). Operative time was significantly increased in the LR group as compared to the RFA group (median range: 190 min *vs* 25 min,  $P = 0.001$ ). In addition, the perioperative blood transfusion rate was markedly higher in the LR group than in the RFA group (17% *vs* 8%,  $P = 0.001$ ).

The estimated 1-, 3-, and 5-year OS rates were 91%, 80.2%, and 76.6% for the LR group and 97.7%, 68.9%, and 40.8% for the RFA group ( $P = 0.001$ , [Figure 3](#)) respectively. The estimated 1-, 3-, and 5-year disease-free survival rates were 84.5%, 60.6%, and 44.4% for the LR group, and 63.2%, 35.7%, and 25.1% for the RFA group ( $P = 0.001$ , [Figure 4](#)) respectively.

### Multivariate analysis

We evaluated factors influencing overall and disease-free survival using univariate and multivariate analyses. Multivariate analyses ([Table 3](#)) showed that the therapeutic choice of radiofrequency [hazard ratio: 1.46; (1.1-1.79),  $P = 0.001$ ], international normalized ratio > 1.3 mg/dL [hazard ratio 1.60, (1.03-2.49),  $P = 0.03$ ], and MELD score > 10 [1.89, (1.21-2.92),  $P = 0.005$ ] were independent risk factors for OS. Concerning the rate of recurrence ([Table 4](#)), radiofrequency [1.37 (1.17-1.60),  $P = 0.0001$ ] and MELD score > 10 [1.51, (1.04-2.17)  $P = 0.0001$ ] were both considered poor prognostic factors.

## DISCUSSION

This study suggested that surgical treatment provided better results in terms of long-term oncological outcomes (OS and disease-free survival) as compared to ablative treatment (RFA) in elderly HCC patients (> 70 years) within the Milan criteria, despite a longer and more complicated postoperative course.



**Table 1 Preoperative and clinical characteristics of patients with hepatocellular carcinoma in Milan criteria who underwent surgical resection and radiofrequency ablation**

	Before PSM			After PSM		
	RFA (n = 165)	Surgery (n = 429)	P value	RFA (n = 136)	Surgery (n = 136)	P value
Male, n (%)	116 (70)	319 (74)	0.35	98 (72)	104 (76)	0.48
Age (yr) median (range)	75 (70-89)	74.9 (70-90)	0.71	75 (70-88)	74.7 (70-86.1)	0.56
BMI (kg/cm <sup>2</sup> ) median (range)	26.7 (19-51)	26.7 (19-52)	0.37	26.7 (19-51)	26 (21-41)	0.85
Co-morbidities > 2, n (%)	107 (64)	142 (33)	0.001	83 (61)	81 (60)	0.90
Cause of Cirrhosis n (%)			0.002			0.11
Hepatitis C virus	89 (54)	217 (50)		73 (54)	68 (50)	
Hepatitis B virus	10 (6)	80 (19)		10 (7)	22 (16)	
Alcohol	37 (22)	60 (14)		31 (23)	23 (17)	
Others	29 (18)	72 (17)		22 (16)	23 (17)	
ASA score, n (%)			0.004			0.59
I-II	45 (27)	172 (40)		41 (30)	36 (26)	
III-IV	120 (73)	257 (60)		95 (70)	100 (74)	
Blood tests median (range)						
Bilirubin (mg/dL)	1 (0.2-2.8)	0.9 (0.18-4.5)	0.41	1 (0.2-2.8)	0.8 (0.2-4.5)	0.02
Creatinine (mg/dL)	0.9 (0.5-2.5)	1 (0.2-2.5)	0.03	0.9 (0.5-2.3)	0.9 (0.4-2.5)	0.02
Platelet count × 10 <sup>9</sup> /L	131 (10-856)	178 (45-900)	0.00	131.5 (10-856)	155 (47-573)	0.57
INR	1.1 (0.9-2.4)	1.2 (0.6-2.5)	0.00	1.1 (0.9-2.4)	1.1 (0.8-2.5)	0.00
Child Pugh, n (%)			0.52			0.87
A	139 (84)	370 (86)		114 (84)	116 (85)	
B	26 (16)	59 (14)		22 (16)	20 (15)	
MELD median (range)	8 (6-18)	6 (6-17)	0.00	8 (6-18)	8 (6-17)	0.05
Tumors number, n (%)			0.07			0.71
Single nodule	142 (86)	392 (91)		117 (86)	120 (88)	
Multi nodules	23 (14)	37 (9)		19 (14)	16 (12)	
Tumor size (mm) n (%)	24 (10-50)	30 (7-50)	0.00	25 (10-50)	24.5 (7-50)	0.9
< 20	49 (30)	33 (8)	0.00	36 (26)	28 (21)	0.31
20-50	116 (70)	396 (92)		100 (74)	108 (79)	
Bilobar tumor, n (%)	8 (5)	8 (2)	0.08	6 (4)	2 (1)	0.28
Tumor location, n (%)			0.28			0.17
1	2 (1)	8 (2)		1 (0.7)	1 (0.7)	
2	14 (8)	41 (10)		13 (9)	14 (10)	
3	12 (7)	42 (10)		10 (7)	20 (15)	
4	20 (12)	53 (12)		15 (11)	13 (9)	
5	28 (17)	63 (15)		21 (15)	27 (19)	
6	27 (16)	87 (20)		23 (17)	29 (21)	
7	18 (11)	60 (14)		16 (12)	11 (8)	
8	44 (28)	75 (17)		37 (27)	21 (15)	
Histologically proven, n (%)	42 (25)	115 (27)	0.75	36 (26)	42 (31)	0.50

Previous treatment, <i>n</i> (%)	53 (32)	53 (12)	0.00	42 (31)	21 (15)	0.004
----------------------------------	---------	---------	------	---------	---------	-------

Continuous variables were compared using an independent sample *t*-test and Mann-Whitney *U* test. Categorical variables were compared using the chi-square test and Kruskal-Wallis test respectively. PSM: Propensity score matching; BMI: Body mass index; ASA: American Society of Anesthesiologists; MELD: Model for End-Stage Liver Disease; RFA: Radiofrequency ablation; INR: International normalized ratio.

**Table 2 Clinical and perioperative characteristics of patients with hepatocellular carcinoma in Milan criteria who underwent surgical resection and radiofrequency ablation**

	Before PSM			After PSM		
	RFA ( <i>n</i> = 165)	Surgery ( <i>n</i> = 429)	<i>P</i> value	RFA ( <i>n</i> = 136)	Surgery ( <i>n</i> = 136)	<i>P</i> value
Operative time (min) median (range)	25 (5-250)	205 (55-600)	0.002	25 (5-250)	190 (55-600)	0.001
Blood transfusion, <i>n</i> (%)	13 (8)	66 (15)	0.01	11 (8)	23 (17)	0.04
Dindo-Clavien Classification, <i>n</i> (%)			0.001			0.002
I-II	163 (99)	378 (91)		134 (98)	121 (89)	
III-IV	2 (1)	38 (9)		2 (1)	15 (11)	
Postoperative complication, <i>n</i> (%)			0.001			0.002
Yes	31 (19)	188 (44)		28 (21)	75 (55)	
No	134 (81)	241 (56)		108 (79)	61 (45)	
Type of complication, <i>n</i> (%)						
Liver failure	1 (1)	35 (8)	0.002	1 (0.7)	14 (10)	0.001
Ascites	3 (2)	60 (14)	0.003	3 (2)	17 (12)	0.002
Biliary leakage	0 (0)	9 (2)	0.064	0 (0)	3 (2)	0.25
Hemorrhage	4 (2)	19 (4)	0.340	3 (2)	11 (8)	0.51
Systemic Infection	4 (2)	30 (7)	0.03	4 (3)	14 (10)	0.03
Intra-abdominal abscess	0 (0)	23 (5)	0.00	0 (0)	8 (6)	0.007
Wound infection	2 (1)	12 (3)	0.37	2 (1)	7 (5)	0.17
Portal thrombosis	1 (1)	3 (1)	1.007	1 (0.7)	2 (1)	1
Pulmonary	7 (4)	33 (8)	0.15	6 (4)	15 (11)	0.07
Cardiac	1 (1)	18 (4)	0.03	1 (0.7)	8 (6)	0.03
Renal	1 (1)	18 (4)	0.03	1 (0.7)	6 (4)	0.12
Reoperation, <i>n</i> (%)	0 (0)	7 (2)	0.19	0 (0)	2 (1)	0.5
Postoperative treatment, <i>n</i> (%)	3 (2)	19 (4)	0.15	3 (2)	10 (7)	0.08
Length of hospital stay median (range)	2 (1-23)	6 (1-203)	0.00	2 (1-23)	7 (1-203)	0.00
Mortality 90 d, <i>n</i> (%)	3 (2)	13 (3)	0.001	3 (2)	4 (3)	1

Continuous variables were compared using an independent sample *t*-test and Mann-Whitney *U* test. Categorical variables were compared using the chi-square test and Kruskal-Wallis test respectively. PSM: Propensity score matching; RFA: Radiofrequency ablation.

Increased life expectancy, ageing, and the accumulation of chronic pathologies, such as obesity, diabetes, and some inadequate living habits (excess alcohol and smoking) led to the establishment of conditions of oxidative stress and inflammation which seemed to be the substratum favouring the onset of HCC, despite the reduction in the incidence rate of HBV and HCV-related liver disease, especially in Western countries[11].

**Table 3 Univariate and multivariate models for survival**

	Univariate analysis	Multivariate analysis	
	P value	RR (95%CI)	P value
RFA	0.001	1.46 (1.1-1.79)	0.001
Age ≤ 75 yr	0.63		
Male	0.001		
Co-morbidity ≥ 2	0.001		
BMI < 24	0.001		
ASA score III-IV	0.07		
TBil (mg/dL > 2)	0.001		
Crea (mg/dL > 1)	0.57		
PLT (U/μL > 150 × 10 <sup>3</sup> )	0.001		
INR (> 1.3)	0.001	1.60 (1.03-2.49)	0.03
Tumor size < 3 cm	0.001		
Multiple nodule	0.001	1.19 (1.08-4.17)	0.03
Child Pugh A	0.001		
MELD > 10	0.007	1.89 (1.21-2.92)	0.005

The relative prognostic significance of the variables in predicting overall survival and overall recurrence was established using univariate and multivariate Cox proportional hazards regression models. Radiofrequency ablation, international normalized ratio > 1.3 mg/dL, and Model for End-Stage Liver Disease score >10 were independent risk factors for overall survival. RFA: Radiofrequency ablation; INR: International normalized ratio; MELD: Model for End-Stage Liver Disease; RR: Relative risk; CI: Confidence interval; BMI: Body mass index; ASA: American Society of Anesthesiologists; PLT: Platelets; TBil: Total bilirubin; Crea: Creatinine.

For this reason, our study aimed to examine a part of the population still growing today, that of the elderly, (≥ 70 years), and namely patients within Milan criteria unsuitable for liver transplantation due to a reached limit of age and who should be managed either with RFA or LR. We analyzed short-term outcomes, namely perioperative characteristics (operative time, postoperative complications, length of hospital stay, and mortality within 90 d), as well as long-term outcomes, namely oncological results (OS and disease-free survival). LR was the treatment of choice in patients with very early and early-stage HCC, with a well-preserved liver function and sufficient residual liver volume. Radiofrequency was indicated in patients who were not candidates to surgery, and who presented with higher rates of local disease control and OS than other local ablative therapies[2,12,13] inducing a tumor necrosis, which guarantees a valid control of margin[14]. Microwave ablation is an alternative procedure, equally based on induction tumor destruction with heat generation, but with a different mechanism, and which seems to show promising performances although in treatment of HCC of 3-5 cm size, adjacent to vessels or gallbladder[15].

The most effective therapeutic strategy in the very early and early stages of HCC was still a matter for debate.

Radiofrequency made use of less invasiveness, thereby presenting a shorter hospital stay, fewer costs, a lower rate of major complications, as shown in multiple randomized clinical trials and meta-analyses[16-20]. On the other hand, LR provided better oncological outcomes in terms of local disease control[17,19,21] and in long-term OS[17,22,23], as reported in randomized controlled trials and meta-analyses, also and above all, considering the characteristics of HCC which presented a tendency to micro-dissemination in portal and hepatic veins and to the generation of micro-metastases around the lesion[24,25].

Recent studies have shown that this therapeutic algorithm can also be extended to elderly patients[26-29]. Old age represented an important risk factor concerning postoperative morbidity and mortality, especially in association with major surgical procedures, but thanks to the evolution of surgical techniques and an increasingly careful postoperative management, it was possible to extend the resective treatment even to the most advanced age groups. According to these findings, our data also showed a shorter postoperative course in patients undergoing RFA, in terms of major

Table 4 Univariate and multivariate models for recurrence

	Univariate analysis	Multivariate analysis	
	<i>P</i> value	RR (95%CI)	<i>P</i> value
RFA	0.001	1.37 (1.17-1.60)	0.0001
Age ≤ 75 yr	0.28		
Male	0.91		
Co-morbidity ≥ 2	0.01		
BMI < 24	0.61		
ASA score III-IV	0.61		
Bilirubin (mg/dL > 2)	0.37		
Creatinine (mg/dL > 1)	0.62		
PLT (U/μL > 150 × 10 <sup>3</sup> )	0.001		
INR (> 1.3)	0.02		
Tumor size < 3 cm	0.001		
Multiple nodule	0.07		
Child Pugh A	0.26		
MELD > 10	0.01	1.51 (1.04-2.17)	0.03

The relative prognostic significance of the variables in predicting overall survival and overall recurrence was established using univariate and multivariate Cox proportional hazards regression models. Radiofrequency ablation and Model for End-Stage Liver Disease score > 10 were considered poor prognostic factors. RFA: Radiofrequency ablation; INR: International normalized ratio; MELD: Model for End-Stage Liver Disease; RR: Relative risk; CI: Confidence interval; BMI: Body mass index; ASA: American Society of Anesthesiologists; PLT: Platelets.

postoperative complications (Clavien-Dindo III-IV) (1% *vs* 9%,  $P = 0.001$ ), length of hospital stay (median range: 2 d *vs* 6 d,  $P = 0.001$ ), and also mortality rate within 90 d (0% *vs* 3%,  $P = 0.02$ ).

Directly related to the type of procedure, data regarding operative time (median range: 25 min *vs* 205 min,  $P = 0.001$ ) and percentage of perioperative blood transfusions (8% *vs* 15%,  $P = 0.001$ ) highlighted the lower invasiveness of the ablative strategy. Although there were studies which showed overlapping[30] or even more satisfactory[31] results in the long-term outcomes of RFA managed patients, our work resulted in a clear superiority in patients managed with LR with a 1-, 3-, 5-year OS of 91.9%, 84%, and 75.5% as compared to 92%, 66.4%, and 37.8% for the RFA group ( $P = 0.001$ ), and a 1-, 3-, and 5-year disease-free survival rate of 85.7%, 63.7%, and 50.3% for the LR group, and 66.7%, 37.8%, and 27.7% for the RFA group ( $P = 0.001$ ).

To prevent any potential selection bias, we applied a PSM. Once co-morbidities, ASA and MELD score, tumor number, and tumor size of both groups had become balanced, we confirmed that LR provided better OS and disease-free survival than RFA treatment in elderly HCC patients with Milan criteria. On the other hand, the percentage of postoperative complications and blood transfusions, operative time, and length of hospital stay were also higher in the resection group even after PSM while the mortality value within 90 d was no longer significant. These data put emphasis on how important it was not only for the preoperative assessment of patients, which allowed us to choose a targeted and tailored therapeutic strategy, but also for the preoperative preparation of patients, which was related to the chosen procedure and made them less susceptible to any events secondary to the treatment itself, especially in elderly patients.

Elderly patients were often considered a high risk group for major surgery regarding the higher incidence of co-morbidities. In the past, this assumption seemed to have been a limit in the evaluation of the therapeutic choice. As a result, this category of patients was often undertreated, and this attitude may have distorted the previous results in terms of overall and recurrent survival.

This study had some limitations. First of all, because of its retrospective nature, there was a possibility of unavoidable selection bias. In addition, only 25.4% of patients undergoing RFA had a biopsy, although they had received a radiological diagnosis according to guidelines. Third, the surgical procedures adopted were very

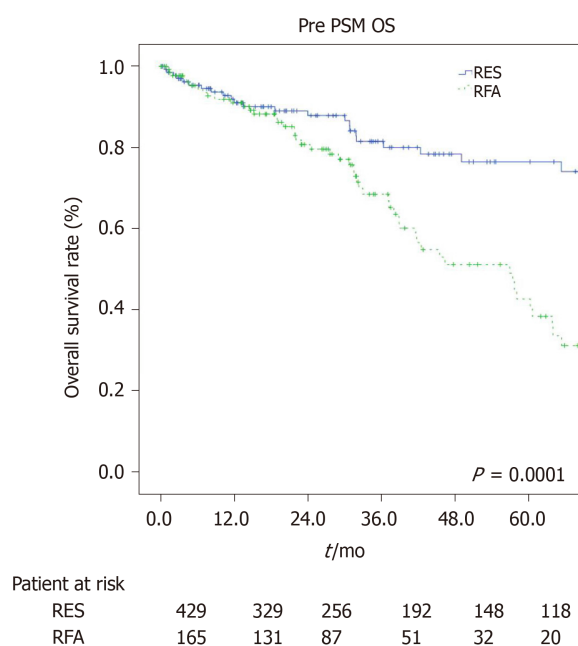


**Figure 1 Survival curves (Kaplan-Meier method) of patients with hepatocellular carcinoma in Milan criteria who underwent surgical resection and radiofrequency ablation before propensity score matching.** Overall survival curves were constructed using the Kaplan-Meier method and compared using the log-rank test. Overall survival significantly differs between the two groups. PSM: Propensity score matching; OS: Overall survival; RES: Resection; RFA: Radiofrequency ablation.

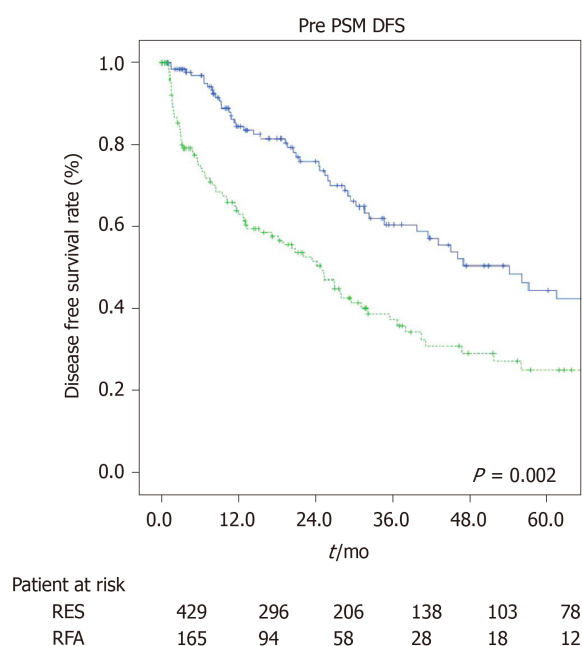


**Figure 2 Tumor recurrence curves (Kaplan-Meier method) of patients with hepatocellular carcinoma in Milan criteria who underwent surgical resection and radiofrequency ablation before propensity score matching.** Recurrence-free survival curves were constructed using the Kaplan-Meier method and compared using the log-rank test. hepatocellular carcinoma recurrence significantly differs between the two groups. PSM: Propensity score matching; DFS: Disease-free survival; RES: Resection; RFA: Radiofrequency ablation.

different, from anatomical to non-anatomical ones. In addition to this, there was the multicentric nature of the study which could be a determining factor in further bias in selection and evaluation criteria.



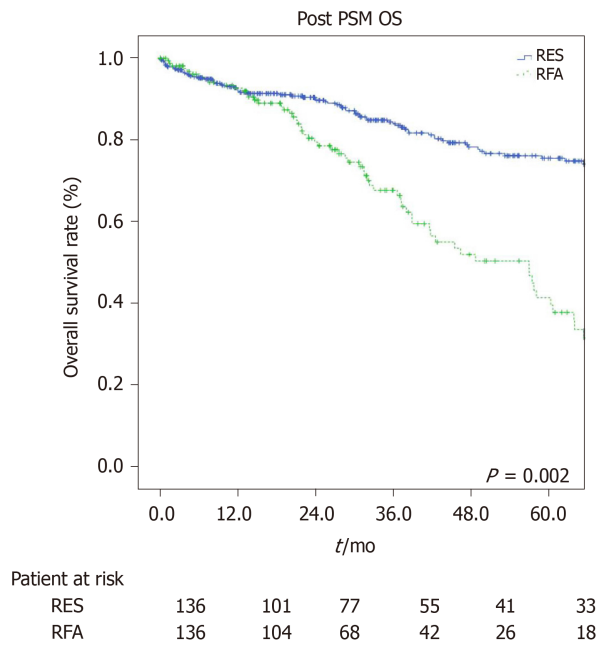


**Figure 3 Survival curves (Kaplan-Meier method) of patients with hepatocellular carcinoma in Milan criteria who underwent surgical resection and radiofrequency ablation after propensity score matching.** Overall survival curves were constructed using the Kaplan-Meier method and compared using the log-rank test. After propensity score matching, survival remained significantly different. PSM: Propensity score matching; OS: Overall survival; RES: Resection; RFA: Radiofrequency ablation.

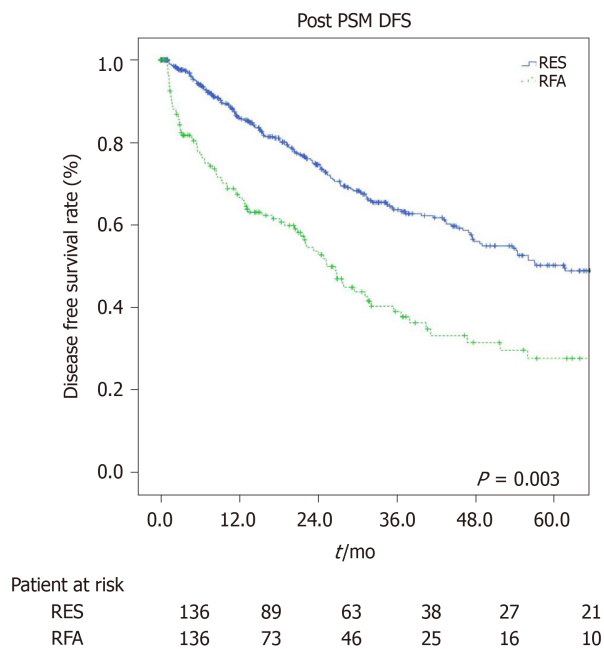


**Figure 4 Tumor recurrence curves (Kaplan-Meier method) of patients with hepatocellular carcinoma in Milan criteria who underwent surgical resection and radiofrequency ablation after propensity score matching.** Recurrence-free survival curves were constructed using the Kaplan-Meier method and compared using the log-rank test. After propensity score matching, recurrence remained significantly different. PSM: Propensity score matching; DFS: Disease-free survival; RES: Resection; RFA: Radiofrequency ablation.

## CONCLUSION

In conclusion, our work reached similar results to the ones of several recent studies which had it that LR guaranteed better outcomes in terms of overall and disease-free survival than RFA in elderly HCC patients within Milan criteria, and so it was mandatory to outline the best therapeutic strategy without foreclosures, rather

respecting the parameters of patient selection and tailored treatment. LR should be considered for patients with a better liver function and a longer life expectancy, in order to balance the postoperative risk of treatment with benefits in long-term overall and disease-free survival.

## ARTICLE HIGHLIGHTS

### Research background

Surgical resection and radiofrequency ablation represent two alternative treatment for hepatocellular carcinoma.

### Research motivation

Evaluation between surgery and radiofrequency ablation in elderly patients with hepatocellular carcinoma within Milan criteria.

### Research objectives

To evaluate short- and long-term outcome in elderly patients (> 70 years) with HCC in Milan criteria, which underwent liver resection (LR) or radiofrequency ablation.

### Research methods

Analysis of results from multicentric data about overall and disease-free survival linked to the two strategy.

### Research results

Our data before and after propensity score matching show a better overall survival and disease-free survival at 1, 3, and 5 years in patient who underwent LR compared to ablation group.

### Research conclusions

This retrospective multicenter study shows that LR provides better overall and disease-free survival despite a higher rate of post-operative complications and longer hospital stay when compared with ablation in elderly patients.

### Research perspectives

With data from this retrospective multicenter study, a purpose of multicenter randomized controlled trials should be considered.

## REFERENCES

- 1 Jemal A, Bray F, Center MM, Ferlay J, Ward E, Forman D. Global cancer statistics. *CA Cancer J Clin* 2011; **61**: 69-90 [PMID: 21296855 DOI: 10.3322/caac.20107]
- 2 European Association for the Study of the Liver. EASL Clinical Practice Guidelines: Management of hepatocellular carcinoma. *J Hepatol* 2018; **69**: 182-236 [PMID: 29628281 DOI: 10.1016/j.jhep.2018.03.019]
- 3 Cherqui D, Laurent A, Mocellin N, Tayar C, Luciani A, Van Nhieu JT, Decaens T, Hurtova M, Memeo R, Mallat A, Duvoux C. Liver resection for transplantable hepatocellular carcinoma: long-term survival and role of secondary liver transplantation. *Ann Surg* 2009; **250**: 738-746 [PMID: 19801927 DOI: 10.1097/SLA.0b013e3181bd582b]
- 4 Sogawa H, Shrager B, Jibara G, Tabrizian P, Roayaie S, Schwartz M. Resection or transplant-listing for solitary hepatitis C-associated hepatocellular carcinoma: an intention-to-treat analysis. *HPB (Oxford)* 2013; **15**: 134-141 [PMID: 23036070 DOI: 10.1111/j.1477-2574.2012.00548.x]
- 5 Spolverato G, Vitale A, Ejaz A, Kim Y, Maithel SK, Cosgrove DP, Pawlik TM. The relative net health benefit of liver resection, ablation, and transplantation for early hepatocellular carcinoma. *World J Surg* 2015; **39**: 1474-1484 [PMID: 25665675 DOI: 10.1007/s00268-015-2987-7]
- 6 Tandon P, Garcia-Tsao G. Prognostic indicators in hepatocellular carcinoma: a systematic review of 72 studies. *Liver Int* 2009; **29**: 502-510 [PMID: 19141028 DOI: 10.1111/j.1478-3231.2008.01957.x]
- 7 Zhao LY, Huo RR, Xiang X, Torzilli G, Zheng MH, Yang T, Liang XM, Huang X, Tang PL, Xiang BD, Li LQ, You XM, Zhong JH. Hepatic resection for elderly patients with hepatocellular carcinoma: a systematic review of more than 17,000 patients. *Expert Rev Gastroenterol Hepatol* 2018; **12**: 1059-1068 [PMID: 30145919 DOI: 10.1080/17474124.2018.1517045]
- 8 Terminology Committee of the International Hepato-Pancreato-Biliary Association; Strasberg SM, Belghiti J, Clavien P-A, Gadzijev E, Garden JO, Lau WY, Makuuchi M, Strong RW. The

- Brisbane 2000 Terminology of Liver Anatomy and Resections. *HPB* 2000; **2**: 333-339
- 9 **Dindo D**, Demartines N, Clavien PA. Classification of surgical complications: a new proposal with evaluation in a cohort of 6336 patients and results of a survey. *Ann Surg* 2004; **240**: 205-213 [PMID: 15273542 DOI: 10.1097/01.sla.0000133083.54934.ae]
  - 10 **Llovet JM**, Lencioni R. mRECIST for HCC: Performance and novel refinements. *J Hepatol* 2020; **72**: 288-306 [PMID: 31954493 DOI: 10.1016/j.jhep.2019.09.026]
  - 11 **Petrick JL**, Florio AA, Znaor A, Ruggieri D, Laversanne M, Alvarez CS, Ferlay J, Valery PC, Bray F, McGlynn KA. International trends in hepatocellular carcinoma incidence, 1978-2012. *Int J Cancer* 2020; **147**: 317-330 [PMID: 31597196 DOI: 10.1002/ijc.32723]
  - 12 **Lau WY**, Leung TW, Yu SC, Ho SK. Percutaneous local ablative therapy for hepatocellular carcinoma: a review and look into the future. *Ann Surg* 2003; **237**: 171-179 [PMID: 12560774 DOI: 10.1097/01.SLA.0000048443.71734.BF]
  - 13 **Bruix J**, Sherman M; American Association for the Study of Liver Diseases. Management of hepatocellular carcinoma: an update. *Hepatology* 2011; **53**: 1020-1022 [PMID: 21374666 DOI: 10.1002/hep.24199]
  - 14 **Ng KK**, Lam CM, Poon RT, Ai V, Tso WK, Fan ST. Thermal ablative therapy for malignant liver tumors: a critical appraisal. *J Gastroenterol Hepatol* 2003; **18**: 616-629 [PMID: 12753142 DOI: 10.1046/j.1440-1746.2003.02991.x]
  - 15 **Yu J**, Yu XL, Han ZY, Cheng ZG, Liu FY, Zhai HY, Mu MJ, Liu YM, Liang P. Percutaneous cooled-probe microwave vs radiofrequency ablation in early-stage hepatocellular carcinoma: a phase III randomised controlled trial. *Gut* 2017; **66**: 1172-1173 [PMID: 27884919 DOI: 10.1136/gutjnl-2016-312629]
  - 16 **Livraghi T**, Meloni F, Di Stasi M, Rolle E, Solbiati L, Tinelli C, Rossi S. Sustained complete response and complications rates after radiofrequency ablation of very early hepatocellular carcinoma in cirrhosis: Is resection still the treatment of choice? *Hepatology* 2008; **47**: 82-89 [PMID: 18008357 DOI: 10.1002/hep.21933]
  - 17 **Huang J**, Yan L, Cheng Z, Wu H, Du L, Wang J, Xu Y, Zeng Y. A randomized trial comparing radiofrequency ablation and surgical resection for HCC conforming to the Milan criteria. *Ann Surg* 2010; **252**: 903-912 [PMID: 21107100 DOI: 10.1097/SLA.0b013e3181efc656]
  - 18 **Feng K**, Yan J, Li X, Xia F, Ma K, Wang S, Bie P, Dong J. A randomized controlled trial of radiofrequency ablation and surgical resection in the treatment of small hepatocellular carcinoma. *J Hepatol* 2012; **57**: 794-802 [PMID: 22634125 DOI: 10.1016/j.jhep.2012.05.007]
  - 19 **Wang Y**, Luo Q, Li Y, Deng S, Wei S, Li X. Radiofrequency ablation vs hepatic resection for small hepatocellular carcinomas: a meta-analysis of randomized and nonrandomized controlled trials. *PLoS One* 2014; **9**: e84484 [PMID: 24404166 DOI: 10.1371/journal.pone.0084484]
  - 20 **Fang Y**, Chen W, Liang X, Li D, Lou H, Chen R, Wang K, Pan H. Comparison of long-term effectiveness and complications of radiofrequency ablation with hepatectomy for small hepatocellular carcinoma. *J Gastroenterol Hepatol* 2014; **29**: 193-200 [PMID: 24224779 DOI: 10.1111/jgh.12441]
  - 21 **Xu XL**, Liu XD, Liang M, Luo BM. Radiofrequency Ablation vs Hepatic Resection for Small Hepatocellular Carcinoma: Systematic Review of Randomized Controlled Trials with Meta-Analysis and Trial Sequential Analysis. *Radiology* 2018; **287**: 461-472 [PMID: 29135366 DOI: 10.1148/radiol.2017162756]
  - 22 **Ueno S**, Sakoda M, Kubo F, Hiwatashi K, Tateno T, Baba Y, Hasegawa S, Tsubouchi H; Kagoshima Liver Cancer Study Group. Surgical resection vs radiofrequency ablation for small hepatocellular carcinomas within the Milan criteria. *J Hepatobiliary Pancreat Surg* 2009; **16**: 359-366 [PMID: 19300896 DOI: 10.1007/s00534-009-0069-7]
  - 23 **Yun WK**, Choi MS, Choi D, Rhim HC, Joh JW, Kim KH, Jang TH, Lee JH, Koh KC, Paik SW, Yoo BC. Superior long-term outcomes after surgery in child-pugh class a patients with single small hepatocellular carcinoma compared to radiofrequency ablation. *Hepatol Int* 2011; **5**: 722-729 [PMID: 21484104 DOI: 10.1007/s12072-010-9237-8]
  - 24 **Shi M**, Zhang CQ, Zhang YQ, Liang XM, Li JQ. Micrometastases of solitary hepatocellular carcinoma and appropriate resection margin. *World J Surg* 2004; **28**: 376-381 [PMID: 15022021 DOI: 10.1007/s00268-003-7308-x]
  - 25 **Sasaki A**, Kai S, Iwashita Y, Hirano S, Ohta M, Kitano S. Microsatellite distribution and indication for locoregional therapy in small hepatocellular carcinoma. *Cancer* 2005; **103**: 299-306 [PMID: 15578688 DOI: 10.1002/cncr.20798]
  - 26 **Oweira H**, Petrausch U, Helbling D, Schmidt J, Mannhart M, Mehrabi A, Schöb O, Gyryes A, Abdel-Rahman O. Early stage hepatocellular carcinoma in the elderly: A SEER database analysis. *J Geriatr Oncol* 2017; **8**: 277-283 [PMID: 28389117 DOI: 10.1016/j.jgo.2017.03.002]
  - 27 **Lim KC**, Chow PK, Allen JC, Siddiqui FJ, Chan ES, Tan SB. Systematic review of outcomes of liver resection for early hepatocellular carcinoma within the Milan criteria. *Br J Surg* 2012; **99**: 1622-1629 [PMID: 23023956 DOI: 10.1002/bjs.8915]
  - 28 **Kishida N**, Hibi T, Itano O, Okabayashi K, Shinoda M, Kitago M, Abe Y, Yagi H, Kitagawa Y. Validation of hepatectomy for elderly patients with hepatocellular carcinoma. *Ann Surg Oncol* 2015; **22**: 3094-3101 [PMID: 25582743 DOI: 10.1245/s10434-014-4350-x]
  - 29 **Pompili M**, Saviano A, de Matthaeis N, Cucchetti A, Ardito F, Federico B, Brunello F, Pinna AD, Giorgio A, Giulini SM, De Sio I, Torzilli G, Fornari F, Capussotti L, Guglielmi A, Piscaglia F, Aldrighetti L, Caturelli E, Calise F, Nuzzo G, Rapaccini GL, Giuliani F. Long-term effectiveness of resection and radiofrequency ablation for single hepatocellular carcinoma  $\leq 3$  cm. Results of a

- multicenter Italian survey. *J Hepatol* 2013; **59**: 89-97 [PMID: [23523578](#) DOI: [10.1016/j.jhep.2013.03.009](#)]
- 30 **Chen MS**, Li JQ, Zheng Y, Guo RP, Liang HH, Zhang YQ, Lin XJ, Lau WY. A prospective randomized trial comparing percutaneous local ablative therapy and partial hepatectomy for small hepatocellular carcinoma. *Ann Surg* 2006; **243**: 321-328 [PMID: [16495695](#) DOI: [10.1097/01.sla.0000201480.65519.b8](#)]
- 31 **Peng ZW**, Lin XJ, Zhang YJ, Liang HH, Guo RP, Shi M, Chen MS. Radiofrequency ablation vs hepatic resection for the treatment of hepatocellular carcinomas 2 cm or smaller: a retrospective comparative study. *Radiology* 2012; **262**: 1022-1033 [PMID: [22357902](#) DOI: [10.1148/radiol.11110817](#)]



## Clinical Trials Study

# Responses to faecal microbiota transplantation in female and male patients with irritable bowel syndrome

Magdy El-Salhy, Christina Casen, Jørgen Valeur, Trygve Hausken, Jan Gunnar Hatlebakk

**ORCID number:** Magdy El-Salhy 0000-0003-3398-3288; Christina Casen 0000-0002-7632-8251; Jørgen Valeur 0000-0001-7193-7069; Trygve Hausken 0000-0001-7080-8396; Jan Gunnar Hatlebakk 0000-0001-9710-7733.

**Author contributions:** El-Salhy M designed the study, obtained the funding, administered the study, recruited the patients, performed faecal microbiota transplantation, collected, analyzed and interpreted the data, and drafted the manuscript; Casen C contributed to the design of the study, analyzed the faecal bacteria and critically revised the manuscript for important intellectual content; Valeur J contributed to the design of the study, analyzed the short-chain fatty acids and critically revised the manuscript for important intellectual content; Hausken T and Hatlebakk JG contributed to the design of the study and to the analysis and interpretation of the data, and critically revised the manuscript for important intellectual content.

**Institutional review board statement:** The study was reviewed and approved by the Institutional Review Board of the University of Bergen.

**Clinical trial registration statement:**

**Magdy El-Salhy**, Department of Medicine, Stord Helse-Fonna Hospital, Stord 5416, Norway

**Magdy El-Salhy, Trygve Hausken, Jan Gunnar Hatlebakk**, Department of Clinical Medicine, University of Bergen, Bergen 5020, Norway

**Magdy El-Salhy, Trygve Hausken, Jan Gunnar Hatlebakk**, National Centre for Functional Gastrointestinal Disorders, Department of Medicine, Haukeland University Hospital, Bergen 5020, Norway

**Christina Casen**, Genetic Analysis AS, Oslo 0485, Norway

**Jørgen Valeur**, Unger-Vetlesen Institute, Lovisenberg Diaconal Hospital, Oslo 0440, Norway

**Corresponding author:** Magdy El-Salhy, BSc, MD, PhD, Chief Doctor, Professor, Department of Medicine, Stord Helse-Fonna Hospital, Tysevegen 64, Stord 5416, Norway.  
[magdy.elsalhy@sklbb.no](mailto:magdy.elsalhy@sklbb.no)

## Abstract

### BACKGROUND

Faecal microbiota transplantation (FMT) seems to be a promising treatment for irritable bowel syndrome (IBS) patients. In Western countries (United States and Europe), there is a female predominance in IBS. A sex difference in the response to FMT has been reported recently in IBS patients.

### AIM

To investigate whether there was a sex difference in the response to FMT in the IBS patients who were included in our previous randomized controlled trial of the efficacy of FMT.

### METHODS

The study included 164 IBS patients who participated in our previous randomized controlled trial. These patients had moderate-to-severe IBS symptoms belonging to the IBS-D (diarrhoea-predominant), IBS-C (constipation-predominant) and IBS-M (mixed) subtypes, and had not responded to the National Institute for Health and Care Excellence (NICE)-modified diet. They belonged in three groups: placebo (own faeces), and active treated group (30-g or 60-g superdonor faeces). The patients completed the IBS severity scoring system (IBS-SSS), Fatigue Assessment Scale (FAS) and the IBS quality of life scale (IBS-QoL) questionnaires



This study is registered at [www.clinicaltrials.gov](http://www.clinicaltrials.gov) (NCT03822299) and [www.cristin.no](http://www.cristin.no) (ID657402).

**Informed consent statement:** All study participants, or their legal guardian, provided informed written consent prior to study enrolment.

**Conflict-of-interest statement:** The authors declare that they have no conflict of interest.

**Data sharing statement:** No additional data are available.

**CONSORT 2010 statement:** The authors have read the CONSORT 2010 statement, and the manuscript was prepared and revised according to the CONSORT 2010 statement.

**Open-Access:** This article is an open-access article that was selected by an in-house editor and fully peer-reviewed by external reviewers. It is distributed in accordance with the Creative Commons Attribution NonCommercial (CC BY-NC 4.0) license, which permits others to distribute, remix, adapt, build upon this work non-commercially, and license their derivative works on different terms, provided the original work is properly cited and the use is non-commercial. See: <http://creativecommons.org/licenses/by-nc/4.0/>

**Manuscript source:** Invited manuscript

**Specialty type:** Gastroenterology and hepatology

**Country/Territory of origin:** Norway

**Peer-review report's scientific quality classification**

Grade A (Excellent): 0  
Grade B (Very good): B  
Grade C (Good): 0  
Grade D (Fair): D  
Grade E (Poor): 0

**Received:** January 25, 2021

**Peer-review started:** January 25, 2021

at the baseline and 2 wk, 1 mo and 3 mo after FMT. They also provided faecal samples at the baseline and 1 mo after FMT. The faecal bacteria profile and dysbiosis were determined using the 16S rRNA gene polymerase chain reaction DNA amplification covering V3-V9; probe labelling by single nucleotide extension and signal detection. The levels of short-chain fatty acids (SCFAs) were determined by gas chromatography and flame ionization.

## RESULTS

There was no sex difference in the response to FMT either in the placebo group or active treated group. There was no difference between females and males in either the placebo group or actively treated groups in the total score on the IBS-SSS, FAS or IBS-QoL, in dysbiosis, or in the faecal bacteria or SCFA level. However, the response rate was significantly higher in females with diarrhoea-predominant (IBS-D) than that of males at 1 mo, and 3 mo after FMT. Moreover, IBS-SSS total score was significantly lower in female patients with IBS-D than that of male patients both 1 mo and 3 mo after FMT.

## CONCLUSION

There was no sex difference in the response to FMT among IBS patients with moderate-to-severe symptoms who had previously not responded to NICE-modified diet. However, female patients with IBS-D respond better and have higher reduction of symptoms than males after FMT.

**Key Words:** Dysbiosis; Fatigue; Microbiome; Quality of life; Short-chain fatty acids; Superdonor

©The Author(s) 2021. Published by Baishideng Publishing Group Inc. All rights reserved.

**Core Tip:** A sex difference in the response to faecal microbiota transplantation (FMT) was previously reported for a subgroup of refractory irritable bowel syndrome (IBS) patients with severe bloating who had not responded to at least three conventional therapies for IBS. This subgroup only contained patients with diarrhoea-predominant (IBS-D) or mixed (IBS-M) IBS. The present study found no sex difference in the response to FMT among IBS patients with moderate-to-severe symptoms of IBS-D, constipation-predominant (IBS-C) and IBS-M. However, female patients with IBS-D respond better and have higher reduction of symptoms than males after FMT.

**Citation:** El-Salhy M, Casen C, Valeur J, Hausken T, Hatlebakk JG. Responses to faecal microbiota transplantation in female and male patients with irritable bowel syndrome. *World J Gastroenterol* 2021; 27(18): 2219-2237

**URL:** <https://www.wjgnet.com/1007-9327/full/v27/i18/2219.htm>

**DOI:** <https://dx.doi.org/10.3748/wjg.v27.i18.2219>

## INTRODUCTION

The gut microbiota plays an important role in the pathophysiology of irritable bowel syndrome (IBS)[1,2]. The composition of the gut bacteria in IBS patients differs from that of healthy subjects[2-6]. IBS patients have lower abundances of the butyrate-producing bacteria, *Erysipelotrichaceae* and *Ruminococcaceae* compared with healthy controls[7,8]. Methane-producing bacteria, *Methanobacteriales* were found to be more abundant in IBS patients with constipation as a predominant symptom (IBS-C) and less abundant in IBS patients with diarrhoea as a predominant symptom (IBS-D) compared with healthy individuals[7,8]. Moreover, IBS patients have been found to have increased abundances of *Veillonella*, *Lactobacillus* and *Ruminococcus* bacteria and decreased abundances of *Bifidobacterium*, *Faecalibacterium* and *Erysipelotrichaceae* methanogens[7,8]. IBS patients also have a lower diversity of gut bacteria (dysbiosis) than healthy subjects[4-6,9].

Faecal microbiota transplantation (FMT) has previously been performed in IBS patients in seven randomized controlled trials (RCTs)[10-16]. Four of these RCTs

**First decision:** February 27, 2021**Revised:** March 13, 2021**Accepted:** April 22, 2021**Article in press:** April 22, 2021**Published online:** May 14, 2021**P-Reviewer:** Huang MC, Melchior C**S-Editor:** Gao CC**L-Editor:** A**P-Editor:** Liu JH

showed that FMT had good effects on symptoms and the quality of life[10,12,15,16], while the other three RCTs found no effects[11,13,14]. It soon became clear that carefully selecting the donor based on clinical and microbial criteria as well as the dose of the transplant are important for a successful outcome of FMT[17].

In Western countries (United States and Europe) there is a sex difference in IBS, with a female:male ratio of 2:1[18-20]. However, in Asia there is no such female predominance[21-24]. A recently published RCT on FMT in IBS found that females responded better to FMT than did males[16]. A recent RCT of IBS patients performed by our group found that FMT led to marked reductions in IBS symptoms and fatigue and an improvement in the quality of life[12]. These improvements were accompanied by marked changes in the faecal bacteria profile and the profile of short-chain fatty acids (SCFAs) of the patients[12,25].

The present study investigated whether there is a sex difference in the response to FMT in terms of symptoms, dysbiosis, and bacteria and SCFA profiles in the same cohort of patients that we had investigated in our previous study[12].

## MATERIALS AND METHODS

### *Study design and randomization of patients*

The design of this study has been described in detail previously[12]. In brief, patients completed three questionnaires to assess their symptoms and quality of life at the baseline and 2 wk, 1 mo and 3 mo after FMT. They also provided faecal samples at the baseline and 1 mo after FMT. Polyethylene glycol and loperamide were allowed as rescue medication during the study. The patients were randomized 1:1:1 to placebo (own faeces), 30-g (superdonor faeces) or 60-g (superdonor faeces) FMT[12]. The 30- and 60-g superdonor-faeces groups were pooled together and called the active treated group in order to increase the sample size and reduce the probability of type-II statistical errors.

### *Patients*

This study included 164 patients who had participated in our previous study[12]. The characteristics of these patients are given in Table 1. The patients enrolled in this study have been described in detail previously[12]. In brief, patients attending the outpatient clinic at Stord Hospital who fulfilled the Rome IV criteria for a diagnosis of IBS were recruited. All of the recruited patients had previously not responded to consuming the National Institute for Health and Care Excellence (NICE)-modified diet for at least 3 mo[12]. They also received a course of IBS treatment that slightly improved their symptoms.

The inclusion criteria were being aged between 18 and 75 years and having moderate-to-severe IBS symptoms, as indicated by a score of 175 on the IBS severity scoring system (IBS-SSS). The exclusion criteria were being pregnant or planning pregnancy, lactating, the presence of systemic disease, having immune deficiency or being treated by immune-modulating medication, or having a psychiatric illness, excessive alcohol consumption or drug abuse. Patients who took probiotics, antibiotics or IBS medications within 8 wk prior to study inclusion were also excluded[12].

### *Donor*

The single superdonor used in this study has been described in detail previously[12]. Briefly, he was screened according to the European guidelines for FMT donors[26]. He was a healthy 36-year-old male, non-smoker, not taking any medication regularly and had a normal body mass index. He had been born *via* a vaginal delivery, breastfed and had taken only a few courses of antibiotics during his life. He exercised regularly and took sport-specific dietary supplements, which made his diet richer than average in protein, fibre, minerals and vitamins. He was normobiotic, but his faecal bacteria profile deviated from the healthy subjects abundance in 14 of the 39 bacteria markers[12].

### *Collection, preparation and administration of faecal samples*

Faecal samples were frozen immediately and kept at -20 °C until they were delivered frozen to the laboratory, where they were kept at -80 °C. The process of FMT has been described in detail previously[12]. In brief, the patients randomized to the placebo FMT group received 30 g of their own faeces (autologous), while those in the 30-g and 60-g FMT groups received 30 g and 60 g of the superdonor's faeces (allogenic),

**Table 1 Characteristics of the patients in the placebo and active treated groups**

	Placebo			P value	Active treated			P value
	Total	Females	Males		Total	Females	Males	
<b>n</b>	<b>55</b>	<b>47</b>	<b>8</b>		<b>109</b>	<b>85</b>	<b>24</b>	
Age, yr (median, range)	38.5 (18-75)	38.0 (18-73)	47.0 (20-75)	0.3	39.0 (18-73)	40.0 (18-73)	32.0 (21-65)	0.07
IBS-D	21	19	2	0.7	42	30	12	0.4
IBS-C	22	18	4		40	32	8	
IBS-M	12	10	2		27	23	4	
IBS duration, yr	15.5 ± 7.9	16.2 ± 8.0	15.0 ± 9.0	0.9	17.3 ± 8.9	16.8 ± 8.2	18.0 ± 9.2	0.9
Age at IBS onset, yr (median, range)	20.0 (15-35)	20.5 (16-35)	19.0 (15-30)	0.4	20.0 (15-36)	20.0 (16-35)	20 (15-33)	0.6
IBS-SSS total score	315.2 ± 77.1	320.1 ± 77.8	286.9 ± 69.3	0.5	312.9 ± 82.0	319.1 ± 77.3	297.7 ± 82.0	0.4
Moderate symptoms <sup>1</sup> (%)	23 (42)	17 (36)	6 (75)	0.06	45 (41)	30 (35)	13 (54)	0.1
Severe symptoms <sup>2</sup> (%)	32 (58)	30 (64)	2 (25)		64 (59)	55 (65)	11 (46)	

Data are *n*, *n* (%) or mean ± SD values.

<sup>1</sup>Irritable bowel syndrome severity scoring system total score between 175 and 300.

<sup>2</sup>Irritable bowel syndrome severity scoring system total score of ≥ 300. IBS: Irritable bowel syndrome; IBS-D: Irritable bowel syndrome with diarrhoea-predominant; IBS-C: Irritable bowel syndrome with constipation-predominant; IBS-M: Irritable bowel syndrome with mixed diarrhoea and constipation; IBS-SSS: Irritable bowel syndrome severity scoring system.

respectively. The transplant was administered to the distal duodenum *via* a gastroscopel[12].

### Symptom and quality-of-life assessments

Symptoms were assessed using the IBS-SSS and the Fatigue Assessment Scale (FAS)[27-31]. Quality of life was measured using the IBS quality of life scale (IBS-QoL)[32-34]. Response was defined as a decrease of ≥ 50 points in the IBS-SSS total score after FMT.

### Microbiome analysis and dysbiosis index

The faecal bacteria profile and dysbiosis were determined by the GA-map Dysbiosis Test (Genetic Analysis, Oslo, Norway) using the 16S rRNA gene polymerase chain reaction DNA amplification covering V3-V9; probe labelling by single nucleotide extension and signal detection by BioCode 1000A 128-Plex Analyzer (Applied BioCode, Santa Fe Springs, CA, United States)[6]. The bacterial markers used detected bacteria within 5 phyla (Firmicutes, Proteobacteria, Bacteroidetes, Tenericutes and Verrucomicrobia) that cover 10 bacterial classes, 36 genera and 32 species[6]. This test assesses > 300 bacteria at different taxonomic levels[9]. The dysbiosis index (DI) was measured on a 5-point scale from 1 to 5, where DI values 1-2 indicates normobiosis, 3-5 indicates dysbiosis[6].

### Determination of faecal SCFA levels

The method used to determine faecal SCFA levels has been described in detail previously[25]. Briefly, the faecal samples were homogenized with a solution containing 3 mmol/L 2-ethylbutyric acid and 0.5 mmol/L H<sub>2</sub>SO<sub>4</sub>. The homogenate was vacuum distilled, and the SCFA levels were determined by gas chromatography (Agilent 7890 A, Agilent, CA, United States) using a capillary column (serial no. USE400345H, Agilent J&W GC columns, Agilent) and flame ionization[35,36] levels of total SCFAs, acetic, propionic, iso-butyric, n-butyric, iso-valeric, n-valeric acid, isocaproic and n-caproic acids, were determined and were expressed in units of mmol/kg wet weight.

### Statistical analysis

The sample size required in each arm of the previously published trial was calculated by assuming that a placebo effect was 40% and an effect response was 80%. The total

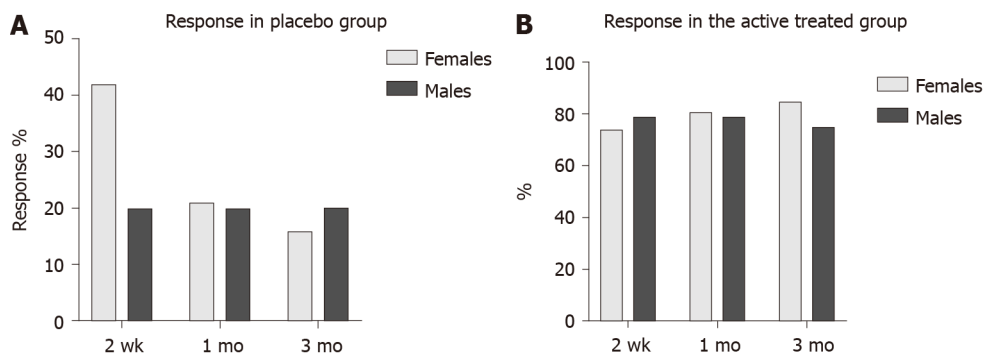


**Figure 1** Response to faecal microbiota transplantation in females and males at different intervals after faecal microbiota transplantation in the two groups. A: Placebo group; B: Active treated group.

sample size was estimated to be 60 patients, with 20 in each arm ( $\alpha = 0.05$ ,  $1-\beta = 0.80$ )[12]. In the present study a new calculation for the sample size was done based on the response rates obtained from our previous RCT[12]. Thus, assuming that the females' response is 90% and males' response is 60%, The total sample size was estimated to be 22 with 11 females and 11 males ( $\alpha = 0.05$ ,  $1-\beta = 0.80$ ). The 30- and 60-g superdonor-faeces groups were pooled together and called the active treated group in order to increase the sample size and reduce the probability of type-II statistical errors. Differences in response and dysbiosis between females and males in the placebo and the active treated group were analyzed using the  $\chi^2$  test. Differences between females and males in the total scores on the IBS-SSS, FAS and IBS-QoL, and in faecal bacteria and SCFA levels were analyzed using the Mann-Whitney test. These analyses were performed using GraphPad Prism (version 8, La Jolla, CA, United States).

### Ethics

The Regional Committee for Medical and Health Research Ethics West, Bergen, Norway approved the study (approval No. 2017/1197/REK vest). All subjects provided both oral and written consents to participate. The study was registered at [www.clinicaltrials.gov](http://www.clinicaltrials.gov) (NCT03822299) and [www.cristin.no](http://www.cristin.no) (ID657402).

## RESULTS

### Symptom and quality-of-life assessments

In the placebo group, the response did not differ between females and males at 2 wk, 1 mo and 3 mo after FMT ( $P = 0.4$ ,  $0.9$  and  $0.8$ , respectively). The responses in the active treated group did not differ between females and males after 2 wk, 1 mo and 3 mo ( $P = 0.6$ ,  $0.8$  and  $0.3$ , respectively) (Figure 1). The response rate was significantly higher in females with IBS-D than that of males at 1 mo, and 3 mo after FMT (Table 2 and Figure 2). There was no significant difference of response rates between female and male patients with either moderate or severe IBS symptoms (Table 3 and Figure 3).

The IBS-SSS total score did not differ significantly between female and male IBS patients in either the placebo or the active treated group (Table 4 and Figure 4). However, IBS-SSS total score was significantly lower in female patients with IBS-D than that of male patients both 1 mo and 3 mo after FMT (Table 5 and Figure 5). The IBS-SSS total score did not differ significantly between females and males in patients with moderate or severe IBS symptoms (Table 6 and Figure 3).

The FAS total score also did not differ significantly between female and male IBS patients in the active treated group (Table 7 and Figure 6), but it was lower in males than females in the placebo group at 3 mo after FMT. This could have been due to a type-I statistical error. There was no significant difference between female and male IBS patients belonging to different IBS-subtypes IBS symptoms (Table 8 and Figure 7). However, the FAS total score was lower in males IBS patients with IBS-D than that of females 2 wk after FMT.

The IBS-QoL total score did differ between females and males in both the placebo and active treated groups (Table 9 and Figure 8), being higher in males than in females at the baseline. IBS-QoL total scores did not differ significantly between female and male patients belonging to different IBS-subtypes (Table 10 and Figure 9).

**Table 2** The response rates of females and males in different irritable bowel syndrome-subtypes at different intervals after faecal microbiota transplantation

Time after FMT	IBS-D			IBS-C			IBS-M		
	Females	Males	P value	Females	Males	P value	Females	Males	P value
2 wk (%)	73	58	0.3	65	50	0.7	72	55	0.3
1 mo (%)	90	42	0.0003	69	75	0.7	65	60	0.9
3 mo (%)	90	42	0.0003	70	75	0.3	63	80	0.6

IBS-D: Irritable bowel syndrome with diarrhoea-predominant symptom; IBS-C: Irritable bowel syndrome with constipation-predominant symptom; IBS-M: Irritable bowel syndrome with mixed diarrhoea and constipation; FMT: Faecal microbiota transplantation.

**Table 3** The response rates in females and males with either moderate or severe irritable bowel syndrome symptoms

Time after FMT	Moderate symptoms <sup>1</sup>			Severe symptoms <sup>2</sup>		
	Females	Males	P value	Females	Males	P value
2 wk (%)	58	61	0.999	78	91	0.4
1 mo (%)	61	61	0.999	78	91	0.4
3 mo (%)	63	56	0.778	77	82	0.999

<sup>1</sup>Irritable bowel syndrome severity scoring system total score between 175 and 300.

<sup>2</sup>Irritable bowel syndrome severity scoring system total score of  $\geq 300$ . FMT: Faecal microbiota transplantation.

**Table 4** Irritable bowel syndrome severity scoring system total scores of females and males in the two study groups at different times after faecal microbiota transplantation

Time	Placebo			Active treated		
	Females	Males	P value	Females	Males	P value
0	320 $\pm$ 78	287 $\pm$ 69	0.2	319 $\pm$ 77	297 $\pm$ 82	0.3
2 wk	254 $\pm$ 106	256 $\pm$ 90	0.9	199 $\pm$ 102	205 $\pm$ 95	0.6
1 mo	277 $\pm$ 98	272 $\pm$ 89	0.8	196 $\pm$ 108	193 $\pm$ 94	0.9
3 mo	288 $\pm$ 90	266 $\pm$ 100	0.6	173 $\pm$ 116	183 $\pm$ 105	0.5

Data are mean  $\pm$  SD values.

### Microbiome analysis

The faecal bacteria levels in the placebo group did not differ between female and male IBS patients at the baseline and 1 mo after FMT (Table 11 and Figure 10). Similarly, there were no differences in the faecal bacteria levels between female and male IBS patients in the active treated group (Table 12 and Figure 11).

In the placebo group, 26 females (55%) and 4 males (50%) had dysbiosis ( $P = 0.8$ ) at the baseline, while 25 females (53%) and 4 males (50%) had dysbiosis ( $P = 0.9$ ) at 1 mo after FMT. In the active treated group, 52 females (61%) and 13 males (54%) had dysbiosis ( $P = 0.3$ ) at the baseline, while 41 females (48%) and 9 males (38%) had dysbiosis ( $P = 0.2$ ) at 1 mo after FMT.

### Faecal SCFA levels

The faecal levels of total SCFAs and acetic, propionic, isobutyric, butyric, isovaleric, valeric, isocaproic and caproic acids did not differ between female and males IBS patients in both the placebo and active treated groups at the baseline and 1 mo after FMT (Table 13 and Figure 12).



**Table 5 The irritable bowel syndrome severity scoring system total scores in females and males belonging to different irritable bowel syndrome-sub-types**

Time after FMT	IBS-D			IBS-C			IBS-M		
	Females	Males	P value	Females	Males	P value	Females	Males	P value
2 wk	190.5 ± 191.4	204.0 ± 92.2	0.6	228.1 ± 116.2	239.2 ± 113.8	0.5	202.8 ± 121.3	225.0 ± 65.8	0.5
1 mo	177.8 ± 94.9	226.9 ± 73.3	<b>0.02</b>	228.8 ± 118.1	215.8 ± 115.7	0.6	219.9 ± 136.6	197.0 ± 65.2	0.8
3 mo	157.8 ± 102.9	212.3 ± 96.9	<b>0.03</b>	212.8 ± 124.0	234.6 ± 131.8	0.5	219.2 ± 146.3	149.0 ± 36.0	0.5

Data are mean ± SD values. IBS-D: Irritable bowel syndrome with diarrhoea-predominant symptom; IBS-C: Irritable bowel syndrome with constipation-predominant symptom; IBS-M: Irritable bowel syndrome with mixed diarrhoea and constipation; FMT: Faecal microbiota transplantation.

**Table 6 Irritable bowel syndrome severity scoring system total scores in females and males with moderate or severe irritable bowel syndrome symptoms**

Time after FMT	Moderate symptoms <sup>1</sup>			Severe symptoms <sup>2</sup>		
	Females	Males	P value	Females	Males	P value
2 wk	166.5 ± 70.0	167.2 ± 55.8	0.8	225.1 ± 114.0	259.5 ± 102.3	0.3
1 mo	162.1 ± 73.1	179.4 ± 63.8	0.5	229.2 ± 120.2	214.1 ± 118.1	0.7
3 mo	155.3 ± 76.9	175.3 ± 100.2	0.5	214.6 ± 131.8	202.3 ± 120.6	0.8

Data are mean ± SD values.

<sup>1</sup>Irritable bowel syndrome severity scoring system total score between 175 and 300.

<sup>2</sup>Irritable bowel syndrome severity scoring system total score of ≥ 300. FMT: Faecal microbiota transplantation.

**Table 7 Fatigue Assessment Scale total scores of females and males in the two study groups at different times after faecal microbiota transplantation**

Time	Placebo			Active treated		
	Females	Males	P value	Females	Males	P value
0	31 ± 5	29 ± 4	0.3	32 ± 5	30 ± 5	0.09
2 wk	31 ± 6	29 ± 6	0.2	28 ± 6	28 ± 5	0.5
1 mo	31 ± 6	27 ± 7	0.1	27 ± 7	29 ± 5	0.5
3 mo	30 ± 4	26 ± 4	<b>0.01</b>	29 ± 6	27 ± 5	0.7

Data mean ± SD values.

## DISCUSSION

The present study found that the response to FMT did not differ between females and males. Furthermore, the total scores on the IBS-SSS, FAS and IBS-QoL did not differ between females and males in the active treated groups before FMT and at different times after FMT. In the placebo group, the total score of IBS-QoL was higher in males than males and the FAS total score was lower in males than females 3 mo after FMT. This indicates that the effects of active treated FMT did not differ between males and females regarding IBS symptoms, fatigue and quality of life. Moreover, there was no difference between females and males regarding dysbiosis or the faecal bacteria.

SCFA profiles following FMT did not differ between females and males in both the placebo and the active treated groups. SCFAs regulate intestinal motility and the secretion and absorption of water and electrolytes[37,38]. Moreover, SCFAs increase also the secretion and up-regulate the gene expression of peptide YY (PYY)[39,40]. PYY is a mediator of the ileal brake and stimulates the absorption of water and electrolytes in the colon[37]. The faecal level of total SCFAs increased significantly in IBS patients after 1 mo and remained elevated at 1 year after FMT (unpublished

**Table 8 Fatigue Assessment Scale total scores of females and males irritable bowel syndrome patients belonging to different irritable bowel syndrome-subtypes**

Time after FMT	IBS-D			IBS-C			IBS-M		
	Females	Males	P value	Females	Males	P value	Females	Males	P value
2 wk	30.1 ± 3.6	27.0 ± 3.6	0.04	28.0 ± 6.3	29.3 ± 7.4	0.5	26.7 ± 5.4	26.3 ± 2.1	0.9
1 mo	27.1 ± 5.2	26.6 ± 4.6	0.6	27.1 ± 6.7	31.3 ± 6.1	0.1	28.3 ± 8.3	28.3 ± 4.0	0.9
3 mo	27.5 ± 5.7	27.8 ± 5.0	0.4	26.0 ± 6.2	29.2 ± 5.0	0.2	26.8 ± 7.6	24.8 ± 2.2	0.7

Data are mean ± SD values. IBS-D: Irritable bowel syndrome with diarrhoea-predominant symptom; IBS-C: Irritable bowel syndrome with constipation-predominant symptom; IBS-M: Irritable bowel syndrome with mixed diarrhoea and constipation; FMT: Faecal microbiota transplantation.

**Table 9 Irritable bowel syndrome quality of life scale total scores of females and males in the two study groups at different times after faecal microbiota transplantation**

Time	Placebo			Active treated		
	Females	Males	P value	Females	Males	P value
0	116 ± 20	130 ± 11	0.03	111 ± 23	114 ± 21	0.9
2 wk	123 ± 29	120 ± 23	0.7	122 ± 24	118 ± 27	0.6
1 mo	123 ± 26	121 ± 26	0.8	126 ± 24	119 ± 29	0.4
3 mo	112 ± 24	118 ± 26	0.2	132 ± 23	131 ± 25	0.9

Data are mean ± SD values.

**Table 10 Irritable bowel syndrome quality of life scale total scores of females and males irritable bowel syndrome patients belonging to different irritable bowel syndrome-subtypes**

Time after FMT	IBS-D			IBS-C			IBS-M		
	Females	Males	P value	Females	Males	P value	Females	Males	P value
2 wk	123.3 ± 98	123.7 ± 25.5	0.8	120.5 ± 23.1	102.4 ± 28.0	0.06	123.1 ± 24.6	131.5 ± 13.0	0.4
1 mo	131.3 ± 20.8	129.6 ± 28.2	0.9	121.9 ± 24.4	111.4 ± 29.1	0.1	125.4 ± 25.2	130.5 ± 11.3	0.8
3 mo	136.4 ± 16.6	134.5 ± 22.7	0.9	128.7 ± 24.4	129.1 ± 31.3	0.6	129.5 ± 28.6	124.8 ± 22.0	0.5

Data are mean ± SD values. IBS-D: Irritable bowel syndrome with diarrhoea-predominant symptom; IBS-C: Irritable bowel syndrome with constipation-predominant symptom; IBS-M: Irritable bowel syndrome with mixed diarrhoea and constipation; FMT: Faecal microbiota transplantation.

data)[25]. Similarly, the faecal level of butyric acid increased in IBS patients after 1 mo and remained elevated at 1 year after FMT (unpublished data)[25]. Butyrate is a major energy source for colonic epithelial cells, interacts with the immune response, modulates the oxidative stress, and decreases both intestinal-cell permeability and intestinal motility[41]. Butyrate modulates also colonic hypersensitivity[42-44]. At 1 year after FMT levels of isobutyric and isovaleric acids were increased in IBS patients, indicating a shift in microbial fermentation from a saccharolytic to a proteolytic pattern[45]. It is worthy of note that in IBS patients, who adhered to a low-FODMAPs (fermentable oligosaccharides, disaccharides, monosaccharides, and polyols) diet an increase in the levels of isobutyric and isovaleric acids have been found[46]. Moreover, the level of acetic acid which induces visceral hypersensitivity decreased significantly at 1 year after FMT[47]. These changes in SCFAs after FMT appear to be one of the mechanisms underlying the effects seen in IBS patients after FMT. That is why the difference between females and males regarding the changes in SCFAs was assessed.

Holvoet *et al*[16] reported that females responded better to FMT than did males. That RCT differed from the present study in terms of the characteristics of the included patients, the size of the patient cohort and the dose of the faecal transplants[16]. The trial of Holvoet *et al*[16] included a subgroup of refractory IBS

**Table 11 Faecal bacteria levels in the female and male irritable bowel syndrome patients in the placebo group at the baseline and 1 mo after faecal microbiota transplantation**

Bacteria	Baseline		1 mo after FMT	
	Females	Males	Females	Males
<i>Actinobacteria</i>	-0.235 ± 0.763	-0.365 ± 0.768	-0.250 ± 0.954	-0.375 ± 0.838
<i>Actinomycetales</i>	0.118 ± 0.382	-0.212 ± 0.536	0.175 ± 0.594	0.100 ± 0.496
<i>Bifidobacterium spp.</i>	-0.020 ± 0.607	-0.154 ± 0.539	0.025 ± 0.660	-0.075 ± 0.572
<i>Alistipes</i>	-0.863 ± 0.895	-0.885 ± 0.900	-0.875 ± 0.853	-0.800 ± 0.709
<i>Alistipes onderdonkii</i>	-0.667 ± 0.792	-0.615 ± 0.718	-0.650 ± 0.834	-0.550 ± 0.783
<i>Bacteroides fragilis</i>	-0.255 ± 0.689	-0.212 ± 0.637	0.175 ± 0.501	0.050 ± 0.221
<i>Bacteroides spp. and Prevotella spp.</i>	-0.980 ± 1.157	-0.885 ± 1.182	-0.750 ± 1.032	-0.900 ± 0.687
<i>Bacteroides stercoris</i>	-0.137 ± 0.448	-0.154 ± 0.415	0.025 ± 0.158	0.100 ± 0.304
<i>Bacteroides zoogloformans</i>	0.078 ± 0.272	0.038 ± 0.194	0.025 ± 0.158	0 ± 0
<i>Parabacteroides johnsonii</i>	0.039 ± 0.196	0.077 ± 0.269	0.050 ± 0.221	0.100 ± 0.304
<i>Parabacteroides spp.</i>	-0.451 ± 0.642	-0.327 ± 0.706	-0.425 ± 0.747	-0.225 ± 0.480
<i>Firmicutes</i>	-0.431 ± 0.575	-0.385 ± 0.566	-0.325 ± 0.526	-0.400 ± 0.591
<i>Bacilli</i>	0.235 ± 1.124	0.192 ± 0.991	0.271 ± 1.132	0.150 ± 1.001
<i>Catenibacterium mitsuokai</i>	0.000 ± 0.400	0.135 ± 0.525	0.050 ± 0.289	0.100 ± 0.441
<i>Clostridia</i>	-0.020 ± 0.244	-0.077 ± 0.269	-0.025 ± 0.276	0.0 ± 0.036
<i>Clostridium spp.</i>	0.039 ± 0.196	0.038 ± 0.194	0.0 ± 0.0	0.050 ± 0.316
<i>Dialister invisus</i>	0.118 ± 0.381	-0.173 ± 0.474	0.200 ± 0.405	0.225 ± 0.158
<i>Dialister invisus and Megaspheara micronuciformis</i>	0.059 ± 0.238	0.173 ± 0.474	0.125 ± 0.335	0.025 ± 0.158
<i>Dorea spp.</i>	0.569 ± 0.700	0.500 ± 0.700	0.625 ± 0.628	0.667 ± 0.806
<i>Eubacterium bifforme</i>	0.412 ± 0.753	0.269 ± 0.598	0.275 ± 0.640	0.400 ± 0.633
<i>Eubacterium hallii</i>	0.804 ± 0.939	0.673 ± 0.879	0.655 ± 0.730	0.650 ± 0.597
<i>Eubacterium rectale</i>	0.078 ± 0.337	0.058 ± 0.235	0.050 ± 0.221	0.025 ± 0.158
<i>Eubacterium siraeum</i>	-1.412 ± 0.963	-1.288 ± 0.161	-1.475 ± 1.086	-1.200 ± 1.265
<i>Faecalibacterium prausnitzii</i>	-0.431 ± 0.671	-0.500 ± 0.804	-0.550 ± 0.745	-0.500 ± 0.599
<i>Lachnospiraceae</i>	0.196 ± 0.566	0.269 ± 0.630	0.325 ± 0.730	0.275 ± 0.640
<i>Lactobacillus ruminis and Pediococcus acidilactici</i>	0.059 ± 0.311	0.077 ± 0.334	0.0 ± 0.0	0.025 ± 0.158
<i>Lactobacillus spp.</i>	0.353 ± 0.594	0.269 ± 0.528	0.325 ± 0.616	0.475 ± 0.680
<i>Phascolarctobacterium spp.</i>	0.078 ± 0.337	0.077 ± 0.337	0.125 ± 0.404	0.075 ± 0.350
<i>Ruminococcus albus and Ruminococcus bromii</i>	0.353 ± 0.658	0.404 ± 0.721	0.325 ± 0.616	0.450 ± 0.749
<i>Ruminococcus gnavus</i>	0.431 ± 0.878	0.577 ± 0.878	0.450 ± 0.815	0.325 ± 0.764
<i>Streptococcus agalactiae &amp; Eubacterium rectale</i>	0.157 ± 0.367	0.250 ± 0.480	0.110 ± 0.304	0.125 ± 0.345
<i>Streptococcus salivarius ssp. Thermophilus and Streptococcus sanguinis</i>	0.412 ± 0.606	0.346 ± 0.556	0.675 ± 0.888	0.475 ± 0.751
<i>Streptococcus salivarius ssp. thermophilus</i>	0.628 ± 0.871	0.577 ± 0.915	0.500 ± 0.934	0.600 ± 0.928
<i>Streptococcus spp.</i>	0.471 ± 0.833	0.423 ± 0.696	0.400 ± 0.709	0.450 ± 0.815
<i>Veillonella spp.</i>	-0.177 ± 0.518	-0.173 ± 0.648	-0.175 ± 0.385	-0.150 ± 0.534
<i>Proteobacteria</i>	0.294 ± 0.576	0.289 ± 0.499	0.275 ± 0.599	0.325 ± 0.616
<i>Shigella spp. and Escherichia spp.</i>	-0.275 ± 0.940	-0.212 ± 0.893	-0.200 ± 0.853	-0.335 ± 0.920
<i>Mycoplasma hominis</i>	-0.451 ± 0.503	-0.404 ± 0.496	-0.450 ± 0.504	-0.450 ± 0.503

<i>Akkermansia muciniphila</i>	0.471 ± 0.644	0.365 ± 0.627	0.450 ± 0.714	0.650 ± 0.802
--------------------------------	---------------	---------------	---------------	---------------

The bacterial levels are mean ± SD relative values to a normobiotic microbiota profile of 165 healthy subjects. FMT: Faecal microbiota transplantation.

patients with severe bloating who had not responded to at least three conventional therapies for IBS. This subgroup contained only patients with the IBS-D or mixed (IBS-M) subtypes. The patients included in the present study had moderate-to-severe IBS symptoms belonging to the IBS-D, IBS-C and IBS-M subtypes, and had not responded to the NICE-modified diet. The patient cohort investigated by Holvoet *et al*[16] included 62 patients: 19 in the placebo group and 43 in the active treated group. The present study investigated a cohort of 164 patients: 55 in the placebo group and 109 in the active treated group. It is worthy of note that in the trial of Holvoet *et al*[16] included 30 females and 13 males in the active treated group and 8 females and 11 males in the placebo group. The present study included 85 females and 24 males in the active treated group and included 47 females and 8 males in the placebo group. Thus, this makes the present study less constrained than the RCT of Holvoet *et al*[16] regarding power and sample sizes. Moreover, the dose of the faecal transplant from the donor was not reported for the RCT by Holvoet *et al*[16], while in the present study the active treated group received either 30 g or 60 g of a superdonor transplant. In our previously published RCT we showed that the response rates increased with increased dose[12]. These differences make it difficult to compare the outcomes of the present study with those of Holvoet *et al*[16]. However, in the present study, female patients with IBS-D had a significant higher response rate to FMT and lower IBS-SSS score after FMT than males. These observations could explain the discrepancy between the findings of Holvoet *et al*[16] and the present study as in Holvoet *et al*[16] study the cohort of patients included were only IBS-D and IBS-M IBS-subtypes.

## CONCLUSION

In conclusion, there is no sex difference in the response to FMT in IBS patients with moderate-to-severe IBS symptoms belonging to the three of IBS subtypes of IBS-C and IBS-M in patients who did not responded to NICE-modified diet. Female patients with IBS-D had a significant higher response rate to FMT and lower IBS-SSS score after FMT than males.

**Table 12 Gut bacteria levels in female and male irritable bowel syndrome patients in the active treated group at the baseline and 1 mo after faecal microbiota transplantation**

Bacteria	Baseline		1 mo after FMT	
	Females	Males	Females	Males
<i>Actinobacteria</i>	-0.250 ± 0.954	-0.375 ± 0.838	-0.250 ± 0.719	-0.2350 ± 0.636
<i>Actinomycetales</i>	0.175 ± 0.594	0.100 ± 0.496	0.068 ± 0.255	0.145 ± 0.412
<i>Bifidobacterium spp.</i>	0.025 ± 0.660	-0.075 ± 0.572	-0.045 ± 0.526	-0.063 ± 0.433
<i>Alistipes</i>	-0.875 ± 0.853	-0.800 ± 0.709	-0.886 ± 0.869	-0.783 ± 0.821
<i>Alistipes onderdonkii</i>	-0.650 ± 0.834	-0.550 ± 0.783	-0.523 ± 0.699	-0.354 ± 0.565
<i>Bacteroides fragilis</i>	0.175 ± 0.501	0.050 ± 0.221	0.159 ± 0.480	0.104 ± 0.371
<i>Bacteroides spp. and Prevotella spp.</i>	-0.750 ± 1.032	-0.800 ± 0.687	-1.091 ± 1.996	-0.708 ± 0.967
<i>Bacteroides stercoris</i>	0.025 ± 0.158	0.100 ± 0.304	0.023 ± 0.151	0.146 ± 0.357
<i>Bacteroides zoogloformans</i>	0.025 ± 0.158	0 ± 0	0.091 ± 0.291	0.083 ± 0.347
<i>Parabacteroides johnsonii</i>	0.050 ± 0.221	0.100 ± 0.304	0.045 ± 0.302	0.021 ± 0.144
<i>Parabacteroides spp.</i>	-0.425 ± 0.747	-0.225 ± 0.480	-0.455 ± 0.504	-0.313 ± 0.468
<i>Firmicutes</i>	-0.325 ± 0.526	-0.400 ± 0.591	-0.546 ± 0.627	-0.454 ± 0.483
<i>Bacilli</i>	0.271 ± 1.132	0.150 ± 1.001	0.205 ± 1.047	0.042 ± 0.824
<i>Catenibacterium mitsuokai</i>	0.050 ± 0.289	0.100 ± 0.441	0.023 ± 0.151	0.104 ± 0.515
<i>Clostridia</i>	-0.025 ± 0.276	0.0 ± 0.036	0.068 ± 0.255	0.021 ± 0.252
<i>Clostridium spp.</i>	0.0 ± 0.0	0.050 ± 0.316	0.223 ± 0.151	0.063 ± 0.245
<i>Dialister invisus</i>	0.200 ± 0.405	0.225 ± 0.158	0.091 ± 0.362	0.146 ± 0.505
<i>Dialister invisus and Megaspheara micronuciformis</i>	0.125 ± 0.335	0.025 ± 0.158	0.068 ± 0.034	0.104 ± 0.308
<i>Dorea spp.</i>	0.625 ± 0.628	0.667 ± 0.806	0.727 ± 0.758	0.663 ± 0.796
<i>Eubacterium bifforme</i>	0.275 ± 0.640	0.400 ± 0.633	0.477 ± 0.791	0.563 ± 0.769
<i>Eubacterium hallii</i>	0.655 ± 0.730	0.550 ± 0.597	0.886 ± 0.993	0.979 ± 1.021
<i>Eubacterium rectale</i>	0.050 ± 0.221	0.025 ± 0.158	0.068 ± 0.255	0.042 ± 0.202
<i>Eubacterium siraeum</i>	-1.475 ± 1.086	-1.200 ± 1.265	-1.295 ± 0.930	-1.208 ± 0.988
<i>Faecalibacterium prausnitzii</i>	-0.550 ± 0.745	-0.500 ± 0.599	-0.568 ± 0.759	-0.521 ± 0.825
<i>Lachnospiraceae</i>	0.325 ± 0.730	0.275 ± 0.640	0.205 ± 0.553	0.125 ± 0.489
<i>Lactobacillus ruminis and Pediococcus acidilactici</i>	0.0 ± 0.0	0.025 ± 0.158	0.021 ± 0.146	0.188 ± 0.571
<i>Lactobacillus spp.</i>	0.325 ± 0.616	0.475 ± 0.680	0.500 ± 0.731	0.583 ± 0.679
<i>Phascolarctobacterium spp.</i>	0.125 ± 0.404	0.075 ± 0.350	0.091 ± 0.362	0.083 ± 0.347
<i>Ruminococcus albus and Ruminococcus bromii</i>	0.325 ± 0.616	0.450 ± 0.749	0.205 ± 0.553	0.271 ± 0.574
<i>Ruminococcus gnavus</i>	0.450 ± 0.815	0.325 ± 0.764	0.364 ± 0.810	0.250 ± 0.636
<i>Streptococcus agalactiae &amp; Eubacterium rectale</i>	0.110 ± 0.304	0.125 ± 0.345	0.267 ± 0.495	0.083 ± 0.279
<i>Streptococcus salivarius ssp. thermophilus and Streptococcus sanguinis</i>	0.675 ± 0.888	0.475 ± 0.751	0.455 ± 0.504	0.292 ± 0.459
<i>Streptococcus salivarius ssp. thermophilus</i>	0.500 ± 0.934	0.600 ± 0.928	0.523 ± 0.821	0.604 ± 0.844
<i>Streptococcus spp.</i>	0.400 ± 0.709	0.450 ± 0.815	0.444 ± 0.841	0.396 ± 0.610
<i>Veillonella spp.</i>	-0.175 ± 0.385	-0.150 ± 0.534	-0.273 ± 0.544	-0.208 ± 0.504
<i>Proteobacteria</i>	0.275 ± 0.599	0.325 ± 0.616	0.717 ± 0.750	0.583 ± 0.498
<i>Shigella spp. and Escherichia spp.</i>	-0.200 ± 0.853	-0.335 ± 0.920	-0.151 ± 1.077	-0.188 ± 0.790
<i>Mycoplasma hominis</i>	-0.450 ± 0.504	-0.450 ± 0.503	-0.500 ± 0.506	-0.479 ± 0.505



<i>Akkermansia muciniphila</i>	0.450 ± 0.714	0.650 ± 0.802	0.741 ± 0.713	0.813 ± 0.915
--------------------------------	---------------	---------------	---------------	---------------

The bacterial levels are relative values to a normobiotic microbiota profile of 165 healthy subjects (mean ± SD). FMT: Faecal microbiota transplantation.

**Table 13** The short-chain fatty acids concentration in the faeces of the placebo group and the patients that received donor's faeces (faecal microbiota transplantation) at the baseline and 1 mo after faecal microbiota transplantation

Acids	Placebo				Active treated			
	Baseline		1 mo after FMT		Baseline		1 mo after FMT	
	Females	Males	Females	Males	Females	Males	Females	Males
Total SCFAs	72 ± 37	69 ± 23	73 ± 37	69 ± 23	77 ± 40	72 ± 40	87 ± 42	89 ± 26
Acetic acid	42 ± 18	40 ± 15	41 ± 17	40 ± 14	44 ± 21	44 ± 20	46 ± 13	40.2 ± 15.0
Propionic acid	12 ± 8	11 ± 5	12 ± 8	11 ± 5	13 ± 10	13 ± 8	14 ± 4	11 ± 7
Iso-butyric acid	2 ± 2	1 ± 1	1 ± 2	1 ± 1	1 ± 1	1 ± 1	2 ± 2	1 ± 1
Butyric acid	14 ± 9	12 ± 6	13 ± 8	12 ± 6	11 ± 8	12 ± 9	18 ± 14	16 ± 10
Iso-valeric acid	2 ± 2	2 ± 1	2 ± 2	2 ± 1	2 ± 1	2 ± 2	2 ± 2	2 ± 1
Valeric acid	2 ± 2	1 ± 1	2 ± 2	1 ± 1	2 ± 2	2 ± 2	2 ± 1	2 ± 1
Iso-capronic acid	0.1 ± 0.04	0.01 ± 0.07	0.5 ± 0.7	0.4 ± 0.7	0.0 ± 0.0	0.02 ± 0.08	0.01 ± 0.04	0.0 ± 0.0
Capronic acid	0.5 ± 0.7	0.5 ± 0.7	0.01 ± 0.04	0.1 ± 0.08	0.7 ± 1.3	0.6 ± 0.8	0.6 ± 0.9	0.5 ± 0.9

The values were expressed as mmol/kg wet weight (mean ± SD). FMT: Faecal microbiota transplantation; SCFAs: Short-chain fatty acids.

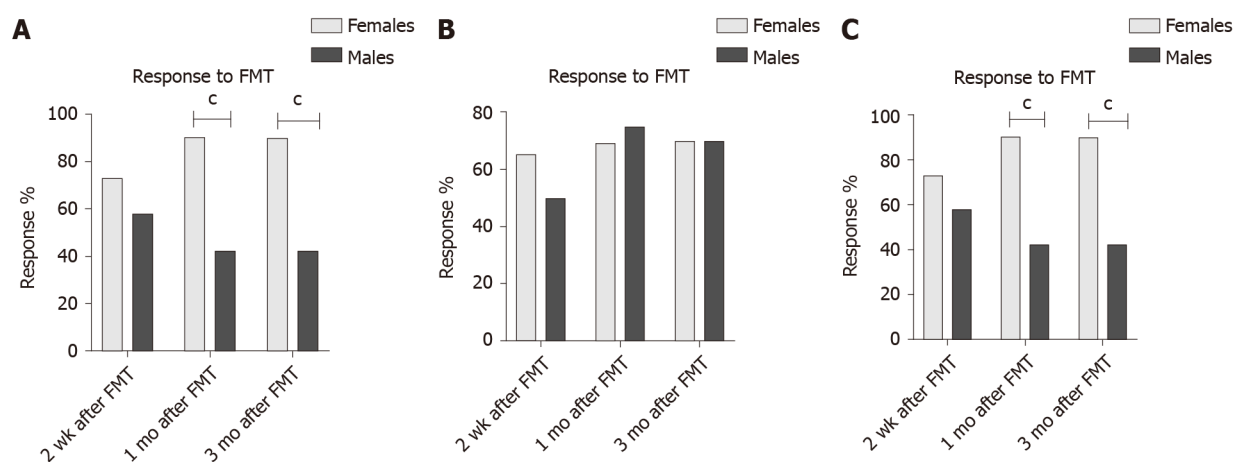


**Figure 2** Response rates to faecal microbiota transplantation of female and male irritable bowel syndrome patients. A: Irritable bowel syndrome with diarrhoea-predominant; B: Irritable bowel syndrome with constipation-predominant; C: Irritable bowel syndrome with mixed diarrhoea and constipation. <sup>a</sup>*P* < 0.001. FMT: Faecal microbiota transplantation.

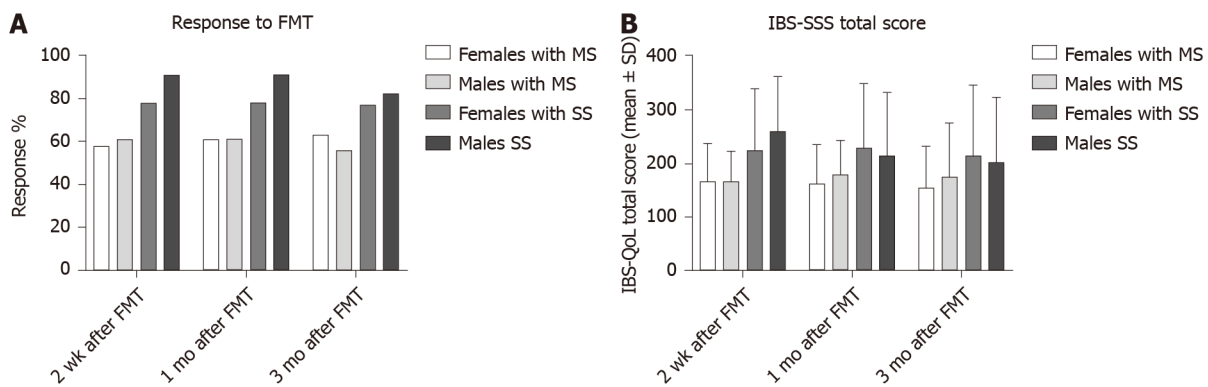


**Figure 3** Response rates to faecal microbiota transplantation and the total irritable bowel syndrome-severity scoring system scores of irritable bowel syndrome patients with moderate irritable bowel syndrome symptoms (irritable bowel syndrome-severity scoring system total score between 175 and 300) and with severe irritable bowel syndrome symptoms (irritable bowel syndrome-severity scoring system total score of  $\geq 300$ ). A: Faecal microbiota transplantation; B: Irritable bowel syndrome severity scoring system total score. MS: Moderate irritable bowel syndrome symptoms; SS: Severe irritable bowel syndrome symptoms; FMT: Faecal microbiota transplantation.

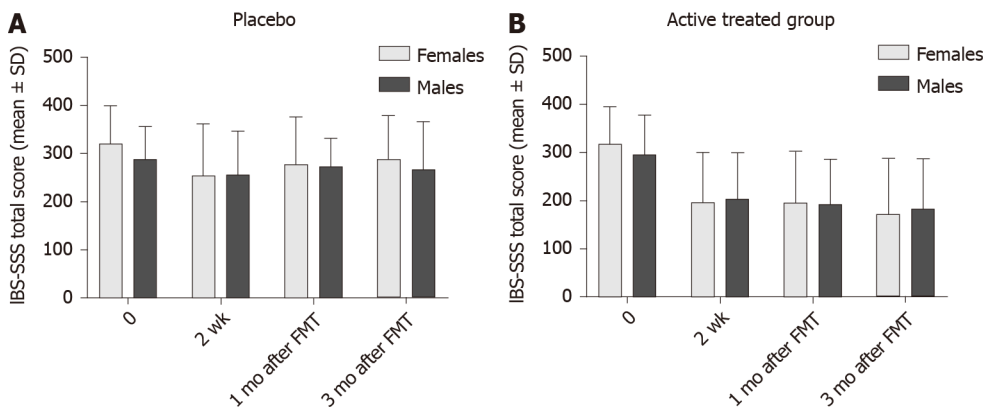


**Figure 4** The total irritable bowel syndrome-severity scoring system scores in females and males. A: Placebo group; B: Active treated group. FMT: Faecal microbiota transplantation.

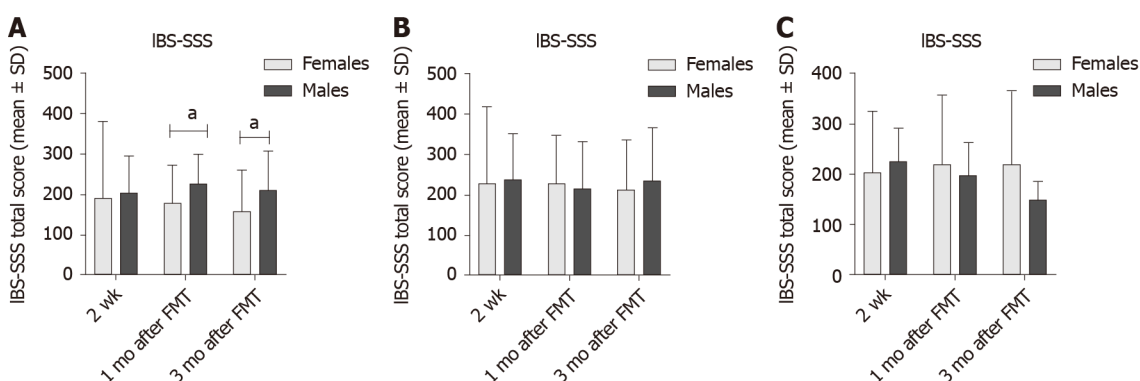


**Figure 5** The total irritable bowel syndrome-severity scoring system scores in females and males. A: Irritable bowel syndrome with diarrhoea-predominant; B: Irritable bowel syndrome with constipation-predominant; C: Irritable bowel syndrome with mixed diarrhoea and constipation. <sup>a</sup> $P < 0.05$ . IBS-SSS: Irritable bowel syndrome-severity scoring system; FMT: Faecal microbiota transplantation.

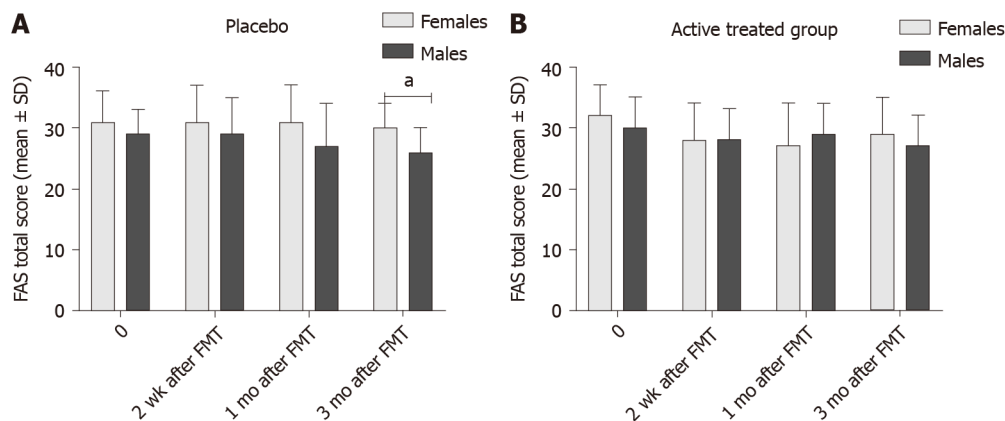


**Figure 6** The total Fatigue Assessment Scale scores in female and male irritable bowel syndrome patients. A: Placebo group; B: Active treated group. <sup>a</sup>P < 0.05. FAS: Fatigue Assessment Scale; FMT: Faecal microbiota transplantation.

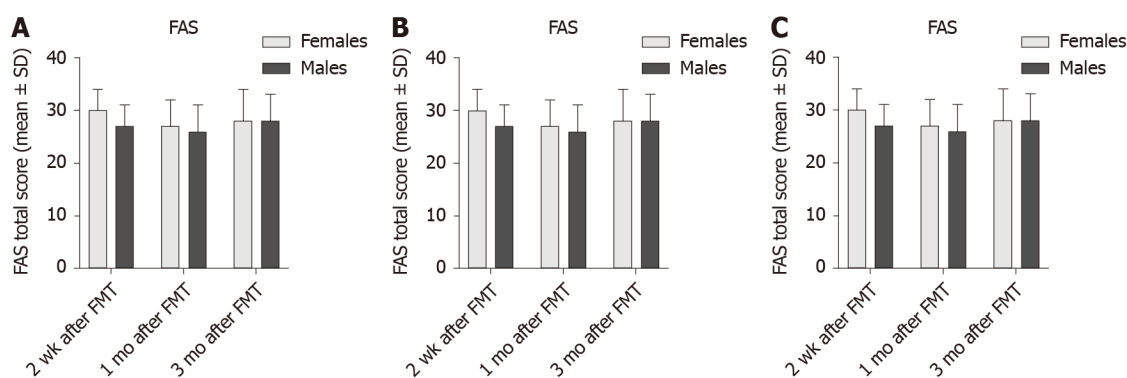


**Figure 7** Total Fatigue Assessment Scale scores in female and male patients. A: Irritable bowel syndrome with diarrhoea-predominant; B: Irritable bowel syndrome with constipation-predominant; C: Irritable bowel syndrome with mixed diarrhoea and constipation. FAS: Fatigue Assessment Scale; FMT: Faecal microbiota transplantation.

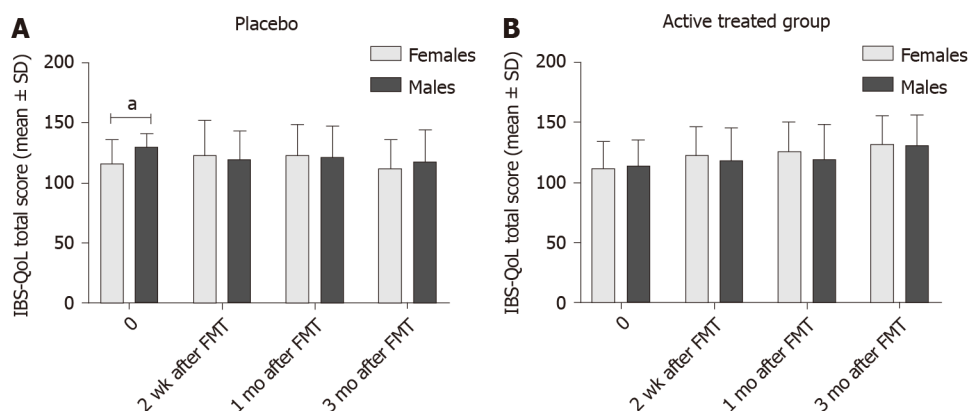


**Figure 8** Total irritable bowel syndrome quality of life scale scores in female and male patients. A: Placebo group; B: Active treated group. <sup>a</sup>P < 0.05. IBS-QoL: Irritable bowel syndrome quality of life scale; FMT: Faecal microbiota transplantation.

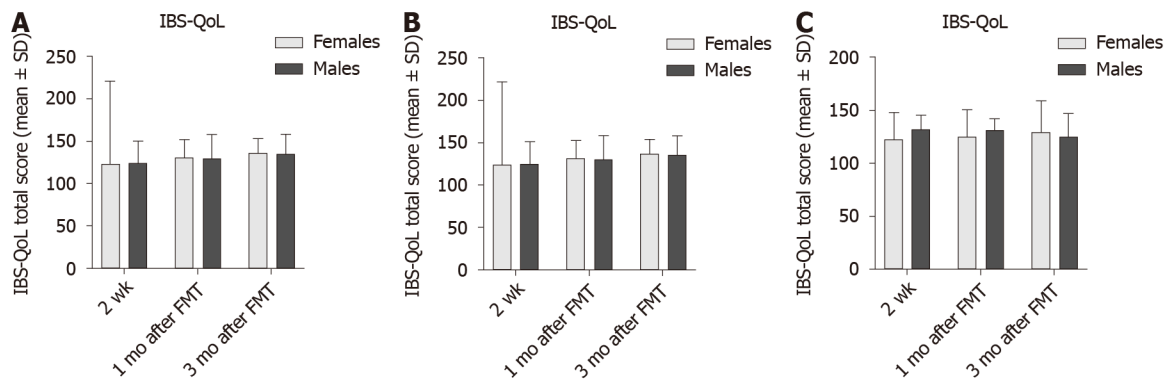


**Figure 9** Total irritable bowel syndrome quality of life scale scores in females and males. A: Irritable bowel syndrome with diarrhoea-predominant; B: Irritable bowel syndrome with constipation-predominant; C: Irritable bowel syndrome with mixed diarrhoea and constipation. IBS-QoL: Irritable bowel syndrome quality of life scale; FMT: Faecal microbiota transplantation.

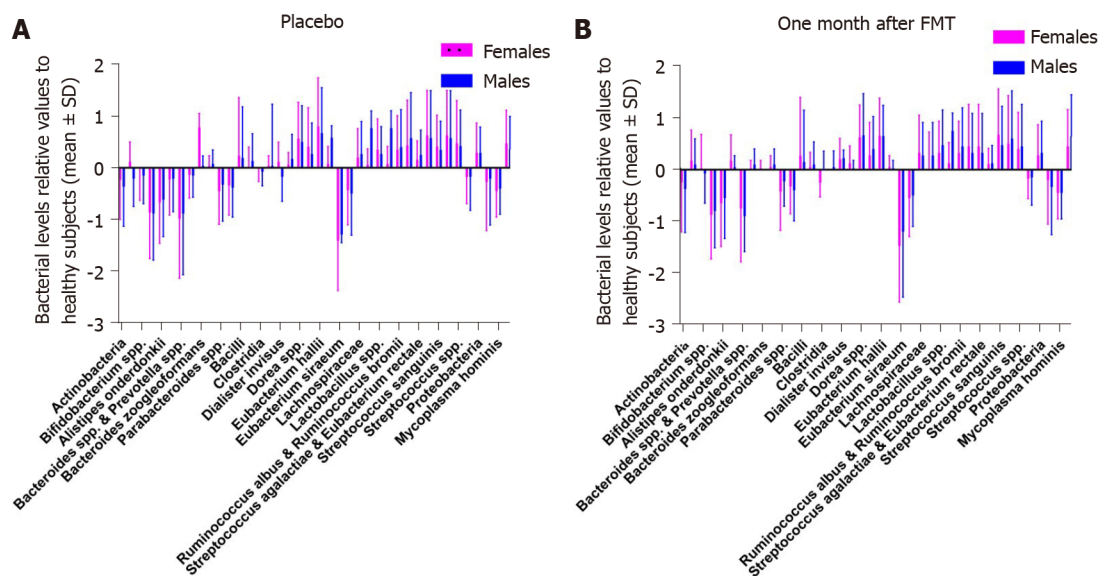
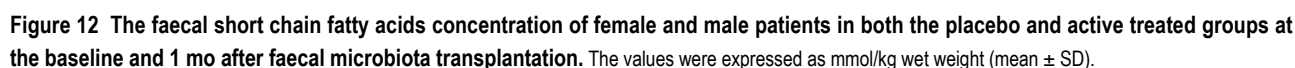
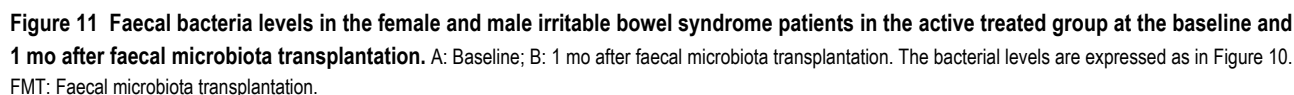


**Figure 10** Bacteria levels in the faeces of female and male irritable bowel syndrome patients in the placebo group at the baseline and 1 mo after faecal microbiota transplantation. A: Baseline; B: 1 mo after faecal microbiota transplantation. The bacterial levels are relative values to a normobiotic microbiota profile of 165 healthy subjects. FMT: Faecal microbiota transplantation.



## Research background

### Research motivation

### **Research objectives**

We aimed to investigate whether there is a sex difference in the response to FMT in terms of symptoms, dysbiosis, and bacteria and short-chain fatty acids (SCFAs) profiles in the same cohort of patients that we had investigated in our previous randomized controlled trial.



### Research methods

This study included 164 patients who fulfilled the Rome IV criteria for the diagnosis of IBS. These patient's cohort included IBS diarrhoea-predominant (IBS-D), IBS-constipation predominant (IBS-C) and mixed diarrhoea and constipation (IBS-M) subtypes. They were randomized to placebo (own faeces), 30 g or 60 g donor's faeces at a ratio of 1:1:1. The faecal transplant was administered *via* gastroscope to the duodenum. Patients completed IBS severity scoring system (IBS-SSS), the Fatigue Assessment Scale (FAS) and the IBS quality of life scale (IBS-QoL) questionnaires at the baseline and 2 wk, 1 mo and 3 mo after FMT. They also provided faecal samples at the baseline and 1 mo after FMT. Response was defined as a decrease of  $\geq 50$  points in the IBS-SSS total score after FMT. The faecal bacteria profile and dysbiosis were determined by the GA-map Dysbiosis Test (Genetic Analysis, Oslo, Norway) using the 16S rRNA gene. The levels of faecal SCFAs were determined by gas chromatography.

### Research results

There was no sex difference in the response to FMT either in the placebo group or active treated group. There was no difference between females and males in either the placebo group or actively treated groups in the total score on the IBS-SSS, FAS or IBS-QoL, in dysbiosis, or in the faecal bacteria or SCFA level. However, the response rate was significantly higher in females with IBS-D than that of males at 1 mo, and 3 mo after FMT. Moreover, IBS-SSS total score was significantly lower in female patients with IBS-D than that of male patients both 1 mo and 3 mo after FMT.

### Research conclusions

There is no sex difference in the response to FMT in IBS patients with moderate-to-severe IBS symptoms belonging to the three of IBS subtypes of IBS-C and IBS-M in patients who did not responded to National Institute for Health and Care Excellence-modified diet. However, female patients with IBS-D had a significant higher response rate to FMT and lower IBS-SSS score after FMT than males.

### Research perspectives

The present observation that female patients with IBS-D respond better to FMT than males raise several questions as to the cause of this difference. Further studies are needed to explore the difference in diet and life style between females and males as possible causes for this difference.

## REFERENCES

- 1 El-Salhy M. Recent developments in the pathophysiology of irritable bowel syndrome. *World J Gastroenterol* 2015; **21**: 7621-7636 [PMID: 26167065 DOI: 10.3748/wjg.v21.i25.7621]
- 2 Ohman L, Simrén M. Intestinal microbiota and its role in irritable bowel syndrome (IBS). *Curr Gastroenterol Rep* 2013; **15**: 323 [PMID: 23580243 DOI: 10.1007/s11894-013-0323-7]
- 3 Öhman L, Törnblom H, Simrén M. Crosstalk at the mucosal border: importance of the gut microenvironment in IBS. *Nat Rev Gastroenterol Hepatol* 2015; **12**: 36-49 [PMID: 25446728 DOI: 10.1038/nrgastro.2014.200]
- 4 Wilson BC, Vatanen T, Cutfield WS, O'Sullivan JM. The Super-Donor Phenomenon in Fecal Microbiota Transplantation. *Front Cell Infect Microbiol* 2019; **9**: 2 [PMID: 30719428 DOI: 10.3389/fcimb.2019.00002]
- 5 Maier L, Pruteanu M, Kuhn M, Zeller G, Telzerow A, Anderson EE, Brochado AR, Fernandez KC, Dose H, Mori H, Patil KR, Bork P, Typas A. Extensive impact of non-antibiotic drugs on human gut bacteria. *Nature* 2018; **555**: 623-628 [PMID: 29555994 DOI: 10.1038/nature25979]
- 6 Casén C, Vebø HC, Sekelja M, Hegge FT, Karlsson MK, Cierniejewska E, Dzankovic S, Frøyland C, Nestestog R, Engstrand L, Munkholm P, Nielsen OH, Rogler G, Simrén M, Öhman L, Vatn MH, Rudi K. Deviations in human gut microbiota: a novel diagnostic test for determining dysbiosis in patients with IBS or IBD. *Aliment Pharmacol Ther* 2015; **42**: 71-83 [PMID: 25973666 DOI: 10.1111/apt.13236]
- 7 Pozuelo M, Panda S, Santiago A, Mendez S, Accarino A, Santos J, Guarner F, Azpiroz F, Manichanh C. Reduction of butyrate- and methane-producing microorganisms in patients with Irritable Bowel Syndrome. *Sci Rep* 2015; **5**: 12693 [PMID: 26239401 DOI: 10.1038/srep12693]
- 8 Chong PP, Chin VK, Looi CY, Wong WF, Madhavan P, Yong VC. The Microbiome and Irritable Bowel Syndrome - A Review on the Pathophysiology, Current Research and Future Therapy. *Front Microbiol* 2019; **10**: 1136 [PMID: 31244784 DOI: 10.3389/fmicb.2019.01136]
- 9 Enck P, Mazurak N. Dysbiosis in Functional Bowel Disorders. *Ann Nutr Metab* 2018; **72**: 296-306 [PMID: 29694952 DOI: 10.1159/000488773]
- 10 Johnsen PH, Hilpüsch F, Cavanagh JP, Leikanger IS, Kolstad C, Valle PC, Goll R. Faecal microbiota

- transplantation vs placebo for moderate-to-severe irritable bowel syndrome: a double-blind, randomised, placebo-controlled, parallel-group, single-centre trial. *Lancet Gastroenterol Hepatol* 2018; **3**: 17-24 [PMID: 29100842 DOI: 10.1016/S2468-1253(17)30338-2]
- 11 **Halkjær SI**, Christensen AH, Lo BZS, Browne PD, Günther S, Hansen LH, Petersen AM. Faecal microbiota transplantation alters gut microbiota in patients with irritable bowel syndrome: results from a randomised, double-blind placebo-controlled study. *Gut* 2018; **67**: 2107-2115 [PMID: 29980607 DOI: 10.1136/gutjnl-2018-316434]
- 12 **El-Salhy M**, Hatlebakk JG, Gilja OH, Bråthen Kristoffersen A, Hausken T. Efficacy of faecal microbiota transplantation for patients with irritable bowel syndrome in a randomised, double-blind, placebo-controlled study. *Gut* 2020; **69**: 859-867 [PMID: 31852769 DOI: 10.1136/gutjnl-2019-319630]
- 13 **Aroniadis OC**, Brandt LJ, Oneto C, Feuerstadt P, Sherman A, Wolkoff AW, Kassam Z, Sadovsky RG, Elliott RJ, Budree S, Kim M, Keller MJ. Faecal microbiota transplantation for diarrhoea-predominant irritable bowel syndrome: a double-blind, randomised, placebo-controlled trial. *Lancet Gastroenterol Hepatol* 2019; **4**: 675-685 [PMID: 31326345 DOI: 10.1016/S2468-1253(19)30198-0]
- 14 **Holster S**, Lindqvist CM, Repsilber D, Salonen A, de Vos WM, König J, Brummer RJ. The Effect of Allogenic Versus Autologous Fecal Microbiota Transfer on Symptoms, Visceral Perception and Fecal and Mucosal Microbiota in Irritable Bowel Syndrome: A Randomized Controlled Study. *Clin Transl Gastroenterol* 2019; **10**: e00034 [PMID: 31009405 DOI: 10.14309/ctg.0000000000000034]
- 15 **Lahtinen P**, Jalanka J, Hartikainen A, Mattila E, Hillilä M, Punkkinen J, Koskenpato J, Anttila VJ, Tillonen J, Satokari R, Arkkila P. Randomised clinical trial: faecal microbiota transplantation vs autologous placebo administered *via* colonoscopy in irritable bowel syndrome. *Aliment Pharmacol Ther* 2020; **51**: 1321-1331 [PMID: 32343000 DOI: 10.1111/apt.15740]
- 16 **Holvoet T**, Joossens M, Vázquez-Castellanos JF, Christiaens E, Heyerick L, Boelens J, Verhasselt B, van Vlierberghe H, De Vos M, Raes J, De Looze D. Fecal Microbiota Transplantation Reduces Symptoms in Some Patients With Irritable Bowel Syndrome With Predominant Abdominal Bloating: Short- and Long-term Results From a Placebo-Controlled Randomized Trial. *Gastroenterology* 2021; **160**: 145-157. e8 [PMID: 32681922 DOI: 10.1053/j.gastro.2020.07.013]
- 17 **Benech N**, Sokol H. Fecal microbiota transplantation in gastrointestinal disorders: time for precision medicine. *Genome Med* 2020; **12**: 58 [PMID: 32605650 DOI: 10.1186/s13073-020-00757-y]
- 18 **Grundmann O**, Yoon SL. Irritable bowel syndrome: epidemiology, diagnosis and treatment: an update for health-care practitioners. *J Gastroenterol Hepatol* 2010; **25**: 691-699 [PMID: 20074154 DOI: 10.1111/j.1440-1746.2009.06120.x]
- 19 **Camilleri M**. Diagnosis and Treatment of Irritable Bowel Syndrome: A Review. *JAMA* 2021; **325**: 865-877 [PMID: 33651094 DOI: 10.1001/jama.2020.22532]
- 20 **Canavan C**, West J, Card T. The epidemiology of irritable bowel syndrome. *Clin Epidemiol* 2014; **6**: 71-80 [PMID: 24523597 DOI: 10.2147/CLEP.S40245]
- 21 **Kwan AC**, Hu WH, Chan YK, Yeung YW, Lai TS, Yuen H. Prevalence of irritable bowel syndrome in Hong Kong. *J Gastroenterol Hepatol* 2002; **17**: 1180-1186 [PMID: 12453277 DOI: 10.1046/j.1440-1746.2002.02871.x]
- 22 **Husain N**, Chaudhry IB, Jafri F, Niaz SK, Tomenson B, Creed F. A population-based study of irritable bowel syndrome in a non-Western population. *Neurogastroenterol Motil* 2008; **20**: 1022-1029 [PMID: 18492027 DOI: 10.1111/j.1365-2982.2008.01143.x]
- 23 **Xiong LS**, Chen MH, Chen HX, Xu AG, Wang WA, Hu PJ. A population-based epidemiologic study of irritable bowel syndrome in South China: stratified randomized study by cluster sampling. *Aliment Pharmacol Ther* 2004; **19**: 1217-1224 [PMID: 15153175 DOI: 10.1111/j.1365-2036.2004.01939.x]
- 24 **Chang FY**, Lu CL, Chen TS. The current prevalence of irritable bowel syndrome in Asia. *J Neurogastroenterol Motil* 2010; **16**: 389-400 [PMID: 21103420 DOI: 10.5056/jnm.2010.16.4.389]
- 25 **El-Salhy M**, Valeur J, Hausken T, Gunnar Hatlebakk J. Changes in fecal short-chain fatty acids following fecal microbiota transplantation in patients with irritable bowel syndrome. *Neurogastroenterol Motil* 2021; **33**: e13983 [PMID: 32945066 DOI: 10.1111/nmo.13983]
- 26 **Cammarota G**, Ianiro G, Tilg H, Rajilić-Stojanović M, Kump P, Satokari R, Sokol H, Arkkila P, Pintus C, Hart A, Segal J, Aloï M, Masucci L, Molinaro A, Scaldaferri F, Gasbarrini G, Lopez-Sanroman A, Link A, de Groot P, de Vos WM, Högenauer C, Malfetherneiner P, Mattila E, Milosavljević T, Nieuwdorp M, Sanguinetti M, Simren M, Gasbarrini A; European FMT Working Group. European consensus conference on faecal microbiota transplantation in clinical practice. *Gut* 2017; **66**: 569-580 [PMID: 28087657 DOI: 10.1136/gutjnl-2016-313017]
- 27 **Francis CY**, Morris J, Whorwell PJ. The irritable bowel severity scoring system: a simple method of monitoring irritable bowel syndrome and its progress. *Aliment Pharmacol Ther* 1997; **11**: 395-402 [PMID: 9146781 DOI: 10.1046/j.1365-2036.1997.142318000.x]
- 28 **Roalfe AK**, Roberts LM, Wilson S. Evaluation of the Birmingham IBS symptom questionnaire. *BMC Gastroenterol* 2008; **8**: 30 [PMID: 18651941 DOI: 10.1186/1471-230X-8-30]
- 29 **Hendriks C**, Drent M, Elfferich M, De Vries J. The Fatigue Assessment Scale: quality and availability in sarcoidosis and other diseases. *Curr Opin Pulm Med* 2018; **24**: 495-503 [PMID: 29889115 DOI: 10.1097/MCP.0000000000000496]
- 30 **Drent M**, Lower EE, De Vries J. Sarcoidosis-associated fatigue. *Eur Respir J* 2012; **40**: 255-263 [PMID: 22441750 DOI: 10.1183/09031936.00002512]
- 31 **Atkins C**, Fordham R, Clark AB, Stockl A, Jones AP, Wilson AM. Feasibility study of a randomised controlled trial to investigate the treatment of sarcoidosis-associated fatigue with methylphenidate

- (FaST-MP): a study protocol. *BMJ Open* 2017; **7**: e018532 [PMID: 29208618 DOI: 10.1136/bmjopen-2017-018532]
- 32 **Drossman DA**, Patrick DL, Whitehead WE, Toner BB, Diamant NE, Hu Y, Jia H, Bangdiwala SI. Further validation of the IBS-QOL: a disease-specific quality-of-life questionnaire. *Am J Gastroenterol* 2000; **95**: 999-1007 [PMID: 10763950 DOI: 10.1111/j.1572-0241.2000.01941.x]
  - 33 **Wong RK**, Drossman DA. Quality of life measures in irritable bowel syndrome. *Expert Rev Gastroenterol Hepatol* 2010; **4**: 277-284 [PMID: 20528115 DOI: 10.1586/egh.10.19]
  - 34 **Arslan G**, Lind R, Olafsson S, Florvaag E, Berstad A. Quality of life in patients with subjective food hypersensitivity: applicability of the 10-item short form of the Nepean Dyspepsia Index. *Dig Dis Sci* 2004; **49**: 680-687 [PMID: 15185878 DOI: 10.1023/b:ddas.0000026318.81635.3b]
  - 35 **Zijlstra JB**, Beukema J, Wolthers BG, Byrne BM, Groen A, Dankert J. Pretreatment methods prior to gaschromatographic analysis of volatile fatty acids from faecal samples. *Clin Chim Acta* 1977; **78**: 243-250 [PMID: 884859 DOI: 10.1016/0009-8981(77)90312-6]
  - 36 **Høverstad T**, Fausa O, Bjørneklett A, Böhmer T. Short-chain fatty acids in the normal human feces. *Scand J Gastroenterol* 1984; **19**: 375-381 [PMID: 6740214]
  - 37 **Soret R**, Chevalier J, De Coppet P, Poupeau G, Derkinderen P, Segain JP, Neunlist M. Short-chain fatty acids regulate the enteric neurons and control gastrointestinal motility in rats. *Gastroenterology* 2010; **138**: 1772-1782 [PMID: 20152836 DOI: 10.1053/j.gastro.2010.01.053]
  - 38 **Hamer HM**, Jonkers D, Venema K, Vanhoutvin S, Troost FJ, Brummer RJ. Review article: the role of butyrate on colonic function. *Aliment Pharmacol Ther* 2008; **27**: 104-119 [PMID: 17973645 DOI: 10.1111/j.1365-2036.2007.03562.x]
  - 39 **Zhou J**, Martin RJ, Tulley RT, Raggio AM, McCutcheon KL, Shen L, Danna SC, Tripathy S, Hegsted M, Keenan MJ. Dietary resistant starch upregulates total GLP-1 and PYY in a sustained day-long manner through fermentation in rodents. *Am J Physiol Endocrinol Metab* 2008; **295**: E1160-E1166 [PMID: 18796545 DOI: 10.1152/ajpendo.90637.2008]
  - 40 **Karaki S**, Mitsui R, Hayashi H, Kato I, Sugiyama H, Iwanaga T, Furness JB, Kuwahara A. Short-chain fatty acid receptor, GPR43, is expressed by enteroendocrine cells and mucosal mast cells in rat intestine. *Cell Tissue Res* 2006; **324**: 353-360 [PMID: 16453106 DOI: 10.1007/s00441-005-0140-x]
  - 41 **Zhou J**, Martin RJ, Raggio AM, Shen L, McCutcheon K, Keenan MJ. The importance of GLP-1 and PYY in resistant starch's effect on body fat in mice. *Mol Nutr Food Res* 2015; **59**: 1000-1003 [PMID: 25631638 DOI: 10.1002/mnfr.201400904]
  - 42 **Zhang J**, Song L, Wang Y, Liu C, Zhang L, Zhu S, Liu S, Duan L. Beneficial effect of butyrate-producing Lachnospiraceae on stress-induced visceral hypersensitivity in rats. *J Gastroenterol Hepatol* 2019; **34**: 1368-1376 [PMID: 30402954 DOI: 10.1111/jgh.14536]
  - 43 **Long X**, Li M, Li LX, Sun YY, Zhang WX, Zhao DY, Li YQ. Butyrate promotes visceral hypersensitivity in an IBS-like model via enteric glial cell-derived nerve growth factor. *Neurogastroenterol Motil* 2018; **30**: e13227 [PMID: 29052293 DOI: 10.1111/nmo.13227]
  - 44 **Banasiewicz T**, Krokowicz L, Stojcev Z, Kaczmarek BF, Kaczmarek E, Maik J, Marciniak R, Krokowicz P, Walkowiak J, Drews M. Microencapsulated sodium butyrate reduces the frequency of abdominal pain in patients with irritable bowel syndrome. *Colorectal Dis* 2013; **15**: 204-209 [PMID: 22738315 DOI: 10.1111/j.1463-1318.2012.03152.x]
  - 45 **Tana C**, Umesaki Y, Imaoka A, Handa T, Kanazawa M, Fukudo S. Altered profiles of intestinal microbiota and organic acids may be the origin of symptoms in irritable bowel syndrome. *Neurogastroenterol Motil* 2010; **22**: 512-519, e114 [PMID: 19903265 DOI: 10.1111/j.1365-2982.2009.01427.x]
  - 46 **Valeur J**, Røseth AG, Knudsen T, Malmstrøm GH, Fiennes JT, Midtvedt T, Berstad A. Fecal Fermentation in Irritable Bowel Syndrome: Influence of Dietary Restriction of Fermentable Oligosaccharides, Disaccharides, Monosaccharides and Polyols. *Digestion* 2016; **94**: 50-56 [PMID: 27487397 DOI: 10.1159/000448280]
  - 47 **Winston J**, Shenoy M, Medley D, Naniwadekar A, Pasricha PJ. The vanilloid receptor initiates and maintains colonic hypersensitivity induced by neonatal colon irritation in rats. *Gastroenterology* 2007; **132**: 615-627 [PMID: 17258716 DOI: 10.1053/j.gastro.2006.11.014]



## Observational Study

# Standard vs magnifying narrow-band imaging endoscopy for diagnosis of *Helicobacter pylori* infection and gastric precancerous conditions

Jun-Hyung Cho, Seong Ran Jeon, So-Young Jin, Suyeon Park

**ORCID number:** Jun-Hyung Cho 0000-0003-2075-2333; Seong Ran Jeon 0000-0001-6970-9737; So-Young Jin 0000-0002-9900-8322; Suyeon Park 0000-0002-6391-557X.

**Author contributions:** Cho JH was involved in the study design, performing the study, data collection and analyses, writing and revising the manuscript; Jeon SR and Jin SY were involved in the study design and revising the manuscript; Park S was involved in statistical analyses; all of the authors approved the final version of the manuscript.

**Supported by** the Soonchunhyang University Research Fund, No. 20200023.

**Institutional review board statement:** The study was reviewed and approved by the Institutional Review Board of Soonchunhyang University Hospital (No. SCHUH 2016-05-001).

**Informed consent statement:** All study participants, or their legal guardian, provided informed written consent prior to study enrollment.

**Conflict-of-interest statement:** The

**Jun-Hyung Cho, Seong Ran Jeon**, Digestive Disease Center, Soonchunhyang University Hospital, Seoul 04401, South Korea

**So-Young Jin**, Department of Pathology, Soonchunhyang University Hospital, Seoul 04401, South Korea

**Suyeon Park**, Department of Medical Biostatistics, Soonchunhyang University Hospital, Seoul 04401, South Korea

**Corresponding author:** Jun-Hyung Cho, MD, PhD, Associate Professor, Digestive Disease Center, Soonchunhyang University Hospital, No. 59 Daesagwan-ro, Yongsan-gu, Seoul 04401, South Korea. [chojhmd@naver.com](mailto:chojhmd@naver.com)

## Abstract

### BACKGROUND

Advances in endoscopic imaging enable the identification of patients at high risk of gastric cancer. However, there are no comparative data on the utility of standard and magnifying narrow-band imaging (M-NBI) endoscopy for diagnosing *Helicobacter pylori* (*H. pylori*) infection, gastric atrophy, and intestinal metaplasia.

### AIM

To compare the diagnostic performance of standard and M-NBI endoscopy for *H. pylori* gastritis and precancerous conditions.

### METHODS

In 254 patients, standard endoscopy findings were classified into mosaic-like appearance (type A), diffuse homogenous redness (type B), and irregular redness with groove (type C). Gastric mucosal patterns visualized by M-NBI were classified as regular round pits with polygonal sulci (type Z-1), more dilated and linear pits without sulci (type Z-2), and loss of gastric pits with coiled vessels (type Z-3).

### RESULTS

The diagnostic accuracy of standard and M-NBI endoscopy for *H. pylori* gastritis was 93.3% and 96.1%, respectively. Regarding gastric precancerous conditions,



authors declare that they have no competing interest.

**Data sharing statement:** The datasets used and analyzed during the current study are available from the corresponding author on reasonable request.

**STROBE statement:** The authors have read the STROBE Statement checklist of items, and the manuscript was prepared and revised according to the STROBE Statement-checklist of items.

**Open-Access:** This article is an open-access article that was selected by an in-house editor and fully peer-reviewed by external reviewers. It is distributed in accordance with the Creative Commons Attribution NonCommercial (CC BY-NC 4.0) license, which permits others to distribute, remix, adapt, build upon this work non-commercially, and license their derivative works on different terms, provided the original work is properly cited and the use is non-commercial. See: <http://creativecommons.org/licenses/by-nc/4.0/>

**Manuscript source:** Invited manuscript

**Specialty type:** Gastroenterology and hepatology

**Country/Territory of origin:** South Korea

**Peer-review report's scientific quality classification**

Grade A (Excellent): 0  
Grade B (Very good): B, B, B  
Grade C (Good): 0  
Grade D (Fair): 0  
Grade E (Poor): 0

**Received:** January 27, 2021

**Peer-review started:** January 27, 2021

**First decision:** March 29, 2021

**Revised:** March 31, 2021

**Accepted:** April 23, 2021

**Article in press:** April 23, 2021

**Published online:** May 14, 2021

**P-Reviewer:** Peruhova M, Ulaşoğlu C

the accuracy of standard and M-NBI endoscopy was 72.0% vs 72.6% for moderate to severe atrophy, and 61.7% vs. 61.1% for intestinal metaplasia in the corpus, respectively. Compared to type A and Z-1, types B+C and Z-2+Z-3 were significantly associated with moderate to severe atrophy [odds ratio (OR) = 5.56 and 8.67] and serum pepsinogen I/II ratio of  $\leq 3$  (OR = 4.48 and 5.69).

## CONCLUSION

Close observation of the gastric mucosa by standard and M-NBI endoscopy is useful for the diagnosis of *H. pylori* gastritis and precancerous conditions.

**Key Words:** Endoscopy; Magnifying narrow-band imaging; *Helicobacter pylori*; Gastric atrophy; Intestinal metaplasia; Pepsinogen

©The Author(s) 2021. Published by Baishideng Publishing Group Inc. All rights reserved.

**Core Tip:** In Correa's model of gastric carcinogenesis, *Helicobacter pylori* infection, gastric atrophy and intestinal metaplasia are linked to gastric cancer development. The low level of serum pepsinogens was known to be highly associated with extensive atrophic gastritis. High-resolution and magnifying narrow-band imaging (M-NBI) facilitate the detailed examination of gastrointestinal mucosa. However, there was no comparative data regarding the usefulness of standard and M-NBI endoscopy for *H. pylori* infection and gastric precancerous conditions. We found the significant relationship between endoscopic mucosal patterns and degree of gastric precancerous conditions (moderate to severe gastric atrophy and serum pepsinogen I/II ratio of  $\leq 3$ ). These results seem to be valuable for identifying a group at risk of gastric cancer using high quality endoscopy.

**Citation:** Cho JH, Jeon SR, Jin SY, Park S. Standard vs magnifying narrow-band imaging endoscopy for diagnosis of *Helicobacter pylori* infection and gastric precancerous conditions. *World J Gastroenterol* 2021; 27(18): 2238-2250

**URL:** <https://www.wjgnet.com/1007-9327/full/v27/i18/2238.htm>

**DOI:** <https://dx.doi.org/10.3748/wjg.v27.i18.2238>

## INTRODUCTION

The global prevalence of *Helicobacter pylori* (*H. pylori*) infection is reportedly > 50%[1]. In the *H. pylori*-infected stomach, chronic active inflammation of the mucosa becomes persistent, leading to gastric atrophy and intestinal metaplasia (IM)[2]. According to Correa's model of gastric carcinogenesis, gastric atrophy and IM are linked to progression to gastric cancer[3]. Advanced gastric atrophy and IM are considered to be precancerous conditions because they correlate with gastric carcinogenesis[4-6]. Accurate diagnosis of gastric precancerous conditions is essential for identifying patients at risk of gastric cancer[7].

Narrow-band imaging (NBI) is an innovative optical method that facilitates detailed examination of the gastric mucosa[8]. Furthermore, magnifying NBI (M-NBI) endoscopy with 80-fold magnification can visualize the fine mucosal structure and microvessels[9]. M-NBI endoscopy can be used to diagnose *H. pylori* infection and classify gastritis by histological severity[10]. Recent improvements in the resolution (> 1 million pixels) of gastrointestinal endoscopy have enhanced image quality, facilitating characterization of the gastric mucosal pattern[11]. Close observation of the gastric corpus mucosa by standard endoscopy without magnification enables prediction of *H. pylori* gastritis[12]. Moreover, the severity of gastric atrophy and IM differ according to the endoscopic mucosal pattern. In a systematic review, standard endoscopy was effective as an alternative method for diagnosing *H. pylori* infection[13]. However, there are no comparative data on the utility of standard and M-NBI endoscopy for diagnosing *H. pylori* infection, gastric atrophy, and IM.

In this study, we evaluated the diagnostic performance of standard and M-NBI endoscopy for *H. pylori* infection and advanced gastritis, and investigated the association between the endoscopic mucosal pattern and gastric precancerous



S-Editor: Yan JP

L-Editor: A

P-Editor: Wang LL



conditions.

## MATERIALS AND METHODS

### *Patients and study design*

From June 2016 to April 2020, we prospectively enrolled patients who underwent gastroscopy for epigastric symptoms, diagnostic work-up for gastric neoplasia, and gastric cancer screening. Before endoscopic examination, all patients had the informed consents about the evaluation of *H. pylori* infection status and gastric precancerous conditions. We performed a complete blood cell count, blood chemistry assays, coagulation test, chest X-ray, and electrocardiogram. The exclusion criteria were: Age < 20 or > 80 years, anemia, severe systemic disease, current use of proton pump inhibitors, history of *H. pylori* eradication, and history of gastric surgery. The study protocol was approved by the Institutional Review Board of our hospital (SCHUH 2016-05-001) and was registered at ClinicalTrials.gov (NCT04489030).

### *Endoscopic equipment and procedure*

Endoscopic procedures were performed using a high-resolution endoscope (GIF-H260Z, H290Z; Olympus, Tokyo, Japan). The whole stomach was examined in a routine manner by a single experienced endoscopist (Cho JH). First, we performed close-up observation of the mucosal patterns at the greater curvature of the middle or lower corpus *via* non-magnified white-light imaging in structural enhancement mode A5. We captured endoscopic images while maintaining a distance of  $\leq 10$  mm between the endoscope tip and mucosal surface. We previously classified abnormal mucosal patterns using a simple standard endoscopy technique (Figure 1)[12]. When a regular arrangement of numerous minute red dots (normal pattern) was absent, abnormal patterns were categorized as mosaic-like appearance (type A), diffuse homogenous redness (type B), or irregular redness with groove (type C). After completing the mucosal examination by standard endoscopy, the greater curvature side of the gastric corpus was observed by M-NBI. Before the procedure, a soft black hood was attached to the endoscope tip to fix the distance between the endoscope tip and mucosal surface to about 2 mm. When white-light endoscopic image was magnified 80-fold (Supplementary Figure 1), we pressed the NBI button on the handle for the enhanced visualization of mucosal structures and microvessels[14]. NBI was set in enhancement mode A7 and color mode 2. Next, we classified the M-NBI still images as normal or one of three abnormal patterns according to Yagi's classification (Figure 2)[15]. A regular arrangement of collecting venules (RAC) and honeycomb-like subepithelial capillary network was considered a normal pattern. If RAC was not visualized by M-NBI endoscopy, abnormal mucosal patterns were classified as regular round pits with polygonal sulci (type Z-1), more dilated and linear pits without sulci (type Z-2), or loss of gastric pits with coiled vessels (type Z-3). In cases of mixed mucosal patterns, the most prominent was reported after discussion with another expert endoscopist (Jeon SR).

### *Evaluation of *H. pylori* infection and gastric precancerous conditions*

To increase the *H. pylori* detection rate, a biopsy was taken from the greater curvature of the gastric corpus. *H. pylori* infection status was confirmed by rapid urease test (Pronto Dry; Gastrex Sarl, Gilly les Citeaux, France) or molecular test (Seeplex® *H. pylori*-ClaR ACE Detection; Seegene Inc., Seoul, South Korea). For the histological assessment of glandular atrophy and IM, biopsy specimens were obtained from the lesser curvature of the gastric antrum and corpus. The specimens were fixed in 10% formalin and embedded in paraffin wax, and 5- $\mu$ m sections were stained with hematoxylin and eosin. The gastric atrophy was defined as loss of glandular tissue and scored on a four-point scale in accordance with the updated Sydney System[16]. The degree of atrophy was classified as mild (1-2), moderate (3-4), or severe (5-6) by summing the scores of the antrum (score 0-3) and corpus (score 0-3). IM was diagnosed by the presence of goblet cells in foveolar epithelium[17]. The pathological examination was performed by an expert pathologist (Jin SY), who was blinded to the patients' data and endoscopic findings.

Before endoscopy, blood samples were collected during a 12-h fasting period. Blood samples were immediately centrifuged at 4 °C and stored at -70 °C until required. Serum pepsinogen (PG) I and PG II levels were measured by latex turbidimetric immunoassay (HiSens; HBI, Anyang, South Korea), and the PG I/II ratio was calculated[18]. A serum PG I level of  $\leq 70$  ng/mL and PG I/II ratio of  $\leq 3$  are highly

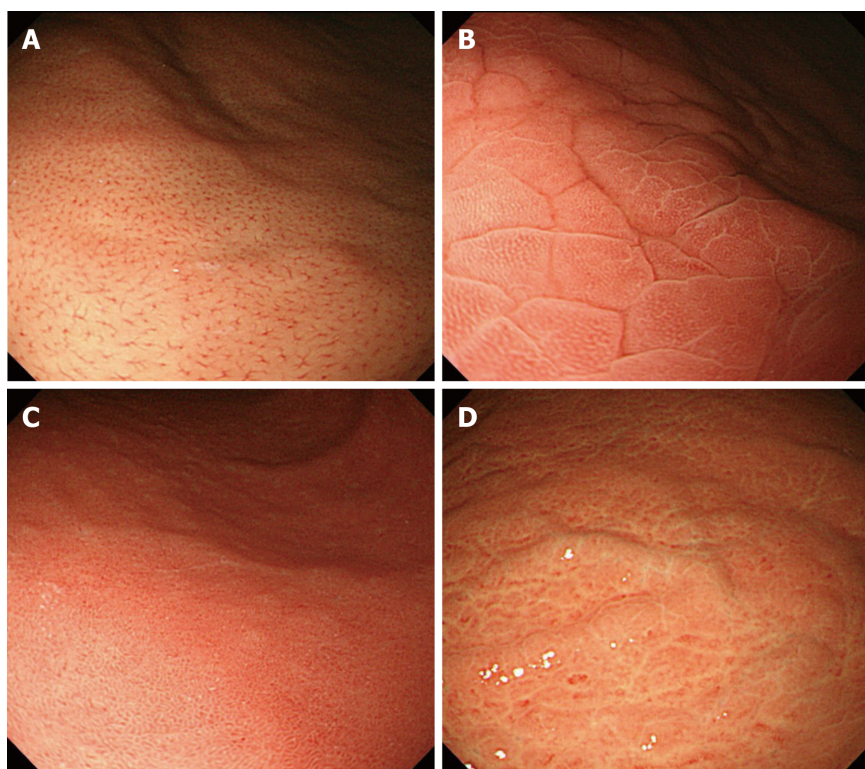


**Figure 1** Normal and three abnormal mucosal patterns in the gastric corpus by standard endoscopy. A: Normal pattern, numerous minute red dots; B: Type A, mosaic-like appearance; C: Type B, diffuse homogenous redness; D: Type C, irregular redness with grooves.

associated with extensive atrophic gastritis[19]. A cutoff PG I/II ratio of  $\leq 3$  was used to assess the risk of gastric precancerous conditions.

### Statistical analysis

Continuous data are presented as means and standard deviations and categorical data as numbers and percentages. The Pearson chi-squared test or linear-by-linear association was used to analyze categorical data. The sensitivity, specificity, positive predictive value (PPV), negative predictive value (NPV), and accuracy of the two endoscopic classifications were compared by McNemar test. Diagnostic performance was assessed by computing area under the curve (AUC) values. The adjusted odds ratios (ORs) of endoscopic mucosal patterns for predicting gastric precancerous conditions were calculated by logistic regression analysis. Statistical analysis was conducted using SPSS software (version 19.0; IBM Corp., Armonk, NY, United States). A value of  $P < 0.05$  was considered indicative of statistical significance.

## RESULTS

### Characteristics of the study population

A total of 254 patients was eligible for the study (Table 1). The mean age was  $45.9 (\pm 14.6)$  years and the proportion of male patients was 46.9%. The most frequent endoscopic findings were chronic active gastritis (53.1%), peptic ulcer (4.3%), gastric neoplasia (9.8%), and non-neoplastic polyp (7.5%). Current *H. pylori* infection was confirmed in 64.2% of the patients. According to the degree of gastric atrophy, 117 patients (66.9%) were classified into the none/mild atrophy group, 37 (21.1%) into the moderate atrophy group, and 21 (12.0%) into the severe atrophy group. Regarding the extent of IM, 115 patients (65.7%) had no IM in the antrum or corpus, and 22 (12.6%) and 38 (21.7%) patients had IM in the antrum only and in both the antrum and the corpus, respectively. The mean serum PG I and PG II concentrations and PG I/II ratio were  $64.4 \pm 32.4$  ng/mL,  $20.5 \pm 14.7$  ng/mL, and  $4.11 \pm 2.2$ , respectively. The mean serum gastrin concentration was  $123.1 \pm 149.9$  pg/mL.

**Table 1** Baseline characteristics of the study population

Characteristic	<i>n</i> = 254
Age (yr, mean $\pm$ SD)	45.9 $\pm$ 14.6
Sex, male, <i>n</i> (%)	119 (46.9)
<b>Indication for endoscopy, <i>n</i> (%)</b>	
Screening	132 (52.0)
Dyspepsia	42 (16.5)
Abdominal pain	47 (18.5)
Other	33 (13.0)
<b>Endoscopic diagnosis, <i>n</i> (%)</b>	
Peptic ulcer	11 (4.3)
Gastric neoplasia	25 (9.8)
Non-neoplastic polyp	19 (7.5)
Chronic active gastritis	135 (53.1)
<i>Helicobacter pylori</i> infection, <i>n</i> (%)	163 (64.2)
<b>Gastric atrophy, <i>n</i> (%)</b>	
None/mild	117 (66.9)
Moderate	37 (21.1)
Severe	21 (12.0)
<b>Intestinal metaplasia, <i>n</i> (%)</b>	
None	115 (65.7)
Antrum only	22 (12.6)
Corpus	38 (21.7)
<b>Serum PG (ng/mL, mean <math>\pm</math> SD)</b>	
PG I	64.4 $\pm$ 32.4
PG II	20.5 $\pm$ 14.7
PG I/II ratio	4.11 $\pm$ 2.2
Serum gastrin (pg/mL, mean $\pm$ SD)	123.1 $\pm$ 149.9

SD: Standard deviation; PG: Pepsinogen.

**Diagnostic performance of standard and M-NBI endoscopy**

By standard endoscopy, the *H. pylori* infection rate was 91.5% (*n* = 43/47) for type A, 100% (*n* = 84/84) for type B, and 100% (*n* = 23/23) for type C (Table 2). By M-NBI endoscopy, the proportion of *H. pylori* infection was 97.6% (*n* = 124/127) for type Z-1, 96.3% (*n* = 26/27) for type Z-2, and 100% (*n* = 7/7) for type Z-3. The rate of advanced gastritis was calculated according to the endoscopic mucosal pattern among 175 patients whose samples were subjected to pathologic examination. Moderate to severe gastric atrophy and the presence of IM in the corpus were considered to be advanced gastritis with a high risk of gastric cancer. By standard endoscopy, the proportions of patients with moderate to severe atrophy were 27.3% (*n* = 9/33) for type A, 74.0% (*n* = 37/50) for type B, and 50.0% (*n* = 10/20) for type C. By M-NBI endoscopy, the proportions of patients with moderate to severe atrophy were 45.9% (*n* = 39/85) for type Z-1, 88.2% (*n* = 15/17) for type Z-2, and 100% (*n* = 4/4) for type Z-3. If the gastric mucosal pattern was normal, however, the rate of moderate to severe atrophy was 2.8% (*n* = 2/72) by standard endoscopy and 0% (*n* = 0/69) by M-NBI endoscopy. Similarly, the rate of IM in the corpus differed significantly between normal and abnormal mucosal patterns by both standard (types A+B+C, *P* < 0.001) and M-NBI endoscopy (types Z-1+Z-2 +Z-3, *P* < 0.001).



**Table 2** *Helicobacter pylori* gastritis, gastric atrophy, and intestinal metaplasia observed by standard and magnifying narrow-band imaging endoscopy

Endoscopy	<i>H. pylori</i> gastritis		Gastric atrophy		Intestinal metaplasia	
	Negative	Positive	None/mild	Moderate/severe	None/antrum	Corpus
	( <i>n</i> = 91)	( <i>n</i> = 163)	( <i>n</i> = 117)	( <i>n</i> = 58)	( <i>n</i> = 137)	( <i>n</i> = 38)
<b>Standard</b>						
Normal	87/100 (87.0)	13/100 (13.0)	70/72 (97.2)	2/72 (2.8)	71/72 (98.6)	1/72 (1.4)
Type A	4/47 (8.5)	43/47 (91.5)	24/33 (72.7)	9/33 (27.3)	25/33 (75.8)	8/33 (24.2)
Type B	0/84 (0)	84/84 (100)	13/50 (26.0)	37/50 (74.0)	24/50 (48.0)	26/50 (52.0)
Type C	0/23 (0)	23/23 (100)	10/20 (50.0)	10/20 (50.0)	17/20 (85.0)	3/20 (15.0)
<b>M-NBI</b>						
Normal	87/93 (93.5)	6/93 (6.5)	69/69 (100)	0/69 (0)	69/69 (100)	0/69 (0)
Type Z-1	3/127 (2.4)	124/127 (97.6)	46/85 (54.1)	39/85 (45.9)	59/85 (69.4)	26/85 (30.6)
Type Z-2	1/27 (3.7)	26/27 (96.3)	2/17 (11.8)	15/17 (88.2)	7/17 (41.2)	10/17 (58.8)
Type Z-3	0/7 (0)	7/7 (100)	0/4 (0)	4/4 (100)	2/4 (50.0)	2/4 (50.0)

M-NBI: Magnifying narrow-band imaging; *H. pylori*: *Helicobacter pylori*.

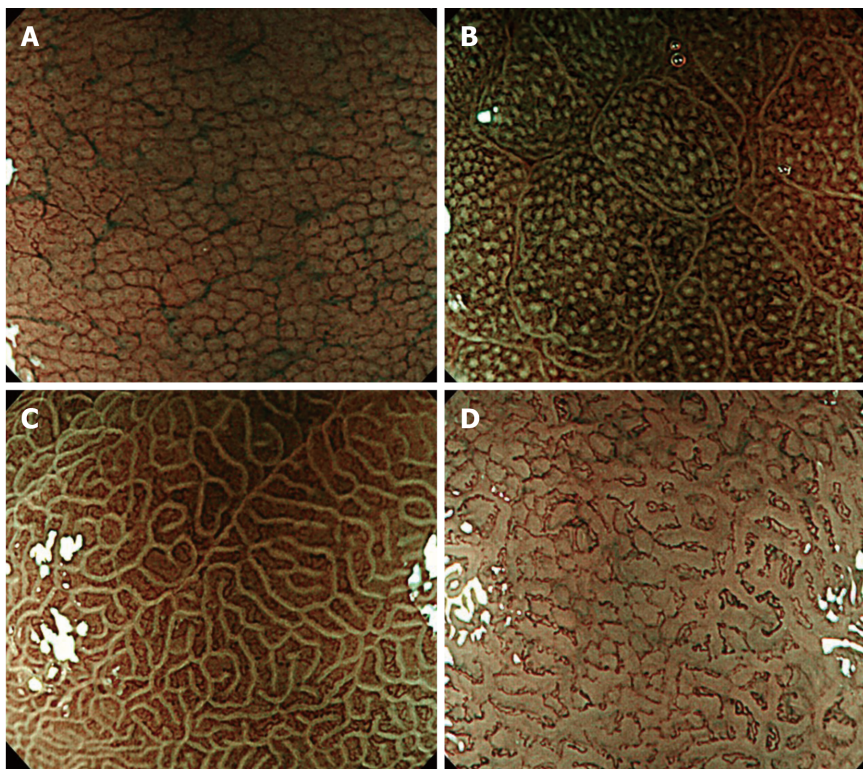


**Figure 2** Micromucosal patterns in the gastric corpus observed by magnifying narrow-band imaging endoscopy. A: Normal pattern characterized by regular arrangement of collecting venules and honeycomb-like subepithelial capillary network; B: Type Z-1, regular round pits with polygonal sulci; C: Type Z-2, more dilated and linear pits without sulci; D: Type Z-3, loss of gastric pits with coiled microvessels.

For the diagnosis of *H. pylori* gastritis, the sensitivity of standard endoscopy was 92.0%, while the specificity was 95.6%, the PPV was 97.4%, the NPV was 87.0%, and the accuracy was 93.3%. The sensitivity of M-NBI endoscopy was 96.3%, while the specificity was 95.6%, the PPV was 97.5%, the NPV was 93.5%, and the accuracy was 96.1%. The sensitivity of M-NBI endoscopy was significantly greater than that of standard endoscopy ( $P = 0.016$ ; Table 3). For the diagnosis of moderate to severe atrophy, the sensitivity of standard endoscopy was 96.6%, while the specificity was

**Table 3** Diagnostic performance of standard and magnifying narrow-band imaging endoscopy for *Helicobacter pylori* gastritis, gastric atrophy, and intestinal metaplasia

Endoscopy	Diagnosis	Sensitivity (%)	Specificity (%)	PPV (%)	NPV (%)	Accuracy (%)	AUC
Standard	<i>H. pylori</i> gastritis	92.0 <sup>a</sup>	95.6	97.4	87.0	93.3	0.93
	Moderate to severe atrophy	96.6	59.8	54.4	97.2	72.0	0.78
	Intestinal metaplasia, corpus	97.4	51.8	35.9	98.6	61.7	0.74
M-NBI	<i>H. pylori</i> gastritis	96.3 <sup>a</sup>	95.6	97.5	93.5	96.1	0.96
	Moderate to severe atrophy	100	59.0	54.7	100	72.6	0.79
	Intestinal metaplasia, corpus	100	50.4	35.8	100	61.1	0.75

<sup>a</sup>*P* = 0.016, McNemar test indicated a significant difference in sensitivity for diagnosis of *Helicobacter pylori* infection between standard and magnifying narrow-band imaging endoscopy. M-NBI: Magnifying narrow-band imaging; PPV: Positive predictive value; NPV: Negative predictive value; AUC: area under the curve; *H. pylori*: *Helicobacter pylori*.

59.8%, the PPV was 54.4%, the NPV was 97.2%, and the accuracy was 72.0%. The sensitivity of M-NBI endoscopy was 100%, while the specificity was 59.0%, the PPV was 54.7%, the NPV was 100%, and the accuracy was 72.6%. For diagnosis of IM in the corpus, the sensitivity of standard endoscopy was 97.4%, while the specificity was 51.8%, the PPV was 35.9%, the NPV was 98.6%, and the accuracy was 61.7%. The sensitivity of M-NBI endoscopy was 100%, while the specificity was 50.4%, the PPV was 35.8%, the NPV was 100%, and the accuracy was 61.1%. The diagnostic performance of standard and M-NBI endoscopy for moderate to severe atrophy and IM in the corpus was not significantly different. The AUC values of standard and M-NBI endoscopy were 0.93 and 0.96 for *H. pylori* gastritis, 0.78 and 0.79 for moderate to severe atrophy, and 0.74 and 0.75 for IM in the corpus, respectively.

### Association of endoscopic patterns with gastric precancerous conditions

Table 4 shows the relationships between endoscopic mucosal patterns and a serum PG I/II ratio of  $\leq 3$ . Among 127 patients who underwent measurement of serum PG concentration, 44.1% (*n* = 56) had a PG I/II ratio of  $\leq 3$ . Of patients with a normal mucosal pattern, the rate of a PG I/II ratio of  $\leq 3$  was 2.6% (*n* = 1/39) by standard endoscopy and 0% (*n* = 0/36) by M-NBI endoscopy. By standard endoscopy, the rate of a PG I/II ratio of  $\leq 3$  was 36.0% (*n* = 9/25) for type A, 71.7% (*n* = 33/46) for type B, and 76.5% (*n* = 13/17) for type C. By M-NBI endoscopy, the rate of a PG I/II ratio of  $\leq 3$  was 54.2% (*n* = 39/72) for type Z-1, 86.7% (*n* = 13/15) for type Z-2, and 100% (*n* = 4/4) for type Z-3. The rate of a PG I/II ratio of  $\leq 3$  differed between normal and abnormal mucosal patterns according to two endoscopic classifications (*P* < 0.001).

The age- and sex-adjusted ORs of abnormal mucosal patterns for gastric precancerous conditions were calculated by logistic regression analyses (Table 5). Compared to type A, the OR for moderate to severe atrophy was 5.56 [95% confidence interval (CI): 2.07-14.92, *P* = 0.001] for types B+C. Compared to type Z-1, the OR for moderate to severe atrophy was 8.67 (95% CI: 1.82-41.30, *P* = 0.007) for types Z-2+Z-3. Compared to type A, the OR for a serum PG I/II ratio of  $\leq 3$  was 4.48 (95% CI: 1.60-12.54, *P* = 0.004) for types B+C. Compared to type Z-1, the OR for a serum PG I/II ratio of  $\leq 3$  was 5.69 (95% CI: 1.19-27.18, *P* = 0.029) for types Z-2+Z-3. For IM in the corpus, there was no significant difference in abnormal mucosal patterns according to two endoscopic classifications (type A *vs* types B+C, *P* = 0.189; and type Z-1 *vs* types Z-2+Z-3, *P* = 0.162, respectively).

## DISCUSSION

Pathological examination plays an important role in the diagnosis of gastrointestinal diseases by endoscopy[20]. Endoscopists tend to focus on detecting abnormal lesions, and macroscopic examination by conventional endoscopy has limitations for characterizing mucosal lesions. Therefore, the final diagnosis of detected lesions is dependent



**Table 4 Serum pepsinogen I/II ratio according to gastric mucosal pattern observed by standard and magnifying narrow-band imaging endoscopy**

PG I/II ratio	Standard (%)				M-NBI (%)			
	Normal	Type A	Type B	Type C	Normal	Type Z-1	Type Z-2	Type Z-3
> 3 ( <i>n</i> = 71)	38/39 (97.4)	16/25 (64.0)	13/46 (28.3)	4/17 (23.5)	36/36 (100)	33/72 (45.8)	2/15 (13.3)	0/4 (0)
≤ 3 ( <i>n</i> = 56)	1/39 (2.6)	9/25 (36.0)	33/46 (71.7)	13/17 (76.5)	0/36 (0)	39/72 (54.2)	13/15 (86.7)	4/4 (100)

PG: Pepsinogen; M-NBI: Magnifying narrow-band imaging.

**Table 5 Logistic regression analysis of the associations of endoscopic mucosal patterns with gastric precancerous conditions**

Mucosal pattern	Moderate to severe atrophy		Intestinal metaplasia, corpus		PG I/II ratio ≤ 3	
	OR (95%CI)	<i>P</i> value	OR (95%CI)	<i>P</i> value	OR (95%CI)	<i>P</i> value
<b>Standard</b>		0.001		0.189		0.004
Type A	1 (ref.)		1 (ref.)		1 (ref.)	
Type B + C	5.56 (2.07-14.92)		1.96 (0.72-5.33)		4.48 (1.60-12.54)	
<b>M-NBI</b>		0.007		0.162		0.029
Type Z-1	1 (ref.)		1 (ref.)		1 (ref.)	
Type Z-2 + Z-3	8.67 (1.82-41.30)		2.12 (0.74-6.07)		5.69 (1.19-27.18)	

M-NBI: Magnifying narrow-band imaging; PG: Pepsinogen; OR: Odds ratio; CI: Confidence interval.

on the pathological report. To identify those at risk of gastric cancer, the presence of precancerous conditions is evaluated by non-targeted protocol-guided biopsies in different areas[21]. However, multiple mucosal biopsies increase medical costs and the procedure time.

High-resolution and high-magnification endoscopy facilitate detailed examination of the gastrointestinal mucosa[22]. In 2002, Yagi *et al*[23] used magnifying endoscopy to show that RAC was a characteristic finding in the normal stomach without *H. pylori* infection. Abnormal mucosal patterns without RAC were classified as Z-1 to Z-3 in accordance with the degree of mucosal damage in the *H. pylori*-infected stomach[24]. Anagnostopoulos *et al*[25] demonstrated that magnifying endoscopic examination could identify normal gastric mucosa, *H. pylori*-related gastritis, and gastric atrophy in a Western population. The severity of chronic gastritis has been investigated based on the micro-mucosal patterns observed by M-NBI[26]. Kanzaki *et al*[27] reported that groove-type mucosa had a higher grade of atrophy and IM compared to foveolar-type mucosa. However, M-NBI endoscopy is not available in all endoscopy units and training program is required prior to its clinical application[28].

In a previous study, we determined *H. pylori* infection status by close observation of the gastric corpus mucosa by high-resolution endoscopy without magnification[12]. The sensitivity and specificity of all abnormal patterns for predicting *H. pylori* infection were 93.3% and 89.1%, respectively, and the overall diagnostic accuracy was 91.6%. The inter- and intra-observer agreement for the endoscopic mucosal patterns was 91.7% and 90.0%, respectively. This simplified endoscopic technique has enabled reliable prediction of gastric *H. pylori* infection in other countries[29,30]. Recent advances in endoscopic imaging technology have increased the diagnostic accuracy for *H. pylori* infection[13,31]. To our knowledge, this is the first study comparing diagnostic performance between standard and M-NBI endoscopy for *H. pylori* infection. We also analyzed the degree of gastric atrophy, IM, and serum PG levels according to two endoscopic classifications. A decrease in the serum PG I/II ratio is reportedly a non-invasive marker for advanced corpus gastritis and gastric cancer[32,33]. Wang *et al*[34] reported that the serum PG level was strongly correlated with the Operative Link for Gastritis Assessment (OLGA) and Operative Link for Gastric Intestinal Metaplasia (OLGIM) stage. Therefore, a serum PG I/II ratio of ≤ 3 is a serologic marker of gastric precancerous conditions.

Except for sensitivity, the diagnostic performance for *H. pylori* infection was similar between standard and M-NBI endoscopy. Seven patients with a normal pattern by standard endoscopy had *H. pylori* infection. In contrast, these patients were classified as type Z-1 ( $n = 4$ ), type Z-2 ( $n = 2$ ), and type Z-3 ( $n = 1$ ) by M-NBI endoscopy. This is likely because of the ability of M-NBI to examine the superficial microanatomy of the areae gastricae and the pit pattern, which is not possible with standard endoscopy. Nevertheless, standard endoscopy may enable detection of *H. pylori* infection in routine clinical practice (diagnostic accuracy, 93.3%).

For diagnosis of gastric atrophy and IM, standard and M-NBI endoscopy had excellent sensitivity, NPV ( $> 95\%$ ), and AUC ( $> 0.7$ ) values; however, the specificity and PPV values were not acceptable. According to the Kimura-Takemoto classification, gastric atrophy progresses more frequently along the lesser curvature than the greater curvature of the corpus[35]. When atrophic change extends into the anterior and posterior mucosa of the corpus, the topographic pattern of IM becomes more diffuse throughout the stomach[36]. In this study, we focused on the mucosal pattern in the greater curvature of the gastric corpus. Atrophy of the gastric mucosa and transformation to IM occur last at the greater curvature of the corpus, hampering evaluation of gastric precancerous conditions. A systematic screening protocol for the stomach has been developed to ensure high-quality endoscopic evaluation[37], and enables detection of gastric atrophy and IM in various areas of the stomach[38]. Using NBI without magnification, Pimentel-Nunes *et al*[39] created an endoscopic classification to grade gastric IM; a tubulovillous mucosal pattern was highly concordant with histological IM. However, image-enhanced endoscopic findings for diagnosing and grading gastric atrophy remain to be established[40].

The *H. pylori*-infected stomach exhibits redness and swelling of the corpus mucosa[41,42]. Histologically, *H. pylori* infection causes infiltration of neutrophils and mononuclear cells in the gastric mucosa[43]. In biopsy specimens, lymphoid hyperplasia is a specific immunological reaction to *H. pylori* infection[44]. During long-term *H. pylori*-induced inflammation, the presence of lymphoid hyperplasia decreased with increasing severity of gastric atrophy and IM. In young women, nodular gastritis is induced by *H. pylori* infection and lymphoid follicles in nodular lesions can be detected histologically[45]. Miyamoto *et al*[46] reported that nodular gastritis showed a lower atrophic score than other forms of *H. pylori*-related gastritis. Similarly, we postulated that a swollen areae gastricae would be present in early stage *H. pylori* infection. Therefore, type A was used as a reference for evaluating the risk of gastric cancer according to abnormal mucosal pattern by standard endoscopy. By M-NBI endoscopy, type Z-1 was reported to correlate with less severe gastric atrophy and IM compared to other types[27]. In this study, types A and B+C showed significantly different serum PG I/II ratios (3.82 *vs* 2.74,  $P = 0.007$ ), as did types Z-1 and Z-2+Z-3 (3.24 *vs* 2.28,  $P = 0.005$ ). However, there was no significant difference among abnormal mucosal patterns for IM in the corpus. Based on the multifocal patterns of IM, an endoscopic mucosal examination of the entire stomach is recommended[47]. Marcos *et al*[48] reported that NBI endoscopic grading of IM was useful for risk assessment of early gastric neoplasia.

This study had several limitations. First, we did not evaluate the severity of gastric atrophy and IM using the OLGA and OLGIM staging systems. Second, only *H. pylori* treatment-naïve patients were enrolled. Therefore, the results may be not be applicable to endoscopic surveillance after *H. pylori* eradication. Finally, this study was conducted in a single center. A multicenter trial involving endoscopists with varying levels of experience is required to confirm the reliability of the results.

## CONCLUSION

In conclusion, close observation of the gastric corpus mucosa by standard and M-NBI endoscopy enables diagnosis of *H. pylori* infection and gastric precancerous conditions. Furthermore, our results suggest an association of endoscopic mucosal patterns with moderate to severe atrophy and a serum PG I/II ratio of  $\leq 3$ .

## ARTICLE HIGHLIGHTS

### Research background

In Correa's model of gastric carcinogenesis, *Helicobacter pylori* (*H. pylori*) infection,

gastric atrophy and intestinal metaplasia (IM) are linked to gastric cancer development. The low level of serum pepsinogens (PG) was known to be highly associated with extensive atrophic gastritis.

### Research motivation

High-resolution and magnifying narrow-band imaging (M-NBI) facilitate the detailed examination of gastrointestinal mucosa. M-NBI endoscopy can be used to diagnose *H. pylori* infection and classify gastritis by histological severity. Moreover, recent improvements in the resolution (> 1 million pixels) of gastrointestinal endoscopy have enhanced image quality, facilitating characterization of the gastric mucosal pattern. Close observation of the gastric corpus mucosa by standard endoscopy without magnification enables prediction of *H. pylori* gastritis and precancerous lesions.

### Research objectives

To date, there was no comparative data regarding the usefulness of standard and M-NBI endoscopy for *H. pylori* infection and gastric precancerous conditions. We compared the diagnostic performance of standard and M-NBI endoscopy for *H. pylori* gastritis and precancerous conditions.

### Research methods

In total, 254 patients who underwent gastroscopy were prospectively enrolled. Standard endoscopy findings of the gastric mucosal surface were classified into mosaic-like appearance (type A), diffuse homogenous redness (type B), and irregular redness with groove (type C). Gastric mucosal patterns visualized by M-NBI endoscopy were classified as regular round pits with polygonal sulci (type Z-1), more dilated and linear pits without sulci (type Z-2), and loss of gastric pits with coiled vessels (type Z-3). We evaluated the utility of the two endoscopic classifications for the diagnosis of *H. pylori* gastritis, gastric atrophy, IM, and a serum PG I/II ratio of  $\leq 3$ .

### Research results

The diagnostic accuracy of standard and M-NBI endoscopy for *H. pylori* gastritis was 93.3% and 96.1%, respectively. Regarding gastric precancerous conditions, the diagnostic accuracy of standard and M-NBI endoscopy was 72.0% vs 72.6% for moderate to severe atrophy, and 61.7% vs 61.1% for IM in the corpus, respectively. Compared to type A and Z1, types B+C and Z-2+Z-3 were significantly associated with moderate to severe atrophy [odds ratio (OR) = 5.56,  $P = 0.001$ ; OR = 8.67,  $P = 0.007$ ] and a serum PG I/II ratio of  $\leq 3$  (OR = 4.48,  $P = 0.004$ ; OR = 5.69,  $P = 0.029$ ).

### Research conclusions

Close observation of the gastric corpus mucosa by standard and M-NBI endoscopy enables diagnosis of *H. pylori* infection and gastric precancerous conditions. Furthermore, our results suggest an association of endoscopic mucosal patterns with moderate to severe atrophy and a serum PG I/II ratio of  $\leq 3$ .

### Research perspectives

By gastric mucosal observation in detail, optical diagnosis of *H. pylori*-related gastritis may be achieved in real time. In the future, a multicenter trial is required to confirm the reliability of our results.

## REFERENCES

- 1 Hooi JKY, Lai WY, Ng WK, Suen MMY, Underwood FE, Tanyingoh D, Malfertheiner P, Graham DY, Wong VWS, Wu JCY, Chan FKL, Sung JJY, Kaplan GG, Ng SC. Global Prevalence of Helicobacter pylori Infection: Systematic Review and Meta-Analysis. *Gastroenterology* 2017; **153**: 420-429 [PMID: 28456631 DOI: 10.1053/j.gastro.2017.04.022]
- 2 Kuipers EJ, Uytendaele AM, Peña AS, Roosendaal R, Pals G, Nelis GF, Festen HP, Meuwissen SG. Long-term sequelae of Helicobacter pylori gastritis. *Lancet* 1995; **345**: 1525-1528 [PMID: 7791437 DOI: 10.1016/s0140-6736(95)91084-0]
- 3 Correa P, Piazuelo MB. The gastric precancerous cascade. *J Dig Dis* 2012; **13**: 2-9 [PMID: 22188910 DOI: 10.1111/j.1751-2980.2011.00550.x]
- 4 Kaji K, Hashiba A, Uotani C, Yamaguchi Y, Ueno T, Ohno K, Takabatake I, Wakabayashi T, Doyama H, Ninomiya I, Kiriya M, Ohya S, Yoneshima M, Koyama N, Takeda Y, Yasuda K. Grading of Atrophic Gastritis is Useful for Risk Stratification in Endoscopic Screening for Gastric Cancer. *Am J Gastroenterol* 2019; **114**: 71-79 [PMID: 30315306 DOI: 10.1038/s41395-018-0259-5]

- 5 **Shichijo S**, Hirata Y, Sakitani K, Yamamoto S, Serizawa T, Niikura R, Watabe H, Yoshida S, Yamada A, Yamaji Y, Ushiku T, Fukayama M, Koike K. Distribution of intestinal metaplasia as a predictor of gastric cancer development. *J Gastroenterol Hepatol* 2015; **30**: 1260-1264 [PMID: 25777777 DOI: 10.1111/jgh.12946]
- 6 **Uemura N**, Okamoto S, Yamamoto S, Matsumura N, Yamaguchi S, Yamakido M, Taniyama K, Sasaki N, Schlemper RJ. *Helicobacter pylori* infection and the development of gastric cancer. *N Engl J Med* 2001; **345**: 784-789 [PMID: 11556297 DOI: 10.1056/NEJMoa001999]
- 7 **Pimentel-Nunes P**, Libânio D, Marcos-Pinto R, Areia M, Leja M, Esposito G, Garrido M, Kikuste I, Megraud F, Matysiak-Budnik T, Annibale B, Dumonceau JM, Barros R, Fléjou JF, Carneiro F, van Hoof JE, Kuipers EJ, Dinis-Ribeiro M. Management of epithelial precancerous conditions and lesions in the stomach (MAPS II): European Society of Gastrointestinal Endoscopy (ESGE), European Helicobacter and Microbiota Study Group (EHMSG), European Society of Pathology (ESP), and Sociedade Portuguesa de Endoscopia Digestiva (SPED) guideline update 2019. *Endoscopy* 2019; **51**: 365-388 [PMID: 30841008 DOI: 10.1055/a-0859-1883]
- 8 **Gono K**, Obi T, Yamaguchi M, Ohyama N, Machida H, Sano Y, Yoshida S, Hamamoto Y, Endo T. Appearance of enhanced tissue features in narrow-band endoscopic imaging. *J Biomed Opt* 2004; **9**: 568-577 [PMID: 15189095 DOI: 10.1117/1.1695563]
- 9 **Muto M**, Horimatsu T, Ezoe Y, Morita S, Miyamoto S. Improving visualization techniques by narrow band imaging and magnification endoscopy. *J Gastroenterol Hepatol* 2009; **24**: 1333-1346 [PMID: 19702901 DOI: 10.1111/j.1440-1746.2009.05925.x]
- 10 **Tahara T**, Shibata T, Nakamura M, Yoshioka D, Okubo M, Arisawa T, Hirata I. Gastric mucosal pattern by using magnifying narrow-band imaging endoscopy clearly distinguishes histological and serological severity of chronic gastritis. *Gastrointest Endosc* 2009; **70**: 246-253 [PMID: 19386303 DOI: 10.1016/j.gie.2008.11.046]
- 11 **ASGE Technology Committee**. High-definition and high-magnification endoscopes. *Gastrointest Endosc* 2014; **80**: 919-927 [PMID: 25442091 DOI: 10.1016/j.gie.2014.06.019]
- 12 **Cho JH**, Chang YW, Jang JY, Shim JJ, Lee CK, Dong SH, Kim HJ, Kim BH, Lee TH, Cho JY. Close observation of gastric mucosal pattern by standard endoscopy can predict *Helicobacter pylori* infection status. *J Gastroenterol Hepatol* 2013; **28**: 279-284 [PMID: 23189930 DOI: 10.1111/jgh.12046]
- 13 **Glover B**, Teare J, Patel N. A systematic review of the role of non-magnified endoscopy for the assessment of *H. pylori* infection. *Endosc Int Open* 2020; **8**: E105-E114 [PMID: 32010741 DOI: 10.1055/a-0999-5252]
- 14 **Cho JH**, Jeon SR, Jin SY. Clinical applicability of gastroscopy with narrow-band imaging for the diagnosis of *Helicobacter pylori* gastritis, precancerous gastric lesion, and neoplasia. *World J Clin Cases* 2020; **8**: 2902-2916 [PMID: 32775373 DOI: 10.12998/wjcc.v8.i14.2902]
- 15 **Yagi K**, Nakamura A, Sekine A. Comparison between magnifying endoscopy and histological, culture and urease test findings from the gastric mucosa of the corpus. *Endoscopy* 2002; **34**: 376-381 [PMID: 11972268 DOI: 10.1055/s-2002-25281]
- 16 **Dixon MF**, Genta RM, Yardley JH, Correa P. Classification and grading of gastritis. The updated Sydney System. International Workshop on the Histopathology of Gastritis, Houston 1994. *Am J Surg Pathol* 1996; **20**: 1161-1181 [PMID: 8827022 DOI: 10.1097/00000478-199610000-00001]
- 17 **Correa P**, Piazuelo MB, Wilson KT. Pathology of gastric intestinal metaplasia: clinical implications. *Am J Gastroenterol* 2010; **105**: 493-498 [PMID: 20203636 DOI: 10.1038/ajg.2009.728]
- 18 **Cho JH**, Jeon SR, Kim HG, Jin SY, Park S. The serum pepsinogen levels for risk assessment of gastric neoplasms: New proposal from a case-control study in Korea. *Medicine (Baltimore)* 2017; **96**: e7603 [PMID: 28723806 DOI: 10.1097/MD.0000000000007603]
- 19 **Kodori A**, Yoshihara M, Sumii K, Haruma K, Kajiyama G. Serum pepsinogen in screening for gastric cancer. *J Gastroenterol* 1995; **30**: 452-460 [PMID: 7550854 DOI: 10.1007/BF02347560]
- 20 **Carpenter HA**, Talley NJ. Gastroscopy is incomplete without biopsy: clinical relevance of distinguishing gastropathy from gastritis. *Gastroenterology* 1995; **108**: 917-924 [PMID: 7875496 DOI: 10.1016/0016-5085(95)90468-9]
- 21 **El-Zimaity HM**, Graham DY. Evaluation of gastric mucosal biopsy site and number for identification of *Helicobacter pylori* or intestinal metaplasia: role of the Sydney System. *Hum Pathol* 1999; **30**: 72-77 [PMID: 9923930 DOI: 10.1016/s0046-8177(99)90303-9]
- 22 **Kiesslich R**, Goetz M, Hoffman A, Galle PR. New imaging techniques and opportunities in endoscopy. *Nat Rev Gastroenterol Hepatol* 2011; **8**: 547-553 [PMID: 21894196 DOI: 10.1038/nrgastro.2011.152]
- 23 **Yagi K**, Nakamura A, Sekine A. Characteristic endoscopic and magnified endoscopic findings in the normal stomach without *Helicobacter pylori* infection. *J Gastroenterol Hepatol* 2002; **17**: 39-45 [PMID: 11895551 DOI: 10.1046/j.1440-1746.2002.02665.x]
- 24 **Yagi K**, Honda H, Yang JM, Nakagawa S. Magnifying endoscopy in gastritis of the corpus. *Endoscopy* 2005; **37**: 660-666 [PMID: 16010611 DOI: 10.1055/s-2005-861423]
- 25 **Anagnostopoulos GK**, Yao K, Kaye P, Fogden E, Fortun P, Shonde A, Foley S, Sunil S, Atherton JJ, Hawkey C, Ragunath K. High-resolution magnification endoscopy can reliably identify normal gastric mucosa, *Helicobacter pylori*-associated gastritis, and gastric atrophy. *Endoscopy* 2007; **39**: 202-207 [PMID: 17273960 DOI: 10.1055/s-2006-945056]
- 26 **Kawamura M**, Abe S, Oikawa K, Terai S, Saito M, Shibuya D, Kato K, Shimada T, Uedo N, Masuda T. Topographic differences in gastric micromucosal patterns observed by magnifying endoscopy with

- narrow band imaging. *J Gastroenterol Hepatol* 2011; **26**: 477-483 [PMID: 21155881 DOI: 10.1111/j.1440-1746.2010.06527.x]
- 27 **Kanzaki H**, Uedo N, Ishihara R, Nagai K, Matsui F, Ohta T, Hanafusa M, Hanaoka N, Takeuchi Y, Higashino K, Iishi H, Tomita Y, Tatsuta M, Yamamoto K. Comprehensive investigation of areae gastricae pattern in gastric corpus using magnifying narrow band imaging endoscopy in patients with chronic atrophic fundic gastritis. *Helicobacter* 2012; **17**: 224-231 [PMID: 22515361 DOI: 10.1111/j.1523-5378.2012.00938.x]
  - 28 **Nakanishi H**, Doyama H, Ishikawa H, Uedo N, Gotoda T, Kato M, Nagao S, Nagami Y, Aoyagi H, Imagawa A, Kodaira J, Mitsui S, Kobayashi N, Muto M, Takatori H, Abe T, Tsujii M, Watari J, Ishiyama S, Oda I, Ono H, Kaneko K, Yokoi C, Ueo T, Uchita K, Matsumoto K, Kanesaka T, Morita Y, Katsuki S, Nishikawa J, Inamura K, Kinjo T, Yamamoto K, Yoshimura D, Araki H, Kashida H, Hosokawa A, Mori H, Yamashita H, Motohashi O, Kobayashi K, Hirayama M, Kobayashi H, Endo M, Yamano H, Murakami K, Koike T, Hirasawa K, Miyaoka Y, Hamamoto H, Hikichi T, Hanabata N, Shimoda R, Hori S, Sato T, Kodashima S, Okada H, Mannami T, Yamamoto S, Niwa Y, Yashima K, Tanabe S, Satoh H, Sasaki F, Yamazato T, Ikeda Y, Nishisaki H, Nakagawa M, Matsuda A, Tamura F, Nishiyama H, Arita K, Kawasaki K, Hoppo K, Oka M, Ishihara S, Mukasa M, Minamino H, Yao K. Evaluation of an e-learning system for diagnosis of gastric lesions using magnifying narrow-band imaging: a multicenter randomized controlled study. *Endoscopy* 2017; **49**: 957-967 [PMID: 28637065 DOI: 10.1055/s-0043-111888]
  - 29 **Yumang ZL**, Panglinan JA. Close observation endoscopy of gastric mucosal pattern in predicting *Helicobacter pylori* infection a single center cross-sectional study (a preliminary report). *Gut Liver* 2018; **12**: S26
  - 30 **Garcés-Durán R**, García-Rodríguez A, Córdova H, Cuatrecasas M, Ginès À, González-Suárez B, Araujo I, Llach J, Fernández-Esparrach G. Association between a regular arrangement of collecting venules and absence of *Helicobacter pylori* infection in a European population. *Gastrointest Endosc* 2019; **90**: 461-466 [PMID: 31108089 DOI: 10.1016/j.gie.2019.05.027]
  - 31 **Qi Q**, Guo C, Ji R, Li Z, Zuo X, Li Y. Diagnostic Performance of Magnifying Endoscopy for *Helicobacter pylori* Infection: A Meta-Analysis. *PLoS One* 2016; **11**: e0168201 [PMID: 27992489 DOI: 10.1371/journal.pone.0168201]
  - 32 **Gantuya B**, Oyuntsetseg K, Bolor D, Erdene-Ochir Y, Sanduijav R, Davaadorj D, Tserentogtokh T, Uchida T, Yamaoka Y. Evaluation of serum markers for gastric cancer and its precursor diseases among high incidence and mortality rate of gastric cancer area. *Gastric Cancer* 2019; **22**: 104-112 [PMID: 29934751 DOI: 10.1007/s10120-018-0844-8]
  - 33 **Kang JM**, Kim N, Yoo JY, Park YS, Lee DH, Kim HY, Lee HS, Choe G, Kim JS, Jung HC, Song IS. The role of serum pepsinogen and gastrin test for the detection of gastric cancer in Korea. *Helicobacter* 2008; **13**: 146-156 [PMID: 18321304 DOI: 10.1111/j.1523-5378.2008.00592.x]
  - 34 **Wang X**, Lu B, Meng L, Fan Y, Zhang S, Li M. The correlation between histological gastritis staging- 'OLGA/OLGIM' and serum pepsinogen test in assessment of gastric atrophy/intestinal metaplasia in China. *Scand J Gastroenterol* 2017; **52**: 822-827 [PMID: 28436254 DOI: 10.1080/00365521.2017.1315739]
  - 35 **Kimura K**. Chronological transition of the fundic-pyloric border determined by stepwise biopsy of the lesser and greater curvatures of the stomach. *Gastroenterology* 1972; **63**: 584-592 [PMID: 5077145 DOI: 10.1016/S0016-5085(19)33241-X]
  - 36 **Cassaro M**, Rugge M, Gutierrez O, Leandro G, Graham DY, Genta RM. Topographic patterns of intestinal metaplasia and gastric cancer. *Am J Gastroenterol* 2000; **95**: 1431-1438 [PMID: 10894575 DOI: 10.1111/j.1572-0241.2000.02074.x]
  - 37 **Yao K**. The endoscopic diagnosis of early gastric cancer. *Ann Gastroenterol* 2013; **26**: 11-22 [PMID: 24714327 DOI: 10.1016/S0016-5107(79)73384-0]
  - 38 **Banks M**, Graham D, Jansen M, Gotoda T, Coda S, di Pietro M, Uedo N, Bhandari P, Pritchard DM, Kuipers EJ, Rodriguez-Justo M, Novelli MR, Ragunath K, Shepherd N, Dinis-Ribeiro M. British Society of Gastroenterology guidelines on the diagnosis and management of patients at risk of gastric adenocarcinoma. *Gut* 2019; **68**: 1545-1575 [PMID: 31278206 DOI: 10.1136/gutjnl-2018-318126]
  - 39 **Pimentel-Nunes P**, Libânio D, Lage J, Abrantes D, Coimbra M, Esposito G, Hormozdi D, Pepper M, Drasovean S, White JR, Dobru D, Buxbaum J, Ragunath K, Annibale B, Dinis-Ribeiro M. A multicenter prospective study of the real-time use of narrow-band imaging in the diagnosis of premalignant gastric conditions and lesions. *Endoscopy* 2016; **48**: 723-730 [PMID: 27280384 DOI: 10.1055/s-0042-108435]
  - 40 **Rodríguez-Carrasco M**, Esposito G, Libânio D, Pimentel-Nunes P, Dinis-Ribeiro M. Image-enhanced endoscopy for gastric preneoplastic conditions and neoplastic lesions: a systematic review and meta-analysis. *Endoscopy* 2020; **52**: 1048-1065 [PMID: 32663879 DOI: 10.1055/a-1205-0570]
  - 41 **Uchiyama K**, Ida K, Okuda J, Asai Y, Ohyama Y, Kuroda M, Matsumoto N, Takami T, Ogawa T, Takaori K. Correlations of hemoglobin index (IHb) of gastric mucosa with *Helicobacter pylori* (H. pylori) infection and inflammation of gastric mucosa. *Scand J Gastroenterol* 2004; **39**: 1054-1060 [PMID: 15545161 DOI: 10.1080/00365520410009645]
  - 42 **Kato T**, Yagi N, Kamada T, Shimbo T, Watanabe H, Ida K; Study Group for Establishing Endoscopic Diagnosis of Chronic Gastritis. Diagnosis of *Helicobacter pylori* infection in gastric mucosa by endoscopic features: a multicenter prospective study. *Dig Endosc* 2013; **25**: 508-518 [PMID: 23369058 DOI: 10.1111/den.12031]
  - 43 **Wyatt JL**. Histopathology of gastroduodenal inflammation: the impact of *Helicobacter pylori*.



- Histopathology* 1995; **26**: 1-15 [PMID: 7713479 DOI: 10.1111/j.1365-2559.1995.tb00614.x]
- 44 **Chen XY**, Liu WZ, Shi Y, Zhang DZ, Xiao SD, Tytgat GN. Helicobacter pylori associated gastric diseases and lymphoid tissue hyperplasia in gastric antral mucosa. *J Clin Pathol* 2002; **55**: 133-137 [PMID: 11865009 DOI: 10.1136/jcp.55.2.133]
  - 45 **Shiotani A**, Kamada T, Kumamoto M, Nakae Y, Nakamura Y, Kakudo K, Haruma K. Nodular gastritis in Japanese young adults: endoscopic and histological observations. *J Gastroenterol* 2007; **42**: 610-615 [PMID: 17701123 DOI: 10.1007/s00535-007-2073-5]
  - 46 **Miyamoto M**, Haruma K, Yoshihara M, Hiyama T, Sumioka M, Nishisaka T, Tanaka S, Chayama K. Nodular gastritis in adults is caused by Helicobacter pylori infection. *Dig Dis Sci* 2003; **48**: 968-975 [PMID: 12772798 DOI: 10.1023/a:1023016000096]
  - 47 **Correa P**, Haenszel W, Cuello C, Zavala D, Fontham E, Zarama G, Tannenbaum S, Collazos T, Ruiz B. Gastric precancerous process in a high risk population: cohort follow-up. *Cancer Res* 1990; **50**: 4737-4740 [PMID: 2369748 DOI: 10.1097/00002820-199008000-00007]
  - 48 **Marcos P**, Brito-Gonçalves G, Libânio D, Pita I, Castro R, Sá I, Dinis-Ribeiro M, Pimentel-Nunes P. Endoscopic grading of gastric intestinal metaplasia on risk assessment for early gastric neoplasia: can we replace histology assessment also in the West? *Gut* 2020; **69**: 1762-1768 [PMID: 32051208 DOI: 10.1136/gutjnl-2019-320091]



Published by **Baishideng Publishing Group Inc**  
7041 Koll Center Parkway, Suite 160, Pleasanton, CA 94566, USA

**Telephone:** +1-925-3991568

**E-mail:** [bpgoffice@wjgnet.com](mailto:bpgoffice@wjgnet.com)

**Help Desk:** <https://www.f6publishing.com/helpdesk>

<https://www.wjgnet.com>

